

University of Warwick institutional repository: <http://go.warwick.ac.uk/wrap>

A Thesis Submitted for the Degree of PhD at the University of Warwick

<http://go.warwick.ac.uk/wrap/67112>

This thesis is made available online and is protected by original copyright.

Please scroll down to view the document itself.

Please refer to the repository record for this item for information to help you to cite it. Our policy information is available from the repository home page.

**An Investigation into the Structure and
Function of VanS proteins involved in the
Two-Component VanS/VanR Regulatory
System controlling Antibiotic Resistance**

Richard James Edwards, MChem (Distinction)

A thesis submitted in partial fulfilment
of the requirements for the degree of
Doctor of Philosophy in Chemistry and Biological Sciences

University of Warwick

Department of Chemistry and School of Life Sciences

September 2014

TABLE OF CONTENTS

LIST OF TABLES	ix
LIST OF FIGURES	x
ACKNOWLEDGEMENTS	xix
DECLARATION.....	xx
ABSTRACT.....	xxi
ABBREVIATIONS.....	xxii
CHAPTER 1: INTRODUCTION.....	1
1.1 Antimicrobials and Bacterial Antibiotic Resistance	1
1.1.1 Historical Background and Current Context.....	1
1.1.2 The Impact of Antibacterial Resistance on Healthcare.....	4
1.1.3 Mechanisms of Action of Antimicrobial Agents	5
1.1.4 Emergence of Antibiotic Resistance	7
1.1.5 Development of Bacterial Resistance	10
1.1.6 Bacterial Resistance Mechanisms to Antibiotics	11
1.2 Peptidoglycan as an Antimicrobial Target	13
1.2.1 The Cell Wall.....	13
1.2.2 The Molecular Structure of Peptidoglycan	14
1.2.3 Synthesis of Nucleotide precursors to Peptidoglycan.....	15
1.2.4 Synthesis of lipid-linked intermediates to Peptidoglycan.....	16
1.2.5 Polymerisation Reactions to form Peptidoglycan.....	16
1.3 Glycopeptide Antibiotics and Resistance Mechanisms.....	18
1.3.1 Structure and Function	18
1.3.2 Vancomycin: A History	19
1.3.3 Mode of Action and Development of Resistance to Vancomycin	19
1.3.4 Vancomycin resistance transfer across species.....	22
1.3.5 Vancomycin resistance in actinomycetes.....	22
1.3.6 The van resistance genes.....	23

1.4	Inducers of the VanS/VanR system.....	26
1.4.1	VanA-type resistance	26
1.4.2	VanB-type resistance	29
1.4.3	Summary of Antibiotic Inducers.....	32
1.5	Two Component Regulatory Systems	34
1.5.1	Diversity of Bacterial Two-Component Systems	34
1.5.2	Domain Architecture and Function.....	35
1.5.3	Histidine Kinase.....	37
1.5.4	Response Regulator (RR).....	42
1.5.5	Insights into Signal Transduction Mechanisms	44
1.5.6	A Full-Length Histidine Kinase.....	50
1.5.7	Cross-Talk within Two Component Systems	51
1.6	Strategies for the Discovery and Development of Novel Antimicrobials	52
1.6.1	Platforms for Antibiotic Discovery.....	52
1.6.2	Underexplored antibiotic targets	54
1.7	Aims and Outline of Thesis	56
1.7.1	Aims.....	56
1.7.2	Outline.....	59
CHAPTER 2:	MATERIALS AND METHODS.....	60
2.1	Suppliers of Chemicals and Reagents	60
2.2	Escherichia coli Strains	60
2.2.1	Bacterial Growth Media.....	60
2.2.2	Bacterial Strains	61
2.2.3	Preparation of Chemically Competent Bacterial Cells for Transformations .	62
2.3	DNA Transformation of <i>E. coli</i>.....	62
2.3.1	Preparation of Glycerol Stocks	63

2.4	DNA Manipulation and Cloning Techniques	63
2.4.1	Polymerase Chain Reaction (PCR)	65
2.4.2	Site-directed Mutagenic PCR ('Round-the-Horn')	66
2.4.3	Restriction Enzyme Digestion of DNA.....	67
2.4.4	Preparation of Plasmid DNA	67
2.4.5	Purification of DNA from PCR and Restriction Digests	68
2.4.6	Agarose Gel Electrophoresis.....	68
2.4.7	Ligation of DNA Fragments with Complementary Ends	68
2.4.8	DNA Sequencing of Plasmid Constructs	69
2.5	Membrane Protein Expression and Purification	71
2.5.1	Protein Over-Expression	71
2.5.2	Preparation of Membrane Protein Lysates	73
2.5.3	Large-Scale Membrane Protein Preparations.....	73
2.5.4	Protein Solubilisation using Membrane Mimetics	74
2.6	Protein Analysis and Detection.....	75
2.6.1	Sodium Dodecyl Sulphate-Polyacrylamide Gel Electrophoresis.....	75
2.6.2	Blue Native PAGE	76
2.6.3	Western Blotting for Histidine-tagged proteins	77
2.6.4	Western blotting for MBP-tagged proteins	79
2.6.5	Detergent Screening by Western Blotting.....	80
2.6.6	Immobilised Metal Affinity Chromatography	81
2.6.7	Analytical Gel Filtration Chromatography	83
2.6.8	Protein Sample Desalting, Concentrating and Dialysing	83
2.6.9	Staining of SDS-PAGE Gels.....	85
2.6.10	Determination of Protein Concentration	85

2.7	ToxCAT assays.....	86
2.7.1	Cloning VanS transmembrane domains into the ToxCAT plasmid.....	87
2.7.2	Maltose malE Complementation assay	90
2.7.3	Expression check.....	90
2.7.4	Proteolysis of Spheroplasts	91
2.7.5	Disk Diffusion Assay	92
2.7.6	Quantitative CAT Assay	93
2.8	Mass Spectrometry	94
2.8.1	Full-length protein identification by Mass Spectroscopy	94
2.8.2	Protein Identification by Tryptic Digest and nanoLC-ESI-MS/MS.....	94
2.9	Protein Activity Determination using Coupled Enzymatic Assays	95
2.9.1	Continuous ADP Release Assay	95
2.9.2	Continuous Inorganic Phosphate Release Assay	96
2.9.3	Identification of Assay products by Anion Exchange Chromatography.....	98
2.10	Circular Dichroism	99
2.11	Fluorescence Spectroscopy.....	101
2.12	Site-specific Enzymatic Tag-Cleavage	103
2.12.1	Enzymatic digestion with in-house synthesised TEV protease.....	103
2.12.2	3C Protease Expression and Purification	104
2.12.3	Enzymatic Digestion with 3C Protease.....	105
2.13	Protein Crystallisation.....	106
2.13.1	Vapour Diffusion Crystallisation	108
2.13.2	Sparse Matrix Screening	108
2.13.3	Data Collection	109
2.14	Solution State Nuclear Magnetic Resonance Spectroscopy	110
2.14.1	2D ¹ H- ¹⁵ N HSQC NMR Spectra of VanS proteins in detergent micelles	112
2.14.2	Ligand-based Titrations by 2D ¹ H- ¹⁵ N HSQC spectroscopy	113
2.14.3	Analysis of NMR-based ligand titration data.....	114

CHAPTER 3: CLONING, EXPRESSION, PURIFICATION AND FUNCTIONAL CHARACTERISATION OF VANS PROTEINS FROM ENTEROCOCCI AND STREPTOMYCES	115
3.1 Introduction.....	115
3.2 Aims.....	121
3.3 Cloning <i>vanS</i> genes into Expression Vectors.....	122
3.4 Expression of VanS constructs.....	124
3.5 Western Blotting for His-tagged VanS proteins.....	129
3.6 Purification of VanS Membrane Proteins by IMAC	131
3.7 Purification of VanS proteins by Gel Filtration Chromatography	140
3.8 Histidine Tag Cleavage for Crystallisation Trials.....	143
3.9 Identification of Full-length VanS Proteins by Mass Spectrometry.....	145
3.10 Secondary structure of VanS proteins by Circular Dichroism.....	146
3.11 Determination of VanS Protein Activity by Coupled Enzymatic Assays.....	149
3.11.1 ADP Release Assay	152
3.11.2 Phosphate Release Assay	156
3.11.3 Assessing the Autophosphorylation of VanS.....	157
3.11.4 Identifying Nucleotide products using Anion Exchange Chromatography .	160
3.12 Crystallisation Screens	167
3.13 Discussion.....	170
3.13.1 Approaches to express and purify VanS proteins for crystal studies.....	171
3.13.2 Screening crystallisation of VanS proteins from multiple species.....	172
3.13.3 Activity of VanS and its crystallisation is affected by detergent micelles ...	173
3.13.4 Possibility of secondary reactions during VanS autophosphorylation.....	174

CHAPTER 4: STRUCTURAL STUDIES OF THE VANS SENSOR DOMAIN BY SOLUTION-STATE NMR SPECTROSCOPY	177
4.1 Introduction.....	177
4.2 Aims.....	180
4.3 Gene Modification of <i>vanS</i> sequences to create NMR-relevant constructs ..	181
4.4 M9 Minimal Media Expression of <i>vanS</i> genes.....	192
4.5 M9 Minimal Media Expression of mutant <i>vanS</i> genes for Enzymatic Cleavage and Purification of the isolated VanS sensor domain	198
4.6 2D Solution State NMR studies of the VanS sensor domain and Optimisation of Solution Conditions by Temperature, Detergent and Buffer Screening	204
4.6.1 Effect of magnetic field strength and temperature	204
4.6.2 Effect of detergent.....	207
4.6.3 Effect of pH.....	214
4.6.4 Analysis of protein fold in NMR samples.....	217
4.7 Discussion.....	219
4.7.1 Optimal routes to obtain and selectively purify the VanS sensor domain ...	220
4.7.2 Optimised protocols for the expression of ¹⁵ N-labelled VanS proteins	222
4.7.3 Obtaining high resolution 2D NMR spectra of the VanS sensor domain	224
CHAPTER 5: ANALYSIS OF RECEPTOR-LIGAND BINDING AND EXAMINATION OF THE ROLE OF OLIGOMERISATION IN SIGNALLING	227
5.1 Introduction.....	227
5.2 Aims.....	232
5.3 Analysis of Ligand Binding by Fluorescence Spectroscopy	233
5.4 Analysis of Ligand Binding by Solution State NMR Spectroscopy	239
5.4.1 Chemical Shift Perturbation NMR Analysis.....	240
5.4.2 Analysis of Full-length VanS proteins by NMR Spectroscopy	257
5.4.3 NMR Titration of the Lipid II cell wall precursor	262
5.4.4 NMR Titration of other glycopeptide antibiotics.....	264

5.5	The Role of VanS Oligomerisation in Ligand Binding and Signalling.....	266
5.5.1	Analysis of VanS Oligomerisation by Blue Native PAGE	267
5.5.2	Analysis of VanS Homo-Oligomerisation using ToxCAT Assays	270
5.6	Discussion.....	280
5.6.1	New evidence for a direct interaction between vancomycin and VanS	281
5.6.2	The role of transmembrane domains upon signal transduction.....	283
5.6.3	The role of vancomycin dimerization in ligand binding	286
CHAPTER 6:	SUMMARY AND CONCLUSIONS.....	290
6.1	Background and Objectives	290
6.2	Efforts towards Crystallisation or an NMR Structure of a VanS protein	290
6.3	Characterising the Mechanism of VanS autophosphorylation	292
6.4	Assessing the Binding of Potential Antibiotic Ligands to VanS proteins.....	293
6.5	Assessing the role of TM domain association in Signal transduction.....	294
6.6	Recommendations for Future Work	296
BILIOGRAPHY	301
APPENDIX	328

List of Tables

Chapter 1 : Introduction

Table 1.1.1.1: Antibiotic classes, their deployment year and observed clinical resistance.....	3
Table 1.1.3.1: Major classes of antibiotics; their targets and mechanism of action.....	5
Table 1.3.3.1: VRE Phenotypes, adapted from Sujatha & Praharaj (2012).....	21
Table 1.4.3.1: Induced vancomycin resistance in the <i>E. faecium</i> VanA phenotype by various antibiotics, according to reporter or assay based systems.....	32
Table 1.4.3.2: Induced vancomycin resistance in the <i>E. faecalis</i> VanB phenotype by various antibiotics, according to reporter or assay based systems.....	33
Table 1.4.3.3: Induced vancomycin resistance in the <i>S. coelicolor</i> VanB-like phenotype by various antibiotics, according to reporter or assay based systems.....	33
Table 1.5.1.1: Examples of bacterial two-component signalling systems.....	35

Chapter 2 : Materials and Methods

Table 2.2.2.1: <i>E. coli</i> strains used in this project.....	61
Table 2.4.1: Synthesised oligonucleotide sequences used in this project.....	63
Table 2.4.8.1: Initial gene constructs and constructs created.....	70
Table 2.13.1: Factors affecting crystallisation.....	107

Chapter 3 : Cloning, Expression, Purification and Functional Characterisation of VanS proteins from Enterococci and Streptomyces

Table 3.11.3.1: ADP and phosphate release per assay for VanS _A in DDM or DPC and VanS _{SC} in DPC, recorded at 25, 60 or 120 minutes.....	159
Table 3.11.4.1A:Relative peak integrals of nucleotide products observed over time by anion exchange chromatography upon addition of ATP to VanS _A	163
Table 3.11.4.1B:Relative peak integrals of nucleotide products observed over time by anion exchange chromatography upon addition of ADP to VanS _A	165
Table 3.12.1: Concentrations of detergent-purified, tag-cleaved VanS _A proteins used in crystallisation screens.....	169

List of Figures

Chapter 1 : Introduction

Figure 1.1.6.1: A schematic illustration of the five families of drug efflux pumps involved in antibiotic resistance.....	13
Figure 1.2.1.1: Structures of Gram-positive (a) and Gram-negative (b) bacterial cell walls, reproduced from Soloman <i>et al.</i> , (1999).....	14
Figure 1.2.5.1: Steps and enzymes involved in the biosynthesis of peptidoglycan.....	17
Figure 1.3.1.1: Structures of vancomycin and teicoplanin.....	18
Figure 1.3.3.1: (left) Vancomycin binding to the D-Ala-D-Ala N-terminus of Lipid II PG precursor and (right) a resistant D-Ala-D-Lac form.....	20
Figure 1.3.6.1: A comparison of van gene clusters from <i>Enterococcal</i> VanA and VanB strains and actinomycetes.	24
Figure 1.3.6.2: (left) A model of the VanRS two-component system controlling antibiotic resistance (right) the function of enzymes encoded by van resistance genes	26
Figure 1.4.1.1: A petri plate assay for vancomycin resistance induction, reproduced from Lai & Kirsch (1996).....	28
Figure 1.4.2.1: Schematic diagram of a direct binding between VPP and VanS _{SC} protein...	31
Figure 1.5.2.1: Domain architecture and signalling in two-component systems.....	36
Figure 1.5.3.1: The dimerisation and phosphotransfer domain of EnvZ HK	38
Figure 1.5.3.2: Ribbon diagram of the ATP binding domain of DesK HK from <i>B. subtilis</i> with bound ATP (PDB: 3EHG).....	39
Figure 1.5.3.3: X-ray crystal structures of monomeric sensor domains of histidine kinases..	40
Figure 1.5.4.1: Structures of the <i>E. coli</i> receiver domain of the PhoB response regulator...	43
Figure 1.5.4.2: Structure of the dimeric effector domain of NarL RR binding to DNA.....	44
Figure 1.5.5.1: Schematic of histidine kinase modular architecture.....	45
Figure 1.5.5.2: Ribbon diagram of the dimeric cytoplasmic portion of HK853.....	47
Figure 1.5.5.3: Ribbon representation of the crystal structure of HK853-RR468 complex...	48
Figure 1.5.5.4: Signal transduction model, adapted from Casino <i>et al.</i> , (2009).....	49
Figure 1.5.6.1: Ribbon diagram of the X-ray crystal structure of the dark-adapted sensor kinase YF1 (PDB: 4GCZ).....	51
Figure 1.6.1.1: Structures of Platensimycin and Bedaquiline.....	54
Figure 1.6.2.1: A synthetic amidine vancomycin aglycone which binds to D-Ala-D-Lac...	55
Figure 1.7.1.1: Schematic diagram showing the predicted topology of VanS, which is activated by vancomycin antibiotics, to transduce a signal to VanR.....	58

Chapter 2 : Materials and Methods

Figure 2.4.2.1: 3C site insertion by “Round-the-Horn” mutagenic PCR.....	67
Figure 2.6.6.1: Model of the interaction between Ni NTA and a His-tag.....	81
Figure 2.7.1.1: Expression of chimeric fusion proteins using the pccKan plasmid.....	87
Figure 2.7.1.2: Example of annealed oligonucleotide sequences of the VanS _A TM1 domain for inserting into pccKan plasmids.....	88
Figure 2.7.1.3: A 0.8% agarose gel stained with ethidium bromide, showing undigested pccKan plasmid, and double-digested pccKan plasmid.....	89
Figure 2.9.1.1: Reaction pathway involved in ADP production by ATP hydrolysis, as described by Wampler and Westhead (1968).....	95
Figure 2.9.2.1: Reaction pathway involved in inorganic phosphate release by ATP hydrolysis, as described by Webb (1992).....	97
Figure 2.11.1: BODIPY-Vancomycin structure, drawn in IsisDraw.....	101
Figure 2.13.1: Two-dimensional Phase diagram for Crystal growth.....	106
Figure 2.13.1.1: The Vapour diffusion method.....	108
Figure 2.14.1: Representation of nuclear spin relative to an axis of rotation, upon irradiation with a 90° pulse at the Larmor frequency (rf).....	110
Figure 2.14.2: An example 2D COSY pulse program.....	111

Chapter 3 : Cloning, Expression, Purification and Functional Characterisation of VanS proteins from Enterococci and Streptomyces

Figure 3.1.1: Model of phosphotransfer relay in the VanS-VanR two-component system.....	116
Figure 3.1.2: Schematic representation of the VanS protein and predicted topology.....	118
Figure 3.1.3: CLUSTALW2 sequence alignment of the VanS _A , VanS _B and VanS _{SC} protein sequences.....	119
Figure 3.3.1: Restriction map of the pProEx HTa plasmid between bases 251 and 450...122	
Figure 3.3.2: A 0.8% agarose gel (inverted image) showing the PCR amplification of (a) vanS _A and (b) vanS _{SC} genes.....	123
Figure 3.3.3: A 0.8% agarose gel (inverted image) showing correctly-sized gene sequences after NcoI/HindIII double-digestion.....	124
Figure 3.4.1: A 12% SDS-PAGE gel showing proteins overexpressed in C41 or C43 (DE3) pRIL cell lines after Water Lysis preparations.....	125

Figure 3.4.2:	(a) An SDS-PAGE gel showing overexpressed proteins from pttQ18::vanS _A in C41pRIL cells at varying [IPTG] and (b) corresponding growth curves.	126
Figure 3.4.3:	12% SDS-PAGE gel showing overexpression from pProEx::vanS _A or pProEx::vanS _{SC} constructs in C41pRIL cells, after Water Lysis.	127
Figure 3.4.4:	A 12% SDS-PAGE gel showing expression from pProEx::vanS _A at 25°C overnight prepared by Water Lysis.	128
Figure 3.5.1:	(left) 12% SDS-PAGE gel of Water Lysis preparations, and (right) equivalent Western blot developed using Roche non-specific anti-His antibodies.	129
Figure 3.5.2:	(left) 12% SDS-PAGE gel of Water Lysis preparations, and (right) equivalent Western blot developed using Sigma N-term preferential anti-His antibodies.	130
Figure 3.6.1:	A 12% SDS-PAGE gel showing N-His ₆ -VanS _A purification by affinity chromatography.	132
Figure 3.6.2:	A 12% SDS-PAGE gel of N-His ₆ -VanS _A extraction into DDM micelles.	133
Figure 3.6.3:	(a) Western blots showing detergent solubilisation of VanS _{SC} (left) or VanS _A (right) membrane pellets, and (b) corresponding bar charts of the relative percentages of soluble and insoluble protein.	134
Figure 3.6.4:	Molecular structures of DPC and DDM detergents, drawn in ISISDraw.	135
Figure 3.6.5:	Crystallisation conditions for C-His ₆ -VanS _A at 18°C, identified by Dr Marek Brzozowski and Justyna Korczynska at York University.	137
Figure 3.6.6:	A 12% SDS-PAGE gel showing the purification of N-His ₆ -VanS _A by affinity chromatography.	138
Figure 3.6.7:	Western blot showing attempted purification of N-His ₆ -VanS _{SC} proteins expressed at 37°C.	139
Figure 3.6.8:	Western blot showing attempted purification of N-His ₆ -VanS _{SC} proteins expressed at 16°C.	139
Figure 3.6.9:	A 12% SDS-PAGE gel showing purification of N-His ₆ -VanS _{SC} proteins by affinity chromatography.	140
Figure 3.7.1:	Gel Filtration Chromatograms for protein samples of VanS _A (black) and VanS _{SC} (red) applied to a Superose 12 column.	141
Figure 3.7.2:	A calibration curve of gel filtration standards, plotted by the log of their weights against their elution times (V _e), relative to a void volume (V _o).	141
Figure 3.7.3:	A 12% SDS-PAGE gels showing aliquots of 0.3 mL gel filtration elutions collected under the main peak (~10 -12 mL).	142
Figure 3.8.1:	A 12% SDS-PAGE gel to test conditions for VanS _A tag-cleavage.	143
Figure 3.8.2:	A 12% SDS-PAGE gel showing tag-cleavage of VanS _A with TEV.	144

Figure 3.9.1: Mass averaged, deconvoluted ESI-TOF mass spectra of tag-cleaved wild-type VanS _A (a) and VanS _{SC} (b) proteins.....	145
Figure 3.10.1: CD spectra of 5 μM N-His ₆ -VanS _A and N-His ₆ -VanS _{SC} in HEPES or phosphate buffer pH 7.5, containing 2 mM DPC.....	147
Figure 3.10.2: CD spectra of 5 μM N-His-tagged and tag-cleaved VanS _A in phosphate buffer pH 7.5 or TFE, containing 2 mM DPC.....	148
Figure 3.11.1: 14% acrylamide SDS-PAGE gel phosphoimage of VanS _A Δ110 autophosphorylation with time, reproduced from Quigley (2010).....	150
Figure 3.11.2: ADP release profile of C-His ₆ -VanS _A full-length (green), VanS _A Δ110 (blue) and VanS _A Δ155 (red), extracted from Quigley (2010).....	151
Figure 3.11.1.1: Reaction pathways involved in (a) ADP production by ATP hydrolysis and (b) inorganic phosphate release by ATP hydrolysis.....	153
Figure 3.11.1.2: ADP release profile for full-length VanS _A protein in 6 mM DDM (0.03 %, red) or 2 mM DPC (0.07%, green), and VanS _{SC} protein in 2 mM DPC (0.07%, blue).....	154
Figure 3.11.1.3: ADP release profile for full-length VanS _A protein in 6 mM DDM (0.03 %) produced upon initiation by either enzyme (green) or substrate (red).....	156
Figure 3.11.2.1: Phosphate release profile for full-length VanS _A in 6 mM DDM (0.03%, red) or 2 mM DPC (0.07%, green), and full-length VanS _{SC} in 2 mM DPC (0.07%, blue).....	157
Figure 3.11.4.1: MS-MS spectra of ATP phosphorylation reaction of VanS _A 100 630 m/z, reproduced from Quigley (2010).....	161
Figure 3.11.4.2: Anion-exchange chromatography profiles for nucleotide standards (200 μM) applied to a pre-equilibrated MonoQ 5/50 GL column.....	162
Figure 3.11.4.3: Overlaid anion exchange chromatograms collected at timepoints during reaction of VanS _A with ATP, showing the relative amounts of nucleotide products.....	163
Figure 3.11.4.4.: Overlaid anion exchange chromatograms collected at timepoints during reaction of VanS _A with ADP, showing the relative amounts of nucleotide products.....	165
Figure 3.12.1: AMP-PNP structure.....	168
Figure 3.12.2: A selection of promising crystallisation conditions for VanS _A proteins solubilised in 0.07% DPC on MemGold 96-well screens.....	169

Chapter 4 : Structural Studies of the VanS sensor domain by solution-stated NMR spectroscopy

Figure 4.1.1:	NMR backbone structures of TM domains of two classes of histidine kinase.....	178
Figure 4.3.1:	Purified PCR products from amplification of <i>vanS_A</i> , encoding the N-terminal His ₆ tag, TEV site and the first 110, 120 or 130 amino acids of the protein sequence.....	182
Figure 4.3.2:	Western blots showing levels of overexpression of VanSA110, 120 or 130 after Water Lysis preparation.....	183
Figure 4.3.3:	Disorder prediction plots for VanS _A (a) and VanS _{SC} (b) using RONN software.....	184
Figure 4.3.4:	Western blot showing overexpression of SA120 at 16 or 25°C, at varying IPTG concentrations.....	185
Figure 4.3.5:	Schematic representation of a VanS protein and the proposed position for insertion of an enzymatic cleavage site.....	187
Figure 4.3.6:	(left) A 15% SDS-PAGE gel containing digested samples of N-His ₆ -VanS _A collected over timepoints, (right) the corresponding Western blot.....	188
Figure 4.3.7:	Map of peptide fragments identified by MS/MS analysis of excised gel bands from digestion of VanS _A or VanS _{SC}	189
Figure 4.3.8:	Secondary structure prediction for VanS _A (a) and VanS _{SC} (b) proteins between residues 80-160, generated using PSIPred software.....	190
Figure 4.3.9:	Sequencing data showing a section of the VanS _A DNA sequence containing an inserted TEV site (GAG AAC CTG TAC TTC CAG AGT) encoding for ENLYFQS.....	191
Figure 4.4.1:	A diagram of the optimised high-cell-density method used for production of uniformly ¹⁵ N-labelled VanS proteins.....	195
Figure 4.4.2:	(left) A 12% SDS-PAGE gel of VanS _A and VanS _{SC} overexpression in M9 minimal media, at different IPTG concentrations, and (right) corresponding Western blot.....	196
Figure 4.4.3:	A bar chart showing relative band intensities for full-length VanS _A proteins overexpressed under different conditions in ¹⁵ N M9 minimal media.....	197
Figure 4.5.1:	(left) A 12% SDS-PAGE gel showing overexpression of VanS _A and VanS _{SC} mutants in ¹⁵ N-labelled M9 minimal media, and (right) the corresponding Western blot.....	198

Figure 4.5.2:	(left) A 15% SDS-PAGE gel showing initial products from digestion of VanS _A -3C after 4 hours, (right) corresponding western blot.....	199
Figure 4.5.3:	(left) A 15% SDS-PAGE gel showing initial products from TEV digestion of VanS _A -TEV after 4 hours, (right) corresponding western blot.....	199
Figure 4.5.4:	A 12% SDS-PAGE gel showing selective purification of the VanS _A N-terminal 'sensor' domain away from the C-terminal domain and 3C enzyme.....	201
Figure 4.5.5:	Gel filtration chromatograms of protein samples containing the N-terminal sensor domain of ¹⁵ N-labelled VanS _A (black line) or VanS _{SC} (red line) in DPC micelles, applied to a Superose 12 10/300 GL column.....	202
Figure 4.5.6:	A 15% SDS-PAGE gel showing digestion and subsequent purification of the N-terminal 'sensor' domain of VanS _A	202
Figure 4.6.1.1:	2D ¹ H- ¹⁵ N HSQC spectrum of 140 μM VanS _A sensor domain collected at (a) 298K on a 500 MHz spectrometer, or (b) 310K on a 700 MHz spectrometer.....	205
Figure 4.6.1.2:	2D ¹ H- ¹⁵ N HSQC spectrum of 200 μM VanS _{SC} sensor domain in 50 mM DPC, collected at 310K on a 700 MHz spectrometer.....	206
Figure 4.6.2.1:	Molecular structures of LPPG and DPPG detergents, drawn in ISISDraw208	
Figure 4.6.2.2:	Bar charts showing the relative percentages of soluble (red) and insoluble (blue) protein for (a) VanS _A or (b) VanS _{SC} in different detergents.....	209
Figure 4.6.2.3:	Overlaid 2D ¹ H- ¹⁵ N HSQC spectra of VanS _A sensor domain solubilised in 50 mM DPC at 140 μM (red) or in 50 mM LPPG at 200 μM (green).....	211
Figure 4.6.2.4:	Overlaid 2D ¹ H- ¹⁵ N HSQC spectra of (a) 200 μM VanS _A sensor domain (b) 150 μM VanS _{SC} sensor domain, at selected temperatures between 288K and 318 K.....	213
Figure 4.6.3.1:	Overlaid 2D ¹ H- ¹⁵ N HSQC spectra of (a) 200 μM VanS _A N-terminal sensor domain, or (b) 150 μM VanS _{SC} N-terminal sensor domain, obtained at selected pHs between pH 4.6 and 6.3 in 50 mM LPPG.....	215
Figure 4.6.3.2:	Overlaid 2D ¹ H- ¹⁵ N HSQC spectra of 140 μM VanS _A N-terminal sensor domain obtained at selected pHs between 4.6 and 6.3 in 50 mM DPC.....	217
Figure 4.6.4.1:	Overlaid CD spectra for VanS _A and VanS _{SC} sensor domains purified in different detergents.....	218
Figure 4.7.1.1:	An illustration of the purification route used to express, cleave and purify the N-terminal sensor domain of VanS.....	221
Figure 4.7.3.1:	Optimal 2D ¹ H- ¹⁵ N HSQC spectra of the N-terminal sensor domains of VanS _A and VanS _{SC} proteins purified in various detergents and collected on a 700 MHz spectrometer at 310K.....	226

Chapter 5 : Analysis of Receptor-Ligand Binding and Examination of the Role of Oligomerisation State in Receptor Signalling

Figure 5.3.1:	Overlaid emission spectra upon excitation of BODIPY-vancomycin dye in HEPES buffer and/or DPC.....	234
Figure 5.3.2:	Overlaid emission spectra upon excitation of BODIPY-vancomycin dye in HEPES buffer containing DPC, and increasing concentrations of detergent-solubilised Lipid II.....	235
Figure 5.3.3:	Overlaid emission spectra upon excitation of BODIPY-vancomycin dye in HEPES buffer containing DPC, and increasing concentrations of detergent-solubilised VanS _A	236
Figure 5.3.4:	Overlaid emission spectra upon excitation of BODIPY-vancomycin dye in HEPES buffer containing DPC, and increasing concentrations of detergent-solubilised VanS _{SC}	237
Figure 5.4.1.1:	Overlaid 2D ¹ H- ¹⁵ N HSQC spectra of 120 μM VanS _A N-terminal domain solubilised in 50 mM DPC, before and after addition of detergent-solubilised vancomycin.....	242
Figure 5.4.1.2:	The appearance of 2D NMR peak shape under different rates of exchange.....	243
Figure 5.4.1.3:	Overlaid 2D ¹ H- ¹⁵ N HSQC spectra of (a) 600 μM VanS _A N-terminal domain solubilised in 50 mM DPC, 20 mM HEPES pH 6.85, or (b) 700 μM VanS _A N-terminal domain solubilised in 50 mM LMPG, 50 mM sodium acetate pH 5.5, during titration of detergent-solubilised vancomycin.....	245
Figure 5.4.1.4:	Overlaid 2D ¹ H- ¹⁵ N HSQC spectra of 200 μM VanS _{SC} N-terminal domain solubilised in 50 mM LPPG, 50 mM phosphate pH 6.1, during titration of detergent-solubilised vancomycin.....	247
Figure 5.4.1.5:	Chemical shift changes observed for individual peaks in the ¹ H- ¹⁵ N HSQC spectrum of VanS _A protein in LMPG (Fig. 5.4.1.3B) upon addition of vancomycin, represented by a bar chart of peak number (in ascending ¹ H ^N) against chemical shift change (Δδ).....	250
Figure 5.4.1.6:	Overlaid 2D ¹ H- ¹⁵ N HSQC spectra of 700 μM VanS _A N-terminal domain in 50 mM LMPG during titration of vancomycin, zoomed in to the region of 7.5-8.4 ppm in ¹ H and 127-110 ppm in ¹⁵ N, in Figure 5.4.1.3B.....	251
Figure 5.4.1.7:	Overlaid 2D ¹ H- ¹⁵ N HSQC spectra of 600 μM VanS _A N-terminal domain in 50 mM DPC during titration of vancomycin, zoomed in to the region of 7.5-8.2 ppm in ¹ H and 125-110 ppm in ¹⁵ N, in Figure 5.4.1.3A.....	252

Figure 5.4.1.8: Overlaid 2D ^1H - ^{15}N HSQC spectra of 200 μM VanS _{SC} N-terminal domain in 50 mM LPPG during titration of vancomycin, zoomed in to the region of 7.4-8.2 ppm in ^1H and 123-108 ppm in ^{15}N , in Figure 5.4.1.4.....	253
Figure 5.4.1.9: Overlaid 2D ^1H - ^{15}N HSQC NMR spectra for VanS proteins during titration of vancomycin, showing individual peak shifts with high calculated CSP256	
Figure 5.4.1.10: Predicted domain positions in the VanS _{SC} protein sequence, showing residues 17 to 85.....	257
Figure 5.4.2.1: (a) Overlaid 2D ^1H - ^{15}N HSQC spectra of 700 μM VanS _A N-terminal domain (red) or 600 μM full-length protein (green), (b) Overlaid 2D ^1H - ^{15}N HSQC spectra of the VanS _A full-length protein during titration of detergent-solubilised vancomycin.....	259
Figure 5.4.2.2: Vancomycin (left) and Desleucyl vancomycin (right) structures, drawn in ISISDraw.....	261
Figure 5.4.3.1: Overlaid 2D ^1H - ^{15}N HSQC spectra of (a) 600 μM VanS _A N-terminal sensor domain solubilised in 50 mM DPC, or (b) 500 μM VanS _{SC} full-length protein solubilised in 50mM DPC, during titration of detergent-solubilised vancomycin and Lipid II-Lys.....	263
Figure 5.4.4.1: Overlaid 2D ^1H - ^{15}N HSQC spectra of 600 μM VanS _A N-terminal domain in 50 mM LMPG, 50 mM phosphate buffer pH 6.0, during titration of detergent-solubilised teicoplanin.....	265
Figure 5.5.1.1: (left) BN-PAGE 4-16% gradient gel loaded with purified His-tagged full-length VanS _A samples in DPC at 0.1% w/v (~2x CMC), or in DDM at 0.05% w/v (~3x CMC) (right) corresponding Western blot.....	268
Figure 5.5.1.2: BN-PAGE 4-16% gradient gel loaded with purified His-tagged full-length VanS _A (left) or VanS _{SC} (right) samples in DPC detergent at 0.1% w/v (~2x CMC).....	269
Figure 5.5.2.1: A schematic diagram of the basis for the ToxCAT assay.....	272
Figure 5.5.2.2: The <i>malE</i> complementation assay.....	273
Figure 5.5.2.3: Anti-MBP Western blots showing (a) the expression of chimeric fusion proteins in NT326 cells (normalised by OD ₆₀₀) or (b) a spheroplast assay for one fusion protein.....	274
Figure 5.5.2.4: The disk diffusion assay.....	275
Figure 5.5.2.5: Fluorescence emission spectra collected upon excitation of samples containing chimeric fusion proteins at 495 nm.....	276

Figure 5.5.2.6: Normalised ToxCAT activity for each chimeric fusion protein.....	277
Figure 5.5.2.7: A comparison of the predicted TM sequences for VanS _A and VanS _{SC} proteins, highlighting helix-helix packing motifs.....	279
Figure 5.6.2.1: (a) Overlaid backbone structures of CitA ligand-free monomers (magenta) and ligand-bound dimers (green), reproduced from Wang (2012) and (b) the hypothetical model of TM signalling in CitA.....	285
Figure 5.6.3.1: A back-to-back dimer of the vancomycin aglycone induced by an acetate ligand, represented by sticks and a cartoon ribbon.....	287
Figure 5.6.3.2: Stereo view of the “face-to-face” dimer present for vancomycins 4 and 6 in a six-vancomycin-asymmetric unit (PDB: 1FVM), with hydrogen bonding to DALAA ligands.....	288

Chapter 6 : Summary and Conclusions

Figure 6.6.1: Conceptual representation of the protein-tethered lipid bilayer, reproduced from Giess <i>et al.</i> , (2004).....	299
--	-----

Acknowledgements

First and foremost I would like to thank my supervisors Dr Ann Dixon and Dr David Roper for providing me with the opportunity to do a PhD at Warwick University, and for their continued support and guidance throughout the last four years. I would also like to thank everyone in the Roper and Dixon research groups for providing a great environment to work in, and for helping motivate me to keep going in my research studies and finish my thesis.

I would particularly like to thank the following: Dr Gemma Warren for support with cloning, Dr Karen Ruane for assistance in purifications and crystallisations, Michael Chow for help with screening detergents for NMR, Dr Adrian Lloyd and Dr David Roper for guidance with expression and activity assays, and Dr Ann Dixon for help analysing the reams of NMR data.

I would also like to thank my collaborators: Dr Andrew Quigley and Dr Liz Carpenter at the Integral Membrane Protein Department (SGC, Oxford) for their expertise in purifying active proteins, and for the use of their mass spectrometry and crystallisation facilities, and within Warwick: Dr Susan Slade at the Warwick/Waters Centre for help analysing protein gel bands, and Anita Catherwood at the Bacwan Facility for providing Lipid II samples.

Thanks also to my sponsor, the Medical Research Council for providing me with the financial backing for this PhD and the opportunity to attend and present my studies at national and international conferences. And special thanks to Dr John Blood, Conor Proud and Dr Dean Rea, for the numerous chats and the occasional beer to help me face the challenge of membrane protein research!

Lastly, I would like dedicate this thesis to my parents; Alison Edwards and Martin Edwards, and my girlfriend; Amy O'Reilly, for all their love and support during this challenging time.

Declaration

This thesis is submitted to the University of Warwick in support of my application for the degree of Doctor of Philosophy. It has been composed by myself and has not been submitted in any previous application for any degree or at any other university.

I hereby declare that the research submitted in this thesis was conducted by myself, under the supervision of Dr David Roper at the School of Life Sciences and Dr Ann Dixon at the Department of Chemistry (University of Warwick), or was conducted by myself during collaborative research at the Structural Genomics Consortium (University of Oxford), which is fully acknowledged.

All sources of information, including the work of others, are acknowledged in the form of references, and can be found in the bibliography.

Richard Edwards

September 2014

Abstract

VanS is a sensor histidine kinase which forms part of a Two-Component System, with the response regulator, VanR. This system regulates inducible transcription of genes responsible for glycopeptide resistance in enterococci and actinomycetes. In the presence of an antibiotic inducer, VanS autophosphorylates at a conserved histidine residue, and transfers this phosphate to VanR. This phosphorylated form of VanR activates transcription of *vanHAX* genes, which confer resistance to glycopeptide antibiotics.

This research investigates the structure and function of VanS proteins derived from *E. faecium* and *S. coelicolor*, which exhibit different antibiotic resistance phenotypes. The focus is on improving understanding of how glycopeptide antibiotics can either, directly or indirectly, induce VanS activity in each species, and if direct, to identify any ligand binding sites. To date, only one study has shown a direct binding between VanS (derived from *S. coelicolor*) and a vancomycin glycopeptide (Koteva *et al.*, 2010), so this protein (termed VanS_{SC}) was chosen as a control in ligand binding assays, alongside VanS proteins derived from *E. faecium* (termed VanS_A).

Full-length VanS proteins were purified in a functionally-active state and analysed for their structure and ligand binding properties by NMR spectroscopy. High resolution 2D NMR spectra of the isolated VanS sensor domains in each protein have been collected for the first time, and provided a platform for conducting NMR-based ligand titrations. Chemical Shift Perturbation Analysis of the resulting NMR titration data indicates several residues in VanS involved in binding to vancomycin. In conjunction with fluorescence assays, this data newly suggests that both VanS_A and VanS_{SC} can interact directly with vancomycin. This challenges consensus belief in the literature that VanS_A should only be activated indirectly. NMR-based assays outlined here now pave the way for further in-depth studies of the ligand binding mechanism and putative identification of other ligands in this Two-Component System.

Abbreviations

^{13}C	carbon-13
^{15}N	nitrogen-15
$^1\text{H}^{\text{N}}$	amide proton
2D	two-dimensional
3D	three-dimensional
$A_{340\text{nm}}$	absorbance at a wavelength of 340 nm
$A_{360\text{nm}}$	absorbance at a wavelength of 360 nm
ADP	adenosine diphosphate
AGP	antimicrobial growth promoter
AMP	adenosine monophosphate
AMP-PNP	adenyl- β - γ -imidodiphosphate
AP4	adenosine 5'-tetrphosphate
ATP	adenosine triphosphate
BN-PAGE	Blue Native Polyacrylamide electrophoresis
BODIPY	Boron dipyrromethene dye
bp	base pair
BSA	bovine serum albumin
CA	<u>C</u> atalytic and <u>A</u> TP-binding domain
CAT	Chloramphenicol acetyltransferase
CD	Circular dichroism
CMC	Critical Micellar Concentration
CLSI	Clinical and Laboratory Standards Institute
CSP	Chemical Shift Perturbation
C-terminal	Carboxy terminus
δ	Chemical shift in parts per million
$\Delta\delta$	Change in chemical shift in parts per million
D-Ala	D-Alanine
Da	Dalton
DDM	n-dodecyl β -D-maltoside
DHp	<u>D</u> imerisation and <u>h</u> istidine phosphotransfer domain
D-Lac	D-Lactate
DNA	Deoxyribonucleic acid
DNase	Deoxyribonuclease I enzyme
DPC	n-dodecyl phosphocholine
ECL	Electrochemical luminescence
EDTA	ethylenediaminetetraacetic acid
ESI	Electrospray ionisation mass spectrometry

FID	Free induction decay
FRET	Fluorescence resonance energy transfer
γ - ³² P	Phosphorus-32 radioisotope
G83I	Glycine-83 point mutant of Glycophorin A protein
GFC	Gel Filtration Chromatography
GFP	Green fluorescent protein
GlcNAc	N-acetylglucosamine
GpA	Glycophorin A protein
GRE	Glycopeptide resistant enterococci
H	Histidine
HAMP	In <u>H</u> Ks, <u>A</u> denyl cyclases, <u>M</u> ethyl-accepting proteins, <u>P</u> hosphatases
HEPES	N-(2-Hydroxyethyl) piperazine-N'-(2-ethanesulfonic acid)
HK	Histidine kinase
HSQC	Heteronuclear Single Quantum Coherence
IMAC	Immobilised metal affinity chromatography
IMP	Integral membrane protein
IPTG	Isopropyl- β -D-thiogalactopyranoside
K	Kelvin
kb	Kilobase
K _D	Dissociation constant
kDa	Kilodalton
L-Ala	L-Alanine
LB	Luria Broth
LMPG	1-myristoyl-2-hydroxy- <i>sn</i> -glycero-3-[phospho-1'-rac-glycerol]
LPPG	1-palmitoyl-2-hydroxy- <i>sn</i> -glycero-3-[phospho-1'-rac-glycerol]
mAU	Milli-absorbance unit
MBP	Maltose-binding protein
MDR	Multi-drug resistant strain
MESG	Methylthioguanosine
MHz	Megahertz
MIC	Minimum inhibitory concentration
MRE	Mean residue ellipticity
MRSA	Methicillin-resistant <i>Staphylococcus aureus</i>
MS	Mass spectrometry
MurNAc	N-acetylmuramic acid
MWCO	Molecular weight cut-off
m/z	Mass to charge ratio
NADH	Nicotinamide adenine dinucleotide
NMR	Nuclear Magnetic Spectroscopy

NOESY	Nuclear Overhauser Effect Spectroscopy
N-terminal	Amino terminus
OD ₆₀₀	Optical density at a wavelength of 600 nm
PAGE	Polyacrylamide electrophoresis
PAS	Fold present in <u>P</u> ER, <u>A</u> RNT and <u>S</u> IM proteins
PBP	Penicillin-binding protein
PCR	Polymerase chain reaction
PDC	Fold present in <u>P</u> hoQ, <u>D</u> cuS and <u>C</u> itA proteins
PDB	Protein Data Bank
PG	Peptidoglycan, or phosphoglycerol detergent
Pi	Inorganic phosphate
PMSF	Phenyl methyl sulphonyl fluoride
REC	Receiver domain
RR	Response regulator
SDS	Sodium dodecyl sulphate
Sp.	Species
TAE	Tris acetate ethylenediaminetetraacetic acid
TBS-T	Tris-buffered saline with 0.1% w/v Tween-20
TCS	Two-component system
TEV	Tobacco etch virus protease
TFE	2, 2, 2-trifluoroethanol
TM	Transmembrane domain
TOCSY	Total correlation spectroscopy
<i>Tn</i>	Transposon
Tris	Tris(hydroxymethyl)aminomethane
UDP	Uridine diphosphate
UV	Ultraviolet spectroscopy
<i>van</i>	Vancomycin-resistance gene cluster
VanS _A	VanS protein derived from <i>Enterococcus faecium</i>
VanS _B	VanS protein derived from <i>Enterococcus faecalis</i>
VanS _{SC}	VanS protein derived from <i>Streptomyces coelicolor</i>
VPP	Vancomycin photoaffinity probe
VRE	Vancomycin resistant enterococci
VRSA	Vancomycin resistant <i>Staphylococcus aureus</i>
v/v	Volume to volume ratio
w/v	Weight to volume ratio
XRD	X-ray diffraction

Other abbreviations are explained, where appropriate, within the text.

1 Introduction

1.1 Antimicrobials and Bacterial Antibiotic Resistance

1.1.1 Historical Background and Current Context

Dame Sally Davies, the UK chief medical officer, has said the threat from infections that are resistant to frontline antibiotics is so serious the issue should be added to the government's national risk register of civil emergencies. She went on to say: "There are few public health issues of potentially greater importance for society than antibiotic resistance. It means we are at increasing risk of developing infections that cannot be treated." (Sample, 2013)

Despite advances in medical science and technology over the centuries, the threat to the human population from bacterial and viral diseases is as great as ever. As human population density has increased, so has the emergence of infectious disease, which has evolved to such a degree that many microbial strains challenge all current drug treatment options. A poignant example is the outbreak of Ebola Virus Disease in Africa this year, for which there is no proven treatment, and which has caused many countries to close their borders, and set up quarantine camps (WHO, 2014a). It is clear that greater research and development of new antimicrobials is required to provide options for treating evolving disease pathogens.

The discovery and development of successful antimicrobial drugs has been accomplished historically by two main routes. Firstly, medicinal chemistry was used to design synthetic compounds for specific targets (Walsh, 2003), which led to the discovery of the first class of antimicrobials, the arsenicals. These include Paul Ehrlich's 'magic bullet', Salvarsan, which was used in the treatment of syphilis (Schwartz, 2004). This was followed by the discovery of the sulphonamide antibiotic, Protonsil in 1935 by Gerhard Domagk, which was heavily prescribed during the Second World War to treat infections from streptococci (Iyer, 2008).

Secondly, chemists used the antibacterial activity of natural products, and developed assays to purify these agents (Walsh, 2003). This approach is highlighted by the work of Sir Alexander Fleming, Sir Howard Florey and Ernst Chain, who were jointly awarded the Nobel Prize in 1945 for their novel work relating to “the discovery of penicillin and its curative effects in various infectious diseases” (Fleming, 1980). Fleming discovered penicillin quite fortuitously whilst working with *Staphylococcus* spp. variants. After mistakenly leaving open the lid from a petri dish containing *Staphylococcus* culture, he noticed a mould growing, around which a halo had formed, where growth of the culture was inhibited. This mould contained *Penicillium notatum*, which exuded a substance with antibacterial properties, repressing growth and lysing the bacteria (Fleming, 1980). Further development of penicillin as a medicine was then pioneered by Florey and Chain, who isolated and purified penicillin for clinical use (as Penicillin G) (Chain *et al.*, 1993).

In 1944, Selman Waksman and his colleagues initiated a screening program to discover new antibiotics, by isolating chemical substances from soil bacteria (actinomycetes), recognising the activity of actinomycetes against other microorganisms (Rubin, 2007). This led to the discovery of streptomycin (Schatz *et al.*, 2005), the first aminoglycoside, which was highly effective against tuberculosis (Feldman and Hinshaw, 1948). Waksman was the first to use the term ‘antibiotic’ to describe its actions, envisioning the drug as ‘a substance produced by one microorganism that antagonized the effect of another’ (Rubin, 2007).

After identification of antibiotics in academic labs, pharmaceutical companies such as Glaxo, Beecham, Eli Lilly and Merck conducted intensive screening programs to identify further antibiotic classes. They were responsible for compound scale-up, formulation and clinical development, allowing antibacterial drug research to gain prominence as a viable area for investment, and led to the ‘golden era’ of antibiotic discovery between 1950 and 1960 (see Table 1.1.1.1).

Table 1.1.1.1: Antibiotic classes, their deployment year and observed clinical resistance

Adapted from Palumbi et al., 2001; Walsh & Wencewicz, 2014. Note: The table shows when clinical resistance was observed, but the first report of resistance may be earlier.

Antibiotic	Year Deployed	Clinical Resistance Observed
Sulfonamides	1930s	1940s
Penicillin G	1943	1946
Streptomycin	1943	1959
Chloramphenicol	1947	1959
Tetracycline	1948	1953
Erythromycin	1952	1988
Vancomycin	1956	1988
Methicillin	1960	1961
Ampicillin	1961	1973
Cephalosporins	1960s	Late 1960s
Nalidixic acid	1962	1962
Fluoroquinolones	1980s	1980s
Linezolid	1999	1999
Daptomycin	2003	2003
Retapamulin	2007	2007
Fidaxomicin	2011	2011
Bedaquiline	2013	?

Resistance has developed to every class of antibiotic, natural and synthetic, over time courses from a year to around a decade (Table 1.1.1.1), with the exception of erythromycin and vancomycin for which resistance was not reported for 30 years. It therefore appears not a matter of *if* but *when* resistance will occur. The first reported case was that of sulphonamide-resistant *Streptococcus pyogenes*, which emerged in military hospitals in the 1940s (Damrosch, 1946). Later that decade, even before FDA approval of penicillin to treat *Staphylococcal* infections, an enzyme was identified (a β -lactamase), which enabled penicillin resistance in *Staphylococcus aureus* (Abraham & Chain, 1988).

As bacterial resistance was identified for each antibiotic, the pharmaceutical industry responded by treating patients with multiple antibiotics, in some cases up to seven drugs. Although initially successful, multiple drug resistant (MDR) strains were observed from the 1950s to 1960s. Resistance to multiple drugs was first detected among enteric bacteria e.g. *Escherichia coli*, *Shigella* and *Salmonella* in the late 1950s to early 1960s (Levy, 2001), posing severe clinical problems and claiming lives, particularly in developing countries.

Furthermore in the 1970s, *H. influenzae* and *Neisseria gonorrhoeae* organisms (Levy & Marshall, 2004) emerged with resistance to ampicillin. By the 1980s, *M. tuberculosis* had re-appeared often with multi-drug resistance, along with widespread methicillin-resistant *S. aureus* (MRSA). This brought multi-drug resistant bacteria to the forefront of international news, leading to the acknowledgment of a new age of antibiotic resistance.

1.1.2 The Impact of Antibacterial Resistance on Healthcare

Infection by a resistant organism increases the chance of hospitalisation, and makes prognosis more difficult for doctors and nurses. This often results in multiple drug therapy with increased patient side-effects. Individuals may succumb to MDR infections because all available drugs have failed (Levy & Marshall, 2004). Global examples of MDR strains include the ‘ESKAPE’ organisms (*Enterococcus* spp., *S. aureus*, *K. pneumoniae*, *A. baumannii*, *P. aeruginosa* and *Enterobacter* spp.) (Boucher *et al.*, 2009), as well as strains of *M. tuberculosis* and *Neisseria gonorrhoea* (WHO, 2014b). A report by the Centre for Disease Control (CDC, 2013) has for the first time, prioritized concern over bacterial infections into three categories: urgent, serious, and concerning. Within the ‘urgent’ category are MDR *Neisseria gonorrhoea*, *C. difficile* and carbapenem-resistant Gram-negative bacteria, showing antibiotic resistance is not a problem confined to developing countries.

The cost of antibiotic resistance puts a significant burden on government budgets, and one estimate for the annual societal cost-of-illness for antimicrobial resistance is \$55 billion for the US alone (Smith & Coast, 2013). Within the UK National Health Service, the best estimate suggests that healthcare-associated infections in hospitals costs at least £1 billion per year (House of Commons, 2009), with at least 300,000 patients affected per year (House of Commons, 2009). Of those affected around 9000 were reported as having died from antibiotic resistant, hospital acquired MRSA and *C. difficile* infections. This clearly demonstrates a need to develop novel antimicrobials to treat these types of infection.

1.1.3 Mechanisms of Action of Antimicrobial Agents

Antimicrobials act selectively on a target present in bacteria but not in humans, to affect vital microbial functions with minimal effects to the host. The drugs can be broadly described as bacteriostatic (inhibiting bacterial growth) or bactericidal (killing bacteria). A summary of current antimicrobial drugs, their mechanisms and targets is given in Table 1.1.3.1.

Table 1.1.3.1: Major classes of antibiotics; their targets and mechanism of action. Adapted from Walsh, 2003; Mulvey & Simor, 2009; Kohanski et al., 2010; Lewis, 2013. *F₁F₀ ATPase catalyses cellular ATP synthesis from ADP, coupled with H⁺ flux.

Target	Antibiotic Class; examples	Mechanism of Action
Cell Wall Biosynthesis	β-lactams; penicillins, cephalosporins, carbapenems	Mimics D-Ala-D-Ala peptidoglycan chain and inhibits cross-linking.
	Glycopeptides; vancomycin, teicoplanin	Binds to the D-Ala-D-Ala peptide chain of peptidoglycan precursors
Protein Synthesis	Aminoglycosides; streptomycin	Bind to 30S ribosomal subunit and blocks translation
	Tetracyclines; chlortetracycline	
	Macrolides; erythromycin	Binds to 50S ribosomal subunit of ribosome and blocks translation.
	Streptogramins; quinupristin	
	Phenicols: chloramphenicol	
Oxazolidinones; linezolid		
DNA synthesis	Fluoroquinolones; cefotaxime, nalidixic acid	Binds to DNA gyrase, blocking DNA replication
RNA synthesis	Rifamycins; rifampicin	Binds to RNA polymerase and prevents attachment to DNA
	Fidaxomicins; fidaxomicin	Binds to RNA polymerase and specifically targets <i>C. difficile</i>
Folic acid synthesis	Sulphonamides; sulphamethoxazole	Blocks folate metabolism which is essential in DNA replication
Cell membrane integrity and permeabilization	Lipopeptides; daptomycin	Binds to and depolarises the cell membrane
	Polymyxins; colistin	Permeabilises the cell membrane, allowing components to diffuse out
Inhibition of ATP synthetase	Diarylquinolines; bedaquiline	Inhibits the F ₁ F ₀ -ATPase* and specifically targets <i>M. tuberculosis</i>

The table lists a number of classes of antibiotics developed to inhibit different targets, of which classically, there were three: cell wall synthesis, protein synthesis, DNA replication.

(i) Inhibitors of Protein Synthesis

Drugs that target protein synthesis inhibit either the 50S or 30S subunit of bacterial ribosomes (Kohanski *et al.*, 2010). Proteins are synthesised from mRNA over three phases (initiation, elongation and termination) involving the ribosome and cytoplasmic factors. The ribosome contains ribosomal RNA (rRNA) and consists of two subunits: 30S which binds and reads messenger RNA (mRNA) (initiation), and 50S which binds transfer RNA (tRNA) and links amino acids to form a polypeptide chain (elongation) (Vannuffel & Cocito, 1996).

The 50S is the larger subunit containing 23S rRNA; to which inhibitors e.g. macrolides and oxazolidinones bind. These either physically block access to the ribosome tunnel to prevent initiation, or sterically hinder translocation of the polypeptide chain, inhibiting peptide bond formation and elongation. The 30S is the smaller subunit containing 16S rRNA, to which inhibitors e.g. aminoglycosides and tetracyclines bind. Aminoglycosides are the best studied, and cause inappropriate amino acids to be added into the elongating polypeptide (Kohanski *et al.*, 2010), leading to mistranslation and protein misfolding. Misfolded membrane proteins also increase membrane permeability allowing greater antibiotic uptake (Davis *et al.*, 1986a).

(ii) Inhibitors of DNA synthesis

To enable the chromosome to be contained within a bacterium, DNA must be supercoiled. However, supercoiling presents a problem as it prevents access to the genome, which is required by DNA polymerases during replication and repair (Champoux, 2001). Supercoiling is modulated by DNA topoisomerases, which are able to insert temporary breaks in the DNA helix, which can later be re-joined (Kohanski *et al.*, 2010). These reactions are exploited by the fluoroquinolones, which target the DNA-topoisomerase complexes. This includes topoisomerase IV and DNA gyrase, which are essential in relieving strain during uncoiling, and are critical to DNA replication and bacterial viability (Kohanski *et al.*, 2010). The quinolones interfere with maintenance of chromosomal topology by trapping these enzymes at the DNA cleavage stage and preventing strand re-joining (Drlica & Zhao, 1997).

(iii) Inhibitors of cell wall biosynthesis

The bacterial cell is encased by layers of peptidoglycan, a covalently cross-linked polymer matrix. Maintenance of the peptidoglycan cell wall is accomplished by the activity of transglycosylases and penicillin-binding proteins. Antibiotics that interfere with steps in cell wall synthesis include β -lactams and glycopeptides (Kahne *et al.*, 2005), for example β -lactams block crosslinking of peptidoglycan by inhibiting the peptide bond formation reaction, as catalysed by penicillin-binding proteins (PBPs) (Tipper & Strominger, 1965). The action of glycopeptides, including vancomycin, on cell wall biosynthesis is discussed in more detail in section 1.3.

1.1.4 Emergence of Antibiotic Resistance

(i) Antibiotic Prescription in Humans

The main factor to the resistance problem is the use and overuse, of massive quantities of antimicrobials in the treatment of people, animals and agriculture globally (Levy & Marshall, 2004), which kills susceptible strains and selects resistant ones. This is particularly common in intensive care units (ICUs), where patients are immunocompromised and require strong antibiotic treatment. Furthermore, the close proximity of wards causes the spread of resistant organisms (Harbarth & Samore, 2005).

The wide-spread prescription of antibiotics in the community results in antibiotic misuse, and misunderstanding, with patients failing to complete treatment courses, resulting in a sub-inhibitory concentrations and increasing selection and evolution of resistant bacteria (Palumbi, 2001). Failing to complete an antibiotic course has been associated with increased emergence of drug-resistant TB and HIV (Wong *et al.*, 1997; Martin & Lazarus, 2000).

(ii) Antibiotic use in Livestock and Agriculture

The use of antimicrobials in agriculture, combined with high numbers of livestock in confined environments (factory farming) has promoted the spread of infectious disease (Wegener, 2003). Antibiotics have often been prescribed as growth promoters for livestock, and used to circumvent disease development and cut the cost of a full treatment. In doing so this provides a source for the acquisition of resistance genes. The use of antibiotics in feedstocks has contributed to the development of clinically relevant resistance in bacteria such as *Salmonella*, *Campylobacter*, and *E. coli* (Levy & Marshall, 2004). Therefore the transfer of resistance from animals to humans may occur through the food chain, by direct interaction or when spreading antibiotic-laden manure on crops (Levy & Marshall, 2004).

Recommendations from the ‘Swann Report’ in the 1970s caused changes in EU regulation on growth promoters in feedstocks, and several antibiotics such as penicillin and tetracycline were banned from agricultural use, and reserved only for use in human medicine (National Academy of Sciences, 1980). However, these regulations did not withdraw approvals of antimicrobial growth promoters (AGPs) that were members of the same class used by humans. Therefore initially when glycopeptide antibiotics that were used for growth promotion (e.g. avoparcin) became important therapeutic drugs (i.e. vancomycin) for drug-resistant strains in hospital infections, AGPs still remained in use (Wegener, 2003).

It was not until 1994 (Bates *et al.*, 1994; Klare *et al.*, 1995) that the first wake up call came, showing that glycopeptide-resistant enterococci (GRE) were present in isolates from food-animals, and that these animals may harbour the GRE infections that were rapidly spreading across hospitals. Studies of animal isolates in different continents confirmed the association of avoparcin, with the occurrence of GRE in chickens and pigs (Bager *et al.*, 1997; Aarestrup, 2000). This led to a ban on avoparcin and all AGPs in the EU (but not in the US), and has greatly reduced levels of resistance in animals (Klare *et al.*, 1999).

(iii) Development of New Antibiotics

The development of antibiotics also contributes to the emergence of resistance. Historically, a dominant strategy has been to utilise the antibacterial activity of natural products e.g. aminoglycosides or glycopeptides, to create semi-synthetic derivatives based on their structural scaffolds. These scaffolds have distinct architectures and many functional groups, for recognition and specific interaction with targets in pathogenic bacteria (Walsh, 2003). Therefore they act as platforms for re-modelling to create generations of semi-synthetic variants, e.g. erythromycin to clarithromycin to telithromycin (Fischbach & Walsh, 2009).

Although mining natural product scaffolds has been a successful strategy up until the 1960s, it has resulted in an 'innovation gap' of 40 years between the last synthetic antibiotic class, the fluoroquinolones (based upon nalidixic acid in 1962), and the introduction of a novel synthetic antibacterial, the oxazolidinones (based on linezolid in 1999) (Walsh, 2003). During this gap, pharmaceutical companies de-emphasised their screening programs, and began research into more profitable areas such as cardiovascular and neurodegenerative disorders (CNS) (Bush, 2004; Walsh, 2003), which require long-term treatments.

The last clinically useful antibiotic in a new class was daptomycin (in 1986); a lipopeptide based on vancomycin and teicoplanin structures, but this was not approved until 2003 (Lewis, 2013). And until 2012, when bedaquiline was approved (a new drug for TB), the last class of narrow-spectrum antibiotics (acting against a specific target) to be discovered was the streptogramins (in 1964), of which streptogramin B was not introduced into the clinic until 30 years later (Lewis, 2013). The lack of novel classes has resulted in the spread of antibiotic resistance outpacing the rate of antibiotic drug discovery, and although new antibiotics are being released, the majority of these target Gram-positive infections and the current pipeline prospects for those drugs that target Gram-negative bacteria is less promising (Arias & Murray, 2009).

1.1.5 Development of Bacterial Resistance

(i) Inherent resistance

Intrinsic resistance applies to a member of a bacterial species that is resistant to an antimicrobial without additional gene modification. For example, mycoplasma bacteria (e.g. *M. tuberculosis*) are always resistant to β -lactam antibiotics since they lack peptidoglycan (the drug target) in their cell wall (Normark & Normark, 2002; Alekshun & Levy, 2007).

(i) Mutations

The selective pressure of the antibiotic can result in acquired resistance by spontaneous mutations, which may be point mutations, deletions or insertions within the bacterial genome (Normark & Normark, 2002). Virtually all resistance to fluoroquinolones can be attributed to mutations within the drug's targets; DNA gyrase and topoisomerase IV (see section 1.1.3).

These complexes involve the genes: *gyrA* and *gyrB* for DNA gyrase, and *parC* and *parE* for topoisomerase IV (Alekshun & Levy, 2007), which are required for DNA replication.

Mutations giving rise to quinolone resistance occur for specific amino acids in the DNA binding domain, resulting in sequential mutations, so as to 'train' resistance in the bacterium.

(ii) Horizontal resistance gene transfer

Drug resistance is mobile, and resistance genes borne on bacteriophages, plasmids, naked DNA and transposons, and can be transferred among bacteria (Levy & Marshall, 2004). This can occur through transduction, conjugation or transformation (Alekshun & Levy, 2007).

Conjugation is the direct transfer of DNA between two bacterial cells in a mating process.

Transduction requires a DNA carrier (bacteriophage) to transfer genetic material into another bacterium, and transformation involves the uptake of DNA from the environment.

Transposons have been known to carry resistance genes to β -lactams (*Tn1* and *Tn3*), streptomycin (*Tn5* and *Tn7*) and glycopeptides (*Tn1546/1547*) (Alekshun & Levy, 2007).

1.1.6 Bacterial Resistance Mechanisms to Antibiotics

Antibiotic resistance can occur through three main mechanisms: (1) modification of the antibiotic, (2) prevention of interaction with the antibiotic target or (3) active efflux of the antibiotic from the cell and reduced antibiotic uptake.

(i) Modification of the Antibiotic

Modifying enzymes are involved in antibiotic inactivation by several routes, including hydrolysis, group transfer and redox mechanisms (Wright, 2005). Many antibiotics have hydrolytically susceptible chemical bonds (e.g. esters and amides), whose integrity is essential to biological activity. For instance amidase enzymes have evolved to cleave the β -lactam ring of penicillins and cephalosporins, and β -lactamases hydrolytically cleave the β -lactam ring using either an active site serine nucleophile or a nucleophilic water molecule (activated via a Zn^{2+} centre). Metallo- β -lactamases utilise the latter mechanism to confer resistance to the last line of β -lactam antibiotics, the carbapenems (Wright, 2011).

(ii) Modification of the Antibiotic Target

Modification of target sites confers resistance by preventing the antibiotic from recognising or associating with the target, leading to diminished activity. Peptidoglycan in the bacterial cell wall is a great example of this as it is essential for growth and survival of most bacteria and has a vastly different chemical structure to any mammalian macromolecule (Lambert, 2005). Therefore enzymes involved in its synthesis and assembly are great targets for selective inhibition. The most important of which are the transpeptidases; targets of the β -lactams, and transglycosylases; substrates of which are the targets for the glycopeptides.

For example, β -lactam resistance can occur through modification of the penicillin-binding proteins (PBPs), which are a group of enzymes involved in assembly of peptidoglycan (by transpeptidation and transglycosylation) (Lambert, 2005). Interaction of a β -lactam with a PBP usually involves a rapid formation of a non-covalent complex, which blocks the function of PBP. However many PBPs have emerged with decreased antibiotic affinities. One example is the altered transpeptidase in *S. aureus*, PBP2a, which causes resistance to methicillin as its rate constant for transpeptidation is reduced 1000-fold (Lambert, 2005).

Target modifications are also involved in resistance to glycopeptide antibiotics, whereby the terminating D-Ala-D-Ala group of peptidoglycan precursors is altered to inhibit binding. This is discussed in section 1.3.3, and directly relates to studies carried out in this thesis.

(iii) Active Efflux and Reduced Antibiotic Uptake

Efflux pumps are found in all bacteria, but most cannot respond to an antibiotic without specific mutations (Normark & Normark, 2002). The combination of reduced uptake and efflux is most prominent in the action of the outer membrane permeability barrier and active efflux, within Gram negative bacteria (Kumar & Schweizer, 2005). The permeability barrier in Gram-negative species is the outer membrane, containing phospholipids and lipopolysaccharides (LPS). In order to enter the cell, drug molecules must penetrate the membrane by diffusing through porins (water-filled channels) (Kumar & Schweizer, 2005). In *P. aeruginosa*, absorption through these porin channels has been found to be 10-100 times less efficient than those of *E. coli* (Hancock & Speert, 2000). These barriers only slow down the rate of absorption of the antibiotic though, so are often coupled with efflux pumps.

There are five families of membrane-spanning efflux pumps, which are able to expel a broad range of compounds (see Figure 1.1.6.1) (Kumar & Schweizer, 2005). Three single-component pumps couple drug efflux with a counterflow of protons or sodium ions, while one pump uses hydrolysis of ATP to provide energy for the active transport of the antibiotic. The multi-component pumps (e.g. RND) function in association with an outer membrane protein pore (OMP), and efflux occurs across the entire cell envelope.

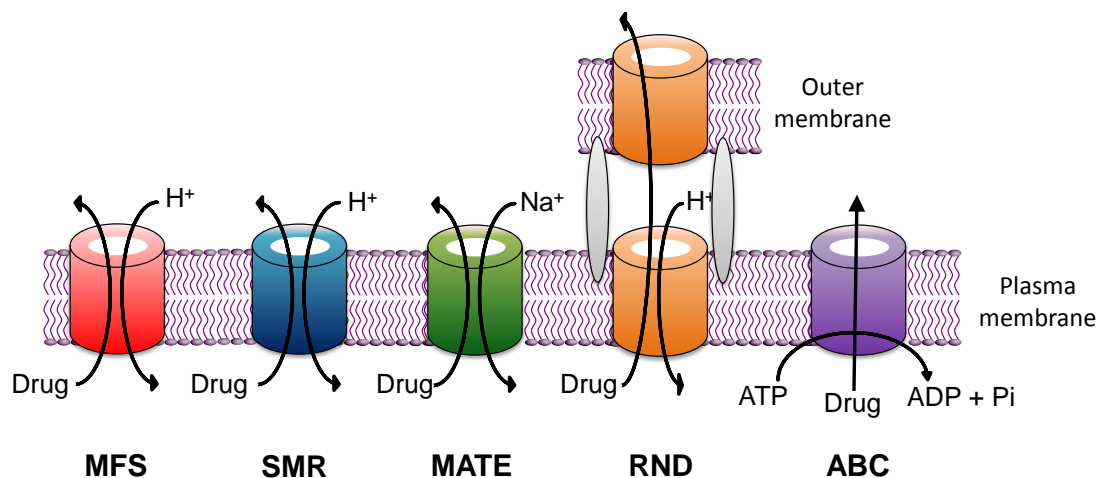


Figure 1.1.6.1: A schematic illustration of the five families of drug efflux pumps involved in antibiotic resistance. Adapted from Kumar & Schweizer, 2005. Efflux pumps are represented by cylinders and for the RND class, accessory proteins are also shown.

1.2 Peptidoglycan as an Antimicrobial Target

1.2.1 The Cell Wall

Bacteria are classified by their reaction to a Gram stain (Gram, 1884). The stain involves the use of a crystal violet dye, and differentiates between Gram-negative and Gram-positive bacteria due to the chemical and physical properties of their cell walls, by detecting peptidoglycan. Gram-positive bacteria have a thick peptidoglycan layer and retain the violet dye, whereas Gram-negative bacteria have a much thinner peptidoglycan layer (~1/10th the size), and do not retain the dye (once a decolouriser e.g. alcohol has been added) (Figure 1.2.1.1). The colouration of stained cells is then produced by addition of a counterstain.

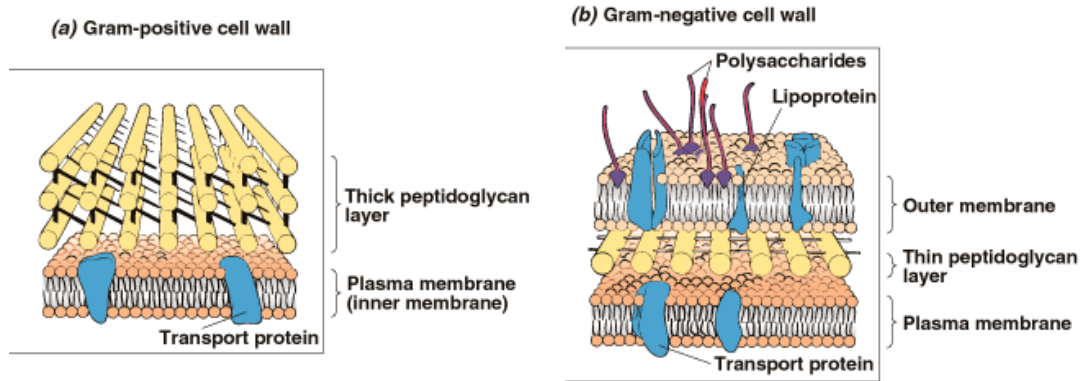


Figure 1.2.1.1: Structures of Gram-positive (a) and Gram-negative (b) bacterial cell walls, reproduced from Soloman et al., (1999).

1.2.2 The Molecular Structure of Peptidoglycan

Peptidoglycan is an essential part of the bacterial cell wall, and consists of polymerised linear glycan chains cross-linked by peptide bonds, which provides high mechanical strength to resist the internal osmotic pressure. The glycan strands consist of alternating N-acetylglucosamine (GlcNAc) and N-acetylmuramic acid (MurNAc) residues, linked by β -1,4-glycosidic bonds. Each MurNAc residue is appended to a pentapeptide chain, of the form L-Ala-D-Glu-X-D-Ala-D-Ala, where X is either L-Lysine in Gram-positive bacteria or *meso*-diaminopimelic acid (*meso*-DAP) in Gram-negative bacteria. During cross-linking, the terminal D-Ala is removed when direct covalent bond forms between the third amino acid (X) and the fourth D-Ala residue of a neighbouring strand (Vollmer *et al.*, 2008).

Peptidoglycan biosynthesis can be considered to occur via three stages:

- i) On the cytoplasmic side; synthesis of nucleotide precursors
- ii) In the cell membrane; synthesis of lipid-linked intermediates
- iii) On the periplasmic side; polymerisation reactions

1.2.3 Synthesis of Nucleotide precursors to Peptidoglycan

The biosynthesis of peptidoglycan involves around 20 different reactions in the cytoplasm alone, and is represented in Figure 1.2.5.1. The cytoplasmic steps in peptidoglycan assembly are outlined below. Initially, uridine diphosphate N-acetylglucosamine (UDP-GlcNAc) is produced from fructose-6-phosphate, which can then be used to form uridine diphosphate N-acetyl muramic acid (UDP-MurNAc), to begin peptidoglycan synthesis. The enzymes responsible for conversion of UDP-GlcNAc to UDP-MurNAc-pentapeptide during cytoplasmic steps in peptidoglycan assembly are the ‘Mur’ proteins (Barreteau *et al.*, 2008).

The first committed step towards the synthesis of peptidoglycan is the conversion of UDP-GlcNAc to UDP-MurNAc by MurA enzymes. MurA catalyses transfer of enolpyruvate from phosphoenolpyruvate (PEP) to the 3-hydroxyl group of UDP-GlcNAc, releasing inorganic phosphate and forming UDP-GlcNAc-enol-pyruvate. This is reduced by the MurB enzyme using one equivalent of NADPH to form UDP-MurNAc (Barreteau *et al.*, 2008). The peptide stem of peptidoglycan is then assembled by the Mur ligases (Mur C, D, E, F), which sequentially add the amino acids to UDP-MurNAc to produce the UDP-MurNAc-pentapeptide, otherwise known as Park’s nucleotide (Park, 1952) (see Figure 1.2.5.1).

Mur ligases catalyse the formation of an amide or peptide bond driven by ATP, and in the presence of a divalent cation. Mur C ligase adds the first residue usually L-alanine, to form UDP-MurNAc-L-Ala (Schleifer & Kandler, 1972). MurD then adds D-glutamic acid and MurE adds an L-lysine (in Gram-positive bacteria), or a *meso*-DAP (in Gram-negative bacteria). Finally, MurF adds the dipeptide D-Ala-D-Ala to the terminus of the growing chain, to produce UDP-MurNAc-L-Ala-D-Glu-L-Lys-D-Ala-D-Ala (in Gram-positive bacteria). The D-Ala-D-Ala dipeptide is normally formed by a DdlA (D-Ala-D-Ala) ligase, but D-Ala-D-Lac and D-Ala-D-Ser are observed in vancomycin-resistant strains (Healy *et al.*, 2000), and are discussed later in this thesis (see section 1.3.6)

1.2.4 Synthesis of lipid-linked intermediates to Peptidoglycan

The Park's nucleophile is next attached to a membrane-bound lipid carrier. The transferase *MraY* catalyses transfer of the phospho-MurNAc-pentapeptide moiety of Park's nucleophile (UDP-MurNAc-pentapeptide) to the membrane acceptor undecaprenyl phosphate (C₅₅-P), with the loss of UMP. This produces a membrane bound intermediate; undecaprenyl-pyrophosphoryl-MurNAc-pentapeptide (known as Lipid I) (Bouhss *et al.*, 2008). A second transferase, *MurG*, catalyses transfer of the GlcNAc moiety from UDP-GlcNAc to Lipid I yielding undecaprenyl-pyrophosphoryl-GlcNAc-MurNAc-pentapeptide (known as Lipid II). Lipid II is then flipped through the membrane, and used in polymerisation reactions.

The translocation of Lipid II across the membrane must be assisted by a flippase protein, which shields the disaccharide-pentapeptide as it crosses the hydrophobic core of the membrane (Butler *et al.*, 2013). Two candidates appear to be capable of this role; *FtsW* (Mohammadi *et al.*, 2011), an essential protein in division, and *MurJ* (Butler *et al.*, 2013), an essential enzyme in PG synthesis and a member of the MATE drug exporter class (Kuroda & Tsuchiya, 2009). Despite a recent paper in which *MurJ* was stated to be the flippase (Sham *et al.*, 2014), there is still heated debate over this and further studies are ongoing.

1.2.5 Polymerisation Reactions to form Peptidoglycan

The final steps of peptidoglycan assembly involve polymerisation of the glycan strand (transglycosylation), then cross-linking between glycan strands (transpeptidation), catalysed by the penicillin-binding proteins (Sauvage *et al.*, 2008) (see Figure 1.2.5.1). PBPs have been historically numbered according to their molecular weight by SDS-PAGE, however, it is more informative to categorise them into classes according to their actions. High molecular weight PBPs are subdivided into either class A (glycosyltransferase and transpeptidase enzymes) or class B (transpeptidase only) (Sauvage *et al.*, 2008).

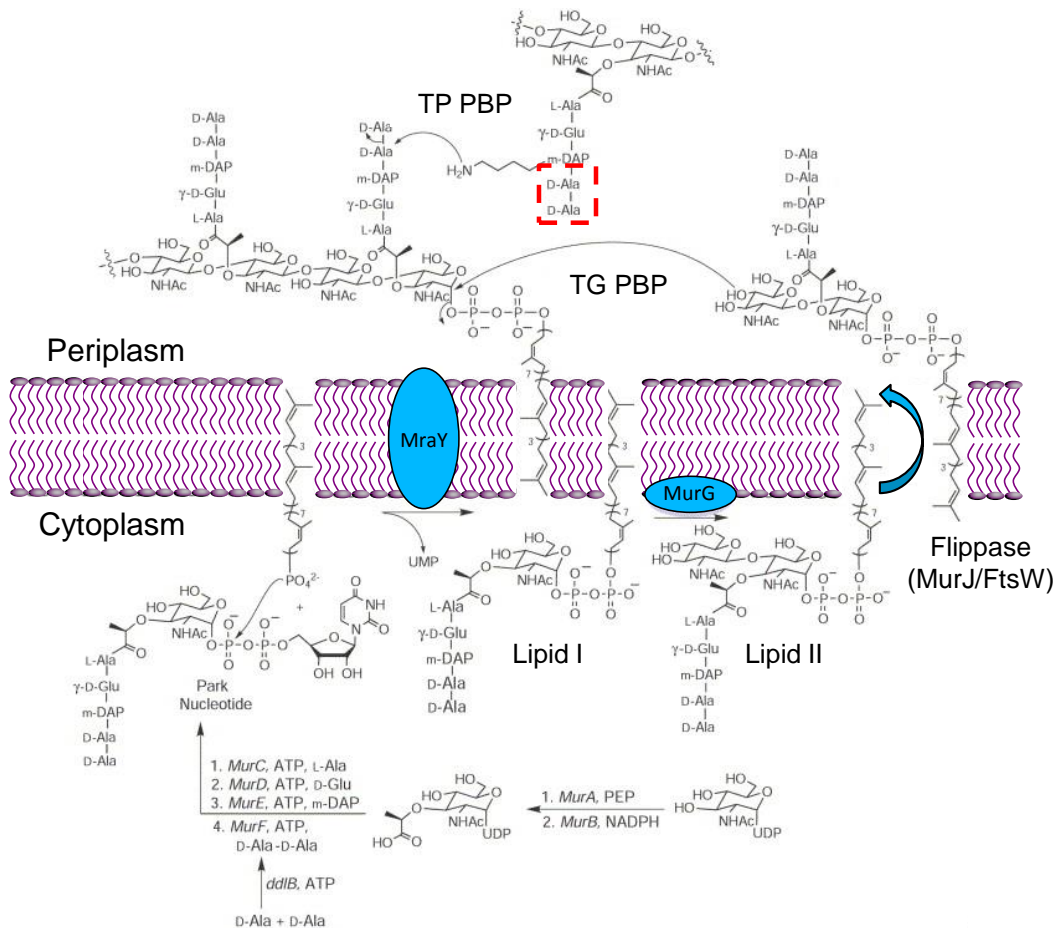


Figure 1.2.5.1: Steps and enzymes involved in the biosynthesis of peptidoglycan. Adapted from Lazar & Walker, 2002; Kahne *et al.*, 2005. The D-Ala-D-Ala binding site for glycopeptide antibiotics including vancomycin is highlighted with a red box.

Transglycosylation involves elongation of the glycan chain by successive attacks of the growing chain (donor) on Lipid II (acceptor), catalysed by formation of a glycosidic bond between the disaccharide pentapeptide chain and the 4-hydroxyl group of the GlcNAc strand. This is followed by transpeptidation, which is catalysed by a three-step mechanism: the rapid formation of a noncovalent complex, followed by attack of an active serine in the PBP on the carbonyl atom of the D-Ala-D-Ala terminus of the strand, leading to formation of an acyl-enzyme intermediate, and finally loss of the terminal D-Ala (Sauvage *et al.*, 2008). This deacylation step forms the cross-link between the fourth position D-Ala and the third position residue in a second stem pentapeptide. The joint transpeptidation and transglycosylation activities, lead to maturation of the peptidoglycan and provide its strength and stability.

1.3 Glycopeptide Antibiotics and Resistance Mechanisms

1.3.1 Structure and Function

Glycopeptide antibiotics act upon the N-terminal D-Ala-D-Ala in the peptidoglycan cell wall, and are crucial in the treatment of serious (e.g. β -lactam resistant) infections caused by Gram-positive bacteria. These antibiotics were developed from natural products in the 1950s such as vancomycin and teicoplanin (Kahne *et al.*, 2005). Only a few glycopeptide antibiotics have been approved for clinical use, including vancomycin, teicoplanin, telavancin (Corey *et al.*, 2009), and oritavancin (FDA, 2014). Vancomycin is approved for human use in many countries, whereas teicoplanin is widely prescribed in Europe but was never FDA approved in the US (Kahne *et al.*, 2005).

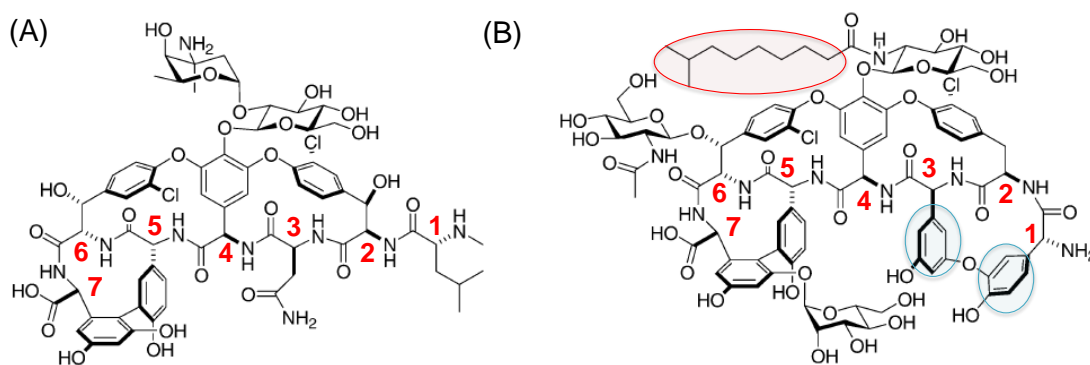


Figure 1.3.1.1: Structures of vancomycin and teicoplanin. Adapted from Kahne *et al.*, (2005). The C₁₀ acyl chain (red) and extra aromatic groups (blue) in teicoplanin are circled.

Vancomycin and teicoplanin have closely related structures, containing a heptapeptide core with five (vancomycin) or seven (teicoplanin) aromatic residues (Figure 1.3.1.1) (Kahne *et al.*, 2005). The peptide framework is glycosylated too, by a disaccharide chain on residue 4 in vancomycin or by three monosaccharides at residues 4, 6 and 7 in teicoplanin. It should be noted that teicoplanin, but not vancomycin, is a lipoglycopeptide, as it has a C₁₀ fatty acyl chain linked to its glucosamine sugar moiety, which is believed to anchor the antibiotic in the membrane, whilst interacting with the D-Ala-D-Ala terminus (Kahne *et al.*, 2005).

1.3.2 Vancomycin: A History

Vancomycin is a natural product, first isolated from soil samples containing *Streptomyces orientalis* obtained from South East Asia in 1952, by Eli Lilly and Company (Moellering, 2006). The drug was isolated, purified and approved by the FDA for clinical use in 1958. Vancomycin was effective against most gram-positive infections e.g. penicillin resistant *Staphylococcus*. However, methicillin was also approved in this period, and due to the perceived toxicity of vancomycin it was reserved for cases of serious β -lactam resistance (Levine, 2006). The toxicity of vancomycin has been reduced through improved purification, but treatment is still associated with nephrotoxicity (Levine, 2006) and ‘red man syndrome’; an infusion-related reaction causing a red burning rash across the body (Davis *et al.*, 1986b).

In 1961, methicillin-resistant *S. aureus* (MRSA) was first reported, and by the 1970s and 1980s, the worldwide emergence of MRSA as well as *C. difficile* infections, rekindled interest in vancomycin (Moellering, 2006). This led to a dramatic increase in vancomycin use to treat these infections, with a 100-fold increase occurring between 1980 and 2000 (Kirst *et al.*, 1998). The exponential increase in vancomycin usage during this period, inevitably led to the emergence of vancomycin-resistant strains, including vancomycin-resistant enterococci (VRE) in the 1980s (Gerding, 1997; Levine, 2006).

1.3.3 Mode of Action and Development of Resistance to Vancomycin

The first studies of the mechanism of action of vancomycin were reported by Perkins & Chatterjee, (1966) who analysed stepwise degradation of the UDP-MurNAc-pentapeptide, and found that vancomycin bound to peptidoglycan precursors at the D-Ala-D-Ala terminus. Structural features of vancomycin were then determined by X-ray diffraction analysis in 1982 by the Harris and Williams labs (Williamson & Williams, 1981; Harris & Harris; 1982). One year later, the Williams lab demonstrated the binding interaction between vancomycin and the D-Ala-D-Ala dipeptide by solution state NMR (Williams *et al.*, 1983).

Intermolecular distances within the complex showed that binding occurred via five hydrogen bonds between the D-Ala-D-Ala dipeptide and amide groups in the vancomycin heptapeptide core (Figure 1.3.3.1). The bound glycopeptide sterically impedes Lipid II chains from interacting, thereby inhibiting peptidoglycan cross-linking and causing cell wall instability and eventual cell lysis.

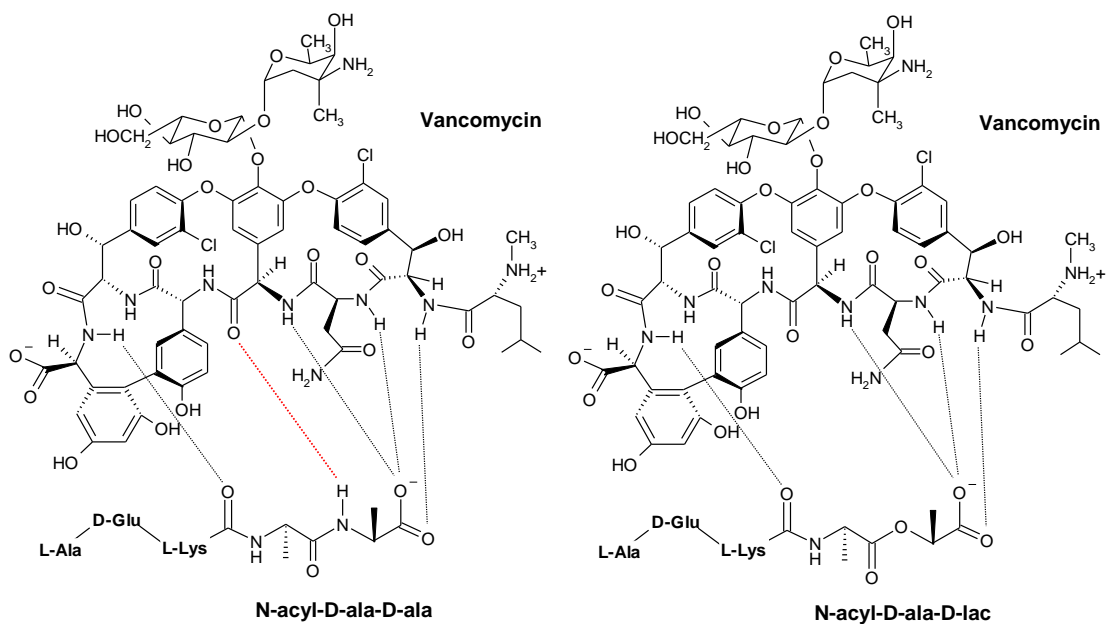


Figure 1.3.3.1: (left) Vancomycin binding to the D-Ala-D-Ala N-terminus of Lipid II PG precursor and (right) a resistant D-Ala-D-Lac form. The hydrogen bond disrupted in VRE is highlighted in red. Adapted from Bugg *et al.*, 1991.

The mechanism of action of glycopeptide antibiotics, unlike the β -lactams, did not appear to be susceptible to modifications that would inactivate them and it was widely believed that microorganisms could not easily alter the drug target, as that would involve multiple enzymes in the pathway to alter peptidoglycan synthesis (Kahne *et al.*, 2005). However, in 1986, vancomycin resistance in enterococci (VRE) was reported in Europe and the US (Murray, 2000), with the first recorded hospital case in the UK in 1988 (Uttley *et al.*, 1989). Since then resistance has been reported in streptococci, staphylococci and actinomycetes.

Vancomycin-resistant enterococci display inducible resistance to glycopeptides such as vancomycin and teicoplanin, and have been observed across the world, with 6 recognised resistance phenotypes – designated ‘VanA’ through ‘VanE’ (Levine, 2006). In all of these resistance phenotypes, the basic mechanism of resistance is the alteration of the terminal D-Ala-D-Ala of the peptidoglycan chain to either a D-Ala-D-Lac form (VanA, B, D) (see Figure 1.3.3.1), or a D-Ala-D-Ser form (Van C, E, G). This results in decreased binding of vancomycin and decreased inhibition of cell wall synthesis. In the case of the D-Ala-D-Lac precursor, binding affinity is reduced 1000-fold (Bugg *et al.*, 1991), due to the loss of just one hydrogen bond, as a result of the ester linkage in D-Ala-D-Lac (Figure 1.3.3.1). In contrast, the D-Ala-D-Ser substitution shows only a 6-fold reduction in binding affinity, since the hydroxymethyl group of serine is bulkier than the methyl group of alanine (Reynolds & Courvalin, 2005). The *van* resistance phenotypes, their MICs and resistance levels are shown in Table 1.3.3.1.

Table 1.3.3.1: VRE Phenotypes, adapted from Sujatha & Praharaj (2012). MIC criteria for resistance are from the CLSI (sensitive: ≤ 4 , intermediate: 8-16, and resistant ≥ 32 $\mu\text{g/ml}$)

Phenotype	Type of resistance	MIC ($\mu\text{g/ml}$)	
		Vancomycin resistance	Teicoplanin resistance
VanA	Inducible	64-1000 (High)	16-512 (High)
VanB	Inducible	4-512 (High)	0.5 (Sensitive)
VanC	Constitutive	2-32 (Low)	0.5 (Sensitive)
VanD	Inducible	64-256 (Moderate-High)	4-32 (Low)
VanE	Inducible	16 (Low)	0.5 (Sensitive)
VanG	Inducible	16 (Low)	0.5 (Sensitive)

VanA and VanB phenotypes are of most clinical relevance and are associated with pathogenic strains of *E. faecium* and *E. faecalis* respectively, which are one focus of this PhD. VanA-type strains are inducibly resistant to high levels of vancomycin and teicoplanin, whereas VanB-type strains are inducibly resistant to vancomycin, but only sensitive to teicoplanin. The *van* genes responsible for glycopeptide resistance are located on a transposon, which allows a route for gene transfer across species.

1.3.4 Vancomycin resistance transfer across species

Vancomycin resistance was observed in *S. aureus* in Japan in 1996 (Hiramatsu, 2001) and later in the US, with an MIC of 8 µg/ml, and so it was classed as vancomycin-intermediate *S. aureus* (VISA). By 2002, vancomycin-resistant *S. aureus* (VRSA) emerged, with several cases in Michigan in the USA (Chang *et al.*, 2003), and 12 further cases observed over the next decade (Sujatha & Praharaj, 2012). In almost all cases, in addition to VRSA, a VRE isolate was recovered from the patient, and it appears that high-level vancomycin resistance in *Staphylococcus* is the result of acquisition of the VanA phenotype, transferred by mobile genetic elements (Perichon & Courvalin, 2009). Because vancomycin is still a front-line therapy for treating problematic MRSA infections, the spread of vancomycin resistance to other bacterial species such as *S. aureus* (VRSA) is a major concern to public health.

1.3.5 Vancomycin resistance in actinomycetes

Vancomycin resistance has also been found in soil-dwelling actinomycetes, which produce most of the natural glycopeptide antibiotics. This includes *Streptomyces orientalis* (producer of vancomycin), *Actinoplanes teichomyceticus* (producer of teicoplanin) *Streptomyces toyocaensis* (producer of A47934), and *Streptomyces coelicolor* (non-producer) (Hong *et al.*, 2008). Glycopeptide resistance in these strains is often essential to survival, as activation of the resistance genes by the antibiotics produced prevents auto-toxicity (Hong *et al.*, 2008).

S. coelicolor is the model species of a Gram-positive, fungal soil bacterium, responsible for producing two thirds of the commercially important antibiotics (Hong *et al.*, 2008). *S. coelicolor* is non-pathogenic like most other actinomycetes, and lives in the soil, where it is likely that it encounters glycopeptide producers and the vancomycin resistance (*van*) gene cluster confers selective advantage. It is also widely believed that all glycopeptide genes are ultimately derived from actinomycete glycopeptide producers.

Over 80% of all antibiotics in clinical use originate from soil bacteria (D'Costa *et al.*, 2007) and extensive studies of the soil resistome by D'Costa *et al.*, (2006) showed that strains of soil organisms were on average resistant to seven to eight antibiotics. It has been suggested that horizontal gene transfer among bacteria may account for the presence of *van* resistance genes in actinomycetes, enterococci and other species. Indeed there is high primary sequence homology between the *vanHAX* resistance strains in pathogenic and soil actinomycetes, with ~60% similarity between resistance genes in the VanA phenotype and those of *S. toyocaensis* and *A. orientalis* (Marshall *et al.*, 1998).

Resistance between species varies, for instance *S. toyocaensis* is resistant to A47934 but is sensitive to both vancomycin and teicoplanin, whereas *S. coelicolor* exhibits high-level resistance to vancomycin, but is sensitive to teicoplanin (Hong *et al.*, 2008), and could therefore be said to have 'VanB-type' resistance. Interestingly, *A. teichomyceticus* exhibits 'pan resistance' to all glycopeptides tested, which is believed to arise from constitutive expression of *van* resistance genes, even in the absence of antibiotic (Hong *et al.*, 2008).

1.3.6 The *van* resistance genes

Vancomycin resistance is conferred by a set of genes contained upon a transposon (a mobile genetic element). The number of genes present in each *van* cluster varies (Figure 1.3.6.1) but the 'core' consists of five genes – *vanS/vanR*, plus a *vanHAX* operon, which encode the three enzymes required for altering cell wall precursors to a D-Ala-D-Lac (or D-Ala-D-Ser) form (Walsh *et al.*, 1996; Healy *et al.*, 2000). VanH is a reductase which converts pyruvate into D-lactate, VanA is a D-Ala-D-Lac ligase, and VanX is a D-Ala-D-Ala dipeptidase that cleaves any residual D-Ala-D-Ala (Gao *et al.*, 2002). The result is that peptidoglycan precursors accumulate which terminate uniformly in D-Ala-D-Lac.

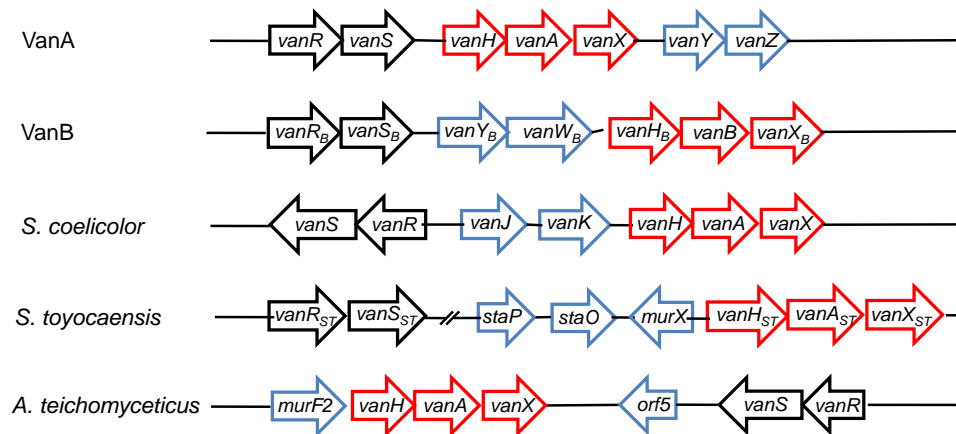


Figure 1.3.6.1: A comparison of van gene clusters from Enterococcal VanA and VanB strains and actinomycetes. Adapted from Hong *et al.*, 2008.

The VanA and VanB phenotypes are found on transposons *Tn1546* and *Tn1547* respectively (Quintiliani & Courvalin, 1996). The VanA transposon encodes two accessory proteins, VanY and VanZ, which are not required for resistance, but can contribute to high-level resistance to vancomycin and teicoplanin. VanZ confers low-level resistance to teicoplanin in the absence of other resistance proteins (Arthur *et al.*, 1995), by an as yet unknown mechanism. VanY is a carboxypeptidase that can cleave the terminal D-Ala of peptidoglycan precursors, but cannot cleave the D-Ala-D-Ala dipeptide, unlike VanX (Wright *et al.*, 1992).

The *S.coelicolor* van gene cluster also adds two additional genes to the conserved *vanRSHAX* genes, which are *vanJ* and *vanK*. *vanK* is an interesting gene as it is essential to vancomycin resistance in *S. coelicolor*, but has no orthologues in the van gene cassette of pathogenic enterococci (Hong *et al.*, 2004). VanK is a member of the Fem family of enzymes, and is responsible for adding ‘branch’ amino acid(s) to the pentapeptide PG precursors. In *S. coelicolor* this branch is a glycine residue which, under normal growth conditions, is added by an enzyme called FemX. However, FemX can only recognise precursors terminating in D-Ala-D-Ala in *S. coelicolor*, and therefore VanK is required for vancomycin resistance as it alone can add the branch glycine to precursors terminating in D-Ala-D-Lac (Hong *et al.*, 2005); precursors lacking this bridge would be lethal to the cell.

VanJ is a membrane protein with its C-terminal active site exposed in the periplasm, and was recently shown to be the sole mediator of teicoplanin resistance in *S. coelicolor* (Novotna *et al.*, 2012). Although *S. coelicolor* carries a complete set of glycopeptide resistance genes, it is sensitive to teicoplanin, because teicoplanin fails to induce expression of the *van* gene cluster (Hong *et al.*, 2008). Novotna *et al.* (2012) showed that exposing a plate containing *S. coelicolor* spores to paper discs containing vancomycin and teicoplanin side-by-side led to a D-shaped (rather than O-shaped) inhibition zone around the teicoplanin disc. This indicates that wild-type cells growing in the presence of vancomycin (as a result of the induction of *van* gene expression) were also able to grow in the presence of teicoplanin. Furthermore in a *vanJ* null mutant strain, the O-shaped zone of inhibition was observed around the teicoplanin disc, which could be restored by supplying a copy of *vanJ* in *trans*. Therefore VanJ alone causes resistance to teicoplanin in *S. coelicolor*.

The main point about the vancomycin resistance genes is that they are only expressed in the presence of an extracellular antibiotic and that signal transduction is effected by a two-component system (TCS, see section 1.5) consisting of a membrane-bound sensor kinase (VanS) and its cytosolic response regulator (VanR) (Healy *et al.*, 2000; Bugg *et al.*, 1991), which regulate the transcription of *vanHAX* (and other genes in the cassette) (see Figure 1.3.6.2). These two-component signal transduction systems are observed for a wide variety of bacteria, in response to stress, for osmoregulation, in quorum sensing, and in many other stimulus and response mechanisms. The focus for this PhD is the two-component VanS-VanR system regulating resistance to glycopeptide antibiotics. The mechanism of two-component systems, their architecture and the proteins involved, including the VanS/R system, is detailed in section 1.5.

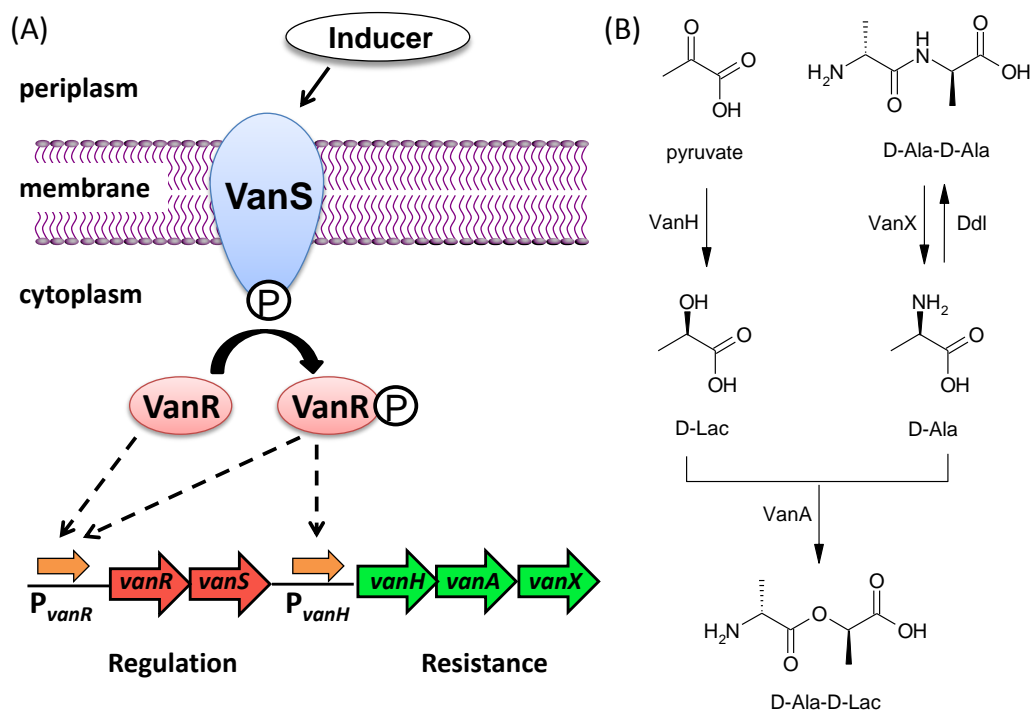


Figure 1.3.6.2: (left) A model of the VanRS two-component system controlling antibiotic resistance, (right) the function of enzymes encoded by van resistance genes. Adapted from Hong *et al.*, 2008 and Gao *et al.*, 2002.

1.4 Inducers of the VanS/VanR system

1.4.1 VanA-type resistance

A number of biochemical assays have been conducted in the literature to determine antibiotic inducers of VanS proteins from different bacterial strains, which are summarised in Table 1.4.3.1 for the VanA phenotype (VanS_A). The first assays were growth-based (Handwerger & Kolokathis, 1990; Allen & Hobbs, 1995), and involved treatment of cell cultures containing vancomycin-resistant VanA-type *E. faecium* strains with potential inducers. Handwerger & Kolokathis (1990) showed that growth of cell wall precursors occurred in the presence of vancomycin or moenomycin A, and Allen & Hobbs (1995) demonstrated the build-up of Lac-containing precursors in the presence of vancomycin, moenomycin A, and antibiotics affecting polymerisation steps in cell wall synthesis e.g. penicillin. However, growth-based assays cannot be used reliably to identify antibiotics that induce the resistance-related enzymes as cells often fail to survive induction (Ulijasz *et al.*, 1996).

A better way to test for inducers is by using gene reporter assays, which do not depend on cell survival to monitor activity. These include a *lacZ:vanH* fusion in *B. subtilis* (Ulijasz *et al.*, 1996; De Pascale *et al.*, 2007) and *E. faecium* (Mani *et al.*, 1998), a *lucA:vanH* fusion in *E. faecium* (Grissom-Arnold *et al.*, 1997) and a chloramphenicol acetyltransferase (CAT) based assay system in *E. faecium* (Lai & Kirsch, 1996).

In the *lacZ:vanH* fusions, the *E. faecium vanRS* operon regulates expression of LacZ from the coupled *E. faecium vanH* promoter. β -galactosidase activity (from LacZ expression) was measured in these assays, however, there are significant differences between the observed inducers in the *B. subtilis* system (Ulijasz *et al.*, 1996; De Pascale *et al.*, 2007) and those in *E. faecium* (Mani *et al.*, 1998). For instance, induced LacZ activity in the *B. subtilis* strain was observed upon addition of inhibitors of cytoplasmic (D-cycloserine and fosfomycin), membrane-bound (bacitracin) and periplasmic steps (glycopeptides, penicillin) in cell wall assembly, (Ulijasz *et al.*, 1996; De Pascale *et al.*, 2007), whereas LacZ activity in *E. faecium* strains was only induced by vancomycin and to a lesser degree by moenomycin A (Mani *et al.*, 1998). The authors propose that species differences between *B. subtilis* and *E. faecium* may have contributed to the differences in observed inducers. By far the strongest inducers of activity in the *lacZ:vanH* fusion are the glycopeptides, and possibly moenomycin A, both of which are involved in inhibiting PBP transglycosylation activity (through different mechanisms). The *lucA:vanH* assay by Grissom-Arnold *et al.*, (1997), which measures luciferase A expression under control of the *vanH* promoter, also supports this theory.

In a CAT-based radioisotopic assay (Shaw, 1975) conducted by Lai and Kirsch (1996), a total of 6800 compounds were screened for inducers of an *E. faecium* strain, containing a *cat* gene placed into an operon with the *vanHAX* genes. Eight active compounds were found to show significant CAT activity, including structurally-related glycopeptides (ristocetin, avoparcin, vancomycin) and cell-wall acting agents (moenomycin, bacitracin, methicillin).

Close examination of the relative CAT activities compared to untreated cells, showed that vancomycin was increased at least 6-fold (or 38-fold according to Arthur *et al.*, 1992), 18-fold for avoparcin and 8-fold for ristocetin. In contrast, the activities were only around 3-fold for bacitracin and moenomycin A, and therefore much weaker than glycopeptide antibiotics (Lai & Kirsch, 1996). In fact, the authors also used a second assay; a petri plate induction assay, which measured CAT activity as a function of colour change, resulting from bacterial growth in the presence of chloramphenicol and esculin. The culture was applied to plates, and an inducer-soaked disc placed on top (Figure 1.4.1.1). The figure clearly shows that although growth in the presence of chloramphenicol (by CAT expression) is observed for discs containing glycopeptide antibiotics (and robenidine; an agent against Protozoa), there is no growth or colour change for moenomycin, or other non-glycopeptide antibiotics.

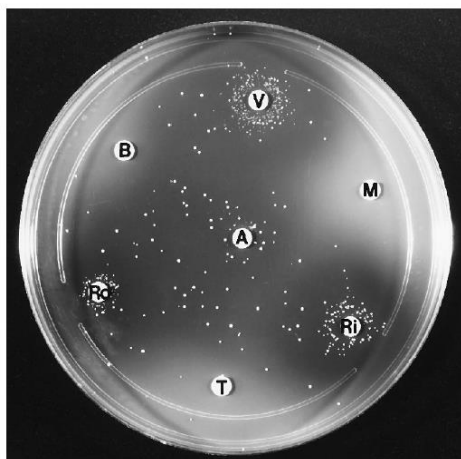


Figure 1.4.1.1: A petri plate assay for vancomycin resistance induction, reproduced from Lai & Kirsch (1996). A – avoparcin, B – bacitracin, M – moenomycin A, Ri – ristocetin, Ro – robenidine, T – tetracycline, V – vancomycin.

Inducers of the VanRS system therefore appear to be the glycopeptide antibiotics, but assays are not wholly consistent as an inducer in one assay is not necessarily an inducer in another. It should be noted that these methods are limited to their reliance on the induction of reporter genes rather than direct measurement of expressed proteins involved in vancomycin resistance. For this reason, further assays were developed by Baptista *et al.*, (1996) and Arthur *et al.*, (1999) which measured activity of the resistance gene, *vanX*, directly.

VanX enzymatic activity in cell extracts was monitored upon addition of potential antibiotic inducers, and is theoretically more reliable than cell reporter systems, as they require the antibiotic tested not to target any other mechanism to survive. It was shown that accumulation of cytoplasmic PG precursors cannot be the signal that triggers induction, since D-cycloserine, ramoplanin, bacitracin and penicillin all failed to act as inducers, whereas moenomycin A, vancomycin and teicoplanin were inducers of VanX activity (Baptista *et al.*, 1996; Arthur *et al.*, 1999). Since moenomycin A inhibits transglycosylase, both glycopeptides and moenomycin A are likely to lead to an accumulation of Lipid II (the lipid-anchored cell wall precursor) on the periplasmic side of the membrane, which could be the direct effector ligand of VanS (Baptista *et al.*, 1999; Hong *et al.*, 2008). Interestingly though, Arthur *et al.*, (1999) showed that although VanX activity was induced by moenomycin in the *E. faecium* VanRS system, activity was minimal (18 +/- 4 nmol min⁻¹ mg⁻¹) compared to vancomycin (190 +/- 31) or teicoplanin (280 +/- 55), and similar to uninduced cells (5 +/- 1).

It is therefore difficult to conclude from biochemical data alone, whether VanS_A is induced by a direct interaction with glycopeptide antibiotics, or whether it is activated by an indirect signal (e.g. by sensing accumulation of a cell wall intermediate such as Lipid II from inhibition of TG activity, or perhaps by interaction with Lipid II in complex with the antibiotic) (Hong *et al.*, 2008). Biophysical data is clearly required in order to ascertain whether a direct interaction is occurring at the VanS sensor domain (which is exposed to antibiotics) to induce gene expression, or if there is an indirect route for activation.

1.4.2 VanB-type resistance

The VanB resistance phenotype shows higher specificity for inducers of glycopeptide resistance (see Table 1.4.3.2 and Table 1.4.3.3). Both reporter assays and direct measurements of expressed proteins have shown that only vancomycin antibiotics induce resistance gene production in the *E. faecalis* VanB phenotype.

CAT radioactivity assays (Evers & Courvalin, 1996) initially showed that VanS_B expression was induced by vancomycin, but was only sensitive to teicoplanin. This was confirmed by VanX activity measurements by Baptista *et al.* (1996), who showed that all non-glycopeptides tested, including moenomycin A, failed to induce VanS_B. Since all identified inducers of VanS_B are structurally related glycopeptides, it seems likely that it should be induced directly by vancomycin itself. Baptista *et al.* (1999) also showed by fluorescence measurements using a *gfpmut1* gene (encoding GFP) fused to the *vanB* resistance gene promoter, that VanS_B was also only induced by vancomycin. However, six different point mutations in the gene resulted in either a vancomycin- and teicoplanin-resistant VanB strain (VanS_BA₁₆₇S), constitutively active VanB strains (VanS_BT₂₃₇M) or intermediate resistance, and it is unclear how VanS_B could be directly inducible by both antibiotics, especially when the point mutations occur in the cytoplasmic region (which cannot be accessed by glycopeptide antibiotics), so an indirect mechanism of induction is also conceivable.

For the VanB-like phenotype in *S. coelicolor*, inducers were identified from a reporter assay which involved the expression of a *neo* gene, conferring resistance to neomycin and kanamycin, under control of a *vanJ* resistance gene promoter (*vanJ_P*) (Hong *et al.*, 2004). *vanJ_P-neo*-containing plasmids were spread onto plates containing a lethal dose of kanamycin and potential inducers were applied on paper disks. The assay found that several glycopeptides induced vancomycin expression, whereas penicillin and teicoplanin did not. In a further optimised assay, a direct measurement of VanK resistance gene expression was made, by spreading strains containing a *femX* null mutant onto plates and applying potential inducers on paper disks (Hutchings *et al.*, 2006). In the absence of vancomycin, FemX enzymes add the single Gly amino acid branch to the pentapeptide cell wall precursor, to allow transpeptidation reactions. However, in the *femX* null mutants, the *vanK* gene must be expressed in order to add this branch amino acid. Inducers of this system were also only glycopeptide antibiotics, and not antibiotics targeting earlier or later steps in PG synthesis. Therefore VanS_{SC} should be activated by a direct interaction with glycopeptide antibiotics.

In fact, recently, fluorescent labelling strategies were applied to study the VanS_{SC} proteins in the presence of a glycopeptide ligand (Koteva *et al.*, 2010) and it was demonstrated for the first time that a direct binding occurs between *S. coelicolor* VanS and a fluorescent vancomycin analogue (a vancomycin photoaffinity probe, VPP) (Figure 1.4.2.1). This VPP ligand contained a biotin tether for purification and visualisation on anti-biotin blots, and a benzophenone ((C₆H₅)₂CO) probe for covalent labelling of protein-probe complexes (VanS-benzophenone). By incubating the ligand with membranes isolated from *E. coli* (containing overexpressed His₆-VanS_{SC} proteins) and irradiating with UV light, the fluorescent biotinylated VPP was observed to covalently bind to the VanS protein (Koteva *et al.*, 2010). Using a gene reporter assay it was shown that VPP was a bioactive ligand of VanS, able to induce *vanH* resistance gene expression in vancomycin-resistant *S. coelicolor* *in vivo*. The synthetic VPP ligand is, however, structurally different from naturally expressed vancomycin, so there is a possibility that vancomycin molecules will not interact via the same mechanism. One of the goals of this PhD is therefore to determine by biophysical studies whether VanS proteins can bind directly to natural glycopeptide antibiotics, or whether a signalling molecule or cell wall intermediate is involved in the activation of VanS.

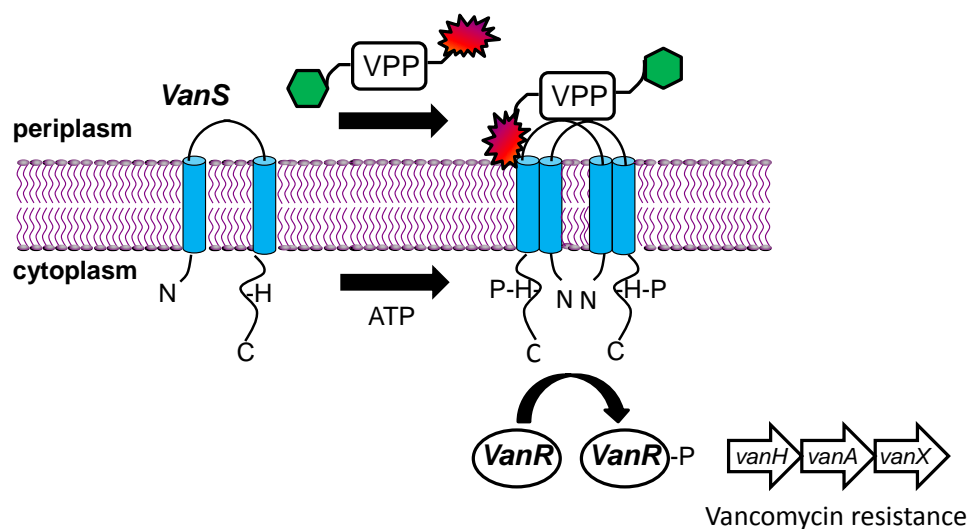


Figure 1.4.2.1: Schematic diagram of the direct binding between VPP and VanS_{SC} protein. VPP binding activates the protein causing auto-phosphorylation and phosphotransfer to VanR, resulting in resistance gene expression. Adapted from Koteva *et al.*, 2010. Biotin tether – green, Benzophenone probe – Purple.

1.4.3 Summary of Antibiotic Inducers

Table 1.4.3.1: Induced vancomycin resistance in the *E. faecium* VanA phenotype by various antibiotics, according to reporter or assay based systems.

Note: Moenomycin A and glycopeptide antibiotics are highlighted in red throughout (as they are potentially both inducers of the VanS_A protein).

Antibiotic Targets in Cell Wall Assembly	Nucleotide Precursors		Lipid-linked Intermediates	Lipid II					PBPs (TG/TP)		
	D-cycloserine	Fosfomycin		Bacitracin	Ramoplanin	Vancomycin	Teicoplanin	Avoparcin	Ristocetin	Moenomycin	Penicillin
Lac-containing precursors (Allen & Hobbs, 1995)	X	X	✓	-	✓	-	-	-	✓	✓	-
LacZ reporter in <i>B. subtilis</i> (Ulijasz <i>et al.</i> , 1996)	✓	✓	✓	-	✓	✓	-	✓	-	✓	-
LacZ reporter in <i>E. faecium</i> (Mani <i>et al.</i> , 1998)	X	X	X	-	✓	✓	-	-	✓	-	-
LucA reporter (Grissom-Arnold <i>et al.</i> , 1997)	-	-	✓ low	✓ low	✓	✓	-	-	✓ low	X	X
CAT radioactivity assay (Lai & Kirsch, 1996)	-	-	✓ low	-	✓	-	✓	✓	✓ low	-	X
CAT-induced petri plate assay (Lai & Kirsch, 1996)	-	-	X	-	✓		✓	✓	X	-	-
VanX activity (Baptista <i>et al.</i> , 1996)	X	-	X	X	✓	✓	-	-	✓	X	-
VanX activity (Arthur <i>et al.</i> , 1999)	-	-	-	-	✓	✓	-	-	X low/none	-	-

Table 1.4.3.2: Induced vancomycin resistance in the *E. faecalis* VanB phenotype by various antibiotics, according to reporter or assay based systems.

Antibiotic Targets in Cell Wall Assembly	Nucleotide Precursors		Lipid-linked Intermediates	Lipid II					PBPs (TG/TP)			
	D-cycloserine	Fosfomycin		Bacitracin	Ramoplanin	Vancomycin	Teicoplanin	Ristocetin	Avoparcin	Moenomycin	Penicillin	Methicillin
Assay method / Reporter												
CAT radioisotope assay (Evers & Courvalin, 1996)	-	-	-	-	✓	X	-	-	-	-	-	-
VanX activity (Baptista <i>et al.</i> , 1996)	X	-	X	X	✓	X	-	-	X	X	-	-
VanX activity (Arthur <i>et al.</i> , 1999)	-	-	-	-	✓	X	-	-	X	-	-	-
<i>Gfpmut1</i> fused to <i>vanB</i> operon (Baptista <i>et al.</i> , 1999)	-	-	-	-	✓	X	-	-	-	-	-	-

Table 1.4.3.3: Induced vancomycin resistance in the *S. coelicolor* VanB-like phenotype by various antibiotics, according to reporter or assay based systems

Antibiotic Targets in Cell Wall Assembly	Nucleotide Precursors		Lipid-linked Intermediates	Lipid II						PBPs (TG/TP)		
	D-cycloserine	Fosfomycin		Bacitracin	Ramoplanin	Vancomycin	Teicoplanin	A47934	Ristocetin	Chloro-eremomycin	Moenomycin	Penicillin
Assay method / Reporter												
VanK activity (Hutchings <i>et al.</i> , 2006)	X	-	X	X	✓	X	✓	✓	✓	X	-	X
<i>vanJp-neo</i> fusion assay (Hong <i>et al.</i> , 2004)	-	-	-	-	✓	X	✓	✓	✓	-	X	-

1.5 Two Component Regulatory Systems

Bacteria, yeast, fungi, archae and some plants (e.g. *Arabidopsis thaliana*) use two-component signal transduction systems (TCSs) to regulate physiological and molecular processes, by sensing and responding to a specific signal (Gao & Stock, 2009). The prototypical TCS is composed of a membrane-bound sensor kinase, which is autophosphorylated on a conserved histidine residue upon induction by a specific stimulus, and is therefore named a histidine kinase (HK). The second component is a response regulator protein (RR), which accepts the phosphate from the kinase, onto a conserved aspartate residue (Walsh *et al.*, 1996). The response regulator proteins are transcription factors, which control expression of target genes. Upon phosphorylation the response regulator changes its conformation, activating an effector domain, to elicit a response.

1.5.1 Diversity of Bacterial Two-Component Systems

Two-component signalling is implicated in many vital cellular processes e.g. in response to changes in osmolarity (e.g. EnvZ/OmpR), chemical gradients (CheA/CheY), cell density and a vast number of other responses (see Table 1.5.1.1). Bacterial adaptation to environmental changes occurs on the level of (a) individual genes and proteins, (b) global regulons, (c) whole-cell level (e.g. motility or sporulation), or (d) multicellular level (e.g. quorum sensing or biofilm formation) (Perry *et al.*, 2011). There are more than 200 structures of two-component proteins identified (Gao & Stock, 2009), and the number of TCSs differs greatly between species, which seems to correlate with the variety of environmental signals bacteria are exposed to. For instance, *Mycoplasma genitalium* has 0 TCSs, whereas *Escherichia coli* has 30/32 (HKs/RRs), and *Myxococcus xanthus* has 132/119 (HKs/RRs) (Jung *et al.*, 2012). Because as many as one hundred TCSs can co-exist in a cell, a key characteristic of TCSs is their exquisite specificity for their cognate response regulator, in order to elicit the correct response amongst such a diverse range of systems (Casino *et al.*, 2010).

Table 1.5.1.1: Examples of bacterial two-component signalling systems. Adapted from Pirrung, 1999; Perry et al., 2011.

Histidine Kinase	Control Function	Response Regulator	Organism
NarX	Anaerobic respiration	NarQ	<i>E. coli</i>
TorS		TorR	<i>E.coli</i>
CitA	Citrate fermentation	CitB	<i>K. pneumoniae</i>
LuxQ	Quorum sensing (Cell density)	LuxR	<i>Many species</i>
VanS	Antibiotic Sensing	VanR	<i>Many species</i>
CheA	Chemotaxis (flagella motility)	CheY	<i>E. coli</i>
EnvZ	Osmosensing	OmpR	<i>E. coli</i>
KinA		Spo0F	<i>E.coli</i>
PhoR	Phosphate metabolism	PhoB	<i>E. coli</i>
BvgS	Virulence	BvgS (internal)	<i>B. pertussis</i>

1.5.2 Domain Architecture and Function

The core of the TCS pathway is the phosphotransfer reaction(s) between a homodimeric histidine kinase and a response regulator. Typically the HK is the input component, designed to sense stimuli and regulate the signalling pathway, and the RR is typically the output of the system, regulated by the HK and effecting cellular response (Gao & Stock, 2009). The HK has kinase and phosphotransferase activities, and also functions as a phosphatase. The HK can autophosphorylate or dephosphorylate (as a ‘phosphatase’) the RR, to control the level of phosphorylation and hence the output response. Additional proteins can also regulate the activities of the HK or RR, to augment this basic scheme. Furthermore, besides systems with a single phosphotransfer step, the phosphotransfer pathway can be expanded to include phosphorelay pathways (with two or more steps) between multiple His- and Asp- residues (Figure 1.5.2.1). Examples of the prototypical class I HKs include EnvZ, HK853 (from *Thermotoga maritima*) and VanS. Class I hybrid HKs include TorS and ArcB, and class II HKs are essentially represented by the CheA chemotaxis system (Gao & Stock, 2009).

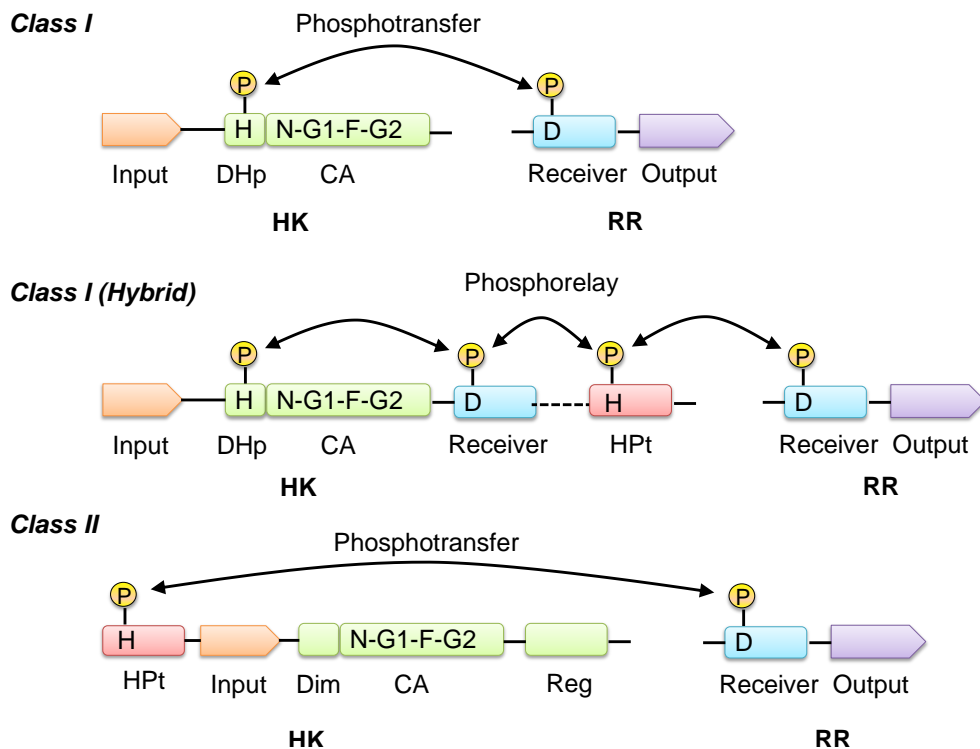


Figure 1.5.2.1: Domain architecture and signalling in two-component systems. Adapted from Jung *et al.*, 2012; Gao & Stock, 2009. In class I HKs, the kinase core has two domains; a DHp domain, connected via a linker to the CA domain. In class II HKs, the His residue (H) is in a histidine phospho-transfer (HPt) domain, separated from the CA domain by an input domain and a dimerisation (Dim) domain.

In prototypical HKs, the cytoplasmic kinase core consists of two domains: a well-conserved C-terminal catalytic ATP-binding domain (CA), and a less-conserved dimerisation and histidine phosphotransfer (DHp) domain, as shown in Figure 1.5.2.1. The DHp domain contains the His residue for phosphorylation, and the CA domain exhibits the catalytic activity to transfer a phosphoryl group from ATP to the His residue. In around 5% of HKs in the SMART database (Letunic *et al.*, 2004), a different organisation of the kinase core exists in which the phosphorylation site is located on a histidine phosphotransfer (HPt) domain, distant from the CA domain, and is transferred to the RR. The class I hybrid HKs, represent around 25% of all HKs and incorporate a receiver domain (REC) of RRs to form hybrid kinases. These are believed to function with linked or individual HPt domains to use a more elaborate phosphorelay system.

1.5.3 Histidine Kinase

Several characteristic sequence motifs are conserved across kinase domains of HKs, termed the H, N, G1, F and G2 boxes, based on their amino acid sequences (Stock *et al.*, 2000). The H box containing the primary phosphorylation site is in the DHp domain, and the rest are located in the CA domain. The CA domain contains the N box, G1, F and G2 boxes (Dutta *et al.*, 1999) and alone exists as a monomer in solution, capable of binding ATP and transferring phosphoryl groups to the dimeric DHp domain. Common to all classes of HK are the dimerisation domain, catalytic ATP binding domain, and the sensor domain.

Atomic structures have been reported for the isolated DHp, CA, or sensor domains of a number of HK sensors (Tomomori *et al.*, 1999, Bilwes *et al.*, 1999, Marina *et al.*, 2005) and more recently a handful of structures of histidine kinases with bound response regulators (Casino *et al.*, 2009, Yamada *et al.*, 2009). Furthermore in 2013, the first full-length structure of a histidine kinase was published (Diensthuber *et al.*, 2013). Taken together these structures have improved understanding of two-component signal transduction systems and enable greater knowledge of ways to inhibit these systems in bacteria. The structures and mechanistic insights into the function of the domains are discussed below.

(i) *Dimerisation and Histidine Phosphotransfer Domain (DHp)*

Histidine kinases are active in the form of a dimer, which is controlled by the interaction of the dimerisation domains of each monomer HK subunit. One of the first high resolution structures of the dimerisation domain produced was that of EnvZ, a class I HK (hybrid) outer membrane protein (OMP) from *E. coli* (Tomomori *et al.*, 1999), which is involved in osmoregulation (see Figure 1.5.3.1). Dimerisation of the transmembrane protein is essential for its autophosphorylation and phosphorelay signal transduction to its response regulator OmpR, to control expression of porin proteins OmpC and OmpF, which form an efflux pump in Gram-negative bacteria (Hall & Silhavy, 1981; Nikaido, 2003).

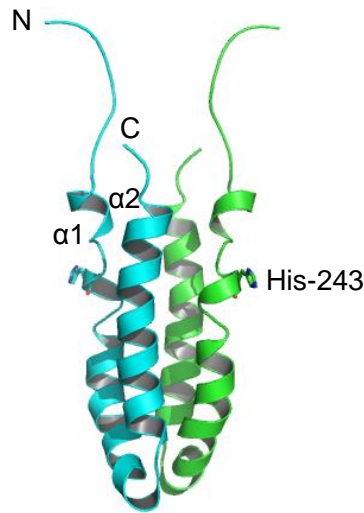


Figure 1.5.3.1: The dimerisation and phosphotransfer domain of EnvZ HK. The His residue is shown in stick representation on helix $\alpha 1$ of each subunit (cyan or green) of the dimeric EnvZ DHp domain (residues 223-289, PDB: 1JOY), produced in PyMol.

The homodimeric DHp structure of EnvZ includes a solvent-exposed His-243 site of autophosphorylation and comprises two antiparallel coiled-coils (or ‘helical hairpins’) (Helix I and II), which form a four-helix bundle. The two active His sites are located near the middle of Helix I (nearest N-terminus) within the dimeric kinase, which appears more mobile than Helix II, which could be important in signalling. Similar structures are also observed for Spo0B, a histidine phosphotransferase (without kinase activity), involved in phosphorelay with its response regulator, Spo0F in *B. subtilis* (Zapf *et al.*, 2000).

(ii) *Catalytic and ATP binding domain (CA)*

The C-terminal catalytic domain proceeds after the dimerisation domain and contains the ATP binding site. A number of structures of the CA domain have been solved including EnvZ (Tanaka *et al.*, 1998) and PhoQ (Marina *et al.*, 2001) from *E. coli*, HK853 (Marina *et al.*, 2005) and CheA (Bilwes *et al.*, 1999) from *Thermotoga maritima*, and DesK (Trajtenberg *et al.*, 2010) from *B. subtilis*. All CA domains have a characteristic α/β sandwich fold, consisting of three alpha-helices covered with a five-stranded β -sheet (see Figure 1.5.3.2), which are distinct from any known Ser/Thr kinases (Dutta & Inouye, 2000).

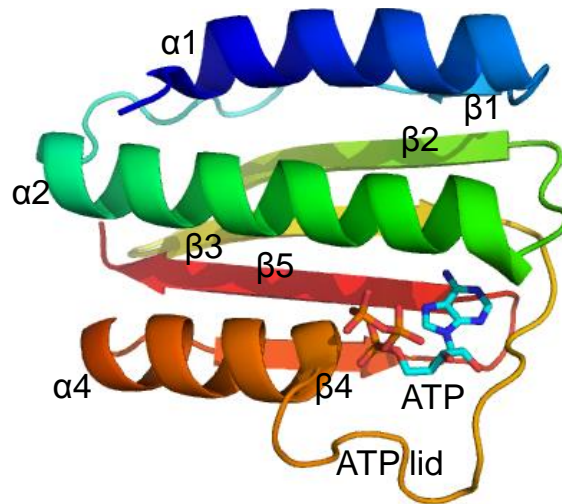


Figure 1.5.3.2: Ribbon diagram of the ATP binding domain of DesK HK from *B. subtilis* with bound ATP (PDB: 3EHG). Each domain is coloured in a rainbow spectrum with blue for the N-terminus and red for the C-terminus, adapted from Wang, (2012).

The highly conserved ATP binding cavity is defined by the conserved residues in the N, G1, F and G2 boxes (Gao & Stock, 2009). Between the F and G2 boxes is a flexible region named the ATP lid, which can adopt different conformations upon nucleotide binding. This domain binds ATP, and donates a γ -phosphate group to the His residue on the DHp domain.

The CA domain for DesK from *B. subtilis* has the shortest known sequence and represents the minimal core structure for this domain. Upon binding ATP and a divalent cation (e.g. Mg^{2+}) structural changes occur at the ‘ATP lid’ (a highly mobile loop) (Yamada & Shiro, 2008), giving it an ‘open’ or ‘closed’ (ATP bound) state. In the absence of ATP, this loop is partially disordered in crystal structures. Even in the presence of ATP, the lid shows flexibility, allowing ATP to bind and interact with the DHp domain for phosphotransfer. The ATP-lid also allows the CA domain to adopt multiple positions relative to the DHp domain, to function as a kinase, phosphotransferase or phosphatase in response to external stimuli.

(iii) *Sensor Domain*

Histidine kinases detect environmental input at their sensor domain and must adapt to changes in their environment by modifying gene expression levels, using the two-component system. Despite the great diversity of sequences found within sensor domains, to detect a specific ligand, there are patterns of domain organisation which be sorted into discrete structural classes. The prototypical HK is a homodimeric membrane protein in which the sensor domain is positioned between two transmembrane helices, as a periplasmic loop, and the DHP domain follows the last transmembrane helix and is located in the cytoplasm (Cheung & Hendrickson, 2010). However, some histidine kinases deviate from the model, and have sensor domains either within the membrane or in the cytoplasm.

Periplasmic sensory HKs include VanS (the subject of this thesis), NarX and TorS (Cheung & Hendrickson, (2009)), which have an all α -helical fold, and PhoQ, DcuS and CitA (Cheung & Hendrickson, 2010) which are the first three members of the PDC mixed α/β -fold (see Figure 1.5.3.3).

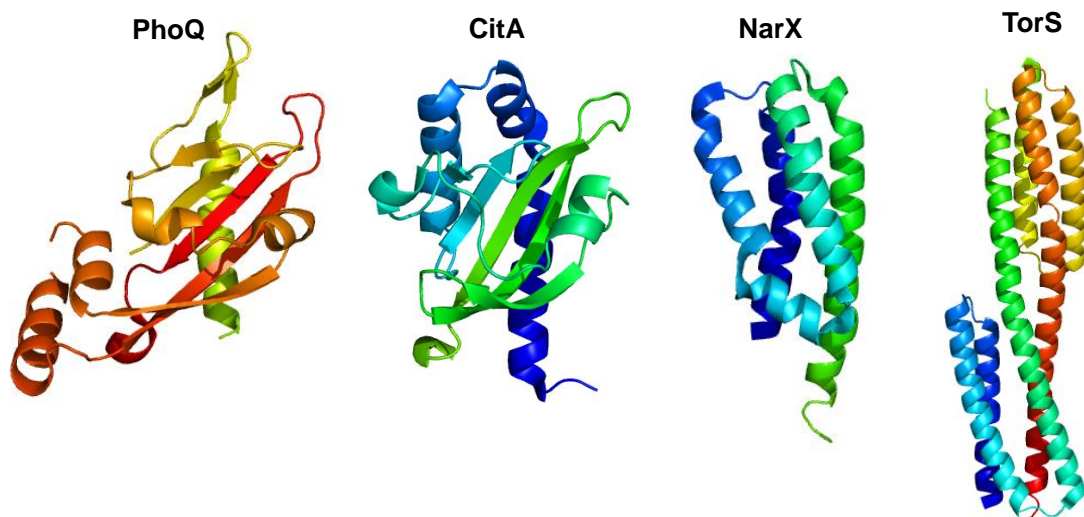


Figure 1.5.3.3: X-ray crystal structures of monomeric sensor domains of histidine kinases. Cartoon representation of the PDC sensor domains of PhoQ (PDB: 3BQ8) and CitA (2J80) and all-helical NarX (3EZH) and TorS (3I9Y) were prepared in PyMol.

Cytoplasmic sensory HKs can have a PAS-type fold (present in PER, ARNT and SIM proteins) (Hefti *et al.*, 2004) e.g. FixL (Ayers & Moffat, 2008), which senses oxygen through heme. The other cytoplasmic sensor structure is a GAF-type fold (present in cGMP phosphodiesterases, Adenyl cyclases and FhlA) e.g. DosS and DosT (Podust *et al.*, 2008), which detect changes in the redox state of a bound iron or in bound oxygen. The PAS domain structure has the same mixed α/β -fold as the PDC domain, but also has other distinctive features. The GAF domain structure consists of a six-stranded anti-parallel β -sheet core (Cheung & Hendrickson, 2010). The majority of kinase sensors have a PAS domain (~33%), which can sense changes in light, oxygen and redox potential in the cell. The GAF domain is present in ~9% of HKs, and can also sense a variety of ligands. Both PAS and GAF domains have high structural plasticity and sequence variability, which is important for stimuli recognition and signal transduction (Cheung & Hendrickson, 2010). HAMP domains are also present in ~31% of HKs, which are implicated in signalling and follow the last TM helix of the sensor domain, and are discussed in section 1.5.5.

In contrast, there is little information on membrane-embedded sensor domains, as no crystal structure exists for a transmembrane sensor domain (Cheung & Hendrickson, 2010).

Structural data on these systems does however suggest that most transmembrane sensors exhibit an all-helical fold. For example, sensory rhodopsin II (SrII) (Gordeliy *et al.*, 2002), which is involved in chemotaxis, forms a dimeric four-helix bundle (within the membrane), to transduce signals downstream.

1.5.4 Response Regulator (RR)

Response regulators are simpler in structure than histidine kinases. The RR superfamily is composed of two main domains; a receiver domain (REC) and an effector domain. A prototypical RR (e.g. VanR) has an N-terminal receiver domain that participates in catalysis of phosphotransfer by accepting a phosphoryl group from its cognate HK onto a conserved aspartate residue. Phosphorylation of the receiver domain changes its conformation, and causes activation of its C-terminal effector domain in a phosphorylation-dependent manner (Wang, 2012). The effector domain is variable in sequence and elicits the output of the signalling event, allowing for a diverse array of output functions. The majority of RRs (~63%) are transcription regulators with their effector domains acting as DNA-binding regions (Gao & Stock, 2009), or have enzymatic effector domains (~13%).

(i) *Receiver domain (REC)*

The REC domain acts as a phosphorylation-induced switch. Phosphorylation in the REC domain occurs at a conserved Asp residue, generating a high-energy acyl-phosphate. It is thought that this acyl phosphate provides the energy to drive a conformational change in the REC domain (Gao & Stock, 2009). The REC domain has enzymatic activity, catalysing phosphotransfer and dephosphorylation. Phosphotransfer from HK to RR involves a complex of the two, where both proteins contribute to the active site. The catalytic activity of the RR is exemplified by its ability to autophosphorylate at the Asp residue using small-molecule phosphodonors such as acetyl phosphate too. However the rate of phosphotransfer is much slower (~100 times) than that of the cognate HK (Lukat *et al.*, 1992).

The REC domain has a α/β -fold, with alternating β -strands and α -helices folding into a central five-stranded parallel β -sheet, surrounded by α -helices 1 and 5 on one side and α -helices 2, 3 and 4 on the other (Wang, 2012) (Figure 1.5.4.1).

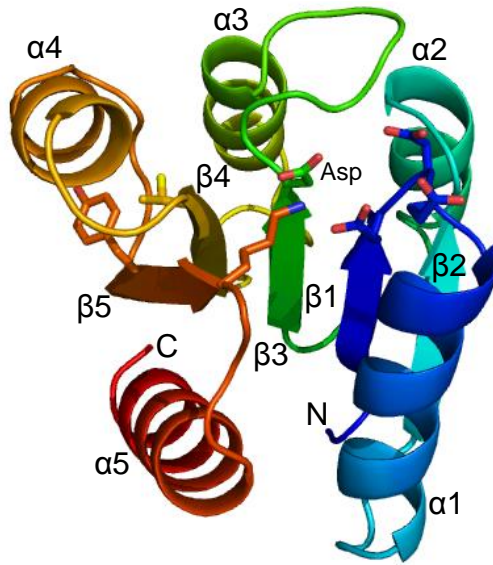


Figure 1.5.4.1: Structures of the *E. coli* receiver domain of the PhoB response regulator. Adapted from Wang, (2012) and coloured in a rainbow spectrum (PDB: 1B00). Phosphorylation site and switch residues are shown as sticks.

The β -sheet consists of mostly hydrophobic side chains, which form a hydrophobic core, as shown in the figure. Most of the conserved binding residues are at the C-terminal ends of β -strands 1, 3, 5. Helix $\alpha 1$ is involved in binding to the DHp domain of HK (Casino *et al.*, 2009) and is likely to play an important role in the specificity of HK-RR pairs. In addition to the Asp site of phosphorylation on the $\beta 3$ strand (Figure 1.5.4.1), the active site contains two Asp/Glu residues on the $\beta 1$ strand, that coordinate a Mg^{2+} ion (Gao & Stock, 2009).

(ii) *Effector Domain*

The effector domains are diverse in structure, in order to provide a variety of output responses. However they are dominated by a small number of structural families, named after highly characterised members. These include the OmpR/PhoB ‘winged-helix’ domain (30% of RRs) and the four-helix NarL/FixJ ‘helix-turn-helix’ domain (17%) (Figure 1.5.4.2).

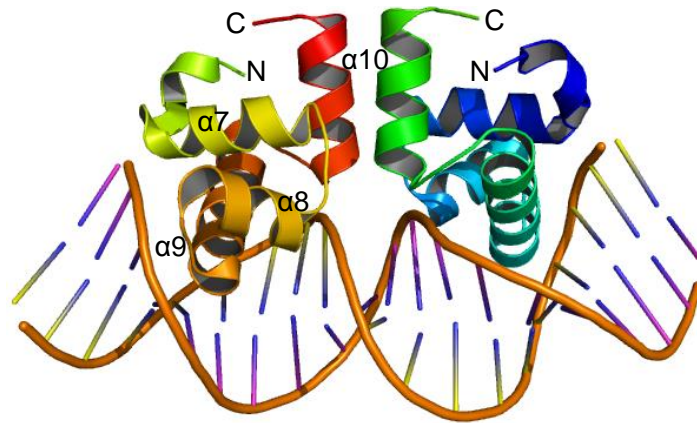


Figure 1.5.4.2: Structure of the dimeric effector domain of NarL RR binding to DNA. NarL (PDB: 1JE8) is drawn in ribbon form, adapted from Wang, (2012).

The C-terminal DNA-binding domain of the NarL/FixJ sub-family is a compact bundle of 4 α -helices (Maris *et al.*, 2005). In the inactive form, the REC and effector domains interact, masking the DNA-recognition helix (Maris *et al.*, 2002). However in the active phosphorylated state, the RRs dimerise and the DNA recognition helix (α 9) from both monomers inserts into the major groove of DNA, leading to transcription.

1.5.5 Insights into Signal Transduction Mechanisms

(i) Sensor Domain to Catalytic Domain

For a sensor HK to conduct its catalytic functions, a mechanism must exist by which the periplasmic loop and transmembrane domains can sense and transduce a signal to the catalytic core. Conformational changes must occur from the sensor loop to the kinase core, to transduce the signal. As stated in section 1.5.3 a number of sensory domains e.g. PAS and GAF domains are involved in sensing signals, which are believed to allow signal transduction through their structural plasticity and flexibility. An additional domain involved in signal transmission is a HAMP domain (present in Histidine kinases, Adenyl cyclases, Methyl-accepting chemotaxis proteins and Phosphatases) (Szurmant *et al.*, 2007).

HAMP domains connect the last transmembrane helix of the sensor domain to the catalytic domain. They consist of two helices which form a parallel four-helical coiled coil in the homodimeric active state, and are proposed to control signal transmission to the catalytic core (Hulko *et al.*, 2006; Ferris *et al.*, 2012) (see Figure 1.5.5.1).

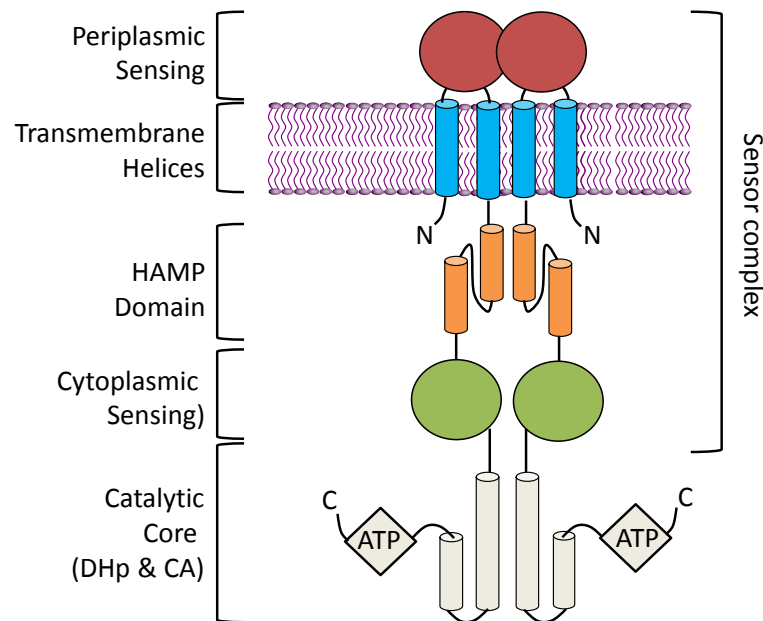


Figure 1.5.5.1: Schematic of histidine kinase modular architecture. Adapted from Szurmant *et al.*, (2007).

Two possible models exist for the function of the HAMP domains: a cog-like rotation of each helix relative to one another (‘gearbox model’) (Hulko *et al.*, 2006) or a combination of vertical movement and helical rotation (‘screw-like motion’) (Airola *et al.*, 2010). The gearbox model was proposed from studies of the first HAMP structure, of Af1503, a receptor from the archaeon *Archaeoglobus fulgidus*. Crystal structures of this receptor indicate that an axial rotation of the four-helix bundle by 26° occurs in the active state to transmit a signal to the kinase domain (Hulko *et al.*, 2006). This rotation converts the domain packing from a ‘complementary x-da’ packing to a ‘knobs-into-holes’ geometry.

The screw-like signalling mechanism is based on the crystal structure of the receptor Aer2 from *P. aeruginosa*, which has three connected HAMP domains, each containing a parallel four-helix bundle. However, in middle of HAMP2, there is an offset in the helical register between the first and second helix, which leads to a combination of vertical and helical rotation to transduce signals, i.e. a screw-like motion (Airola *et al.*, 2010). Therefore it is likely that structural changes in the sensor region upon ligand binding could trigger rotations of the TM helices and HAMP domain, or structural changes in PAS/GAF or other domains, to transduce signals to the kinase domain (Cheung & Hendrickson, (2010), Zhang & Hendrickson, (2010).

(ii) *Catalytic Domain to Dimerisation Domain*

Downstream structural changes in the dimerisation domain induced by signalling elements such as the HAMP domains are likely to alter the regulation of interactions between the DHP and CA domains. The changes triggered by different HAMP conformations do not appear to perturb the active-site histidine or the lower half of the DHP domain (Wang, 2012), but the CA domain must rotate to transfer a phosphate to the active His site in the DHP domain. As stated in section 1.5.3, numerous atomic structures exist for the isolated cytoplasmic domains of different HKs including EnvZ (Tomomori *et al.*, 1999), PhoQ (Marina *et al.*, 2001) and HK853 (Marina *et al.*, 2005). The crystal structure of HK853 from *T. maritima* is particularly useful for discussion since a recent co-crystal structure of the kinase and its cognate response regulator RR468 has been published (Casino *et al.*, 2009). The crystal structure of the entire cytoplasmic portion of HK853 is shown in Figure 1.5.5.2, which represents a dimeric conformational state ready for phosphotransfer (Marina *et al.*, 2005).

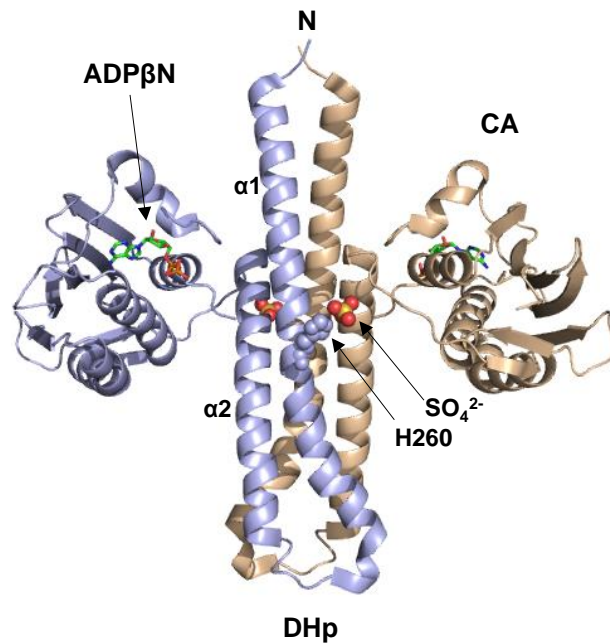


Figure 1.5.5.2: Ribbon diagram of the dimeric cytoplasmic portion of HK853. Adapted from Casino *et al.*, 2009. Each subunit is coloured in pale blue or light brown, with the H260 site and bound phosphate mimic (SO_4^{2-}) shown as spheres, drawn in PyMol (PDB: 2C2A).

The CA domain characteristically hosts one ATP molecule between its ATP lid and a central helix, which can be exposed for attack. In this instance the structure contains an ADP β N, instead of ATP. The CA domain is also connected to the DHp domain via a mobile hinge, which has been observed in other HKs to adopt multiple conformations for phosphotransfer. The H260 side chain is exposed to the surface of the protein and there is a sulphate ion in the structure bound to H260, mimicking the phosphorylated histidine.

As HKs are homodimeric, there are two mobile phosphorylating domains (CA) and two phospho-accepting exposed His residues (DHp). Therefore *cis*- or *trans*-phosphorylation could occur. *Cis*-phosphorylation is the phosphorylation of one HK monomer by itself, whereas *trans*-phosphorylation is phosphorylation of one HK monomer by the other. In the HK853 structure, the His residue and ATP binding site are 19Å apart, requiring a rotation of domains of 70° for *trans*- phosphorylation (Marina *et al.*, 2005). This is not consistent with 26° rotations observed in HAMP domains, so *cis*-phosphorylation is the preferred model.

However, there has been debate over which model applies, since e.g. EnvZ and DesK (Tomomori *et al.*, 1999; Trajtenberg *et al.*, 2010) autophosphorylate in a *trans*-mechanism, whereas HK853 and PhoR (Casino *et al.*, 2009; 2010) autophosphorylate in *cis*. In fact, a recent paper has demonstrated that the mechanism of autophosphorylation is independent of the *cis*- or *trans*-directionality since the catalytic centre of HK853 and EnvZ appear identical in functional and structural data (Casino *et al.*, 2014), and that the directionality is dependent on the left or right handedness of the DHp $\alpha 1$ and $\alpha 2$ helices.

(iii) *Dimerisation Domain to Response Regulator*

The crystal structure of the HK853-RR468 complex is shown in Figure 1.5.5.3, and shows that the response regulator molecules are positioned on opposite sides of the DHp domain dimer and sit below the phosphorylatable His260 residue.

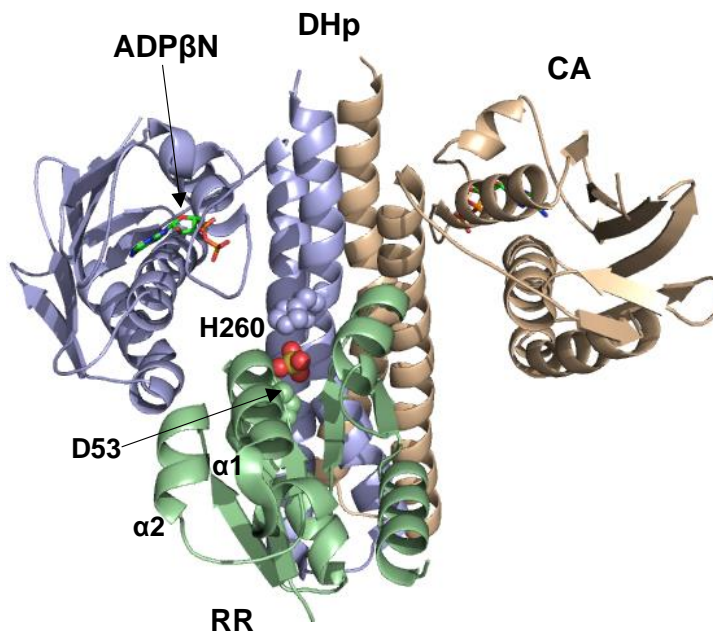


Figure 1.5.5.3: Ribbon representation of the crystal structure of the HK853-RR468 complex. Adapted from Casino *et al.*, 2009. The complex is viewed perpendicular to the DHp axis, and one RR molecule is shown in the structure for clarity. Each subunit of the HK is coloured in blue or light brown, and the RR is in green.

In this orientation the Asp53 site of the RR is aligned with a phosphoryl mimic and the H260 site of the HK (shown by spheres), favouring phosphoryl transfer (Casino *et al.*, 2009). The RR clings to the helical stem of one HK subunit by inserting the $\alpha 1$ helix of the RR next to the two helices of the HK, forming a six-helix bundle (Wang, 2012).

Overall the crystal structures of HK853 with and without bound RR, show conformational changes in accordance with the different functional states (phosphorylated by ATP, and phosphotransfer to the RR). These contacts should vary with the reaction occurring and confer specificity between the HK and its cognate RR. Similar interactions are observed for the catalytic domains of other histidine kinases with their cognate response regulators, e.g. in the Spo0B-Spo0F complex in *B. subtilis* (Zapf *et al.*, 2000) and in the ThkA-TrrA complex in *T. maritima* (Yamada *et al.*, 2009). Based on the HK853-RR468 complex and previous structures, Casino *et al.*, (2009), propose a model for TCS signalling (see Figure 1.5.5.4).

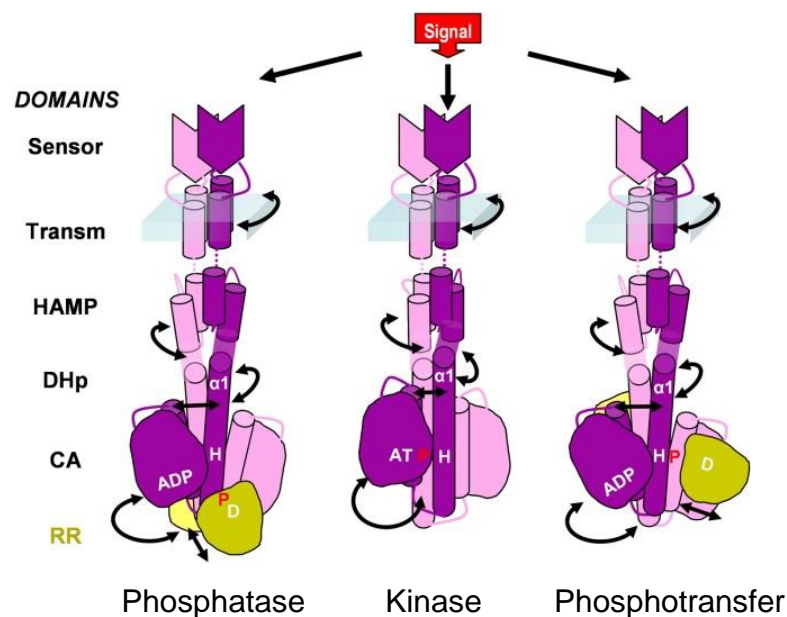


Figure 1.5.5.4: Signal transduction model, adapted from Casino *et al.*, (2009). Signal transduction involves rotation of coiled coils at the top of the DHp domain, altering its packing. This causes the CA domain to either approaches the His residue, activating the kinase (centre), or moves away to generate site for unphosphorylated RR, for phosphotransfer (right), or phosphorylated RR, triggering phosphatase function (left).

1.5.6 A Full-Length Histidine Kinase

During these studies, the first structure of a full-length histidine kinase, a photosensor kinase YF1, was published by Diensthuber *et al.*, (2013) (see Figure 1.5.6.1). The group demonstrated that a ‘rotary-switch’ mechanism is involved in its function, whereby rotation of helical connectors and coiled coils (e.g. PAS domains) is crucial to transduce signals to the kinase domain, to effect a response under different light conditions. YF1 is an engineered histidine kinase whereby the oxygen-sensitive PAS-B domain of the *B. japonicum* FixL HK is replaced with a light-oxygen-voltage (LOV) photosensor domain which also adopts a PAS fold, and is activated by binding flavin-mononucleotide (FMN) ligands. The resulting YF1 protein phosphorylates the cognate FixJ RR with similar activity to FixL in the dark. Upon exposure to blue light, the LOV sensor domain binds FMN, and compared to FixL, YF1 has a 1000 times increased phosphatase activity. Therefore the kinase and phosphatase states can be easily distinguished by switching from dark to light conditions.

In the structure, upon light absorption, a signal is transduced from the A’ α helices (N-terminus) which modulate the activity of the LOV (PAS) domain. Crucially the A’ α and J α coiled coils are precisely aligned and form a continuous helical spine, which rotates around the central axis to transduce signals, resulting in an increase in the crossing angle at the A’ α domains and J α . This rotary-switch model has also been proposed to occur in other HKs e.g. the Af1503 HK (Ferris *et al.*, 2012), involving HAMP domain signalling. It therefore appears that the alterations in the helical connectors and coiled coils (such as DHp, PAS and HAMP domains) are crucial to signal transduction. It has been shown in several studies that point mutations in coiled coil regions (Havranek & Harbury, 2003, Skerker *et al.*, 2008, Ferris *et al.*, 2012, Diensthuber *et al.*, 2013) can completely alter or ‘rewire’ the signal response of receptors, and this reprogramming could be used to engineer proteins in the same way as YF1, and perhaps act as a route to inhibit histidine kinase function, for instance those involved in bacterial antibiotic resistance.

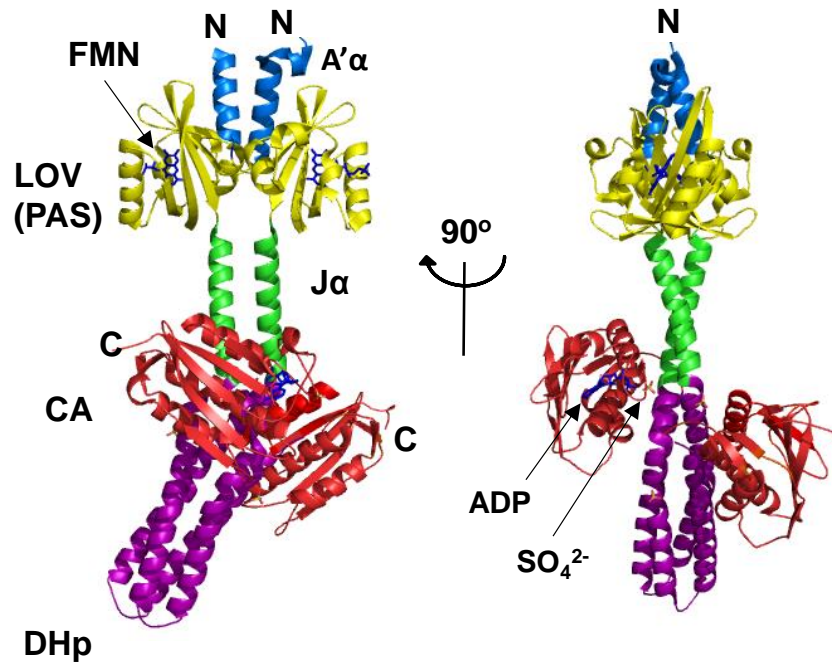


Figure 1.5.6.1: Ribbon diagram of the X-ray crystal structure of the dark-adapted sensor kinase YF1 (PDB: 4GCZ). Adapted from Diensthuber et al., 2013 and drawn in PyMol.

1.5.7 Cross-Talk within Two Component Systems

Most bacterial genomes encode dozens of TCSs to respond to a variety of stimuli. As a result, multiple HK/RR proteins are present from paralogous gene families. This makes it possible for cross-phosphorylation or ‘cross-talk’ between proteins in different TCS pathways, at highly similar DHp and REC domains (Gao & Stock, 2009). Cross-talk is different from ‘cross-regulation’ which occurs in branched TCSs, through necessity for a proper response by the organism. For instance cross-regulation occurs in ‘one-to-many’ systems such as the CheA HK chemotaxis system, which can phosphorylate CheY and CheB to control motility (Laub & Goulian, 2007). Cross-talk by comparison involves a deviation from a specific pathway by cross-phosphorylation from another TCS, and can be detrimental to cellular response. Several groups have reported cross-talk to non-cognate substrates *in vitro*, but usually only after protein overexpression, so it is not clear to what extent it occurs *in vivo*, but it is likely minimal to ensure specificity (Laub & Goulian, 2007).

One example of cross-talk is between VanS and the response regulator PhoB in *E. coli*, which only occurs in the absence of the PhoR histidine kinase (Fisher *et al.*, 1995; Silva *et al.*, 1998). Similarly the kinase, PhoR, can cross-talk to VanR, but only in the absence of VanS (Fisher *et al.*, 1996; Haldimann *et al.*, 1997). Therefore cross-talk is likely a consequence of eliminating the phosphatase activity normally provided by the other HK. In the VanS-VanR TCS in enterococci, VanS was also found to phosphorylate VanR with a 10,000-fold preference over non-cognate PhoB (Fisher *et al.*, 1995; 1996), demonstrating the inherent preference of a kinase for its cognate substrate, to prevent cross-talk.

1.6 Strategies for the Discovery and Development of Novel Antimicrobials

1.6.1 Platforms for Antibiotic Discovery

As stated in section 1.1.1, the discovery of the first aminoglycoside, streptomycin, by Selman Waksman in the 1940s was the first example of a robust discovery platform. The Waksman platform involved simply screening soil-derived *streptomycetes* for antimicrobial activity against a susceptible test organism by detecting zones of inhibition on an overlay plate. This platform of mining soil-derived actinomycetes was widely used by the pharmaceutical industry and produced most of the major classes of antibiotics during the golden era (Lewis *et al.*, 2013), but after 20 years of success, the returns diminished due to the rediscovery of known compounds. In the 1990s, the pharmaceutical industry de-emphasised its microbial screening programs and focussed on developing synthetic antibiotics using high-tech screening approaches based on genomics, high-throughput screening (HTS) using robotic technologies, and rational drug design. It was thought that essential conserved bacterial proteins identified through genomics would serve as targets for HTS and drug design with the aim of producing novel antibiotics. However, since the discovery of daptomycin, no novel drugs with broad spectrum activity against important pathogens have emerged from this platform (Clardy *et al.*, 2006).

A recent comprehensive HTS program of chemical libraries by GSK in 2007, examining 500,000 small molecules against a range of antibacterial targets did not find any new drugs worthy of development (Payne *et al.*, 2007). However, bedaquiline, a novel diarylquinoline antibiotic (Figure 1.6.1.1), was obtained through a focussed high-throughput screen using a commercially available library, and has been FDA approved for MDR-TB treatment (FDA, 2012). These focussed libraries, more suited for a specific target class, could hold more promise. For instance, the discovery of natural product platensimycin from *Streptomyces platensis*, with new terpenoid scaffold architecture (see Figure 1.6.1.1) was made by scientists at Merck using their old collection that had been previously screened for growth-inhibitory activity against *S. aureus* (Wang *et al.*, 2006; Young *et al.*, 2006).

Platensimycin was discovered by a targeted ‘smart’ screen using gene ‘knock-downs’, which lower the level of essential gene expressions in MRSA, one at a time, and render a particular step in a pathway rate limiting. A knockdown of the FabF and FabB enzymes in the fatty acid biosynthetic pathway made FabF the rate-limiting step in *S. aureus* lipid biosynthesis, and made bacterial growth sensitive to inhibition of this step (Walsh & Wencewicz, 2014).

There is a clear need to develop reliable discovery platforms, using focused compound libraries for HTS discovery and the use of structure-based rational design. X-ray structure and NMR structure determination of small-molecule ligands bound to target proteins has become a widely used tool for drug discovery, and *in silico*-based modelling methods supplement this (Clardy *et al.*, 2006). These techniques allow design of potential inhibitors that can be synthesised and evaluated in targeted biochemical screens. Structure-based approaches were responsible for revealing that platensimycin binds specifically to the FabF acyl-S-intermediate, and a C₁₆₃Q mutant of *E. coli* FabF mimicked the acyl-enzyme conformation well-enough to provide crystals in complex with platensimycin, revealing the unique structural features of platensimycin (Wang *et al.*, 2006).

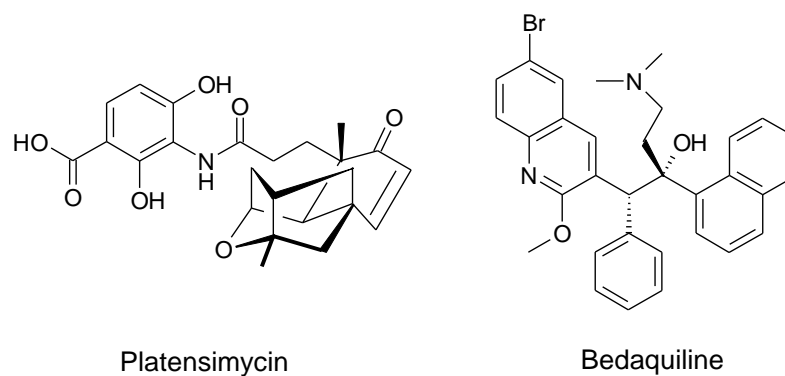


Figure 1.6.1.1: Structures of Platensimycin and Bedaquiline. *Platensimycin has an unusual pentacyclic terpenoid-like structure, whereas bedaquiline has two naphthalene-like rings and is a novel class called diarylquinolines.*

1.6.2 Underexplored antibiotic targets

There is potential to re-explore conventional targets to develop antimicrobials, given the wealth of new structural data available on drug targets and new mechanistic data on antibiotic action. For instance, in the early 2000s, a high resolution structure was published of the 50S ribosomal subunit from the archaeon *Haloarcula marismortui* (Ban *et al.*, 2000), and the 30S ribosomal subunit from *Thermus thermophilus* (Wimberly *et al.*, 2000). This could enable improved drug targeting at these sites by structure-based approaches. Recent data on the mechanism of action of the prototype lantibiotic nisin, which targets Lipid II, has also shown a new, additional mode of function. The lantibiotics, along with glycopeptides, mannopeptimycins and ramoplanins are thought to bind Lipid II preventing one or more steps in the Lipid II cycle or blocking peptidoglycan precursors from crosslinking (Breukink & Kruiff, 2006). New NMR evidence shows that the A and B rings of nisin form a pyrophosphate cage which binds the pyrophosphate of Lipid II, and that nisin uses Lipid II as a docking molecule to create a pore, disturbing cell integrity and leading to cell death (Hsu *et al.*, 2004). Nisin has promising activity against clinical isolates of MRSA and VRE, so nisin or its derivatives could be used therapeutically (Brumfitt *et al.*, 2002).

One advance of particular relevance to this PhD is the work of Boger's group (Xie *et al.*, 2011; James *et al.*, 2012) who generated a new synthetic version of the vancomycin aglycone: an amidine derivative (see Figure 1.6.2.1). The design took inspiration from the lowered affinity of vancomycin for D-Ala-D-Lac-terminating cell wall precursors. The loss of a critical hydrogen bond is compensated in the amidine derivative. This version shows activity against VRE, and retains acceptable activity against D-Ala-D-Ala PG precursors. Addition of the disaccharide moiety back onto the amidine aglycone could therefore lead to a new generation of glycopeptide antibiotics, to combat VRE, and perhaps VRSA infections. Further insight into the mechanism of binding of vancomycin to VanS (which is a major focus of this PhD) could therefore help improve structure-based design of novel glycopeptide antibiotics.

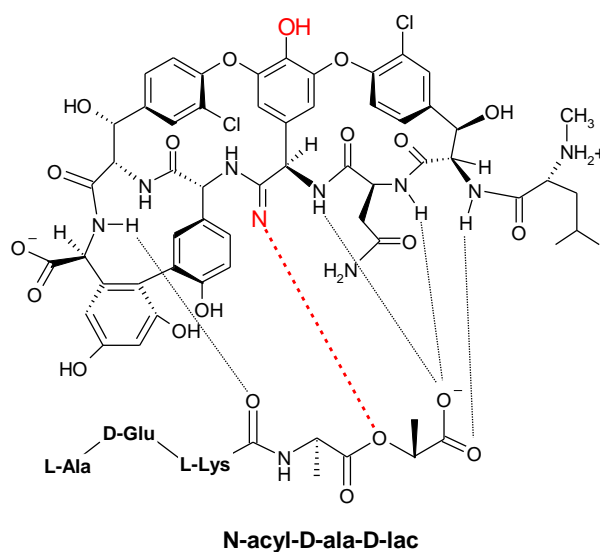


Figure 1.6.2.1: A synthetic amidine vancomycin aglycone which binds to D-Ala-D-Lac. Adapted from Walsh & Wenczewicz, 2014. The modification of a carbonyl group allows a key hydrogen bond (red) to be restored for high affinity in vancomycin resistant strains.

1.7 Aims and Outline of Thesis

1.7.1 Aims

The literature review above details advances in the field of drug discovery and development to combat the continued threat posed by antimicrobial resistance. The intricate architecture of two-component systems in bacteria shows how they have become tuned to sense slight changes in their environment and adapt through expression of individual genes or even on a whole cell level. The VanS-VanR TCS is one such example, which responds to the presence of glycopeptide antibiotics through expression of *van* resistance genes to alter the structure of the antibiotic target. This has led to the emergence of glycopeptide resistance in clinically relevant *Enterococcal* strains (GRE/VRE), and in more virulent *S. aureus* strains (VRSA). Vancomycin resistance has also been observed in soil-dwelling bacteria e.g. *Streptomyces*, which are often intrinsically resistant. The increasing emergence of glycopeptide resistance is a public health concern, and is particularly alarming given vancomycin's current status as a drug of last defence against serious Gram-positive infections e.g. MRSA. There is therefore a need to develop novel antimicrobials to combat infections from MRSA, VRE and VRSA, and to improve understanding of the associated resistance mechanisms.

Using a structural biology based approach, improved knowledge of the structure and function of different VanS proteins could contribute toward rational design of novel inhibitors. If successful these inhibitors could be used in conjunction with current antibiotics or as stand-alone therapies to combat glycopeptide resistance mechanisms. Towards this general aim, the work of this thesis focuses on the study of the sensor histidine kinase, VanS, derived from two bacterial strains (*E. faecium* and *S. coelicolor*), by biophysical and biochemical methods. These strains were chosen represent two different antibiotic resistance phenotypes (VanA and VanB-type respectively), and therefore proteins derived from these may interact with glycopeptide antibiotics by different mechanisms. Proteins derived from *E. faecium* are termed 'VanS_A', and those from *S. coelicolor*, are termed 'VanS_{SC}' throughout.

Literature on the VanS-VanR TCS demonstrates current knowledge of how extracellular glycopeptide and non-glycopeptide antibiotics activate VanS directly or indirectly via another signalling molecule such as Lipid II, and improvements in the understanding of structure-activity relationships for these systems. However, there are many questions that remain unanswered (see below). These are summarised schematically in Figure 1.7.1.1.

1. What is the atomic structure of the VanS membrane protein?

As a membrane protein, a long-term goal of any studies would be to determine the structure, function and dynamics of this protein kinase. In particular structure-function studies could reveal how vancomycin and other potential ligands activate VanS proteins in different species. Towards this goal, attempts were made to crystallise the full-length VanS protein and analyse the structure (and antibiotic binding properties) of its sensor domain by NMR spectroscopy.

2. What is the nature of the inducer that activates VanS, and if induced by a direct binding to the antibiotic, where are the binding sites located?

Biochemical screens for antibiotic inducers of the *Enterococcal* VanS_A protein are not consistent (see section 1.4), and biophysical experiments are required to provide conclusive evidence for a direct or indirect induction mechanism. Fluorescence- and NMR-based titration experiments are described in this thesis to test for a direct interaction between VanS and potential vancomycin ligands. Titration studies are conducted with VanS proteins derived from *S. coelicolor* (VanS_{SC}) to act as a positive control when assessing VanS proteins derived from *E. faecium* (VanS_A), since VanS_{SC} has recently been shown to bind directly to a vancomycin analogue (see section 1.4.2). NMR-based titration data is analysed to determine which residues (if any) can interact directly with vancomycin antibiotics.

3. By what mechanism are signals transduced across the transmembrane domain, upon induction by glycopeptide antibiotics?

There is evidence in many two-component systems that conformational changes are propagated throughout the sensor kinase upon induction. It is therefore likely that the sensor domain alters its conformation to propagate a signal downstream to the kinase domain. The transmembrane helices are positioned between these domains and could either associate with one another, or exhibit displacements/rotations relative to the bilayer to transduce this signal. To examine the propensity of these helices to self-associate, *in vivo* oligomerisation assays (ToxCAT) are conducted, with the aim of improving understanding of signal transduction across this domain.

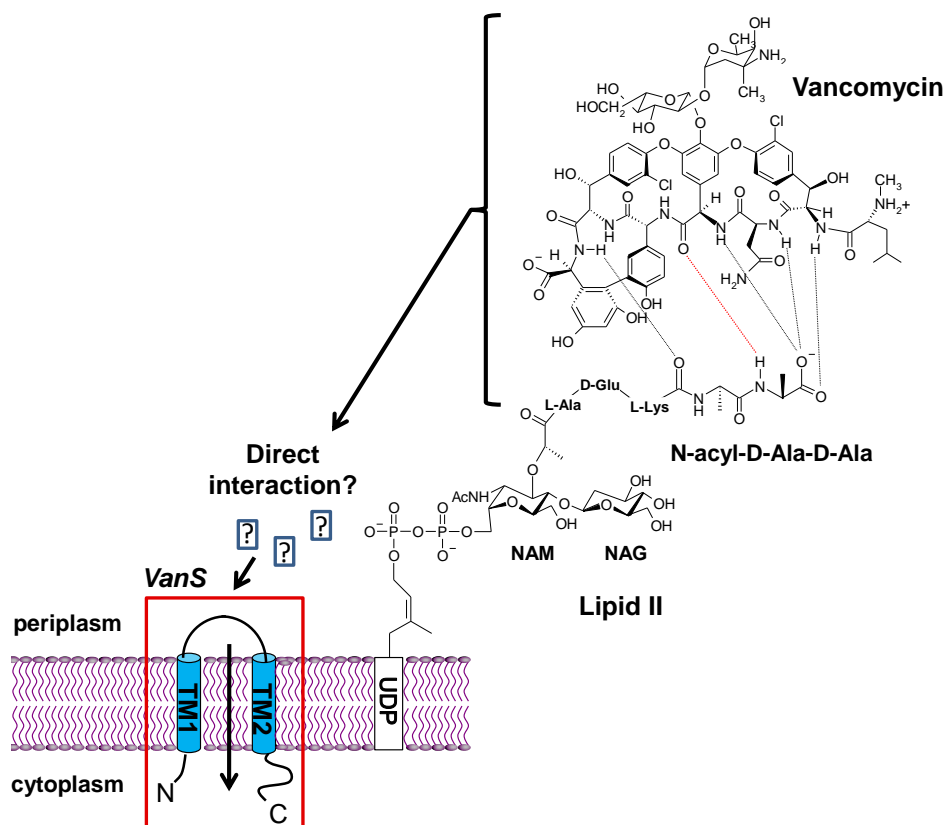


Figure 1.7.1.1: Schematic diagram showing the predicted topology of VanS, which is activated by vancomycin antibiotics, to transduce a signal to VanR. Vancomycin is known to bind to Lipid II to inhibit cell wall biosynthesis, but it is not clear whether VanS indirectly senses the action of vancomycin on the cell wall, or if it binds to vancomycin directly.

1.7.2 Outline

The expression and purification of full-length VanS membrane proteins from two bacterial species (*E. faecium* and *S. coelicolor*) with different phenotypic backgrounds is discussed in Chapter 3. Appropriate vectors are chosen for selective purification of VanS proteins by affinity chromatography and subsequent tag cleavage. Detergent-solubilised VanS proteins are assessed for their autophosphorylation activity using coupled enzymatic assays developed within the Warwick group, and tag-cleaved proteins are placed into crystallisation trials (using membrane protein screens). The main aim of these studies was to obtain a diffraction-quality crystal of a VanS protein, with improved resolution, compared to crystal hits identified (8Å) during previous studies by Dr. Michael Williams (Warwick University).

Chapter 4 describes cloning techniques used to modify the *vanS* gene sequence, in order to isolate the VanS sensor domain for use in NMR studies (see Figure 2.4.2.1). The main goal of which is to provide structural data on the sensor region and conformational changes at this domain upon titration of potential glycopeptide ligands. Routes towards overexpression and purification of this domain in isotopically labelled media, as required for NMR, are outlined. NMR spectral quality is also optimised by screening detergent, pH and buffer conditions.

In Chapter 5, fluorescence assays are applied to qualitatively test for any interaction between VanS proteins and a labelled vancomycin analogue. NMR-based titration experiments are then conducted to determine any residues that interact between the VanS sensor domain and vancomycin. These NMR assays involved the use of ¹⁵N-labelled VanS protein, and monitored for changes in peak chemical shift of the protein (on ¹H-¹⁵N HSQC spectra) upon titration of unlabelled vancomycin antibiotic. Additionally, oligomerisation assays are presented which aimed to further elucidate the mechanism by which signals are transduced from the sensor domain across the membrane, upon ligand activation. These assays quantify association between VanS transmembrane helices using an *in vivo* ToxCAT reporter system.

2 Materials and Methods

2.1 Suppliers of Chemicals and Reagents

All chemicals and reagents used were of analytical grade, and were obtained from the following sources unless otherwise stated:

Promega Corporation; Madison, Wisconsin, USA

Sigma-Aldrich Company Ltd.; Dorset, UK

New England Biolabs (UK) Ltd; Hitchin, Hertfordshire, UK

Perkin Elmer; Waltham, Massachusetts, USA

Affymetrix (formerly Anatrace); Maumee, Ohio, USA

GE Healthcare; Little Chalfont, Buckinghamshire, UK

Avanti Polar Lipids, Alabaster, AL, USA

Integrated DNA Technologies, Coralville, Iowa, USA

Roche, Basel, Switzerland

Invitrogen Life Technologies Ltd., Paisley, UK

2.2 Escherichia coli Strains

2.2.1 Bacterial Growth Media

LB Broth (Bertani, 2004) was composed of 10 g Tryptone, 5 g Sodium Chloride, 5 g Yeast Extract, prepared to one litre in water and autoclaved.

Super Optimal Broth with Catabolites (SOC) (Hanahan, 1983) was composed of 20 g Tryptone, 0.5 g Sodium Chloride, 5 g Yeast Extract, 0.2 g Potassium Chloride, 3.6 g Glucose and 1 g Magnesium Chloride and made up to 1 L with double-distilled water and autoclaved.

LB Agar Plates were composed of LB media, to which 15 g of bacto-agar was added to 1 L of media and autoclaved. Mediums were cooled to around 50°C at which point appropriate antibiotics were added and poured into sterile Petri-dishes and stored at 4°C until use.

5x M9 salts (Sambrook, 1989) were composed of 85 g Na₂HPO₄.12H₂O or 64 g Na₂HPO₄.7H₂O, 15 g KH₂PO₄, 2.5 g NaCl, prepared to one litre in water and autoclaved.

2.2.2 Bacterial Strains

Table 2.2.2.1 E. coli strains used in this project

Strain	Genotype	Reference
TOP10	<i>F</i> - <i>mcrA</i> Δ (<i>mrr</i> - <i>hsdRMS</i> - <i>mcrBC</i>) ϕ 80 <i>lacZ</i> Δ <i>M15</i> Δ <i>lacX74</i> <i>nupG</i> <i>recA1</i> <i>araD139</i> Δ (<i>ara-leu</i>)7697 <i>galE15</i> <i>galK16</i> <i>rpsL</i> (<i>Str</i> ^R) <i>endA1</i> λ ⁻	Grant <i>et al.</i> , 1990
DH5 α	<i>F</i> <i>endA1</i> <i>glnV44</i> <i>thi-1</i> <i>recA1</i> <i>relA1</i> <i>gyrA96</i> <i>deoR</i> <i>nupG</i> Φ 80 <i>dlacZ</i> Δ <i>M15</i> Δ (<i>lacZYA</i> - <i>argF</i>) <i>UI69</i> , <i>hsdR17</i> (<i>r_K⁻</i> <i>m_K⁺</i>), λ ⁻	Hanahan, 1985
NT326	<i>F</i> - <i>araD139</i> Δ <i>lacUl69</i> <i>rpsL</i> <i>thi</i> Δ <i>malE444</i> <i>recA1</i>	Treptow <i>et al.</i> , 1985
C41(DE3)	Derivative of E. coli BL21(DE3): <i>F</i> <i>ompT</i> <i>hsdSB</i> (<i>r_B⁻</i> <i>m_B⁻</i>) <i>gal</i> <i>dcm</i> (DE3). Contains at least one uncharacterised mutation - prevents cell death associated with expression of toxic recombinant proteins.	Miroux & Walker, 1996
C43(DE3)	Derivative of C41 (DE3) obtained using F-ATPase subunit gene.	Miroux & Walker, 1996
BL21 (DE3)	<i>F</i> ⁻ <i>ompT</i> <i>gal</i> <i>dcm</i> <i>lon</i> <i>hsdS_B</i> (<i>r_B⁻</i> <i>m_B⁻</i>) λ . An E. coli strain with DE3, a λ prophage carrying the T7 RNA polymerase gene and <i>lacI</i> ^q . Transformed plasmids containing T7 promoter driven expression are repressed until IPTG induction of T7 RNA polymerase from a <i>lac</i> promoter.	Studier & Moffat, 1986
BL21 (DE3) pLysS	<i>F</i> ⁻ <i>ompT</i> <i>gal</i> <i>dcm</i> <i>lon</i> <i>hsdS_B</i> (<i>r_B⁻</i> <i>m_B⁻</i>) λ (DE3) <i>pLysS</i> (<i>cm^R</i>). The pLysS plasmid is chloramphenicol resistant, and encodes T7 phage lysozyme, an inhibitor for T7 polymerase which reduces and almost eliminates expression from transformed T7 promoter containing plasmids when not induced.	Moffatt & Studier, 1987

2.2.3 Preparation of Chemically Competent Bacterial Cells for Transformations

Based upon the protocol outlined by Hanahan (1985), several methods for competent cell production exist. To produce ultracompetent cells, a method was followed using Promega Protocols and Applications Guide (Doyle, 1996). 10 ml of sterile Luria broth (LB) 10:5:5 was inoculated with 100 μ l of the required *E. coli* strain from a glycerol stock (stored at -80°C) and incubated at 37°C with shaking at 180 rpm overnight, until mid-OD phase.

250 mL sterile LB was inoculated with 2.5 mL of the overnight culture and incubated at 37°C with shaking at 180 rpm until the optical density at 600 nm reached between 0.4 and 0.6. The culture was then centrifuged at 4,500 g for 10 minutes to pellet cells, and resuspended in 100 ml of TFB1 buffer (30 mM potassium acetate, 10 mM calcium chloride, 50 mM manganese chloride, 100 mM rubidium chloride, 15% (v/v) glycerol, pH 5.8), centrifuged and resuspended in 10ml of TFB2 buffer (10 mM MOPS or PIPES pH 6.5, 75 mM calcium chloride, 10 mM rubidium chloride, 15% (v/v) glycerol). Competent cells were snap-frozen in 200 μ l aliquots in liquid nitrogen and stored at -80°C.

2.3 DNA Transformation of *E. coli*

Chemically competent cells (prepared as described in section 2.2.3) were thawed on ice and 100 μ L of cells was incubated with 10-100 ng of plasmid DNA for 20 minutes. Cells were heat-shocked at 42°C for 45 seconds and returned to ice for 2-3 minutes. 500 μ L of autoclaved LB media or 300 μ L of autoclaved SOC buffer was added and cells were incubated at 37°C, with shaking at 180 rpm, for 30-45 minutes. 100 μ L of transformation mixture was plated using aseptic technique onto LB agar plates containing the appropriate antibiotic selection for the transformed plasmid. Plates were incubated at 37°C overnight.

2.3.1 Preparation of Glycerol Stocks

5 mL sterile LB was inoculated with a single *E. coli* colony from a fresh transformation (see section 2.3) and grown to mid-log phase in the presence of appropriate antibiotic for plasmid selection with shaking at 37°C. 0.8 mL of culture was aseptically mixed with 0.2 mL sterile analytical reagent grade 80% (v/v) glycerol in a Corning cryo-vial and frozen at -80°C.

2.4 DNA Manipulation and Cloning Techniques

Oligonucleotides were designed against the appropriate gene target with relevant restriction enzyme sites included and ordered from Integrated DNA Technologies (IDT) or Invitrogen.

Table 2.4.1: Synthesised oligonucleotide sequences used in this project. For -forward (5') primer; Rev- reverse (3') primer, FL- Full-length gene, 4aa/3aa – Section of DNA encoding for 4 or 3 amino acids of an enzymatic cleavage site, Tm- melting temperature. Primers for Van_{S_A} and Van_{S_{SC}} were designed against *E. faecium* 'VanA' phenotype and *S. coelicolor* 'VanB' phenotype respectively. Restriction sites are underlined, mutations highlighted, and stop codons in red. CCATGG:- NcoI, AAGCTT:- HindIII.

Primer Name	Sequence 5' to 3'	Tm (°C)	Use in Project
pttQ18 For	CAT CGG CTC GTA TAA TGT GTG G	60.3	Sequencing
pttQ18 Rev	GGC GAA AGG GGG ATG TGC TG	63.4	Sequencing
pProEx For	AGC GGA TAA CAA TTT CAC ACA GG	55.7	Sequencing
pProEx Rev	CTG CGT TCT GAT TTA ATC TGT AGG C	63.7	Sequencing
Van _{S_A} FL For	TTT GCG <u>CCA TGG</u> TTA TAA AAT TGA AAA ATA AAA AAA ACG ACT ATT CC	61.4	Construct Creation
Van _{S_A} FL Rev	TTT GCG <u>AAG CTT</u> AGG ACC TCC TTT TAT CAA CCA AGT CTG GCA TCG CTG	69.1	Construct Creation
Van _{S_{SC}} FL For	TTT GCG <u>CCA TGG</u> ATA GGC GCC CCG GTC TGA GCG TCC GCC TCA AG	75.2	Construct Creation
Van _{S_{SC}} FL Rev	TTT GCG <u>AAG CTT</u> ACC TGC CGG TGT GCG GAG CGG CCG CGG GCA G	77.1	Construct Creation
Van _{S_A} 110 Rev	GCG GCG <u>AAG CTT</u> TTA AAT GCC GGT ATT TAT CTC GTC AAA GTA TTT TGC GAA TTT	66.8	Construct Creation

VanS _A 120 Rev	GCG GCG AAG CTT TTA TTG TTT ATC TTC GTT CTG AAT AAG TAC ATC AAT GCC GGT	67.0	Construct Creation
VanS _A 130 Rev	GCG GCG AAG CTT TTA CAT AAC ATC CAT TTC CGC AGA AAG CTC AAT TTG TTT AGC	67.7	Construct Creation
VanS _{sc} 100 Rev	GCG GCG AAG CTT TTA GCG GGT GGC CTC GGT GAT GCG GTC CAG GGG	76.0	Construct Creation
VanS _{sc} 110 Rev	GCG GCG AAG CTT TTA CCG GTG GGA GAG GGA TCC GGT CGC CGC CGT GCG	76.8	Construct Creation
VanS _{sc} 120 Rev	GCG GCG AAG CTT TTA GTA CTC GTC CCT GCG GCC CGG CAG CCG GAT GCG GTG	76.5	Construct Creation
VanS _A 3C 4aa For	TTC CAG GGA CCT ATT GAG CTT TCT GCG GAA ATG GAT GTT ATG GAA	67.0	Mutagenesis
VanS _A 3C 4aa Rev	CAG CAC CTC CAG TTG TTT ATC TTC GTT CTG AAT AAG TAC ATC AAT GCG GG	66.4	Mutagenesis
VanS _A TEV 4aa For	TAC TTC CAG AGT ATT GAG CTT TCT GCG GAA ATG GAT GTT ATG GAA C	65.0	Mutagenesis
VanS _A TEV 3aa Rev	CAG GTT CTC TTG TTT ATC TTC GTT CTG AAT AAG TAC ATC AAT GCC GG	64.2	Mutagenesis
VanS _{sc} 3C 4aa For	TTT CAA GGA CCT AGG GAC GAG TAC CGA GAA CTC GCC GAT GCC	68.6	Mutagenesis
VanS _{sc} 3C 4aa Rev	CAG CAC CTC CAG GCG GCC CGG CAG CCG GAT	70.0	Mutagenesis
pccKan For	CCT TCA TCA GCC ACT GTA GTG AAC	66.0	ToxCAT
pccKan Rev	CGA CTT CAG CGA GAC CGT TAT AG	66.0	ToxCAT
VanS _A TM1 For	CTA GCC TGT ATA TGT ATA TTG TGG CGA TTG TGG TGG TGG CGA TTG TTG TGC TGT ATA TTG G	67.0	ToxCAT
VanS _A TM1 Rev	GAT CCC AAT ATA CAG CAC AAA CAC AAT CGC CAC CAC CAC AAT CGC CAC AAT ATA CAT ATA CAG G	67.0	ToxCAT
VanS _A TM2 For	CTA GCA TTT TTA TTT ATG TGG CGA TTG TGA TTA GCA TTC TGA TTC TGT GCC GCG TGA TGC TGA GCG G	68.0	ToxCAT
VanS _A TM2 Rev	GAT CCC GCT CAG CAT CAC GCG GCA CAG AAT CAG AAT GCT AAT CAC AAT CGC CAC ATA AAT AAA AAT G	68.0	ToxCAT
VanS _{sc} TM1 For	CTA GCG GCT TTC TGA CCC TGG CGG GCG TGC TGC TGC TGG TGG CGG TGG GCG TGT TTC TGC TGG G	78.0	ToxCAT
VanS _{sc} TM1 Rev	GAT CCC CAG CAG AAA CAC GCC CAC CGC CAC CAG CAG CAG CAC GCC CGC CAG GGT CAG AAA GCC G	78.0	ToxCAT
VanS _{sc} TM2 For	CTA GCT GGG TGA TGG CGT TTC TGC TGG TGT TTG GCC TGG TGG GCG GCT GGT TTC TGG CGG GCG G	68.0	ToxCAT
VanS _{sc} TM2 Rev	GAT CCC GCC CGC CAG AAA CCA GCC GCC CAC CAG GCC AAA CAC CAG CAG AAA CGC CAT CAC CCA G	68.0	ToxCAT

2.4.1 Polymerase Chain Reaction (PCR)

DNA amplification was carried out using the specific enzymes for each PCR according to the manufacturer's guide. Initially Accuprime High-Fidelity *Taq* polymerase (Invitrogen) and Accuprime GC-rich *Taq* polymerase (Invitrogen) were used to amplify full-length or truncated *vanS* genes and clone into pProEx vectors. Each PCR reaction contained 5 μL of 10x Accuprime PCR buffer I (containing 2mM dNTPs, 20mM MgSO_4), 2 μL of a mix of forward and reverse primers from Table 2.4.1 (stock concentration 10 μM), 1 μL of *vanS* template DNA (25-50 ng/ μL) and 0.2 μL of *Taq* polymerase, and were made up to 50 μL with nuclease-free water. Reaction mixtures were centrifuged briefly at 10 krpm, before heating in an Eppendorf Mastercycler Gradient thermal cycler with an initial denaturation of 95°C for 2 minutes, then cycling 25 times from 94°C for 30 seconds, to annealing at 58-68°C (i.e. 5°C below the lowest T_m of the primer pair) for 45 seconds, to extending at 68°C for 90 seconds.

For PCR reactions involving site-directed mutagenesis, Phusion High-Fidelity polymerase (NEB) was used according to the manufacturer's guide. Each PCR reaction contained 10 μL of 5x Phusion HF or GC-rich buffer (containing 15mM MgSO_4), 1 μL of dNTPs (stock concentration of 10 μM), 5 μL of a mix of forward and reverse primers (stock concentration of 10 μM), 1.5 μL DMSO and 0.5 μL Phusion DNA polymerase, and were made up to 50 μL with nuclease-free water. Reaction mixtures were centrifuged briefly at 10 krpm, before heating in an Eppendorf Mastercycler Gradient thermal cycler with an initial denaturation of 98°C for 45 seconds, then cycling 30 times from 98°C for 10 seconds, to annealing and extending at 72°C (i.e. 5°C below the lowest T_m of the primer pair) for 90 seconds.

2.4.2 Site-directed Mutagenic PCR ('Round-the-Horn')

This 'Round-the-Horn' technique is based on the protocol created by Sean Moore (http://openwetware.org/wiki/'Round-the-horn_site-directed_mutagenesis), and the phrase originally referred to "Rounding Cape Horn"; a very difficult but rewarding journey. The method enabled insertion of a TEV or 3C proteolysis site directly into the *vanS* gene sequence, for subsequent cleavage, after expression and purification of the full-length protein. A primer pair e.g. "VanSa 3C 4aa For" and "VanSa 3C 4aa Rev" (see Table 2.4.1) was mixed with template DNA (pProEx::*vanS_A*), and used in a PCR reaction. These primers do not fully base-pair with template *vanS* gene sequences (highlighted in Table 2.4.1), and amplification results in linear mutated strands that have to be blunt-end ligated (see Figure 2.4.2.1). After blunt-end ligation, the first 4 amino acids of the 3C cleavage site ('4aa For') and the last 4 amino acids of the 3C cleavage site ('4aa Rev') join to form the full cut site.

PCR reactions were set up as given in section 2.4.1, using Phusion HF polymerase and the phosphorylated, mutagenic primers. To exclude that the template plasmid is transformed, it had to be removed before transformation. The template plasmid is isolated from an *E. coli* strain with active Dam methylase. This enzyme methylates the internal cytosine residues of DNA (plasmids). Because of this, it was possible to selectively digest the template DNA with the restriction enzyme DpnI, which only cleaves when its recognition site is methylated. PCR products were digested with DpnI at 37°C for 1 hour, before running a preparative gel (see section 2.4.6), excising the band and purifying (see section 2.4.5). Purified, linear mutated strands were subsequently circularised by blunt-end ligation overnight at 25°C using T4 DNA Ligase (see section 2.4.7). The ligation mixture was transformed into *E. coli* Top10 competent cells (Invitrogen) and DNA minipreparations were extracted from positive transformants (section 2.4.4). Extracted plasmids were restriction digested (section 2.4.3) and analysed by agarose gel electrophoresis (section 2.4.6) to determine the presence of a correctly-sized insert.

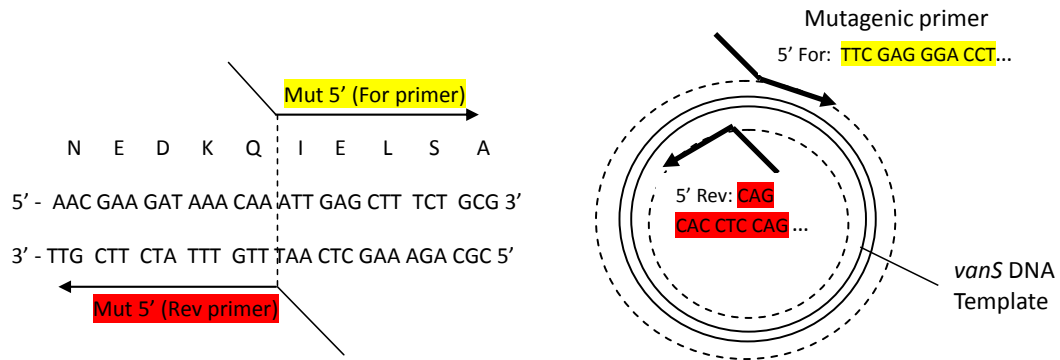


Figure 2.4.2.1: 3C site insertion by “Round-the-Horn” mutagenic PCR. The direction of transcription (arrows) of the forward (highlighted yellow) and reverse (highlighted red) mutagenic primers designed is shown, as well as the position of insertion into the protein.

2.4.3 Restriction Enzyme Digestion of DNA

Restriction digests (including double digests containing two restriction enzymes) were carried out using restriction enzymes (NEB, UK) in the appropriate buffer system, according to the manufacturer's guide. 1 µl of restriction enzyme and 100-500 ng of plasmid DNA or PCR product was used and reactions incubated at 37°C for 1-2 hours.

2.4.4 Preparation of Plasmid DNA

Plasmid DNA was extracted from *E. coli* TOP10 cells grown overnight in LB broth and appropriate antibiotics. Plasmid DNA was extracted using Fermentas or Qiagen miniprep extraction kits or purified by Promega Wizard DNA purification kit, according to the manufacturer's instructions. These kits employ the alkaline lysis method, where DNA is purified by adsorption to a silica matrix under high salt conditions.

2.4.5 Purification of DNA from PCR and Restriction Digests

DNA was purified to remove polymerases and endonucleases after PCR and restriction digests using the Promega Wizard PCR Extraction kit or Qiagen PCR purification kit, according to the manufacturer's instructions. Both methods purify DNA by adsorption to a silica matrix as used in the mini-prep kits above.

2.4.6 Agarose Gel Electrophoresis

A 0.8% (w/v) solution of high-melting point agarose (Sigma-Aldrich) was prepared by dissolving 0.4 g of agarose into 50 mL of 1x Tris-acetate-EDTA (TAE) buffer and heating for 3 minutes in a microwave oven. The solution was cooled to touch and 5 μ L of Ethidium Bromide (10 mg/ml stock) was added. The solution was poured into a gel cast and left to set. The gel was submerged in a gel tank containing 1x TAE buffer, and DNA samples were loaded into wells with 1 μ L of 6x DNA loading dye (Fermentas) per 5 μ L of DNA sample. 5 μ L of a DNA standard 100 bp or 1kb GeneRuler ladder or 1 kb Quick-Load ladder (pre-mixed with loading buffer) (Thermoscientific) was loaded to allow size determination of DNA samples. Electrophoresis was carried out at 100V for 30 minutes, and samples visualised with ultraviolet light using a Syngene G:Box gel illuminator, attached to a camera to allow imaging.

2.4.7 Ligation of DNA Fragments with Complementary Ends

Ligation reactions either involved blunt-end ligation or ligation of 'sticky ends'. Restriction digestion of plasmid DNA and PCR-amplified insert yielded DNA fragments with complementary 'sticky ends'. Digestion was confirmed by visualisation on an agarose gel, and the plasmid DNA band was excised and purified using a QIAquick Gel Extraction Kit, whilst PCR inserts were purified using a Qiagen PCR purification kit. Plasmid DNA and

insert were ligated at a nanogram ratio of 3:1 PCR insert: DNA plasmid, in the presence of T4 DNA ligase (Fermentas) according to the manufacturer's instructions, in a volume of 10 μ L. For blunt-end ligation, only T4 DNA ligase was added. Reaction mixtures were incubated at 25°C for 4 hours or overnight.

The ligation mixture was used to transform *E. coli* TOP10 cells as described in section 2.3. Transformed colonies were picked and cultured overnight in 5ml LB with appropriate antibiotics and plasmid DNA extracted by minipreparation (section 2.4.4). Extracted plasmids were restriction digested (section 2.4.3) and analysed by agarose gel electrophoresis (section 2.4.6) to determine the presence of a correctly-sized insert.

2.4.8 DNA Sequencing of Plasmid Constructs

To check that a cloned gene had been inserted correctly into the plasmid vector, start and stop codons were present and no mutations were incorporated by PCR errors, constructs were sequenced. 100 - 250 ng of plasmid DNA and 5-10 pmol of primer per sequencing reaction was mixed together and submitted to the Genomics Facility (University of Warwick) or GATC Biotech (London). Primers were either those used in the initial PCR, or specific for pProEx HTa vectors. Reactions were carried out using an ABI PRISM 3130xl or 3730xl Genetic Analyser. Resulting sequences were blasted against a database (www.uniprot.org/blast) and aligned with the database sequence using *ClustalW* (Larkin *et al.*, 2007) to check for point mutations introduced by PCR. Sequences were also manually checked (using BioEdit by Tom Hall, Ibis Biosciences from www.mbio.ncsu.edu/bioedit) to identify the presence of start and stop codons and correct gene orientation.

Table 2.4.8.1 Initial gene constructs and constructs created. Note: For details on the creation of *vanS* gene truncates (e.g. *vanS_A100-130*) and rationale behind their selection, refer to section 4.3.

Construct	Antibiotic gene	Description
pTTQ18:: <i>vanS_A</i>	Ampicillin	pTTQ18 vector containing <i>E. faecium vanS_A</i> wild-type gene
pGEM-T:: <i>vanS_{SC}</i>	Ampicillin	pGEM-T Easy vector containing <i>S. coelicolor vanS_{SC}</i> wild-type gene
pProEx:: <i>vanS_{SC}</i>	Ampicillin	pProEx HTA vector containing <i>E. faecium vanS_A</i> wild-type gene
pProEx:: <i>vanS_{SC}</i>	Ampicillin	pProEx HTA vector containing <i>S. coelicolor vanS_{SC}</i> wild-type gene
pProEx:: <i>vanS_A110</i>	Ampicillin	pProEx HTA vector containing <i>E. faecium vanS_A</i> gene truncated after 110 th residue (Met-1 to Ile-110)
pProEx:: <i>vanS_A120</i>	Ampicillin	pProEx HTA vector containing <i>E. faecium vanS_A</i> gene truncated after 120 th residue (Met-1 to Gln-120)
pProEx:: <i>vanS_A130</i>	Ampicillin	pProEx HTA vector containing <i>E. faecium vanS_A</i> gene truncated after 130 th residue (Met-1 to Met-130)
pProEx:: <i>vanS_{SC}100</i>	Ampicillin	pProEx HTA vector containing <i>S. coelicolor vanS_{SC}</i> gene truncated after 100 th residue (Met-1 to Arg-100)
pProEx:: <i>vanS_{SC}110</i>	Ampicillin	pProEx HTA vector containing <i>S. coelicolor vanS_{SC}</i> gene truncated after 110 th residue (Met-1 to Arg-110)
pProEx:: <i>vanS_{SC}120</i>	Ampicillin	pProEx HTA vector containing <i>S. coelicolor vanS_{SC}</i> gene truncated after 120 th residue (Met-1 to Tyr-120)
pProEx:: <i>vanS_A-TEV</i>	Ampicillin	pProEx HTA vector containing <i>E. faecium vanS_A</i> gene with an inserted TEV-specific proteolysis site
pProEx:: <i>vanS_A-3C</i>	Ampicillin	pProEx HTA vector containing <i>E. faecium vanS_A</i> gene with an inserted 3C-specific proteolysis site
pProEx:: <i>vanS_{SC}-TEV</i>	Ampicillin	pProEx HTA vector containing <i>S. coelicolor vanS_{SC}</i> gene with an inserted TEV-specific proteolysis site
pProEx:: <i>vanS_{SC}-3C</i>	Ampicillin	pProEx HTA vector containing <i>S. coelicolor vanS_{SC}</i> gene with an inserted 3C-specific proteolysis site
pccKan:: <i>vanS_ATM1</i>	Ampicillin	pccKan vector encoding for the predicted first transmembrane helix of <i>E. faecium vanS_A</i> gene (residues L19 to I37) with an N-terminal ToxR domain and C-terminal MBP domain (see section 5.5.2)
pccKan:: <i>vanS_ATM2</i>	Ampicillin	pccKan vector encoding for the predicted second transmembrane helix of <i>E. faecium vanS_A</i> gene (residues I78 to S97) with an N-terminal ToxR domain and C-terminal MBP domain (see section 5.5.2)
pccKan:: <i>vanS_{SC}TM1</i>	Ampicillin	pccKan vector encoding for the predicted first transmembrane helix of <i>S. coelicolor vanS_{SC}</i> gene (residues G19 to L37) with an N-terminal ToxR domain & C-terminal MBP domain (see section 5.5.2)
pccKan:: <i>vanS_{SC}TM2</i>	Ampicillin	pccKan vector encoding for the predicted second transmembrane helix of <i>S. coelicolor vanS_{SC}</i> gene (residues W68 to G86) with an N-terminal ToxR domain & C-terminal MBP domain (see section 5.5.2)

2.5 Membrane Protein Expression and Purification

2.5.1 Protein Over-Expression

Proteins were expressed (from gene constructs in Table 2.4.8.1 above) in *E. coli* strains grown in LB media, at levels amenable to purification by Immobilised Metal Affinity Chromatography (IMAC, see section 2.6.6). Increased levels of soluble protein was achieved by modifying these protocols, and allowed expression of both proteins in M9 minimal media. Recombinant proteins were over-expressed in a number of *E. coli* strains (Table 2.2.2.1) using IPTG induction. Strains were made competent (section 2.2.3) and transformed with an expression plasmid containing the recombinant gene (section 2.3) (in some cases with a second plasmid to aid expression) and plated on LB agar plates with appropriate antibiotics.

(i) Overexpression in LB media

A single colony was picked for a small-scale pre-culture and grown, at 37°C, 180 rpm, overnight in 5 or 10 ml of LB media and appropriate antibiotics. The pre-culture was diluted at 1 in 50 or 1 in 100 into LB media containing the appropriate antibiotics (and 0.2% glucose for VanS_A), and grown at 37°C, 180 rpm, before induction with IPTG to a final concentration of 0.2 mM or 1 mM when the optical density of a culture, at a wavelength of 600nm, was between 0.5 and 0.6. Expressions were initially grown for 4 hours at 37°C, but it was found that 12-16 hours at 25°C (for VanS_A) or 20-24 hours at 16°C (for VanS_{SC}) gave higher yields of soluble protein, before harvesting at 10,000g, 15 mins using a Beckmann JA14 rotor.

Cell pellets were washed in ice-cold phosphate-buffered saline (PBS) and the pellet was resuspended in 3 mL of resuspension buffer per gram of wet cell weight. To prevent protein degradation, protease inhibitors (2µM leupeptin, 2µM pepstatin, 0.2mM PMSF final concentrations) were added. Resuspended cells were snap-frozen and stored at -80°C.

(ii) Overexpression in M9 Minimal Media

Both pProEx::*vanS_A* and pProEx::*vanS_{SC}* were transformed onto LB plates containing 100 µg/ml of ampicillin and 35 µg/ml of chloramphenicol (see section 2.3). A scraping of colonies was taken using an inoculation loop, and added to 10 mL starter cultures in LB containing the appropriate antibiotics with addition of 2 g/L glucose for those containing *vanS_A*. Starter cultures were grown at 37°C for 12-14 hours and used to inoculate 800mL cultures at a starting optical density at 600nm of ~0.01. These larger cultures were grown at 37°C until an optical density at 600nm of ~ 0.7-0.8, at which point media was switched to M9 (see section 2.2.1) from LB, by pelleting at 3000 g for 10 minutes in a Beckmann benchtop centrifuge, washing and resuspending twice in M9 media. In the final resuspension step, the pellet was resuspended in either 800ml ('1x'), 400ml ('2x'), or 200ml ('4x') of M9 minimal media containing: 1x BME vitamins (Sigma), 1 g/L unlabelled or ¹⁵N-labelled NH₄Cl, 4 g/L glucose, 0.1 mM CaCl₂, 2mM MgSO₄, 50 µM FeCl₃, 1x M9 salts, 100 µg/ml Ampicillin, 35 µg/ml Chloramphenicol and pH adjusted to 7.5 or 8.0 for higher buffering capacity.

Cells were incubated at the induction temperature for 1-2 hours prior to induction to discharge unlabelled metabolites, and overexpressed with IPTG for 16-20 hours (0.2 mM IPTG and 25°C for VanS_A and 1mM IPTG and 18°C for VanS_{SC}). Cultures were then pelleted at 3000 g for 10 minutes, and aliquots taken for SDS-PAGE (section 2.6.1) and Western Blot analysis (section 2.6.3). Cell pellets were resuspended in 10 mL/L of resuspension buffer, and to prevent protein degradation, protease inhibitors (2µM leupeptin, 2µM pepstatin, 0.2mM PMSF final concentrations) were added. Resuspended cells were snap-frozen and stored at -80°C.

2.5.2 Preparation of Membrane Protein Lysates

For small-scale production, membrane protein lysates were prepared, as described in Ward *et al.* (2000), using the 'Water Lysis' method. 100 mL of an overnight expression (section 2.5.1) was centrifuged at 10,000 g, 10 mins at 10°C in a JA14 rotor with the cell pellet resuspended in 0.2 M Tris-HCl (pH 7.8). At time zero, 9.7 mL of sucrose buffer (1M sucrose, 1mM EDTA, 0.2M Tris-HCl, pH7.8) was added, followed by 1 mL of 1.3 mg/mL lysozyme at 1.5 minutes and 20 mL of deionised water at 2 minutes and left to shake for one hour at 25°C to form spheroplasts, due to the high osmotic shock experienced by the cells. Spheroplasts were sedimented at 20,000 g, 20 mins at 10°C in a Beckman JA25.50 rotor. The pellet was re-suspended, using a hand-held homogeniser, in 30 mL of water until cloudy and no lumps present and left to stand for 30 minutes at 25°C.

Membranes were sedimented at 30,000 g, 20 mins at 4°C in a JA 25.50 rotor and the resulting pellet resuspended in membrane resuspension buffer (0.1 M Sodium phosphate, pH 7.2, 1 mM 2-mercaptoethanol). Membranes were washed twice in 15 mL of membrane resuspension buffer using a hand-held homogeniser each time to resuspend the pellet. Finally washed membranes were resuspended in 1 – 5 mL (depending on the weight of protein obtained) of membrane resuspension buffer containing 1 mM MgCl₂ to which DNase was added to a final concentration of 20 µg/mL. Preparations were incubated at 37°C for 30 minutes before addition of EDTA to a final concentration of 1 mM. Preparations were analysed using SDS-PAGE (section 2.6.1) and stored at -80°C.

2.5.3 Large-Scale Membrane Protein Preparations

Large-scale membrane protein preparations followed the protocol given by Quigley (2010). The expressed cell pellet (from one or more litres of culture) was mixed with resuspension buffer (20 mM HEPES pH 7.8 or 50 mM phosphate buffer pH 7.5, 300 mM NaCl) in the

ratio of 3mL per gram of wet cell pellet, before snap-freezing and storing at -80°C. Upon thawing, DNase (20 µg/ml final concentration, Roche), magnesium chloride (10 mM final concentration) and chicken egg lysozyme (2.5 mg/ml final concentration, Calbiochem) were added. After rocking at 4°C for 30 mins, cells were lysed by passing through a continuous cell disrupter (Constant Cell Disruption Systems) three times at 30 kpsi and 4°C. Lysate was centrifuged at 10,000g for thirty minutes using a Beckman JA14 rotor to pellet cell debris before the supernatant was transferred to ultracentrifuge tubes and centrifuged at 40 krpm for two hours using a Beckman Ti45 rotor in an ultracentrifuge (Beckman Optima L90K) to pellet the membrane fraction. Membranes were resuspended in 20 mM HEPES pH 7.8, 300 mM NaCl, 20 mM Imidazole and 20% Glycerol, in 10 mL of buffer per litre for VanS_A or per three litres for VanS_{SC}, before storing at -80°C.

2.5.4 Protein Solubilisation using Membrane Mimetics

Membrane proteins are naturally embedded in a complex and dynamic lipid bilayer, limiting their analysis by standard biophysical techniques. *In vitro* studies are reliant on successful solubilisation of membrane proteins, using appropriate membrane mimicking environments. These must consist of a solubilising component and satisfy the hydrophobic nature of TM segments, while bringing loop regions into contact with an aqueous phase. Therefore lipid and detergent systems are often chosen.

Detergents are amphipathic with polar head groups and a single hydrophobic tail, and can spontaneously form spherical, micellar structures (Seddon *et al.*, 2004) above a Critical Micelle Concentration (CMC) (Bhairi, 1997). The number of solubilised monomers contained in a micelle is known as the mean aggregation number (\bar{n}), and is related to bulk molar detergent concentration (d) and micelle concentration (m) by Equation 1.

$$m = \frac{d - C}{a} \quad (1)$$

Detergents tested include dodecylphosphocholine (DPC) ($a = 56$ and $CMC = 1.1-1.2$ mM) (Wüthrich, 1986), dodecylmaltoside (DDM) ($a = 98$ and $CMC = 0.17-0.3$ mM), octylglucoside (OG) ($a = 84$, $CMC = 18-20$ mM) (Bhairi, 1997) and sodium dodecyl sulphate (SDS) ($a = 62$ and $CMC = 8-14$ mM, at 298K) (Nishikido, 1983). A full list of all detergents tested is given in Appendix Table 1.

Prepared membranes were thawed and detergent added to a final concentration of 0.5-1% w/v, before membranes were incubated at 4°C on a roller rocker for two hours. Solubilised membranes were centrifuged at 40 krpm for 45 mins using a Beckman TLA 100.3 rotor and benchtop ultracentrifuge (< 20ml volume) or Beckman Ti45 rotor and Beckmann T90K ultracentrifuge (< 350ml volume). The resulting supernatant was added to charged nickel, high performance agarose (Qiagen) or sepharose (GE Healthcare) slurry (ratio of 1mL slurry per mg of expected VanS protein) pre-equilibrated in 20 mM HEPES pH 7.8, 300 mM NaCl, 10% Glycerol, 20 mM Imidazole, 0.1% w/v detergent). This protein-resin mix was left to rock for 1-2 hours at 4°C before pouring into a column and allowing the resin bed to settle.

2.6 Protein Analysis and Detection

2.6.1 Sodium Dodecyl Sulphate-Polyacrylamide Gel Electrophoresis

For SDS-PAGE experiments, either a Tris-Glycine buffer system (Laemmli, 1970) or Bis-Tris system (Invitrogen) was used to separate and visualise polypeptides under denaturing conditions on a discontinuous gel system. For the Tris-Glycine system, the resolving gel is at pH 8.8 and the stacking gel at pH 6.8. 11 mL of 355 mM Tris-HCl pH 8.8, 0.1% SDS and 12% or 15% acrylamide: bis-acrylamide (29:1) was prepared allowing resolution of proteins between 4 and 100 kDa. Gels were cast using the Hoeffer Mighty Small gel kit, polymerised with 10 µL TEMED and 120 µL 10% APS, then overlaid with ethanol to remove the

meniscus. 3.5 mL stacking gel mix was prepared with 610 mM Tris-HCl pH 6.8, 0.1% SDS and 3% acrylamide:bisacrylamide (29:1), polymerised with 10 μ L TEMED and 50 μ L 10% APS and pipetted on top of the polymerised resolving gel, where a plastic comb was added to form the wells. For the Bis-Tris system, which was used for Blue Native PAGE and prior to anti-MBP Western blots (see section 2.6.4), NuPAGE Novex 12 % Bis-Tris 10-well precast gels were used. Gels were run in an Invitrogen XCell SureLock Mini-Cell electrophoresis kit according to manufacturer's instructions.

Protein samples were usually standardised to 20 μ g/ml concentration per lane (unless specified), and prepared in 6 x loading buffer (62.5 mM Tris-HCl pH 6.8, 10% glycerol, 0.1% SDS, 2.5% bromophenol blue and 5% β -mercaptoethanol) and either heat denatured at 60°C in a heat block for 5 minutes or 37°C for 15 minutes. The gel comb was removed, wells were washed with SDS-PAGE running buffer (25 mM Tris, 192 mM Glycine, 0.1% SDS pH 8.3) to remove unreacted and samples were pipetted into the wells. Gels were run in SDS-PAGE running buffer at 180V for 1 hour or until the gel front reached the cast base. SDS-PAGE ladders used were either LMW-SDS standard (GE Healthcare, 14-90 kDa range), SeeBlue Plus2 Standard (Invitrogen, 3-188 kDa), or the ColorPlus Broad Range Marker (NEB, 7-175 kDa). SDS-PAGE gels were stained to visualize protein bands in either Coomassie Brilliant Blue or Instant Blue stain (see section 2.6.9).

2.6.2 Blue Native PAGE

VanS protein samples that had been purified in detergent micelles, by IMAC and Gel Filtration Chromatography (see section 2.6.7) (conducted at 4°C), were analysed using the NativePAGE Novex Bis-Tris system (Invitrogen). This system is based on the blue native polyacrylamide electrophoresis (BN-PAGE) technique developed by Schägger and von Jagow (1991), and allows an estimation of the oligomeric states of native proteins and their protein complexes relative to molecular weight markers.

Samples were applied to a 4 - 16 % precast Bis-Tris gradient gel, and proteins are separated based on size under electrophoresis at 4°C in NativePAGE running buffer (1M Bis-Tris-HCl pH 7.0, 1M Tricine pH 7.0). Sample migration through the gel involves addition of a non-denaturing Coomassie G-250 dye to protein samples, at 1/4 to 1/10th of the detergent concentration, which confers a net negative charge while maintaining the proteins in their non-denatured native state. Protein molecular weights were estimated relative to prestained markers (High MW Standards, Amersham). After electrophoresis, separated proteins were either analysed by Coomassie Brilliant Blue staining (see section 2.6.9), or by Western blotting. For Western blotting, bands were transferred onto a PVDF membrane (Hybond-P, GE Healthcare) under an applied current of 110 mA for 90 mins in an X-Cell II Blot Module (Invitrogen). After transfer membranes were incubated in 8% acetic acid for 15 mins, rinsed with de-ionised water and air-dried, then rewet in methanol (to remove background dye) and rinsed once more before blocking with 10% milk powder. Immunodetection followed the same protocols outlined in section 2.6.3.

2.6.3 Western Blotting for Histidine-tagged proteins

The method for Western blotting was originally developed by Towbin *et al.*, (1979). The procedure allows determination of protein molecular weights and quantification of relative amounts of proteins in each sample. Initially, proteins are separated by SDS-PAGE (section 2.6.1) then protein bands in the gel are directly transferred under an applied voltage onto a nitrocellulose or PVDF membrane which is placed on top of the gel, all within a transfer cassette. All sites except protein bands are then blocked in a milk solution, and a primary antibody is added which binds to specific protein tags. A secondary antibody containing an attached alkaline phosphatase or horseradish peroxidase enzyme is then added which binds to the primary. This enzyme allows detection of tagged protein bands by chromogenic techniques or electrochemical luminescence, in a reaction between enzyme and developing reagents, which can be visualised on X-ray films or directly depending on technique used.

In this study, Western blotting procedures have been used and optimised to reduce background and decrease experiment time, using the methods below. Proteins were resolved by SDS-PAGE or NativePAGE as described in section 2.6.1 or 2.6.2, against His-tagged protein markers (Benchmark or MagicMark, Invitrogen) or prestained markers (High MW Standards, Amersham) or and the resulting gel was washed in transfer buffer (100mM Tris base, 80mM Glycine and 20% methanol). Polypeptides were transferred from the gel to a PVDF membrane (Hybond-P, GE Healthcare) at a constant voltage of 120 V in transfer buffer for 70 mins, using a BioRad electroblotting kit.

Before transfer, the membrane was activated by placing in methanol for 5 mins, washing with deionised water then adding to transfer buffer for 2 mins. After transfer, membranes were blocked in 25 mL of 10% Milk powder in TBS containing 0.1% Tween-20 (TBST-T) and rocked for 1 hour, before washing with 20mL of TBS-T for a further 15 min. The TBS-T wash step was repeated twice more. 20mL of TBS-T containing 20µL of anti-his IgG mouse monoclonal non-preferential antibody (Roche) or 8 µl anti-His IgG mouse monoclonal N-terminal preferential antibody (Sigma, H1029), and left to shake for one hour. Three 20 mL TBS-T wash steps of 15 mins each followed. Subsequently, 10 mL of TBS-T containing 5 µl of anti-mouse IgG conjugated to horseradish peroxidase derived from sheep (Sigma, A5906) was added and left to shake for two hours before three further TBS-T wash steps.

For the final wash step, membranes were left to rock overnight to reduce background from unbound proteins. For development either 5 mL of blotting reagent 1 (GE Healthcare) and 5 mL of blotting reagent 2 (GE Healthcare), or 1ml of ECL Solution A (Biological Industries) and 1ml of ECL Solution B (Biological Industries) was added to the membrane and allowed to develop for 90 seconds. Membranes were dried on their edge on a tissue held by tweezers then wrapped in cling film and exposed to X-ray films (Super-RX NIF, Fujifilm), generally for 10 seconds to 5 mins, but sometimes up to 30 mins. Observed bands resulted from electrochemical luminescence (ECL).

2.6.4 Western blotting for MBP-tagged proteins

Western blotting antibodies were chosen depending on the protein tag involved. Both the TOXCAT constructs and the 3C enzyme construct, encoded for an MBP-tag, therefore anti-MBP western blots were run. Proteins were resolved by SDS-PAGE using a 12% NuPAGE gel, against ColorPlus prestained markers (7-175 kDa) or SeeBlue Plus2 Prestained markers (3-188 kDa) and the resulting gel was washed in transfer buffer (see section 2.6.3).

Polypeptides were transferred from the gel to a Nitrocellulose or PVDF membrane (Hybond, GE Healthcare) at a constant voltage of 120 V in transfer buffer for 90 mins, using an X-Cell II Blot module. Before transfer, the membrane was activated by placing in methanol for 5 mins (for PVDF membranes only) then washed with deionised water, and added to transfer buffer for 2 mins. After transfer, membranes were blocked in 20 mL of 3-5% Milk powder in TBS containing 0.1% Tween-20 (TBS-T) and rocked for 1 hour, before washing with 20 mL of TBS-T for a further 15 mins. The TBS-T wash step was repeated twice more. 10 mL of TBS-T containing 2.5 µL of anti-MBP antibody (Sigma) was added, and left to shake for one hour. Three 20 mL TBS-T wash steps of 15 minutes each followed. Subsequently, 10 mL of TBS-T containing 1 µL of anti-mouse IgG conjugated to alkaline phosphatase (Sigma) was added and left to shake for two hours before three further TBS-T wash steps.

3mL of SigmaFAST BCIP/NBT (5-Bromo-4-chloro-3-indolyl phosphate/Nitro blue tetrazolium) chromogenic solution was added to the membrane and allowed to develop for between 1 - 2 mins, before washing with distilled water and immersing in 1x TBS-T. Observed bands resulted from electrochemical luminescence (ECL).

2.6.5 Detergent Screening by Western Blotting

VanS proteins were expressed on a large-scale (2-6 L) in LB media and membranes extracted and resuspended in 10-20 mL total buffer (see section 2.5.3). Membrane samples (1-2 mL) at a total protein concentration of 3 mg/ml were dissolved in 1% w/v detergent (except for octylglucoside detergent, which has a high CMC, so 1.8% was used) and centrifuged at 100,000 g (~35000 rpm) in a TLA100.3 rotor in a benchtop Beckmann ultracentrifuge. The supernatant was pipetted off, and the pellet remaining was resuspended to the same initial volume (prior to centrifugation) in HEPES buffer (20 mM HEPES pH 7.8, 300 mM NaCl) with a homogeniser in order to obtain a homogenous mixture for loading onto SDS-PAGE gels or Western blots.

For Western blots, a known fixed volume (of either 10 or 20 μ L, depending on band intensity) was added into each lane in order to ~20 μ g of total protein per lane. For each detergent, the soluble (supernatant) fraction was loaded next to the pellet fraction, both with the same volume but not necessarily the same concentration, as this is dependent on solubility in the selected detergent. Blotting was carried out according to the protocol in section 2.6.3. Bands on the X-ray films were imaged and analysed for each detergent using a band-sizing technique (quantified by ImageJ analysis software), to determine the relative amounts of VanS protein in supernatant and pellet fractions, and therefore establish the protein's solubility in each detergent. Detergents were selected from three classes: anionic, zwitterionic and non-ionic, and those used were commonly tested in detergent screens in the literature (Bhairi, 1997; Newby, 2009; Oliver *et al.*, 2013), either prior to NMR experiments or crystallisation trials. A full list of all detergents used in this thesis and their properties is given in Appendix Table 1.

2.6.6 Immobilised Metal Affinity Chromatography

The concept of immobilized-metal affinity chromatography (IMAC) was first formulated and its feasibility shown by Porath *et al.* (1975). It was based on the known affinity of transition metal ions such as Ni^{2+} and Co^{2+} for histidine and cysteine residues in aqueous solutions. In the 1980s, improvements in the design of chelating ligands provided nitrilotriacetic acid (NTA) (Hochuli *et al.*, 1987) and recombinant proteins were produced containing genetic modifications to their DNA template to give His-tagged polypeptides that could be purified on NTA-based supports (Hochuli *et al.*, 1988) (see Figure 2.6.6.1).

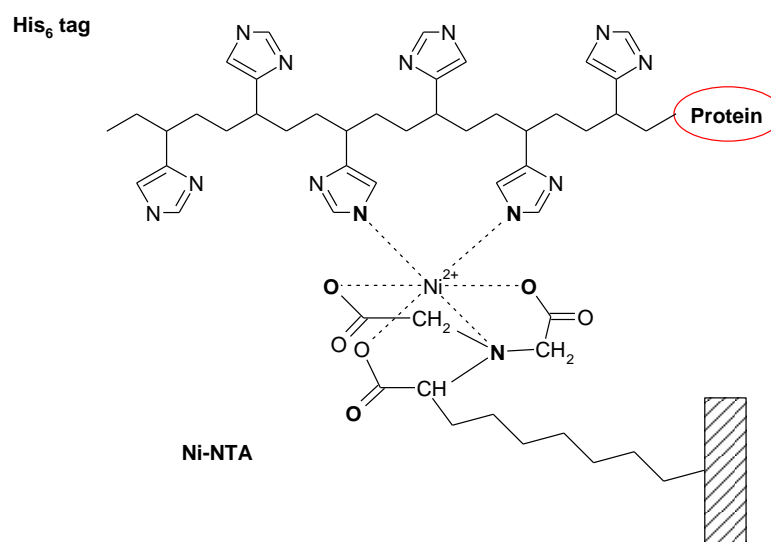


Figure 2.6.6.1: Model of the interaction between Ni NTA and a His-tag. Adapted from Block *et al.*, 2009.

In this study, pProEx HTa constructs were used with encode for a TEV-cleavable N-terminal hexahistidine tag in front of the *vanS* gene. Purification of hexahistidine-tagged proteins was carried out using chelating high performance Nickel NTA agarose (Qiagen) or Chelating Sepharose (GE Healthcare), with the exception of his-tagged 3C protease which was purified with Cobalt resin (TALON, ClonTech). Columns were resolved by gravity-flow using imidazole-containing buffers which compete for the his-tag to bind to Nickel (II) ions. Resin was added at a ratio of 1 mL slurry per mg of expected VanS protein.

Chelating sepharose resin required charging with Nickel prior to use, according to the manufacturer's guide. Resin was added to the column and washed with 20 column volumes (CV) of water then charged with 1 CV of a 0.2 M NiCl₂ solution. Excess nickel chloride was then washed off with 10 CV of water and 5 CV of 50 mM sodium acetate pH 4.0 added. The column was then equilibrated with 5 CV of the binding buffer (20 mM HEPES pH 7.8, 300 mM sodium chloride, 20 mM imidazole pH 8.0, 10% glycerol and 0.1% detergent). Ni-NTA resin was charged by washing with 20 CV of water, and 10 CV of binding buffer.

Once equilibrated, solubilised protein-resin mix was loaded onto the column and the flow-through collected under gravity and retained for analysis before the column was developed by washing with gradient steps of equilibration buffer and elution of the hexahistidine-tagged protein. Initially, 30 CV of low imidazole wash buffer (20 mM HEPES pH 7.8, 400 mM NaCl, 10% Glycerol, 0.075% w/v detergent and 20 mM Imidazole pH 8.0) was added. This was followed by a wash step with this buffer but containing high salt (1M NaCl, 20 CV), and a final wash step with this buffer but containing intermediate imidazole (50 mM Imidazole pH 8.0, 15 CV), before elution with 2.5 ml volumes of the buffer containing high (250 mM) Imidazole pH 8.0. The high salt wash removes ionically bound proteins, and the intermediate imidazole wash removes weakly bound histidine-rich *E. coli* proteins. Eluted fractions were retained for analysis using SDS-PAGE. Eluted protein was desalted immediately (and imidazole removed) in a desalting PD10 gel filtration column (GE Healthcare). A final wash with 500 mM Imidazole pH 8.0 removed any residual protein.

After use, affinity chromatography columns containing chelating sepharose were stripped with 5 CV of stripping buffer (20 mM NaPO₄ pH 7.4, 50 mM EDTA and 0.5 M NaCl) to remove any chelated metal ions with bound protein, followed by 3 CV of 0.5 M NaCl to remove residual EDTA, then 10 CV of water. Ni-NTA resin was washed with 1 CV of 0.5 M NaOH for 30 mins, then 10 CV of water. Resins were stored at 4°C in 20% filter-sterilised ethanol solution. Columns were recharged as described above.

2.6.7 Analytical Gel Filtration Chromatography

Proteins were separated based on their molecular size using a Superose 6 or Superose 12 resin (GE Healthcare), on a 10/300 mm GL, 24mL bed volume column, attached to a GE Healthcare AKTA Prime system. Superose resin consists of a composite of highly cross-linked porous agarose beads. Columns were washed with 2.5 CV of distilled water, then equilibrated with 2.5 CV of the appropriate buffer (20 mM HEPES pH 7.8, 200 mM NaCl, 0-10% glycerol, and 0.05-0.1% detergent) before samples were loaded (using a Hamilton syringe and adaptor), via an injection loop in volumes of 0.2 or 0.5 mL to prevent loss of resolution due to sample smearing. Buffer was pumped through the column at a rate of 0.3 mL/min under an isocratic gradient of 100% Buffer A for 1.5 column volumes and 0.3 ml fractions collected, with absorbance traces recorded at wavelengths of 280 nm and 254 nm. Fractions collected were analysed for purity by SDS-PAGE.

After each run, the column was washed with 1.5 CV of water, then 1.5 CV of 20% ethanol for storage. After 10-20 runs, rigorous cleaning was conducted, involving washing with 1 CV of 0.5 M NaOH at 0.3 mL/min, prior to a water/ethanol wash for storage.

2.6.8 Protein Sample Desalting, Concentrating and Dialysing

To exchange buffers or to remove imidazole from protein samples that had been purified by IMAC techniques, a PD10 Desalting column (GE Healthcare) was used. All protein samples were initially solubilised with DPC or DDM detergent, and purified with the same detergent throughout (to avoid the formation of mixed micellar species). The eluted 2.5 mL fractions from IMAC were directly applied to the PD10 Desalting column, which had been equilibrated with 25 mL of detergent-containing buffer. Once applied, the flow through was collected and discarded, and 3.5 mL of the equilibration buffer applied to the PD10 to elute the protein sample in the new buffer.

For detergent exchange, protein purified in DPC micelles (after IMAC at 0.075 % w/v) was diluted to below the CMC for the detergent (<1mM) with an appropriate buffer. This was applied to a PD10 desalting column equilibrated with the new detergent-containing buffer (containing detergent at 2-5 times its CMC). Proteins purified in DDM detergent were not exchanged in these studies (as they have a micellar size greater than most concentrators).

Protein solutions that had been desalted were subsequently concentrated using either Corning centrifugal concentrators, with polyethersulfonate (PES) membranes at a molecular weight cut-off (MWCO) of 10, 30, 50 or 100kDa, depending on the size of detergent molecules bound. Concentrators were washed twice by centrifuging for 10 minutes at 3000g and 4°C in a bench-top centrifuge (Labofuge 400R, Heraeus Instruments) filled with MilliQ water, then the water was discarded and the concentrators were centrifuged once more, filled with detergent-containing buffer for 10 minutes at 3000 g, prior to addition of protein solution and centrifugation at 3000g. Protein solution was concentrated to ~0.5 ml for application to a gel filtration column or ~0.1 mL for application to 96-well membrane protein crystallisation trays. In general, activity assays, NMR and gel filtration required protein at between 2 and 10 mg/mL and crystallography trials required protein ~10mg/ml.

For protein samples, dialysis was not routinely used as it would require large amounts of detergent, which is not cost-effective. However, for soluble proteins e.g. 3C protease, dialysis was conducted immediately after IMAC, to remove all imidazole and exchange into an appropriate buffer for long-term storage. Dialysis tubing (19 mm and 12-14 kDa MWCO) was pre-boiled, and stored in 10 mM EDTA pH 7.4, 0.05% sodium azide solution. The tubing was rinsed with and immersed in 1L of distilled water, and one end tied before use. The solution to be dialysed was added into the open end by pipette, and air bubbles removed before tying the other end. The tubing was immersed in 1L of buffer to exchange into, stirred for 1 hour, then placed into 1L of fresh buffer and stirred for a further hour. 20% w/v ice-cold glycerol was added to the dialysed solution, which was aliquoted and stored at -80°C.

2.6.9 Staining of SDS-PAGE Gels

Proteins resolved by SDS-PAGE were stained overnight in Colloidal Coomassie stain (Neuhoff *et al.*, 1988) or for 1 hour in Instant Blue stain (Expedeon Protein solutions, UK) before destaining for overnight in MilliQ water. For NativePAGE, gels were fixed for 30 minutes (50% methanol, 10% acetic acid), stained overnight in Coomassie Brilliant Blue (0.01g Coomassie blue R-250, 4ml acetic acid, in 40ml of deionised water), and destained over several hours (20% methanol, 7% acetic acid). Gels were imaged using a Syngene G:Box illuminator, attached to a camera under a yellow UV filter.

2.6.10 Determination of Protein Concentration

Three methods for protein concentration determination were conducted. The BioRad reagent method, is based on a protein's reaction to Coomassie Brilliant Blue G-250 dye, which has an absorbance maximum at 465 nm, which shifts to 595 nm once it binds protein. 2-10 μL of protein solution was added to 200 μL BioRad reagent in a cuvette and topped up to 1000 μL total volume, mixed and the absorbance measured at 595 nm using a Phamacia Biotech UltraSpec 2000. For protein solution giving a reading greater than the linear range of the assay (> 0.6), solutions were diluted and readings repeated. Protein concentration (in μg protein per mL) was calculated using Equation 2, according to manufacturer's instructions.

$$[\text{Protein}] (\mu\text{g/mL}) = \frac{\text{Absorbance (A595nm)}}{0.1} \times 1.95 \times \text{dilution factor} \times \frac{1000}{\text{assay volume}} \quad (2)$$

The second method involved directly measuring concentrated protein solutions at 280 nm, using 1 mL of undiluted protein in a quartz cuvette, or adding 2 μL to a NanoDrop ND2000 (ThermoScientific) device. The extinction coefficient was assumed to be $1.0 \text{ cm}^{-1} \text{ mg}^{-1} \text{ mL}$ and the protein concentration was directly calculated from the absorbance at 280 nm.

The preferred assay though was the BCA (bicinchoninic acid) assay, which is not affected by the presence of detergent in protein samples and therefore gives the most accurate representation. This method follows the reduction of Cu^{2+} to Cu^+ by proteins in an alkaline medium (the biuret reaction) with the colorimetric detection of the cuprous cation using a reagent containing bicinchoninic acid. The BCA assay was carried out as described by the manufacturer's (Pierce) guide. Reagents A and B were mixed at a 50:1 ratio for 1 minute and 1mL of subsequent working reagent was added to a known volume of each protein sample in a 1.5ml Eppendorf, and vortexed to mix. Reactions were left to incubate at 37°C in a water bath for exactly 30 mins before allowing to cool to room temperature. Absorbance was measured against a blank (exposed to similar conditions) at 562 nm using a Pharmacia Biotech Ultraspec 2000. Protein concentrations were calculated based upon a BSA (bovine serum albumin) standard curve. The assay working range is between 20 and 2000 $\mu\text{g mL}^{-1}$.

2.7 ToxCAT assays

The TOXCAT assay is used to quantify transmembrane (TM) helix-helix self-association in the *E. coli* inner membrane. It can discriminate between strongly associating and weakly associating transmembrane α -helices within a natural membrane environment (Russ & Engelman, 1999). Fusion constructs are designed to contain wild-type (*wt*) TM domains of interest flanked by a C-terminal maltose binding protein (MBP) domain and an N-terminal DNA binding domain from ToxR, within the ToxCAT plasmid, *pccKan* (see Figure 2.7.1.1).

In these studies, oligonucleotides encoding individual predicted TM domains of VanS proteins were cloned into the *pccKan* plasmid (provided by Prof. Donald Engelman (Yale University) (see section 2.7.1). The resulting chimera were then expressed in *E. coli* strain NT326, and quantitative CAT assays were performed using the FAST CAT kit (Invitrogen) (see section 2.7.6). In these assays, activation of the CAT reporter gene depends on the extent of TM-driven dimerization, which is measured by fluorescence intensity.

Prior to performing ToxCAT assays, membrane insertion of all constructs was confirmed using the *malE* complementation assay (see section 2.7.2), and correct orientation of the chimera in the membrane was confirmed via protease sensitivity in a spheroplast assay as described in Russ & Engelman (1999) (see section 2.7.4). Expression levels for all constructs were similar and confirmed via Western analysis against the MBP domain (see section 2.7.3). The extent of TM dimerization as a function of chloramphenicol resistance was determined by Disk Diffusion assays (by measuring the zone of inhibition) (see section 2.7.5), and quantified by measuring CAT activity in cell-free extracts (see section 2.7.6). All resulting CAT activities were normalized to total fusion protein expression levels using the ImageJ software (Abramoff *et al.*, 2004) by analyzing band intensities after anti-MPB western blotting, and percentage error calculated over three repeat measurements.

2.7.1 Cloning VanS transmembrane domains into the ToxCAT plasmid

The chimeric *pccKan* construct is composed of the N-terminal DNA binding domain of ToxR (a dimerization-dependent transcriptional activator) fused to a transmembrane domain (TM) of interest and a monomeric periplasmic anchor (MBP) (see Figure 2.7.1.1). TM association causes ToxR-mediated activation of a reporter gene encoding chloramphenicol acetyltransferase (CAT), the level of which indicates the strength of oligomerisation.

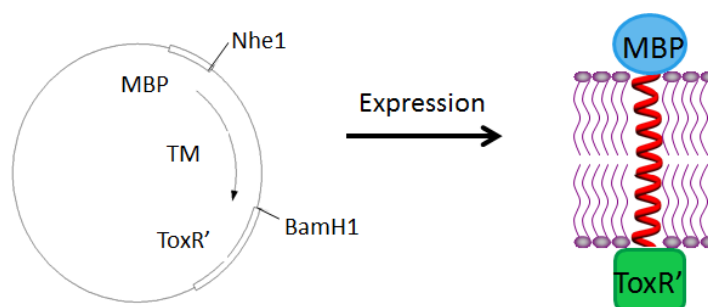


Figure 2.7.1.1: Expression of chimeric fusion proteins using the *pccKan* plasmid. (left) *pccKan* plasmid with inserted VanS TM domain of interest between NheI and BamHI, which expresses (right) a chimeric fusion protein with C-terminal MBP (blue circle) and N-terminal ToxR' (green square) domains flanking the TM section (red helix).

(i) *Phosphorylation and Annealing of ToxCAT primers*

Oligonucleotides listed in Table 2.4.1 were used as inserts for the DNA ligation reaction, along with double-digested (BamH1, Nhe1) pccKan vectors. Primers were designed to insert into the digested pccKan vector by having 'sticky ends' (Figure 2.7.1.2), and all sequences were optimised by removing any rare codons present. Primers were initially phosphorylated and annealed to create double-stranded inserts. 5 µL of each primer (at 10 µM concentration) was added to 2 µL of 10x T4 PNK reaction buffer, 1 µL of 10mM ATP, 2 µL of T4 PNK (Fermentas) and 10 µL of water. The tubes were briefly sonicated before incubation for 30 mins at 37°C, followed by 10 mins at 56°C to quench the reaction. From each tube, 4 µL of forward primer and 4 µL of reverse primer were added together, along with 2 µL of annealing buffer (made with 200 µL 1M Tris-HCl pH7.5, 20 µL 1M MgCl₂, 166 µL 3M NaCl and 614 µL water) and 10 µL of water into PCR tubes. Primer mixes were incubated at 95°C for 7 minutes to denature any base pairing, before cooling to room temperature over time to anneal strands. Annealed oligonucleotides were ligated and stored at -20°C.

```
5' CTAGCctgtatatgtatatattgtggcgattgtggtggtggcgattgtgtttgctgtatatattGG
3' GgacatatacatataaacaccgctaacaccaccaccgctaacacaaacacgacatataaCCTAG
```

Figure 2.7.1.2: Example of annealed oligonucleotide sequences of the VanS_A TMI domain for inserting into pccKan plasmids. 'Sticky ends' (highlighted in yellow) are produced which consist of complementary codons to those at the BamH1 and Nhe1 restriction enzyme sites, to ligate with digested pccKan plasmids. A 'G/C' base (highlighted in red) was also required in the primer design, to ensure codon reading was 'in-frame'.

(ii) *pccKan Plasmid Preparation and Digestion*

The plasmid used to carry out the ToxCAT assay was pccKan. In this study, modifications of the pccKan plasmid were carried out as follows: the Kan cassette was cut out of the plasmid and transmembrane domain (TM) sequences of interest were cloned in. These constructs were then used in quantitative CAT assays to examine the strength of homo-oligomerisation.

A scraping was taken using an inoculation loop from a glycerol stock containing pccKan plasmids in *E. coli* DH5 α cells, and added to 5 mL of LB in a universal tube, under sterile atmosphere. After overnight incubation at 37°C, plasmid DNA was harvested by minipreparation (see section 2.4.4). The plasmid was digested with both restriction enzymes (see section 2.4.3), with the addition of 4 μ L of Tango buffer (Thermo Scientific) to prevent ‘star activity’ of the enzymes (under non-standard reaction conditions, some enzymes cleave sequences which are similar, but not identical, to their defined recognition sequence). In order to check that the plasmids were correctly digested at both sites an agarose DNA gels was run (see section 2.4.6) (see Figure 2.7.1.3). The digested vector was subsequently excised and purified with the Qiagen gel extraction kit (see section 2.4.5). The phosphorylated, annealed TM insert could then be ligated into the digested pccKan vector using the method outlined in section 2.4.7. Finally the ligation mixture was transformed into *E. coli* DH5 α competent cells (see section 2.3) and DNA minipreparations were extracted from positive transformants (section 2.4.4). Extracted plasmids were restriction digested (section 2.4.3) and analysed by agarose gel electrophoresis (section 2.4.6) to determine the presence of a correctly-sized insert, which was confirmed by Sanger sequencing using pccKan primers (see section 2.4.8).

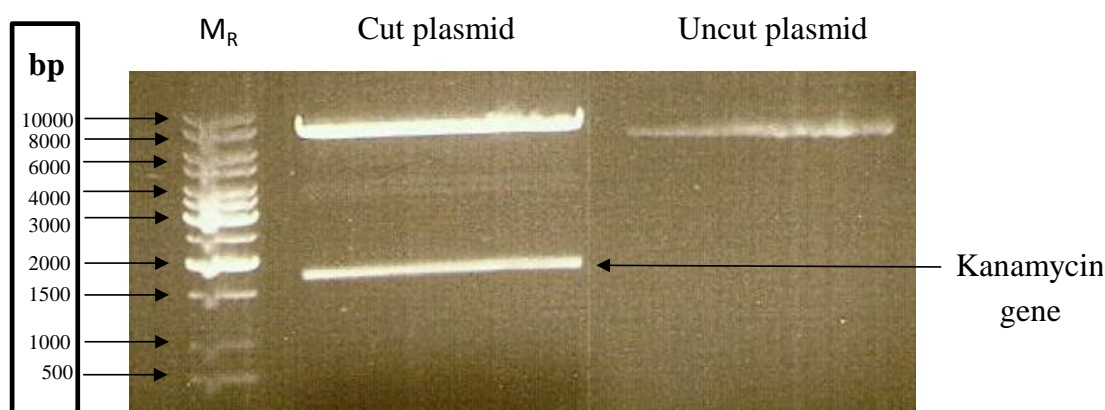


Figure 2.7.1.3: A 0.8% agarose gel stained with ethidium bromide, showing undigested pccKan plasmid, and double-digested pccKan plasmid. M_R - GeneRuler 1kb DNA ladder. The kanamycin gene which is cut out from the pccKan plasmid appears as a band at 1.7 kbp.

2.7.2 Maltose *malE* Complementation assay

To establish whether chimeric fusion proteins for the ToxCAT assay were inserting into *E. coli* membranes with the correct topology, a *malE* complementation assay was conducted. NT326 cells which lack endogenous MBP cannot transport maltose into the cytoplasm for metabolism and therefore cannot grow on maltose/agar plates. However, if the ToxCAT chimera are correctly inserted into the inner membrane, the periplasmic MBP domain will complement the NT326 *malE*-deficient phenotype and support growth on maltose.

Maltose plates were prepared as follows: 100 ml of 5x M9 salts, 1M MgSO₄, 1M CaCl₂ and 20% w/v maltose, were prepared separately by filter sterilising or autoclaving. In another flask, 78 ml water and 1.5 g agar were also autoclaved. The agar/water mix was melted in a microwave and cooled to touch, then 20 ml of 5x M9 salts, 0.2 ml of 1M MgSO₄, 2 ml of 20% maltose and 0.01 ml of 1M CaCl₂ were added, and the solution poured into petri dishes and allowed to solidify. A single colony from an LB plate transformed with NT326 cells containing cloned pccKan plasmids was streaked onto the plate and incubated for 2-3 days at 37°C. Negative controls were also streaked, containing only untransformed NT326 cells.

2.7.3 Expression check

Before conducting the quantitative ToxCAT assay, tests were performed to check that chimeric fusion proteins were being expressed in NT326 cells. Differences in expression level also affect the amount of dimerization, and were therefore determined by Western blotting. An overnight culture of cells was inoculated (1 in 100) into fresh LB, and incubated in a shaker until mid-exponential phase (OD₆₀₀ = 0.6). An aliquot of these cells was taken and diluted to give 1 ml samples at an OD of 0.3. Cells were centrifuged at 13000 rpm and resuspended in 80 µl 1x SDS sample buffer, before loading onto an a NuPAGE 12% Bis-Tris gel in an XCell SureLock Mini-Cell electrophoresis kit (section 2.6.1).

After running, gels were placed in an XCell II Blot Module, and bands transferred under an applied voltage to a Nitrocellulose membrane (Invitrogen LC2000) in 1x transfer buffer (see section 2.6.4). Membranes were then blocked (in 3% w/v milk solution), anti-MBP antibodies bound and blots developed (see section 2.6.4).

2.7.4 Proteolysis of Spheroplasts

To verify that interactions within the membrane are responsible for the observed CAT activity, the membrane insertion and orientation of the MBP chimerae was measured by protease sensitivity assays. The protease sensitivity of a chimera is assayed in cells that have been stripped of their outer membrane and cell wall (spheroplasts). MBP should be detectable in the spheroplast fraction as it is associated with the inner membrane via TM and ToxR domains, and a protease (proteinase K) will liberate the MBP domain from the TM domains as it should be exposed on the periplasmic side of the membrane. SDS-PAGE analysis of proteolysed spheroplast fractions will therefore show MBP as a lower molecular weight fragment.

Overnight cultures containing the chimerae in NT326 cells, were diluted to an OD_{600} of 0.6, and 1 mL of each sample was centrifuged at 13.4 krpm for 1 minute then resuspended in ice-cold buffer (100 mM Tris-acetate pH 8.2, 0.5 M sucrose, 5 mM EDTA). 6 μ L of 10 mg/mL ice-cold lysozyme was added to lyse cells open by dissolving the cell wall, and left to stand for 1 minute. To the lysed samples, 0.5 mL of ice-cold deionised water was added and samples left to stand for 4 minutes (to form spheroplasts from osmotic shock). 20 μ L of 1 M $MgSO_4$ was then added to each sample to stabilise the spheroplasts, before pelleting by centrifugation at 13.4 krpm for 1 minute.

The supernatant will contain the periplasmic fraction, and the pellet can be used to make up three fractions – a spheroplast fraction (sp), a proteolysed spheroplast fraction (sp*) and a broken spheroplast fraction (bp). The pellet was resuspended in 300 μ L of ice-cold buffer (10 mM HEPES pH 7.6, 2 mM EDTA) and split into three aliquots of 100 μ L each. The 'sp' fraction was subjected to TCA precipitation. This involved incubation in 1 mL of 10% TCA for 30 minutes, centrifugation at 13.4 krpm for 15 minutes, and the resultant pellet incubated in 1 mL acetone for 5 minutes. The reaction mixture was centrifuged at 13.4 krpm for 10 minutes, and the pellet fraction dissolved in 80 μ L of SDS loading buffer. The 'bp' fraction was freeze-thawed in liquid nitrogen then 37°C water, five times, to break open spheroplasts.

Now both the 'bp' fraction and 'sp*' fraction were digested with 2.7 μ L of 19.6 mg/mL ProteinaseK enzyme for 30 minutes on ice, and TCA precipitated and dissolved in SDS loading buffer as above. For each chimera, all three fractions were analysed on SDS-PAGE to examine the membrane insertion and orientation of the MBP chimerae.

2.7.5 Disk Diffusion Assay

As a measure of the TM-mediated dimerization of different chimerae, prior to quantitative CAT analysis, disk diffusion assays were carried out. An overnight culture containing chimerae in NT326 cells were diluted to an OD₆₀₀ of 0.1 in a final volume of 1 mL. A 100 μ L aliquot was plated on an LB/ampicillin plate and allowed to dry for 1 hour at room temperature. A chloramphenicol soaked disk was then placed in the centre of the plate (prepared by adding 42 μ L of a 90 mg/mL stock of chloramphenicol in ethanol to a 2 mm Whatman filter-paper disk and allowed to dry for 1 hour). The diameter of the clear zone of inhibition of growth around the disk was then recorded, and the size of the inhibition zone is directly dependent on the strength of TM-dimerisation in the chimera (increased dimerization confers greater CAM resistance, thereby decreasing the diameter of the zone of inhibition).

2.7.6 Quantitative CAT Assay

To quantify the strength of TM-dimerisation, CAT activity was measured in cell-free extracts. Dimerisation of helices brings the ToxR domains into contact and activates the *ctx* promoter, resulting in high levels of CAT expression. The assay is based on the Invitrogen FAST CAT (deoxy, green) system, using xylene phase extraction to isolate product, as described by Seed and Sheen, (1988). The rate of transfer of a butyryl group from butyryl-CoA to chloramphenicol is detected by the rate of color change (at ~520 nm) associated with the reaction of the resulting free coenzyme A with BODIPY-FL-deoxychloramphenicol (Molecular Probes, Cat. No. F6616).

An overnight culture of cells was diluted 1 in 100 and grown to an OD₆₀₀ of 0.7. From these, a 200 µl aliquot of cells was taken and centrifuged at 13.4 krpm for 1 minute to pellet the cells. The pellet was resuspended in 500 µl of 100 mM Tris-HCl pH 8.0 and vortexed, before adding 20 µl of lysis solution (100 mM EDTA, 100 mM DTT, 50 mM Tris-HCl pH8.0) and a drop of toluene. Samples were incubated at 30°C for 30mins to lyse, and then used in the CAT assay. 10 µl of fluorescent CAM (BODIPY-FL-deoxyCAM) was added and incubated at 37°C for 5 minutes. 10 µl of 5 mg/ml butyryl CoA solution was added (Amersham) and samples returned to 37°C for 90 minutes. Samples were centrifuged briefly before terminating reactions by adding 300 µl xylene and vortexing for 30 seconds and centrifuged for a further 3 minutes to collect the upper phase. To this phase, 300 µl Tris buffer was added and samples vortexed for 30 seconds and this procedure repeated. The sample was then assayed for fluorescence by excitation at 495 nm and emission monitored by scanning between 500 and 600 nm, with slit settings = 3.5/2.5 nm. Fluorescence values at the maximum (~520 nm) were recorded and normalized against expression levels.

2.8 Mass Spectrometry

2.8.1 Full-length protein identification by Mass Spectroscopy

Full-length tag-cleaved (wild-type) VanS protein samples were analysed for their identity using ESI-TOF mass spectrometry experiments, with the assistance of the Integral Membrane Protein group at the Structural Genomics Consortium (Oxford University). Samples at 0.5 mg/ml in detergent were diluted by 1 in 50 with 0.1% formic acid, and 40 µl aliquots of these were loaded onto a C3 column and run in methanol/formic acid/water mobile phase on an Agilent LC MSD TOF system. The 0.1% formic acid was added to the analyte solution to enhance protonation and sensitivity. The resulting total ion count (TIC) data (summed intensity across the entire range of masses being detected at every point in the analysis) was extracted and mass averaged in the region containing VanS proteins, and deconvoluted between 4 and 100 kDa using Agilent MassHunter software.

2.8.2 Protein Identification by Tryptic Digest and nanoLC-ESI-MS/MS

Coomassie stained gel pieces were sent to the Warwick/Waters Centre for BioMedical Mass Spectrometry and Proteomics (University of Warwick), where they were processed and tryptically digested using the manufacturer's recommended protocol on the MassPrep robotic protein handling system. The extracted peptides from each sample were analysed by means of nanoLC-ESI-MS/MS using the NanoAcquity/Ultima Global instrumentation (Waters) using a 30 minute LC gradient. All MS and MS/MS data were corrected for mass drift using reference data collected from the [Glu¹]-Fibrinopeptide B (human - F3261 Sigma) sampled each minute of data collection. The data was used to interrogate the *E. coli* BL21 database (<http://www.ebi.ac.uk/integr8>) using the full-length protein sequence using ProteinLynx Global Server v2.5.1.

2.9 Protein Activity Determination using Coupled Enzymatic Assays

2.9.1 Continuous ADP Release Assay

This assay is based on the production of ADP via ATP hydrolysis linked to NADH oxidation, by the coupling enzymes: pyruvate kinase and lactate dehydrogenase (PK/LDH) as described by Wampler and Westhead (1968). If active, VanS proteins should hydrolyse ATP to ADP, and pyruvate kinase will phosphorylate ADP by the catalytic conversion of phospho-enolpyruvate (PEP) to pyruvate, thus regenerating ATP. Lactate dehydrogenase uses pyruvate and converts it to lactate, by oxidising NADH to NAD^+ (see Figure 2.9.1.1).

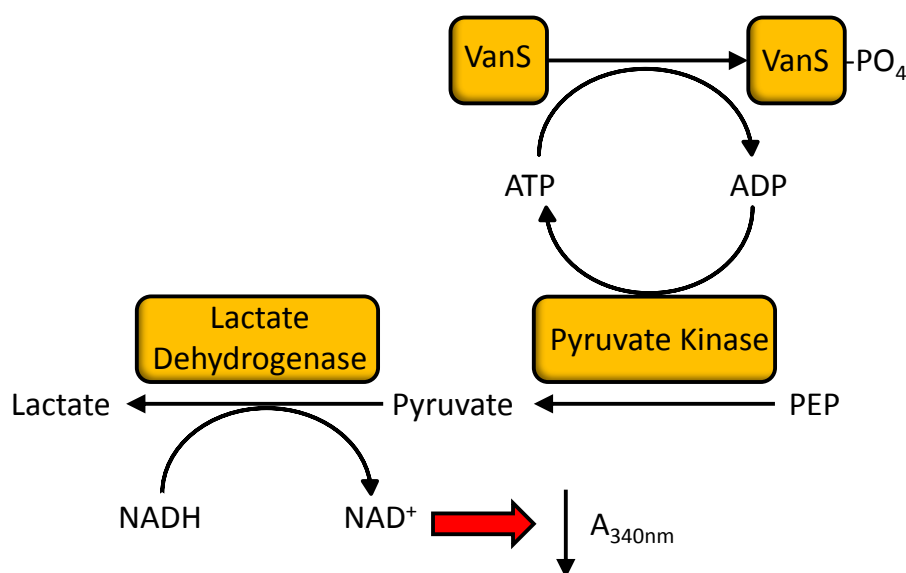


Figure 2.9.1.1: Reaction pathway involved in ADP production by ATP hydrolysis, as described by Wampler and Westhead (1968). VanS or ATP can be used to initiate the reaction, and ATP is catalytically regenerated by pyruvate kinase. The reaction is followed at 340 nm on a UV spectrophotometer, by monitoring oxidation of NADH to NAD^+ .

A reaction mixture typically consisted of 50 mM HEPES pH 7.6, 10 mM MgCl_2 , 50 mM KCl, 2.5 mM phospho-enolpyruvate (PEP), 0.3 mM NADH (freshly prepared daily), 1 μL of pyruvate kinase/lactate dehydrogenase (PK/LDH, Sigma), 3 mM ATP, and 20 μL to 80 μL of purified VanS (at 2-8 mg/ml or 10 nmol final concentration) in 0.03-0.07% w/v detergent, all in a final volume of 200 μL . Assays were performed on a Cary 100 spectrophotometer.

All components except ATP were added to a 1 cm path-length UV-visible quartz cuvette (Hellma), mixed and placed in the cell changer of the spectrophotometer with the temperature controller set at 20°C for all experiments. The cuvette was allowed to equilibrate to 20°C before setting the absorbance at 340 nm to zero. Sample absorbance was followed for 1 – 5 minutes, until a flat baseline, after which the cuvette was quickly removed, ATP substrate added and mixed and placed immediately back into the cell changer. The reaction was followed for at least 60 minutes, up to 300 minutes, and the resulting absorbance changes over the time-course of the assay were recorded using Varian Kinetics software. To demonstrate the dependence of the absorbance decrease on both VanS and ATP components, assays were also initiated by addition of VanS.

2.9.2 Continuous Inorganic Phosphate Release Assay

This assay is based on the utilisation of any free inorganic phosphate by the enzyme MESG (2-amino-6-mercapto-7-methylpurine ribonucleoside) and its subsequent conversion by PNP enzyme (purine nucleoside phosphorylase) to methylthioguanine and ribose-1-phosphate, effecting an increase in absorbance, which may be observed at a wavelength of 360 nm, as detailed by Webb (1992). The MESG enzyme has a strong absorbance at 330 nm, whereas methylthioguanine has an absorbance maximum at 360 nm, therefore a change in absorbance occurs which can be followed spectrophotometrically (see Figure 2.9.2.1).

This assay was conducted as a second measure of protein activity, to complement the ADP production assay. It also enabled quantification of the amount of phosphate released by VanS after autophosphorylation and therefore allowed calculation of how much ATP is turned over from this, giving relative stoichiometries, corrected for any free phosphate release.

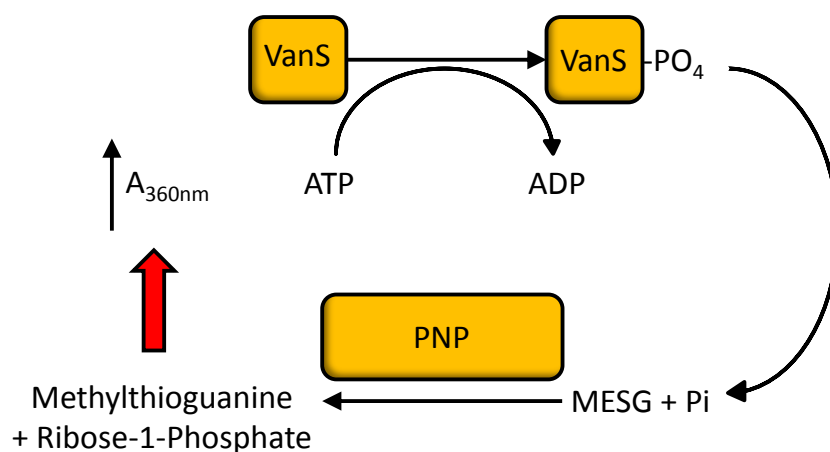


Figure 2.9.2.1: Reaction pathway involved in inorganic phosphate release by ATP hydrolysis, as described by Webb (1992). VanS or ATP can be used to initiate the reaction, but ATP is not regenerated. The reaction is followed at 360 nm on a UV spectrophotometer, by monitoring conversion of MESG to methylthioguanine by PNP enzyme.

All components except ATP were added to the quartz cuvette (Hellma), mixed and placed in the cell changer of the spectrophotometer with the temperature controller set at 20°C for all experiments. The cuvette was allowed to equilibrate to 20°C before setting the absorbance at 360 nm to zero. Sample absorbance was followed for 1 – 5 minutes, until a flat baseline, after which the cuvette was quickly removed, ATP substrate added and mixed and placed immediately back into the cell changer. The reaction was followed for 20-60 minutes and the resulting absorbance changes over the time-course of the assay were recorded using Varian Kinetics software. To demonstrate the dependence of the absorbance decrease on both VanS and ATP components, assays were also initiated with VanS enzyme.

A reaction mixture typically consisted of 50 mM HEPES pH 7.6, 10 mM MgCl₂, 0.2 mM MESG, 1 μL of PNP (160 units/mL), 3 mM ATP, and 20 μL up to a limit of 80 μL of purified VanS enzyme (at 2-8 mg/ml or 10 nmol final concentration) in 0.03-0.07% w/v detergent, all in a final volume of 200 μL. Assays were performed on a Cary 100 spectrophotometer (Varian). In both assays, careful pipetting was required to reduce air bubbles or bubbles in detergent containing samples.

2.9.3 Identification of Assay products by Anion Exchange Chromatography

To identify products of the reaction between VanS and ATP, simplified experiments were conducted involving only VanS enzyme and ATP substrate (i.e. ATP is not regenerated). A reaction mix consisted of 50 mM HEPES pH 7.6, 1 mM MgCl₂, 1 mM KCl, 0.03% DDM detergent, 10 nmol of VanS enzyme purified in 0.03% DDM and 3 mM ATP in a final volume of 200 µL. The reaction time was monitored, from the point at which ATP was added, and all 200 µL samples (aliquoted from a master mix) were maintained at 20°C in a PCR machine for direct comparison with activity data. Control samples were also run and tested simultaneously. These control samples were in-house standards of AMP, ADP or ATP (at 3 mM final concentration) in a reaction mix containing 50 mM HEPES pH 7.6, 1 mM MgCl₂ with a final volume of 200 µL. A reaction mix was also tested involving VanS and ADP; 50 mM HEPES pH 7.6, 1 mM MgCl₂, 1 mM KCl, 0.03% DDM detergent, 10 nmol of VanS enzyme purified in 0.03% DDM and 3 mM ADP in a final volume of 200 µL.

For all samples, a 200 µL aliquot was removed from the PCR machine at specific time points (0, 30, 60, 120, 240, 360 or 480 min) and the reaction was quenched with 25 mM (final concentration) of EDTA pH 8, which chelates to any magnesium ions present. The sample was then applied to a new 5 kDa MWCO concentrator, and concentrated for 20 minutes at 4000 g, to obtain the VanS protein in the upper chamber and the DNA in the lower chamber. nucleotide products of the reaction could then be analysed by Anion Exchange Chromatography (IEX), and identified against standards (AMP/ADP/ATP). 80 µL of the flow through from the concentrator was diluted with 1.3 mL of buffer A (10 mM ammonium acetate pH 7.6), and applied via a 1 mL injection loop onto a pre-equilibrated MonoQ 5/50 GL column (Amersham) on an AKTA purifier at 1 mL/min flow rate. Absorbance at 280 and 254 nm was recorded, and ~10 mL was passed through the column to elute any unbound compounds, before a gradient was started of 100% B (1M ammonium acetate pH 7.6), over 30 minutes, and held at 100% B for 10-15 minutes.

Once all compounds had been eluted, the gradient was lowered to 0% B and the next sample was loaded onto the column when the conductivity reached 0 mS/cm. Absorbance traces were recorded for each sample, and the integrals of all peaks and their retention time (relative to standards) enabled percentages of AMP/ADP/ATP to be calculated.

2.10 Circular Dichroism

To determine the secondary structure in solution and extent of helicity of VanS proteins in different membrane mimetic environments, and for tagged or tag-cleaved samples, Circular Dichroism (CD) experiments were conducted. This phenomenon arises from the difference in absorption of left and right circularly polarized light (Correa & Ramos, 2009). When plane polarized light enters a chiral molecule it is resolved into two perpendicular vibrating waves that propagate at different velocities. Retardation of the slow wave relative to the fast wave generates a phase difference upon emergence. Circular dichroism arises because not only does the phase shift, but the amplitude of incident left and right-hand circularly polarized light changes, giving positive or negative values. Therefore circular dichroism can be measured by the difference in absorbance of the material for circularly polarized light, ΔA , (where $\Delta A = A_L - A_R$), calculated from the Beer-Lambert Law (using $\Delta A = (\Delta \epsilon)cl$). This difference in absorption is easily converted to ellipticity units, θ , and typically spectra are generated by the CD spectropolarimeter as a function of θ (in millidegrees) against wavelength (nm). To provide data of publishable quality, it was converted into standard units of Mean Residue Ellipticity (MRE). To calculate this from raw data (in millidegrees, θ), the equation below was used (Equation 3) (Rodger & Norden, 1997) which incorporates mean residue weight (M_r), concentration ('c' in mg/ml), path length ('l' in cm) and sequence length. N_A is the number of amino acids per peptide and units of MRE are mdeg cm² dmol⁻¹.

$$MRE [\Theta] = \frac{\theta * 100 * M_r}{c * l * N_A} \quad (3)$$

CD spectra were measured using a Jasco 815 spectropolarimeter (Jasco UK, Great Dunmow, UK) at room temperature and using 1.0 mm path-length quartz cuvettes (Starna; Optiglass Ltd., Hainault, UK). All spectra were recorded at room temperature between 190-260 nm, using a data pitch of 0.2 nm, bandwidth of 2 nm, scanning speed of 100 nm/min, response time of 1 second, and either 16 or 32 accumulations. Data was initially acquired in 10 mM HEPES containing 2 mM dodecylphosphocholine (DPC; Avanti Polar Lipids), at a protein concentration of 0.2 mg/ml as measured by BCA assay (section 2.6.10) but required truncation in the region of 195-200 nm and below. To reduce minimal light scattering and obtain data to 190 nm, samples were prepared by exchanging from HEPES buffer into 10mM phosphate buffer using a PD10 column, containing 2 mM DPC. However, for analysing protein samples prior to NMR spectroscopy, the buffer conditions were maintained as much as possible. For NMR samples, an aliquot of protein (2-10 μ L) in the NMR buffer (HEPES/ sodium acetate/ phosphate) was diluted to a final volume of 200 μ L with that buffer but containing 20 mM NaCl and 2 mM detergent (DPC, LMPG or LPPG).

To stabilise the α -helical fold, and increase the strength of helicity, concentrated protein samples were also diluted to 0.2 mg/ml with 100% 2,2,2-trifluoroethanol (TFE) (containing 2 mM detergent to determine the difference between samples with and without TFE), as this reagent is known to induce α -helix formation (Arunkumar *et al.*, 1997). The helicity in TFE could then be compared to that in each detergent to analyse the relative protein folds.

Micelle:protein ratios varied depending on detergent, but were in the range of 3-10, for solubilisation in DPC detergent, (assuming a CMC for DPC of 1.1 mM and an aggregation number of 56) (Wüthrich, 1986). During scans, the high tension voltage remained below 600V down to 200 nm, and often to 190 nm, to obtain reliable, publishable data.

2.11 Fluorescence Spectroscopy

Fluorescence spectroscopy was used as a qualitative test for an interaction between a fluorescently labelled vancomycin probe and a VanS protein. The phenomenon is defined as the re-emission of light by a substance that has absorbed radiation at a fixed wavelength.

Photochemically, fluorescence can occur when an orbital electron of an atom or molecule, relaxes to its ground state (S_0) by emitting a photon of light, after being excited to a higher state (S_1 , the first excited state). For a full review, see e.g. Sharma & Schulman, (1999).

For these studies, a vancomycin analogue was chosen which was available in the laboratory and had been previously used for imaging SDS-PAGE gels (Abrahams, 2011) containing transglycosylated polymerised Lipid II molecules of different chain lengths (visualised under a fluorescent light filter). The vancomycin analogue contains a BODIPY (Boron-dipyrromethene) molecule covalently linked to vancomycin, and is a class of fluorescent dye (BODIPY-vancomycin, Molecular Probes, V-34850) (Figure 2.11.1). The BODIPY-vancomycin dyes have sharp excitation and emission wavelengths at ~504 nm and ~512 nm.

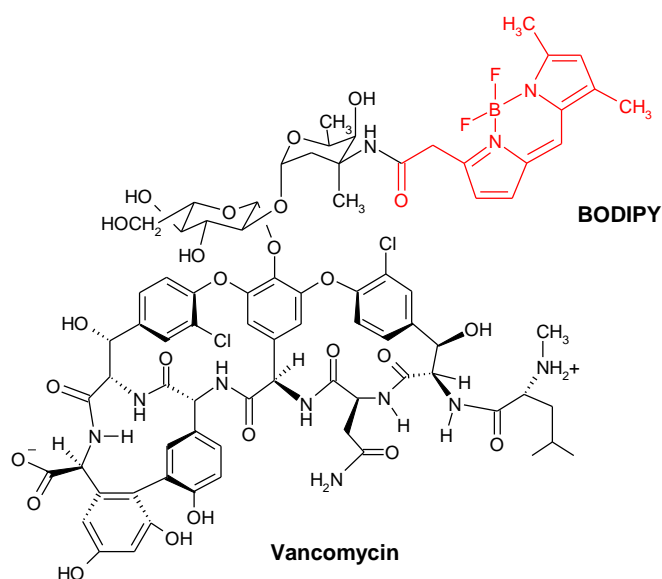


Figure 2.11.1: *BODIPY-Vancomycin structure, drawn in IsisDraw. BODIPY (red) is covalently bonded to the amine group on a sugar moiety of vancomycin, well away from the lipid binding heptapeptide core.*

BODIPY-vancomycin powder showed high solubility in water, and was resuspended in 1mL of 20 mM HEPES pH 7.8 buffer, and centrifuged to remove any undissolved powder, aliquoting the supernatant into a 1.5 mL Eppendorf shielded from light by wrapping in foil. The concentration was determined by testing the absorbance at 504 nm of a number of samples with differing dilution factors, in a 0.1 cm path length quartz cell in a UV spectrophotometer, using the extinction coefficient of $78000 \text{ M}^{-1} \text{ cm}^{-1}$ for BODIPY-vancomycin (Zlotnick *et al.*, 2007), and applying the formula:

$$[BODIPY] = \frac{A_{504}}{78000} \quad (4)$$

The concentration was determined to be $\sim 100 \mu\text{M}$. Initially, BODIPY-vancomycin at $10 \mu\text{M}$ in 20 mM HEPES pH 7.8 was excited at 504 nm with monochromatic light and the emission spectrum collected by measuring the emission intensity between 500 and 600 nm. The slit width was 1 nm, and the scan speed was 50 nm/min, and all samples were collected at 20°C on a Perkin Elmer LS50 fluorimeter. The effect of micelles on the emission spectrum of the vancomycin analogue was next tested by adding microliter volumes (5 -10 μL) of a 2% w/v (40mM) DPC solution in buffer, mixing thoroughly and measuring the emission spectra. Once the concentration of DPC was significantly above the CMC, VanS proteins or Lipid II-Lys molecules were added.

VanS proteins were purified from DPC-solubilised membrane pellets by IMAC techniques (see section 2.6.6), which were applied to a PD10 column and exchanged to a buffer containing 20 mM HEPES pH 7.8 and 2 mM DPC (see section 2.6.8) and then concentrated to 3-6 mg/ml. Lipid II-Lys was synthesised in-house by the Bacwan facility (School of Life Sciences, University of Warwick) and its concentration determined by assay as $660 \mu\text{M}$, in chloroform/methanol/water (2:3:1).

For samples containing BODIPY-vancomycin, DPC and Lipid II, an aliquot of Lipid II was pipetted (from a parafilm glass vial), into a clean glass vial, immediately dried under nitrogen to a film and resuspended with the 200 μ L solution of BODIPY-vancomycin in DPC detergent (10 μ M BODIPY-vancomycin in 20 mM HEPES pH 7.8, 2 mM DPC), and vortexed thoroughly to resuspend the Lipid II fully. Further aliquots of Lipid II were added in the same way, to final concentrations of 10, 20, 30 μ M, and the emission spectra of all samples measured. For samples containing BODIPY-vancomycin, DPC and VanS, an aliquot of VanS in 20 mM HEPES pH 7.8, 2 mM DPC was added directly to 200 μ L containing 10 μ M BODIPY-vancomycin in 20 mM HEPES pH 7.8, 2 mM DPC, mixed thoroughly and the emission spectrum measured. Further aliquots of VanS were added in the same way, until no appreciable changes in the emission spectra were observed.

2.12 Site-specific Enzymatic Tag-Cleavage

2.12.1 Enzymatic digestion with in-house synthesised TEV protease

After IMAC purification of His-tagged VanS proteins, elution fractions were digested with in-house synthesised histidine-tagged tobacco etch virus (TEV). The gene encoding for TEV protease (within a pRK793 vector) was obtained from the David Waugh laboratory deposit at Addgene, and was the S219V mutant version, containing an N-terminal polyhistidine tag and C-terminal polyarginine tag (His₆-TEV (S129V)-Arg₅). TEV protease was expressed in-house from this gene, under assistance from the Roper group (University of Warwick). The gene was expressed in *E.coli* BL21(DE3)pRIL cells in Terrific Broth (12 g Tryptone, 24 g Yeast extract, 4 mL Glycerol per litre of H₂O), and purified by IMAC on a pre-packed nickel His-trap column followed by Gel Filtration Chromatography (data not shown).

Cleavage experiments were conducted for 8-12 hrs at room temperature or overnight at 4°C, at a 1:1 ratio of [protein]:[TEV], in 20mM HEPES pH 7.5, 200mM NaCl, 10% glycerol, 20 mM Imidazole and 2 mM DPC. The mixture was rebound to pre-charged nickel resin over 1 hour rocking, prior to IMAC purification. The flow through was collected, and any weakly bound, cleaved VanS protein was selectively removed from the resin in a low imidazole buffer (20mM HEPES pH 7.5, 200mM NaCl, 10% glycerol, 40 mM Imidazole and 2mM DPC). TEV protease and uncut VanS were only eluted under high imidazole (250 mM).

2.12.2 3C Protease Expression and Purification

Constructs encoding for N-terminal polyhistidine, and C-terminal MBP-tagged 3C protease (N-His₆-3C-MBP-C) tagged protease were sourced from Jim Brannigan's lab in York University. 1L of protease was overexpressed in BL21(DE3) cell line with pRARE codon optimisation, according to published protocols (Alexandrov *et al.*, 2001). All steps were carried out at 4°C. The cell pellet was resuspended in 40mL of buffer A (40mM sodium phosphate pH 7.8, 200 mM NaCl, 5 mM BME, 5% glycerol). Lysozyme was added to 1 mg/ml, and DNase to 2 µg/ml, as well as 1 mM PMSF, 0.2 µM leupeptin, 0.2 µM pepstatin. Cells were sonicated on ice by three bursts of 30 seconds on and off. The lysate was subsequently centrifuged at 17000 g for 30 minutes and rotated for 2 hours with 5 mL bed volume TALON affinity resin (pre-equilibrated with buffer A). The resin was then pelleted at 1500g for 2min, supernatant decanted and washed with 50 mL of buffer A containing 20mM Imidazole, 3 times, each time pelleting at 700g, 2mins.

To elute the protease, 5mL of buffer A containing 1M imidazole was added and the sample was rotated for 20 mins at 4°C. The eluent was collected and dialysed twice for 1 hour each in 1L of buffer A (see section 2.6.8). After adding ice-cold glycerol to a final volume of 20%, the protease was divided into 0.5 mL aliquots (at 3 mg/ml) and stored at -80°C. Total yield was 60 mg protease per litre, with some protease remaining in the flow through.

2.12.3 Enzymatic Digestion with 3C Protease

After IMAC purification of hexahistidine-tagged VanS proteins, elution fractions were digested with in-house synthesised 3C protease (N-His₆-3C-MBP-C) (see section 2.12.2). Cleavage experiments were conducted for 10-12 hrs at room temperature or overnight at 4°C, at a ratio of 1:1 [protein]:[3C], in buffer A (20mM HEPES pH 7.2, 800mM NaCl, 10% glycerol, 1mM DTT, and 2mM DPC). After digestion, the mixture was bound to 10 mL bed volume of pre-charged amylose resin (NEB, UK) (washed with 50 mL of 20mM Tris-HCl pH 7.5, 200mM NaCl, 10% glycerol, 1mM EDTA and 1mM 2-mercaptoethanol) over 2-3 hours rocking at 4°C, in order to remove the MBP-tagged 3C protease.

Once the flow through had been collected, the resin was washed with 20 mL of buffer A to remove residual VanS protein. Fractions were concentrated from ~25 to 2.5mL, and applied to a pre-equilibrated PD10 column (20 mM HEPES pH7.5, 300 mM NaCl, 10% glycerol and 2mM DPC) to remove EDTA which would affect binding to nickel resin.

The elution fraction from the PD10 was then rebound to nickel resin (to remove the C-terminal untagged region) by adding 20mM Imidazole and rocking in 1-1.5mL bed volume of nickel sepharose charged resin for 2 hours. After the rebind, flow through was collected under gravity, the column was washed with 20mL of buffer containing 20mM Imidazole, 20mM HEPES, 300mM NaCl, 10% glycerol and 2mM DPC, then 20mL of this buffer but containing 50mM Imidazole, and finally the protein was eluted with the N-terminal product as the major band using 2.5mL of buffer containing 250mM Imidazole. The product was then applied to a PD10 column before concentrating to 0.5 mL for gel filtration chromatography (section 2.6.7), and applying onto a Superose 6 10/300 GL column, under an isocratic gradient of 100% A (20mM HEPES, 300mM NaCl, 10% glycerol, 2mM DPC).

2.13 Protein Crystallisation

X-Ray crystallography is an effective tool for generating atomic resolution structures of protein structure. However, the rate limiting step is the production of diffraction quality protein crystals, especially when studying membrane proteins, because solubilized protein-detergent complexes do not often form ordered crystal lattices (Newby *et al.*, 2009). It is difficult to rationalise why some proteins crystallise easily and others do not. However, by understanding the crystallisation process, better methods for crystal growth can be created.

The science of crystal growth began in the 1980s and is termed crystallogenesis (Giege & Mikol, 1989). The three stages of crystallisation that are followed by all molecules are nucleation, crystal growth and termination of growth (Russo Krauss *et al.*, 2013). Protein crystal formation requires that interactions between associating molecules are specific, directional and organised to provide the three-dimensional lattice. The full growth process can be visualised in a two-dimensional phase diagram (see Figure 2.13.1).

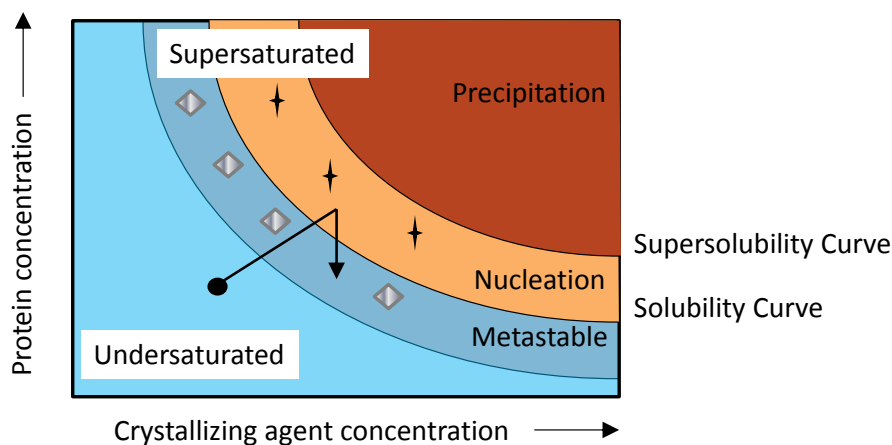


Figure 2.13.1: Two-dimensional Phase diagram for Crystal growth. Adapted from Russo Krauss *et al.*, 2013. The arrow shows the route required for optimal crystal growth by vapour diffusion; the protein solution should reach supersaturation and nucleate, but a crystal only forms if the concentration drops and growth continues in the metastable zone.

As the concentration of a protein solution is brought above the solubility limit, it becomes supersaturated. Depending on the degree of supersaturation, growth will proceed in either the “precipitation” zone (as amorphous aggregates), the “nucleation” zone (where growth and nucleation can occur) or the “metastable” zone (where only growth is supported). There are many factors that affect crystal growth, which include pH, buffer, temperature, viscosity, protein concentration (Table 2.13.1). Any of these can greatly affect success of crystallising a protein, but several effects can be minimized by obtaining highly pure (single band on SDS-PAGE or > 95% purity), homogenous proteins at concentrations of around 10 mg/ml.

In order to rapidly assess a number of conditions, and control some of these factors, sparse matrix screens of 24 to 96 wells can be adopted, and allow determination of conditions that provide crystal ‘hits’. There are also general protocols for the expression, isolation, solubilisation and purification of membrane proteins, with a view towards identification and refinement of conditions suitable for crystallisation (Newby *et al.*, 2009).

Table 2.13.1 Factors affecting crystallisation. Adapted from Russo Krauss *et al.*, (2013).

Physical Factors	Chemical Factors	Biochemical Factors
Temperature (affects vapour diffusion and protein stability)	Precipitant choice and concentration	Sample purity and Degradation rate
Time (equilibration time and growth rate)	pH and Buffer type (affects pI of protein and solubility)	Sample homogeneity and Oligomeric State
Viscosity	Detergents (affects crystal contacts and stability)	Sequence modifications e.g. tags or mutations
Methodology	Sample concentration and drop ratio (affects supersaturation)	Aggregation
Nucleants present	Ionic strength and Purity of chemicals	Ligands, co-factors

A final parameter required for crystallisation is the method chosen to form crystals, which includes Batch, Dialysis, and most the commonly used, Vapour Diffusion.

2.13.1 Vapour Diffusion Crystallisation

Vapour diffusion techniques utilise the evaporation and diffusion of water between a small droplet (10 μL or less) containing protein, buffer and precipitant, and a well solution, under a sealed environment. The well contains similar buffers and precipitant, but at higher concentrations with respect to the droplet. The droplet is equilibrated over the well by a hanging, sitting or sandwich drop method (Figure 2.13.1.1), to allow a slow increase in both protein and precipitant concentration which could cause supersaturation and crystal growth.

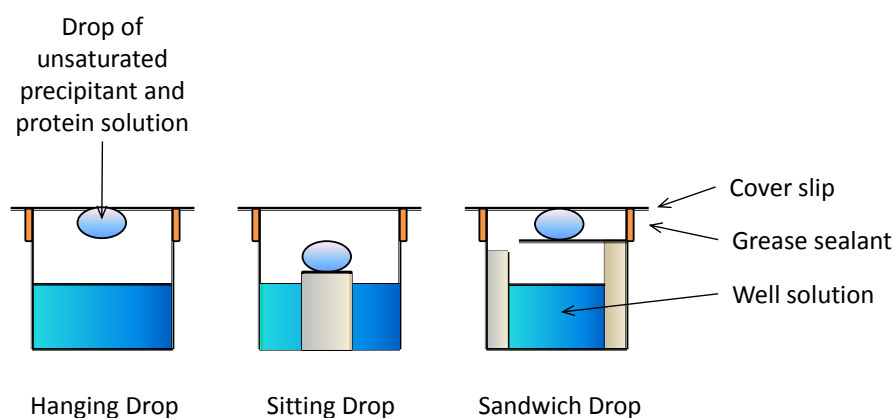


Figure 2.13.1.1: The Vapour diffusion method. Adapted from Russo Krauss et al., 2013. In the 'Hanging' drop technique, the droplet is placed on a cover glass, and turned over to face the well. In the 'Sitting' drop technique, the droplet is placed on a small island inside the well. In the 'Sandwich' drop technique, the droplet is placed between two cover slips, one of which seals the reservoir.

2.13.2 Sparse Matrix Screening

Sparse matrix screens are routinely used when studying a new protein since each protein will often crystallise in different and sometimes multiple conditions. It is therefore a necessity to screen a variety of solutions, and these matrix screens are developed based on documented conditions which have yielded successfully diffracting protein crystals.

Often conditions contain a variety of precipitants such as polyethylene glycols (PEG), as well as salts, buffers such as Tris-HCl or HEPES, or solvents that have shown high success rates. Modern day screens are set-up in 96-well plate format and although there are >30 possible matrix screens, only a few bias towards conditions for membrane protein crystallisation. These include screens developed by the Iwata group, known as MemGold, MemStart, and MemSys (Carpenter *et al.*, 2008). Robotic tools are also available at high-throughput facilities e.g. the Membrane Protein Laboratory (MPL) at Diamond Light Source (UK), which allow automated crystallisation screen set-up and imaging analysis.

During this project, Memgold and MemStart (Molecular Dimensions) matrix screens were tested, which were set-up in 96-well MRC plates, using a 100 μ L volume of precipitant per well. Sitting-drops were dispensed by a Honeybee 963 (University of Warwick) or a Mosquito robot (Structural Genomics Consortium, Oxford University) and consisted of 0.2 μ L of protein mixed with precipitant, at drop ratios of either 1:1, 2:1 or 0.5:1 protein:precipitant, to test a range of concentrations, up to an effective concentration of 28 mg/ml protein. Each 96-well plate therefore required at least 30 μ L of protein solution. All trials were carried out at 18°C.

2.13.3 Data Collection

Microcrystals and nanocrystals of potential hits were collected and transported to Diamond Light Source (Harwell, UK) and exposed to a synchrotron beam line to test for crystal diffraction, under the assistance of the Integral Membrane Protein Department at the Structural Genomics Consortium (Oxford).

2.14 Solution State Nuclear Magnetic Resonance Spectroscopy

NMR spectroscopy can provide three-dimensional structure determination of proteins in the solution phase. In addition, it provides a useful tool for the study of kinetic and ligand binding reactions at the atomic level. In this study, two-dimensional solution state NMR was used as a quantitative test for the interaction between a vancomycin or teicoplanin antibiotic and a VanS protein, to establish if binding was occurring and determine binding affinities.

NMR spectroscopy examines chemical properties by studying individual nuclei. Only those nuclei with a half-spin e.g. ^1H , ^{13}C or ^{15}N will exhibit NMR absorption spectra. The nucleus will have two possible spin states: $m = +\frac{1}{2}$ or $m = -\frac{1}{2}$, which when placed in a magnetic field, will align with or against the applied field (B_0), and the nucleus will precess about the magnetic field on its axis of rotation (in the z-axis). This results in an energy difference with a small population bias toward the lower state, as described by the Boltzmann distribution.

When the correct resonance frequency (matching the Larmor frequency) of radiation is applied to equal the energy difference, at right angles to the external magnetic field, those nuclei in the $+\frac{1}{2}$ state are excited into the higher $-\frac{1}{2}$ state. This excitation shifts the net magnetisation away from the z-axis and toward the x-axis, where the nuclei will precess in the x-y plane, before returning to equilibrium by relaxation processes (see Figure 2.14.1).

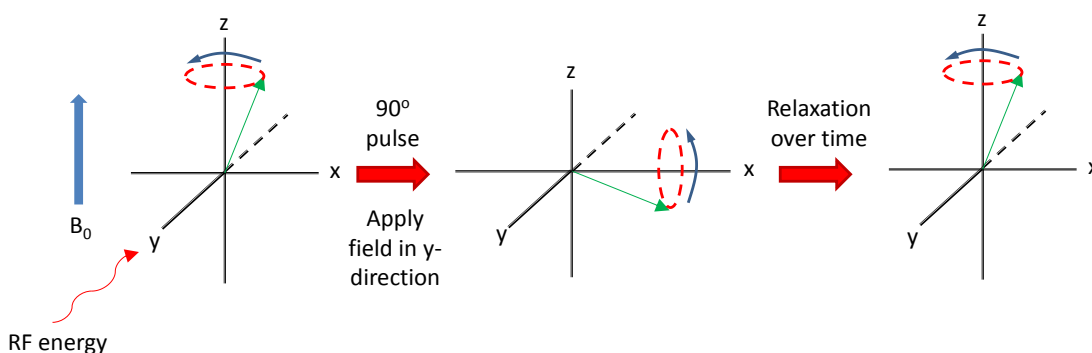


Figure 2.14.1: Representation of nuclear spin relative to an axis of rotation, upon irradiation with a 90° pulse at the Larmor frequency (ν_f).

These are non-radiative relaxation processes and there are two major relaxation processes: spin-lattice (longitudinal) relaxation (T_1), in the z-direction and spin-spin (transverse) relaxation (T_2), in the x-y plane. The relaxation mechanism is a first order process, so the 'rf' signal emitted by the sample decays exponentially, by free induction decay (FID). Each FID signal, generated as excited protons relax, can be stored and averaged, and then converted by Fourier Transform from a time domain signal to a frequency domain spectrum.

By selecting appropriate pulse programs, we can obtain structural information on proteins. A basic one dimensional NMR experiment consists of a simple pulse sequence, involving a delay time (d1), or a presat pulse (p19) in the case of 'zgpr' water suppression pulse, prior to excitation (p1), and acquisition (t2). For two-dimensional NMR experiments, there is also an evolution time, and mixing time, prior to collection of the FID data (see Figure 2.14.2).

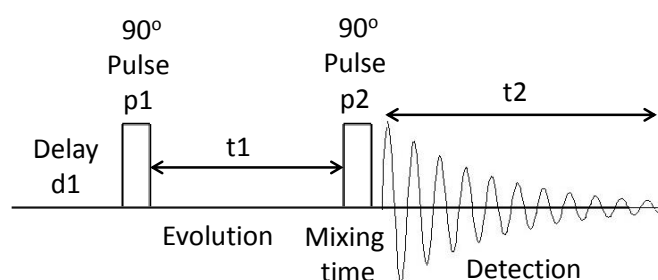


Figure 2.14.2: An example 2D COSY pulse program. The program consists of preparation (p1) and mixing (p2) periods of single 90° pulses separated by evolution time (t1), and the resonance signal from the sample is read during the detection period over a time range (t2).

As stated above, two-dimensional solution state NMR was used for these studies, to identify any interaction of glycopeptide antibiotics with VanS proteins. ^1H - ^{15}N Heteronuclear Single Quantum Coherence (HSQC) experiments were conducted to obtain information on protein fold, in different buffers, detergents, pH environments, temperatures, and determine the optimal conditions. Under these conditions, it was then possible to measure changes to peak chemical shift upon addition of potential ligands such as vancomycin and teicoplanin.

Experimental measurements for all samples (in 10% D₂O, and fixed temperature), involved locking the proton signal, tuning and shimming, then collecting an initial 1D ¹H ‘zgpr’ presaturation pulse sequence (which provided the ‘p1’ value). This was followed by a ‘zggpwg’ Watergate pulse sequence which provided water suppression and gave information on peaks of the protein. From these experiments, values (e.g. p1, o1, sw) were inserted into the ‘hsqcetf3gpsi’ pulse program for the 2D ¹H-¹⁵N HSQC experiment.

2.14.1 2D ¹H-¹⁵N HSQC NMR Spectra of VanS proteins in detergent micelles

Proteins were overexpressed in M9 minimal media, containing ¹⁵N ammonium chloride, as required for NMR experiments (see section 2.5.1). Membrane proteins were extracted by cell disruption and ultracentrifugation (see section 2.5.3), and solubilised in 0.5-1% w/v DPC detergent. After IMAC purification the protein was cleaved with 3C protease at a 1:1 ratio of protein:protease, and the N-terminal His-tagged VanS sensor domain was selectively purified away from the protease and C-terminal domain (see section 2.12.3). At this point detergents were either exchanged on the IMAC resin, or the protein was further purified by Gel Filtration Chromatography. Similarly, the pH, salt and buffer could be altered during IMAC exchange or after it by applying to a pre-equilibrated PD10 column (section 2.6.8).

The ¹⁵N labelled VanS N-terminal sensor domain was then concentrated to ~200 μL or >100-200 μM, centrifuged at 13 krpm for 10 minutes in a Beckmann benchtop centrifuge, to pellet any aggregated material, before pipetting into 3mm BrukerMATCH NMR tubes. 10% v/v D₂O was then added to samples, prior to analysis by solution state NMR on a 500 MHz Bruker NMR spectrometer with a tbi probe, or a 700 MHz Bruker NMR spectrometer with a cyroprobe. Samples were inserted into the spectrometer, and locked, tuned and shimmed, as detailed above, and a 1D ¹H ‘zgpr’ experiment was conducted. These 1D experiments, provided ‘p1’ and ‘o1’ values required to conduct 2D ¹H-¹⁵N HSQC experiments.

2D ^1H - ^{15}N HSQC spectra were collected for VanS samples in different detergents, pHs and temperatures, to determine the optimal conditions for protein fold and to obtain sharp, well-resolved NMR peaks with uniform intensities. Three detergents were analysed: DPC, LMPG and LPPG, and a pH range between 4.6 and 6.9, and temperature range between 288K and 418K was tested. Samples were also buffered in either 50mM sodium acetate (pH 4.6-5.6), 50mM sodium phosphate (pH 5.6-6.6), or maintained in 20mM HEPES buffer throughout (pH 6.6-6.9). These experiments informed decisions on appropriate conditions for conducting ligand-based titration experiments, as detailed in section 2.14.2.

2.14.2 Ligand-based Titrations by 2D ^1H - ^{15}N HSQC spectroscopy

2D ^1H - ^{15}N HSQC spectra were acquired for samples containing isotopically labelled VanS proteins solubilised in micelles, in a known buffer (as detailed above), to which glycopeptide antibiotics were added. The glycopeptide antibiotics tested were vancomycin hydrochloride (Sigma) and teicoplanin (Molekula), which were dissolved in buffer, containing detergent micelles (at a concentration \gg CMC). For instance, a VanS protein sample at $\sim 200 \mu\text{M}$, solubilised in 50 mM DPC, in 50 mM sodium acetate pH 5.6, was analysed by HSQC NMR spectroscopy. A vancomycin solution of 10-20 mM was prepared by dissolution in this buffer (but containing 5 mM DPC) and titrated into the sample, at 1:1 ratio of [protein]:[Vancomycin]. The pH was measured before and after addition of antibiotic on a calibrated pH meter, and adjusted accordingly with microliter volumes of 0.1 M acetic acid or hydrochloric acid, or 0.1 M sodium hydroxide, to within 0.05 pH units (over all titrations).

Each new titration sample was centrifuged to pellet any insoluble material and aggregated protein, and allowed to equilibrate for 15-30 minutes, before being placed into the spectrometer and locked, tuned and shimmed. A new 'p1' value was obtained using 1D ^1H 'zgpr' pulse sequences, before collecting another set of HSQC spectra. The Watergate pulse sequence ('zggpwg') was also collected to examine protein degradation between samples.

NMR samples were also prepared for VanS proteins in the presence of vancomycin and Lipid II-Lys (from Gram-positive bacteria), to determine the effects of interaction of VanS proteins with a complex of vancomycin and Lipid II cell wall precursor by HSQC NMR. Lipid II-Lys was obtained from the Bacwan facility (Warwick) as dissolved lyophilised powder at a concentration of 660 μM . An aliquot of Lipid II was dried to a film in a glass vial under nitrogen, and the NMR sample containing ^{15}N labelled detergent-solubilised VanS protein and vancomycin was added and vortexed thoroughly to resuspend the lipid. Samples were allowed to equilibrate for several hours before analysis. Due to the high cost of the lipid (1 mg \sim £1000), the molar ratio of vancomycin : protein : Lipid II used in experiments was 4:1:0.5, but this should be sufficient to form a complex with the excess vancomycin present.

2.14.3 Analysis of NMR-based ligand titration data

NMR data from the 500 or 700 MHz Bruker NMR spectrometer was collected in Topspin 2. This data was exported into Sparky 3.114 program for analysis of HSQC NMR spectra. The 2D ^1H - ^{15}N HSQC NMR spectra acquired at each titration point were overlaid in Sparky and exported into Microsoft Expression Design 4 for publishing. HSQC spectra were analysed in Sparky by peak picking with all peaks tabulated and numbered according to their chemical shift (δ), in order of ascending $^1\text{H}^{\text{N}}$ value. Changes in the chemical shift (δ) of each peak during ligand titrations were calculated using a Chemical Shift Perturbation (CSP) analysis. For full details of CSP analyses see section 5.4.1. Briefly, this involved calculating the difference in ^1H (δ_{H}^2) or ^{15}N (δ_{N}^2) chemical shift value of each peak (at each titration point), by subtracting against the chemical shift value of the corresponding peak in the spectrum containing only the protein in detergent (i.e. at 0:1 [ligand]:[protein]). The relative chemical shifts of the ^1H and ^{15}N nuclei were then weighted, and the chemical shift change, ($\Delta\delta$), calculated according to Equation 4 (see section 5.4.1). By calculating the chemical shift change ($\Delta\delta$) for each peak, a bar graph was then produced of peak number against CSP, to demonstrate the number and magnitude of shifts observed (e.g. see Figure 5.4.1.5).

3 Cloning, Expression, Purification and Functional Characterisation of VanS proteins from Enterococci and Streptomyces

3.1 Introduction

VanS is an integral membrane protein and sensor histidine kinase, which forms part of a two component system (TCS) (section 1.5), with its cognate cytosolic response regulator, VanR. This system regulates inducible transcription of the genes responsible for glycopeptide resistance in pathogenic strains such as enterococci (GRE) (section 1.3), as well as in some actinomycetes e.g. *Streptomyces*. In the presence of a glycopeptide antibiotic e.g. vancomycin, VanS binds ATP molecules at its cytoplasmic ATP-binding domain and auto-phosphorylates a conserved histidine residue in an adjacent α -helix (Walsh *et al.*, 1996) (Figure 3.1.1). The phosphate is subsequently transferred to a conserved aspartate residue on VanR, resulting in a conformational change in the protein. This increases its affinity for a specific promoter region, effecting transcription of a number of genes (*vanHAX*), responsible for glycopeptide resistance (Walsh *et al.*, 1996; Healy *et al.*, 2000) (section 1.3.3).

The structural genes for this system are found in many bacteria and their identity can vary depending on the bacterial species concerned, for instance additional *vanJ* and *vanK* genes are required for resistance in *Streptomyces coelicolor* (Hutchings *et al.*, 2006; Hong *et al.*, 2008) (section 1.3.5), but generally the *vanRSHAX* resistance genes are conserved throughout all bacterial phenotypes for the core two component systems and D-alanine to D-lactate or D-serine peptidoglycan metabolism. Each phenotype has a different antibiotic sensitivity, for instance in enterococci, the most clinically relevant phenotypes are VanA and VanB. Bacteria carrying the VanA phenotype confer resistance to vancomycin and teicoplanin, whereas those carrying VanB are resistant to vancomycin but sensitive to teicoplanin. In actinomycetes, some species such as *S. coelicolor* bacteria can also be considered as having VanB-type resistance i.e. resistant to vancomycin but not teicoplanin.

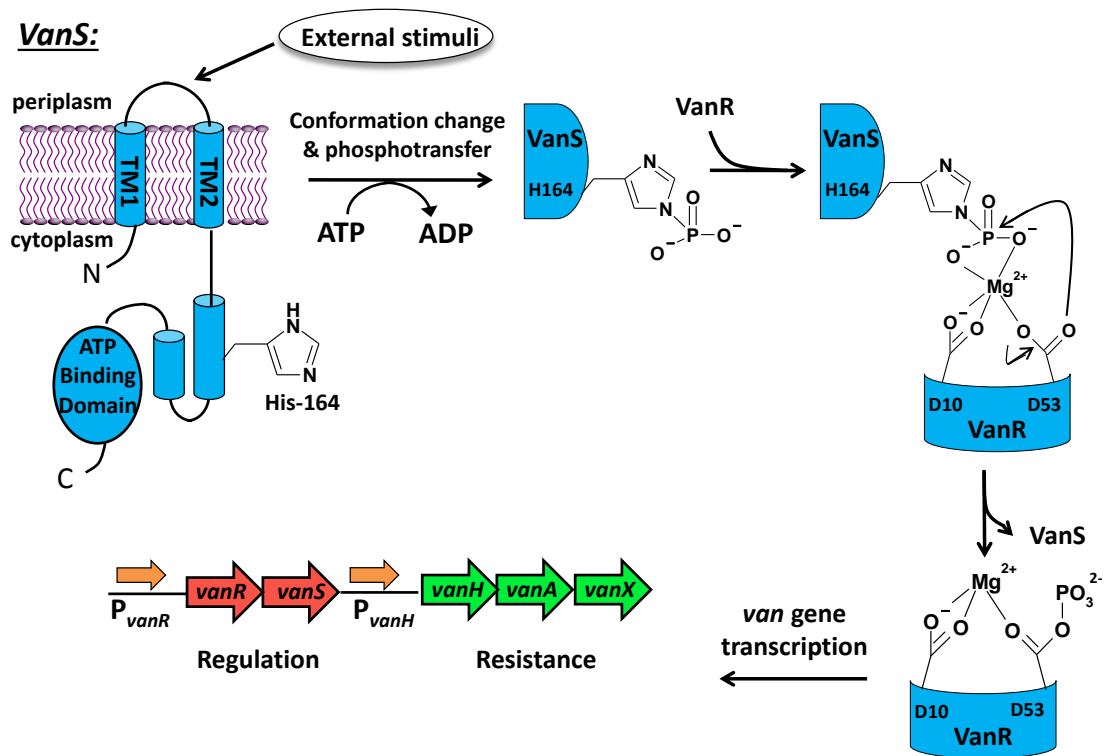


Figure 3.1.1: Model of phosphotransfer relay in the VanS-VanR two-component system.

Adapted from Walsh *et al.*, 1996; Healy *et al.*, 2000. VanS is proposed to consist of a small extracytoplasmic loop region bound by two membrane spanning helices (shown as cylinders) and a large cytoplasmic domain containing the ATP binding site and conserved His residue. Residues shown relate to proteins of the Enterococcal VanA strain (VanS_A and VanR_A).

Biochemical evidence to support the VanRS mechanism includes studies by Wright *et al.*, (1993) on *E. faecium* VanS_A/R_A proteins, Depardieu *et al.*, (2003) on *E. faecalis* VanS_B/R_B and Hutchings *et al.*, (2006) on *S. coelicolor* VanS_{SC}/R_{SC}. Wright *et al.*, (1993) showed that a fusion protein consisting of maltose binding protein (MBP) linked to the cytosolic domain of the Enterococcal VanA species (VanS_A) at Met95, could catalyse both autophosphorylation and rapid phosphotransfer to purified VanR_A using radiolabelled [γ -³²P]ATP assays. The rate of autophosphorylation of MBP-VanS_A Δ 95 was calculated as 0.17 min⁻¹ over a reaction time of one hour. However, even under saturating levels of ATP, only 10-15 % of the protein could be phosphorylated. This suggests the actual fraction of active protein was only ~0.1. Phosphotransfer from MBP-VanS_A~P to VanR_A was also found to exhibit ratio of 0.1-0.15 for phosphate bound to VanR_A, thus indicating a 1:1 transfer from active VanS_A to VanR_A.

In a reverse experiment; adding P~VanR_A to MBP-VanS_A, the group also illustrated the role of VanS_A as a VanR_A-specific phosphatase, which increased the rate of dephosphorylation of VanR_A by 6-fold when present. Similar experiments by Depardieu *et al.*, (2003) showed that the cytosolic domain of *Enterococcal* VanS_B (Met159 to Lys447) also possesses kinase activity and acts as a VanR_B-specific phosphatase, increasing its dephosphorylation by 11-fold when present. Furthermore, Hutchings *et al.*, (2006), showed that the cytosolic domain of *S. coelicolor* VanS_{SC} (Ala85 to Arg364) can autophosphorylate and catalyse rapid phosphotransfer to *S. coelicolor* VanR_{SC}, and subsequent dephosphorylation of VanR_{SC}-P *in vitro*. Biochemical data therefore suggests that VanS is a bifunctional protein that can self-regulate between kinase and phosphatase activities, and can be represented as follows:

- 1) Autophosphorylation: VanS-H + ATP ↔ VanS-H~P + ADP
- 2) Phosphotransfer: VanS-H~P + VanR-D ↔ VanS-H + VanR-D~P
- 3) Phosphatase: VanR-D~P + H₂O ↔ VanR~D + Pi

Further evidence for the phosphatase function of VanS includes experiments involving deletion of *vanS* in *S. coelicolor* (Hong *et al.*, 2004) and in enterococci (Arthur *et al.*, 1997), and the use of a *vanH-lacZ* reporter system (Haldimann *et al.*, 1997). Deletion of *vanS* results in constitutive expression of the *vanHAX* resistance genes, indicating that VanS negatively regulates VanR in the absence of vancomycin. VanR~P can therefore be produced independently of VanS, with VanS acting as a phosphatase in the absence of the antibiotic. In the *lacZ* reporter system (Haldimann *et al.*, 1997), P_{vanH} promoters (expressing VanHAX) drive *lacZ* expression, which can be monitored by β-galactosidase production. It was found that strains expressing VanR_A only were activated by phosphorylation with donor acetyl phosphate molecules, showing increased β-galactosidase production. By contrast, expression of VanRS reduced β-galactosidase levels, showing that VanS_A interferes with the activation of VanR by acetyl phosphate, and illustrating its role as a phosphatase. These experiments indicate that separate mechanisms exist for the phosphatase and kinase activities of VanS.

Sequence alignments of VanS proteins derived from different species shows a number of conserved motifs in the cytoplasmic domain (Figure 3.1.2), which are known to be important to protein function, whereas there are large deviations in sequence identity between the extracytoplasmic sensor domains. The *Enterococcal* VanS_A and VanS_B proteins are structurally related, but have only ~23% overall sequence identity (Depardieu *et al.*, 2007), and no relation in sequence in their sensor loop regions (see Figure 3.1.3), or the length of their sensor loops (103 residues for VanS_B vs. 37 residues for VanS_A) (Hong *et al.*, 2008). *Enterococcal* VanS proteins are also very divergent from their streptomycete equivalents (~15% identity in pairwise comparisons) (Hong *et al.*, 2008). Between actinomycetes there is higher structural similarity, e.g. *S. coelicolor* and *S. toyocaensis* have ~65% identity, but again these differ greatly in the sensor regions (Figure 3.1.3). Structural differences between VanS sensor domains may suggest why each species exhibits a different response to glycopeptide antibiotics (see section 1.4.3), whereas conservation of sequence motifs in the cytoplasmic domain (e.g. the H, N, G1, F, G2 boxes, see section 1.5.3), means that the overall kinase functional mechanism remains the same.

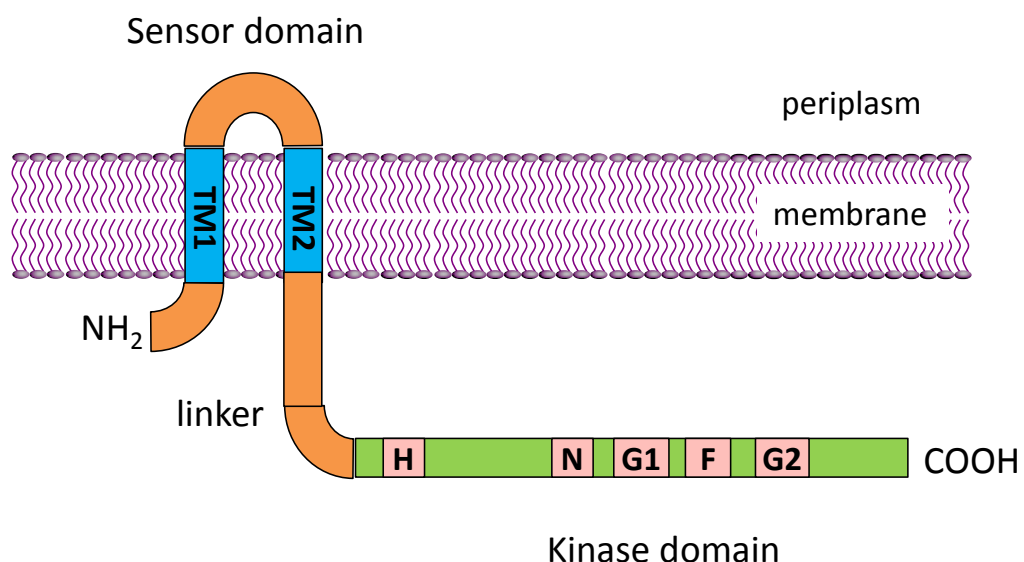


Figure 3.1.2: Schematic representation of the VanS protein and predicted topology. Adapted from Depardieu *et al.*, 2003; 2007. The putative membrane-bound sensor domain (orange) containing transmembrane (TM) helices (blue boxes) is linked to the putative cytoplasmic kinase domain (green) containing conserved sequence motifs (H, N, G1, F, G2).

```

VanSB  --MERKGIFIKVFSYTIIVLLLLLVGVATLFAQQFVSYFRAMEAQQTVKSYQPLVELIQN  58
VanSSC --MDRRPGLSVRLKLT-----LSYAGFLTLAG-  25
VanSA  MVIKLKNKNDYSKLER-----KLYMYIVAIIVVV  29
      : . : . * : : :
VanSB  SDRLDMQEVAGLFHYNNQSFEFYIEDKEGSLVYATPNADTSNSVSRPDFLYVVHRDDNISI  118
VanSSC ---VLLLVAVGVFLLDQG---WLLTNERGAVRATPGT-----  56
VanSA  A-IVFVLYIRSMIRGKLGDWILSILENKYDLNHLDAMK-----  66
      : : . : : . : : . .
VanSB  VAQSKAGVGLLYQGLTIRGIVMIAIMVVFSLLCAYIFARQMTTPIKALADSANKMAN--L  176
VanSSC -----VFLRSFAPTAAWVMAFLLVFGLVGGWFLAGRMLAPLDRITEATRATAATGSL  107
VanSA  -----LYQYSIRNNIDIFIYVAIVISIL---ILCRVMLSKFAYKVFDEINTGIDVLI  114
      : . : . : . * : : : : : : :
VanSB  KEVPPPLERKDELGALAHDMHSMYIRLKETIARLEDEIAREHELEETQRYFFAAASHELK  236
VanSSC SHRIRLPGRRDEYRELADAFDEMLARLEAHVA-----EQRFAANASHELK  153
VanSA  QNEDKQIELSAEMDVMEQKLNLTLEKREKQD-----AKLAEQRKNDVVMYLAHDIK  167
      . . * : . : : * : . . : * : :
VanSB  TPIAAVSVLLEGMLENIGD-YKDH SKYLRECIKMMDRQGKTISEILELVS LNDGRIVPIA  295
VanSSC TPLAVSKAILD--VARTDP-HQDPGE-IIDRLHAVNTRAIIDLTEALLLSR-AGQRSFTR  208
VanSA  TPLTSIIIGYLSLLDEAPDMPVDQKAKYVHITLDAKAYRLEQLIDEFFEITRYNLQTITLTK  227
      * * : : * . . : : : : : * : : :
VanSB  EPLDIGRTVAELLPDFQTLAEANNQRFVTDIPAGQIVLSDPKLIQKALSNVILNAVQN-T  354
VanSSC EQVDMSLLAAEEATETLLPFAEKHGVTLETRG-HVTLALGSPALLQLTTLNLVHNAIVHNL  267
VanSA  THIDLYYMLVQMTDEFYPQLSAHGKQAVIHAPEDLTVSGDPPDKLARVFNNILKNAAY-S  286
      : * : : . . : . . * : : . * : : * *
VanSB  PQGGEVRIWSEPGAKEYRLSVLNMGVHIDDTALS KLFIPF YRIDQARSRKSGRSGLGLAI  414
VanSSC PGRGRVWIHTAAGPRTRLVVENTGDLISPHQASTLLEPFQRGTERIHTDHPGVGLGLAI  327
VanSA  EDNSIIDITAGLSGDVVSIEFKNTG-SIPKDKLAAIFEFKYRLDNARSSDTGGAGLGLAI  345
      . : * : . : . * * * : : * * : . * * * *
VanSB  VQKTLDAMS LQYALEN-TSDGVLEFWLDLPPTSTL-----  447
VanSSC VNTITQAHDGTLTLTPRHSGGLRVTVELPAAAPHTGR---  364
VanSA  AKEIIVQHGGQIYAES-NDNYTTFRVELPAMPDLVDKRRS  384
      . : . . . : * * .

```

Figure 3.1.3: CLUSTALW2 sequence alignment of the VanS_A, VanS_B and VanS_{SC} protein sequences. Extracellular sensor loops are highlighted in green text. Transmembrane-spanning helices are highlighted in red text. HAMP domains are highlighted in blue text. Conserved motifs are outlined in boxes – ‘H’ in brown, ‘N’ in green, ‘G1’ in purple, ‘F’ in pink and ‘G2’ in orange. Transmembrane helices shown were predicted using TMPred software (Hofmann and Stoffel, 1993) (and checked against other software e.g. TopPred (von Heijne, 1992) and PSIPred (Jones, 1999). HAMP domains were predicted using SMART bioinformatic software (Letunic et al., 2012).

Figures 3.1.2 and 3.1.3 show the sequences of conserved regions (H, N, G1, F, and G2 boxes) which identify the proteins as histidine kinases. These regions are involved in autophosphorylation and contain residues that directly interact with ATP. The direct link between the H-box and other four boxes categorises them as class I HKs (Dutta et al., 1999).

Interestingly, the VanS_A protein does not contain a HAMP domain (Hulko *et al.*, 2006), whereas VanS_B and VanS_{SC} proteins do. These domains are believed to possess a role in regulating phosphorylation of kinases by transmitting conformational changes in the periplasmic sensor domain to the cytoplasmic kinase domain (see section 1.5.5). HAMP domains could therefore be implicated in the observed activity of each VanS protein.

Currently, there are no structures of a VanS sensor histidine kinase in the Protein Data Bank (PDB), which would be highly beneficial in order to characterise the structural and mechanistic basis of VanS catalysis. Several crystal or NMR structures do exist though for the soluble cytoplasmic domains of histidine kinases, with and without bound response regulators (Casino *et al.*, 2009; Marina *et al.*, 2005; Tanaka *et al.*, 1998), which have provided structural information on the architecture of the kinase domain and its interaction with the response regulator receiver domain (see section 1.5.5). Recently, the first structure of a full-length histidine kinase (YF1) was published (Diensthuber *et al.*, 2013), which shows that coiled coil regions like those in HAMP domains, are crucial in signalling (section 1.5.6). However, there is little sequence similarity between VanS and YF1, and the precise mechanism of ligand binding and autophosphorylation of VanS is not fully understood, in particular with relation to the nature of the signalling molecule that induces VanS activity.

This chapter details the cloning, expression, purification and crystallisation of full-length VanS enzymes in detergent environments, for structural and mechanistic characterisation, with comparison to previous data by Quigley, (2010) and Wright *et al.*, (1993). The main goal of this work is to obtain a more detailed understanding of the atomic structure of VanS proteins derived from enterococci and *Streptomyces* bacteria and increase knowledge of the signalling mechanism that underpins glycopeptide resistance. This could contribute toward rational design of novel inhibitors of Two-Component Systems and more targeted therapies to combat bacterial resistance mechanisms, which are in critical need due to the recent emergence of VRE and more virulent, VRSA in hospitals (Murray, 2000; Hiramatsu, 2001).

Previous work by Dr. Andrew Quigley at the University of Warwick (Quigley, 2010), provided some biochemical characterisation of full-length VanS from *Enterococcus faecium* (VanS_A) and of truncates containing only the cytoplasmic kinase domain (MBP-VanS_AΔ95 and VanS_AΔ110 – Δ155). Full-length and truncated VanS_A proteins were shown to be active with respect to autophosphorylation and phosphotransfer using coupled enzymatic assays (see section 2.9) or radiolabelling assays using [γ -³²P]ATP. VanS proteins from *E. faecium* (VanS_A) and *S. coelicolor* (VanS_{SC}) were therefore expressed and purified, and tested in the phosphorylation assays developed within the Warwick group (Quigley, 2010) to increase understanding of the mechanism of autophosphorylation in different VanS species.

Prior to Dr. Andrew Quigley, studies were carried out by Dr. Michael Williams at the University of Warwick (Williams, 2007), in collaboration with Dr. Marek Brzozowski and Justyna Korczynska (University of York), which provided several potential crystals of C-His-tagged VanS_A proteins, the best of which diffracted to 8Å. By analysing the conditions that yielded these crystal hits, attempts were made to improve crystal growth and obtain higher resolution diffraction patterns crystals by selecting appropriate membrane mimetics.

3.2 Aims

- (i) To clone *vanS* genes from two different backgrounds (*E. faecium*, *S. coelicolor*) into new, tag-cleavable vectors for high level expression and selective purification of wild-type VanS proteins by affinity chromatography.
- (ii) To test the activity of purified VanS proteins using coupled-enzymatic assays, to improve upon knowledge of the phosphorylation mechanism in different species.
- (iii) To obtain active, homogenous and natively folded wild-type (tag-cleaved) VanS protein samples for use in crystallographic studies on 96-well plates.
- (iv) To crystallise tag-cleaved VanS proteins (and improve upon the 8Å crystals previously obtained for C-His-tagged VanS_A in DDM) by testing conditions that yielded these hits and by screening for hits in other detergent classes.

3.3 Cloning *vanS* genes into Expression Vectors

Full-length wild-type *vanS* genes derived from *Enterococcus faecium* (termed *vanS_A*) and *Streptomyces coelicolor* (termed *vanS_{SC}*) were provided by Dr. David Roper. These genes were contained within a pTTQ18 vector (for *vanS_A*) or a pGEM T-easy vector (for *vanS_{SC}*). Previous studies at Warwick University by Quigley (2010) aimed to obtain crystals of the VanS_A protein by expression and purification from pTTQ18::*vanS_A* constructs. The pTTQ18 vector encodes a C-terminal hexa-histidine tagged protein, but the tag cannot be removed. Therefore, in these PhD studies the *vanS_A* and *vanS_{SC}* genes were amplified by Polymerase Chain Reaction (PCR, section 2.4.1) and cloned into pProEx HTa vectors (Addgene) for recombinant expression. These vectors encode an N-terminal hexa-histidine tag and contain a TEV-cleavable linker in front of the *vanS* gene sequence (Figure 3.3.1). In this way, the N-terminal hexa-histidine tag aids expression of the resulting protein and enables selective purification by immobilised metal affinity chromatography (IMAC, see section 2.6.6), and the tag can subsequently be cleaved (by TEV protease) to obtain the wild-type protein. Cleavage of the His-tag is preferential to obtain protein samples with a more native fold (and to remove impurities) for use in activity assays and crystallisation trials.

```
251 ACACAGGAAACAGACCATGTCGTACTACCATCACCATCACCATCACGATTACGATATCCCAACGACC
                               Start                               His6
318 GAAAACCTGTATTTTCAGGGCGCCATGGATCCGGAATTCAAAGGCCTACGTCGACGAGCTCAACTAG
    TEV protease site      NcoI
385 TCGGCGCCGCTTTTCGAATCTAGAGCCTGCAGTCTCGAGGCATGCGGTACCAAAGCTTGGCTGTTTTGG
                                               HindIII
```

Figure 3.3.1: Restriction map of the pProEx HTa plasmid between bases 251 and 450. Restriction sites are in red, and start codon (ATG), His₆ and TEV cleavage site are underlined. The *vanS* genes were cloned between the two restriction sites, with the region between these sites removed by enzymatic digestion of the pProEx HTa plasmids.

To insert the *vanS* genes into pProEx vectors, forward and reverse oligonucleotides were designed against template *vanS* sequences (Table 2.4.1), incorporating either an *NcoI* restriction site (5' end, forward primer) or a *HindIII* restriction site (3' end, reverse primer). This allowed amplification of plasmid DNA by PCR (section 2.4.1) (Figure 3.3.2) with restriction sites at either end of the gene. The PCR products were then double-digested (*NcoI*, *HindIII*) (section 2.4.3) alongside pProEx HTa plasmids, and provided compatible sticky ends for ligation. The high GC content of *Streptomyces vanS*, relative to *Enterococcal vanS* required higher annealing temperatures (68°C) and the use of GC-rich *Taq* polymerases in order to obtain gene products.

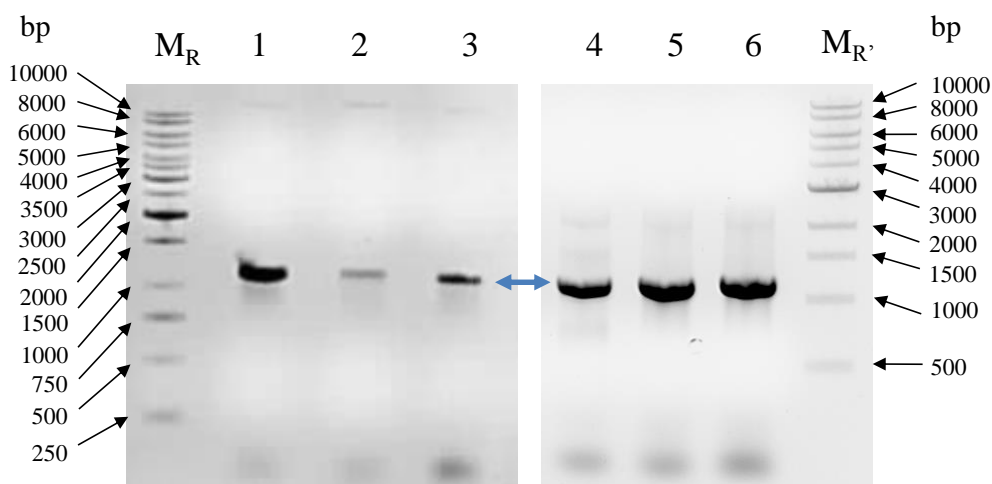


Figure 3.3.2: A 0.8% agarose gel (inverted image) showing the PCR amplification of (a) *vanS_A* and (b) *vanS_{SC}* genes. *M_R* - GeneRuler 1kb DNA ladder, *M_R*' - Quick-Load 1kb ladder, (a) Lane 1-3 *vanS_A* gene (1152 bp length) (b) Lane 1-3 *vanS_{SC}* gene (1104 bp length), showing intense bands of DNA obtained using the GC-rich *Taq* polymerase.

Double-digested PCR products and pProEx plasmids were then ligated (section 2.4.7), and the mixture used to transform *E. coli* TOP10 cells (Table 2.2.2.1) (section 2.3) and extract DNA from positive transformants by minipreparations (section 2.4.4). To check the *vanS* insert was present, minipreparations were digested with *NcoI* and *HindIII* enzymes (Figure 3.3.3), and sequence identity was confirmed by Sanger sequencing (section 2.4.8), which showed in-frame *vanS* sequences, without DNA mutations.

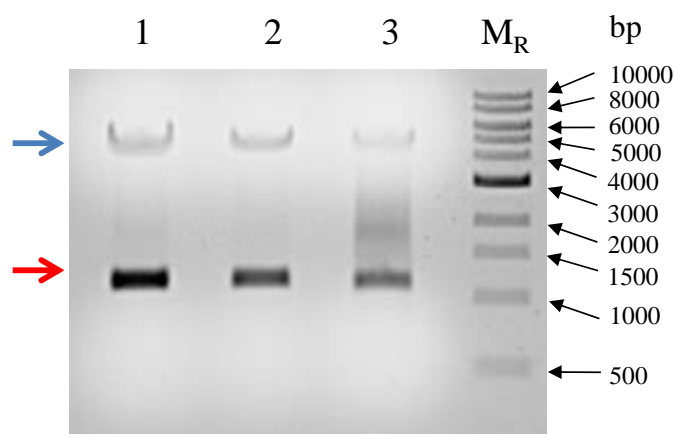


Figure 3.3.3: An 0.8% agarose gel (inverted image) showing correctly-sized gene sequences after *NcoI/HindIII* double-digestion. M_R – Quick-Load 1Kb ladder; Lane 1 – control *pProEx* plasmid containing *ape* gene from *Neisseria gonorrhoeae*, Lane 2 - digested *pProEx::vanS_A* gene, Lane 3 – digested *pProEx::vanS_{SC}* gene. Each digestion shows a gene insert at ~1100 bp (red arrow), and a cut linear vector at ~5000 bp (blue arrow).

3.4 Expression of VanS constructs

Previous work by Dr. Andrew Quigley showed that expression from the *pTTQ18::vanS_A* construct (for C-His₆-VanS_A) using the “Walker strains” (Miroux & Walker, 1996) (C43 or C41(DE3)) co-transformed with *pRIL* plasmids (Table 2.2.2.1) improved expression level of *Enterococcal* VanS proteins, as they are more tolerant to toxic proteins. Therefore the *pTTQ18::vanS_A* construct was used as a guide to test previous conditions, prior to optimising conditions for the new *pProEx::vanS* constructs. C41 and C43(DE3).*pRIL* cell lines were tested for expression from *pTTQ18::vanS_A* constructs by using small-scale trials and analysing on SDS-PAGE gels (see section 2.6.1) (Figure 3.4.1). C41 or C43 cells were added to overnight cultures and used to inoculate 100 ml LB containing ampicillin and chloramphenicol, as described in section 2.5.1. VanS proteins were overexpressed with IPTG for 4 hours at 37°C (as previously used by Dr. Andrew Quigley (Quigley, 2010) in the Warwick group), and analysed by SDS-PAGE after extraction of the membrane fraction from whole cells using a technique known as Water Lysis (Ward *et al.*, 2000) (see section 2.5.2), which produces membrane proteins via an osmotic shock procedure.

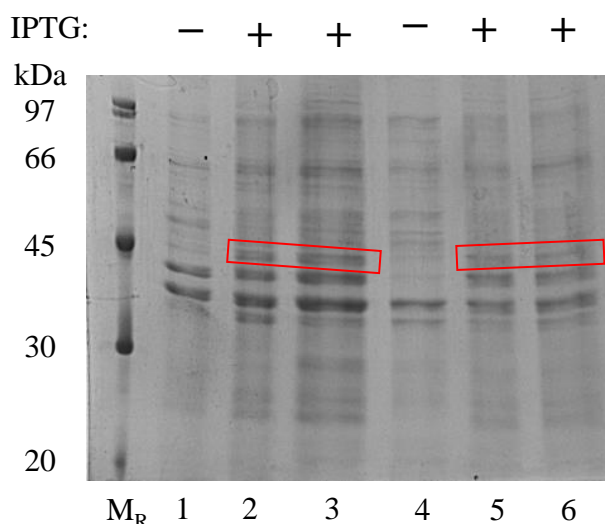


Figure 3.4.1: A 12% SDS-PAGE gel showing proteins overexpressed in C41 or C43 (DE3) *pRIL* cell lines after Water Lysis preparations. VanS proteins overexpressed with IPTG (+) are highlighted in red boxes (~ 44 kDa), against uninduced (-) controls. Mr - Protein ladder (LMW-SDS, GE Healthcare), lanes 1 – 3 - C41 cell line, lanes 4 – 6 – C43 cell line. For lanes 2-3 and 5-6, 0.2 mM IPTG inducer was added.

These membrane preparations showed that VanS proteins were not the major band on SDS-PAGE gels, but were being overexpressed, therefore further optimisation of current protocols was required. It is known that membrane proteins can be toxic to the cell, and these Walker strains can help prevent this, as they are able to tune the rate of transcription to harmonise with translation, such that saturation of the Sec translocon does not occur, and proteins are inserted correctly into the membrane (Wagner *et al.*, 2008). However, transcription prior to induction with IPTG can occur, known as “leaky expression”, in which the cell uses carbon sources such as glycerol to stimulate transcription. This can be reduced by the “glucose effect” or “catabolite repression”, which lowers transcription from the *lac* promoter (Kolb *et al.*, 1993). Therefore 0.2% w/v autoclaved glucose was added and small-scale expression trials repeated. Furthermore, a cell growth curve was constructed to determine the optimal level of inducer (IPTG) for the VanS_A expression system. Growth curves were monitored at different concentrations of IPTG relative to an uninduced control, and the resulting preparations were analysed by SDS-PAGE experiments (Figure 3.4.2).

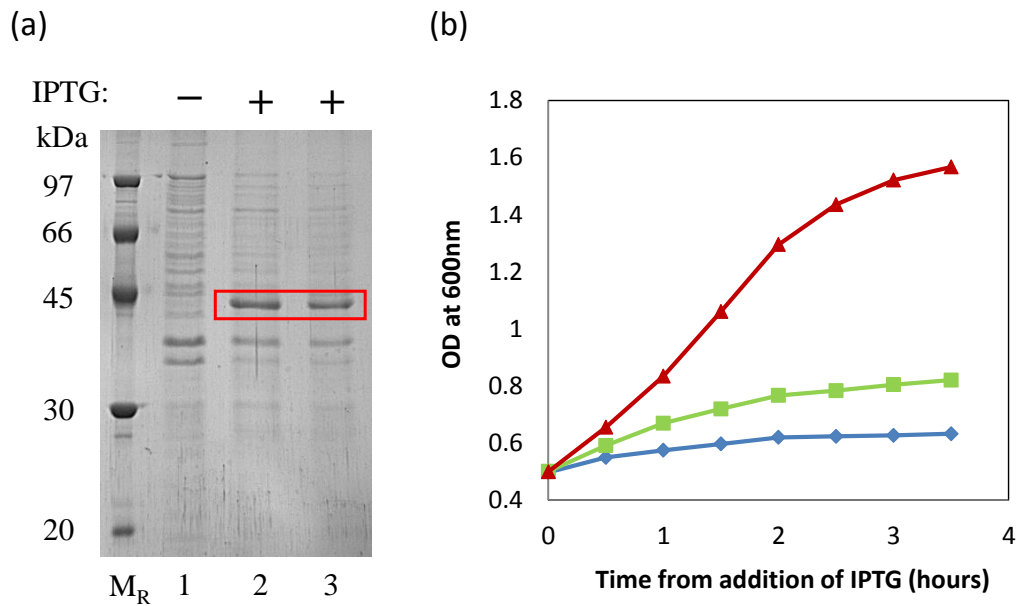


Figure 3.4.2: (a) An SDS-PAGE gel showing overexpressed proteins from *pttQ18::vanS_A* in *C41pRIL* cells at varying [IPTG] and (b) corresponding growth curves. Samples loaded had been processed by Water Lysis, and VanS proteins overexpressed with IPTG (+) are highlighted in red boxes (~ 44 kDa), against uninduced (-) controls. M_R – Protein ladder, lane 1 – 0 mM IPTG added, lane 2 – 0.2 mM IPTG added, lane 3 – 1 mM IPTG added. For the growth curves, each line is a concentration of IPTG inducer; 1 mM (blue line), 0.2 mM (green line), 0 mM (red line).

These trials showed a dramatic effect on expression level upon adding glucose, producing C-His₆-VanS_A proteins as the major species (~ 45kDa, theoretically 43,916 Da); with concomitant reduction in ‘leaky’ expression of other *E. coli* proteins (see Figure 3.4.2). The Water Lysis method also provided a clear visualisation of the protein expression level, as it extracts only soluble proteins in the membrane fraction, and therefore reduces interference from other naturally expressed cytosolic proteins. Growth curves monitored over 4 hours post-induction indicated that upon addition of IPTG, the rate of increase of optical cell density (OD, measured at 600 nm) was lowered, hence the cells were under strain to overexpress VanS proteins. Furthermore, 0.2 mM IPTG inducer gave greater cell densities and increased VanS yield, relative to 1 mM IPTG inducer, and was therefore the optimum concentration of inducer.

With this information in hand, small-scale expression was trialled for the novel pProEx::*vanS_A* and pProEx::*vanS_{SC}* constructs (encoding N-His₆-VanS_A), overexpressed in LB media, with addition of 0.2% w/v glucose and both ampicillin and chloramphenicol antibiotics (section 2.5.1), and processed by Water Lysis (Figure 3.4.3).

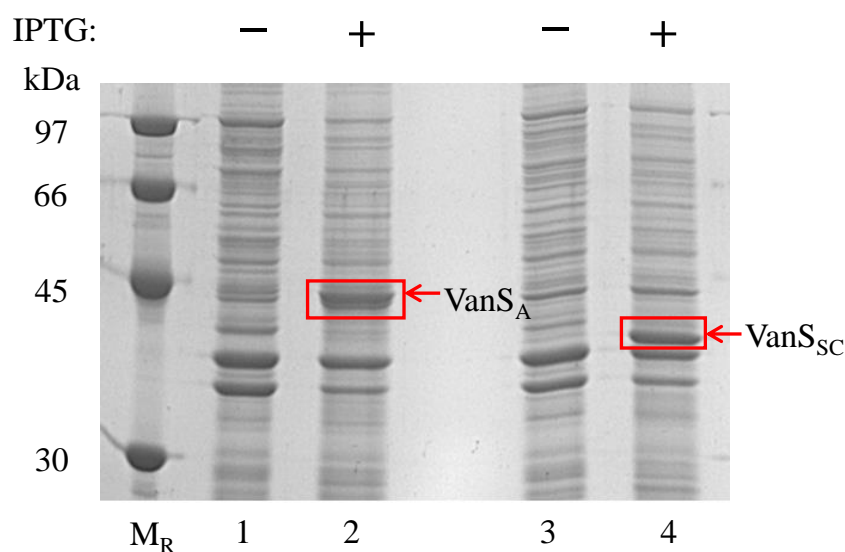


Figure 3.4.3: 12% SDS-PAGE gel showing overexpression from pProEx::*vanS_A* or pProEx::*vanS_{SC}* constructs in C41pRIL cells, after Water Lysis. VanS proteins overexpressed with 0.2 mM IPTG (+) are highlighted in red boxes and labelled, against uninduced (-) controls. Mr – Protein Marker (GE), lanes 1-2 – expression from pProEx::*vanS_A* and lanes 3 – 4 – expression from pProEx::*vanS_{SC}*.

Figure 3.4.3 shows that the major expressed protein bands were at ~45 kDa, which corresponds to the molecular weight of His₆-TEV-VanS_A (47,012 Da theoretically), and at ~40 kDa, which corresponds to the molecular weight His₆-TEV-VanS_{SC} (42,620 Da theoretically). However, to confirm that these observed bands were indeed the His₆-tagged VanS proteins, anti-histidine Western blots were required, which are discussed section 2.6.3.

As a final experiment, the temperature for induction was lowered and cells were grown over a longer time, to reduce the propensity for protein misfolding or unfolding. If proteins are highly overexpressed in *E. coli* but misfolded, this can lead to formation of insoluble aggregates known as inclusion bodies. Therefore the temperature for inductions was lowered to 25°C and small-scale expressions were induced as before at mid-log phase, but allowed to grow for 12-16 hours to increase cell density. SDS-PAGE analyses (Figure 3.4.4) showed marginal increases in expression level of soluble protein compared to those grown at 37°C, and VanS proteins are still the major species. Protein unfolding is increased at higher temperatures, therefore the fold at 25°C is likely to be better stabilised, and was selected in future expressions.

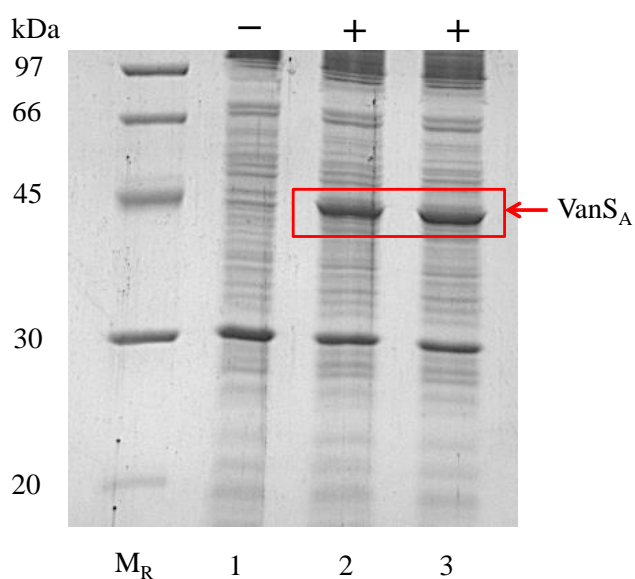


Figure 3.4.4: A 12% SDS-PAGE gel showing expression from *pProEx::vanS_A* at 25°C overnight prepared by Water Lysis. *M_R* – Protein ladder (GE Healthcare), Lane 1 – 0 mM IPTG, Lane 2 – 0.2 mM IPTG, Lane 3 – 1 mM IPTG.

3.5 Western Blotting for His-tagged VanS proteins

To confirm the expression of His-tagged VanS proteins, anti-His Western blots were performed (section 2.6.3) and run alongside SDS-PAGE gels for direct comparison. At this point expression was still carried out at 37°C for 4 hours to confirm the observed bands were indeed VanS proteins. Initial Western blots used primary anti-His antibodies (Roche) to bind to polyHis-tagged proteins, and were developed (after addition of secondary antibody) by electrochemical luminescence (ECL) as described in section 2.6.3. Two SDS-PAGE gels were run simultaneously with identical samples loaded, one of which was blotted.

The positions of bands in the blot corresponded well with SDS-PAGE bands of proposed VanS proteins, and it was observed that C-terminal His-tagged (pTTQ18) VanS_A and N-terminal His-tagged (pProEx) VanS_{SC} were visible from the blot, but no bands were observed for the N-terminal His-tagged (pProEx) VanS_A protein (Figure 3.5.1).

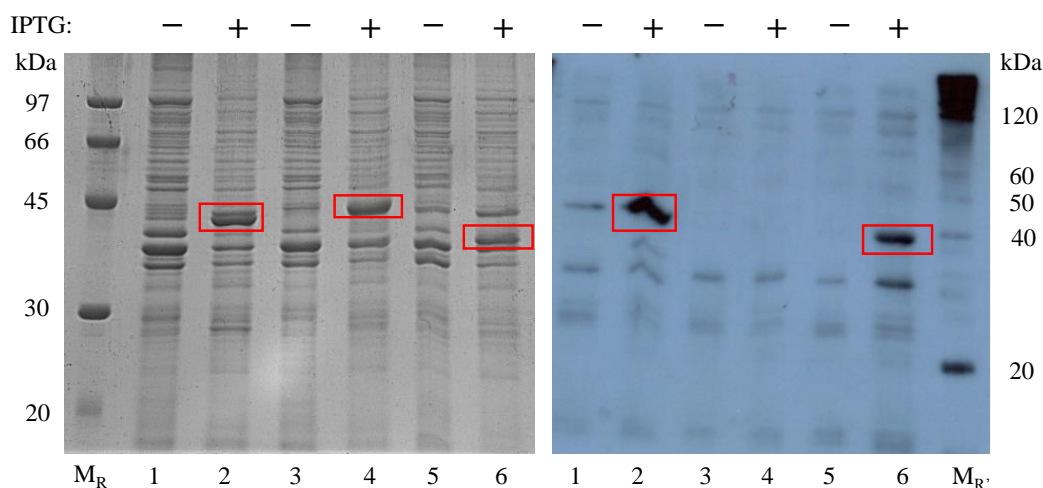


Figure 3.5.1: (left) 12% SDS-PAGE gel of Water Lysis preparations, and (right) equivalent Western blot developed using Roche non-specific anti-His antibodies. All *vanS* constructs were transformed into C41pRIL cells, and either not induced (-) – Lanes 1, 3, and 5, or induced with 0.2mM IPTG (+) – Lanes 2, 4, and 6 for 4 hours at 37°C. Lanes 1 & 2 were transformed with pTTQ18::*vanS_A*, Lanes 3 & 4 were transformed with pProEx::*vanS_A* and Lanes 5 & 6 were transformed with pProEx::*vanS_{SC}*. M_R – Protein marker (GE), M_R' – Benchmark His-tagged Ladder (Invitrogen). VanS proteins are highlighted by red boxes.

Since all three VanS proteins appear to be expressed and only one VanS proteins was not visible on the blot, it was likely that there was reduced interaction between the antibody and the tag, e.g. the protein fold rendering the binding site inaccessible. The manufacturer's instructions stated that these anti-His antibodies were 'non-specific', i.e. can bind to N- or C-terminal His-tags if exposed. By examining commercially available antibodies, it was found that anti-His antibodies have also been designed which bind preferentially to N-terminal tags (Sigma). VanS protein samples were loaded onto SDS-PAGE gels, and analysed by blotting, using the same protocol but adding the novel anti-His primary antibodies (Figure 3.5.2).

The SDS-PAGE gels and corresponding blots demonstrated that the N-terminal His-tagged VanS_A protein was being expressed and the bands were much clearer for the N-terminal tagged proteins, compared to C-terminal, demonstrating the preference of the antibody. Therefore hexa-histidine tagged VanS membrane proteins were being expressed, without cleavage *in vivo*, and in a soluble form, and could now be selectively purified using this tag.

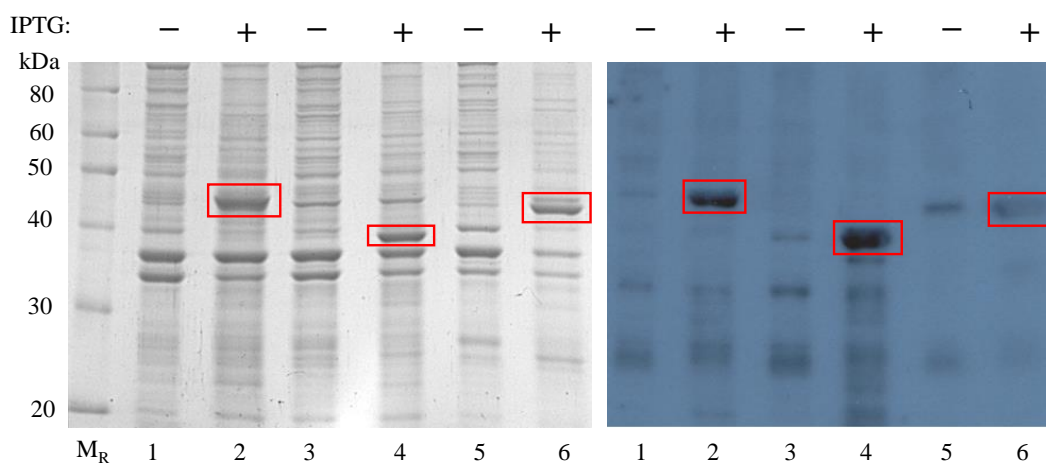


Figure 3.5.2: (left) 12% SDS-PAGE gel for Water Lysis preparations, and (right) equivalent blots developed using Sigma N-term preferential anti-His antibodies. All *vanS* constructs were transformed into C41pRIL cells, and either not induced - Lanes 1, 3, and 5, or induced with 0.2mM IPTG - Lanes 2, 4, and 6 for 4 hours at 37°C. Lanes 1 & 2 were transformed with pProEx::*vanS_A*, Lanes 3 & 4 were transformed with pProEx::*vanS_{SC}* and Lanes 5 & 6 were transformed with pTTQ18::*vanS_A*. M_R - Benchmark His-tagged Ladder (Invitrogen). VanS proteins are highlighted by red boxes.

3.6 Purification of VanS Membrane Proteins by IMAC

Attempts were now made to purify VanS proteins by extracting them from the *E. coli* inner membrane and then selectively purifying the histidine-tagged proteins by immobilised metal affinity chromatography (IMAC). For small-scale purification, published Water Lysis methods, developed in Professor Peter Henderson's laboratory (Leeds University) were used (Ward *et al.*, 2000) (see section 2.5.2). These involve formation of spheroplasts by lysing cells under osmotic shock and subsequent centrifugation (at $\leq 50,000g$) to pellet membranes. However, previous work carried out in the Warwick group by Quigley (2010), showed that scale-up and the use of sucrose gradients (to separate inner and outer membranes), gave low yields of C-His-tagged VanS, due to apparent localisation of VanS to the outer membrane.

By working at the Membrane Protein Laboratory (MPL, Harwell), Quigley (2010) found that higher yields could be obtained by lysing the expressed cell pellet with a continuous cell disruptor (shears cells by forcing them through a mesh), obtaining membrane pellets by ultracentrifugation and solubilising the membranes directly in (DDM) detergent prior to IMAC. This method can impinge on final purity as it gives the opportunity for further contaminants to be solubilised, but extraction with detergents is widely used for membrane proteins both within the research group and wider science community, reflecting its success.

Expressed cell pellets containing N-terminal His-tagged VanS_A proteins were therefore treated this way (see section 2.5.3). Large-scale expressions (1-6 L, section 2.5.1) were induced at 25°C for 12 hours, and cells pelleted, and lysed by cell disruption. Membranes extracted from the lysate by ultracentrifugation were solubilised in 1% w/v DDM overnight. The protein-detergent mix was then ultracentrifuged in order to pellet and remove insoluble material (not bound to detergent micelles), and the supernatant (soluble fraction) was applied to pre-charged, pre-equilibrated nickel-nitrilotriacetic acid (Ni-NTA) agarose resin, at a ratio of 1 mL bed volume of resin per 1 litre of expressed cell pellet.

The mix was allowed to rock for two hours then poured into a column, flow through collected and the resin was washed as described in section 2.6.6, before eluting VanS_A in a high-imidazole buffer. Fractions collected were then analysed by SDS-PAGE (Figure 3.6.1). The Ni-NTA agarose resin was used as it allows high binding capacity and minimal non-specific binding, up to 5-10 mg of His-tagged protein per mL of resin.

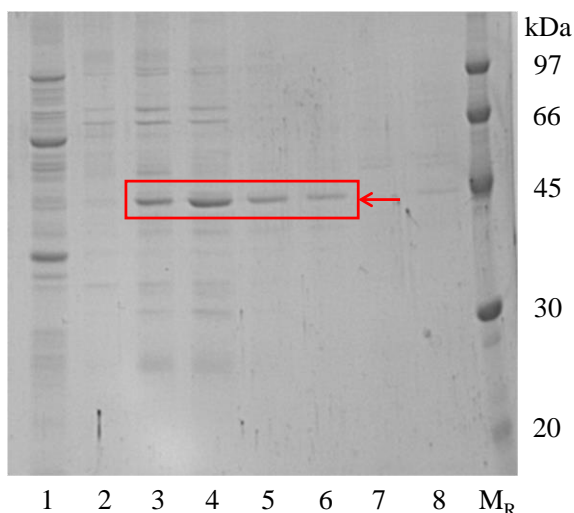


Figure 3.6.1: A 12% SDS-PAGE gel showing N-His₆-VanS_A purification by affinity chromatography. Membranes were solubilised in 1% DDM from 5L of expressed cells containing VanS_A, and purified in buffer containing 0.05% DDM. Lane 1 – 20mM Imidazole eluate, Lane 2 – 50mM Imidazole eluate, Lane 3-6 – 300mM imidazole eluates (2.5 mL volume each). VanS_A protein bands are highlighted.

Unfortunately, even from a 5L expression relatively low yields of around 1-2 mg of purified N-His₆-VanS_A membrane protein were being obtained, as calculated using the BCA protein concentration assay (see section 2.6.10), which was lower than that obtained for the C-His₆-VanS_A protein previously (~1 mg per Litre by Quigley, 2010), and the purity appeared reduced, due to some non-specific binding. By assessing protein yield at each stage, it was found that even after solubilising a freshly expressed and processed membrane pellet in DDM detergent, only ~ 40 % of protein remained in the soluble fraction (Figure 3.6.2), therefore the N-His₆-VanS protein was not stable in DDM micelles.

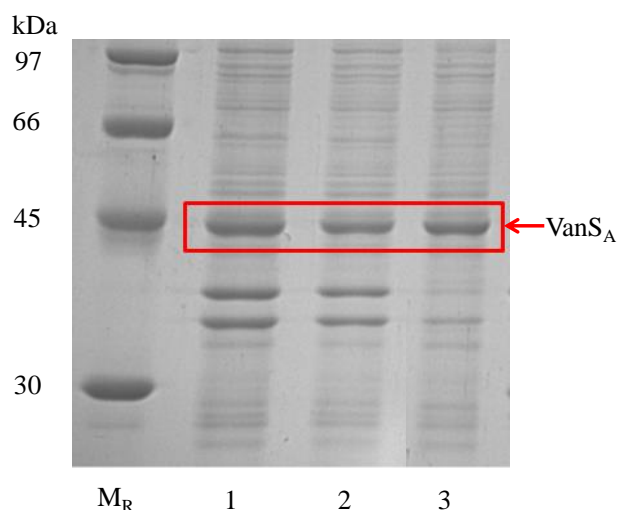


Figure 3.6.2: A 12% SDS-PAGE gel of *N-His₆-VanS_A* extraction into DDM micelles. Membranes were extracted in 1% DDM from 1L of cells containing *VanS_A*, (lane 1) and ultracentrifuged at 40 krpm. Lane 2 – soluble fraction, Lane 3 – insoluble fraction.

In order to select a better detergent for solubilisation, a detergent screen (see section 2.6.5 and Appendix Table 1) was set-up for *VanS_A* as well as *VanS_{SC}* proteins (extracted from membranes by the same method as before, as detailed in section 2.5.3). These screens included higher purity ANA-GRADE DDM (Affymetrix), to ensure the low solubility was not a function of the SOL-GRADE DDM (Melford) used. Detergents tested were chosen based on their success in the literature to extract and reconstitute membrane proteins (Newby *et al.*, 2009). These included LDAO and maltoside detergents (DM, DDM), which are commonly used in protein extraction prior to crystallisation, and DPC detergent, which is routinely used in solution state NMR studies. The selection of a particular detergent for crystallographic study is based on its ability to extract a large quantity of soluble, as well as stable and active protein. In comparison, a suitable detergent for NMR studies is one that has a small micelle size in order to permit rapid tumbling of the associated protein-micelle complex in solution (giving long T_2 spin-spin relaxation rates). For this reason, DDM, which forms micelles of 50-70 kDa is only used in crystallography studies, whereas e.g. DPC detergent, which forms micelles of 15-25 kDa, can be used in both crystallographic and NMR studies.

Detergent screens essentially involved solubilising a fixed volume (1 – 2 mL) of a resuspended membrane pellet in a detergent solution, then ultracentrifuging at 100,000 g, and collecting the supernatant (soluble fraction), and pellet (insoluble fraction). Aliquots of the soluble and insoluble fractions were then loaded onto an SDS-PAGE gel and transferred to PVDF membrane for Western blot analysis (Figure 3.6.3). All lanes contained a fixed volume of protein to directly measure the ratio of VanS proteins in soluble and insoluble fractions, and all pellet fractions were resuspended to the same initial volume in buffer. Unfortunately, LDAO detergents smeared on gels, so these samples were not blotted.

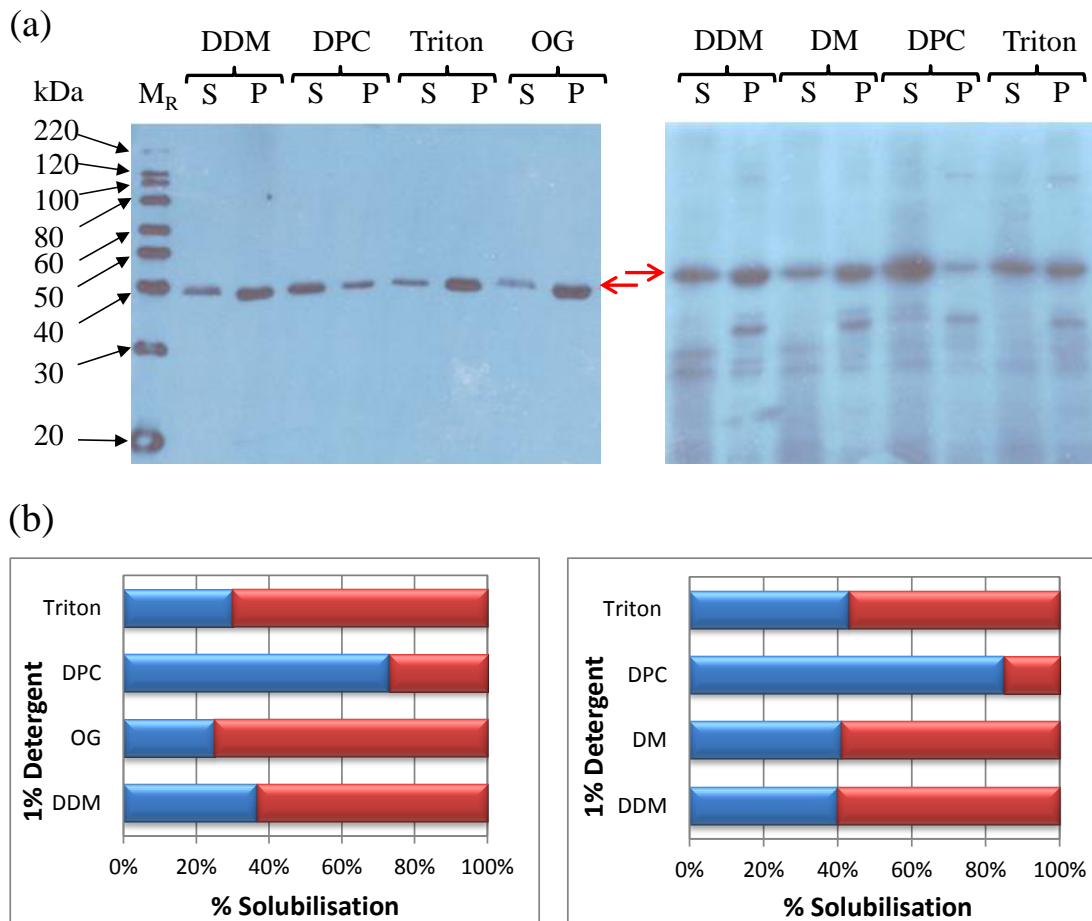


Figure 3.6.3: (a) Western blots showing detergent solubilisation of VanS_{SC} (left) or VanS_A (right) membrane pellets, and (b) corresponding bar charts of the relative percentages of soluble and insoluble protein. Soluble supernatant fraction – S, blue bar, insoluble pellet fraction – P, red bar. Solubilisation (%) was calculated from band sizing of the VanS band (red arrow) using ImageJ software. M_R – MagicMark His-tagged ladder. Western blots for VanS_{SC} showed reduced background as they were washed overnight before developing.

From these detergent screens, it was concluded that the non-ionic maltoside detergents (DM, DDM) could only solubilise ~40% of the VanS proteins, whereas zwitterionic DPC detergent (dodecylphosphocholine) gave the highest protein solubilisation at ~80%. This difference in solubility could be attributed to the head-group, since DPC and DDM have the same hydrocarbon chain, but DPC has a more native, lipid-like PC head-group (Figure 3.6.4).

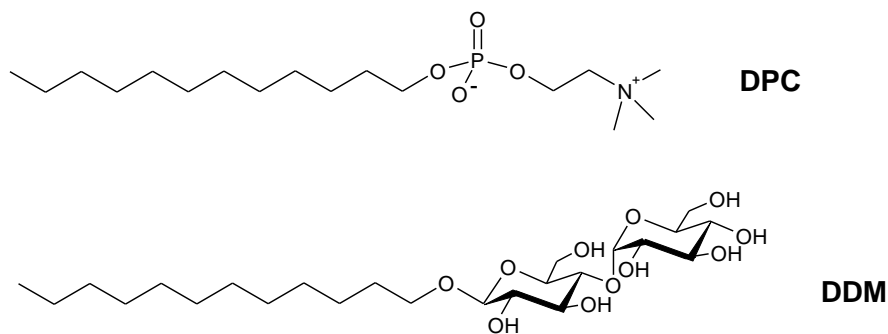


Figure 3.6.4: Molecular structures of DPC and DDM detergents, drawn in ISISDraw.

Previous attempts to crystallise the C-His-tagged VanS_A protein by Dr. Marek Brzozowski and Justyna Korczynska at York University (see Figure 3.6.5) identified several crystal hits in the presence of 0.05% w/v DDM, but the group could only achieve low resolution diffraction patterns ($> 8\text{\AA}$) in this detergent. Further screening by Dr. Andrew Quigley (2010) using the same crystallisation conditions could not repeat these protein crystals, and he concluded that reduced crystal packing, possibly due to the large steric size of DDM micelles (50-70 kDa), may have prevented hydrophilic regions from forming protein-protein contacts in the crystal (and hence giving low diffraction-quality crystals).

From the detergent screens conducted in this thesis, it appears that VanS proteins are relatively unstable in DDM, and the use of other detergents e.g. DPC may provide better conditions for crystal growth. DPC detergents form smaller micelles than those of DDM, which could allow closer protein-protein contacts within the crystal, thereby increasing crystal stability. This does however makes the assumption that the micelle size of each

detergent will be affected in a similar way upon insertion of the protein, but this could only truly be quantified experimentally e.g. by Dynamic Light Scattering (DLS). Both the mass and hydrodynamic radii of micelles will be affected by the addition of the protein, which inserts its transmembrane domains into the hydrophobic core of the micelle, thus altering the packing of the hydrocarbon tails and polar headgroups (Bond *et al.*, 2004). Therefore the actual micelle size is not necessarily predictable once the protein is added to the micelle. As a check of the average micelle size for VanS_A proteins extracted into DPC detergents, DLS measurements were briefly made using a Nano-Series Zetasizer (Malvern). This gave mean particle diameters (termed as ‘Z-average’) of ~13 nm and a particle size distribution dominated by a single population at ~ 10 nm (see Appendix Figure 1), which is within the range expected for DPC micelles (which have hydrodynamic radii of ~3.5 nm before addition of any protein) (Oliver *et al.*, 2013).

Based on the high solubility of VanS proteins in DPC micelles and the favourable hydrodynamic radii of their associated protein-micelle complexes, attempts were therefore made to purify N-His-tagged VanS_A (and VanS_{SC}) proteins in DPC, with a view towards conducting crystal screens in this detergent. As noted earlier, the best detergent for crystallization purposes is one that can solubilise protein at high concentrations, but also provides a homogeneous, stable and functionally-active protein sample. With this in mind, prior to crystallisation trials, VanS proteins were also analysed by Gel Filtration Chromatography (section 3.7); to test for a single sharp (homogeneous) peak, by CD spectroscopy (section 3.10); to test for a native protein fold, and by spectrophotometric assays (section 3.11); to test for functional activity of the kinase.

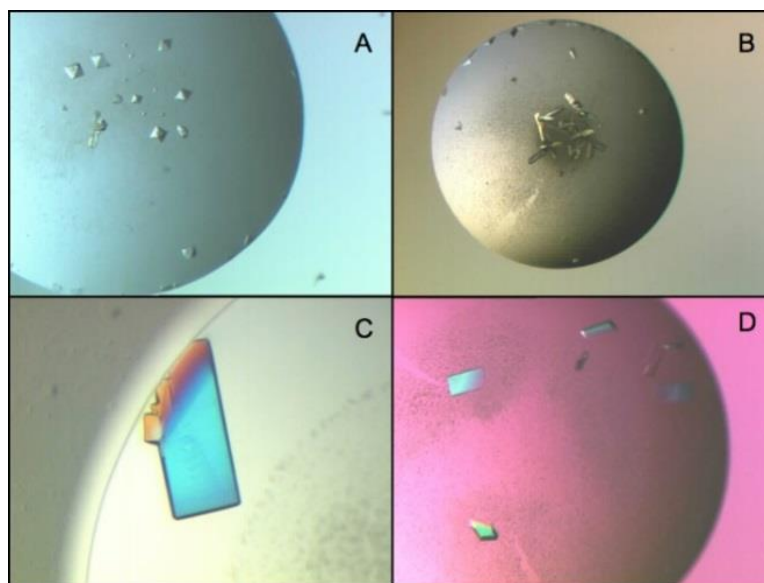


Figure 3.6.5: Crystallisation conditions for C-His₆-VanS_A at 18°C, identified by Dr Marek Brzozowski and Justyna Korczynska at York University. (A): VanS_A in 0.05% DDM, 10% PEG 4000 (w/v), 10% Glycerol, 0.1M Tris/HCl, pH8.5, (B): VanS_A in 0.05% DDM, 14% PEG 2000 (w/v), 0.1M NaCl, 0.1M LiSO₄, 0.1M Tris/HCl pH8.5, (C): VanS_A in 0.05% DDM, 10% PEG 3350 (w/v), 0.1M NaAc pH 4.5, (D): VanS_A in 50mM BOG, 30% PEG 400 (w/v), 0.1M LiSO₄, 0.1M Sodium Citrate pH 4.5.

First of all, N-His₆-VanS_A proteins had to be purified by metal affinity chromatography. Samples were solubilised in 1% w/v DPC detergent and applied to Ni-NTA agarose pre-charged, pre-equilibrated resin, and purified using the protocol given in section 2.6.6. Proteins were eluted in 0.075% DPC (~1.5x CMC), to compare with elution fractions obtained using DDM detergent (0.05%, ~2x CMC), and the resulting fractions were analysed on SDS-PAGE gels, loaded at 20 µg/ml per lane, or if lower concentration, the maximum volume for the lane (~25 µl) (see Figure 3.6.6). As observed from the gel in Figure 3.6.6, the quantity of purified VanS_A protein was vastly greater than in DDM, with around 3-4 mg of pure VanS per litre of culture.

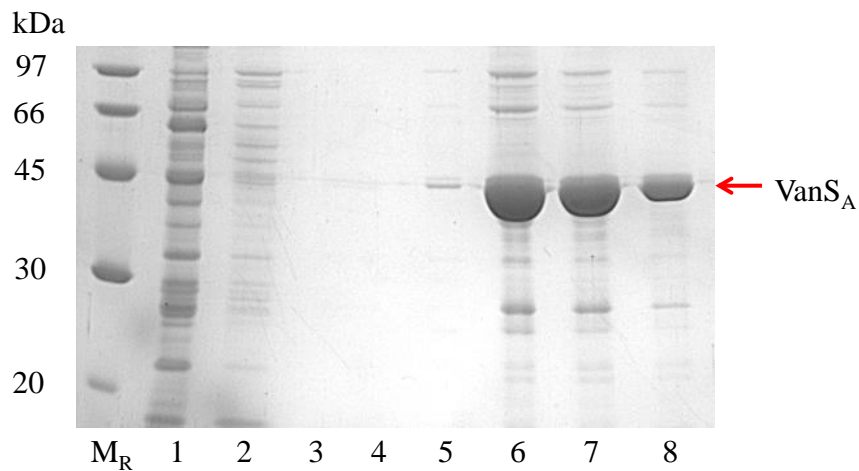


Figure 3.6.6: A 12% SDS-PAGE gel showing the purification of N-His₆-VanS_A by affinity chromatography. Membranes were solubilised in 1% DPC from 2L of expressed cells of VanS_A, and purified in buffer containing 0.075% DPC. M_R – Ladder (GE), Lane 1 – Flow through, Lanes 2-5 – 20 - 50mM Imidazole, Lane 6-8 – 300 mM Imidazole (2.5 mL volumes).

In contrast, attempts to purify N-His₆-VanS_{SC} proteins under the same protocols did not provide any protein in IMAC elution fractions. Examination of the yield of protein at each stage of purification by Western blotting (Figure 3.6.7), revealed that most of the protein expressed at 25°C (or 37°C) was insoluble, and pelleted with cell debris after lysing by cell disruption. In light of this poor solubility, the induction temperature was further decreased to 16°C for 18 hours and overexpressed cells containing VanS_{SC} proteins were purified and blotted (Figure 3.6.8). A much higher proportion of soluble protein was obtained (~50-60%) after cell disruption, which localised to the membrane fraction (lane 6). The resulting membrane pellet was subsequently solubilised in 1% w/v DPC and purified by IMAC and aliquots loaded onto SDS-PAGE gels (Figure 3.6.9).

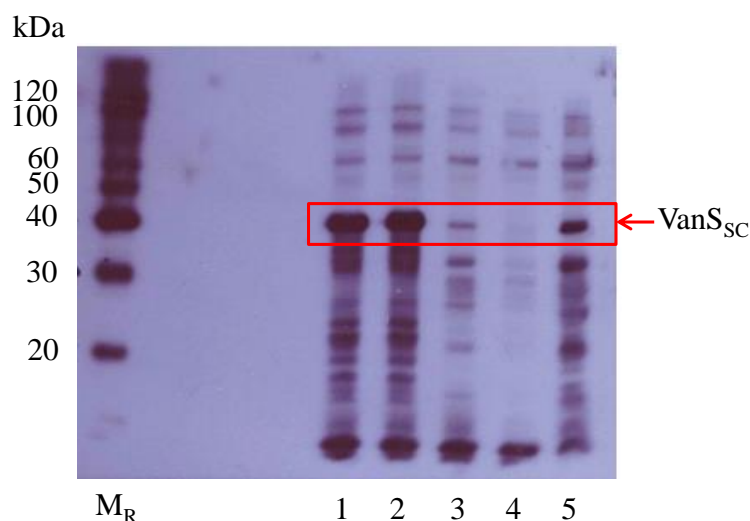


Figure 3.6.7: Western blot showing attempted purification of *N-His₆-VanS_{SC}* proteins expressed at 37°C. Lane 1 – Cell pellet, Lane 2 – Insoluble protein after cell disruption, Lane 3 – Soluble protein after cell disruption, Lane 4 – Supernatant from 40 krpm spin, Lane 5 – Pellet from 40 krpm spin (resuspended in a smaller volume) *M_R* – Benchmark ladder.

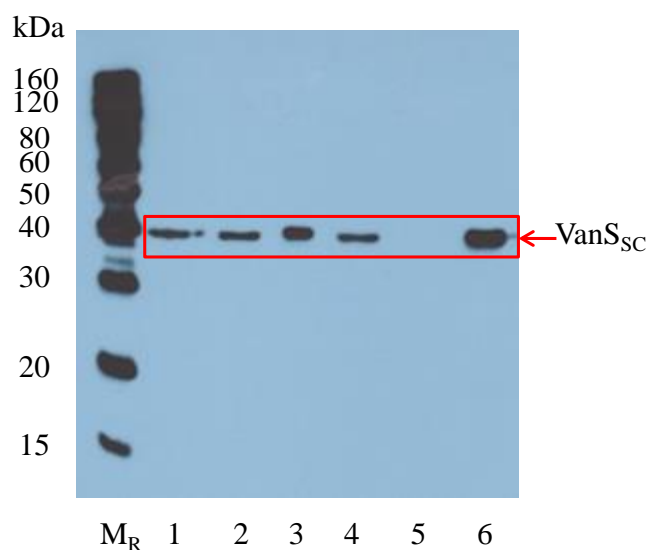


Figure 3.6.8: Western blot showing attempted purification of *N-His₆-VanS_{SC}* proteins expressed at 16°C. Lane 1 – Cell pellet, Lane 2 – Proteins after cell disruption, Lane 3 – Soluble protein, Lane 4 – Insoluble protein, Lane 5 – Supernatant from 40 krpm spin, Lane 6 – Pellet from 40 krpm spin (resuspended in a smaller volume). *M_R* – Benchmark Ladder.

VanS_{SC} protein purified by these methods gave about 1 mg of pure protein per litre in DPC, which is reasonable considering it is one of several major expressed bands and had to be overexpressed at low temperatures. In addition, studies by Koteva *et al.*, (2010), found that VanS_{SC} expressed in their constructs in BL21 (DE3) pLysS was toxic to the cell and also

required induction at 16°C. Therefore the culture size had to be increased to 6L or more to obtain enough protein for biochemical and biophysical studies (see Appendix Figure 2).

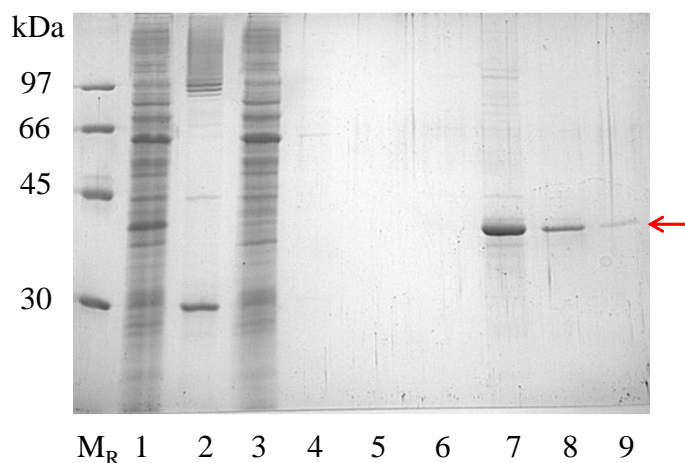


Figure 3.6.9: A 12% SDS-PAGE gel showing purification of N-His₆-VanS_{SC} proteins by affinity chromatography. 1L of cells expressing VanS_{SC} were purified to membranes and solubilised in 1% DPC. Lane 1: Soluble fraction, Lane 2: Insoluble fraction, Lane 3: Flow through, Lane 4-6 : 20 mM Imidazole, Lane 7-9: 300 mM Imidazole (2.5 mL elutions).

3.7 Purification of VanS proteins by Gel Filtration Chromatography

Elution fractions from IMAC containing VanS protein were next applied to PD10 desalting columns (see section 2.6.8) and further purified by Gel Filtration Chromatography (GFC) (see section 2.6.7). Improved separation of VanS proteins was achieved by applying samples that had been concentrated using 30 kDa MWCO concentrators (see section 2.6.8) to a Superose 12 Gel Filtration column (separation range 1-300 kDa), under an isocratic gradient of 100% B. As shown in Figure 3.7.1, the protein eluted as a single peak at elution volumes of 11.5 mL for VanS_{SC} and 11.8 mL for VanS_A (as identified by SDS-PAGE, see Figure 3.7.3). There is one other peak at 9 mL elution time, which contains aggregated protein at high molecular weight (>300 kDa), and represents the void volume of the column (V_0 , 9.0 mL). The single peaks at ~11-12 mL indicate that the protein is predominantly stable in DPC micelles, and should be amenable for crystallisation studies. Since the retention times of both proteins are similar, this could indicate that they exist also in the same oligomeric state.

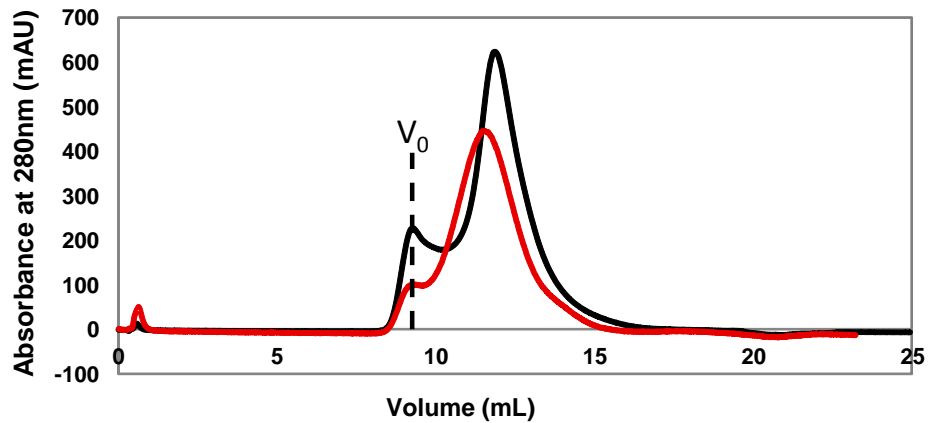


Figure 3.7.1: Gel Filtration Chromatograms for protein samples of VanS_A (black) and VanS_{SC} (red) applied to a Superose 12 column. An isocratic gradient of 100 % B was used (B: 20 mM HEPES pH 7.8, 300 mM NaCl, 0.075% w/v DPC).

By applying Gel Filtration standards to the column and running at the same flow rate and with the same buffer (Appendix Figure 3), it was possible to create a calibration curve of log(molecular weight) against elution volume, assuming a void volume of 9.0 mL (Figure 3.7.2). Plotting the relative retention times of VanS_A and VanS_{SC} proteins on this curve gave predicted molecular weights of around 80-90 kDa, and therefore it is expected the proteins migrate as dimers. However, all standards run were globular proteins, which may migrate differently to VanS membrane proteins, so the molecular weights are only a prediction.

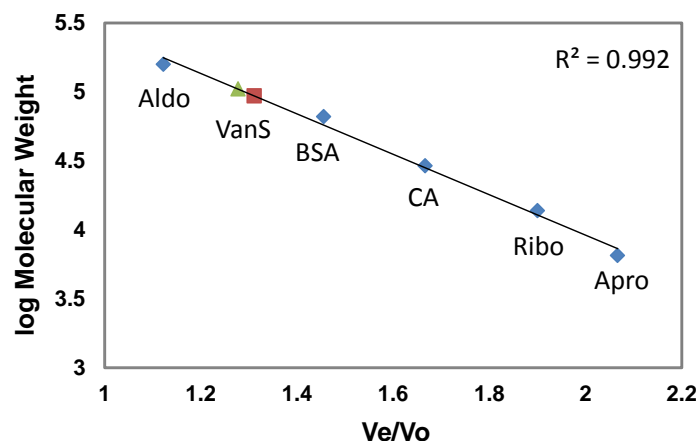


Figure 3.7.2: A calibration curve of gel filtration standards, plotted by the log of their weights against their elution times (V_e), relative to a void volume (V_o). Standards (blue dots) were applied to a Superose 12 column under an isocratic gradient. For full standard names see Appendix Figure 3. Using the equation for the line, values for the log(molecular weight) of VanS_A (red) and VanS_{SC} (green) were calculated and added.

SDS-PAGE analysis of gel filtration samples collected under the main peak confirm a pure band of VanS protein at ~40 -45 kDa, (Figure 3.7.3). There is also an impurity at ~100 kDa which is present throughout purifications, and could not be removed by Gel filtration chromatography. This could be AcrB (110 kDa), a histidine-rich *E. coli* expressed protein which co-elutes with many proteins during IMAC purifications (Veesler *et al.*, 2008). It is a further reason for choosing a construct that has an enzymatic cleavage site after the His-tag, since any AcrB impurities can be removed due to their high affinity for nickel resin, whilst the cleaved VanS wild-type protein is collected in the flow through.

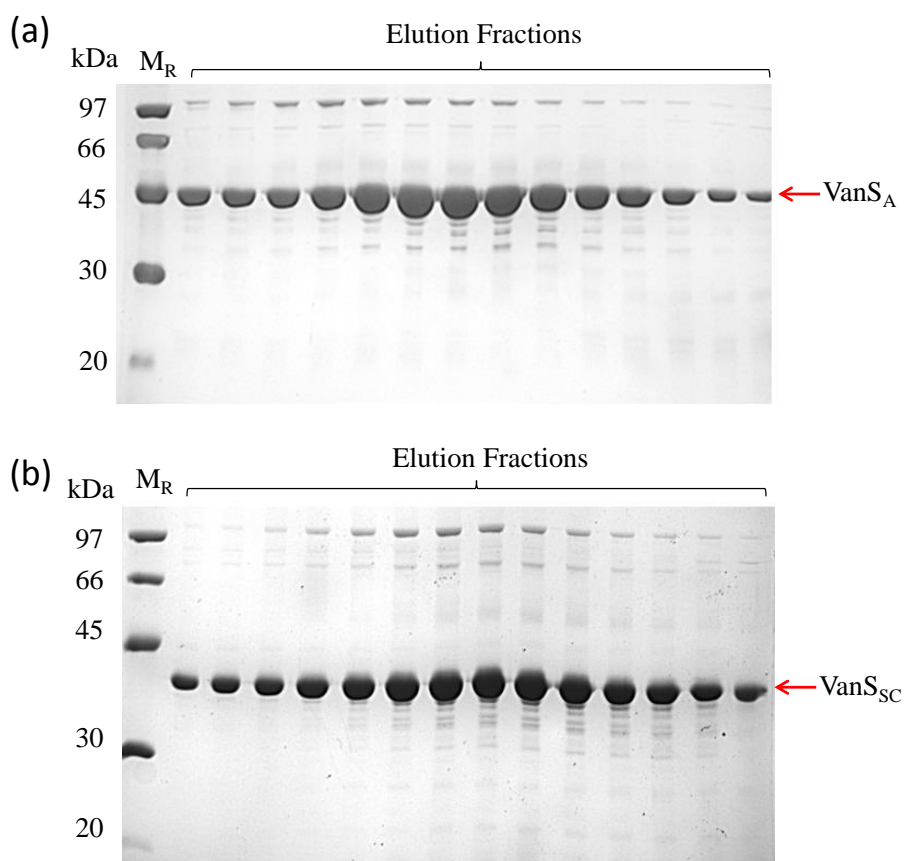


Figure 3.7.3: A 12% SDS-PAGE gels showing aliquots of 0.3 mL gel filtration elutions collected under the main peak (~10 -12 mL). *N-His₆-VanS_A* (a) and *N-His₆-VanS_{SC}* (b) proteins are indicated by red arrows.

3.8 Histidine Tag Cleavage for Crystallisation Trials

As mentioned above, in a number of studies, it has been observed that AcrB proteins spontaneously bind to IMAC resin and co-elute with the protein of interest. AcrB proteins also crystallise preferentially over membrane proteins, even at low concentrations (Bolanos-Garcia & Davies, 2006; Veessler *et al.*, 2008). Therefore by cleaving the His-tag, and subjecting the digest to a further round of IMAC purification, impurities like AcrB can be removed, to improve the chances of crystallising VanS proteins. Experiments to cleave the tag using tobacco etch virus (TEV, 27 kDa) (see section 2.12.1), found that relatively high concentrations were required to access the cut site, possibly due to its close proximity to the micelle surface (Figure 3.8.1). SDS-PAGE gels demonstrate the cleavage, with a mass reduction of ~3 kDa (the His-tag), and show that even 1:2 [TEV]:[protein] ratios did not provide 100 % cleavage (as some uncleaved protein remains bound to the resin).

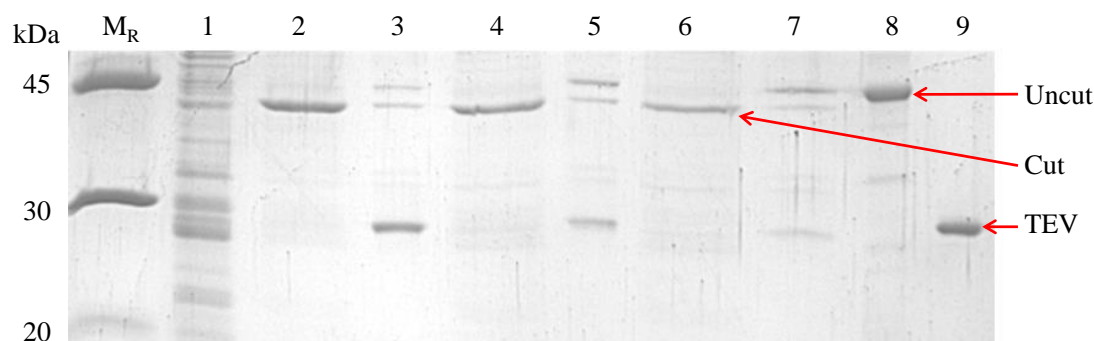


Figure 3.8.1: A 12% SDS-PAGE gel to test conditions for *VanS_A* tag-cleavage. *VanS_A* protein was bound to pre-charged nickel sepharose resin, and digested on-column with different ratios of [TEV]:[protein] (in different columns). Lane 1 – 20 mM Imidazole wash to remove non-specifically bound proteins, Lanes 2, 4, 6 – Flow through after cleavage, Lane 3, 5, 7 – Proteins on the resin after cleavage, Lane 8 – *N-His₆-VanS_A* uncut control, Lane 9 – *His₆-TEV* protease control. Lane 2/3 – 1:2 [TEV]:[protein], Lane 4/5 – 1:4 [TEV]:[protein], Lane 6/7 – 1:8 [TEV]:[protein]. *M_R* – Protein ladder (GE).

Upon discussion with collaborators in the Integral Membrane Protein facility at the Structural Genomics Consortium (SGC, Oxford University), it was found that they often use 1:1 and even 2:1 [TEV]:[protein] ratios in their purifications and overnight cleavage is preferable to achieve optimal yield. Protein samples were therefore cleaved at 1:1 ratios (see section 2.12.1) and run on SDS-PAGE gels (Figure 3.8.2), which showed complete cleavage.

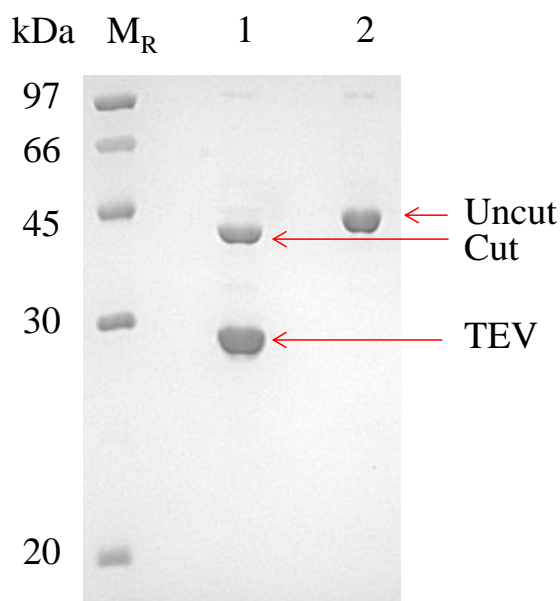


Figure 3.8.2: A 12% SDS-PAGE gel showing tag-cleavage of VanS_A with TEV. Lane 1 – After overnight cleavage with TEV, Lane 2 – before cleavage. Band sizes were ~47 kDa for tagged-VanS and ~44 kDa for tag-cleaved VanS, relative to a GE marker.

Digestion products were subsequently rebound to nickel resin, to remove his-tagged impurities (e.g. AcrB and TEV) and collect cleaved VanS proteins in the flow through. As a final measure, the wild-type VanS proteins were purified by gel filtration chromatography (see Appendix Figure 4), and samples were concentrated to 200 μ L for use in crystallisation trials (see Appendix Figure 5), which showed that the possible AcrB contaminant at ~100 kDa had been removed. Concentrated samples were also analysed by mass spectrometry (see section 2.8.1), to confirm their exact protein identity and by CD spectroscopy (see section 2.10), to ensure the purified proteins remained in their native helical fold.

3.9 Identification of Full-length VanS Proteins by Mass Spectrometry

To confirm the identity of purified VanS proteins, samples were analysed after TEV digestion, by mass spectrometry. An aliquot of tag-cleaved VanS protein purified in DPC detergent was analysed under positive-mode electrospray ionisation on an Agilent LC-MSD TOF instrument (see section 2.8.1). Resulting spectra were averaged and deconvoluted using MassHunter software, as shown in Figure 3.9.1.

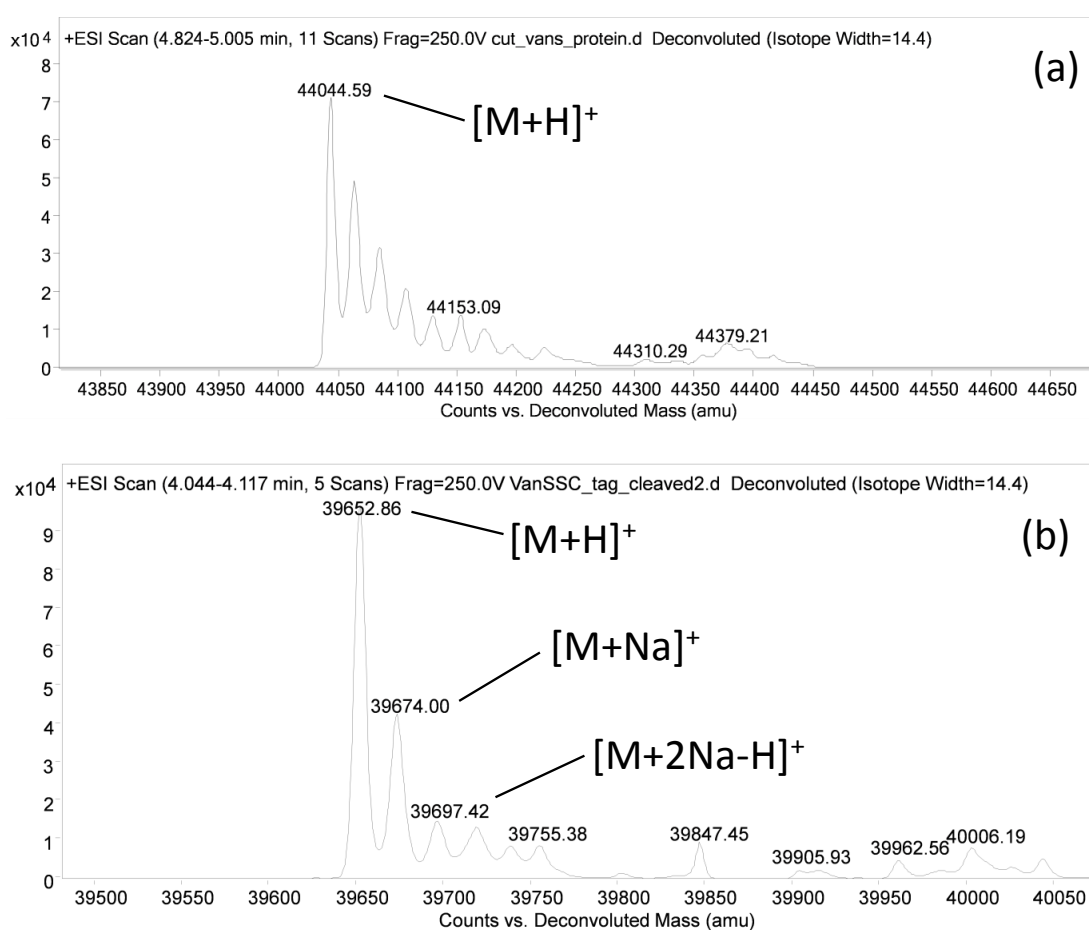


Figure 3.9.1: Mass averaged, deconvoluted ESI-TOF mass spectra of tag-cleaved wild-type VanS_A (a) and VanS_{SC} (b) proteins. The view is enlarged in the m/z region of the molecular ion peak. Major species identified including the $[M+H]^+$ peak are annotated.

Full-length tag-cleaved VanS proteins were identified at the exact molecular mass predicted +/- 1 Dalton, containing the wild-type sequence and an additional two residues (glycine and alanine) prior to the gene sequence (resulting from cleavage at glutamine/glycine in the TEV recognition site). For VanS_A the [M+H]⁺ ion was observed at 44044.6 Da (expected molecular ion mass including the two residues is 44043.9 Da) and for VanS_{SC} at 39652.9 Da (expected molecular ion mass including the two residues is 39651.5 Da). Spectra showed some impurities remaining after gel filtration, but the highest intensity peak was the [M+H]⁺ peak, and shoulder peaks resulting from sodiated species e.g. [M+Na]⁺ (e.g. 39674.0 Da) and [M+2Na-H]⁺ (e.g. 39697.4 Da). Therefore purified VanS proteins had the correct mass and were being cleaved by TEV protease at the correct site, and despite any impurities, did not appear to show any post-translational modifications.

3.10 Secondary structure of VanS proteins by Circular Dichroism

As a pre-requisite to crystallisation and NMR studies, VanS protein samples were analysed by Circular Dichroism (CD) (section 2.10) to ensure the proteins were properly folded, and to compare secondary structure characteristics of both proteins. CD provides information about molecular conformation and protein stability. In the instance of proteins, there are spectral signatures characteristic of alpha-helical, beta-sheet and random coil secondary structures, and fitting software can determine the relative percentages of each in the sample.

Each protein sample was prepared as described in section 2.10. Scans were made in the far UV range (190 - 260 nm) at all data was collected at 20°C. Initially, samples were prepared from VanS proteins that had been purified by gel filtration in a buffer containing 20 mM HEPES pH 7.5, 2 mM DPC, diluted in the same buffer to give a final concentration of 0.1-0.15 mg/ml in 200 µL (4-5 µM). However, it was found that HEPES can cause high scattering at wavelengths around and below 200 nm (Figure 3.10.1) and preferred buffers used in the literature are sodium phosphate, Tris or sodium acetate (Kelly *et al.*, 2005).

Therefore samples in HEPES buffer were exchanged into 20 mM phosphate buffer pH 7.5 (containing 2 mM DPC) using a PD10 column, and diluted to ~0.1 mg/ml, in order to collect data to 190 nm (which is required for most fitting software) (see Figure 3.10.1).

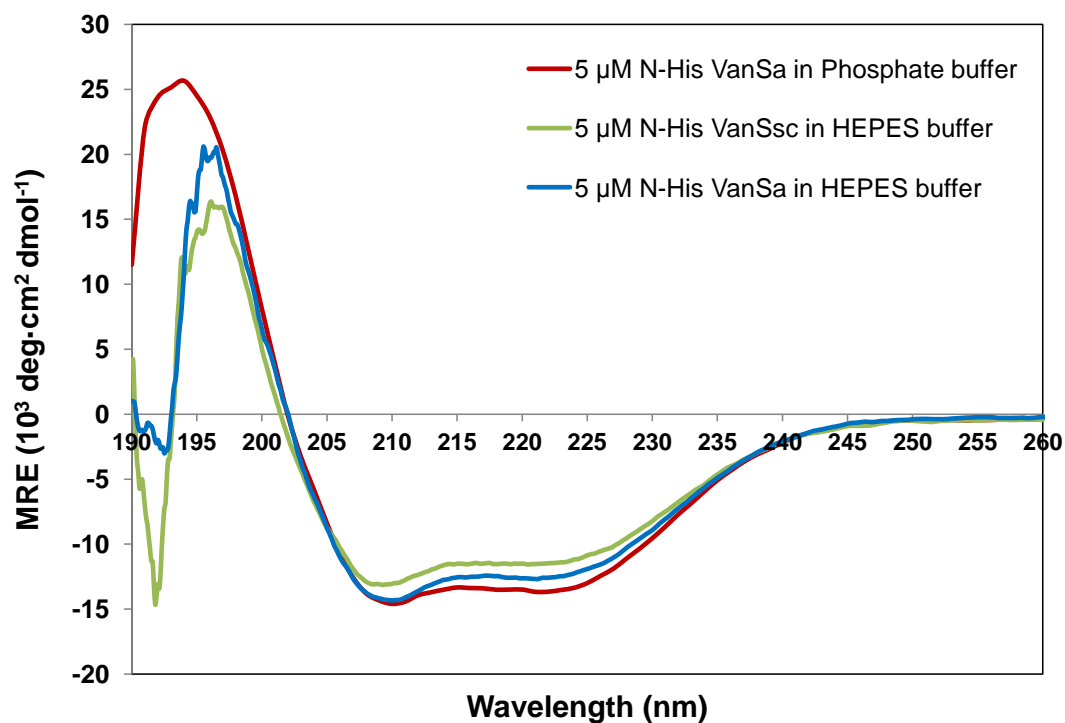


Figure 3.10.1: CD spectra of 5 μM *N-His₆-VanS_A* and *N-His₆-VanS_{SC}* in HEPES or phosphate buffer pH 7.5, containing 2 mM DPC. *VanS_A* in phosphate buffer – red line, *VanS_{SC}* in HEPES buffer – green line, *VanS_A* in HEPES buffer – blue line.

Examination of the CD spectra above for *VanS_A* and *VanS_{SC}* in DPC detergent shows strong peaks at around 208 nm and 222 nm, characteristic of a predominantly α -helical protein.

Analysis of the CD data for *VanS_A* in phosphate buffer, using fitting software (Dichroweb, CDSSTR) (Whitmore & Wallace, 2004) confirms this (60% α -helix, 13% β -strand and 26% β -turn/random coil), and is in close agreement with the predicted secondary structure (using PredictProtein software) (Rost *et al.*, 2004) for the protein sequence alone. Samples of *VanS_{SC}* could not be analysed by a fitting program due to light scattering below 200 nm, but appear to show the characteristic α -helical fold, and have similar MRE values to *VanS_A*, as predicted from protein sequence alone (50% α -helical using PredictProtein software).

In order to assess any changes in secondary structure upon histidine-tag cleavage, tag-cleaved VanS samples purified by gel filtration (see section 3.7) were also analysed under the same conditions, exchanged into phosphate buffer (Figure 3.10.2). Furthermore, 100% 2,2,2-trifluoroethanol (TFE) was added to his-tagged VanS_A samples in DPC, as it is known to induce α -helicity (Shiraki *et al.*, 1995; Arunkumar *et al.*, 1997), in order to provide a measure against which to compare the helicity observed in DPC detergent alone.

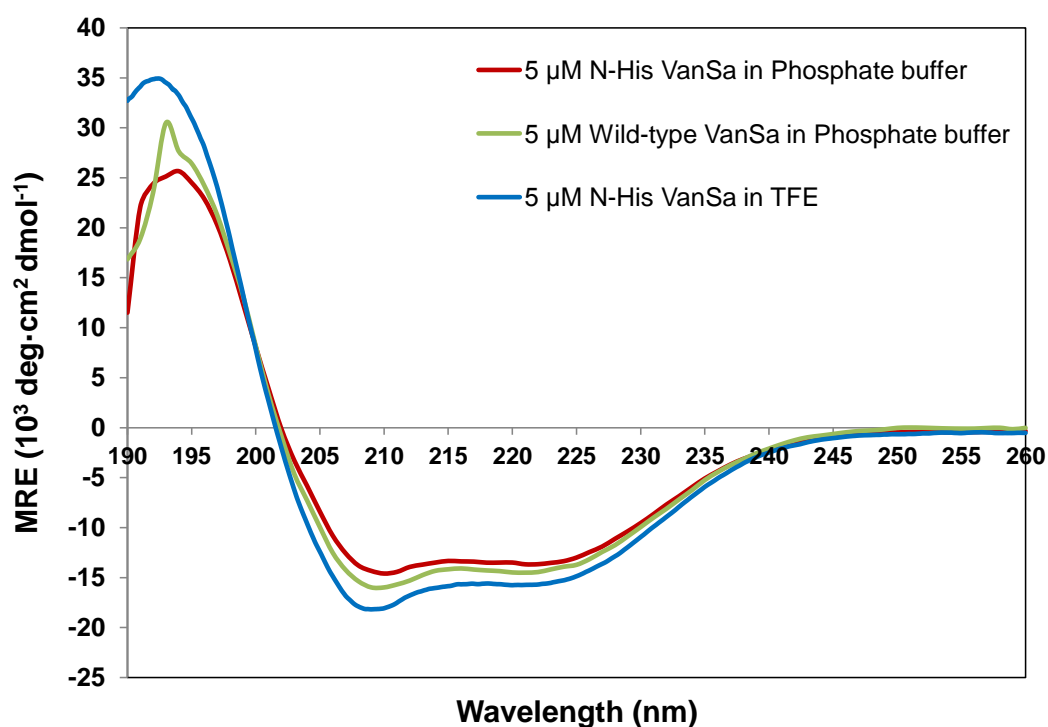


Figure 3.10.2: CD spectra of 5 μ M N-His-tagged and tag-cleaved VanS_A in phosphate buffer pH 7.5 or TFE, containing 2 mM DPC. His-tagged VanS_A in buffer – red line, tag-cleaved VanS_A in buffer – green line, His-tagged VanS_A in TFE solvent – blue line.

Fitting software for tag-cleaved VanS_A gave values of 64% α -helix, 11% β -strand and 25% β -turn/random coil, therefore the cleavage did not greatly affect the fold, and may even improve protein stability. Addition of TFE further stabilises the fold, but only marginally, giving approximately 70% α -helicity, therefore the proteins were well folded in the DPC detergent chosen, and could be placed into crystallisation trials.

3.11 Determination of VanS Protein Activity by Coupled Enzymatic Assays

Although the VanS protein samples are highly pure and well-folded, the ability of the protein to function as a kinase or phosphatase is often reduced when it is extracted from the bacterial membrane. Previous studies within the Warwick group (Quigley, 2010; Williams, 2007) found that the addition of detergent greatly hampered or prevented detection of the autophosphorylation and dephosphorylation rate of VanS proteins. Therefore it was critical to assess the activity of purified VanS proteins within a detergent environment prior to crystallisation or NMR studies, especially if potential ligands were to be added to samples.

The first biochemical characterisation of VanS_A autophosphorylation was conducted by Wright and co-workers (Wright *et al.*, 1993), and similar autophosphorylation assays were adopted by Hutchings *et al.*, (2006) to characterise VanS_{SC} proteins. By adding radiolabelled [γ -³²P]ATP into autophosphorylation reactions, both groups measured the amount of labelled VanS protein present after an incubation period, on SDS-PAGE gels. Phosphotransfer was also shown from the ³²P-radiolabelled VanS protein to a VanR protein after a co-incubation period. In order to avoid the potential difficulty of re-solubilising full-length VanS proteins, the groups studied the soluble C-terminal domain of each protein. Wright *et al.*, (1993) expressed and purified the cytoplasmic C-terminal region of VanS_A (VanS_A Δ 95) containing an N-terminal MBP-tag to assist protein folding, whereas Hutchings *et al.*, (2006), expressed and purified the cytoplasmic domain of VanS_{SC} (VanS_{SC} Δ 84) assisted by an attached His tag.

Incubation of MBP-VanS_A Δ 95 or His-VanS_{SC} Δ 84 with [γ -³²P]ATP, in the presence of Mg²⁺ ions, allowed transfer of the labelled phosphoryl group to the protein, and phosphorylation was essentially complete after ~ 60 minutes. Kinetic parameters for the MBP-VanS_A protein were determined by autoradiography and showed that the initial rate was first-order with respect to ATP, and analysis of the total ³²P incorporated demonstrated that 10-15% of the protein was phosphorylated after one hour under saturating levels of [γ -³²P]ATP.

A previous PhD student in the Warwick group, Dr. Andrew Quigley (2010), studied truncates of the VanS_A protein using radiolabelling assays, to verify these kinetic parameters and examine the role of structural features in the kinase domain on activity. These truncates (and a control protein, MBP-VanS_AΔ95) contained only the cytoplasmic domain (VanS_AΔ95 to VanS_AΔ155) and were all active with respect to autophosphorylation, provided that the histidine site (H164) was present (see Figure 3.11.1). They also showed that ~15% of the MBP-VanS_AΔ95 was phosphorylated after 60 minutes, but significantly less phosphorylation occurred for the truncates. Critically, no autophosphorylation could be observed for the full-length kinase (C-His₆-VanS_A) purified into detergent micelles, and it was concluded that the His-site may have been occluded by the presence of excess detergent micelles.

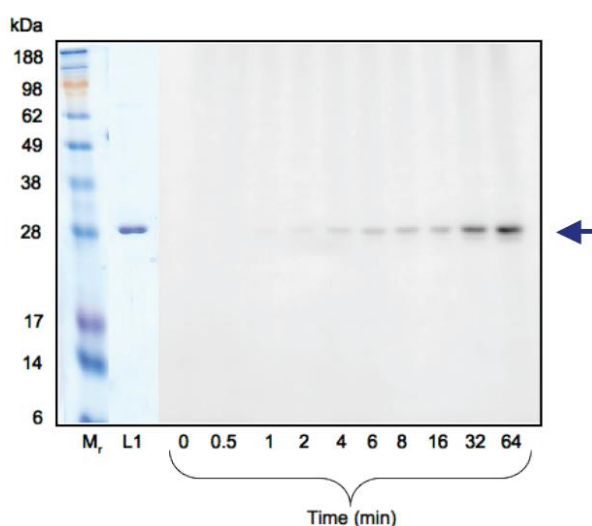


Figure 3.11.1: 14% acrylamide SDS-PAGE gel phosphoimage of VanS_AΔ110 autophosphorylation with time, reproduced from Quigley (2010). An equivalent SDS-PAGE stained gel was used to quantify band position (lane L1).

Although radiolabelling methods are widely used in the literature to determine the activity of sensor kinases (Hastie *et al.*, 2006), the technique does suffer from being non-continuous, and as such the value of the observed autophosphorylation is often undercalculated. The phospho-histidine bond is labile in acidic conditions, such as those during SDS-PAGE analysis, and phosphate can potentially be lost. For instance, Wright *et al.*, (1993), showed by HPLC that the percentage of phosphorylation was underestimated by ~25%.

A more continuous measure of autophosphorylation can be obtained by spectrophotometric assays which can account for phosphate loss. These include quantification of ADP production using a coupled enzymatic assay, as developed by Wampler and Westhead, (1968) (see section 2.9.1), by monitoring changes in absorbance during oxidation of NADH to NAD⁺, as a result of ADP release. This can be coupled to a phosphate release assay, as developed by Webb, (1992), to account for any phosphate loss due to the lability of the phospho-histidine bond (see section 2.9.2). The ADP release assay assumes that resultant ADP is released after autophosphorylation (Marina *et al.*, 2005), and the amount released enables quantification of autophosphorylation rate and stoichiometry. These assays were also tested by Quigley (2010), who found that against expectations, autophosphorylation was observed for purified full-length C-His-VanS_A protein in DDM detergent (see Figure 3.11.2).

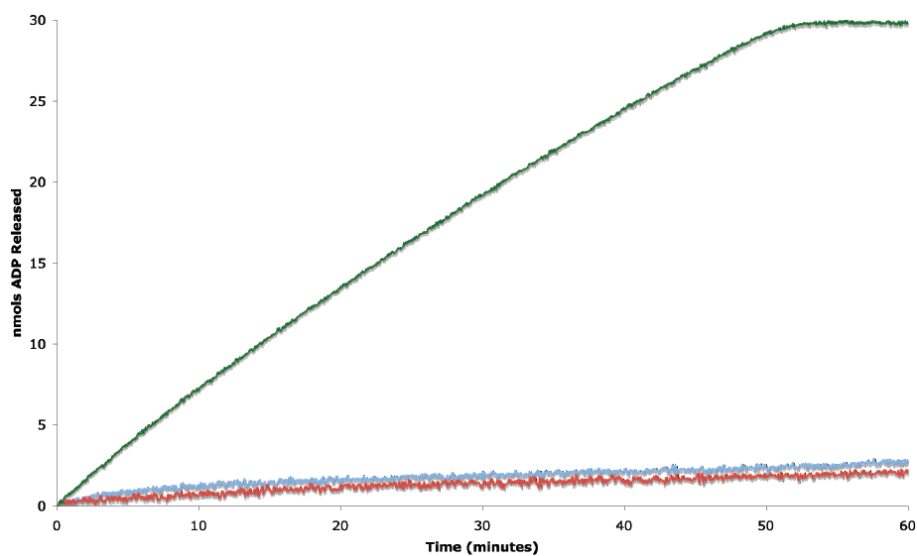
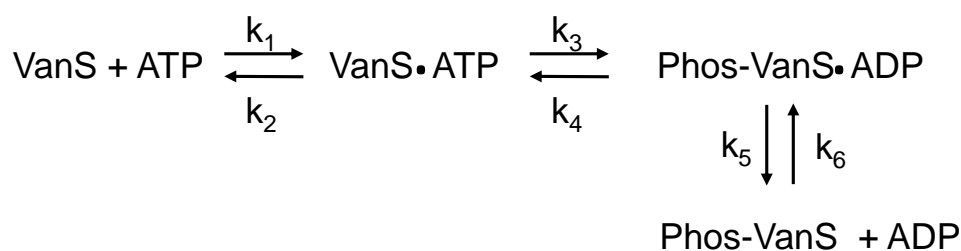


Figure 3.11.2: ADP release profile of C-His₆-VanS_A full-length (green), VanS_AΔ110 (blue) and VanS_AΔ155 (red), extracted from Quigley (2010).

To assess autophosphorylation activity of the N-His₆-VanS_A and N-His₆-VanS_{SC} proteins expressed in this PhD, a combination of ADP release and phosphate release assays were conducted for the full-length proteins purified into detergent micelles. Detergents chosen included DDM as a control, in which activity had already been observed for C-His-tagged VanS_A, and DPC, as this was used throughout the PhD for crystallography and NMR studies.

3.11.1 ADP Release Assay

Using the two continuous spectrometric assays, attempts were made to measure the autophosphorylation of purified VanS proteins in terms of ATP turnover. The assays measure phosphorylation indirectly by recording the release of ADP and inorganic phosphate. By subtracting the molar quantity of inorganic phosphate released from the molar quantity of ADP produced, a value can be obtained, which should correspond to the percentage phosphorylation of VanS_A, provided no other products form. This relationship is shown in Reaction Scheme 1, as proposed by Wright *et al.*, (1993).



Reaction Scheme 1

The assays are represented in Figure 3.11.1.1 ((a) – ADP release, (b) phosphate release). In the ADP release assay a decrease in absorbance at 340 nm is observed, whereas in the phosphate release assay, an increase in absorbance at 360 nm is seen. It is worth noting that the ADP release assay is cyclic as it involves regeneration of ATP, which provides a closer approximation to Michaelis-Menten kinetics. By maintaining the level of ATP present in the cyclic reaction, the reverse reaction should be prevented, and should not affect autophosphorylation kinetics.

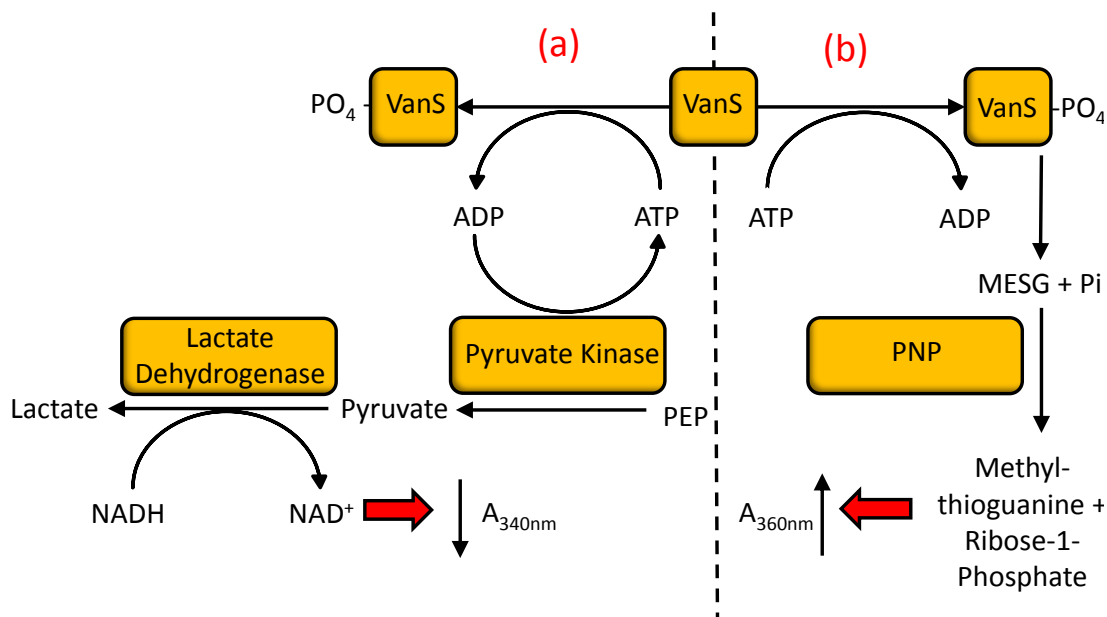


Figure 3.11.1.1: Reaction pathways involved in (a) ADP production by ATP hydrolysis and (b) inorganic phosphate release by ATP hydrolysis. The assays are based on enzymes and substrates described by Wampler and Westhead (1968) and Webb (1992). VanS or ATP can initiate the reaction, which can be followed at 340 nm by monitoring oxidation of NADH to NAD⁺ during ADP release, or at 360 nm by monitoring production of methylthioguanine during phosphate release. In the former reaction, ATP is catalytically regenerated by pyruvate kinase, whereas in the latter, all ATP is converted to ADP.

ADP release was monitored at 340 nm on a UV spectrometer as detailed in section 2.9.1 for VanS_A and VanS_{SC} full-length proteins which had been purified (by IMAC) in 0.03% DDM (for comparison with activity data collected by Quigley, 2010), or in 0.07% DPC detergent (chosen from solubility screens) (Figure 3.11.1.2). Both proteins appeared active in these detergents, although the observed activity varied depending on how much detergent was present, and concentrating the samples sometimes led to unmeasurable rates of activity. It was found that provided the detergent concentration was minimized to 1.5x to 2x CMC (i.e. 0.03% DDM and 0.07% DPC), the rate of ADP release could still be observed over a reasonable timescale. These experiments indicate that ADP is being released from VanS before VanR binding takes place.

As anticipated for a biochemical reaction involving a single substrate, the reaction curves display Michaelis-Menten kinetics, and asymptotically approach a maximum rate, indicating all enzyme has bound to substrate. However, the phosphorylation reaction is only around 50% complete at 60 minutes. This much slower than the reaction observed by Wright *et al.*, (1993) when assessing kinase activity of the cytoplasmic domain of VanS_A, and by Quigley, (2010), when assessing the ADP release activity of full-length VanS_A (see for Figure 3.11.2), who both found that phosphorylation reactions were essentially complete after 1 hour. It should be noted though, that the presence of excess micelles in the samples of detergent-solubilised VanS proteins, is likely to hamper the ability of the VanS catalytic region to phosphorylate the conserved His-164 site.

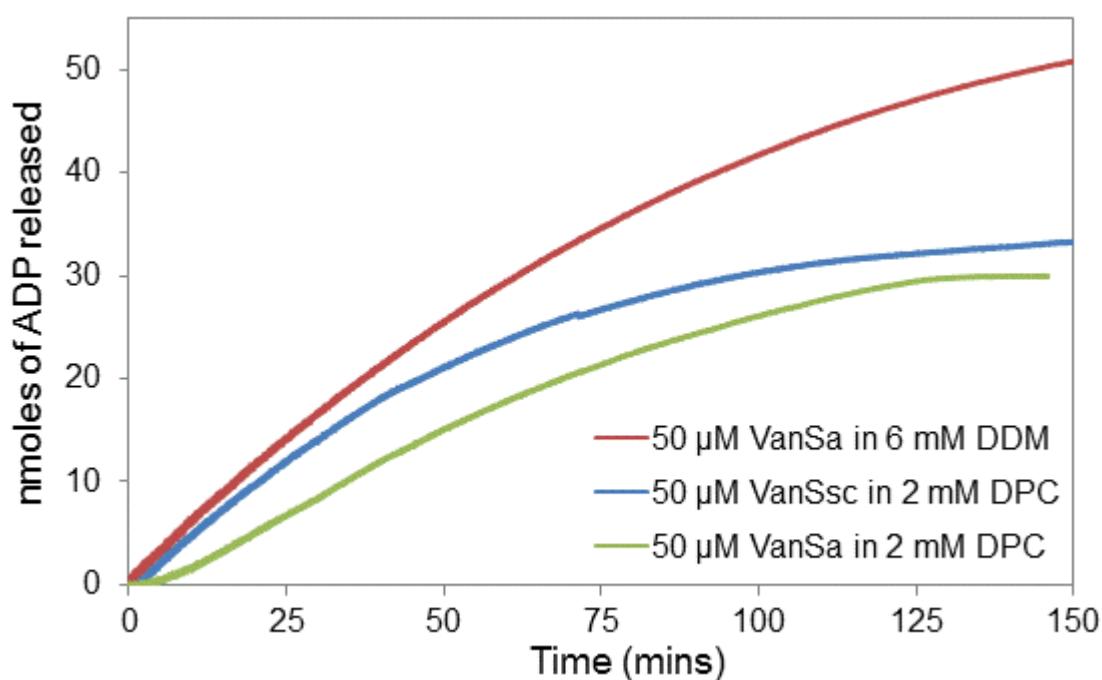


Figure 3.11.1.2: ADP release profile for full-length VanS_A protein in 6 mM DDM (0.03 %, red) or 2 mM DPC (0.07%, green), and VanS_{SC} protein in 2 mM DPC (0.07%, blue). nmoles of ADP released were calculated from the change in absorbance observed at 340 nm, as a result of NADH oxidation to NAD⁺ in the coupled reaction, using an extinction coefficient of 6220 M⁻¹cm⁻¹ at 340 nm for NADH. The reaction was initiated by the addition of 3 mM ATP into the final mix containing 50 μM (10 nmol) of VanS protein, and monitored over 300 minutes or until completion.

The rate and number of nmoles of ADP produced was found to be highest in DDM, over DPC detergent, but the reaction is slow in both detergents, and complete phosphorylation is only observed after ~ 2 hours. Furthermore, the nmoles of ADP produced is much higher than the nmoles of VanS protein used (10 nmoles) in assays, for instance VanS_A in DPC detergent attained a maximum turnover of ATP of 29 nmoles. This indicates that the VanS protein may be losing phosphate at a high rate, which can be tested using the phosphate release assay (see section 3.11.2). It is assumed that the observed change in absorbance occurs from ADP release, and that this release is due to the action of VanS, which is likely, as the protein samples appeared relatively pure by SDS-PAGE, however this cannot be proven without an additional assay technique. As such, the nucleotide products from the reaction were also assessed by Anion Exchange Chromatography (see section 3.11.4).

As a control measure for the ADP release assays, reactions were initiated by addition of ATP or VanS, to demonstrate that the absorbance changes observed are representative of a real event. The reversibility of this system is confirmed in Figure 3.11.1.3, which shows that the reaction can proceed by addition of enzyme or substrate, and ~60 moles of ADP are released in the reaction. There is however a slight difference in the profiles of the reactions, which could be due to differences in the rate of mixing in each reaction; a different volume of enzyme (20 μ L) was added compared to substrate (6 μ L) to initiate the reaction. The temperature for reactions in the spectrophotometer was also controlled and set at 20°C throughout, and the amount of protein per assay was fixed at 10 nmoles, in order to make direct comparisons with data previously collected by Quigley, (2010).

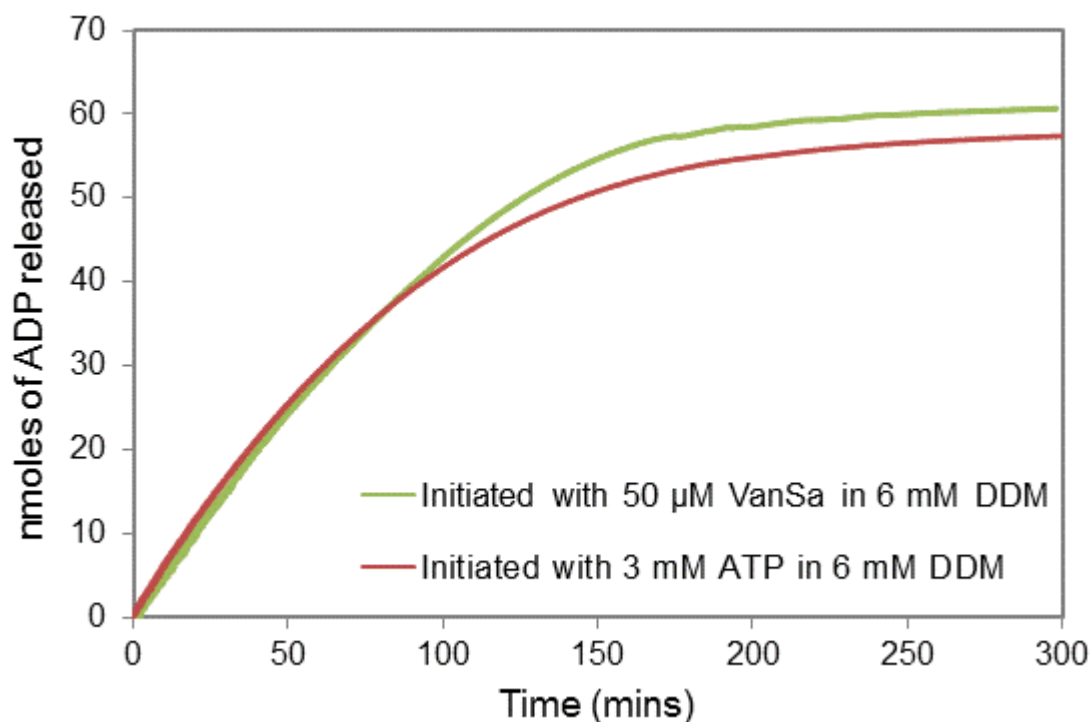


Figure 3.11.1.3: ADP release profile for full-length VanS_A protein in 6 mM DDM (0.03 %) produced upon initiation by either enzyme (green) or substrate (red). nmoles of ADP released were calculated from the change in absorbance observed at 340 nm, as a result of NADH oxidation to NAD^+ in the coupled reaction, and using an extinction coefficient of $6220 \text{ M}^{-1}\text{cm}^{-1}$ at 340 nm for NADH. The reaction was initiated by the addition of VanS_A enzyme at 50 μM (10 nmoles, green line) or ATP at 3 mM (red line) into the final mix.

3.11.2 Phosphate Release Assay

The phosphate release assay was conducted as described in section 2.9.2 for the VanS_A and VanS_{SC} proteins, using consistent amounts of protein (10 nmol) (see Figure 3.11.2.1). In contrast to the ADP release reactions, all phosphate release appeared to be complete within 30 minutes, and reaction profiles all started quickly initially then slowed after the first few minutes, reaching a maximum phosphate release between 6 and 12 nmol at around 25 minutes, which must be related to the enzyme (VanS) or substrate (ATP) present, since the total MESG present in the reaction is 40 nmoles. This suggests that no more phosphate is released after 30 minutes.

For the VanS_A protein in DDM detergent, 1.2 nmoles of phosphate is released for every 1 nmol of protein, which suggests that either the phospho-histidine bond is extremely labile under these conditions, or a secondary reaction is taking place that also produces phosphate.

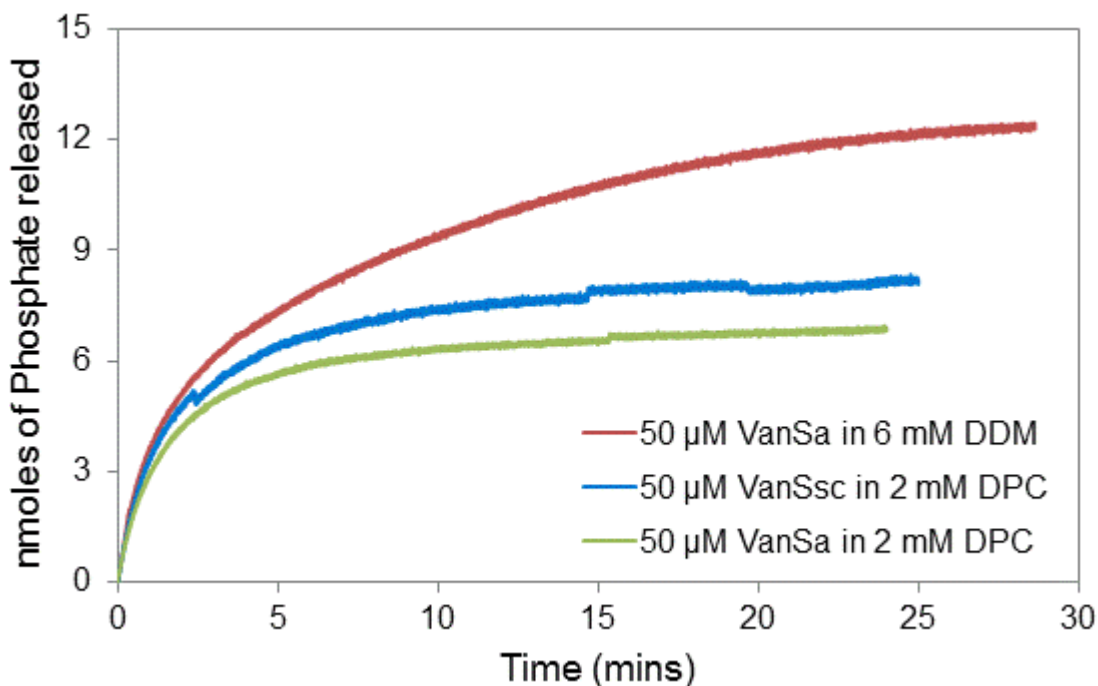


Figure 3.11.2.1: Phosphate release profile for full-length VanS_A in 6 mM DDM (0.03 %, red) or 2 mM DPC (0.07 %, green), and full-length VanS_{SC} in 2 mM DPC (0.07%, blue). nmoles of phosphate released were calculated from the absorbance change observed at 360 nm upon conversion of MESG to methylthioguanine in the coupled reaction, and an extinction coefficient for free phosphate of 10,000 M⁻¹cm⁻¹ at 360 nm.

3.11.3 Assessing the Autophosphorylation of VanS

The ADP release assay continues over a longer time course than the phosphate release assay, which could occur for several reasons. Firstly this could reflect the stability of the ADP bound state (VanS-ADP), over the phosphate bound state (His-P). In the structures of the cytoplasmic domains of histidine kinases (e.g. HK853 from *T. maritima*, see Figure 1.5.5.2), the His site on the dimerisation domain (DHp) is more exposed than the nucleotide binding site in the catalytic binding domain (CA) (see section 1.5.5) and the phospho-His bond

appears very labile (as shown in Figure 3.11.2.1). Therefore the rate of exchange of bound ADP for ATP is unlikely to be the same as the rate of phosphate release. It is possible that VanS exists in an ADP bound state for a long time, and may be quite stable in that state. As the assay continues, the amount of free ATP to exchange with will reduce, and the assay will reach completion, but only after a long time.

Secondly, the ADP release reaction continues even after all phosphate appears to have been released, which means that ATP should still be being turned over to ADP and phosphate, but this phosphate could remain bound to the protein (and not released). This could occur if there are multiple phosphorylation sites in the VanS protein, and would also help explain the very high percentage of protein phosphorylated (> 100 %) in Table 3.11.3.1 below.

To analyse the amount of ADP and inorganic phosphate released during the reaction of VanS with ATP, values are tabulated at timepoints in both assays (see Table 3.11.3.1). Values for ADP release are tabulated at 25 minutes (at the end of the phosphate release reactions), and at 60 and 120 minutes. Approximately half the ADP release reaction was complete for both proteins at 60 minutes, and almost all ADP release had occurred by 120 minutes for VanS in DPC. The values at these timepoints were used to calculate the amount of phosphorylated protein, to compare with data obtained by Wright *et al.*, (1993) and Quigley (2010) for the VanS_A protein. Theoretically, the ratio of ADP release to phosphate release should be 1:0 if all phosphates are transferred to VanS, but it is known from the literature that some phosphate is released (Fisher *et al.*, 1996), so the ratio may be expected to be slightly higher (up to 1:0.5 according to Fisher *et al.*, 1996).

Table 3.11.3.1: ADP and phosphate release per assay for VanS_A in DDM or DPC and VanS_{SC} in DPC, recorded at 25, 60 or 120 minutes. NB Data for phosphate release is given at a 25 min timepoint, at the apparent completion of the reaction.

Assay Time (min)	Protein; Detergent	ADP release (nmol)	Pi release (nmol)	Protein phosphorylated		ADP:Pi ratio
				nmol	%	
25	VanS _A ; DDM	14.40	11.57	2.83	28	1.2:1
	VanS _A ; DPC	6.78	6.75	0.03	0	1:1
	VanS _{SC} ; DPC	11.88	7.95	3.93	39	1.5:1
60	VanS _A ; DDM	29.45	11.57	17.88	180	2.5:1
	VanS _A ; DPC	17.96	6.78	11.18	110	2.5:1
	VanS _{SC} ; DPC	23.77	7.95	15.82	160	3:1
120	VanS _A ; DDM	46.20	11.57	34.63	346	4:1
	VanS _A ; DPC	28.93	6.78	22.15	222	4.3:1
	VanS _{SC} ; DPC	31.81	7.95	23.86	239	4:1

Data in Table 3.11.3.1 shows that over the first 25 minutes, the ratio of ADP:phosphate was around 1:1, and the percentage of protein phosphorylated (except for VanS_A in DPC) is predicted to be around 30%, which indicates a single phosphorylation event. However, the ADP release reaction did not reach completion at this point, which could reflect the stability of the ADP-VanS bond. By 60 minutes, the calculated ratio of ADP:phosphate is around 2.5:1, suggesting a secondary product may also be forming. Dr. Andrew Quigley, (2010) calculated a similar ADP:phosphate ratio (of 3:1) for the MBP-VanS_AΔ95 protein over 60 minutes, and showed that this could result from secondary product formation, by identifying the production of AP₄ (adenine 5'-tetraphosphate) (see section 3.11.4). Finally, by 120 minutes, the ratio of ADP:phosphate was 4:1, leading to a calculated percentage of phosphorylated VanS protein of 350%. This high ratio could simply indicate that ATP hydrolysis is occurring independently of VanS kinase activity, but it does raise the possibility of phosphorylation at multiple sites or the formation of secondary nucleotide products.

Overall the data indicates that the purified VanS proteins are able to turnover ATP and exhibit autokinase activity, but there may be secondary reactions occurring or the protein may be phosphorylated at sites other than the conserved histidine site (His-164 in VanS_A). Although multiple-site phosphorylation could not be assessed within the timecourse of these studies, anion exchange chromatography techniques were conducted to identify the nucleotide products in these reactions, including any secondary products, as detailed below. Methods to analyse phosphorylation at sites other than the active histidine site are outlined in the discussion in section 3.13.4.

3.11.4 Identifying Nucleotide products using Anion Exchange Chromatography

To identify nucleotide products formed during the reaction between VanS and ATP, reaction mixes containing the enzyme and substrate were set up and products formed were analysed by anion exchange chromatography. It was observed in previous autophosphorylation assays (Quigley, 2010) that a secondary product, AP₄, was formed as identified by tandem MS analysis (see Figure 3.11.4.1). This nucleotide product can occur from addition of phosphate onto ATP. Under certain conditions, some enzymes involved in biosynthetic pathways have been shown to produce AP₄, such as MurD (Bouhss *et al.*, 1999) and MurE (Blewett, 2005). Formation of AP₄ could explain the high ratio of ADP:phosphate release observed, and why the ADP release reaction continues to occur over 2 hours, whereas phosphate release appears to stop at 30 minutes, since phosphate produced could recombine with ATP and hence not be observed.

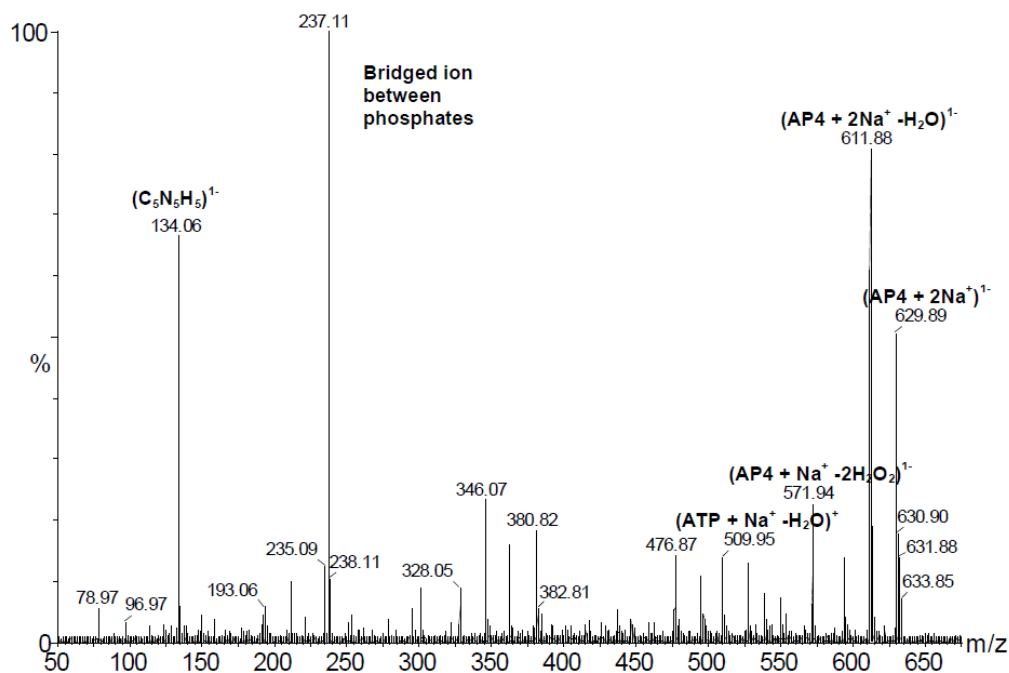


Figure 3.11.4.1: MS-MS spectra of ATP phosphorylation reaction of VanSA100 630 m/z, reproduced from Quigley (2010). Molecular weights can be assigned to fragments of ATP and there is a fragmentation pattern of the suspected AP4, confirming its formation.

Simplified experiments were conducted involving only VanS enzyme and ATP substrate (i.e. ATP is not regenerated), and products were analysed for the presence of e.g. AP4, by anion exchange chromatography. Full details are given in section 2.9.3, but essentially, a reaction mix consisted of identical concentrations of VanS enzyme (10 nmol) and ATP (3mM) in the same buffer as that of the ADP release reaction. Magnesium and potassium ions (important in complex formation) were also present, and the final volume was maintained at 200 μ L and the incubation temperature set at 20°C. The reaction was monitored upon initiation with ATP, and all 200 μ L samples were aliquoted from a master mix.

At timepoints of between 0 and 480 minutes, a 200 μ L aliquot was taken and quenched with 25 mM EDTA (final concentration) pH 8, which chelates to the magnesium ions present. The sample was then applied to a fresh 5 kDa MWCO concentrator, and concentrated for 20 minutes at 4000 g, to obtain the nucleotide products from the reaction in the flow through.

These products were then analysed by Anion Exchange Chromatography (IEX) on a MonoQ 5/50 GL column, and identified against standards (AMP/ADP/ATP) (see Figure 3.11.4.2). To apply samples onto the loop, a fixed volume (of 80 μ L) from the concentrator flow through was diluted with 1.3 mL of buffer A (10 mM ammonium acetate pH 7.6), and injected. Samples were applied under an isocratic gradient of 100% B over 30 minutes, and the absorbance at 280 and 254 nm was recorded.

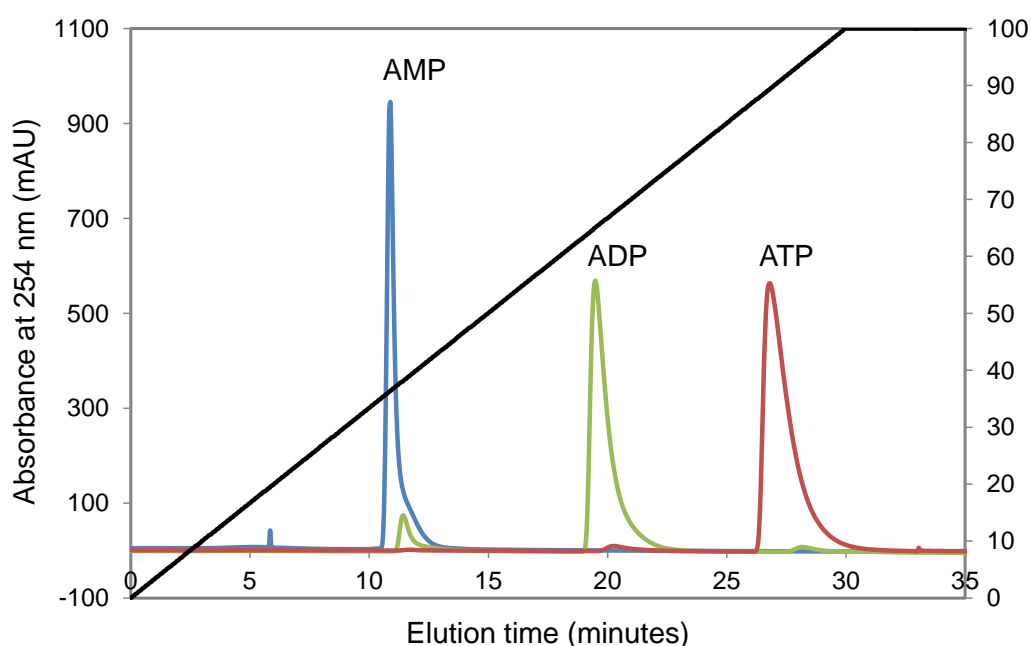


Figure 3.11.4.2: Anion-exchange chromatography profiles for nucleotide standards (200 μ M) applied to a pre-equilibrated MonoQ 5/50 GL column. Standards were run under a linear gradient of 0 to 100% B over 30 minutes, and remained at 100% B to elute any bound nucleotide products. A: 10 mM ammonium acetate pH 7.6, B: 1M ammonium acetate pH 7.6.

For protein-containing samples, it was important to quench the reaction at the exact timepoint, and to use a fresh concentrator for each sample to avoid carryover of nucleotide products. This should enable the same amount of nucleotides to be present in each assay (i.e. the same total integral). The integrals of each peak at 254 nm and their retention time (relative to standards) allowed percentages of AMP/ADP/ATP/AP4 to be quantified (see Table 3.11.4.1A and Appendix Figure 6). Absorbance traces recorded for the ATP standard (0 min), or samples from reaction between protein and ATP are shown in Figure 3.11.4.3.

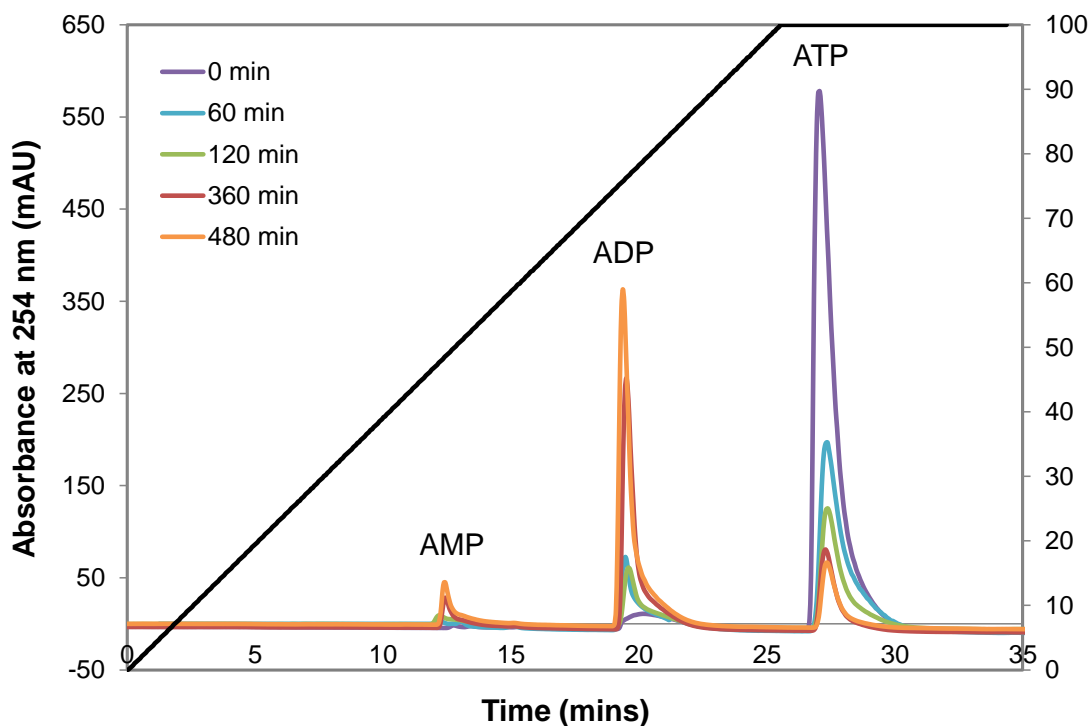


Figure 3.11.4.3: Overlaid anion exchange chromatograms collected at timepoints during reaction of VanS_A with ATP, showing the relative amounts of nucleotide products.

Timepoints (in minutes) are coloured as follows: 0 – purple, 60 – cyan, 120 – green, 360 – red and 480 – orange. The gradient of 0 – 100% B over 30 minutes is shown as a black line against a secondary axis.

Table 3.11.4.1A: Relative peak integrals of nucleotide products observed over time by anion exchange chromatography upon addition of ATP to VanS_A . The relative retention time of each peak is noted in the table at each timepoint.

Aliquot (min)	AMP		ADP		ATP	
	Peak (min)	Area (%)	Peak (min)	Area (%)	Peak (min)	Area (%)
0	12.2	0.0	20.2	5.9	27.1	94.0
60	12.2	1.1	19.5	20.1	27.3	78.8
120	12.2	5.8	19.6	28.8	27.4	65.4
360	12.4	8.1	19.5	65.6	27.3	26.3
480	12.4	9.5	19.4	71.3	28.0	19.2

The overlaid chromatograms of nucleotide products in Figure 3.11.4.3 illustrate the decrease in ATP present and concomitant increase in ADP formation. The turnover of ATP to ADP by the VanS_A kinase is even more apparent when the percentage integrals of each nucleotide product are plotted graphically, as shown in Appendix Figure 6. In the graph, the change in ATP over time is exactly mirrored in the increase in ADP over time, demonstrating that the VanS_A kinase is active with respect to ATP turnover.

Detailed analysis of the reaction products, finds that at 60 minutes around 15% of the ATP moles had been converted to ADP moles (see Table 3.11.4.1A; ATP: 94.0 to 78.8%, and ADP: 5.9 to 20.1%). This reflects well with the stoichiometry of phosphorylated VanS_A reported by Wright *et al.*, (1993) for the VanS_AΔ95 truncate, which showed ~15% of the protein was phosphorylated in one hour. By 120 minutes the level of ADP produced doubled to ~30% (and 30% reduction in ATP present), which also fits well with the activity data in Table 3.11.3.1 (ADP nmoles doubled from 60 to 120 minutes for VanS_A in DDM).

Unfortunately no AP4 reaction products could be observed using this technique, which would elute with a retention time >30 minutes (although a standard was not available to test), but it is possible AP4 may still be produced and requires another technique for identification.

It is worth noting though that the level of AMP increased over time, from 0 to 10 % by the final sample, which may indicate a secondary reaction. To check that this was not just the result of ADP hydrolysis to AMP, control experiments were set up involving only the ATP standard (no VanS present) under identical conditions, which found that the level of AMP did not change significantly (data not shown). This indicated that the VanS protein may have been responsible for the increase in AMP present from ADP. To test this hypothesis, a reaction mix was set up containing 10 nmoles VanS and 3 mM ADP, in the same buffer and to the same final volume of 200 μL. Aliquots were quenched and nucleotide products analysed by anion exchange at each timepoint as before. Overlaid chromatograms are shown in Figure 3.11.4.4 and the integrals of each peak are recorded in Table 3.11.4.1B.

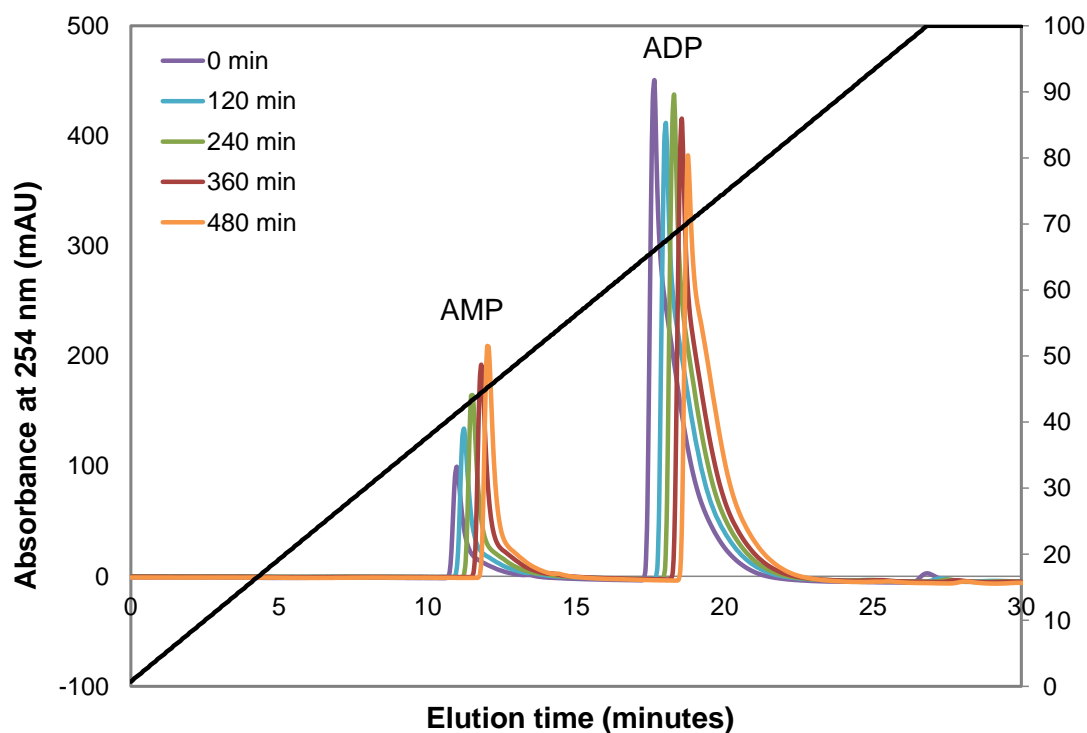


Figure 3.11.4.4.: Overlaid anion exchange chromatograms collected at timepoints during reaction of VanS_A with ADP, showing the relative amounts of nucleotide products.

Timepoints are coloured (in minutes) as follows: 0 – purple, 120 – cyan, 240 – green, 360 – red and 480 – orange. The gradient of 0 – 100% B over 30 minutes is shown as a black line against a secondary axis. Identified peaks of AMP and ADP products are staggered by 0.25 min (15 s) between each set of peaks, in order to show peak changes more clearly.

Table 3.11.4.1B: Relative peak integrals of nucleotide products observed over time by anion exchange chromatography upon addition of ADP to VanS_A . The relative retention time of each peak is noted in the table at each timepoint.

Aliquot (min)	AMP		ADP	
	Peak (min)	Area (%)	Peak (min)	Area (%)
0	11.0	11.6	17.6	88.4
120	11.2	15.2	18.0	84.8
240	11.5	18.1	18.3	81.9
360	11.8	20.1	18.6	79.9
480	12.0	21.0	18.8	79.1

It is apparent from the overlaid chromatograms in Figure 3.11.4.4 that in the presence of ADP, there is a correlation between the level of AMP produced and the reduction in ADP present. As observed for the VanS sample in the presence of ATP, the level of AMP present increases by ~10% by the final sample. To test for ADP hydrolysis, control experiments were again set up involving only ADP standards (no VanS present), under identical conditions, which also did not show any appreciable changes in ADP or AMP present (data not shown). Therefore the AMP produced must result from a reaction between the VanS-containing sample and ADP. There are no reports in the literature of a histidine kinase that is able to convert ADP to AMP, as this would involve removal of a high energy phosphate, and would not be beneficial to cellular response or growth. It therefore remains unclear how the purified VanS protein could cause AMP production.

One kinase that is known to convert ADP to AMP is adenylate kinase, which is present in *E. coli* bacteria (Krishnamurthy *et al.*, 2005) (and in mammalian cells), and responds to a reduction in the level of ATP available in the cell. When the ATP in the cell is consumed faster than it can be replenished (or in this experiment, is not regenerated), and the concentration of ADP is increased, adenylate kinase responds by converting two molecules of ADP, into ATP and AMP. This supplies the cell with energy, and lowers the ADP concentration, with the by-product of AMP. Therefore it is possible that in the anion exchange experiments conducted, an expressed *E. coli* protein such as adenylate kinase may be present in the detergent-solubilised VanS sample, which increases the level of AMP, in the limit of high ADP and very low ATP concentrations. If this is the case, AMP is unlikely to be a secondary product in the ADP release reaction, as ATP is constantly regenerated.

Further techniques are required to identify suspected secondary products in the ADP release reaction, which could include tandem MS analyses, or the use of radiolabelled assays to determine if other impurity proteins extracted in the detergent micelles are also responsible for the high ADP:phosphate ratio calculated and nmoles of ADP produced.

Overall both N-His-tagged VanS proteins have been shown to be active with respect to autophosphorylation, and anion exchange data clearly shows that ATP is being converted by VanS_A to ADP. This indicates that in the presence of detergent micelles, the kinase can still bind ATP molecules and turnover ADP. Crystallisation trials were conducted with the active VanS proteins (after cleavage of the His-tag), with a view to determine the structure of the kinase or fix it into a single state. Active His-tagged protein was also used in NMR titration studies, to assess the potential of antibiotics to bind to VanS (as discussed in chapter 5).

3.12 Crystallisation Screens

Crystallisation trials were set up on 96-well MRC or Greiner plates at either at the University of Warwick using a Honeybee 963 crystallisation robot, or at the Integral Membrane Protein facility, at the Structural Genomics Consortium (Oxford) using a Mosquito robot. MemGold and MemStart screens designed towards crystallisation of membrane proteins were tested, both of which use the sitting drop method of vapour diffusion crystallisation (see section 2.13.1). Initially, active tag-cleaved VanS_A purified in 0.07% w/v DPC detergent (from gel filtration chromatography) was concentrated in a 50 kDa MWCO PES concentrator, and added to MemGold plates using the Mosquito robot (SGC) to give sitting drops of 0.2 µL of protein mixed with mother liquor (100 µL per well), at drop ratios of 1:1, 2:1 or 0.5:1 (protein:precipitant) (effectively 7, 14 and 28 mg/ml). All trials were carried out at 18°C, as this temperature gave hits in previous studies of C-His₆-VanS_A (Williams, 2007).

On a second plate, the same drop ratios were used but with addition of AMP-PNP (an ATP derivative, Figure 3.12.1) (Wikström, 2005) to a final concentration of 5 mM. The ATP derivative is a stable non-hydrolysable analog of ATP, and was used to try to fix the VanS into an active phosphorylated conformation, and provide a ‘snapshot’ of this state during the catalytic cycle. This approach has been successful in studies of other histidine kinases e.g. PhoQ (Marina *et al.*, 2005), HK853 (Marina *et al.*, 2001) and CheA (Bilwes *et al.*, 2001).

It was hoped that by purifying the tag-cleaved VanS_A protein into DPC detergent at the min1.5x CMC), greater protein-protein contacts could be formed than that in DDM detergent, as used in previous trials (see Figure 3.6.5), which could increase stability of the crystal packing.

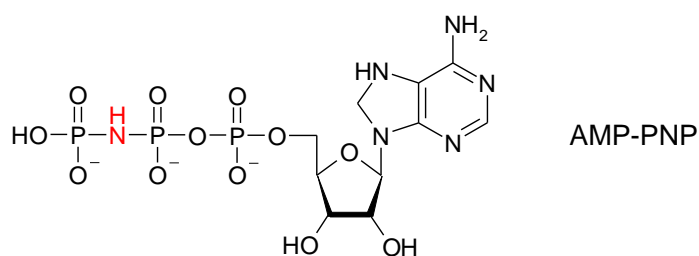


Figure 3.12.1: AMP-PNP structure. This differs from ATP by replacement of an oxygen between β - and γ -phosphate groups with a nitrogen (red), which is very slowly hydrolysed.

Crystal trays were therefore set up at the SGC (Oxford) at 18°C, containing the tag-cleaved VanS_A proteins in DPC (from the pProEx::vanS_A construct), in the presence or absence of AMP-PNP. Some potential crystals or crystallites formed in DPC detergent (see Figure 3.12.2), which were analysed on a beam line at Diamond Light Source (UK), with help from collaborators at the SGC. However, these were all found to be detergent crystals.

Crystallisation trials were repeated with freshly purified tag-cleaved VanS_A proteins using MemStart or MemGold screens at the University of Warwick, in DPC (9.1 mg/ml), or in DDM (6.4 mg/ml) (see Table 3.12.1). But again these also did not provide any crystals.

Protein samples in DDM showed a large proportion of clear drops on crystal trays and may not have reached supersaturation, as the concentration was relatively low. Furthermore drop dispensing using the in-house Honeybee 963 crystallisation robot was not uniform due to the presence of detergent bubbles.

Table 3.12.1: Concentrations of detergent-purified, tag-cleaved VanS_A proteins used in crystallisation screens. All proteins were purified in detergents at 1.5-2 times their CMC.

Construct	Detergent	Screen chosen	Concentration in Screen
VanS _A	0.07% DPC	MemGold	13.8 mg/ml, 9.1 mg/ml
VanS _A	0.07% DPC	MemStart	13.8 mg/ml, 9.1 mg/ml
VanS _A	0.03% DDM	MemGold	6.4 mg/ml
VanS _A	0.03% DDM	MemStart	6.4 mg/ml

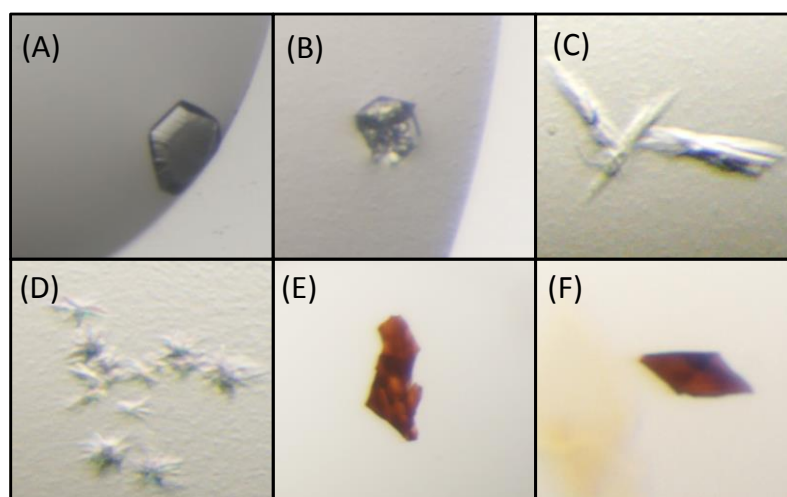


Figure 3.12.2: A selection of promising crystallisation conditions for VanS_A proteins solubilised in 0.07% DPC on MemGold 96-well screens. (A) 0.02 M CaCl₂/0.01 M MgSO₄ /0.02 M NaCl, 0.02 M MES pH 6.5, 7.7% PEG 1500 (w/v), (B, C and D) 0.1 M CaCl₂, 0.1 M Tris pH 6.5, 13% PEG 2000 MME (w/v), (E) 0.2 M MgCl₂, 0.1 M Tris pH 8.5, 25 % PEG 4000 (w/v), (F) 0.1 M NaCl/0.325 M Sodium Acetate, 0.1 M Tris pH 8.0, 21 % PEG 400 (v/v).

A selection of crystallites which appeared promising, and their conditions is given in Figure 3.12.2. In the figure, the crystal in panel A appeared promising, but did not diffract and was found to be a salt crystal. In panels B – D, crystallites appeared at low concentration (D - 7 mg/ml) but more structured crystals were formed at 14 mg/ml and above (B/C). All of these were tested on the beam line but found to be detergent crystals. In panels E and F (14 mg/ml), coloured crystallites formed after several weeks. These were not tested at the time,

but examination by eye of the crystal hits obtained at York University using the C-His-tagged VanS_A sample, finds that either cuboid (Figure 3.6.5 C/D, pH 4.5) or a dipyrnid-like crystallites formed (Figure 3.6.5 A, pH 8.5), and the possible hits in Panels E and F above (Figure 3.12.2 E/F, pH 8 – 8.5) appear to show a similar dipyrnid-like shape. Therefore crystal shape may depend on pH, but the use of DPC detergent does not seem to improve conditions compared to DDM, and the crystal hits obtained previously still appear the most promising. Crystallisation of the VanS membrane protein with or without bound ligand (ATP) clearly requires a wider screen of detergents such as maltosides, glucosides and other classes. Further collaboration with membrane protein research groups such as those at the Structural Genomics Consortium is needed to have a chance of crystallising this protein, as they can provide the specialist expertise and state-of-the-art equipment needed to rapidly screen multiple detergents and conditions for crystal hits.

3.13 Discussion

Recombinant *E. faecium* VanS_A and *S. coelicolor* VanS_{SC} proteins were successfully cloned into pProEx HTa vectors, and overexpressed as N-hexahistidine-tagged proteins with tag-cleavable TEV linkers, in *E. coli* C41(DE3).pRIL cells. Both proteins were purified to homogeneity by two chromatographic steps: immobilised metal affinity chromatography, followed by size exclusion chromatography, and their identities confirmed by LC-MS data. Autophosphorylation activity of purified N-His₆-VanS proteins was assessed by a combination of ADP release and phosphate release spectrophotometric assays and found to be active in DDM and DPC micelles. The protein activity was dependent on the detergent chosen, with a reduced rate observed in DPC micelles, but overall the time course for ATP turnover was ~ 2 hours. Subsequent cleavage of active protein with TEV protease gave the wild-type protein, and a final purification step provided relatively pure (>90%) protein samples, which were applied to sparse matrix screens and allowed to form crystals by vapour diffusion crystallisation, in an attempt to improve on the 8Å resolution previously obtained.

3.13.1 Approaches to express and purify VanS proteins for crystal studies

N-His-tagged VanS_A and VanS_{SC} recombinant proteins were successfully expressed by using the C41 Walker strain, which is optimised for membrane proteins, and by adding 0.2% w/v glucose, to prevent 'leaky' expression. The use of anti-His Western blots showed that VanS protein expressed at 37°C (in line with previous protocols in the Warwick group) was often insoluble and not visible on anti-His antibodies (presumably as the His-tag was occluded). It was found that the level of soluble VanS proteins could be greatly increased by lowering the induction temperature (to 16°C for VanS_{SC} and to 25°C for VanS_A) and growing overnight. The use of novel 'N-terminal preferential' anti-His antibodies also improved visualisation of the N-His-tagged VanS proteins during all stages of purification. In addition, detergent solubilisation of VanS proteins was optimised through screening, and selecting DPC detergent, which was found to solubilise much greater quantities of VanS protein than previously adopted maltoside detergents. This enabled yields of purified VanS_A protein to be increased to 3 mg/L, compared to ~1 mg/L observed by Quigley (2010) in DDM. The high solubility of VanS proteins in DPC is very desirable for NMR studies (see Chapter 5) since a large number of membrane protein NMR structures have been solved in this detergent.

High yields of VanS proteins of potential crystallisation-quality were produced in DPC detergent. These proteins exhibited all the desired qualities for crystallisation; they were homogenous, with the correct helical fold and appeared active with respect to autophosphorylation. The use of a TEV cleavable linker in the expressed protein also enabled cleavage and purification of the wild-type protein for use in crystal trials. This avoided any potential contamination with histidine-rich proteins such as AcrB which often crystallise preferentially. Despite these efforts, no VanS_A crystals were obtained in these studies in DPC or DDM detergents tested, which is a large set back in improving the 8Å resolution of the VanS_A diffraction pattern. The overriding issue appears to be the formation of detergent crystals in crystal screens.

3.13.2 Screening crystallisation of VanS proteins from multiple species

Another approach towards obtaining an X-ray crystal structure is to screen a protein target from multiple species (Benvenuti & Mangani, 2007). It would have been useful to screen VanS proteins derived from *S. coelicolor* (and other species such as *E. faecalis*). However, expression of soluble VanS_{SC} protein proved more difficult than VanS_A, for which initial expression protocols had already been given (Quigley, 2010). Although not discussed at length in this chapter, a number of different routes were pursued to improve VanS_{SC} expression including different cell lines such as BL21(DE3).pLysS, as previously used in expression studies by Koteva *et al.*, (2010), and the use of chaperonins: the GroEL-GroES double-ring system of *E. coli* (Xu *et al.*, 1997, PDB: 1AON) to assist in protein folding. Unfortunately, the level of soluble protein expressed was not greatly increased by these changes, and growth under multiple antibiotics in the GroEL-GroES system actually led to reduced yields. The optimal expression conditions were found to be 16°C in C41 (DE3) pRIL cells for ~ 20 hours (see Figure 3.6.8), which produced around 1 mg of purified VanS_{SC} per litre of culture. As a result of the low yield, crystal trials were not attempted with VanS_{SC}, but if yields could be further improved, it could be a candidate in future screens. It should be noted that the *vanS_{SC}* gene was not codon-optimised, and contained several rare codons, so this could improve expression levels of soluble protein.

Another possibility for crystallising VanS proteins would be to add a fusion tag. Membrane protein-GFP fusions allow monitoring of the protein directly throughout the purification process (Drew *et al.*, 2008) for instance in fluorescence size-exclusion (FSEC) studies. This allows analysis of the effects of different detergents on the chromatogram shape, in order to select those with sharp, single peaks for use in crystal trials (Kawate & Gouaux, 2006). In addition, MBP fusions can be used as ‘scaffolds’ to induce crystallisation (Smyth *et al.*, 2003), e.g. for proteins such as SarR (Liu *et al.*, 2001). MBP crystallises readily and can be attached to proteins of interest to induce crystal contacts and provide co-crystal structures.

3.13.3 Activity of VanS and its crystallisation is affected by detergent micelles

Crystallisation assays have been affected by the presence of excess detergent, which has led to a lack of protein crystals in the screen, and a large number of detergent crystals. Attempts were made to lower the detergent concentration to 2x CMC (0.03 % w/v DDM or 0.07 % w/v DPC), and use appropriate concentrators e.g. 100 kDa MWCO concentrators for samples in DDM detergent (micelle size: 50-70 kDa) to avoid concentrating the detergent. However, no protein crystals were observed in any membrane protein screens.

Activity assays also appeared to be affected by the presence of detergent, which increased the reaction time for autophosphorylation, as measured by ADP release assays, from 60 minutes for the cytoplasmic domain of VanS_A (MBP-VanS_AΔ95 tested by Quigley (2010), (see Figure 3.11.2) to ~120 minutes for the full-length VanS_A protein in DPC micelles (see Figure 3.11.1.2). This may be due to reduced access to the ATP binding site, in the presence of excess detergent micelles, or possibly a long-lived ADP bound state (see section 3.11.3).

The activity data presented in this thesis is however qualitative and requires additional experiments to determine the kinetic parameters for the binding of ATP to VanS, such as the Michaelis-Menten constant (K_M), the turnover number of substrate to product (K_{CAT}) and the maximal velocity (V_{Max}). These values could be obtained by measuring the rate of activity at increasing concentrations of ATP (around the K_M value of 0.62 mM observed by Wright *et al.*, 1993) e.g. 0.25 to 6 mM, and plotting the resulting substrate versus velocity profile. Attempts were made to obtain this data, however measurements of ADP release for VanS_A and VanS_{SC} proteins gave variable rates even at constant ATP concentrations, since the detergent-containing sample was difficult to accurately pipette without creating air bubbles during experiments. Therefore there is a need to obtain consistent measurements in a specific detergent before a full kinetic analysis can be achieved.

In addition to ADP/phosphate release assays, a new antibody has just been developed which allows identification of phospho-Histidine bonds by Western blotting (Kee *et al.*, 2013). Despite the development of a number of assays to identify phosphorylation of serine, threonine and tyrosine kinases, there has been a lack of available tools to study histidine kinase phosphorylation, which has been attributed to the chemical instability of the phosphoramidate linkage at the histidine residue to acid. However, Kee *et al.*, (2013), have raised antibodies which are specific to the pHis modification, and showed that this antibody could be used to detect histidine phosphorylation of the HK KinB *in vitro* and *in vivo* (in native cell lysates) on Western blots. Anti-pHis Western blotting would enable higher throughput studies of the VanS histidine kinase, and is therefore suggested as future work (see section 6.6) to act in place of more hazardous radiolabelling studies using [γ - 32 P]ATP.

3.13.4 Possibility of secondary reactions during VanS autophosphorylation

ADP and phosphate release assays recorded for purified VanS_A and VanS_{SC} proteins gave a ratio of ADP:phosphate of around 1:1 over the first 25 minutes (see Table 3.11.3.1). However, although all phosphate appeared to be released within this time, ADP release did not reach completion until much later. Indeed, the ratios of ADP:Pi were calculated as 4:1 by the completion of the ADP release reaction, and the percentage of VanS phosphorylated was calculated as ~300%. These values are much higher than anticipated, and possible explanations include: the formation of secondary (nucleotide) products, which will affect the observed UV absorbance at 340 nm, or perhaps phosphorylation of VanS at multiple sites, including the active His site, thereby increasing the percentage phosphorylation above 100%.

In order to investigate the possibility of secondary product formation during autophosphorylation, reactions involving samples of VanS_A enzyme and ATP substrate were analysed over a time course by anion exchange chromatography. By adding a fixed amount of ATP into reactions (i.e. ATP is not regenerated), it was shown by this technique that the percentage increase in ADP nucleotides directly correlated with a percentage decrease in ATP substrate present (see Appendix Figure 6).

It was hoped that AP₄ formation could be observed using this method, which is a secondary product that had been observed during autophosphorylation of VanS_A in previous studies (Quigley, 2010). This can form by the recombination of free phosphate with ATP molecules, and would reduce the amount of free phosphate present, and thereby fit with the observed phosphate release data. However, AP₄ could not be identified by this method, and instead the only secondary product that was observed was AMP, which formed even upon addition of ADP (rather than ATP) to purified VanS samples. There are no reports of histidine kinases that can convert ADP to AMP, and the only known enzyme that catalyses this reaction is adenylate kinase, so it remains unclear how AMP is produced in the reaction, and it may only occur in response to conditions of low ATP availability (refer to section 3.11.4). The formation of AP₄ may still be occurring, which may be identified by other techniques such as mass spectrometry, and secondary reactions would account for the high percentages of VanS phosphorylation calculated (> 100%) and ADP:phosphate ratios observed. With hindsight, it would also have been useful to see if the ADP release reaction could be abolished by addition of EDTA (which complexes to Mg²⁺ ions), to see if secondary reactions were occurring, and causing a higher than expected absorbance change.

The second possibility for the observed activity data is multiple-site phosphorylation. This was not assessed in these studies due to time restrictions, but is known to occur for some protein kinases, and at sites other than histidine such as serine, threonine or tyrosine, e.g. the serine/threonine kinase MSK1 is phosphorylated on at least six sites (McCoy et al., 2005).

Multiple-site phosphorylation could be tested by two routes. Firstly, tandem mass spectrometry techniques could be used to identify residues that have been phosphorylated. In the simplest site mapping experiment, a purified protein is proteolytically digested at defined sites to produce small peptides, and tandem mass spectrometry can be used to measure the masses of intact peptides and fragment ions. Computer algorithms are then used to identify phosphopeptides by matching the experimental data to theoretical spectra derived from sequence databases (that consider all possible phosphorylated versions of the peptide). (Dephoure *et al.*, 2013). Secondly, site-directed mutagenesis could be used to identify other phosphorylation sites in the absence of the active histidine residue. Studies by Haldimann *et al.*, (1997) have already shown that replacement of the His-164 site in VanS_A with a glutamine residue (H164Q) led to a loss of kinase activity. Therefore the creation of this mutant could provide support for the observed activity data; no activity should be expected for the detergent-purified VanS_A H164Q mutant unless a secondary phosphorylation reaction is occurring that does not require the presence of the conserved histidine residue.

4 Structural Studies of the VanS sensor domain by solution-state NMR spectroscopy

4.1 Introduction

Membrane proteins include receptors, ion channels, transporters, and enzymes, and constitute a significant fraction (20%–30%) of the proteome (Fagerberg *et al.*, 2010). However they are highly underrepresented, and make up less than 1% of all protein structures solved. As of July 2014, there were 878 published reports of membrane protein structures (491 unique) solved by NMR or crystallographic techniques (<http://blanco.biomol.uci.edu/mpstruc/>), out of a total of 100,000 protein structures deposited in the Protein Data Bank (PDB) (<http://www.rcsb.org/pdb/>). This is not due to a lack of biological importance, since membrane protein receptors represent the targets of over half of all known drugs (Bakheet & Doig, 2009; Yildirim *et al.*, 2007), but due to the challenges associated with expressing and purifying large enough quantities for structural study.

By nature, integral membrane proteins (IMPs) contain hydrophobic regions, and are often flexible and unstable, which causes difficulties in studying them. The proteins are embedded in a lipid membrane which varies in composition and constitutes only ~10% of the cytosolic volume (or ~5% for the plasma membrane) (Alberts *et al.*, 2002) therefore the environment for transmembrane protein function is highly specialized, and there is a need to select appropriate membrane mimetics in order to structurally characterise each membrane protein.

Of the membrane protein structures deposited, structures of the membrane-spanning sensor domains of histidine kinases are poorly represented. Structural analysis by both NMR and X-ray methods is hampered by inherent difficulties. The mobility of TM helices causes strong broadening of NMR signals and reduces spectral quality and resonance assignment, and diffraction quality crystals are hard to obtain because solubilised protein-detergent complexes do not usually form ordered lattices (Maslennikov *et al.*, 2010).

However, a few NMR structures have been obtained for the transmembrane domains of histidine kinases e.g. ArcB, QseC, KpdD (Maslennikov *et al.*, 2010) (see Figure 4.1.1). There are also X-ray crystal structures for HK sensor domains e.g. PhoQ, NarX, TorS (Cheung & Hendrickson, 2009; Moore & Hendrickson, 2009) (see section 1.5.3).

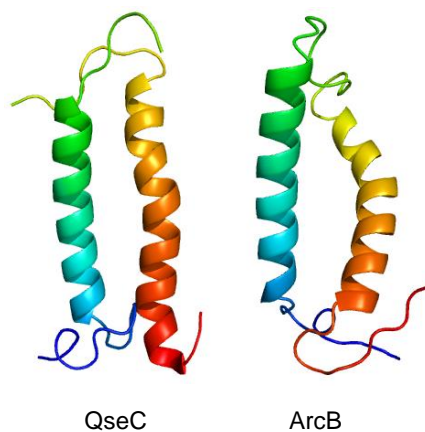


Figure 4.1.1: NMR backbone structures of TM domains of two classes of histidine kinase. *QseC* (class I, PDB: 2KSE) and *ArcB* (class II, PDB: 2KSD) are drawn in cartoon form.

Significant advances in expertise relating to the handling and analysing of membrane proteins *in vitro* over the past few decades have contributed to the solution of membrane protein structures. By screening buffer, pH and detergent conditions in protein analysis, the aggregation (or oligomerisation) state of the material can be monitored using gel filtration, electron microscopy or ultracentrifugation (Gutmann *et al.*, 2007) in order to choose a detergent that extracts a large quantity of soluble, active, homogeneous and stable protein. In addition, improved methods are being developed to address bottlenecks in expression and solubilisation, such as the use of GFP or MBP-fusion constructs (Drew *et al.*, 2008) and novel detergents e.g. lyso-phospholipids (derivatives of natural *E. coli* lipids) (Krueger-Koplin *et al.*, 2004), and in crystallisation, the use of robots for high-throughput screening. The effect of these advances is highlighted by the exponential increase in the number of membrane protein structures deposited in the PDB, since the first structure was added (Deisenhofer *et al.*, 1985) (see <http://blanco.biomol.uci.edu/mpstruc/>). Therefore membrane proteins have become more realistic targets for NMR or crystallographic study.

This chapter details the structural study of the sensor domains of VanS histidine kinases derived from *E. faecium* and *S. coelicolor* by solution state NMR techniques, using a number of these buffer, pH and detergent screens, in order to obtain homogeneous, well-folded and stable proteins. To the best of knowledge, there are currently no NMR structures of VanS_A or VanS_{SC} proteins in the literature, or any details of protocols to overexpress and purify the two proteins in labelled media, as required for NMR analyses. Therefore the data presented in this chapter illustrates a route for high yields of isotopically (¹⁵N) labelled VanS proteins and provides the first high resolution NMR spectrum of VanS_A and VanS_{SC} sensor domains.

The full-length VanS_A/VanS_{SC} proteins are 40-47 kDa in size and would therefore not be easily amenable to study by solution NMR, since the spin-spin relaxation rate (T₂) would be very rapid, causing significant line broadening and overlapping signals from the nuclei. An ideal protein size would be around 10 - 20 kDa (or ~100 residues), to enable individual peak shifts to be discerned and assigned by two- and three-dimensional NMR techniques, especially since solubilisation in detergent micelles will further reduce tumbling rates in solution and hence decrease spectral resolution. Therefore, although the structure of a full-length VanS kinase would be beneficial to understand structural aspects of VanS catalysis, the main area of focus has been to obtain structural information on the isolated sensor domain of the VanS protein, and to examine binding of glycopeptide ligands to this domain. It should be noted that the recent development of TROSY (Transverse Relaxation Optimized Spectroscopy) techniques (Tian *et al.*, 2005; Eletsky *et al.*, 2001) has allowed two-dimensional NMR analyses of proteins above 30 kDa in size, and towards 100 kDa (Riek *et al.*, 2002; Tugarinov *et al.*, 2004), but significant reduction in protein yields are often observed since TROSY techniques usually require protein labelling with addition of ²H, by growing bacteria in D₂O, and were therefore not tested in this study.

Experiments by Koteva *et al.*, (2010) have indicated that *S. coelicolor* VanS proteins bind directly to vancomycin derivatives (see section 1.4.2), therefore this protein could act as a positive control in NMR-based ligand binding experiments, to establish whether VanS_A proteins are also activated by direct binding or if they are activated via an indirect route. NMR studies were therefore conducted on the VanS sensor domain of each protein (without the C-terminal kinase domain), since this is below 20 kDa in size and contains the extracellular loop region of the protein, which is the only domain accessible region to glycopeptide antibiotics. Expression and purification of the isolated sensor domain would then enable protein-ligand binding studies using isotopic labelling methods and two-dimensional solution-state NMR methods. Since it was not known how any ligand binding would affect the conformation of the protein, it was beneficial to study the isolated sensor domain which (due to its size) should allow individual peak shifts to be observed.

4.2 Aims

- (i) To genetically modify *vanS* sequences in order to obtain the isolated sensor domain for structural study by solution state NMR.
- (ii) To provide a route for overexpression and purification of VanS sensor domains in labelled M9 minimal media, for use in solution state NMR studies.
- (iii) To obtain high resolution NMR spectra of the VanS sensor domain in detergent micelles, using two-dimensional NMR methods, and to optimise spectral quality by screening detergents, buffers, pH and temperatures.
- (iv) To assign individual amino acids in the VanS protein using 3D NMR methods.

4.3 Gene Modification of *vanS* sequences to create NMR-relevant constructs

Constructs were created which encoded only the VanS sensor domain, by using PCR techniques (section 2.4.1) to amplify the N-terminal section of the full-length *vanS* gene, contained within pProEx::*vanS* constructs (see section 3.3). PCR reactions were set up using pProEx forward primers ('pProEx For'), and reverse primers that encoded amino acids in the *vanS* sequence directly after the second TM domain (e.g. 'VanS_A110 Rev', see Table 2.4.1). These reverse primers terminated in a Stop codon, and therefore PCR amplification would provide the N-terminal sensor domain, containing both transmembrane helices, followed by the stop codon. The transition from transmembrane to cytoplasmic residues is predicted to occur after Ser-97 in VanS_A and after Gly-86 in VanS_{SC} sequences, but as this is only a prediction, amplified sections of the genes were chosen to include (approximately) a further 10 amino acids after these residues to ensure both transmembrane domains would be complete in the final constructs. Therefore the first PCR products encoded *vanS* gene residues from Met-1 up to Ile-110 (for VanS_A) and Met-1 up to Arg-100 (for VanS_{SC}).

It was also important to design different length *vanS* truncates, and quantify the level of expressed protein from each, since the amount of protein expressed will be reduced when residues in the extramembranous domains are truncated, and the resultant protein may be inserted into the membrane incorrectly or improperly folded. Proper assembly of a truncated membrane protein depends on features charge and hydrophobicity, and other factors e.g. the rate of folding. TM domains have high overall hydrophobicity, and are flanked by hydrophilic loop residues as governed by the "positive inside" rule (non-translocated loops are enriched in positively charged residues compared to translocated loops) (von Heijne G., 1992). Therefore the TM domains reduce protein solubility, whereas the loop regions increase the overall solubility. For these reasons, two additional PCR products were designed from VanS_A and VanS_{SC} sequences, to include residues up to Gln-120 or Met-130 for VanS_A and Arg-110 or Tyr-120 for VanS_{SC}, (see Table 2.4.1) to compare expression levels of each.

PCR products were generated for the N-terminal sensor domains of VanS_A and VanS_{SC} by amplification from the full *vanS* length gene (section 2.4.1), which was subsequently purified (section 2.4.5) and analysed by agarose gel electrophoresis, as shown in Figure 4.3.1. The resulting shortened *vanS* genes were ~400 bp in length, and required further purification by gel extraction. These were ligated into fresh, double-digested (NcoI, HindIII) pProEx HTa vectors, to test expression of the VanS sensor domain (as detailed previously in section 3.3).

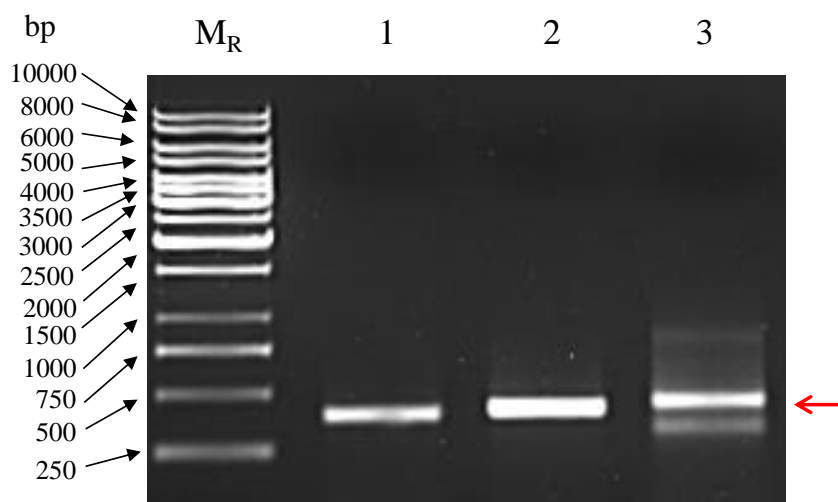


Figure 4.3.1: Purified PCR products from amplification of *vanS*_A, encoding the N-terminal His₆ tag, TEV site and the first 110, 120 or 130 amino acids of the protein sequence. M_R – 1 kb GeneRuler DNA ladder, Lane 1 - SA110, Lane 2 - SA120, Lane 3 - SA130. Position of the N-terminal VanSA bands is indicated by a red arrow at ~400 bp.

The ligation mixture was used to transform *E. coli* TOP10 cells (Table 2.2.2.1) (section 2.3) and extract DNA from positive transformants by minipreparations (section 2.4.4), which were analysed by Sanger sequencing (section 2.4.8), both to confirm sequence identity and ensure the *vanS* sequences were in-frame and without DNA mutations. These constructs were then tested for recombinant expression of the isolated sensor domain in a range of *E. coli* cell lines and at different [IPTG], using the protocol in section 2.5.1. The resulting overexpressions were analysed by Western blotting (section 2.6.3), as shown in Figure 4.3.2.

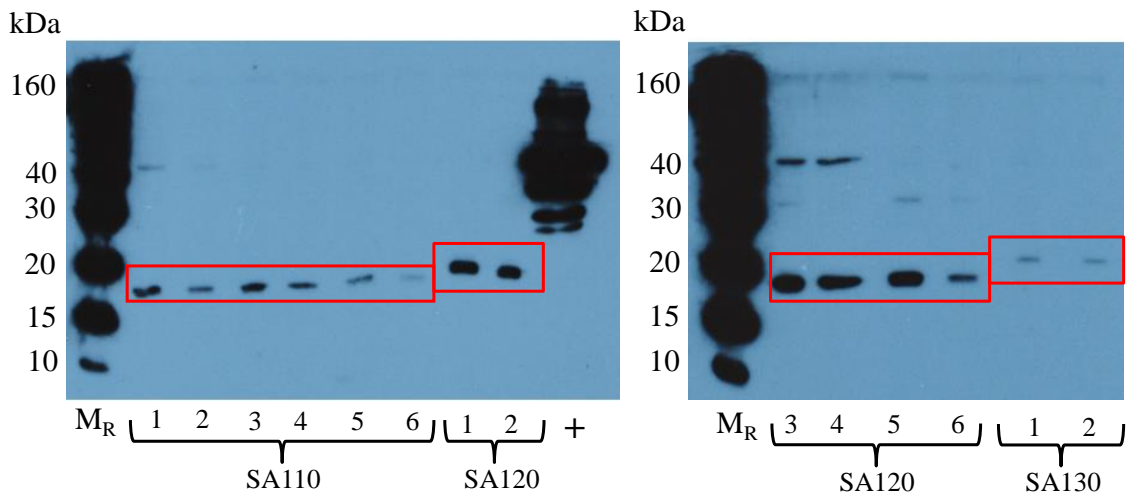


Figure 4.3.2: Western blots showing levels of overexpression of VanSA110, 120 or 130 after Water Lysis preparation. 40mL cultures were grown overnight at 25°C and resuspended in 2ml of phosphate buffer pH7.5 and blotted. Induction was with 0.2mM IPTG (lanes 1, 3, 5) or 1mM IPTG (lanes 2, 4, 6), in BL21(DE3) (Lanes 1, 2), C43(DE3) (Lanes 3, 4) or C41pRIL(DE3) (Lanes 5, 6). M_R – Benchmark His-tagged ladder (Invitrogen). Overexpressed full-length N-His₆-VanS_A was added as a positive standard (+).

In contrast to the positive standard (full-length N-His₆-VanS_A annotated as '+'), which was expressed under the same conditions and loaded at the same volume, the expression levels for VanS_A proteins were greatly reduced, which shows the impact of the soluble C-terminal domain upon expression. In terms of expression level, the SA120 construct produced the highest yield, and as observed with the full-length proteins, 0.2 mM IPTG inducer was again the optimal concentration (see for Figure 3.4.2).

By analysing *vanS* gene sequences using RONN (Regional Order Neural Network) disorder prediction software, it was found that disordered regions are predicted to exist for VanS_A between residues 130-155, and for VanS_{SC} between residues 97-120 and 141-171 (Figure 4.3.3). These disorder predictions suggest a reason why SA130 expresses at far lower levels than SA120, and similarly why SSC 120 expresses better than SSC110 (data not shown). It is also likely that SA110 does not express as highly as SA120, because this truncation is closer to the membrane-spanning residues and could affect protein insertion or folding.

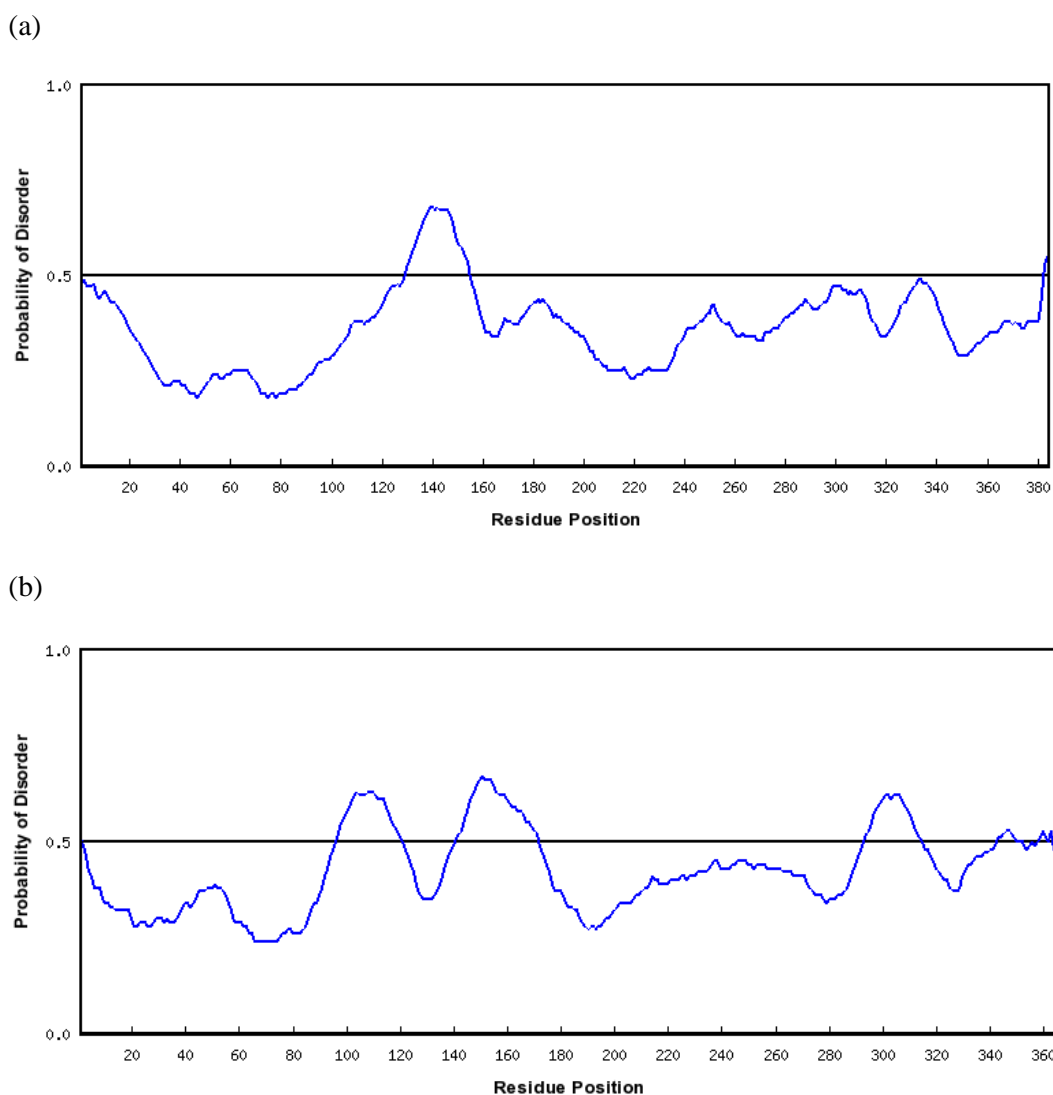


Figure 4.3.3: Disorder prediction plots for $VanS_A$ (a) and $VanS_{SC}$ (b) using RONN software. Major regions of disorder predicted for $VanS_A$ were M130-L150, and for $VanS_{SC}$ were E97-Y120, Q141-H171 and L294-I314.

In an attempt to increase expression level of the VanS sensor domain, further concentrations of IPTG inducer were screened for the most promising constructs (SA120 and SSC120) and cell line (C41(DE3) pRIL), and the temperature for induction was lowered to 16°C to allow time for proper insertion and folding in the membrane (e.g. see Figure 4.3.4). BL21(DE3) pLysS cell lines were also screened for expression, since they encode the gene for T7 lysosyme, a natural inhibitor of T7 RNA polymerase which serves to suppress basal expression of the polymerase prior to induction (Sivashanmugam *et al.*, 2009).

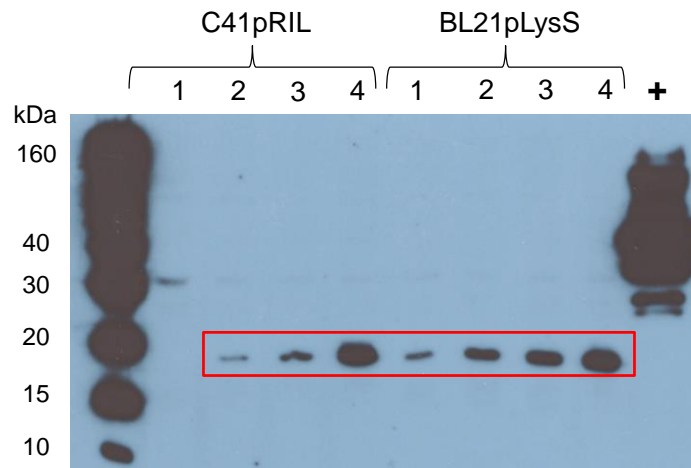


Figure 4.3.4: Western blot showing overexpression of SAI20 at 16 or 25°C, at varying IPTG concentrations. 100 ml cultures were grown overnight and resuspended in 2ml volume, processed by Water Lysis and blotted. Lane 1 – 0.05 mM IPTG added, Lane 2 – 0.1 mM IPTG added, Lane 3 and 4 – 0.2 mM IPTG added. Lanes 1-3 - 16°C induction, Lane 4 – 25°C induction. Overexpressed full-length VanS_A was added as a positive standard (+).

Figure 4.3.4 shows that of the three IPTG concentrations tested, 0.2 mM IPTG was still optimal, and more soluble protein was produced by induction at 25°C, and over a shorter period, than at 16°C. However, the level of soluble protein from these constructs was much lower than that of their full-length counterparts, and would not produce enough yield of protein after purification. From the RONN plots it was apparent that lengthening the sensor domain to e.g. 140 or 150 residues would be likely to only increase disorder for both proteins, and may not improve expression level. It is concluded that expression of the sensor domain requires increased solubility, afforded by the C-terminal cytoplasmic domain.

With this in mind, a new approach was adopted, in which the full-length proteins could be expressed using the already optimized protocols, and subsequently cleaved between the sensor and cytoplasmic kinase regions, to produce the desired sensor domain in a high yield. Using the knowledge gained from the *vanS* truncates, the best position to cleave the protein, and obtain a soluble sensor region, was around the 120th residue of the wild-type sequence. This cleavage would need to be highly specific to avoid multiple digestion products, and require a method to selectively purify the sensor domain or remove the C-terminal domain.

One of the advantages of cloning into the pProEx HTa plasmid, was that the encoded VanS proteins are His-tagged at the N-terminus, and when digested will produce a tagged N-terminal product, and an untagged C-terminal product. The N-terminal product can be selectively purified by Nickel affinity chromatography, and the C-terminal domain will be removed (in the flow through). Furthermore, by choosing an appropriate digestion enzyme, e.g. one that is tagged with e.g. MBP or GST (i.e. not His-tagged), the enzyme can be removed after cleavage using amylose or glutathione resin respectively. Another possibility is to use the His-tagged TEV protease for cleavage. This enzyme will cleave the expressed VanS proteins at the inserted site ~120th residue, and at the TEV-cleavable linker (between the His-tag and *vanS* gene sequence) (see Figure 4.3.5). The TEV protease can then be removed by affinity chromatography, and the remaining untagged N-terminal domain and C-terminal cytoplasmic domain can be separated by size using gel filtration chromatography.

Within the Roper laboratory, glycerol stocks were available which encoded digestion enzymes such as thrombin, enterokinase, 3C, and TEV, each of which act at specific cleavage sites, consisting of a defined sequence of five or more amino acids. Although the serine proteases, enterokinase and thrombin, used to be reagents of choice for removing affinity tags (Waugh, 2011; Gasparian *et al.*, 2003), and should cleave with high specificity, there are several reports of fusion proteins that were cleaved by these proteases at locations other than the designed site (Waugh, 2011). By contrast, few if any reports exist of cleavage at non-canonical sites in designed fusion proteins by the viral proteases, TEV and 3C. This specificity is probably attributed to their low turnover rates (low k_{cat}) (Kapust *et al.*, 2001; Long *et al.*, 1989). For this reason, TEV and 3C enzymes were selected for cleavage of VanS proteins in these studies. The TEV protease is His-tagged and the 3C protease is tagged at either end with Histidine and MBP, so they can both be selectively purified by affinity chromatography, and easily removed on resin after use. The only practical ramification of this choice is that more viral protease than serine protease is required to digest a fixed amount of protein, but far greater expression of viral proteases is achievable in *E. coli*.

A new route was therefore devised to insert a TEV or 3C site into the *vanS* gene sequence (after the second transmembrane helix), as shown in Figure 4.3.5, to cleave with high specificity using the respective enzyme and selectively purify the sensor domain.

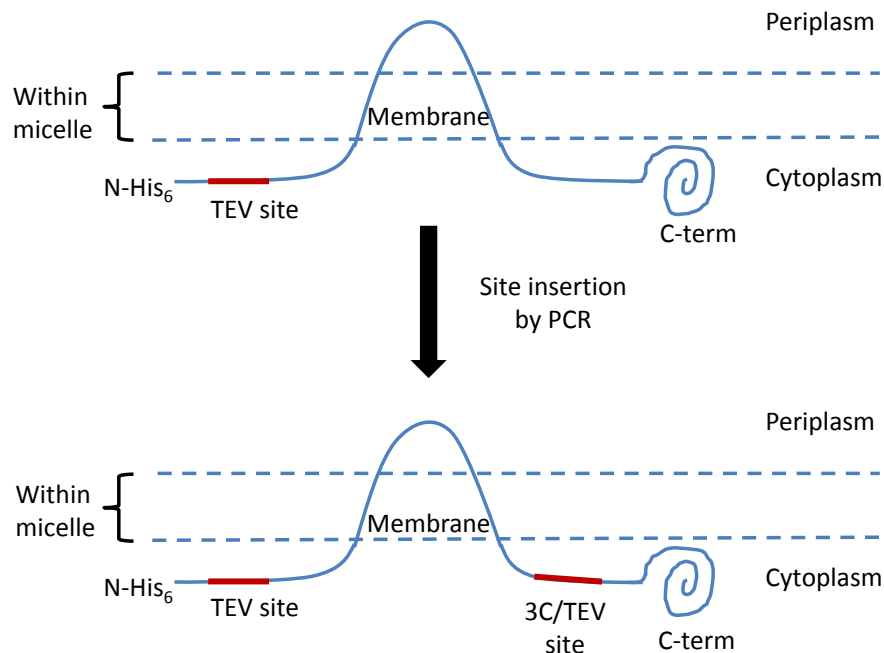


Figure 4.3.5: Schematic representation of a VanS protein and the proposed position for insertion of an enzymatic cleavage site. VanS has a predicted N-in, C-in topology with two transmembrane domains, and the inserted 3C/TEV cleavage site would proceed these in a solvent-exposed region (outside the micelle).

Enzymatic cleavage would be conducted on detergent-solubilised, purified full-length VanS proteins, and hence a further requirement is that the cleavage site must be inserted into a solvent-exposed region (i.e. not enclosed in the micelle), within the cytoplasmic domain. To confirm that this site would be in a solvent-exposed region, protein samples that had been purified in DPC detergent, were digested with trypsin or chymotrypsin, which cleave at multiple positions in the protein, and would show accessible regions. Trypsin cleaves peptide bonds mainly at the carboxyl side of Lys or Arg residues, whereas chymotrypsin preferentially cleaves peptide bonds where the carboxyl side of the bond contains a large hydrophobic residue e.g. Tyr, Trp or Phe.

Digestion experiments were set up with a 1:50 ratio of [tryptic enzyme]:[protein], and aliquots of the mixture were taken at different timepoints and resolved on 15% SDS-PAGE gels and corresponding Western blots (see Figure 4.3.6). The blots would enable identification of peptide fragments containing a His-tag, and therefore fragments from the N-terminal region. Although several bands were observed on SDS-PAGE gels from digestion with chymotrypsin, none of them appeared to be His-tagged proteins (data not shown). Whereas, digestion with trypsin produced two major his-tagged bands (see arrows in Figure 4.3.6 at ~22 and ~16 kDa), which were present at both 1:20 and 1:50 cleavage ratios. The two his-tagged proteins were excised from the corresponding SDS-PAGE gels, and sent for identification by means of fragmentation and mass spectrometric analysis (using nanoLC-ESI-MS/MS, section 2.8.2). Similar bands were observed during trypsin digestion of detergent-solubilised VanS_{SC} proteins which were also sent for identification. From the MS/MS fragmentation data, peptide residues in the cleaved products were identified and mapped onto the full-length sequence (see Figure 4.3.7).

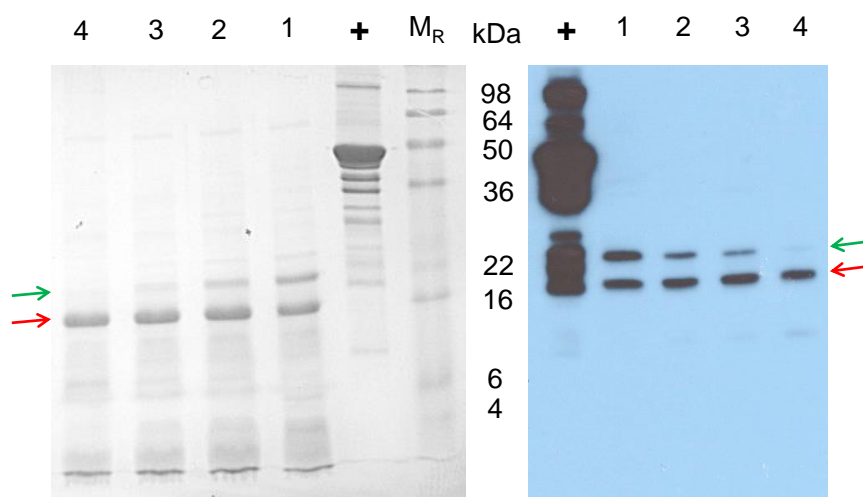


Figure 4.3.6: (left) A 15% SDS-PAGE gel containing digested samples of *N-His₆-VanS_A* collected over timepoints, (right) the corresponding Western blot. Samples were collected after 2, 4, 6 and 16 hours tryptic digestion (labelled 1-4 respectively), at a ratio of 1:50 [trypsin]:[protein]. *M_R* - Prestained SeeBlue Plus2 marker (Invitrogen). Two major digestion products were observed, which were his-tagged (green and red arrow).

(a)	1	MSYYHHHHH	DYDIPTTENL	YFQGAMVIKL	KNKKNDYSKL	ERKLYMYIVA
	51	<u>IVVVAIVFVL</u>	YIRSMIRGKL	GDWILSILEN	<u>KYDLNHLDAM</u>	<u>KLYQYSIRNN</u>
	101	<u>IDIFIYVAIV</u>	<u>ISILILCRVM</u>	LSKFAKYFDE	INTGIDVLIQ	<u>NEDKQIELSA</u>
	151	<u>EMDVMEQKLN</u>	TLKRTLEKRE	QDAKLAEQRK	NDVVMYLAHD	IKTPLTSIIG
	201	YLSLLDEAPD	MPVDQKAKYV	HITLDKAYRL	EQLIDEFFEI	TRYNLQITIL
	251	TKTHIDLYYM	LVQMTDEFYP	QLSAHGKQAV	IHAPEDLTVS	GDPDKLARVF
	301	NNILKNAAAY	SEDNSIIDIT	AGLSGDVVSI	EFKNTGSIPK	DKLAAIFEKF
	351	YRLDNARSSD	TGGAGLGLAI	AKEIIVQHGG	QIYAESNDNY	TTFRVELPAM
	401	PDLVDKRRS				
(b)	1	MSYYHHHHH	DYDIPTTENL	YFQGAMDRRP	GLSVRLKLTIL	SYAGFLTLAG
	51	<u>VLLLVAVGVF</u>	LLDQGWLLTN	ERGAVRATPG	<u>TVFLRSFAPT</u>	<u>AAWVMAFLIV</u>
	101	<u>FGLVGGWFLA</u>	<u>GRMLAPLDRI</u>	TEATRТАATG	SLSHRIRLPG	<u>RRDEYRELAD</u>
	151	<u>AFDEMLARLE</u>	AHVAEQRRFA	ANASHEL RTP	LAVSKAILDV	ARTDPHQDPG
	201	EIIDRLHAVN	TRAILDTEAL	LLLSRAGORS	FTREQVDMSL	LAEATETLL
	251	PFAEKHGVTL	ETRGHVTLAL	GSPALLQLT	TNLVHNAIVH	NLPGRGRVWI
	301	HTAAGPRITR	LVVENTGDLI	SPHQASTLTE	PFQRGTERIH	TDHPGVGLGL
	351	AIVNTITQAH	DGTLTILPRH	SGGLRVIVEL	PAAAPHTGR	

Figure 4.3.7: Map of peptide fragments identified by MS/MS analysis of excised gel bands from digestion of VanS_A or VanS_{SC}. Maps are shown for the His-tagged VanS_A band observed on SDS-PAGE at ~22 kDa (a) and the His-tagged VanS_{SC} band observed at ~17 kDa (b). Peptide fragments are highlighted, and predicted TM domains are underlined.

Maps of peptide fragments identified from excised gel bands show accessible regions either in the periplasmic loop region between the two predicted TM domains, or in the cytoplasmic domain that follows the second TM helix. Importantly, both VanS_A and VanS_{SC} are being cleaved by trypsin at ~20 – 30 residues after the predicted second TM helix (at Q120 for VanS_A and E122 for VanS_{SC}), so a site inserted around this region should be cleavable by the viral proteases. Initial expressions showed that SA120 and SSC120 were the most soluble expressed proteins, so cleavage at ~120th residue should give stable N-terminal products.

Bioinformatic analyses of the protein sequences using PSIPred (and JPred3) software (Jones, 1999; Cole *et al.*, 2008) also revealed that both VanS_A and VanS_{SC} sequences exhibited relatively unstructured, coiled regions in the region of the 110-120th residue (see Figure 4.3.8). A digestion site in the coiled region should not affect protein secondary structure, and will hopefully cleave to leave two separated sections, without any unwanted hydrophobic interactions maintaining the protein structure. The full-length protein should also still express, insert into membranes and obtain its native fold with the cleavage site present.

In this protocol, two primers are designed with different sequences, which do not fully base pair with the template DNA and amplify the template sequence in opposite directions. This results in linear mutated strands with blunt-ends which can be ligated (and re-circularised), to obtain the gene, containing the full stretch of inserted amino acids. For full details and a diagram of the method applied to *vanS* genes, see section 2.4.2.

After transformation of the ligation mixture into *E. coli* TOP10 cells (section 2.4.7), and extraction of positive transformants by minipreparation, the presence of a correctly sized insert was determined from restriction digests (section 2.4.3). DNA sequencing (section 2.4.8) was then used to confirm the addition of a TEV or 3C site, correctly orientated within the vector and in the correct reading frame. 3C and TEV sites were successfully incorporated into both *vanS_A* and *vanS_{SC}* genes (e.g. in Figure 4.3.9) and expression from the constructs could now be tested, prior to digestion at the sites.

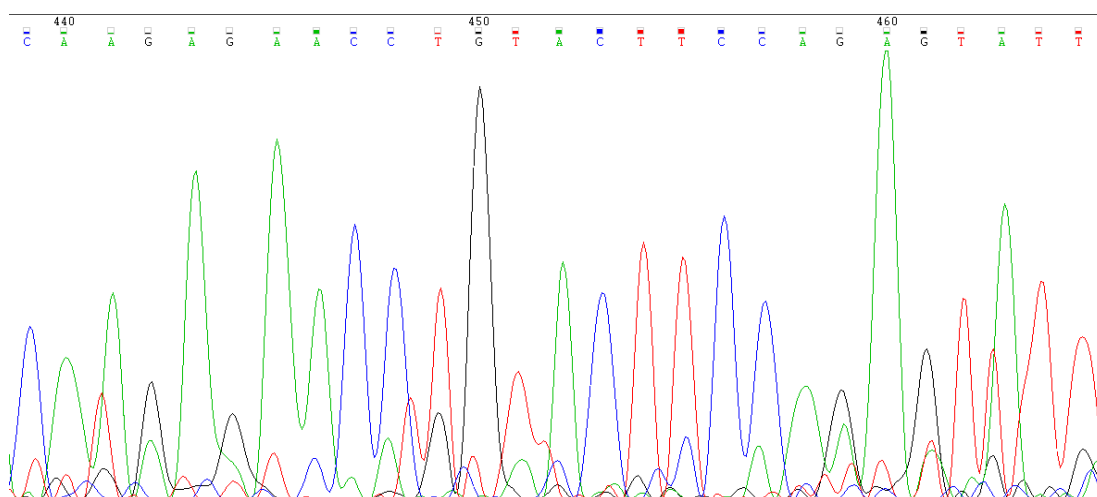


Figure 4.3.9: Sequencing data showing a section of the *VanS_A* DNA sequence containing an inserted TEV site (GAG AAC CTG TAC TTC CAG AGT) encoding for ENLYFQS.

4.4 M9 Minimal Media Expression of *vanS* genes

For isotopic labelling of recombinant VanS proteins, a standard version of the M9 minimal media protocol was followed (Sambrook *et al.*, 1989), which employs ^{15}N ammonium chloride for nitrogen labelling, and if required ^{13}C glucose can be used for carbon labelling, and deuterium oxide for deuteration (see section 2.5.1). Supplements can also be added to the media such as trace metal mixtures and vitamins, which can enhance growth and expression (Jansson *et al.*, 1996; Kainosho, 1997; Cai *et al.*, 1998). For these studies, Basal Medium Eagle (BME) vitamins (Sigma) were chosen which consist of vitamins such as thiamine, riboflavin and folic acid, to stimulate cell growth. The only trace metals tested were calcium chloride and magnesium sulphate, which are commonly used alongside M9 metal salts in minimal media preparations. However, in later expression trials, the addition of iron (III) chloride to media was also analysed.

Isotopically labelled media is expensive, and optimisation of expression conditions and growth media is a necessary requirement, before addition of labelled ammonium chloride and/or glucose. Therefore, expression trials were conducted for the full-length His-tagged VanS proteins in unlabelled M9 minimal media (prior to site insertion). M9 salts were prepared as detailed in section 2.2.1 and used to make a minimal media (see section 2.5.1). This media contains a source of ions (1x M9 salts), a source of carbon for growth (glucose) and a source of nitrogen to synthesise bases and amino acids (ammonium chloride), other metals (CaCl_2 , MgSO_4), vitamins, and antibiotics, as suggested by (Sambrook *et al.*, 1989).

Traditionally for protein NMR, constructs are transformed into *E. coli* and grown on M9 plates, with single colonies used to inoculate M9 starter cultures, which in turn can be used to inoculate larger cultures e.g. 1L. At this point M9 salts are supplemented with metals, vitamins, and labelled ammonium chloride or glucose. The advantage of this route is that cells grow in M9 media throughout, providing a high yield of uniformly labelled protein.

However, unlike rich Luria Broth media, minimal media excludes yeast and other nutrients, and supplies only the exact nutrients needed for bacteria to grow. Therefore slower growth rates are observed, which can result in reduced expression due to cytotoxic effects associated with the plasmid exerting selective pressure (Baneyx, 1999) and reduced viability of cells to overexpress proteins. In a number of recent papers, authors have shown that rich LB media can be used for transformation, inoculation and growth of large-scale cultures then switched to M9 minimal media at the point of induction for overexpression of labelled proteins (Marley *et al.*, 2001; Cai *et al.*, 1998; Sivashanmugam *et al.*, 2009). In this way, high level protein expression can be achieved, in a time-efficient manner by utilising the fast doubling rates of *E. coli* cells in the media. Media is switched by gently pelleting the cells once at the mid-log phase, washing and resuspending in the minimal media, and allowing cells to equilibrate in the new media (usually for one hour) before inducing.

Using this method, Cai *et al.*, (1998) monitored cell growth in fermentors, and measured the decrease in oxygen consumption (which occurs upon exhaustion of essential nutrients) to precisely time the switch between unlabelled and labelled nutrients. Similarly, Marley *et al.*, (2001) monitored cell growth in regular shaker incubators, and found optimal expression levels by growing in unsaturated LB media and exchanging around the mid-log phase ($OD_{600} \sim 0.7$). However, when exchanging media, they also concentrated the cell suspension to 1/2, 1/4 or 1/8th of its original volume, before transferring the bacteria into isotopically labelled media for expression. They stated that exchanging cells into fresh media immediately prior to induction can increase protein expression levels by removing byproducts (e.g. unlabelled metabolites) inhibitory to growth and expression, and prevent problems arising from cells going into the stationary phase. Furthermore, the optimal cell density for induction differs for freshly exchanged media, and allows 'high-cell-density' expression (by concentrating the cells). Overall, a concentration factor of four times (25% of original volume) conferred maximal protein expression for those studied, but this is protein dependent.

Finally, Sivashanmugam *et al.*, (2009) went a step further to generate improved methods for triple-labelled protein expression (incorporating D₂O) and examined two high-cell-density bacterial expression methods: an autoinduction method by Studier (2005), and the IPTG-induction method. The Studier method was advantageous as it achieved high cell densities with minimal handling, as there was no need to monitor growth for induction, however, results were inconsistent with OD₆₀₀ values reaching 8-20, but no protein yield observed. By comparison, the high-cell-density method allowed induction and harvesting of cells (after 4 hours growth at 37°C) within a normal working day, and gave high yields (OD₆₀₀ 5-10 from growth in LB media). For isotopic labelling the group state that a longer period of exchange time e.g. two hours, at a reduced temperature is preferable. This allows clearance of unlabelled metabolites and slows down bacterial growth during the exchange period, preserving nutrients for protein synthesis after IPTG-induction. Two further alterations were the buffer pH in the media and the culture volume. Typically during expression, the pH drops from 7.2 to ~6 at the point of harvest, and should be set a log higher (pH ~8) to increase buffering capacity and prevent plasmid instability and degradation of ampicillin. Cultures volume should also be limited to 1/5th of the flask volume to increase aeration.

Using this literature information, it was possible to combine protocols, to examine high-cell-density protein expression levels in M9 minimal media at different induction temperatures, and with addition of trace metals. The pH for the M9 minimal media was set at pH 8 for higher buffering capacity, and ampicillin was added to initial cultures and in the M9 media to maintain selection pressure. All cultures were grown at 37°C in LB media, and the temperature was reduced for expression in M9 media to obtain high yields of soluble, isotopically labelled proteins. A schematic representation of the optimised, high-cell density method used in these studies, based on literature protocols is given in Figure 4.4.1.

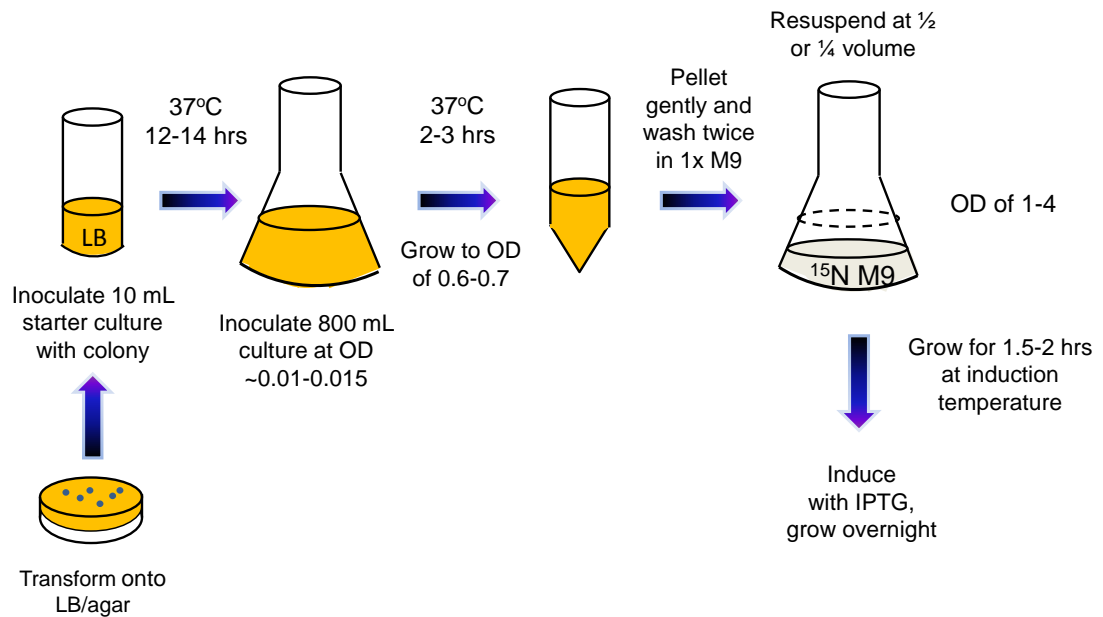


Figure 4.4.1: A diagram of the optimised high-cell-density method used for production of uniformly ^{15}N -labelled VanS proteins. Adapted from methods by Marley et al., (2001) and Sivashanmugam et al., (2009). Constructs are transformed on LB/agar plates, and single colonies added to 10mL starter cultures, which are grown overnight to an $\text{OD}_{600} \sim 1-1.5$. In this way, 800mL cultures of LB media can be inoculated at 1/100 dilution, and grown until mid-log phase ($\text{OD}_{600} \sim 0.6-0.7$) before gentle pelleting, and washing in M9 salts. In the final wash, cells are resuspended at $\frac{1}{2}$ or $\frac{1}{4}$ of the original volume in ^{15}N labelled M9 media containing metals, vitamins and antibiotics to achieve high cell density. The culture is then equilibrated at the induction temperature for 1-2 hours, before induction and growth.

Using the high-cell-density method, expression was initially tested for full-length VanS proteins using unlabelled M9 minimal media (section 2.5.1) and under similar conditions to those that gave favourable expression in *E. coli* C41pRIL. The media was switched from cultures grown in LB to M9 minimal media, (initially without concentrating) and induced with IPTG at an OD_{600} of 0.6-0.7. The cells were allowed to grow at 25°C overnight for VanS_A or 18°C overnight for VanS_{SC} and overexpressions were analysed on SDS-PAGE gels and Western Blots as shown in Figure 4.4.2.

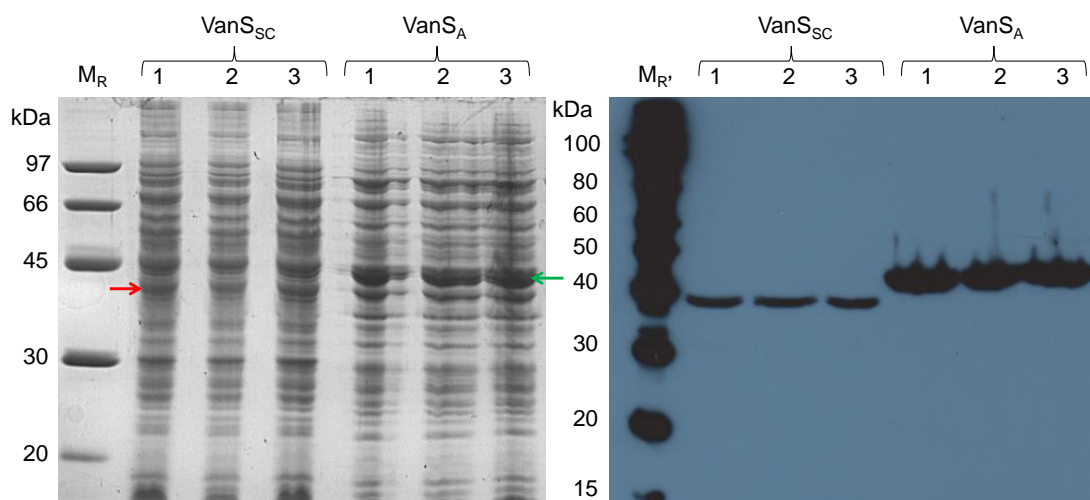


Figure 4.4.2: (left) A 12% SDS-PAGE gel of *VanS_A* and *VanS_{SC}* overexpression in M9 minimal media, at different IPTG concentrations, and (right) corresponding Western blot. *M_R* – GE LMW-SDS marker, *M_{R'}* – Benchmark His-tagged marker, Lane 1 – 0.2 mM IPTG added, Lane 2 – 0.5 mM IPTG added, Lane 3 – 1mM IPTG added. Bands relating to *VanS_A* (green arrow) and *VanS_{SC}* (red arrow) are indicated.

These experiments demonstrated that both *VanS_A* and *VanS_{SC}* proteins could be overexpressed in M9 media, with similar levels to those observed in LB. To further optimise the expression yield, different concentration factors were tested (1x, 2x and 4x), and trace amounts of iron were added to improve bacterial growth. The addition of iron was suggested in an article by Cambridge Isotope Laboratories entitled “Top Ten Tips for Producing ¹³C ¹⁵N Protein in Abundance” (Berthold *et al.*, undated), who stated that, in the absence of trace metals, 50-100 μM FeCl₃ alone will provide the nearly the same increase in expression level (Studier, 2005). 800 mL cultures in 2L flasks were inoculated and grown to an OD₆₀₀ ~ 0.6, and exchanged into 800, 400 or 200 mL of ¹⁵N-labelled M9 minimal media, with and without supplementary iron (III) chloride. After overnight induction at a fixed IPTG concentration (0.2 mM), the resulting expression levels were analysed by SDS-PAGE and quantified by band sizing on the corresponding Western blots (Appendix Figure 7). A plot of normalised expression level relative to the unconcentrated, unsupplemented sample is shown in Figure 4.4.3.

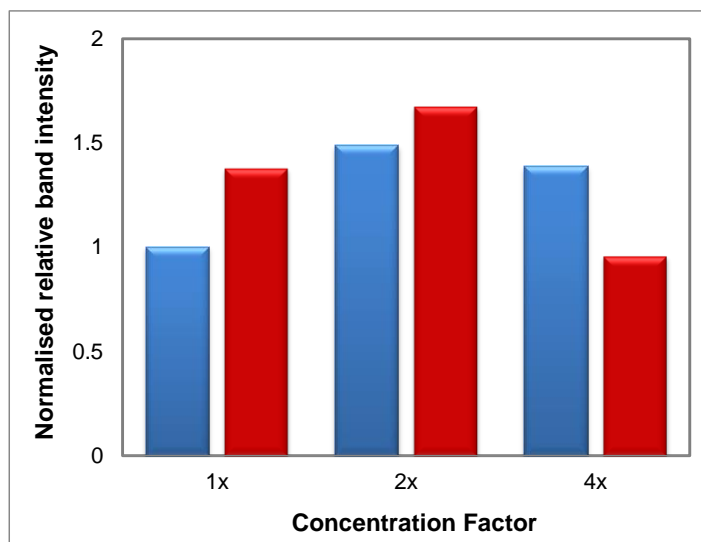


Figure 4.4.3: A bar chart showing relative band intensities for full-length *VanS_A* proteins overexpressed under different conditions in ¹⁵N M9 minimal media. The intensities were quantified from Western blots using ImageJ analysis and normalised against the sample grown in media without iron supplement or concentrating (1x). The concentration factor was either equal to that in LB (1x) or concentrated to half (2x) or quarter (4x) of the initial volume. Some expressions were also supplemented with 75 µM iron (III) chloride (red bars).

In agreement with studies by Marley *et al.*, (2001), concentrating the cell culture during exchange into minimal media significantly increased the expression yield of soluble VanS protein, but above a concentration factor of 2, the level of expression appears to decrease. High-density bacterial cells require more nutrition in the medium for overexpression, therefore an increased amount of carbon source (glucose) could enable healthy cell growth at high concentration factors. Indeed, Sivashanmugam *et al.*, (2009), believe that the amount of glucose is critical for high-cell-density expression, and showed that they could increase cell density at concentration factors of 8x by adding up to 10 g/L of glucose in minimal media. Therefore the addition of 4 g/L of glucose was used in all future expression trials (in place of 2 g/L), to ensure cells would have sufficient nutrients to overexpress VanS proteins upon concentrating two-fold or four-fold. In addition, cells supplemented with iron also increased their expression level, demonstrating it can act in place of a mixture of trace metals.

These findings led to the optimised M9 minimal media expression protocol, as given in Figure 4.4.1 and section 2.5.1. It was now possible to use this protocol to overexpress mutagenic ^{15}N -labelled VanS proteins, containing the newly inserted enzymatic cleavage sites, which could be subsequently digested to obtain the desired ^{15}N -labelled sensor domain.

4.5 M9 Minimal Media Expression of mutant *vanS* genes for Enzymatic Cleavage and Purification of the isolated VanS sensor domain

After cloning in the TEV and 3C sites, expression trials were conducted for the full-length His-tagged VanS proteins in ^{15}N -labelled M9 minimal media. VanS proteins were overexpressed and allowed to grow at 25°C (for VanS_A-3C or VanS_A-TEV) or 18°C (for VanS_{SC}-3C or VanS_{SC}-TEV) overnight. Expression was assessed using SDS-PAGE and Western Blots as shown in Figure 4.5.1.

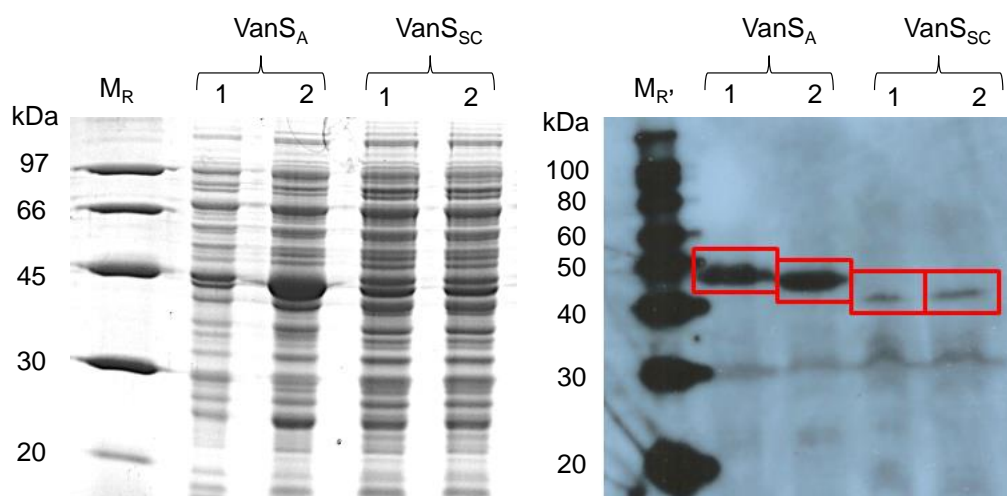


Figure 4.5.1: (left) A 12% SDS-PAGE gel showing overexpression of VanS_A and VanS_{SC} mutants in ^{15}N -labelled M9 minimal media, and (right) the corresponding Western blot. VanS_A and VanS_{SC} proteins are indicated by boxes. Lane 1 – VanS containing TEV site, Lane 2 – VanS containing 3C site, M_R – LMW-SDS Protein Ladder, M_{R'} – Benchmark his-tagged ladder. VanS_A and VanS_{SC} proteins were induced at an [IPTG] of 0.2 and 1mM respectively

These experiments demonstrate that both VanS_A and VanS_{SC} mutants can be overexpressed in ^{15}N -labelled M9 media, with similar levels to that of the wild-type proteins in LB media.

The blots show only marginally higher expression yields for the VanS-3C proteins (compared to VanS-TEV) even though by SDS-PAGE, VanS_A-3C appears by far the most expressed. VanS-TEV and VanS-3C proteins were next solubilised in DPC micelles and purified by nickel affinity chromatography, before digestion with in-house synthesised TEV (section 2.12.1) and 3C protease (sections 2.12.2 & 2.12.3), for the respective constructs. The ratio of [protease]:[protein] was fixed at 1:1. Products were analysed during digestion by SDS-PAGE and Western blotting (see Figures 4.5.2 & 4.5.3, and Appendix Figure 8).

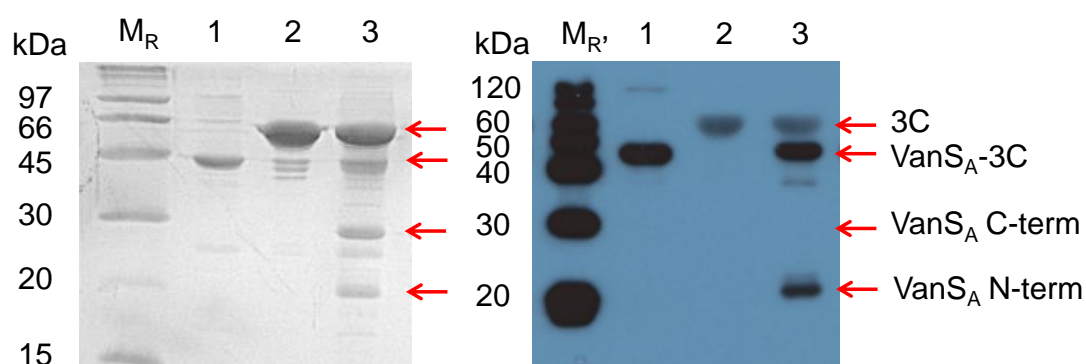


Figure 4.5.2: (left) A 15% SDS-PAGE gel showing initial products from digestion of VanS_A-3C after 4 hours, (right) corresponding western blot. Key bands are labeled with arrows. M_R: LMW-SDS Protein Marker, M_{R'}: MagicMark XP ladder. Lane 1: VanS_A-3C protein, Lane 2: 3C protease (~ 66 kDa), Lane 3: 1:1 Digestion mixture.

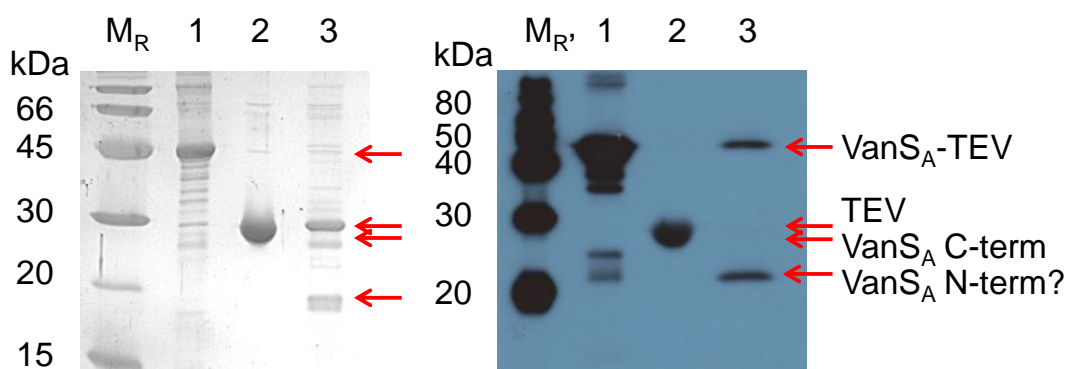


Figure 4.5.3: (left) A 15% SDS-PAGE gel showing initial products from TEV digestion of VanS_A-TEV after 4 hours, (right) corresponding western blot. Key bands are labeled with arrows. M_R: LMW-SDS Protein Marker, M_{R'}: MagicMark XP ladder. Lane 1: VanS_A-TEV protein, Lane 2: TEV protease (~ 27 kDa), Lane 3: 1:1 Digestion mixture. NB: A band for TEV should have been visible in the blot in Lane 3, but must not have transferred properly.

Figure 4.5.2 shows that during digestion of purified VanS_A-3C with 3C protease, two major bands are present at ~ 29 kDa and ~ 17 kDa, with the latter visible on Western blots. These bands correspond well with the predicted molecular weights of the untagged C-terminal cytoplasmic product and the His-tagged N-terminal membrane-bound product. Similar digestion products are also observed for purified VanS_{SC}-3C incubated with 3C protease (see Appendix Figure 8). In Figure 4.5.3, however, VanS_A-TEV is rapidly digested by TEV protease and the production of C-terminal and N-terminal products was not easy to identify by SDS-PAGE or Western blots. The TEV protease should cleave all tags from the protein therefore no protein bands should be visible on a Western blot of the digestion mixture (assuming 100% cleavage). Unexpectedly though, the corresponding Western blot indicated the presence of a possible N-terminal band (~20 kDa) retaining its his-tag, which suggests that the TEV protease accesses the inserted cytoplasmic cut site more readily than the site immediately following the his-tag. Attempts to purify the products from TEV digestion did not appear to produce any yield of the VanS sensor domain, and therefore purification was pursued only for products from 3C digestion.

In contrast to TEV, the 3C protease cleaved the detergent-purified VanS proteins at only one site, giving the desired His-tagged N-terminal product and C-terminal cytoplasmic product. Since the 3C protease synthesised contained a His-tag and an MBP-tag (as confirmed by an anti-MBP blot, see Appendix Figure 9), it was possible to selectively remove the enzyme after digestion using amylose resin (section 2.12.3). This resin has a high affinity for MBP and allowed removal of the protease from the digestion mixture, with the remaining VanS proteins eluting in the flow through and wash steps. This eluent was then rebound to pre-charged nickel resin to remove the untagged C-terminal cytoplasmic domain (see section 2.12.3). The flow through was collected and the column was washed with an imidazole gradient to elute the ¹⁵N-labelled N-terminal His-tagged VanS protein (in DPC micelles) under high imidazole. An SDS-PAGE gel showing products from the amylose binding and subsequent IMAC purification steps is shown in Figure 4.5.4.

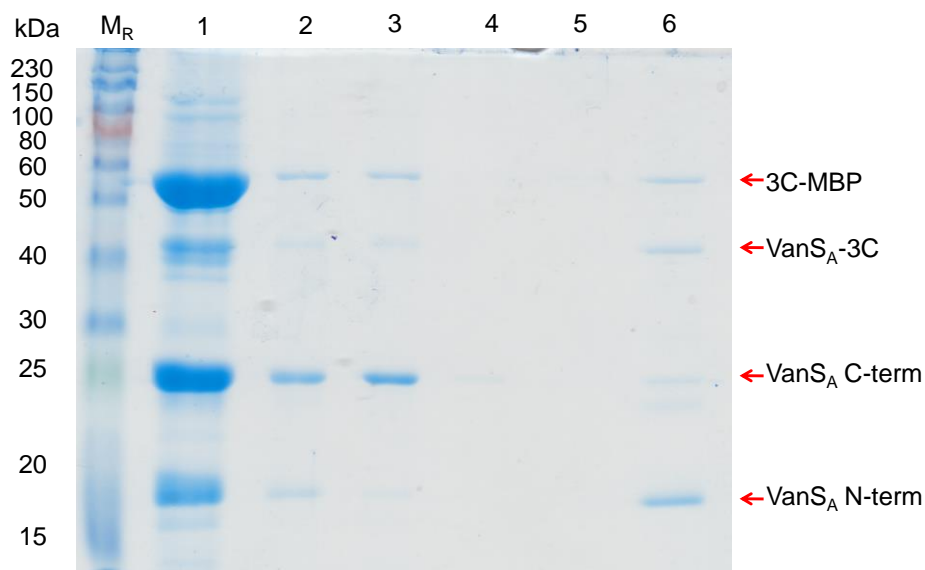


Figure 4.5.4: A 12% SDS-PAGE gel showing selective purification of the VanS_A N-terminal 'sensor' domain away from the C-terminal domain and 3C enzyme. Lane 1 – 1:1 digest of VanS_A-3C with 3C protease overnight, Lane 2 – Flow through upon rocking in amylose resin, Lane 3 – Flow through upon subsequent rocking in nickel sepharose resin, Lane 4 – 20mM Imidazole wash fraction, Lane 5 – 50mM Imidazole wash fraction, Lane 6 – 250mM Imidazole elution fraction. M_R – ColorPlus Prestained Ladder (10-230 kDa).

The eluted N-terminal VanS sensor domain was then concentrated in a 10 kDa MWCO concentrator to 500 μ L for final purification by Gel Filtration Chromatography (see section 2.6.7) on a Superose 6 10/300 GL column, to remove any residual 3C protease and undigested VanS. An example of a typical gel filtration profile acquired is given in Figure 4.5.5, and the overall products from all the purification steps for VanS_A are illustrated on an SDS-PAGE gel (Figure 4.5.6), with the purified N-terminal sensor domain of VanS_A in DPC micelles shown in Lane 6.

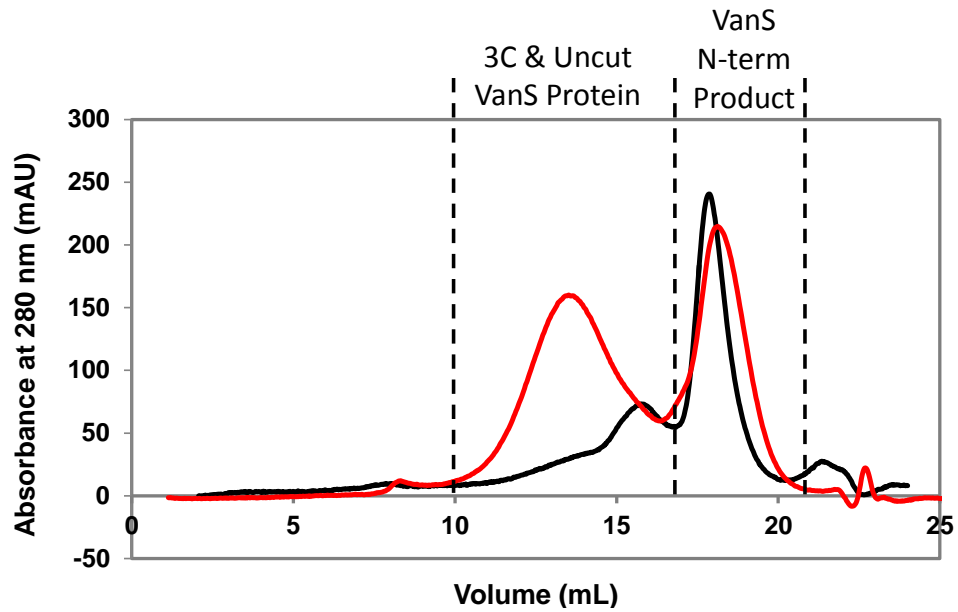


Figure 4.5.5: Gel filtration chromatograms of protein samples containing the N-terminal sensor domain of ^{15}N -labelled VanS_A (black line) or VanS_{SC} (red line) in DPC micelles, applied to a Superose 12 10/300 GL column. Plots were drawn in Microsoft Excel. The VanS sensor domain eluted at 17-18 mL, and undigested full-length protein and 3C protease eluted at 10-16 mL. An isocratic gradient of 100 % B was used to elute the proteins (buffer B: 20 mM HEPES pH 6.8 or 50 mM phosphate pH 6.3, 75-100 mM NaCl, 2 mM DPC).

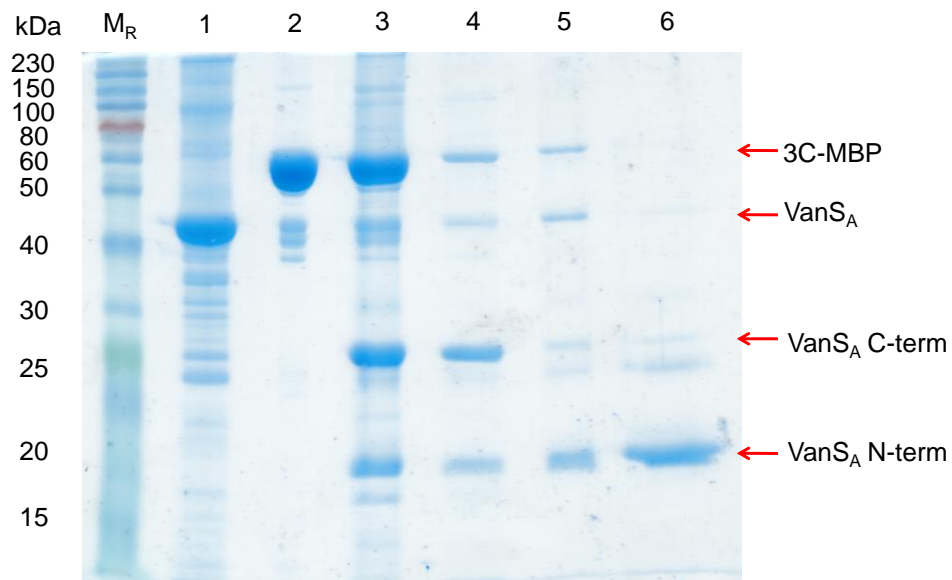


Figure 4.5.6: A 15% SDS-PAGE gel showing digestion and subsequent purification of the N-terminal 'sensor' domain of VanS_A . Lane 1: IMAC purified VanS_A -3C, Lane 2: purified 3C protease, Lane 3: 1:1 Digest of VanS_A -3C with 3C protease after 4 hours incubation, Lane 4: Digest after removal of 3C protease on amylose resin, Lane 5: Digest after removal of C-terminal untagged VanS_A by IMAC, Lane 6: VanS_A sensor domain purified by GFC.

The purified VanS N-terminal product in DPC was eluted from the gel filtration column (at an elution volume of 17 – 20 mL) and was further concentrated to ~ 200 μ L, for application into 3 mm BrukerMATCH NMR tubes, to analyse protein structure and ligand binding properties by solution state NMR spectroscopy (see section 2.14). For NMR studies of alpha-helical membrane proteins such as VanS, the concentration of detergent must be tuned to enable sufficient tumbling of the associated protein-micelle complex in solution, whilst not being excessively high so as to cause denaturing of the native fold of the membrane protein. A list of all current structures for membrane proteins solved by solution state NMR is given at <http://www.drорlist.com/nmr/>. By studying the list of structures it is apparent that the detergent and concentration used successfully for solution NMR structure determination differ greatly, but DPC is the most commonly used detergent, and concentrations are in the order of 50 mM and above (except in mixed micellar systems or nanodiscs). Therefore for these studies, the final concentration of DPC detergent in the NMR sample was adjusted from 2 mM (after gel filtration) to 50 mM, and all samples were analysed by CD spectroscopy (refer to Figure 4.6.4) before analysis in the NMR spectrometer, to ensure the alpha-helical protein fold (~ 60% α -helical) was still maintained.

Initially, NMR was used to analyse purified, uniformly 15 N-labelled VanS sensor domains in 50 mM DPC detergent in HEPES or phosphate buffer. The pH was maintained near physiological values, but was required to be below pH 7, in order to avoid loss of amide (NH) signals due to exchange in solution. From these experiments, several factors required optimisation to achieve high resolution 2D 1 H- 15 N HSQC NMR spectra, with well resolved peaks and uniform peak intensities. These included buffer selection, pH, temperature and detergent, and are detailed in section 4.6.

4.6 2D Solution State NMR studies of the VanS sensor domain and Optimisation of Solution Conditions by Temperature, Detergent and Buffer Screening

To find solution conditions required to produce well-folded and homogeneous samples of the VanS_A sensor domain, the sensitivity-enhanced ¹H-¹⁵N Heteronuclear Single Quantum Coherence (HSQC) experiment was used (see section 2.14). A well-resolved HSQC spectrum containing sharp, well-dispersed signals is a strong predictor of correct folding and is essential for successful structural characterisation. More specifically, when judging the suitability of a set of conditions, the following properties of the spectrum were primarily considered: peak width (narrow peaks are optimal), the number of observable peaks (approximately 112 backbone amide peaks should be observable for VanS_A and 107 for VanS_{SC}, not including the 39/40 predicted transmembrane residues in each protein), chemical shift dispersion (characteristic of a well-folded protein), and homogeneity of peak intensity.

4.6.1 Effect of magnetic field strength and temperature

Initially, the effects of magnetic field strength and temperature were examined for samples of the N-terminal domain of VanS_A in 50 mM DPC detergent, after gel filtration. ¹H-¹⁵N HSQC spectra were acquired on 500 and 700 MHz Bruker spectrometers (see Figure 4.6.1.1A and B). These spectra contain peaks for the backbone amide NH groups (¹Hδ ~ 8-9 ppm) as well as NH-containing functional groups on side-chains of specific residues (¹Hδ < 8 ppm). At 500 MHz, the peaks are broad and difficult to resolve, indicating short spin-spin relaxation times (T₂) and variable (heterogeneous) peak intensities. The chemical shifts are not well-dispersed either, making it difficult to judge the number of peaks in the spectrum. The spectrum is improved at 700 MHz (panel B). In addition to using a higher field strength, which improves resolution, the temperature was increased from 25°C to 37°C, to improve tumbling rates in solution, and reduce line broadening due to rapid spin-spin relaxation rates (T₂). The spectrum shown in Figure 4.6.1.1B clearly contains additional peaks (55 resolvable), which are narrower and more disperse.

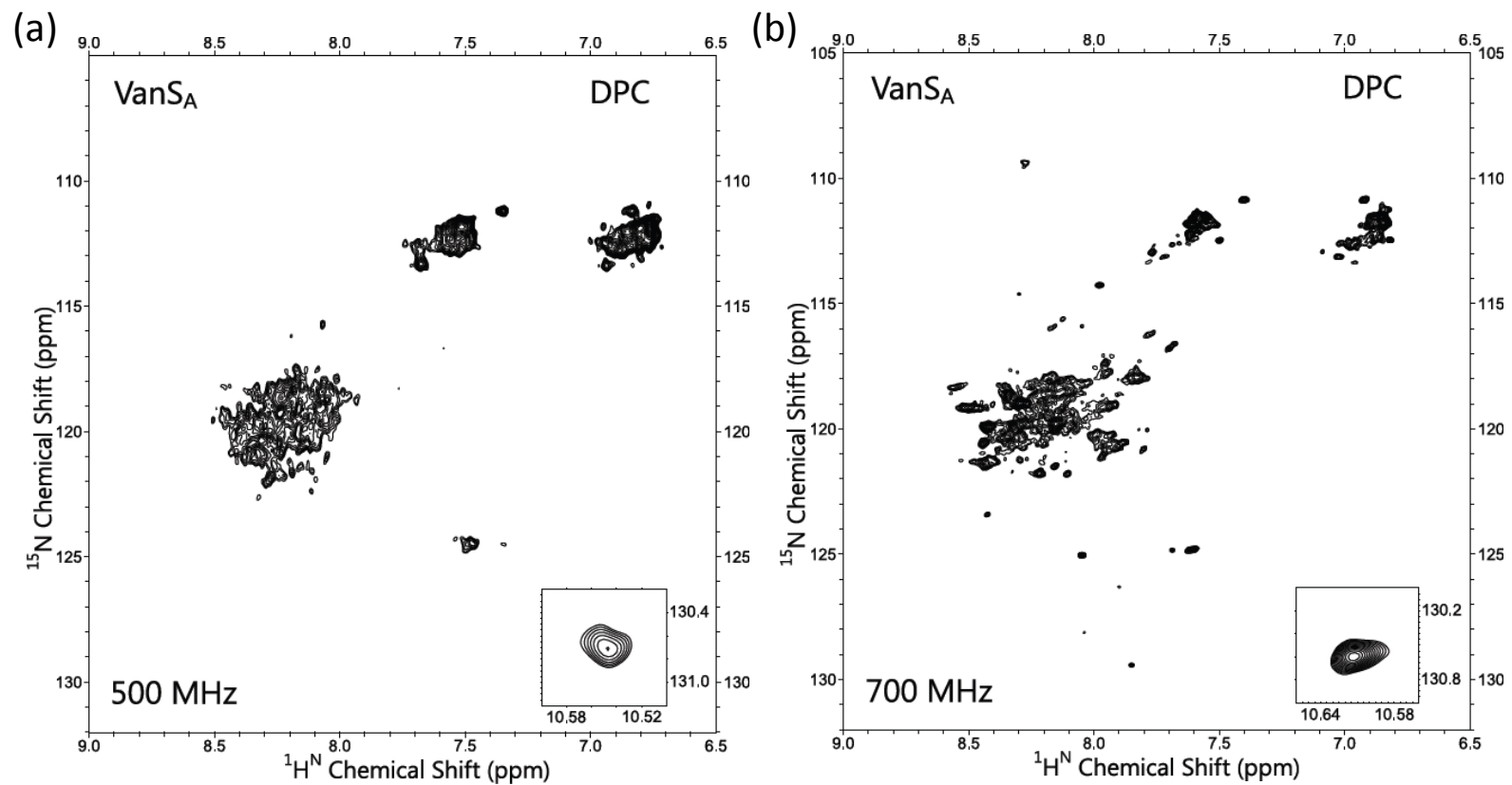


Figure 4.6.1.1: *2D ^1H - ^{15}N HSQC spectrum of 140 μM VanS_A sensor domain collected at (a) 298K on a 500 MHz spectrometer, or (b) 310K on a 700 MHz spectrometer. Both proteins were purified in 50 mM DPC, 50 mM phosphate buffer pH 6.3, 75 mM NaCl.*

The optimal field strength (700 MHz) and temperature (37°C) obtained from these analyses were used to acquire an HSQC spectrum of the VanS_{SC} N-terminal sensor domain, purified and prepared under similar conditions as those for VanS_A. The resulting spectrum is shown in Figure 4.6.1.2. NMR samples of the purified ¹⁵N-labelled samples containing VanS_A and VanS_{SC} sensor domains are given in Appendix Figure 10, which show no obvious impurities, and protein samples appeared stable for up to around two weeks of measurements at 310K.

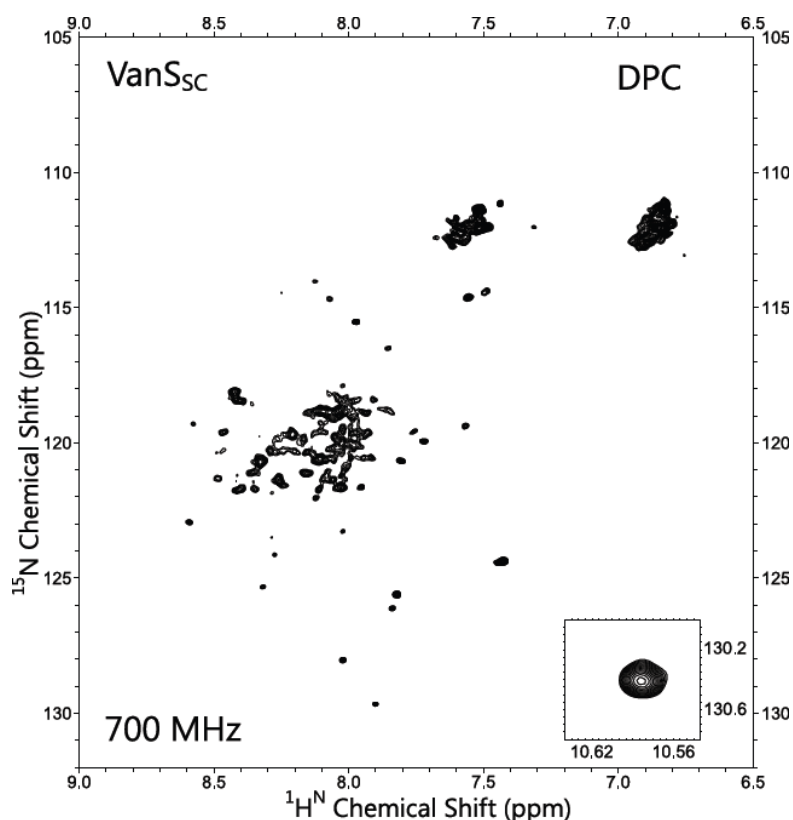


Figure 4.6.1.2: 2D ¹H-¹⁵N HSQC spectrum of 200 μM VanS_{SC} sensor domain in 50 mM DPC, collected at 310K on a 700 MHz spectrometer. Protein was purified into 20 mM HEPES pH 6.8, 75 mM NaCl.

If anything, the spectrum of ¹⁵N-labelled VanS_{SC} in Figure 4.6.1.2, is superior in quality to the VanS_A spectrum (Figure 4.6.1.1B), showing sharp, disperse peaks (78 peaks in total) that are similar in intensity. Overall, it is clear that field strength and temperature are important variables to monitor when optimising spectral quality. The composition, concentration and pH of buffer components can also affect the quality of the NMR spectrum, but there are

currently no firm guides on which buffers are best for a given protein. Unlike sparse matrix screens employed in X-ray crystallisation, there are no simple and rapid analogous buffer screening protocols for NMR analyses, so spectra must be collected for each condition.

4.6.2 Effect of detergent

As demonstrated above, the sensitivity of the spectrometer, the temperature and the buffer choice will influence the spectral quality, but perhaps the most key variable in analysing membrane proteins, is the choice of membrane mimetic (the solubilising detergent). The spectral resolution of a membrane protein within a detergent micelle is directly dependent on the T_2 (spin-spin) relaxation rate. Only those detergents which allow rapid tumbling of the protein-micelle complex in solution can provide long T_2 relaxation times, leading to reduced line broadening and increased signal-to-noise.

Although most NMR structures of membrane proteins have been solved in DPC detergent (see <http://www.drorlist.com/nmr>), it is not the optimal detergent for all proteins, and a number of other detergent classes provide promising membrane mimetics. For instance, Gautier *et al.*, (2010) screened a number of detergents and obtained NMR spectra of a seven-transmembrane-helix GPCR, pSR11, in diheptanoylphosphatidylcholine (DHPC) micelles of a quality that would rival those of 'normal' soluble proteins, despite the fact that the protein-micelle complex was found to be over 70 kDa in size.

In addition, studies by Krueger-Koplin *et al.*, (2004) on three test membrane proteins; the LH1 β -subunit from *R. sphaeroides* (a single TM helix), subunit *c* from *E. coli* (a two TM helix) and the Smr protein from *S. aureus* (a four TM helix), found that by far the highest resolution solution NMR spectra, and most stable protein-micelle complexes were produced in lyso-phospholipid detergents e.g. LPPG and LPPC. These detergents are single chain

analogues of native *E. coli* lipids; dipalmitoylglycerolphosphoglycerol (DPPG) and dipalmitoylglycerolphosphocholine (DPPC) respectively (see Figure 4.6.2.1).

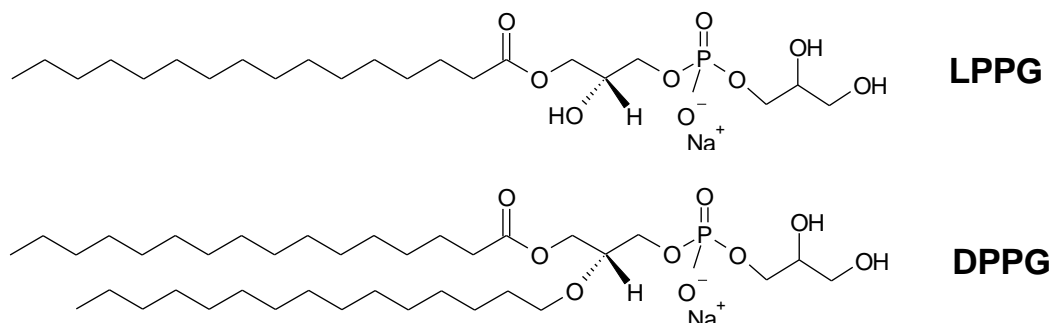


Figure 4.6.2.1: Molecular structures of LPPG and DPPG detergents, drawn in ISISDraw

It is believed that the ability of these lyso-phospholipids to maintain stable, functional protein folds may be closely related to the fact that they are the only class of single-chain detergents that resemble the majority of natural phospholipids, in that they have a polar but uncharged (glycerol) spacer that links the apolar lipid-like C₁₄/C₁₆ tail to the charged headgroup (Krueger-Koplin *et al.*, 2004; Koehler *et al.*, 2010). These long lipid-like tails provide a good match for the hydrophobic span of protein transmembrane domains, whilst the native phospholipid headgroups form favourable interactions with the membrane protein.

Most interestingly, Krueger-Koplin *et al.*, (2004) found that although the protein-lysolipid complexes had diffusion times consistent with molecules > 100 kDa in size, the rotational correlation times for proteins within the micelles (as measured by NOE relaxation experiments) were surprisingly short; on the order of 8 – 12 ns. This is the time anticipated for a 15 – 20 kDa protein tumbling isotropically in solution. It is therefore proposed that the lyso-phospholipids may also be fluid enough to permit rotation of proteins within the confines of the micelle, thus increasing the tumbling rate in solution (reducing line broadening due rapid T₂ spin-spin relaxation) and providing high resolution NMR spectra.

To examine the applicability of the lyso-phospholipids, DHPC and other detergents classes for structural NMR studies, detergent screens were set-up for both VanS proteins. The experimental procedure follows that given in section 2.6.5. Briefly, this involved addition of 1% w/v detergent to a known amount of protein, rocking for 2 hours and then separating the soluble and insoluble fractions by ultracentrifugation. These fractions were loaded in equal volume onto SDS-PAGE gels and blotted (see Appendix Figure 11). The relative percentage of protein solubilised in each detergent (including those tested in section 2.6.5) was calculated from the blots by band sizing, and is represented in the bar chart in Figure 4.6.2.2.

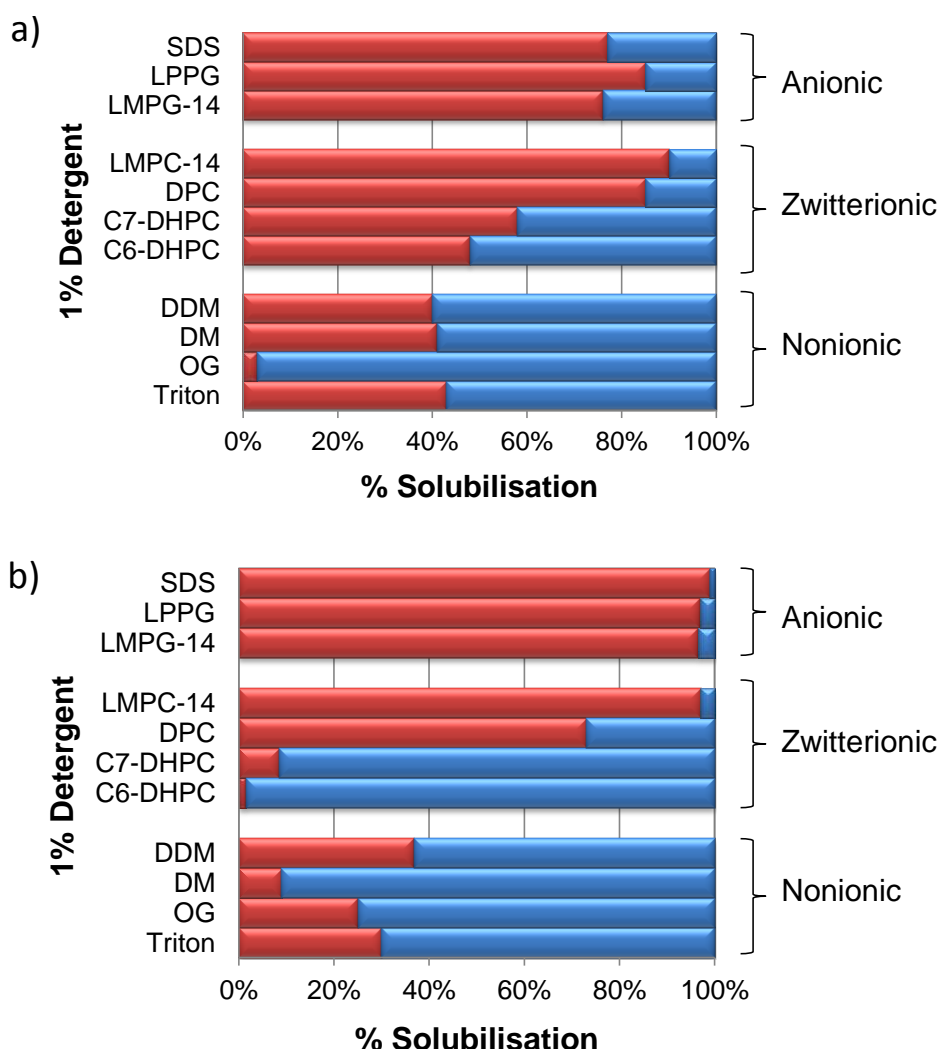


Figure 4.6.2.2: Bar charts showing the relative percentages of soluble (red) and insoluble (blue) protein for (a) VanS_A or (b) VanS_{SC} in different detergents. Percentages were calculated from the intensity of protein bands on Western blots calculated using ImageJ analysis software. Western blots are provided in Appendix Figure 11.

By grouping the detergents into their respective classes, it is clear that anionic (and some zwitterionic) detergents provide optimal solubilisation of the VanS proteins. This is likely to reflect the composition of native *E. coli* and *Enterococcus* membranes. In Gram-negative *E. coli*, the inner membrane is mostly composed of zwitterionic phosphatidylethanolamine lipid (PE, ~ 70%), anionic phosphatidylglycerol lipid (PG, ~ 20%) and cardiolipin (CL, ~ 10%), (Giddey *et al.*, 2009) and there is a net negative charge on the membrane. PE is also converted into zwitterionic PC (phosphatidylcholine) lipid by methylation in cells, which can be found in the inner membrane of some Gram-negative species.

By comparison, although several Gram-positive bacterial membranes contain PG, PE, and CL, they are often enriched with glycolipids (such as lysyl-PG) (Giddey *et al.*, 2009) and lipoteichoic acids (Fabretti *et al.*, 2006), so both membranes have an overall negative charge. It therefore appears that the highest degree of solubility and stability of both VanS proteins is observed in anionic phosphatidylglycerol lipids and some zwitterionic PC lipids, which closely resemble the native functional headgroups present in bacterial membranes.

From the screen above, several candidates for protein solubilisation and NMR analysis were possible e.g. LPPG, LMPG, LMPC and SDS. SDS is a relatively harsh detergent and would destabilise any dimerization of the VanS proteins in solution, which may be required for ligand binding. Whereas, the lyso-phospholipids are detergent analogues of native *E. coli* lipids, and allow protein solubilisation without denaturation. Furthermore, studies by Krueger-Koplin *et al.*, (2004) indicated that for several membrane proteins, the lyso-PG lipids (LMPG/LPPG), provided the highest percentage of resolvable peaks on 2D ^1H - ^{15}N HSQC NMR spectra, and protein lifetimes of one to two months at room temperature (as determined from the quality of 2D ^1H - ^{15}N HSQC spectra observed over the period).

Therefore, new ^{15}N -labelled VanS samples were expressed and purified in lyso-PG detergent, and cleaved and purified as before (see section 2.12.3), in order to obtain the labelled N-terminal sensor domain in 50 mM LPPG. To compare spectra of VanS proteins in LPPG and DPC, the buffer composition was maintained at 50 mM Phosphate pH 6.3, 75 mM NaCl, and the temperature fixed at 310K. An overlaid HSQC is shown in Figure 4.6.2.3.

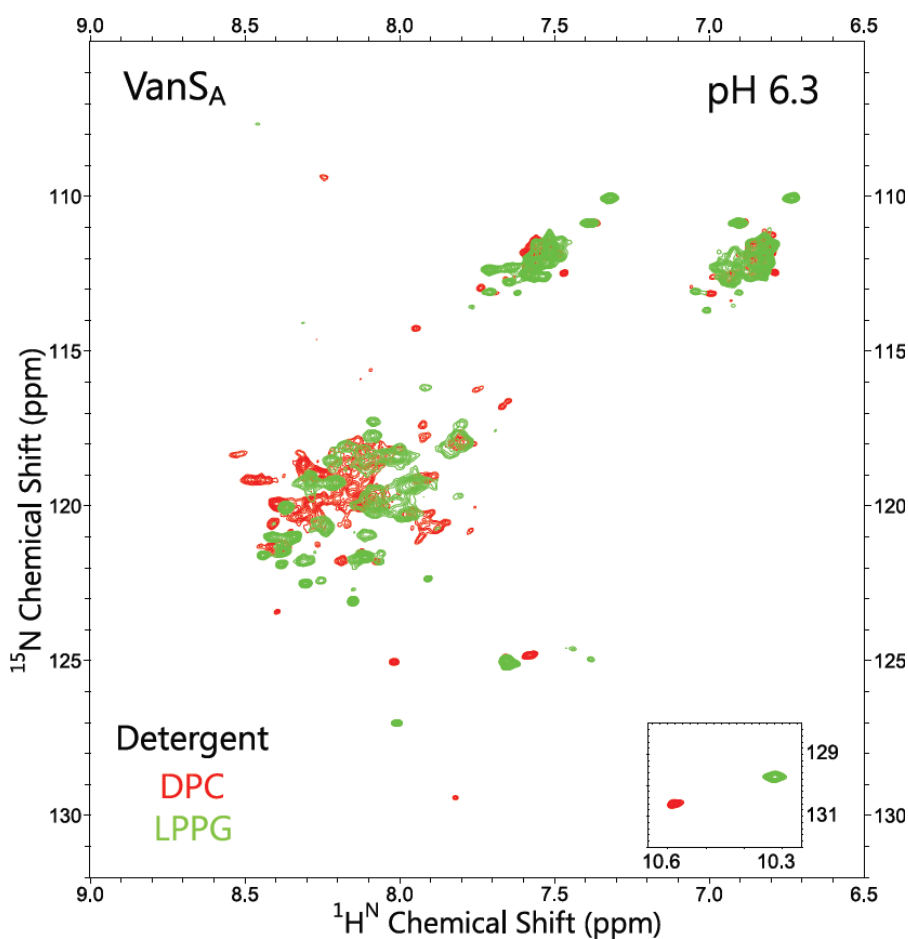


Figure 4.6.2.3: Overlaid 2D ^1H - ^{15}N HSQC spectra of VanS_A sensor domain solubilised in 50 mM DPC at 140 μM (red) or in 50 mM LPPG at 200 μM (green). Both proteins were purified into 50 mM Phosphate pH 6.3, and 75 mM NaCl collected at 310K on a 700 MHz Bruker spectrometer.

A marked improvement in peak resolution is observed for those samples in LPPG detergent (in Figure 4.6.2.3), particularly for those peaks in the backbone amide NH region ($^1\text{H}\delta \sim 8\text{-}9$ ppm). This may be a function of the increased tumbling rate in solution within the micelle, as

postulated by Krueger-Koplin *et al.*, (2004). By peak picking in LPPG, 106 peaks were obtained (including side-chain resonances), which is relatively high considering the N-terminal VanS_A protein has 151 residues in total, of which ~ 40 are present in the transmembrane domains. Therefore an improved NMR spectrum of VanS_A was achieved through detergent selection. To further optimise solution conditions, the effect of temperature was also screened for both proteins in the new detergent.

According to Krueger-Koplin *et al.*, (2004), the quality of 2D ¹H-¹⁵N HSQC spectra for two of their membrane proteins in LPPG improved as the temperature was increased above 25°C, since tumbling rates increased (as observed in DPC in section 4.6.1), however signals were irreversibly lost above 50°C. In agreement with these studies, the list of known membrane protein structures solved by NMR indicates that almost all structures have been produced from spectra collected between 25°C and 50°C. Therefore temperature changes were screened for VanS_A and VanS_{SC} proteins in LPPG detergent, at specific temperatures between 15°C and 45°C (Figure 4.6.2.4A and B), to qualify the effect on the number of peaks observed, and the peak dispersity and intensity.

The number of observable peaks in Figure 4.6.2.4 (A and B) clearly increases with increasing temperature (for the same contour level) up to 310K and the peaks are more disperse. This indicates more rapid tumbling, improving signal to noise. However, comparing the spectra for VanS_{SC} at 310K against that at 318K (in Figure 4.6.2.4B) shows a significant reduction in signal, particularly for those peaks in the backbone amide region, so a temperature of 310K (37°C) is preferential. Protein stability can be reduced at elevated temperatures and often the rate of exchange of labile amide protons with water is increased (Kwan *et al.*, 2011), resulting in loss of signal intensity. These screens were useful to determine the optimal temperature for NMR study, and form a foundation for conducting NMR-based ligand binding experiments, which should be at near physiological conditions and at 37°C, which fortuitously happens to provide the highest quality NMR spectra.

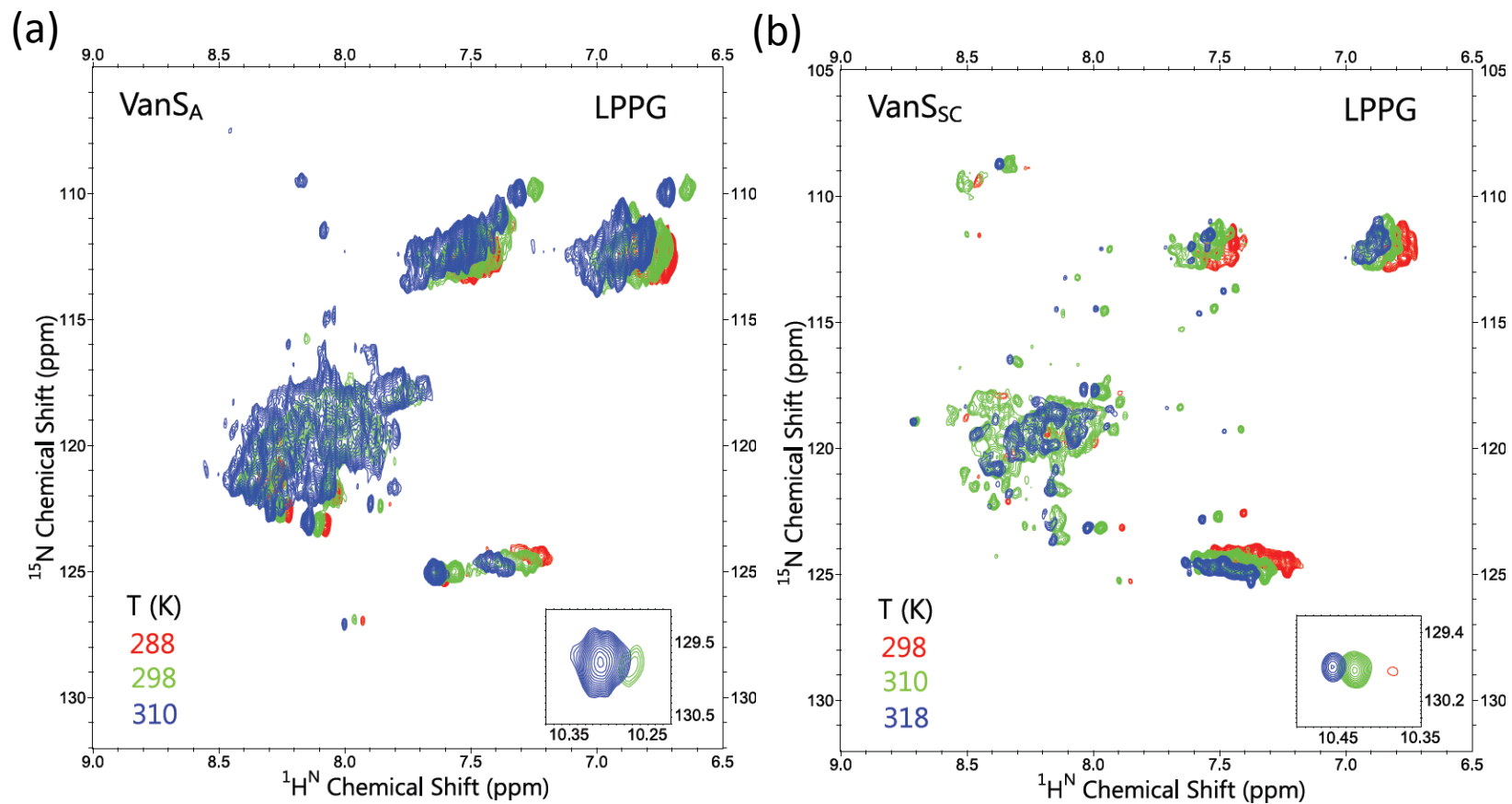


Figure 4.6.2.4: Overlaid 2D ^1H - ^{15}N HSQC spectra of (a) 200 μM VanS_A sensor domain (b) 150 μM VanS_{SC} sensor domain, at selected temperatures between 288K and 318 K. Both proteins were purified in 50 mM LPPG, 50 mM Phosphate pH 6.3, 75 mM NaCl and collected on a 700 MHz Bruker spectrometer. The resolution of spectra in overlay (b) is greater than (a) as it they were collected over 128 planes, rather than 64 planes for (a).

4.6.3 Effect of pH

In addition to temperature screens, pH changes were analysed for both VanS proteins in different detergents. NMR spectra can be recorded at any pH value, however, protons that are chemically labile (e.g. backbone and side-chain amide protons) can exchange with solvent protons, and the rate of this exchange increases logarithmically above pH 2.6 (Kwan *et al.*, 2011). Once the exchange becomes too fast, the signal from the labile proton will merge with that of the solvent, causing the signal to broaden and become unobservable. For these reasons, many studies in the literature are performed at reduced pH, generally between pH 4.0 and 7.5.

A range of pHs were tested for both proteins solubilised in LPPG, with spectra collected between pH 4.6 and 6.3 and overlaid (Figures 4.6.3.1A and B). Phosphate has a buffering capacity in the range of pH 5.8 to 8.0, so to obtain data at lower pH values, the NMR sample was diluted, and exchanged into a buffer containing 50 mM sodium acetate, and concentrated in a 30 kDa MWCO concentrator to ~ 200 μ L. For VanS_A protein solubilised in LPPG detergent (Panel A in Figure 4.6.3.1), a dramatic increase in peak dispersion is observed upon decreasing pH, and the number of resolvable peaks in the backbone amide region is increased (to 113 peaks) with most proton resonances discernable in the backbone amide region. For VanS_{SC} protein solubilised in LPPG (Panel B in Figure 4.6.3.1), there is perhaps a slight improvement is observed in peak dispersion at reduced pH, but much of the backbone amide region remained unresolvable at either pH. In order to distinguish individual protons in the backbone amide region, it may therefore be necessary to produce samples at higher protein concentration, of the order of 0.3-0.5 mM.

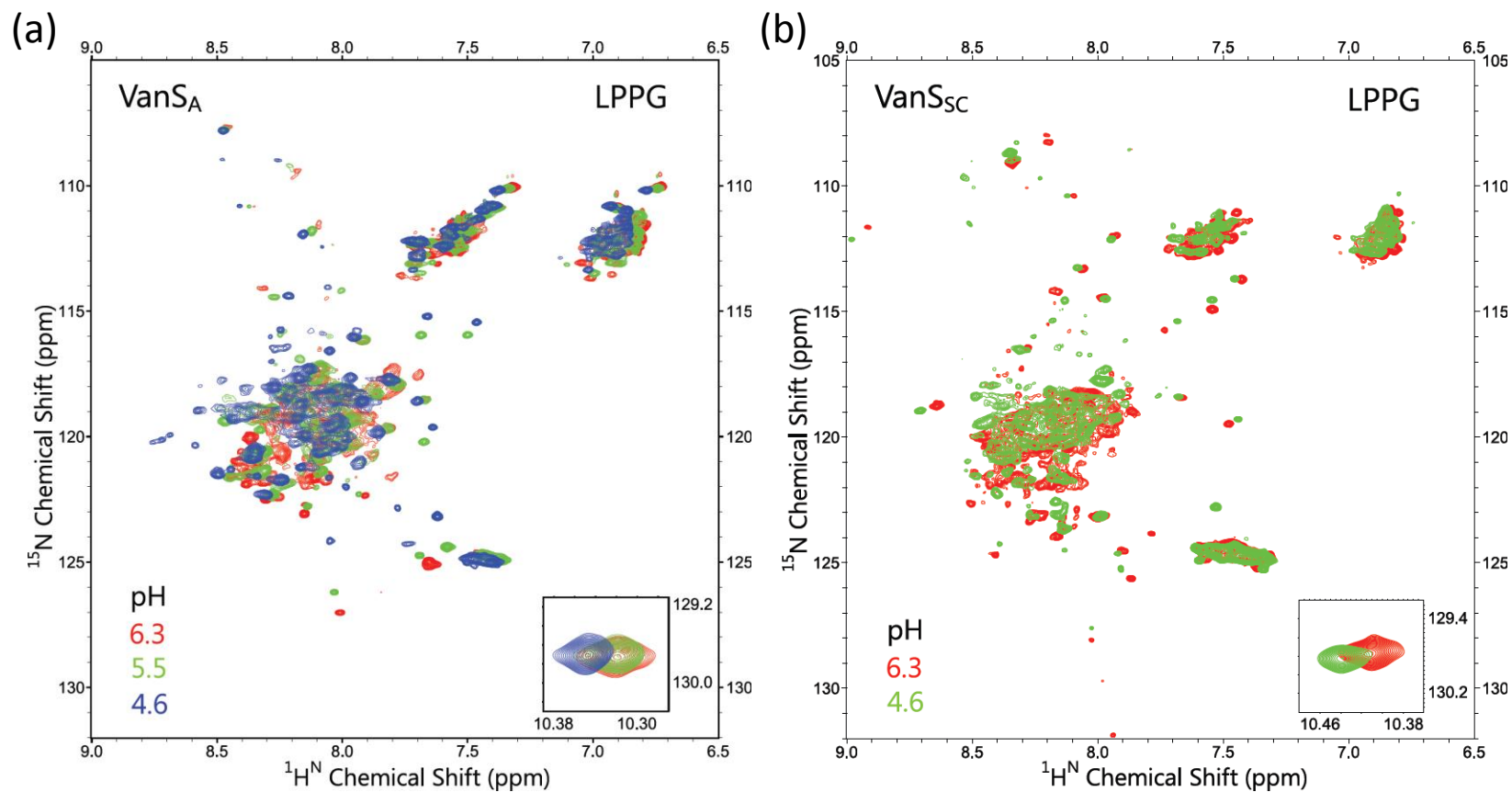


Figure 4.6.3.1: Overlaid 2D ^1H - ^{15}N HSQC spectra of (a) 200 μM VanS_A N-terminal sensor domain, or (b) 150 μM VanS_{SC} N-terminal sensor domain, obtained at selected pHs between pH 4.6 and 6.3 in 50 mM LPPG. Both proteins were purified in 50 mM phosphate pH 6.3 (red) or 50 mM Sodium acetate pH 5.5 or 4.6 (green/blue), containing 75 mM NaCl, and collected at 310K on a 700 MHz Bruker spectrometer.

For studies involving ligand addition, a near-neutral pH would be preferable, as it is known that glycopeptide antibiotics such as vancomycin have reduced solubility in acidic solutions (FDA, 2008). Therefore ideally studies of antibiotic binding to VanS should be conducted at pH 5-7. From temperature and pH screens in LPPG detergent, optimal spectra for both proteins were acquired at a temperature around 310K, and, for VanS_A, at a relatively low pH.

When conducting titrations the pH chosen will depend on the peak shifts observed and if required, it can be lowered to increase peak dispersity and reduce peak linewidth of those residues involved. Furthermore, pH changes in one detergent will affect the NMR spectra differently to those in others, so titrations should be tested for a range of detergents and pHs for comparison. Indeed analysis of the VanS_A protein in DPC detergent, recorded at a range of pH values (Figure 4.6.3.2), illustrates that spectral dispersity is dependent on the detergent chosen. Although a reduced pH does improve peak dispersity in Figure 4.6.3.2, the resolution of the backbone amide region does not appear improved, and a reduction may not be advantageous, since it could destabilise the protein fold. For VanS proteins solubilised in DPC, a near-neutral pH may be preferred for NMR-based ligand binding studies, to be physiologically relevant and reduce sample degradation and increase sample lifetimes.

By conducting NMR-based ligand binding studies in different detergents, it may be possible to identify conserved residues involved in binding to VanS proteins, and hence the position of any binding site, based on the chemical shift change upon titration of the ligand (i.e. using a Chemical Shift Perturbation (CSP) Analysis) (Williamson, 2013). Essentially, this involves measuring and weighting peak shifts in ¹⁵N and ¹H on HSQC spectra, and selecting those residues for which the weighted shift change is greater than the standard deviation for all residues. NMR-based binding studies are detailed in section 5.4, involving VanS proteins and potential glycopeptide antibiotic ligands. Antibiotics were titrated in excess into NMR samples containing the N-terminal VanS sensor domain, in order to allow approach to the binding site, and ensure any binding should be observed.

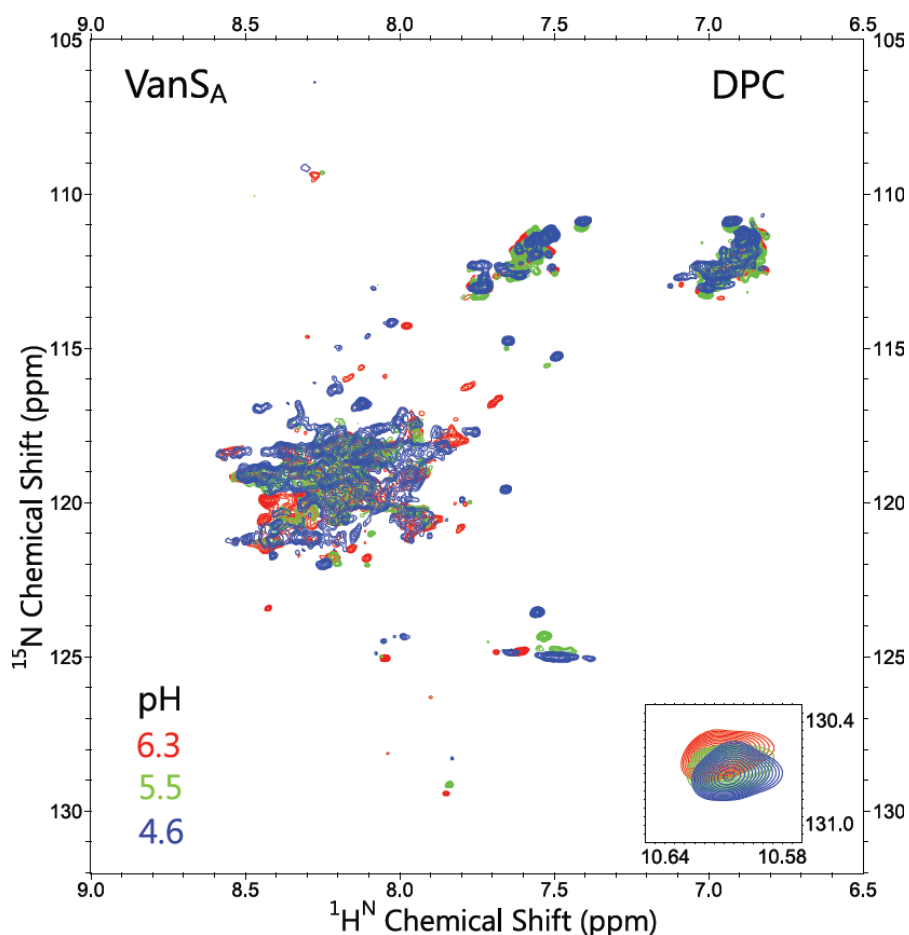


Figure 4.6.3.2: *Overlaid 2D ^1H - ^{15}N HSQC spectra of 140 μM VanS_A N-terminal sensor domain obtained at selected pHs between 4.6 and 6.3 in 50 mM DPC. Protein was purified in 50 mM Phosphate pH 6.3 (red) or 50 mM Sodium acetate pH 5.5 or 4.6 (green/ blue).*

4.6.4 Analysis of protein fold in NMR samples

Prior to NMR analyses, CD spectroscopy was used to analyse the secondary structure content for samples of VanS proteins purified into detergent micelles. The secondary structure of the protein will vary when solubilised in different detergents, as some are ‘harsher’ than others or do not adequately mimic the native bacterial membrane. Therefore as a precaution, VanS proteins were analysed in each detergent by CD spectroscopy. The full-length VanS proteins have an alpha-helical fold (~ 60% alpha-helix) which should be maintained for the truncated N-terminal sensor domain.

An aliquot of the purified protein in 50 mM detergent was diluted to ~ 0.1 mg/ml (~ 5 μ M) in the appropriate sample buffer (containing HEPES/ sodium acetate/ phosphate buffer), and the final detergent concentration was ~ 5 mM (i.e. \gg CMC). For each sample spectra were measured at room temperature as detailed in section 2.10. A selection of CD spectra collected for VanS protein samples solubilised in each detergent, and normalised to MRE values, are shown in Figure 4.6.4.1.

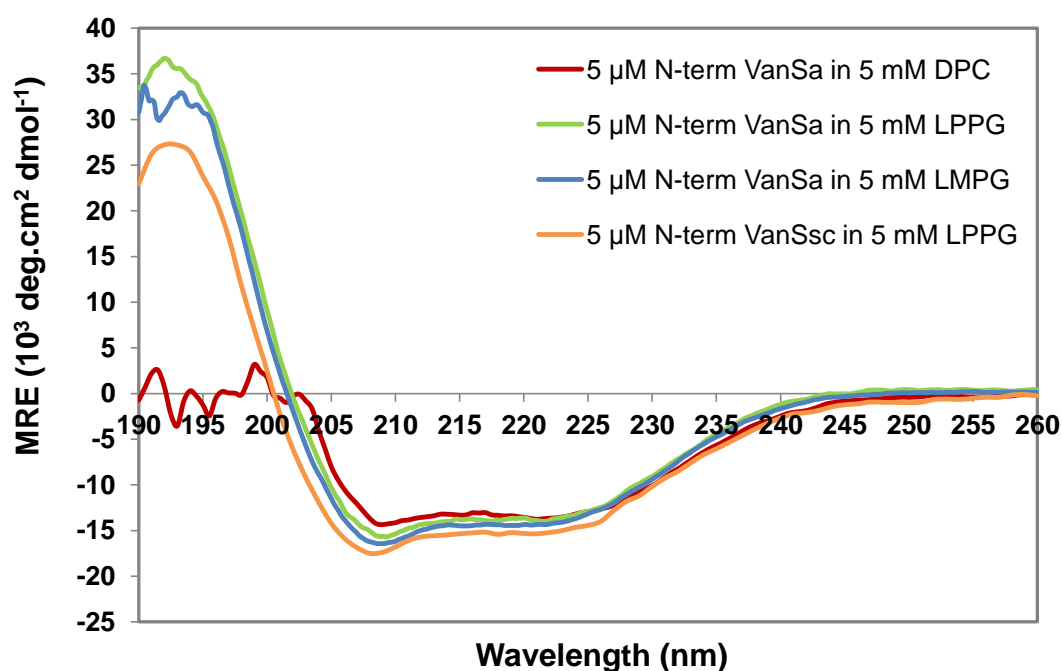


Figure 4.6.4.1: Overlaid CD spectra for $VanS_A$ and $VanS_{SC}$ sensor domains purified in different detergents. The $VanS_A$ N-terminal sensor domain was purified in 20 mM HEPES pH 6.8, 5 mM DPC (red line), 50 mM Sodium acetate pH 4.6, 5 mM LPPG (green line), or 50 mM Sodium acetate pH 5.5, 5 mM LMPG (blue line) is shown, and the $VanS_{SC}$ N-terminal sensor was purified in 50 mM Sodium acetate pH 4.6, 5 mM LPPG (orange line).

As shown in Figure 4.6.4.1, both proteins maintain an alpha-helical fold in all detergents and buffers tested, and across a pH range of 4.6 to 6.8. The spectrum obtained in DPC and HEPES buffer, shows strong light scattering below 200 nm, but peaks at ~208 nm and ~222 nm, characteristic of the alpha helical fold are clearly visible. An increased alpha-helicity is observed in LMPG and LPPG detergents, which may reflect a more lipid-like characteristic of these detergents, compared to DPC detergent.

This CD data, in conjunction with the corresponding HSQC NMR data, confirms that the VanS proteins are well-folded, and the peak dispersity, signal intensity and number of resolvable peaks in the NMR spectrum have been optimised through screening buffer, temperature, pH and detergent conditions. By using DPC and the lyso-lipid detergents, under these optimised conditions, it should be possible to observe the changes in peak chemical shift on HSQC spectra during titration experiments with potential antibiotic ligands (as detailed in section 5.4), and determine any residues which may be involved in binding.

4.7 Discussion

A novel ‘Round-the-Horn’ PCR technique was used in these studies to insert a 3C enzymatic site into full-length *vanS* gene sequences (from *E. faecium* and *S. coelicolor*), and a route was devised to cleave specifically at this site, to obtain and purify the isolated N-terminal VanS sensor domain for NMR analysis. This is the only region that is accessible to bind to glycopeptide ligands, and by truncating the C-terminus, the resulting protein-micelle complexes could tumble in solution on an appropriate timescale for NMR analysis.

Conventional NMR labelling techniques (Sambrook *et al.*, 1989) were applied to produce uniformly ¹⁵N-labelled VanS sensor domains, and expression protocols were optimised, based on recent literature methods (Marley *et al.*, 2001; Sivashanmugam *et al.*, 2009). These labelled samples provided the first known ¹H-¹⁵N HSQC spectrum of a VanS protein from enterococci or *Streptomyces*, and high resolution spectra were achieved by optimising detergent choice and solution conditions. These studies have now provided suitable VanS proteins and NMR conditions to conduct NMR-based titration experiments (see Chapter 5), to determine whether vancomycin and other glycopeptide antibiotics bind directly to VanS, or if the sensor is activated indirectly.

4.7.1 Optimal routes to obtain and selectively purify the VanS sensor domain

Initial routes to obtain the VanS sensor domain by inserting a stop codon into the *vanS* gene sequence, after the second TM domain, and overexpressing the resulting N-terminal product did provide some protein yield. However, the expression level was greatly reduced compared to that of the full-length control (see Figure 4.3.4), and this was concluded to result from the absence of the solubility-enhancing C-terminal cytoplasmic region. Using an unconventional ‘Round-the-Horn PCR’ approach, an enzymatic cleavage site was instead inserted into the *vanS* gene, which allowed the use of already optimised expression protocols to obtain high yields of soluble VanS protein, before truncation of the C-terminus.

The position for the inserted site was also carefully chosen based on disorder prediction plots (RONN), secondary structure predictions (PSIPred/JPred3) and a novel tryptic digest experiment, in order to make sure it would be in a relatively unstructured, unordered region of the protein, and easily accessible for cleavage, without greatly disrupting the overall fold. The tryptic digest experiment involved digesting samples of purified VanS proteins (within detergent micelles) with trypsin or chymotrypsin, and resolving digestion products by SDS-PAGE. Individual protein bands were then excised and analysed for their peptide sequence by tandem MS, and mapped to the full sequence. These maps showed solvent-exposed regions of the VanS proteins, accessible (outside the micelle) for cleavage, and demonstrated that an inserted site at ~ 20 amino acids away from the second TM helix in each VanS protein (at ~120th residue), would be accessible for enzyme cleavage of the C-terminus.

It was decided that it would be most appropriate to insert 3C or TEV protease sites, which are cleaved with high specificity, which were inserted in one step, using an unconventional ‘Round-the-Horn’ PCR technique. Unfortunately, subsequent TEV digestion of the overexpressed VanS protein resulted in a product that could not be easily identified on gels or blots, or purified by IMAC. However, cleavage at the 3C site gave an N-terminal His-

tagged VanS product which was selectively purified from the untagged C-terminal product by IMAC, and the MBP-tagged 3C protease was removed by utilising the strong affinity of amylose resin for MBP. A schematic representation showing the purification route to obtain the isolated purified VanS sensor domain, and the position of the inserted site is illustrated in Figure 4.7.1.1. This route can be applied to study VanS proteins from other species, cloned into pProEx vectors, and shows how important it is to choose appropriate protein tags and cleavage sites, in order to purify individual proteins domains, and still make use of the high solubility afforded by soluble domains in the protein.

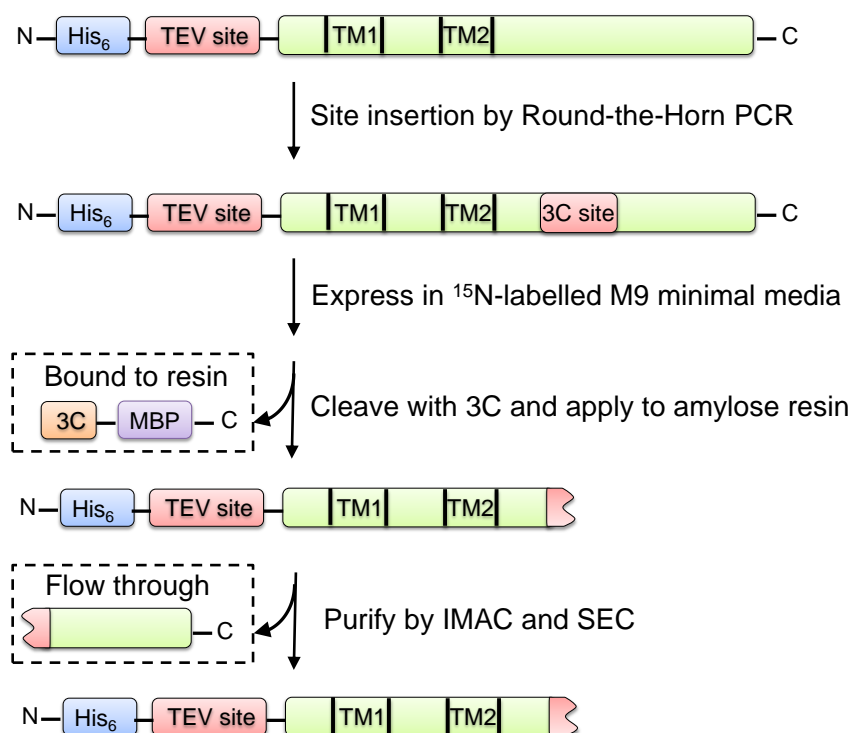


Figure 4.7.1.1: An illustration of the purification route used to express, cleave and purify the N-terminal sensor domain of VanS.

One problem encountered with the purification route above was the cost: DPC is not cheap compared to most detergents (~£60/g) and large quantities are required for purification of the isolated sensor domain. One possible change to the proposed route would therefore be to

screen VanS solubility, stability and activity in other, cheaper detergents such as CHAPS, sodium cholate, LDAO, and purify in the most suitable candidate. Another possibility would be to change the affinity tag in order to reduce the number of purification steps. Sometimes the solubility of a recombinant protein can be improved by fusing it to a highly soluble partner. In particular, MBP tags have been used in several studies as fusion tags to purify aggregation-prone or low solubility polypeptides, by promoting folding of native conformations (Pryor & Leiting, 1997; Sachdev & Chirgwin, 1998; Kapust & Waugh, 1999).

In one such system, which is commercially available (the pMAL Protein Fusion and Purification System, NEB), a gene can be cloned into a pMAL vector downstream from the *malE* gene (encoding for MBP), and an MBP-fusion protein is expressed. Using a pMAL system (e.g. pMAL-p5, NEB), the MBP-fusion protein is expressed which contains a polylinker sequence between MBP and the gene of interest, allowing for recognition by a specific protease and cleavage of MBP after expression. Furthermore, the MBP-fusion protein can be selectively purified using amylose resin, and cleaved, without the need for any vector-derived residues in the protein (e.g. His-tags) and the fusion protein can be purified in one step. This route would reduce the quantity of DPC detergent required and decrease the total time required to express and purify ¹⁵N-labelled VanS proteins for NMR analyses.

4.7.2 Optimised protocols for the expression of ¹⁵N-labelled VanS proteins

¹⁵N protein labelling strategies conducted were based on M9 minimal media preparations detailed in Sambrook *et al.*, (1989), and media was supplemented with vitamins (BME, Sigma-Aldrich) and iron (75 µM iron (III) chloride), which was suggested to be sufficient for expression of membrane proteins in the absence of a trace metal mix (Studier, 2005).

Expression trials initially involved full-length (unmutated) His-tagged VanS proteins, and expression protocols were optimised by testing different approaches given in the literature.

The first of which was a method employed by Cai *et al.*, (1998), in which cell cultures were grown in rich Luria broth, up until the point of induction, when the media was switched to M9 minimal media containing isotopic labels, which greatly reduces the time required for expression. Secondly, Marley *et al.*, (2001), showed that these methods can be further optimised by concentrating the cell suspension prior to exchanging media, giving ‘high-cell-density’ expression which both reduces the amount of labelled media required (and hence the cost) and increases protein yield. And finally, Sivashanmugam *et al.*, (2009) stated that the time between exchanging media and inducing should be lengthened to around two hours and incubating at the temperature for induction, in order to discharge unlabelled metabolites and preserve nutrients for protein synthesis. From all this literature information, protocols were combined and tested to examine protein expression in M9 minimal media (see Figure 4.4.1).

Using these protocols, both VanS_A and VanS_{SC} proteins were overexpressed in ¹⁵N-labelled minimal media and at a similar level to that observed in the much richer LB media. In addition, it was shown that both supplementation with iron chloride in expression media, and concentrating the media to half its initial volume when exchanging into M9 (‘high-cell-density’), almost doubled the yield of VanS protein (see Figure 4.4.3), demonstrating just how effective these strategies are. Even greater yields of the VanS proteins may have been achievable by concentrating cell cultures to 1/4 or 1/8th of their original volume prior to induction, provided that the concentration of glucose and other nutrients (e.g. vitamins) was sufficient to support cell growth, since these concentration factors have been successful in the literature for several membrane proteins (Marley *et al.*, 2001; Sivashanmugam *et al.*, 2009). Increased protein yields (of the order of 1 mM) would be necessary in order to obtain sufficient protein concentrations to assign protons to individual residues in the VanS sensor domain, and enable those residues involved in binding to glycopeptide ligands to be identified. These NMR assignments involve using three-dimensional HSQC techniques e.g. TOCSY-HSQC and NOESY-HSQC (Marion *et al.*, 1989a; 1989b; Zuiderweg & Fesik, 1989), which assign each proton spin system observed to a specific residue.

The assignment procedure simply involves inspecting a series of 2D TOCSY or NOESY spectra collected, viewed as 2D $^1\text{H}(\text{F1})\text{-}^{15}\text{N}(\text{F3})$ slices, edited with respect to the frequency of the ^{15}N heteronucleus in a third dimension (F2). Connections between residues can be identified from through-space (NOESY) correlations. By collecting 2D slices, those peaks in the spectrum with similar or overlapping chemical shift values can be separated in a third dimension, allowing residue assignment (Marion *et al.*, 1989a; 1989b). It should be noted that assignment of the full sequence, including side chain hydrogen atoms may also require additional NMR experiments e.g. HCCH-TOCSY or HCCH-COSY.

4.7.3 Obtaining high resolution 2D NMR spectra of the VanS sensor domain

Initial $^1\text{H}\text{-}^{15}\text{N}$ HSQC NMR spectra were collected for uniformly ^{15}N -labelled VanS sensor domains purified in DPC detergent, since this detergent had provided active (full-length protein) with respect to autophosphorylation, and appeared to produce stable, homogeneous and well-folded samples. HSQC spectra in DPC collected on a 700 MHz spectrometer showed that a number of peaks (~50) could be discerned, but further optimisation was clearly required in order to observe individual peak shifts during titration experiments. Therefore a number of conditions were optimised, including pH, temperature and buffer, and critically different detergents were screened to optimise spectral resolution.

Raising the temperature from 298K to 310K did improve spectral quality, resulting in increased protein-micelle tumbling in solution, but above 310K significant reductions in signal were observed, indicating that 310K (37°C) was the optimal temperature for studies. This is useful as it reflects physiological conditions within bacterial cells. Reducing the pH also increased peak dispersity especially in the lyso-lipid detergent, LPPG, but the result was dependent on the detergent chosen, as the pH affects protein fold and stability. Overall, a near neutral pH is preferential anyway in ligand titration studies, since glycopeptide antibiotics such as vancomycin and teicoplanin are most soluble in the pH range 5 – 7.

For selecting the most suitable membrane mimetic for ligand binding studies, a wide detergent screen was conducted for both VanS proteins, involving detergents from 3 different classes: anionic, zwitterionic and non-ionic. These screens showed that VanS proteins exhibited highest solubility in anionic (LPPG, LMPG, SDS) and (some) zwitterionic detergents (LMPC, DPC), rather than non-ionic ones, which reflects the PC/PG lipid composition of Gram-negative *E. coli* and Gram-positive enterococci and *Streptomyces* bacterial membranes. Of course, the extent of solubilisation is only one measure of a detergent's suitability as a membrane mimetic, and both the stability and activity of the protein should ideally be assessed in each detergent. Although these were not tested in these screens, literature studies suggested that the lyso-phosphatidylglycerols (LPPG, LMPG) have been able to extract many large membrane proteins in a native, functional form and maintain their stability under conditions of high temperature and low pH over days to weeks (Foury *et al.*, 1981; Huang *et al.*, 1998; Krueger-Koplin *et al.*, 2004). NMR spectra were therefore collected for VanS proteins purified into LPPG and LMPG lyso-phospholipid micelles.

The NMR spectral quality of proteins solubilised in LPPG compared to those in DPC was markedly improved, as shown in Figure 4.6.2.3. The number of resolvable peaks was increased to >100 and the peak dispersity was significantly improved. Under these NMR conditions it should now be possible to observe any small conformational changes induced during ligand binding. The success of these lyso-lipids in NMR spectroscopy is thought to be due to their ability to stabilise protein folds through favourable interactions with their native phospholipid headgroups and lipid-like acyl chains, and to permit fluid rotation of proteins within the confines of the micelle (Krueger-Koplin *et al.*, 2004; Koehler *et al.*, 2010).

A selection of the best observed spectra for the VanS proteins studied in different detergents is given in Figure 4.7.3.1, along with the conditions under which the spectra were obtained. Screening a number of factors that affect NMR spectral resolution has now provided optimal solution conditions and detergent selections, in order to study changes in peak chemical shift

on HSQC spectra during ligand titration experiments with antibiotic ligands (as detailed in section 5.4), and determine any residues which may be involved in binding.

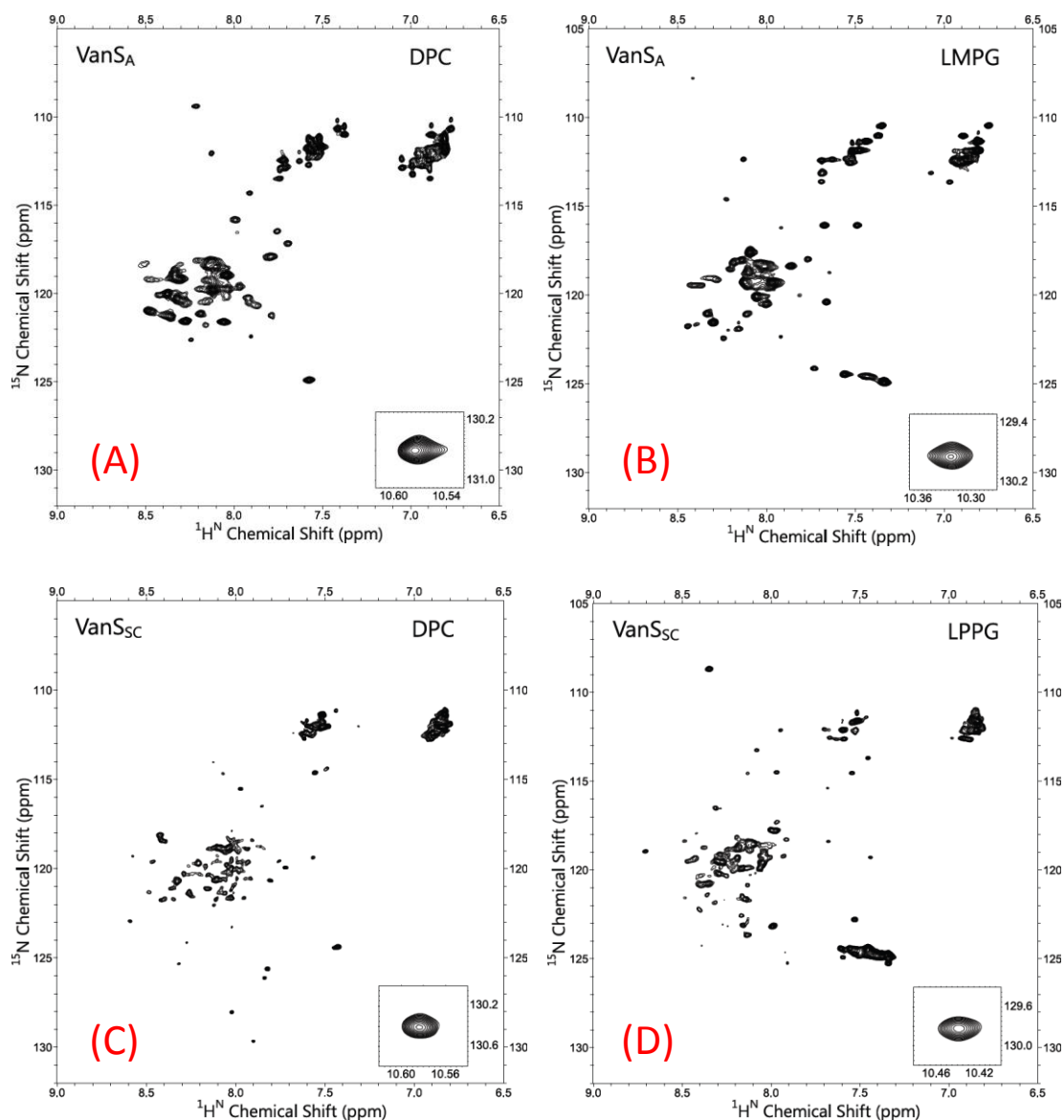


Figure 4.7.3.1: Optimal 2D ^1H - ^{15}N HSQC spectra of the N-terminal sensor domains of *VanS_A* and *VanS_{SC}* proteins purified in various detergents and collected on a 700 MHz spectrometer at 310K. (A) 600 μM *VanS_A* solubilised in 50 mM DPC, 50 mM NaCl, 20 mM HEPES pH 6.85, (B) 700 μM *VanS_A* solubilised in 50 mM LMPG, 50 mM NaCl, 50 mM sodium acetate pH 5.5, (C) 200 μM *VanS_{SC}* N-terminal sensor domain solubilised in 50 mM DPC, 50 mM NaCl, 20 mM HEPES pH 6.8, (D) 200 μM *VanS_{SC}* N-terminal sensor domain solubilised in 50 mM LPPG, 50 mM NaCl, 50 mM phosphate pH 6.1.

5 Analysis of Receptor-Ligand Binding and Examination of the Role of Oligomerisation State in Receptor Signalling

5.1 Introduction

Protein-protein and protein receptor–ligand interactions play a crucial role in biological systems. Testing ligand binding to specific receptors is important both for theoretical studies and for drug development research. The main aspects of receptor-ligand binding interactions include binding affinity and kinetics, binding thermodynamics and conformations of targets (de Jong *et al.*, 2005). Numerous methods are available to study protein-ligand binding, but perhaps the most commonly applied include fluorescent-labelled or radioreceptor assays, label-free chip-based assays such as Surface Plasmon Resonance (SPR) (Wilson, 2002), structure-based assays such as NMR or X-ray diffraction, and thermodynamic assays e.g. Isothermal Titration Calorimetry (ITC) (Rajarathnam & Rosgen, 2014). In this thesis, NMR-based and fluorescence-based ligand binding assays are used to examine the binding of VanS to glycopeptide antibiotics. Details of the methodology for NMR spectroscopy are provided in section 2.14 and 5.4, and fluorescence spectroscopy techniques are outlined below.

Fluorescence spectroscopy techniques involve excitation of a fluorophore, by unpolarised light (or in the case of fluorescence polarisation (FP) (Lea & Simeonov, 2011), linearly polarised light), and measurement of the resulting photons re-emitted. Upon ligand binding, changes will be observed in the light re-emitted, which usually involves an alteration in the emission intensity e.g. due to ‘quenching’, or a shift in emission peak wavelength (de Jong *et al.*, 2005). These fluorescence techniques often do not require separation or washing steps before measurement (so called ‘mix-and-measure’) (de Jong *et al.*, 2005), allowing their application in high-throughput screening (HTS) experiments (Lea & Simeonov, 2011).

In relation to studies in this thesis, one such screening assay was developed by Popienek & Pratt, (1987), in which binding was screened for potential glycopeptide ligands to a fluorescently-labelled (Dansyl) derivative of the pentapeptide terminus of the cell wall precursor (refer to section 1.2). The fluorophore was excited at 330 nm and binding was identified from an increase in the intensity of light emitted at 550 nm, upon changes in the fluorophore environment. Using similar assays it may be possible to test for changes in fluorescence upon addition of potential glycopeptide ligands to VanS protein samples, provided that one of the molecules contains a fluorophore. If a direct interaction did occur, the environment of the fluorophore would be perturbed, altering its emission properties.

As stated in section 1.4.2, fluorescent labelling strategies have recently been successfully applied to study VanS membrane proteins in the presence of glycopeptide ligands. Koteva *et al.*, (2010), demonstrated for the first time, a direct covalent binding between a fluorescently labelled vancomycin analogue (VPP) and the VanS protein derived from *S. coelicolor*. Using a *vanH* gene reporter assay it was also shown that VPP was a bioactive ligand of VanS, able to induce resistance gene expression in vancomycin-resistant *S. coelicolor in vivo*. This VPP ligand is however synthetic and structurally different from natural vancomycin, so it is possible that vancomycin molecules may not interact via the same mechanism. Nonetheless, this VanS_{SC} protein could act as a positive control in NMR-based vancomycin binding experiments, to establish whether other VanS_A proteins are also activated by direct binding.

Despite a number of biochemical assays conducted in the literature to determine the nature of the inducing ligand that activates VanS in *Enterococcus faecium* (VanS_A), screens for antibiotic inducers of this system are not consistent (see section 1.4.1 and Table 1.4.3.1). Inducers have been identified by either assaying VanX activity in cell extracts (Baptista *et al.*, 1996; Arthur *et al.*, 1999), by monitoring induction of Lac-containing precursors (Allen & Hobbs, 1995), or by coupling the *lacZ* promoter under control of VanRS to a reporter gene (Lai & Kirsch, 1996; Ulijasz *et al.*, 1996; Grissom-Arnold *et al.*, 1997; Mani *et al.*, 1998).

Biochemical data from all of these assays suggests that *E. faecium* VanS_A is strongly induced by glycopeptide antibiotics, which would suggest a direct binding. However, in some assays it is also induced by other structurally unrelated compounds involved in late steps in cell wall biosynthesis, in particular, by moenomycin A. This has led to a general consensus in the scientific community that VanS_A should be activated indirectly, either by sensing accumulation of a cell wall intermediate such as Lipid II (as a result of antibiotic inhibition of TG activity) or perhaps by interaction with Lipid II in complex with the glycopeptide antibiotic (Hong *et al.*, 2008). By close examination of each assay technique, it can be seen that the screens provide conflicting evidence (see Table 1.4.3.3), since an inducer in one system is often not an inducer in another, for instance Grissom-Arnold *et al.*, (1997), concluded that ramoplanin was an inducer whereas Baptista *et al.*, (1996), conclude it is not. Even moenomycin A was found to be either weakly inducing (Grissom-Arnold *et al.*, 1997), or in some assays, not inducing at all (Arthur *et al.*, 1999; Lai & Kirsch, 1996) (see section 1.4.1), so it is still possible than VanS_A could be activated by direct glycopeptide binding.

By comparison, similar biochemical assays showed that VanS proteins from *E. faecalis* VanS_B and *S. coelicolor* VanS_{SC} (see section 1.4.2 and Tables 1.4.3.2 & 1.4.3.3) were only induced by structurally related glycopeptides, and other antibiotics tested failed to activate VanS, so it therefore appears that these proteins are activated by direct antibiotic binding (as proposed from biophysical studies by Koteva *et al.*, 2010). During this PhD I therefore hope to determine by biophysical studies including fluorescence- and NMR-based binding assays, whether each VanS protein binds directly to glycopeptide antibiotics or whether another signalling molecule or cell wall intermediate is involved in the activation of VanS. I also hope to improve understanding of the structures of VanS proteins from *Enterococcus* and *Streptomyces* using solution NMR spectroscopy.

Another question that requires investigation is: how does the VanS protein interact with its ligand, to transduce a signal from the sensor domain to the kinase domain and effect a response? The extracytoplasmic sensor domains show little or no sequence homology between VanS proteins and yet can respond to multiple signals. By examining published structures of HK sensor domains there do, however, appear to be several common structural folds, suggesting some conserved signal sensing mechanisms. DHP and CA domains are common elements of HKs and have conserved sequence motifs (as discussed in section 1.5.3) (Dutta *et al.*, 1999). There are also a variety of modular elements that are commonly found N-terminal to the catalytic domains, which are believed to be involved in stimulus perception and transduction, such as PAS, GAF (see section 1.5.3) and HAMP domains (see section 1.5.5). HAMP domains are positioned directly after the second TM domain, and consist of two helices that form a four-helix bundle in the homodimeric active state. They are thought to transduce signals from the extracytoplasmic sensor domain to the catalytic kinase core via either ‘cog-like’ rotations of this bundle (Hulko *et al.*, 2006; Ferris *et al.*, 2012) or a ‘screw-like’ movement (Airola *et al.*, 2010). Therefore a multiplicity of domains exist in the HK sensor complex, to allow multiple signals to be transduced and effect sensor kinase activity. It is likely that structural changes that occur in the extracytoplasmic sensor region upon ligand binding, trigger signal transduction through the TM helices to the kinase domain, via conformational changes in PAS/GAF/HAMP domains (as proposed in a recent TCS signalling model by Casino *et al.*, 2009, shown in Figure 1.5.5.4).

It is still not clear what the role of the TM helices play in the mechanism of signal transduction, but rotations or interactions between TM helices have been suggested (Cheung & Hendrickson, 2010; Zhang & Hendrickson, 2010). Structures of sensor domains in the literature have usually been obtained by truncating these transmembrane regions, and the resulting isolated domains are monomers in solution (see Figure 1.5.3.3) (Cheung *et al.*, 2008; Cheung & Hendrickson, 2009; 2010). However, they are expected to form dimers in the context of the whole protein since the DHP and HAMP domains are homodimers.

Therefore, homo-dimerisation of the TM domains (and the full-length protein) is likely to occur, and requires further investigation to understand its role in the signalling mechanism. To this end, gel-based Blue Native PAGE (BN-PAGE) assays are conducted to assess oligomerisation of full-length VanS, and *in vivo* reporter assays (ToxCAT/ GALLEX) are tested to analyse homo-dimerisation of VanS transmembrane helices (TM-TM interactions).

Blue Native PAGE (BN-PAGE) techniques can identify native membrane protein complexes on PAGE gels, without denaturing the protein (Schagger & von Jagow, 1991) and can be conducted in different detergents, in order to determine protein oligomeric state, relative to standards. Samples of VanS proteins purified into detergent micelles are analysed by BN-PAGE to identify their oligomeric state. The detergents tested included those used in structural (NMR, Crystallography) and enzymatic assays, and therefore could identify if, for instance a homodimeric complex was present, which could be important in ligand binding or in signal transduction mechanisms.

The ToxCAT assay (Russ & Engelman, 1999) (see section 2.7) quantifies the strength of homo-oligomerisation of TM domains, and the GALLEX assay (Schneider & Engelman, 2003; Cymer *et al.*, 2013) quantifies either the homo- or hetero-oligomerisation of TM domains. The two assays differ in the fusion construct design involved and the assay product quantified. For the ToxCAT assay, the TM domain of interest is cloned into a fusion construct flanked by a periplasmic MBP anchor and a cytoplasmic ToxR domain, whereas in GALLEX the ToxR is replaced by LexA (LEX) protein. Upon dimerization, the ToxR or LexA domains come into close contact, and activate transcription of reporter genes encoding either chloramphenicol acetyltransferase (CAT) or β -galactosidase (GAL), which can be assayed by different methods. There are indications in the literature that TM-TM interactions influence downstream signalling to the catalytic kinase domain. For instance Jeffery & Koshland, (1994), found that a single substitution of an isoleucine with a

phenylalanine in the second TM domain (TM2) of the Tar chemotaxis receptor, led to a significant alteration in receptor activation. By conducting ToxCAT and GALLEX assays it should be possible to quantify the level of homo- or hetero-oligomerisation for VanS, to improve understanding of the role of TM-TM interactions in signalling.

This chapter therefore focuses on trying to answer the following questions:

- Does vancomycin bind directly to VanS proteins from different species?
- Do transmembrane helix-helix interactions play a role in signalling and does the oligomerisation state of the VanS sensor affect its ligand binding?

5.2 Aims

- (i) To determine whether binding can be observed between glycopeptide antibiotics and VanS proteins using fluorescence spectroscopy and solution state NMR.
- (ii) To identify any conserved residues in the VanS sensor domain that are involved in binding to glycopeptide ligands, by conducting NMR titration experiments, and analysing changes in peak chemical shift at each titration point.
- (iii) To determine the oligomerisation state of detergent-solubilised full-length VanS proteins using gel-based PAGE techniques, in order to increase understanding of the role of oligomerisation state upon ligand binding.
- (iv) To investigate transmembrane helix-helix association, using *in vivo* reporter assays, to improve knowledge of the means by which signals are transduced across the bacterial membrane to the kinase core.

5.3 Analysis of Ligand Binding by Fluorescence Spectroscopy

Initially, fluorescence spectroscopy was conducted as a qualitative measure to test for an interaction between purified VanS proteins and a fluorescently-tagged vancomycin glycopeptide. In these studies, the fluorescent vancomycin analogue chosen was readily available from Sigma-Aldrich, and was selected based on previous success in the Warwick group, in which the fluorescent probe was used to image SDS-PAGE gels (Abrahams, 2011) containing transglycosylated polymerised Lipid II molecules of different chain lengths (visualised under a fluorescent light filter). The probe contained a BODIPY molecule covalently linked to vancomycin, and is a class of fluorescent dye (BODIPY-vancomycin, Molecular Probes) (for structure, see Figure 2.11.1).

The major use of BODIPY dyes is in cell imaging studies such as fluorescence imaging microscopy (DeDent *et al.*, 2007; Pereira *et al.*, 2007). Despite their small Stokes shift; BODIPY-vancomycin has an excitation wavelength of 504 nm and an emission wavelength ~ 511 nm, the dyes have high fluorescence quantum yields (even in water) and sharp peaks, whose position remain almost unchanged in different solvents, making them ideal for ligand binding studies in detergent environments. BODIPY-vancomycin was solubilised in HEPES buffer and its emission spectrum monitored upon excitation at 504 nm, with and without the addition of detergent, to examine its suitability for these studies. The stock concentration of BODIPY dye in the buffer was calculated as approximately 100 μM , from its observed absorbance at 504 nm using an extinction coefficient of $78000 \text{ M}^{-1} \text{ cm}^{-1}$.

Microliter additions from a 40 mM DPC stock solution were added to the BODIPY-vancomycin at 10 μM in buffer, mixed thoroughly, and the emission spectra recorded (see Figure 5.3.1). As observed from overlaid emission spectra, BODIPY-vancomycin has an emission maximum of 510 nm in buffer, which shifts by less than 1 nm in the presence of detergent micelles showing the low environment dependence of the BODIPY fluorophore.

The CMC of DPC is approximately 1 mM, so all studies were therefore carried out above this, at a final concentration of 2 mM (0.1% w/v DPC) which was maintained throughout. It should be noted that a second peak at ~ 506 nm is present in all detergent-containing samples. However this almost directly overlaps with the excitation wavelength (505 nm) and must result from light scattering in the detergent solution.

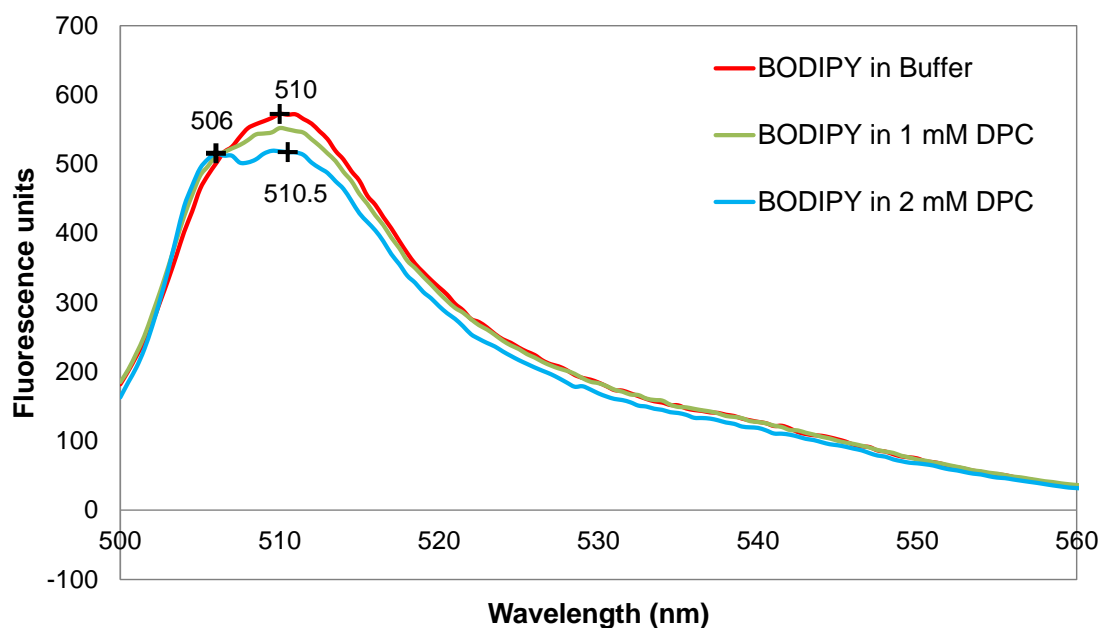


Figure 5.3.1: Overlaid emission spectra upon excitation of BODIPY-vancomycin dye in HEPES buffer and/or DPC. Aliquots of a 40 mM DPC solution were added to 10 μ M BODIPY-vancomycin dissolved in HEPES buffer (red line), to final concentrations of 1 mM (green line) or 2 mM (blue line), and allowed to mix before recording emission spectra.

Since the presence of detergent did not greatly affect the emission spectra, it was possible to test samples containing detergent-solubilised VanS proteins or Lipid II molecules. Adding Lipid II molecules to a solution of BODIPY-vancomycin, would act as a control experiment, since vancomycin is known to bind to the D-Ala-D-Ala N-terminus of Lipid II (Walsh *et al.*, 1996). Binding of proteins to ligands often causes changes in their 3D structures, and if this affects the environment of a fluorophore, it can result in measurable changes in the spectrum, such as a shift in the position of the emission maximum or the emission intensity (Möller & Denicola, 2002). Therefore an interaction between Lipid II and the vancomycin analogue

could influence the environment of the BODIPY fluorophore, and could cause a change in its emission spectrum. Similarly, if an interaction occurred between VanS proteins and the vancomycin analogue, this may also be observed by changes in the spectrum.

Samples were prepared as before by adding DPC detergent into a 10 μM solution of BODIPY-vancomycin, up to a final concentration of 2 mM (2 x CMC), and subsequently titrating in Lipid II or VanS protein (refer to section 2.11). For those samples containing BODIPY-vancomycin, DPC and Lipid II, an aliquot of Lipid II was pipetted into a glass vial, immediately dried under nitrogen to a film and resuspended with vortexing, using the solution of BODIPY-vancomycin (10 μM BODIPY-vancomycin in 20 mM HEPES pH 7.8, 2 mM DPC). Further aliquots of Lipid II were added in the same way, to final concentrations of 10 - 40 μM , and the emission spectra of all samples measured (see Figure 5.3.2).

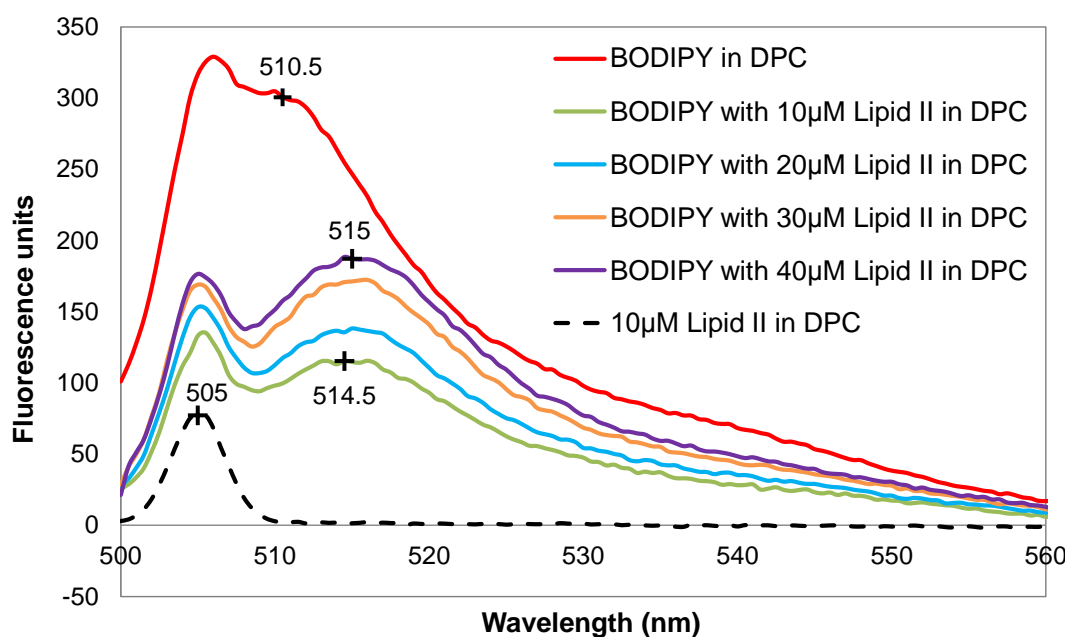


Figure 5.3.2: Overlaid emission spectra upon excitation of BODIPY-vancomycin dye in HEPES buffer containing DPC, and increasing concentrations of detergent-solubilised Lipid II. Aliquots of a 40 mM DPC solution were added and mixed with 10 μM BODIPY-vancomycin dissolved in HEPES buffer to a concentration of 2 mM (red line), and the solution used to resuspend a lipid film to give final concentration of Lipid II of 10 μM (green line), 20 μM (blue line), 30 μM (orange line) or 40 μM (purple line). A control spectrum was also recorded for the excitation of Lipid II solubilised in 2 mM DPC (dashed line).

This experiment showed an appreciable shift in the position of the emission maxima of about 4 nm, which is an indication that the Lipid II and vancomycin dye are interacting. Successive additions of Lipid II did not appear to greatly affect the maxima position, but this may be anticipated since only 1 molecule of Lipid II is able to bind 1 molecule of vancomycin at a time, and at the first addition, the concentration of vancomycin and Lipid II was 10 μM (1:1 ratio). The emission intensity also decreases appreciably upon adding Lipid II, but this quenching does not necessarily indicate an interaction, since BODIPY dyes also self-quench, therefore shifts in the position of the emission maximum are more informative of an interaction. Based on the success of these experiments with Lipid II, similar methods were applied to samples of vancomycin dye and VanS protein (see Figures 5.3.3 and 5.3.4).

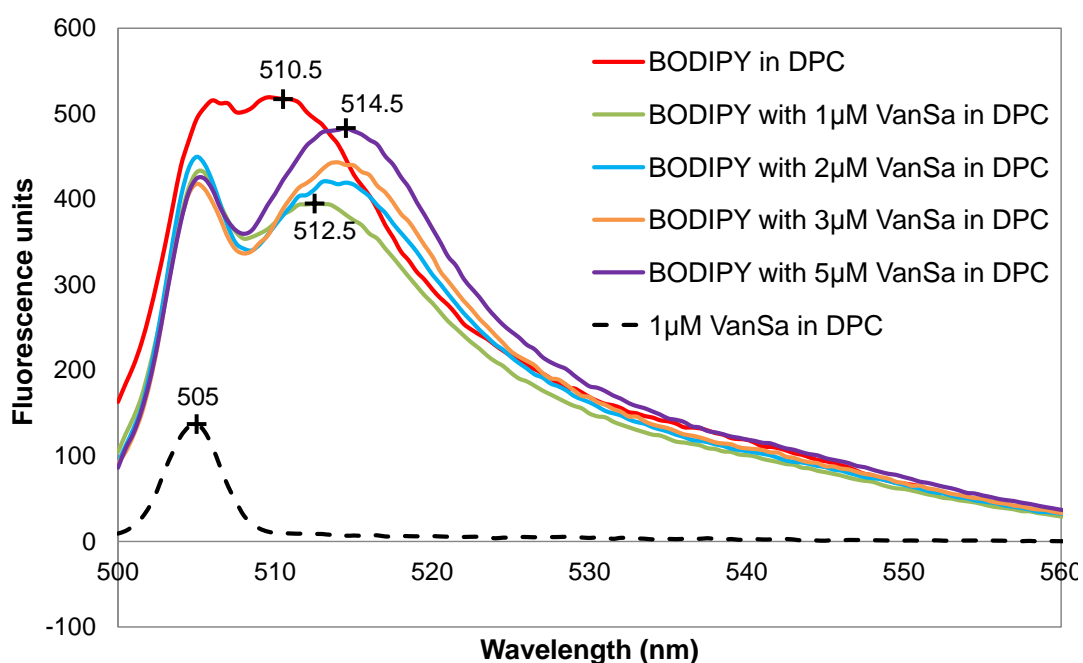


Figure 5.3.3: Overlaid emission spectra upon excitation of BODIPY-vancomycin dye in HEPES buffer containing DPC, and increasing concentrations of detergent-solubilised VanS_A. DPC detergent-containing solution was added and mixed with 10 μM BODIPY-vancomycin dissolved in HEPES buffer to a concentration of 2 mM (red line), to which microliter aliquots of purified detergent-solubilised VanS_A protein was added at final concentrations of 1 μM (green line), 2 μM (blue line), 3 μM (orange line) or 5 μM (purple line). A control emission spectrum was also recorded for excitation of VanS_A solubilised in 2 mM DPC (dashed line).

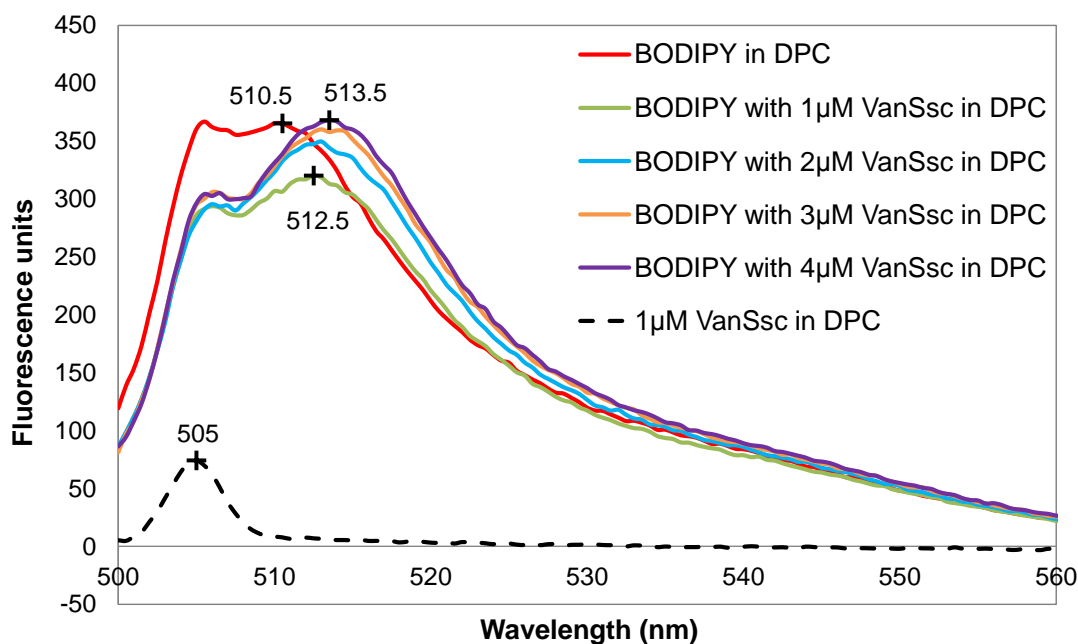


Figure 5.3.4: *Overlaid emission spectra upon excitation of BODIPY-vancomycin dye in HEPES buffer containing DPC, and increasing concentrations of detergent-solubilised VanS_{sc}. DPC detergent-containing solution was added and mixed with 10 μM BODIPY-vancomycin dissolved in HEPES buffer to a concentration of 2 mM (red line), to which microliter aliquots of purified detergent-solubilised VanS_{sc} protein was added at final concentrations of 1 μM (green line), 2 μM (blue line), 3 μM (orange line) or 4 μM (purple line). A control emission spectrum was also recorded for excitation of VanS_{sc} solubilised in 2 mM DPC (dashed line).*

Microliter aliquots of IMAC purified VanS proteins (at 3-6 mg/ml in 20 mM HEPES pH 7.8, 2 mM DPC) were added directly to a solution of detergent-solubilised 10 μM BODIPY-vancomycin dye. After thorough mixing, the emission spectrum was measured upon excitation at 504 nm (Figures 5.3.3 and 5.3.4). Further aliquots of VanS were added until no appreciable changes in the spectra were observed, and the total volume change from additions was maintained below 10%. Emission spectra of the BODIPY dye in the presence of detergent-solubilised VanS proteins did not display the same level of quenching, but importantly, the emission maximum still shifted by a significant amount and continued to shift with increasing concentration of VanS, up to a limit.

For both VanS_A and VanS_{SC}, a cumulative shift in peak wavelength of 3-4 nm was observed at the final addition (4/5 μ M final concentration), which is similar to that of the Lipid II control, and suggests that both full-length VanS proteins could be interacting with the vancomycin analogue. This is in agreement with binding studies conducted by Koteva *et al.*, (2010), who demonstrated covalent binding between VanS_{SC} proteins and a vancomycin derivative (a vancomycin photoaffinity probe). However, no direct binding has been previously observed between VanS_A proteins and vancomycin, so these results contradict the consensus view in the scientific community (based on biochemical data as mentioned above, and in detail in section 1.4.1) that VanS_A should be activated by an indirect mechanism in the presence of vancomycin. The fluorescence data presented therefore suggests a direct interaction (whether it be productive or not) between the vancomycin analogue and both VanS_A and VanS_{SC} proteins. It should however be noted that there are other possible explanations for the changes observed in the fluorescence spectra. For instance, the spectra are detergent sensitive, so if vancomycin binds directly to the micelle, this will alter the micelle structure and dynamics, and indirectly affect the fluorescence observed (rather than the changes resulting purely from direct binding).

Much more data still needs to be collected using other biophysical techniques in order to ascertain if vancomycin can bind directly to VanS, and whether any direct interaction activates the kinase. To this end, the fluorescence data acts as a starting point, prior to more quantitative, ligand-binding studies such as SPR, ITC or solution state NMR, the latter of which is detailed in section 5.4 below.

5.4 Analysis of Ligand Binding by Solution State NMR Spectroscopy

In order to more quantitatively ascertain whether a direct binding is occurring between VanS proteins and vancomycin antibiotics, solution state NMR techniques were applied. NMR spectroscopy is an attractive technique for studying protein-ligand interactions because many molecules have (or can be enriched with) NMR-active nuclei (e.g. $^{13}\text{C}/^{15}\text{N}/^1\text{H}$) and a single analysis can provide a vast amount of structural and binding affinity data without destroying the sample (Lucas & Larive, 2004). In addition, unlike fluorescence or spectrophotometric techniques, it is less prone to giving false positive results (Williamson, 2013), and can provide data on small conformational changes in the protein during ligand binding.

Ligand-based NMR screening and the identification of ligand-binding conformations by NMR are becoming routine in the pharmaceutical industry and are important tools in the rational drug-discovery process (Lucas & Larive, 2004). Combinatorial libraries of thousands of ligands can be synthesised and potential drug candidates screened against a specific target such as an enzyme or cell surface receptor for activity. Several solution-state NMR techniques have therefore been developed to study protein-ligand interactions, which are extensively reviewed in the literature e.g. by Fielding (2003) and Meyer & Peters (2003) and the choice of technique is often based on whether the ligand or the protein is labelled.

Protein-based techniques include monitoring changes in chemical shift (δ) by calculating Chemical Shift Perturbations (CSP) and require isotopically enriched or selectively labelled protein samples. Ligand-based techniques include those based on relaxation (Hajduk *et al.*, 1997), Saturation Transfer Difference (STD) (Mayer & Meyer, 1999) and Pulsed-field gradient (PFG) (Lucas & Larive, 2004) NMR, and can be more desirable as spectra are better resolved than those of large proteins. However, all these techniques require labelled protein or ligand, which must be expressed or synthesised and although ligand-based assays are useful for screening, they cannot identify specific residues of the protein involved in binding.

Therefore, in these studies, protein-based techniques were chosen since VanS proteins had already been successfully isotopically labelled, purified and solution conditions optimised (see section 4.6). Additionally, ligand-based techniques would require the use of labelled (^{13}C)-vancomycin, which is naturally expressed unlabelled, as a vancomycin hydrochloride in *Streptomyces orientalis*, so the bacteria would need to be grown in media containing [1- ^{13}C] or [U- ^{13}C] glucose. Using protein-based methods, the labelled proteins were mixed with unlabelled ligands, and protein-ligand binding was analysed. In this instance, the changes in protein chemical shifts were analysed by a Chemical Shift Perturbation (CSP) experiment.

5.4.1 Chemical Shift Perturbation NMR Analysis

For CSP experiments, the ligand is titrated into a sample containing the protein, and protein chemical shifts are monitored at each stage of the titration by acquiring a series of 2D ^1H - ^{15}N HSQC spectra. The chemical shift is highly sensitive to structural changes, and can be measured accurately, meaning that virtually any genuine binding interaction will produce CSPs. The analysis is also relatively simple in its basic form; measure the chemical shifts at each titration point; follow the movement of peaks in the ^1H and ^{15}N dimensions; those that shift the most are likely to map to the binding site for the ligand. A titration curve (of chemical shift vs. concentration of ligand) can also be fitted to obtain a value for the dissociation constant of the ligand (K_D).

Several issues can still arise from using this analysis technique including scenarios where multiple binding modes occur or when the dynamics of the system change upon binding, e.g. from fast exchange to slow or intermediate exchange (Williamson, 2013). Additionally, several controls must be measured during the titration; the same buffer must be used for both protein and ligand (including detergent present), and the pH should remain constant between ligand additions (or adjusted if necessary), since even small changes in the pH, salt concentration or detergent concentration can alter protein signals and peak positions.

CSP experiments were therefore conducted by collecting initial ^1H - ^{15}N HSQC spectra of ^{15}N -labelled VanS proteins in an appropriate solubilising detergent and buffer. Next, dissolved and detergent-solubilised, vancomycin was titrated into the NMR sample (in the same detergent and buffer) (see section 2.14.2 for full experimental details) and chemical shift changes were monitored at each titration point. The pH was controlled by maintaining it to within 0.05 units over all titrations. Vancomycin stock solutions were prepared at 10-20 mM concentrations by dissolution in an appropriate buffer (containing 5 mM detergent) and titrated into the NMR sample at [vancomycin]:[protein] molar ratios of 1:1, 2:1, or 4:1.

All NMR titrations were allowed to equilibrate after mixing for 15-30 minutes, before centrifuging at 13,000 rpm for 10 minutes in a benchtop centrifuge, to pellet any insoluble material, and loading the supernatant into 3 mm BrukerMATCH NMR tubes for analysis. Initially, vancomycin was titrated into samples containing the sensor domains of VanS_A proteins at ~120 μM which had been solubilised in 50 mM DPC, 50 mM sodium acetate buffer pH 5.5 (Figure 5.4.1.1). The vancomycin was added to a final concentration of 0.48 mM and was soluble in NMR buffer at room temperature and at 310K in the spectrometer.

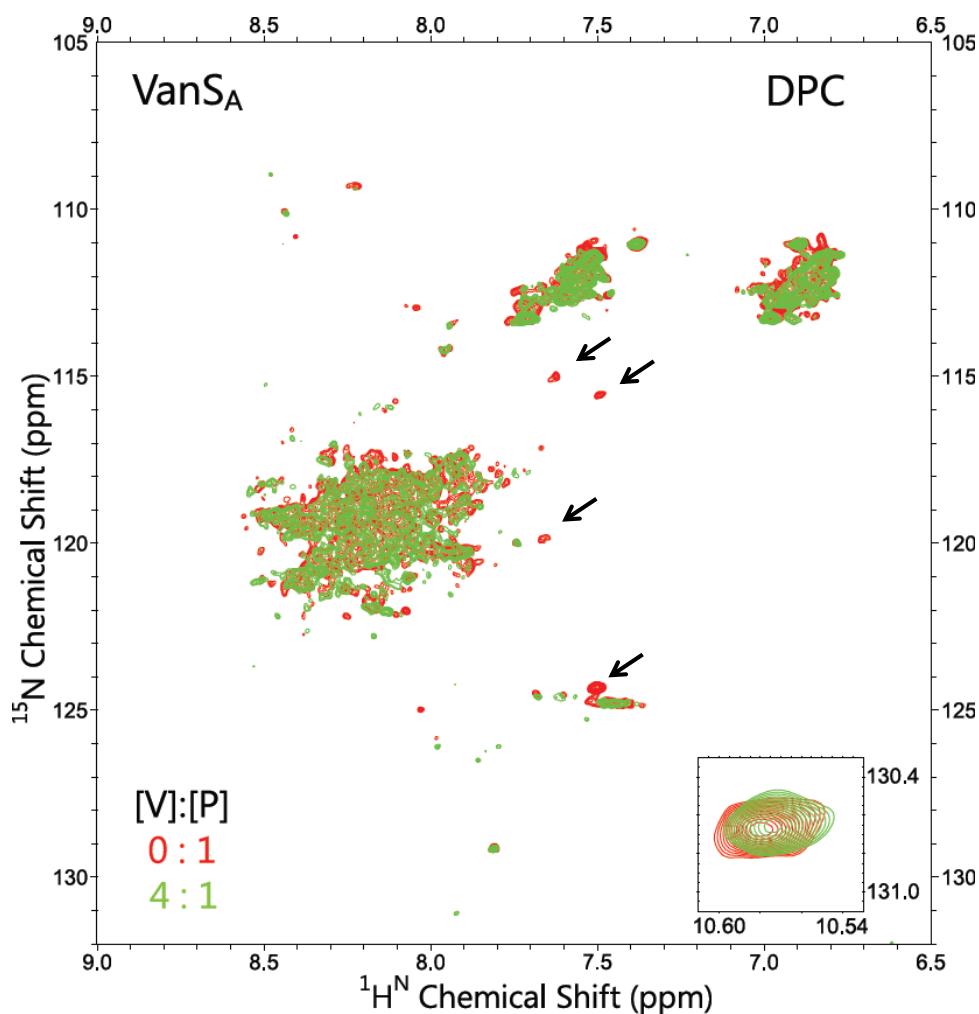


Figure 5.4.1.1: Overlaid 2D ^1H - ^{15}N HSQC spectra of $120\ \mu\text{M}$ VanS_A N-terminal domain solubilised in $50\ \text{mM}$ DPC, before and after addition of detergent-solubilised vancomycin. Both the protein and vancomycin were solubilised in $50\ \text{mM}$ Phosphate pH 5.5 and $75\ \text{mM}$ NaCl. [Vancomycin]:[protein] ratios of 0:1 and 4:1 were tested and spectra collected at 310K on a 700 MHz Bruker spectrometer. Peaks of interest are highlighted with arrows.

It was anticipated that the addition of excess vancomycin would result in multiple peak shifts, and their chemical shifts could be mapped for each titration to conduct a CSP analysis. However, no significant peak shifts were observed, and instead several peaks (marked with arrows on Figure 5.4.1.1) were observed to disappear in the presence of excess antibiotic. It was not possible to determine if those peaks had broadened or become narrower during titrations, as a result of interaction with the antibiotic. However, according to Williamson, (2013), as a ligand is titrated into a sample containing protein, when exchange is fast i.e.

when $k_{\text{off}} \gg \Delta\delta$ (of free and bound ligand), the signals will move smoothly from their position in the free spectrum to their position in the bound spectrum. By contrast, if the exchange rate is slow on the chemical shift timescale i.e. when 'off rate' (k_{off}) $\ll \Delta\delta$ (of free and bound ligand), the free signal gradually disappears and the bound signal appears, with the intensity of the two peaks reflecting the concentrations of free and bound ligand. In the limit of very slow exchange, the peaks may also broaden and disappear. Furthermore, if the exchange rate is similar to the chemical shift difference i.e. when $k_{\text{off}} \sim \Delta\delta$ (of free and bound ligand), signals will broaden and shift simultaneously. Observed peak changes during exchange are illustrated in Figure 5.4.1.2. It is therefore possible that protein-vancomycin interactions occur in DPC detergent, but could involve slow exchange to a bound state.

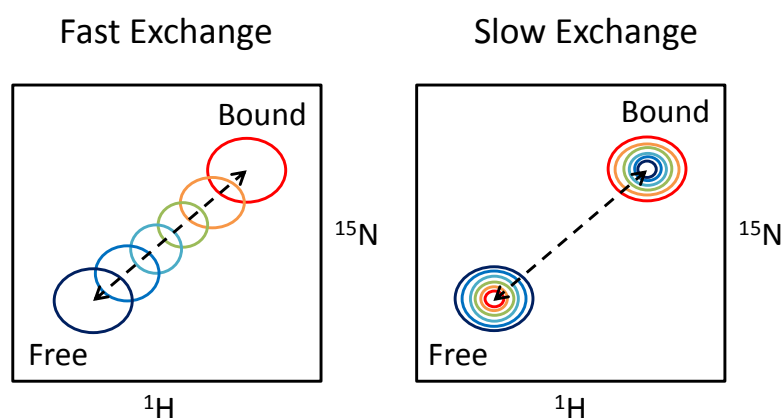


Figure 5.4.1.2: The appearance of 2D NMR peak shape under different rates of exchange. Adapted from Williamson, (2013). (Left): During fast exchange, peaks move smoothly from free (blue) to bound (red) state (see arrows). (Right): During slow exchange, the free peak (blue) decreases in intensity as the bound peak (red) increases.

In order to establish whether the peak disappearances observed for VanS_A in the presence of vancomycin were indicators of ligand binding, and if so, what the rate of exchange between free and bound states was, protein samples containing the VanS_A sensor domain were re-tested in either the same detergent (DPC) but at different pH, or solubilised in another detergent, and spectra collected.

In Figure 5.4.1.1 the solution pH was 5.5, so a more neutral pH of 6.8 was selected for further analysis, in order to provide a more physiologically relevant environment for the ligand to bind to VanS. All titrations were again performed at 0:1, 1:1 and 4:1 ratios of [vancomycin]:[protein] to observe any changes in peak intensity or chemical shift during additions (see Figure 5.4.1.3 Panel A). Solubilisation of VanS_A protein in DPC detergent at the increased pH of 6.8 (Figure 5.4.1.3A) resulted in similar peak changes and disappearances (marked with arrows) to those in Figure 5.4.1.1 (at pH 5.5), although the higher pH led to reduced peak dispersity. Therefore peak changes observed upon vancomycin addition can be seen to occur across the relevant pH range (5-7).

Titrations were next performed for samples of the VanS_A sensor domain in different detergents (LMPG: Figure 5.4.1.3B, and LPPG: Appendix Figure 12), with the aim to investigate antibiotic binding for a range of protein folds. It should be noted that samples in the lyso-phospholipids (LMPG and LPPG) were usually solubilised in sodium acetate buffer at pH ~5.5, because Krueger-Koplin *et al.*, (2004) had shown that for their membrane proteins, sample lifetimes were not significantly affected by buffering in the range of pH 4.5 to 8.0, and reduced amide broadening could be achieved around pH 5-6.

A comparison of samples of VanS_A solubilised in DPC detergent with those solubilised in LMPG detergent (Figures 5.4.1.3A and 5.4.1.3B respectively) also shows a number of peaks that shift and/or disappear during ligand titrations (marked on both figures with arrows), with relatively similar peak positions. In particular, reasonably large peak shifts are observed in LMPG detergent (Figure 5.4.1.3B), which could indicate a direct interaction between vancomycin and the VanS_A protein. The peak shifts also appear to cluster to a particular region of the spectrum (see arrows in Figures 5.4.1.3A and B) for VanS_A protein samples solubilised in different detergents and at different pHs, and therefore may indicate a possible binding site (provided that the identity of the peaks indicated are equivalent residues).

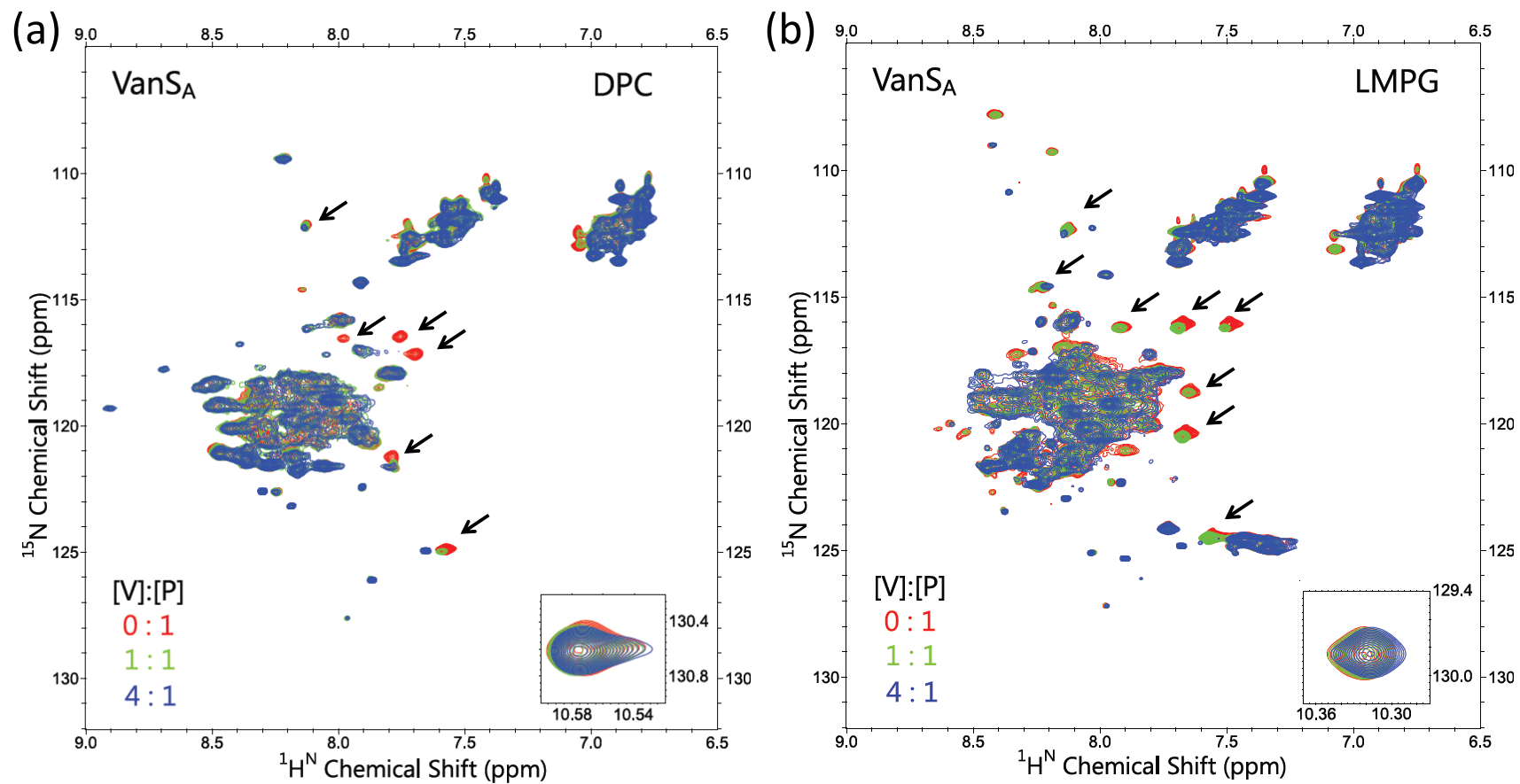


Figure 5.4.1.3: Overlaid 2D ^1H - ^{15}N HSQC spectra of (a) $600\ \mu\text{M}$ VanS_A N-terminal domain solubilised in 50 mM DPC, 20 mM HEPES pH 6.85, or (b) $700\ \mu\text{M}$ VanS_A N-terminal domain solubilised in 50 mM LMPG, 50 mM sodium acetate pH 5.5, during titration of detergent-solubilised vancomycin. [Vancomycin]:[protein] ratios of 0:1 (red), 1:1 (green) and 4:1 (blue). All spectra were collected at 310K and peaks of interest are highlighted with arrows.

As a further test to examine vancomycin binding, samples of VanS_{SC} proteins were solubilised in detergent, and HSQC spectra recorded at each titration point. VanS_{SC} proteins were solubilised in LPPG or DPC detergent, under similar conditions to those for the VanS_A proteins, and titrations conducted at identical molar ratios of vancomycin: protein. Peak shifts of interest were marked with arrows on Figure 5.4.1.4 (in LPPG) and Appendix Figure 13 (in DPC), and it is clear that several of the peaks indicated are observed in similar regions to those in the VanS_A spectra (for the same detergent). It is therefore possible, that vancomycin may be directly interacting with both VanS proteins in detergent micelles, and perhaps even at residues with similar identity. However, other possibilities for observed peak shifts should also be considered. For instance, the position of many peaks in the HSQC spectra of the VanS proteins are affected by the detergent chosen (e.g. comparing Figure 5.4.1.3A with Figure 5.4.1.3B), and if the structure of the detergent micelle is altered e.g. upon binding to vancomycin, this could in turn alter the structure of VanS (within the micelle) and hence indirectly affect peak chemical shifts, rather than necessarily resulting from a direct binding.

In order to identify those peaks which had statistically significant chemical shift changes, and hence provide supporting evidence for a direct binding, a Chemical Shift Perturbation Analysis was conducted for each protein in each detergent (see Figure 5.4.1.5). This identified those peaks with a chemical shift change ($\Delta\delta$) greater than that of the standard deviation for all peaks in the spectrum (using Equation 4, see Figure 5.4.1.5). Ideally, the peaks would be assigned to specific residues in the VanS proteins, however efforts towards assignment are still underway in the laboratory. Optimisation of protein concentration to allow collection of 3D spectra such as TOCSY-HSQC or NOESY-HSQC with improved signal-to-noise ratios is required and was not achievable in the time available, despite considerable efforts. Therefore further discussion of peak perturbation and broadening in this chapter is done in the absence of protein assignments.

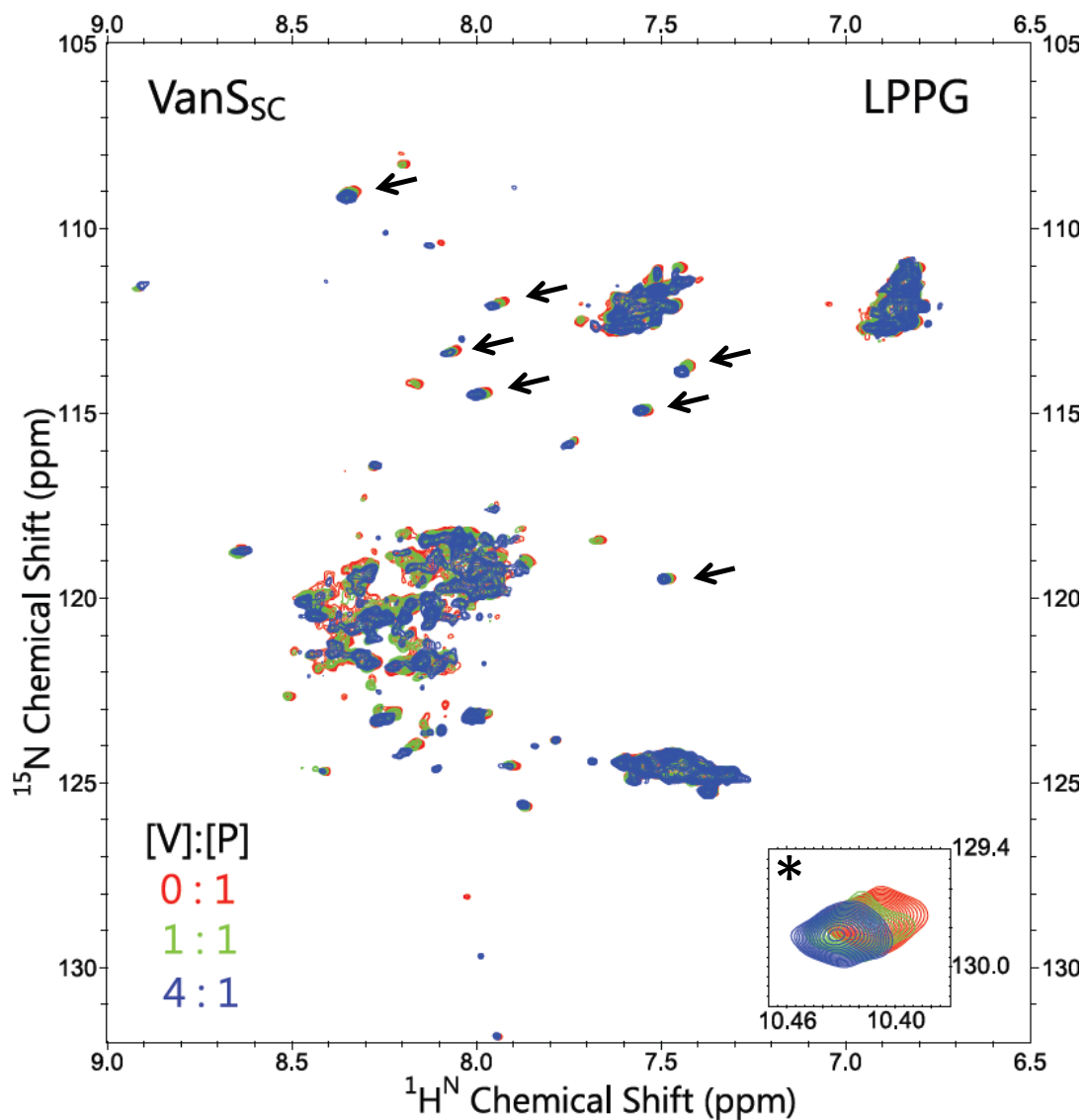


Figure 5.4.1.4: Overlaid 2D ^1H - ^{15}N HSQC spectra of 200 μM VanS_{sc} N-terminal domain solubilised in 50 mM LPPG, 50 mM phosphate pH 6.1, during titration of detergent-solubilised vancomycin. [Vancomycin]:[protein] ratios of 0:1 (red), 1:1 (green) and 4:1 (blue) were tested. All spectra were collected at 310K and peaks of interest are highlighted.

For each CSP analysis, all peaks in the HSQC spectrum were picked at each titration point (0:1, 1:1 and 4:1 [ligand]:[protein] ratios) and the ^1H and ^{15}N peak values were recorded and tabulated. The difference in ^1H (δ_H^2) or ^{15}N (δ_N^2) chemical shift value of each peak (at each titration point) was calculated by subtracting against the chemical shift value of the corresponding peak in the spectrum containing only the protein in detergent (i.e. at 0:1 [ligand]:[protein]). The relative chemical shifts of the ^1H and ^{15}N nuclei were then weighted, and the chemical shift change, ($\Delta\delta$), calculated according to Equation 4 (Grzesiek *et al.*, 1996; Garrett *et al.*, 1997):

$$\Delta\delta = \sqrt{0.5 \cdot [\delta_H^2 - (\alpha \cdot \delta_N^2)]} \quad (4)$$

This equation is standard practice in CSP analysis, and calculates the average (or summed) Euclidean distance moved for each peak in ^1H and ^{15}N dimensions, using an appropriate scaling factor, α , for values in ^{15}N (Williamson, 2013). Although there is no theoretical value for the scaling factor, several groups have taken the chemical shift range for ^1H and ^{15}N , and used this to provide a scale. For example, the range of backbone ^{15}N chemical shifts for both VanS_A and VanS_{SC} is approximately 130 – 105 ppm, and the range of $^1\text{H}^{\text{N}}$ shifts is approximately 10.4 – 6.8 ppm, so the scale factor should be 3.6/25 or approximately 0.14. This is value for α is common in the literature (Williamson, 2013; Williamson *et al.*, 1997), and was used throughout CSP analyses of VanS proteins in this study.

By picking and numbering peaks for VanS proteins at each titration point (in ascending $^1\text{H}^{\text{N}}$ value), and calculating the chemical shift change ($\Delta\delta$) for those peaks, it was possible to produce a bar graph of peak number (as opposed to residue number, for reasons discussed previously) against CSP to illustrate the number and magnitude of shifts observed (Figure 5.4.1.5A and 5.4.1.5B). Peaks displaying the largest CSPs are likely to indicate an amide or side-chain proton involved in binding, however, a threshold value had to be calculated to decide which shifts were large enough to be considered indicators of the binding site.

Generally, the standard deviation of the shift changes (σ) is calculated (Schumann *et al.*, 2007), to identify residues with significant chemical shift change (i.e. those with $\Delta\delta > \sigma$). Typically if the ligand binds in a well-defined binding site, there should be chemical shift changes in excess of 0.2 ppm in $^1\text{H}^{\text{N}}$. However, if the ligand binds in a less well defined orientation, changes will be smaller (Williamson, 2013). For example, Morrison *et al.*, (2003) found that a phenylalanine-containing peptide ligand bound to their protein in a number of conformations, and the largest chemical shift change ($\Delta\delta$) was only 0.08 ppm in $^1\text{H}^{\text{N}}$. Therefore, CSP analysis alone only gives an indication of the region involved in binding, and the absolute shift measured will vary widely for different systems. The chemical shift change calculated also varies depending on the degree of saturation reached, for example, larger shifts will be observed at ligand:protein molar ratios of 4:1 versus 1:1. This is evident in Figure 5.4.1.5, whereby shift changes increase in Panel B (4:1-0:1) versus Panel A (1:1-0:1), because the molar ratio of ligand:protein is greater.

In Figure 5.4.1.5, those peaks with high chemical shift changes during ligand titrations are starred and numbered (in increasing ^1H chemical shift) e.g. 1*, and are annotated onto overlaid HSQC spectra in Figure 5.4.1.6, to highlight shifts that indicate genuine binding. This bar graph for the analysis of CSP values was created based on a paper by Morrison *et al.*, (2003) (mentioned above), who saw similar shifts, often with peak overlap. The group picked peaks and plotted them on bar graphs against calculated chemical shift perturbations, to determine peak changes of relevance. Based on these methods, CSP analyses were conducted for vancomycin titrations into samples of VanS_A protein solubilised in DPC, and VanS_{SC} protein solubilised in LPPG detergent. Shifts significantly above the threshold value (see Appendix Figures 14 and 15) are annotated by stars on the corresponding overlaid HSQC spectra, which are shown in Figures 5.4.1.7 and 5.4.1.8 respectively, zoomed in on the region containing these starred peaks.

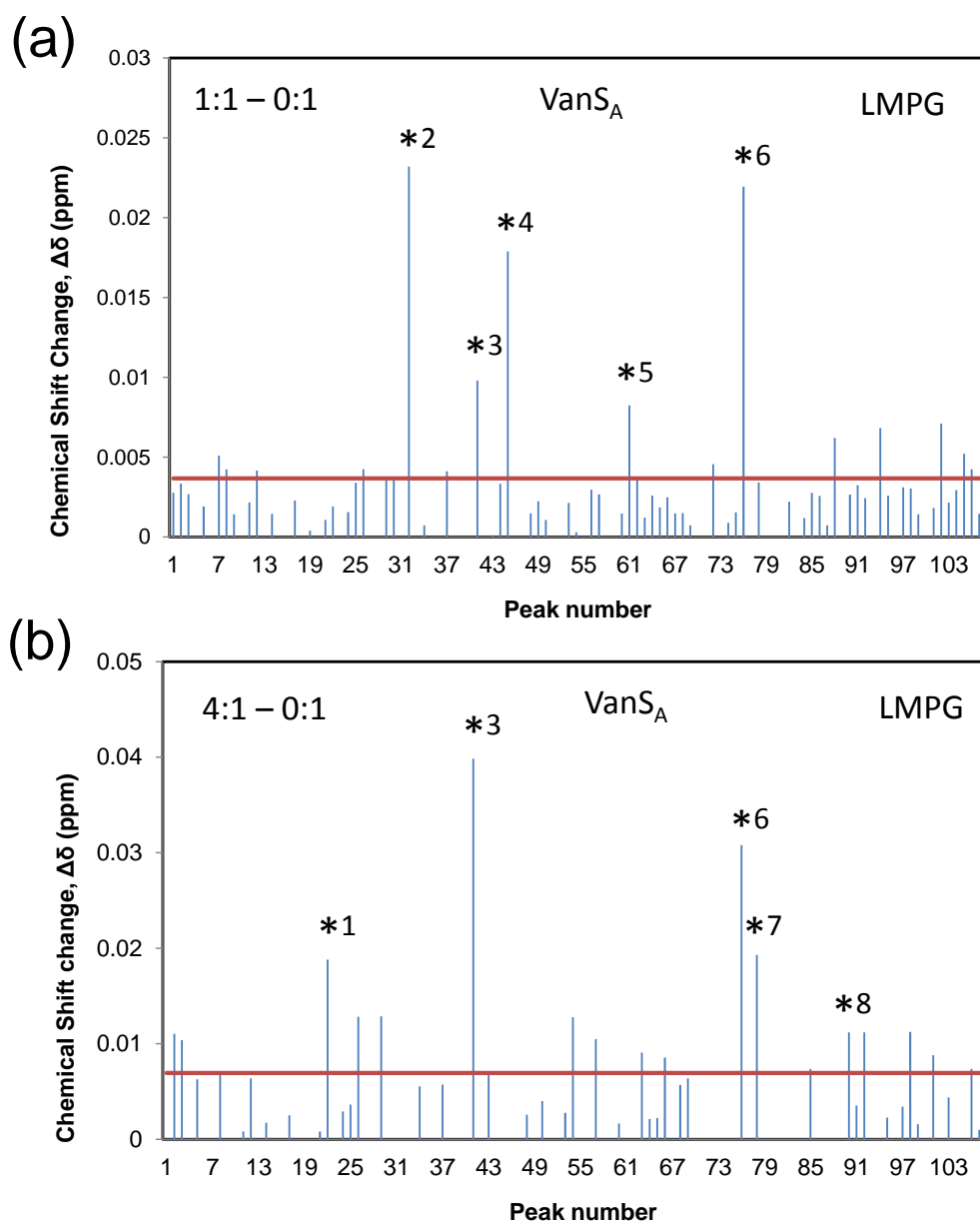


Figure 5.4.1.5: Chemical shift changes for individual peaks in the ^1H - ^{15}N HSQC spectrum of VanS_A protein in LMPG (Fig. 5.4.1.3B) upon addition of vancomycin, represented by a bar chart of peak number (ascending $^1\text{H}^{\text{N}}$) against chemical shift change ($\Delta\delta$). Changes for side-chain and backbone $^1\text{H}^{\text{N}}$ protons were calculated using the equation: $\Delta\delta = \sqrt{0.5 \cdot [\delta_{\text{H}}^2 - (0.14 \cdot \delta_{\text{N}}^2)]}$, against a threshold value (σ , red line). Peaks with significant CSPs are annotated by starring. (A) Chemical shift changes upon adding a 1:1 molar ratio of [vancomycin]:[protein] (B) Chemical shift changes upon adding a 4:1 molar ratio of [vancomycin]:[protein].

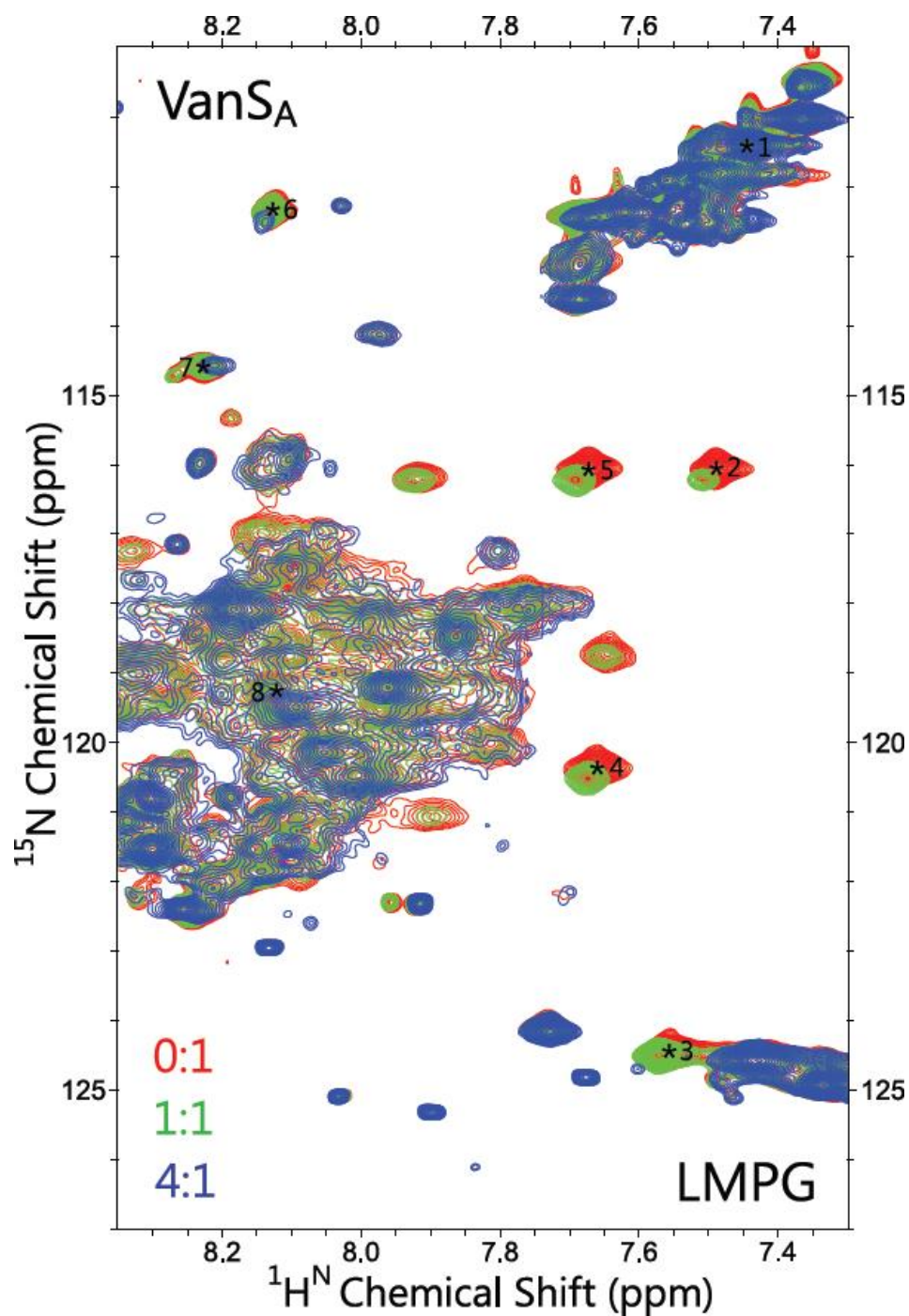


Figure 5.4.1.6: Overlaid 2D ^1H - ^{15}N HSQC spectra of 700 μM VanS_A N-terminal domain in 50 mM LMPG during titration of vancomycin, zoomed in to the region of 7.5-8.4 ppm in ^1H and 127-110 ppm in ^{15}N , in Figure 5.4.1.3B. [Vancomycin]:[protein] ratios of 0:1 (red), 1:1 (green) and 4:1 (blue) were tested at 310K. Peaks with significantly high chemical shift changes, according to CSP analysis, are starred and numbered and their positions (prior to ligand addition) annotated onto the spectra.

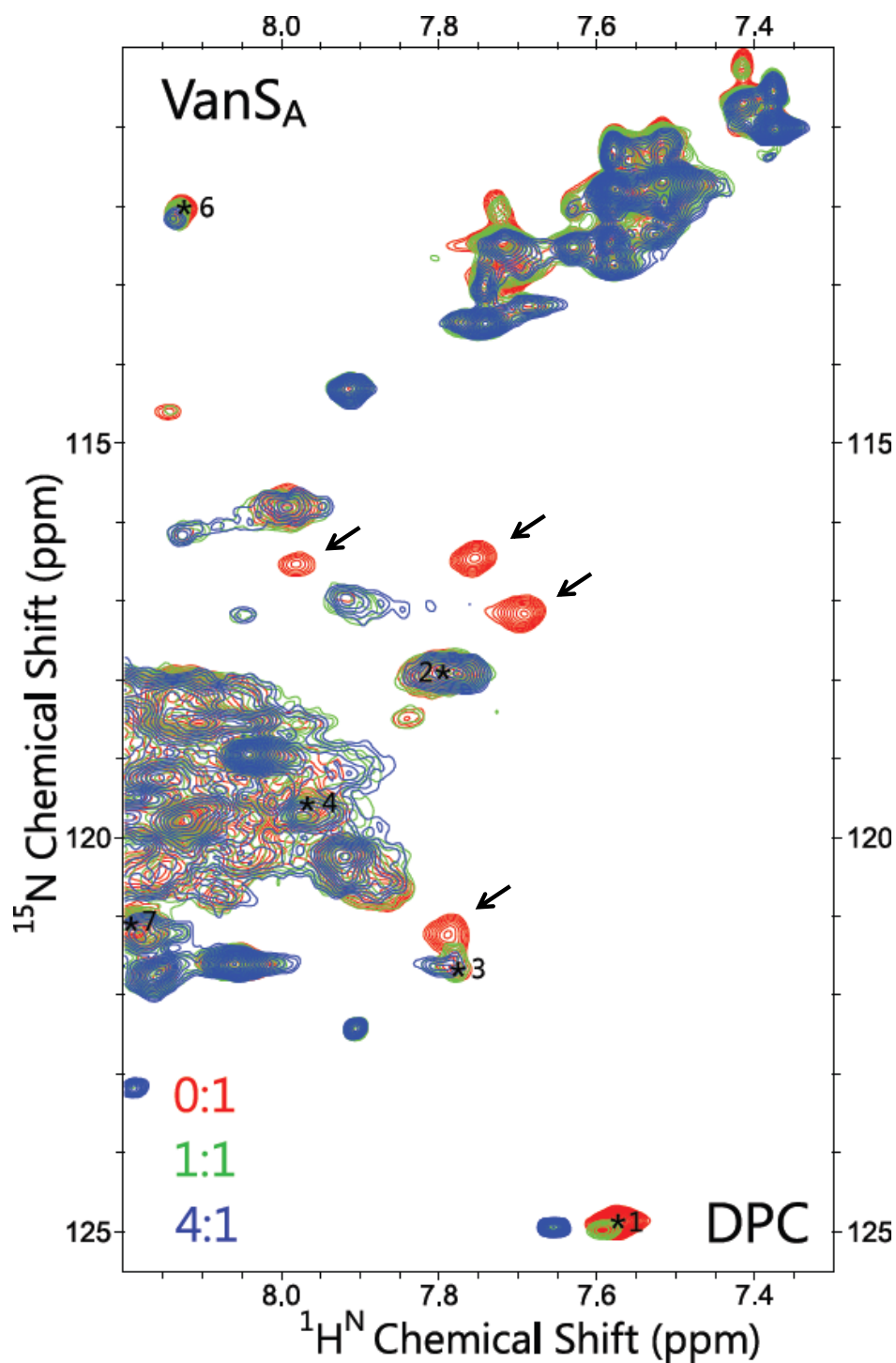


Figure 5.4.1.7: Overlaid 2D ^1H - ^{15}N HSQC spectra of 600 μM VanS_A N-terminal domain in 50 mM DPC during titration of vancomycin, zoomed in to the region of 7.5-8.2 ppm in ^1H and 125-110 ppm in ^{15}N , in Figure 5.4.1.3A. [Vancomycin]:[protein] ratios of 0:1 (red), 1:1 (green) and 4:1 (blue) were tested at 310K. Peaks with significantly high chemical shift changes, according to CSP analysis (see Appendix Figure 14), are starred and numbered and their positions (prior to ligand addition) annotated onto the spectra. Those peaks that do not shift, but instead disappear upon addition of vancomycin are indicated by arrows.

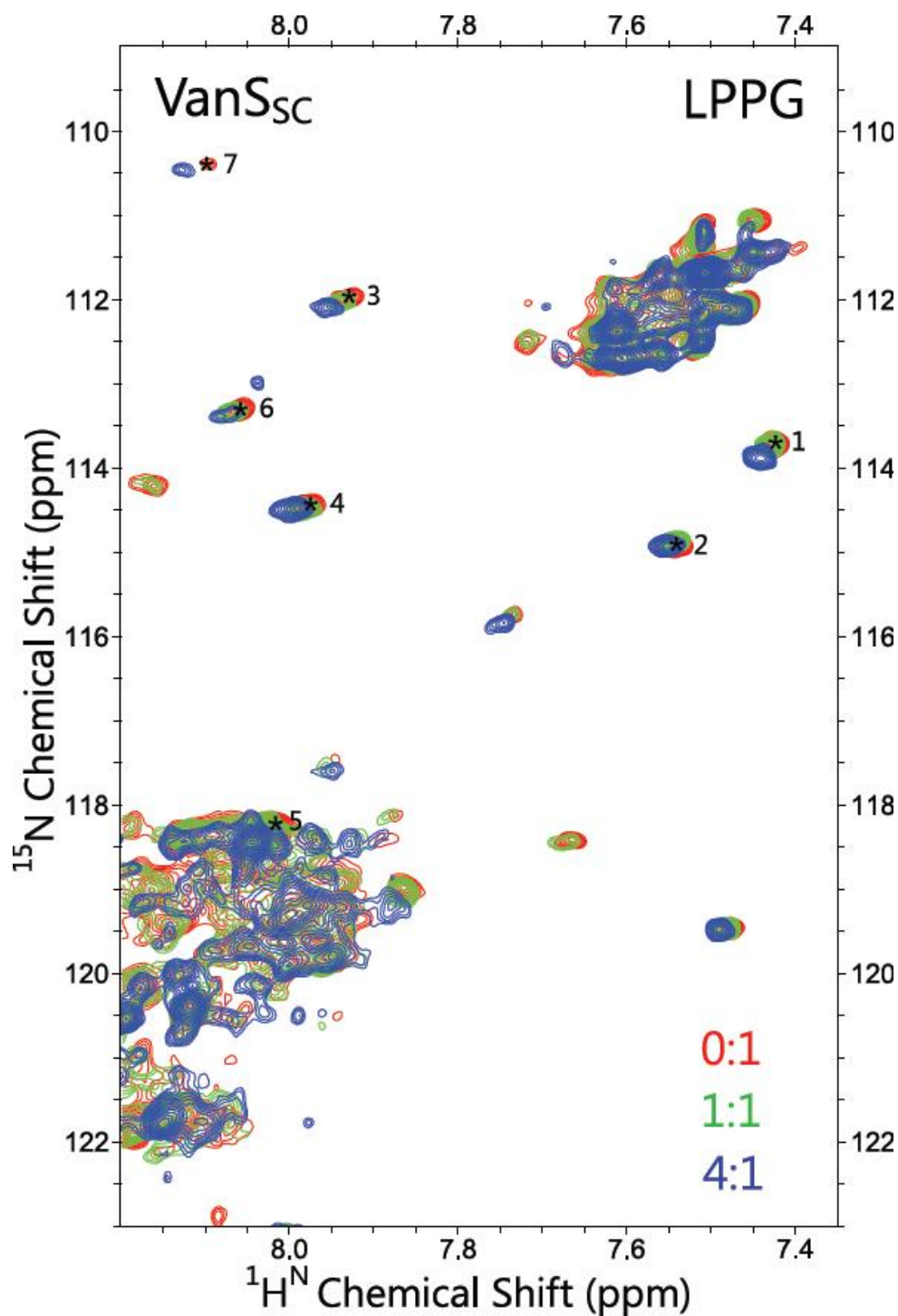


Figure 5.4.1.8: Overlaid 2D ^1H - ^{15}N HSQC spectra of 200 μM VanS_{sc} N-terminal domain in 50 mM LPPG during titration of vancomycin, zoomed in to the region of 7.4-8.2 ppm in ^1H and 123-108 ppm in ^{15}N , in Figure 5.4.1.4. [Vancomycin]:[protein] ratios of 0:1 (red), 1:1 (green) and 4:1 (blue) were tested at 310K. Peaks with significantly high chemical shift changes, according to CSP analysis (see Appendix Figure 15), are starred and numbered and their positions (prior to ligand addition) annotated onto the spectra.

CSP analyses confirmed that several of the perturbations marked with arrows in Figures 5.4.1.3A and B, and 5.4.1.4A were likely to be significant, as they lie well above the calculated standard deviation across all resolvable peaks analysed, and are starred in Figures 5.4.1.6 to 5.4.1.8. The CSP data provides further evidence for a direct interaction between vancomycin and VanS proteins, and several residues (as yet unassigned) in similar chemical environments are indicated to be involved. Despite this statement, the magnitude of the shifts are small (similar to that presented by Morrison *et al.*, 2003), which could mean the vancomycin interacts weakly or transiently with VanS, or presents different conformations (i.e. not a well-defined binding site), but the data does suggest an interaction between VanS and vancomycin, which causes perturbation of a number of proton signals.

Further insight can be gained by examining individual peak shifts in overlaid HSQC spectra. Individual peaks (annotated with stars) were selected from the spectra of VanS_A in LMPG detergent (Figure 5.4.1.6) or VanS_{SC} in LPPG detergent (Figure 5.4.1.8), and are shown in Figure 5.4.1.9, to demonstrate the dependence of chemical shift on vancomycin concentration. Overall, most peaks in the spectra did not shift (above the standard deviation), and some disappeared with excess ligand, which may have resulted from altered dynamics upon binding. However, for those peaks that did display a CSP, the peak position moves roughly along a direct line, as a function of increasing antibiotic concentration, with some peaks broadening during the titration.

As stated earlier, one might expect to see a chemical shift change of 0.2 ppm or above in $^1\text{H}^{\text{N}}$, and 0.9 ppm or above in ^{15}N , for a system in fast exchange between bound and unbound state (Williamson, 2013). Therefore the peak shifts observed for both VanS_A and VanS_{SC} proteins do not represent a system under fast exchange. Instead, several peaks disappear with increasing concentration of vancomycin, which is more indicative of an intermediate-slow exchange to the bound conformation (see Figure 5.4.1.2). Any peak broadening occurring could also result from intermediate-slow exchange or reduced tumbling in solution.

For those peaks that do shift, the signal intensity is often reduced at high concentrations of vancomycin (tested to a final concentration of 2.8 mM), which may result from slow exchange (decreasing peak linewidth), or decreased signal-to-noise (since the antibiotic is added in excess into solution). In contrast, the signal intensity for all peak shifts in Figure 5.4.1.8 does not vary with increasing antibiotic concentration (tested up to 0.8 mM), so changes in signal intensity may only result from decreased antibiotic solubility.

As a final note, in Figure 5.4.1.9 below, the peak shifts in Panel F, resulting from addition of vancomycin to samples of VanS_{SC} protein in LPPG detergent, show relatively large changes in the chemical shift of the peak at ~ 10.4 ppm. This peak must result from the resonance of the indole NH ring proton of a tryptophan residue, as this is the only proton present in that chemical shift region. This is interesting since the N-terminal sensor domain of VanS_{SC} contains only three tryptophan residues (W), at positions 41, 68 and 82 in the wild-type sequence, and only W41 should be exposed outside the micelle and therefore accessible to interact with vancomycin, since residues W68 and W82 occur in the predicted second transmembrane domain (Figure 5.4.1.10).

Additionally, studies by Koteva *et al.*, (2010) which showed the first direct binding of a vancomycin analogue to the VanS_{SC} protein, identified that the only section of the protein covalently labelled by the vancomycin probe was between residues M1 – W41. This consists of the putative first transmembrane helix and the first four residues, DQGW, of the predicted extracytoplasmic loop region (Figure 5.4.1.10). Therefore W41 could potentially be involved in binding to vancomycin, and the peak at 10.4 ppm is likely to represent that residue (as it is the only tryptophan exposed). This provides supporting evidence for a direct interaction of vancomycin with the VanS_{SC} protein *in vitro*.

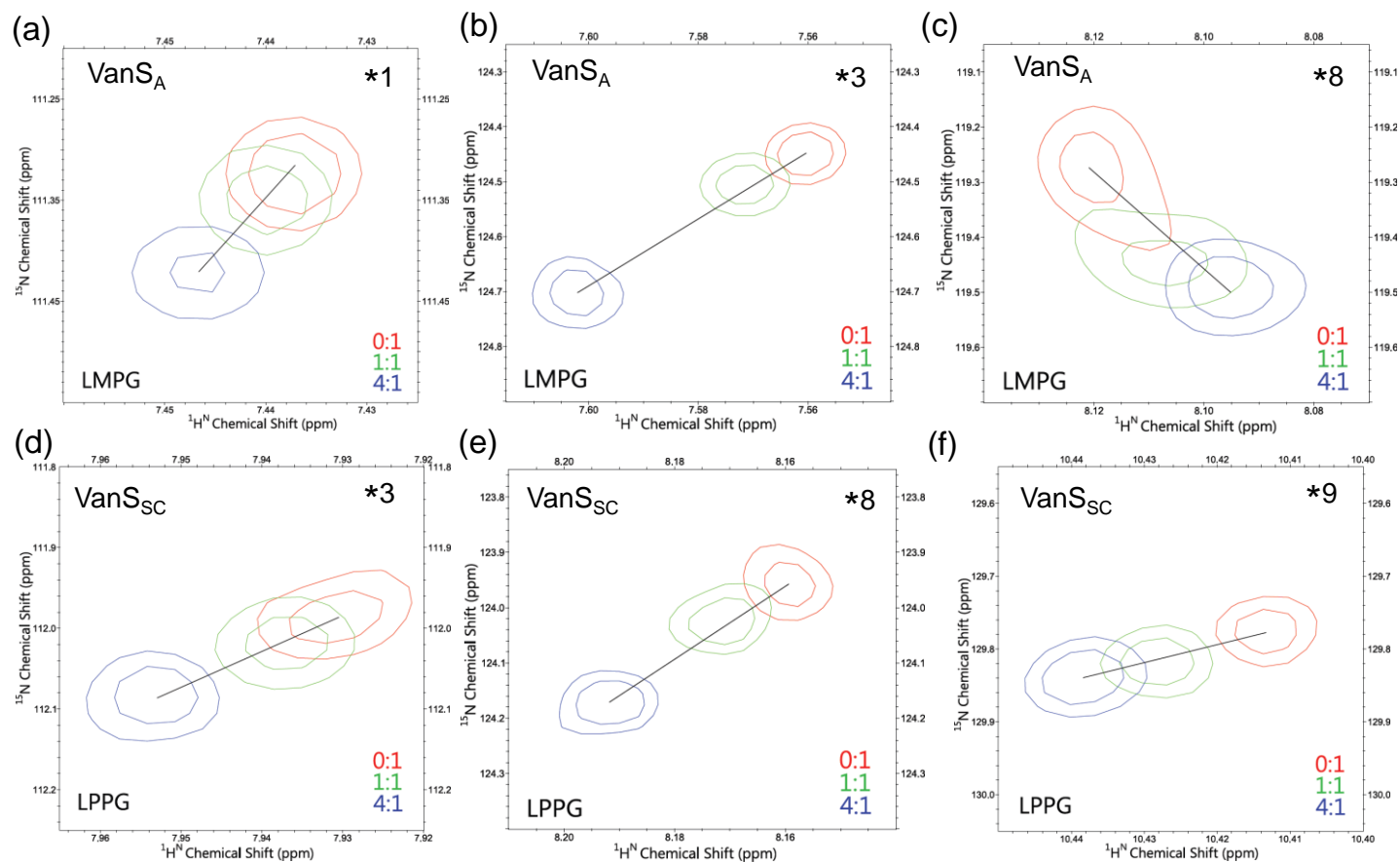


Figure 5.4.1.9: Overlaid 2D ^1H - ^{15}N HSQC NMR spectra for VanS proteins during titration of vancomycin, showing individual peak shifts with high calculated CSPs. (A-C): 600 μM VanS_A N-terminal domain in 50 mM LMPG pH 5.5, (D-F): 200 μM VanS_{sc} N-terminal domain in 50 mM LPPG pH 6.1. [Vancomycin]:[protein] ratios of 0:1 (red), 1:1 (green) and 4:1 (blue) were tested. Peaks were starred and numbered according to data in Figure 5.4.1.5 (A-C) or Appendix Figure 15 (D-F).

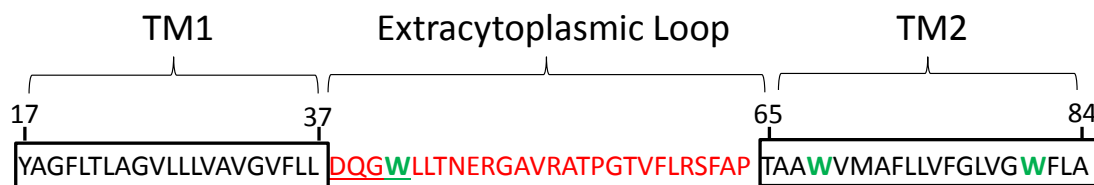


Figure 5.4.1.10: Predicted domain positions in the VanS_{SC} protein sequence, showing residues 17 to 85. Predicted TM domains (according to TMPred, and Koteva et al., 2010) are shown in boxes (residues 17-37 and 65-85) and the extracytoplasmic loop region is highlighted in red. The four residues (DQGW) in the loop region that are proposed by Koteva et al., (2010) to be involved in binding to vancomycin are underlined, and the three tryptophan residues in the sequence are in green.

5.4.2 Analysis of Full-length VanS proteins by NMR Spectroscopy

Sensor histidine kinases such as VanS function as dimers, and in prototypical histidine kinases, the cytoplasmic core consists of a dimerisation domain (DHp) and a C-terminal ATP binding domain (CA) (see section 1.5.3) (Gao and Stock, 2009). The CA domain alone exists as a monomer in solution, and is capable of binding ATP and transferring phosphoryl groups to a conserved histidine residue in the dimeric DHp domain. In the presence of an inducer such as vancomycin, it is not clear whether VanS interacts with vancomycin in a monomeric or dimeric form, but the formation of a dimeric sensor complex is required for signal transduction via the dimeric DHp domains to the catalytic domain, to effect kinase function. It is therefore likely that any binding that does occur between vancomycin and monomeric VanS proteins, will not be productive, i.e. will not cause signal transduction and activation resistance gene transcription.

As observed for the VanS_A and (to a lesser extent) VanS_{SC} N-terminal sensor domains, the addition of vancomycin does perturb the chemical environment of several protons (on different residues), and suggests that the presence of vancomycin does alter the conformation of VanS. Since the functional form of the VanS kinase is a dimer, if

vancomycin is added to the full-length form of VanS, which has been shown in section 3.11 to be functionally active in DPC detergent (with respect to ADP release and phosphate release assays), further changes in conformation would be anticipated as interactions could be more productive, and enable downstream signal transduction. Therefore, full-length VanS proteins overexpressed in ^{15}N labelled M9 minimal media were examined (without enzymatic cleavage) using ^1H - ^{15}N HSQC NMR spectroscopy and spectral changes monitored during ligand titrations. Although spectral crowding would be much greater for the full-length protein and peak linewidths would likely increase due to the increase in size, it was thought that the peaks that had been observed to shift during ligand titrations to samples containing the VanS sensor domain would still remain distinguishable; since they were well-dispersed from the majority of peaks in the backbone amide region and predicted to be in a more flexible region of the protein. Furthermore, even if peaks could not be easily distinguished, the resulting HSQC spectra of the full-length, and isolated sensor domain of VanS, could be overlaid to ensure no changes in protein fold were occurring after cleavage of the C-terminal domain, which could impinge on antibiotic binding.

Samples of full-length detergent-solubilised VanS proteins in DPC detergent (and in LMPG detergent) were purified in the same buffer and detergent conditions as those of the isolated VanS sensor domain (see Figure 5.4.2.1A for VanS_A and Appendix Figure 16 for VanS_{SC}). Overlaid NMR spectra in Figure 5.4.2.1A show that the overall fold of the isolated sensor domain of VanS is highly similar to that of the full-length protein, with overlapping peaks in the side-chain regions and backbone amide region. Additional peaks are also present for the full-length protein, dispersed widely across the ^{15}N axis. However, most of the peaks which are implicated in antibiotic binding to the isolated VanS_A sensor domain (starred and annotated), are either not observed in the spectrum of full-length VanS_A or appear at a different chemical shift value. It is therefore difficult to see if interaction with these residues is conserved for the full-length protein.

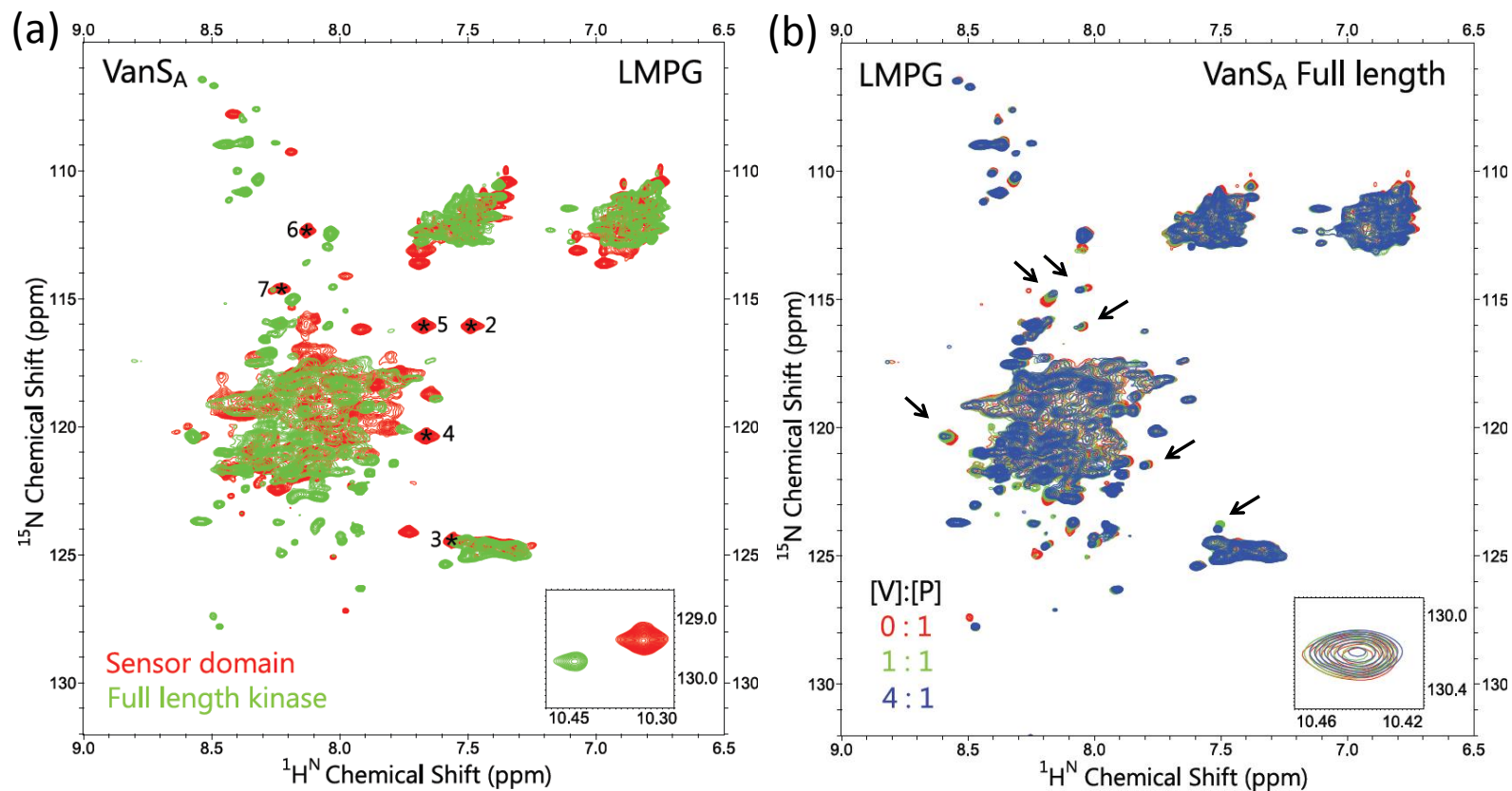


Figure 5.4.2.1: (a) Overlaid 2D ^1H - ^{15}N HSQC spectra of 700 μM VanS_A N-terminal domain (red) or 600 μM full-length protein (green), (b) Overlaid 2D ^1H - ^{15}N HSQC spectra of the VanS_A full-length protein during titration of detergent-solubilised vancomycin. Both protein samples were solubilised in 50 mM LMPG, 50 mM sodium acetate pH 5.5 collected at 310K. Peaks with significantly high chemical shift changes (according to CSP analyses) during vancomycin titration into samples containing the VanS_A sensor domain in (a), are starred and numbered and their positions annotated onto the spectrum. [Vancomycin]:[protein] ratios of 0:1 (red), 1:1 (green) and 4:1 (blue) were tested in (b), and peaks of interest are highlighted with arrows.

Nevertheless, vancomycin was added to samples of the VanS_A full-length protein in LMPG detergent at molar ratios of 0:1, 1:1, 4:1 (vancomycin:protein). Chemical shift changes were monitored during titrations and the resulting overlaid spectra are given in Figure 5.4.2.1B. The figure shows a handful of peaks (marked with arrows) that display chemical shift changes during the titration, some of which appear in similar chemical environment to those in the isolated sensor domain (e.g. near *6, *7 or *3). However, the magnitude of the chemical shift changes remains small, despite the presence of the full-length VanS_A protein, and it appears that any interaction with vancomycin is not altered by the presence of the kinase domain. This suggests that any binding between VanS_A (whether full-length or truncated) and vancomycin involves only a few residues (similar to the DQGW binding region proposed by Koteva *et al.*, (2010) for VanS_{SC}) and exchange rate to the bound form is likely to be slow.

However, these are *in vitro* studies using purified and detergent-solubilised proteins, whereas direct binding to a VanS protein has only been confirmed *in vivo* from unpurified membrane preparations (Koteva *et al.*, 2010). This raises the possibility that the membrane preparations used may still contain cell wall precursors, such as Lipid II, which may also be required in order to facilitate binding to the protein. Therefore three distinct models can be proposed: (i) direct induction; in which the kinase is activated by direct binding of antibiotic to the sensor domain, (ii) indirect induction; in which the kinase is activated by binding a cell wall metabolite which is either an intermediate in cell wall biosynthesis or accumulates as a result of antibiotic action, or (iii) induction by the vancomycin-cell wall metabolite complex; in which the kinase is activated by the glycopeptide antibiotic when it is bound to a D-Ala-D-Ala-containing cell wall precursor.

In a recent paper by Kwun *et al.*, (2013), *in vivo* activation of the *van* cluster in the VanB-type resistance system of *S. coelicolor* was found to require vancomycin binding to the D-Ala-D-Ala termini of cell wall PG precursors, to be perceived by the VanS_{SC} sensor domain.

By manipulating the amounts of D-Ala-D-Ala and D-Ala-D-Lac-containing precursors in the cell, the group showed that induction of *van* gene expression by vancomycin was significantly reduced in cells where D-Ala-D-Lac-containing precursors were more abundant than D-Ala-D-Ala, consistent with model (iii) for VanS sensing. Furthermore, induction of *vanH* transcription was readily observable upon addition of vancomycin to *S. coelicolor* wild-type cells, but when a vancomycin derivative was added, which cannot bind to D-Ala-D-Ala termini (desleucyl vancomycin, Figure 5.4.2.2), no *vanH* transcript was detectable. This showed that the D-Ala-D-Ala binding pocket of vancomycin is important not only for the mode of action but also for inducing the *van* resistance system, and supports the view that a vancomycin-cell wall metabolite complex should be required for activation of VanS_{SC}.

With this knowledge it was important to conduct a further experiment, involving addition of Lipid II cell wall precursor to NMR samples containing VanS and vancomycin, in case activation is triggered by formation of a vancomycin-cell wall PG precursor complex, which could be observed by chemical shift changes in the spectrum.

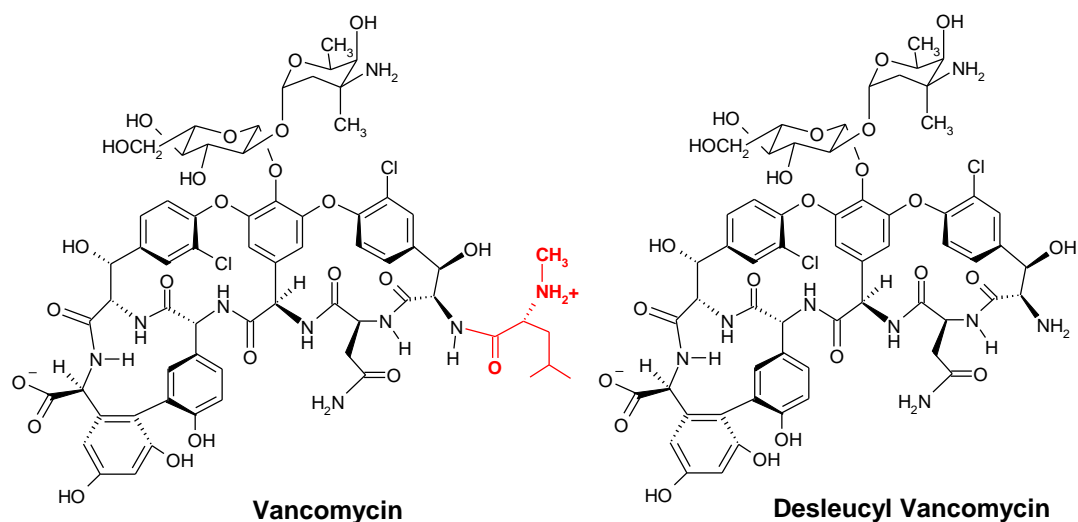


Figure 5.4.2.2: Vancomycin (left) and Desleucyl vancomycin (right) structures, drawn in ISISDraw. The desleucyl vancomycin has a modified peptide-binding pocket and is unable to bind to the of extracellular PG precursors. The difference in the two structures is highlighted by the moiety in red, which forms one of the five hydrogen bonds to the D-Ala-D-Ala N-terminus of PG precursors.

5.4.3 NMR Titration of the Lipid II cell wall precursor

Samples were prepared for VanS proteins in the presence of vancomycin and Lipid II-Lys (naturally found in the cell wall of Gram-positive bacteria) and analysed by 2D HSQC NMR, in order to test for any interaction of the VanS proteins with a complex of vancomycin and the Lipid II cell wall precursor. Lipid II-Lys was obtained from the Bacwan synthesis facility (School of Life Sciences, University of Warwick) as a dissolved lyophilised powder (in chloroform/methanol/water). An aliquot of Lipid II was dried to a film in a glass vial, and the NMR sample containing ^{15}N labelled detergent-solubilised VanS protein and vancomycin, was added to the vial and vortexed to resuspend the lipid (see section 2.14.2).

HSQC spectra for samples of VanS_A protein or VanS_{SC} protein solubilised in DPC detergent during titration of vancomycin, and subsequent addition of Lipid II, are overlaid and shown in Figure 5.4.3.1A or Figure 5.4.3.1B respectively. For the sample containing VanS_A protein, only the N-terminal sensor domain was present (since full-length VanS proteins had not been tested at this time), and Lipid II was added after vancomycin titrations in order to see if further peak shifts were observed. Although one or two peaks (marked with arrows in Figure 5.4.3.1A) were perturbed by the addition of Lipid II, the overall protein conformation remained unchanged. It was therefore not possible to state whether a complex of Lipid II and vancomycin are causing the peak shifts observed.

As stated in section 5.4.2, a possible issue with using the VanS sensor domain, is that the protein may not be able to dimerise which is important for kinase function, and vancomycin might only interact with dimeric VanS. Therefore in a second test, vancomycin was added to a sample containing full-length VanS_{SC} protein in DPC detergent (in which the protein appeared active), and subsequently Lipid II was added (Figure 5.4.3.1B). This would enable interactions to occur between a dimeric VanS_{SC} protein and a vancomycin-lipid complex, which is believed to be required for activation of the kinase *in vivo* (Kwun *et al.*, 2013).

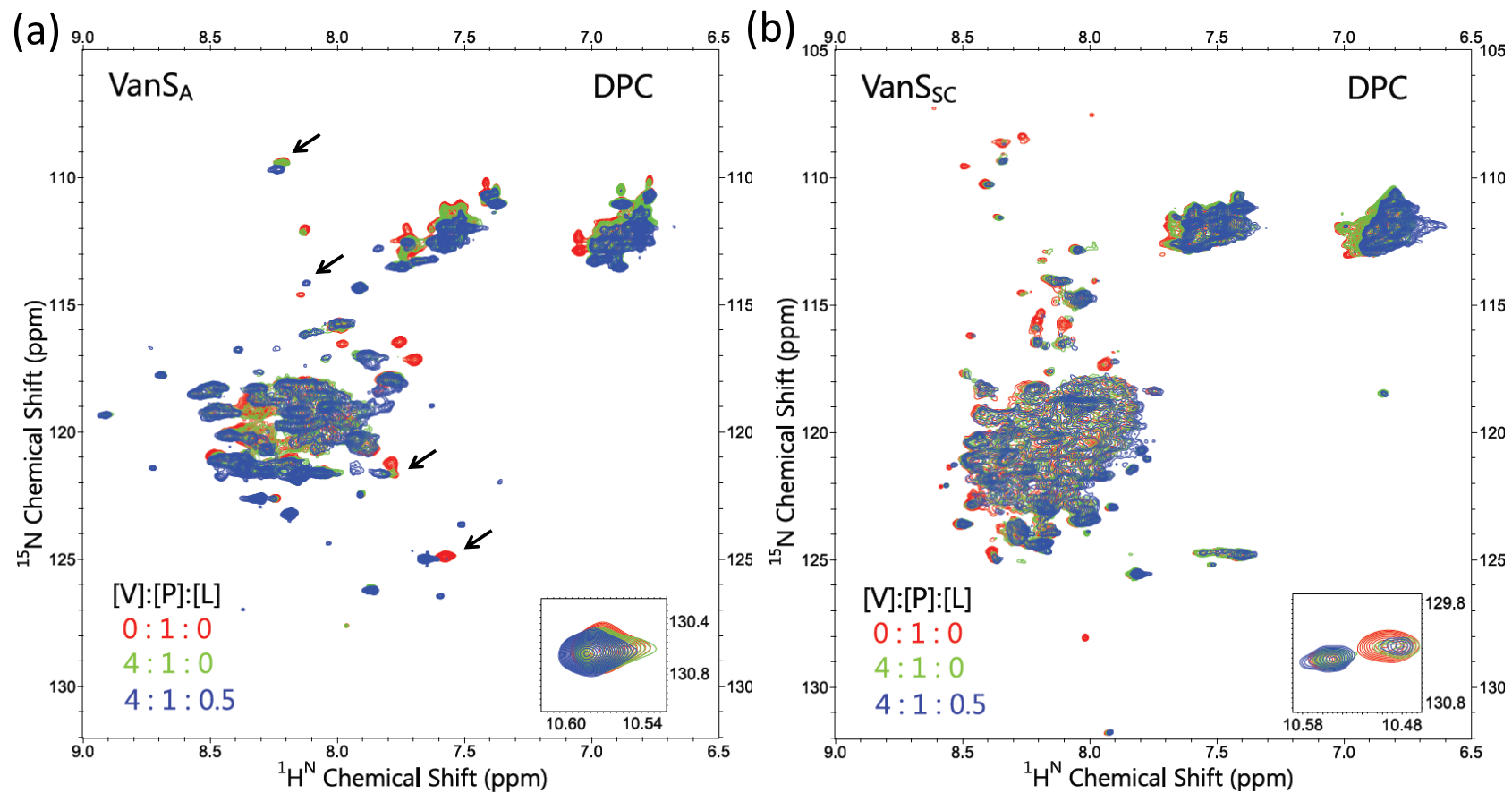


Figure 5.4.3.1: Overlaid 2D ^1H - ^{15}N HSQC spectra of (a) $600\ \mu\text{M}$ VanS_A N-terminal sensor domain solubilised in $50\ \text{mM}$ DPC, or (b) $500\ \mu\text{M}$ VanS_{sc} full-length protein solubilised in $50\ \text{mM}$ DPC, during titration of detergent-solubilised vancomycin and Lipid II-Lys. [Vancomycin]:[protein]:[Lipid II] ratios of 0:1:0 (red), 4:1:0 (green) and 4:1:0.5 (blue) were tested, and all data collected at $310\ \text{K}$. Both proteins were solubilised in $20\ \text{mM}$ HEPES pH 6.85.

Minimal changes in the position of peaks in Figure 5.4.3.1B are observed upon addition of vancomycin to full-length VanS_{SC}, and no significant changes occurred after subsequent addition of Lipid II. It is therefore not possible to ascertain from the data whether complexation of vancomycin to Lipid II is required to activate VanS_{SC} or not. It appears that technical difficulties associated in working with a membrane-localised sensor protein and a lipidated PG ligand, have prevented collection of *in vitro* data to support the *in vivo* vancomycin-VanS_{SC} binding studies by Kwun *et al.*, (2013) and Koteva *et al.*, (2010). Trying to recreate appropriate cell conditions *in vitro* for ligand binding to occur, will require the selection of a more suitable membrane mimetic (e.g. one that provides a more native environment for PG lipids) and perhaps the addition of other cell wall metabolites.

5.4.4 NMR Titration of other glycopeptide antibiotics

All NMR studies presented so far have concentrated on interactions between VanS proteins and vancomycin, since a direct binding of VanS to a glycopeptide antibiotic has only been shown with vancomycin analogues. However, both VanS_A and VanS_{SC} are activated by other glycopeptide antibiotics, and are classed as VanA- or VanB-type phenotypes based on their resistance to teicoplanin antibiotics. VanS_A is resistant to teicoplanin, whereas VanS_{SC} is only sensitive to teicoplanin, and therefore teicoplanin should only induce kinase activity in VanS_A. This could therefore provide a useful control experiment in NMR titration studies, as changes in the chemical shifts of VanS proteins on HSQC NMR spectra, should only be observed upon addition of teicoplanin to VanS_A proteins.

NMR ligand titration experiments were conducted as stated previously (see section 2.14.2) and teicoplanin was dissolved to a stock concentration of 10-20 mM and solubilised in 5 mM LMPG detergent micelles. The teicoplanin was added to NMR samples containing VanS_A (solubilised in LMPG detergent) at molar ratios of 1:1 and 4:1 of teicoplanin:protein and HSQC spectra collected at each titration point and overlaid, as shown in Figure 5.4.4.1.

Teicoplanin was obtained from Molekula (Dorset, UK) and comprises of a mixture of different compounds, including five major (termed teicoplanin A₂-1 through A₂-5) and four minor (termed teicoplanin R_S-1 through R_S-4), which all share the same glycopeptide core termed A₃-1 (a fused ring to which two carbohydrates are attached). The antimicrobial action of teicoplanin is tuned by using the proper ratio of A₂ and A₃ compounds (marketed as Targocid by Sanofi Aventis).

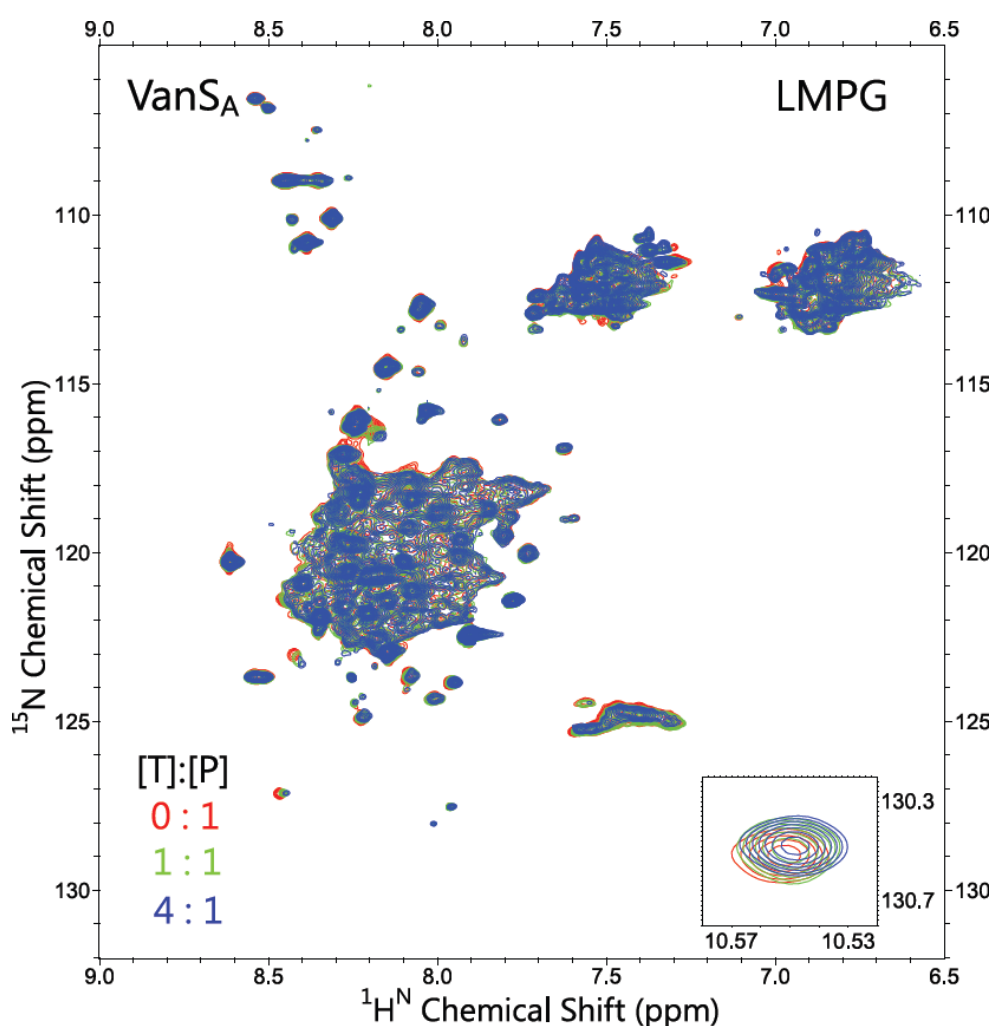


Figure 5.4.4.1: Overlaid 2D ¹H-¹⁵N HSQC spectra of 600 μM VanS_A N-terminal domain in 50 mM LMPG, 50 mM phosphate buffer pH 6.0, during titration of detergent-solubilised teicoplanin. [Teicoplanin]:[protein] ratios of 0:1 (red), 1:1 (green) and 4:1 (blue) were tested and all spectra were collected at 310K.

No peak shifts of significance are observed during titration of teicoplanin to VanS_A in LMPG detergent, in comparison to the many shifts observed during addition of vancomycin under similar conditions. The effect if any, of adding the teicoplanin cannot be determined, but a possible conclusion that could be drawn is that peak shifts of VanS_A proteins are observed in the presence of a dimeric glycopeptide antibiotic (vancomycin). Teicoplanin is unique among the vancomycin group of antibiotics in that it shows no appreciable propensity to dimerise (Gerhard, 1993a) and carries a glucosamine acylated by a C₁₀ or a C₁₁ fatty acid (Barna *et al.*, 1984). It is postulated that the fatty acid side chain acts as a membrane anchor, to enable the binding of the antibiotic to the pentadyl-D-Ala-D-Ala terminus of a growing cell wall to be effectively intramolecular (Beauregard *et al.*, 1995; MacKay *et al.*, 1994). Therefore in the membrane mimic chosen (detergent micelles), the teicoplanin may not be able to anchor into the membrane and interact with VanS. Additionally, no data to suggest a direct interaction of a VanS protein with teicoplanin antibiotic is present in the literature, so a lack of peak shifts may have been anticipated.

5.5 The Role of VanS Oligomerisation in Ligand Binding and Signalling

As stated in section 1.5.3, a number of common HK structural motifs have been identified (Gao & Stock, 2009) that are believed to possess a role in regulating phosphorylation of kinases by transmitting conformational changes in the periplasmic sensor domain to the cytoplasmic kinase domain. For instance, ~33% of HKs contain at least one PAS domain (Taylor & Zhulin, 1999), and ~31% of HKs contain a HAMP domain (Hulko *et al.*, 2006; Szurmant *et al.*, 2007), both of which are implicated in signalling in dimeric sensor kinases, by providing movements in the protein which are transduced to the kinase domain. It has been proposed that these movements cause conformational changes in the ATP binding domain which are necessary to position the histidine residue optimally for phosphotransfer. Therefore knowledge exists of conserved features required for signal transduction through the kinase, which should be critical to expression of resistance genes. However, little is

known about how the signal is transferred across the membrane from the extracytoplasmic loop region through the transmembrane helices, to the dimerization domain. Through a combination of *in vitro* and *in vivo* oligomerisation assays, VanS histidine kinases were therefore analysed for their oligomerisation state, and the strength of oligomerisation of their transmembrane helices, to improve understanding of the role of oligomerisation in ligand binding and in signal transduction.

5.5.1 Analysis of VanS Oligomerisation by Blue Native PAGE

The oligomerisation state of VanS proteins can be investigated by a number of techniques such as Analytical Ultracentrifugation (AUC) (Macfarlane, 2007), Native PAGE, Native Mass Spectrometry (Laganowsky *et al.*, 2013) and Gel Filtration Chromatography. As seen in section 3.7, VanS proteins purified in membrane mimetics appear to elute as dimers by gel filtration chromatography (at ~ 90 kDa size relative to gel filtration standards), but further methods are required to support this data, one of which is Blue Native PAGE (BN-PAGE). This technique provides identification of native membrane protein complexes and determination of purity on PAGE gels, without denaturing the protein (Schagger & von Jagow, 1991). Coomassie G-250 is present as the charge-shift molecule in the NativePAGE Gel system, which binds to proteins and confers a net negative charge while maintaining the proteins in their native state (Schagger *et al.*, 1994). BN-PAGE was therefore conducted to characterise the oligomeric state of VanS proteins in different detergents, and determine their molecular size relative to Native PAGE standards (see section 2.6.2). Samples of VanS proteins purified by IMAC techniques were loaded onto NativePAGE gels (Invitrogen) and protein bands were visualised by Coomassie staining or Western blotting (see Figure 5.5.1.1).

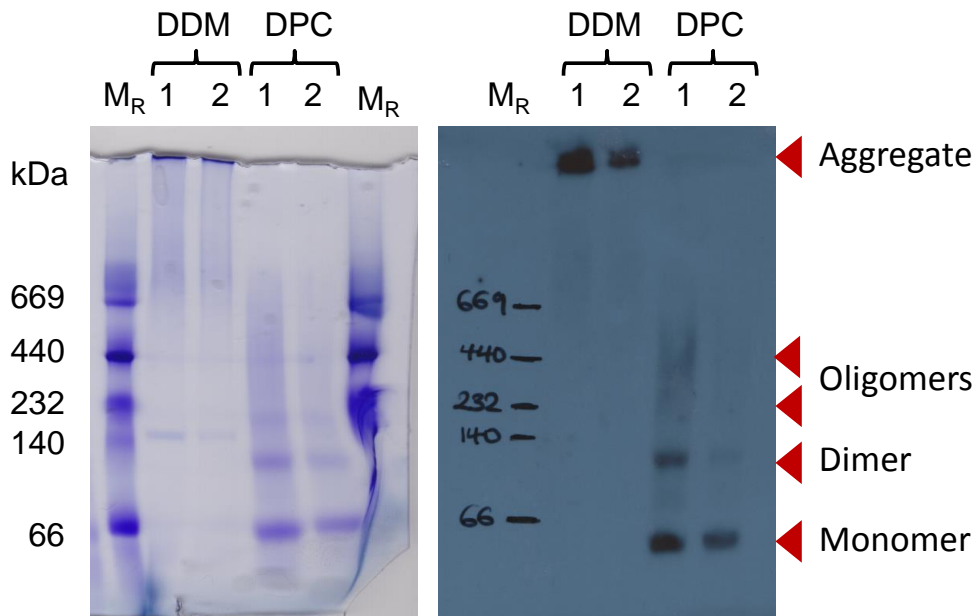


Figure 5.5.1.1: (left) BN-PAGE 4-16% gradient gel loaded with purified His-tagged full-length VanS_A samples in DPC at 0.1% w/v (~2x CMC), or in DDM at 0.05% w/v (~3x CMC) (right) corresponding Western blot. In each lane 5 μ g (1) or 15 μ g (2) VanS protein was loaded, and an estimate of protein molecular weight was provided by a NativePAGE protein marker (M_R , Amersham), solubilised in DDM and loaded at 0.05% w/v. Bands at molecular sizes which would correlate with a monomer, dimer or higher oligomer are indicated by arrows.

VanS proteins are proposed to be homo-dimeric in their active state and the BN-PAGE gel and blot (Figure 5.5.1.1) shows that VanS_A exists in DPC in different oligomeric forms, with protein sizes indicating dimeric and monomeric, and possibly higher oligomeric states. The higher oligomers are unlikely to form in native bacterial membranes, but instead indicate that the DPC detergent micelles are able to stabilise trimer or higher oligomeric structures. Ideally, however, only one band for VanS (dimer) should be observed, since this is the form that has kinase activity. Interestingly VanS_A protein in DDM detergent (at roughly the same [protein]:[detergent] ratio), appears to be aggregated since very little enters the resolving gel, which indicates that either the protein is unstable in the detergent environment, or that it also forms high order oligomers. This result helps to explain why a large proportion of the protein

pelleted as insoluble material, when testing in DDM detergent during the initial solubility screens (see section 3.6), and could be a reason for the poor crystal growth observed in previous studies in DDM.

VanS_{SC} proteins in DPC detergent display similar oligomeric complexes to that of VanS_A (see Figure 5.5.1.2), and indicate that DPC detergent is capable of stabilising VanS proteins in a functional dimeric form (although some monomer is also present). There also appears to be a higher ratio of dimer to monomer for VanS_{SC} proteins compared to VanS_A proteins in Figure 5.5.1.2, which could indicate a higher strength of oligomerisation between VanS_{SC} monomers or increased oligomer stability.

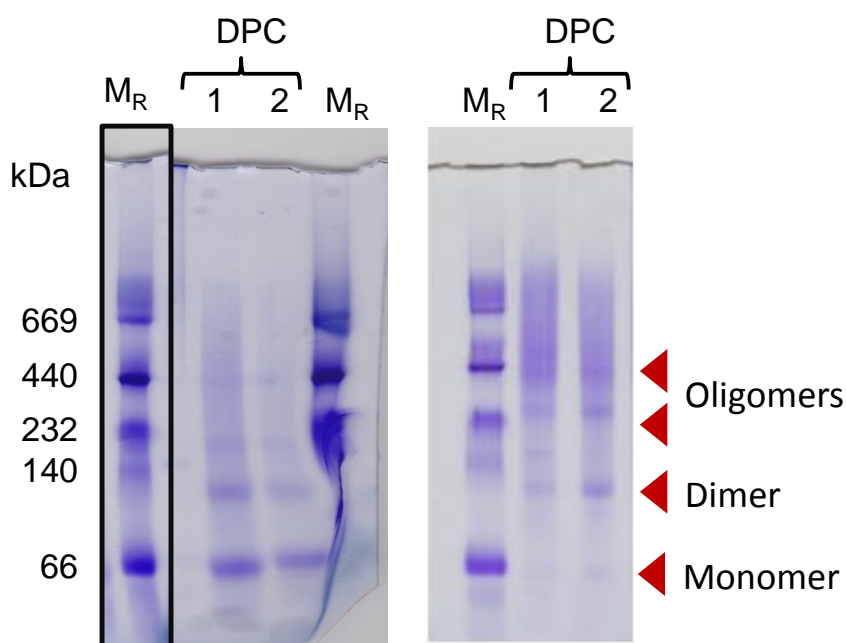


Figure 5.5.1.2: BN-PAGE 4-16% gradient gel loaded with purified His-tagged full-length VanS_A (left) or VanS_{SC} (right) samples in DPC detergent at 0.1% w/v (~2x CMC). In each lane 5 μg (1) or 15 μg (2) of VanS protein was loaded, and an estimate of protein molecular weight was provided by a NativePAGE protein marker (M_R, Amersham). Bands at molecular sizes corresponding to monomer, dimer or higher oligomer are indicated by arrows.

5.5.2 Analysis of VanS Homo-Oligomerisation using ToxCAT Assays

Native PAGE and gel filtration data presented indicate that dimeric VanS proteins are one species being formed *in vitro*, and these have been shown to be active with respect to ADP release and phosphate release through the use of coupled enzymatic assays (see section 3.11). As a further test of homo-dimerisation *in vivo*, another assay was performed, known as the ToxCAT assay (Russ & Engelman, 1999). This assay determines whether homo-oligomerisation is occurring between transmembrane (TM) domains within the VanS protein and quantifies the strength of association relative to a strongly dimerising control protein, glycophorin A (GpA) (Russ & Engelman, 1999). NMR data has shown that the association between GpA TM monomers is mediated by a seven residue motif presented on one face of each TM helix (Russ & Engelman, 1999) which is tightly packed at the interface, making it an ideal positive control protein of a strongly dimerising system. A point mutation in GpA at residue Gly-83 to an isoleucine (G83I) has also been found to disrupt the dimer interface, and therefore provides a good negative control in assays. It was hoped that the ToxCAT assay would provide an insight into the mechanism of signal transduction across the bacterial membrane via the membrane-spanning helices.

In the first instance bioinformatic software was used to predict the position of transmembrane residues, and the most appropriate prediction was found using TMPred software (Hofmann & Stoffel, 1993), which predicted an anticipated N-in, C-in topology and predicted sequences also followed the “positive inside rule” i.e. TM domains had high overall hydrophobicity, and were often flanked by hydrophilic residues (von Heijne G., 1992). This directed the synthesis of corresponding primers (given in Table 2.4.1), which were then cloned into a pccKan DNA vector (section 2.7.1), between two restriction sites (NheI and BamHI) to create a chimeric fusion protein (refer to Figure 2.7.1.1).

Full details of primer phosphorylation, annealing and ligation into digested pccKan plasmids are given in sections 2.7.1. The predicted TM sequences are given below, and the residue numbers are 19-37 and 78-97 for VanS_A proteins, and 19-37 and 68-86 for VanS_{SC} proteins:

VanS_{SC} TM1: GFLTLAGVLLLVAVGVFLL
VanS_{SC} TM2: WVMAFLLVFGLVGGWFLAG

VanS_A TM1: LYMYIVAIVVVAIVFVLYI
VanS_A TM2: IFIYVAIVISILILCRVMLS

The pccKan construct is composed of the N-terminal DNA binding domain of ToxR (a dimerization-dependent transcriptional activator), termed ToxR', which is fused to a transmembrane domain (TM) of interest (i.e. TM 1 and 2 of VanS) and a monomeric periplasmic anchor (the maltose binding protein, MBP) as shown in Figure 5.5.2.1. MBP directs the fusion protein across the inner membrane of *E. coli* and association of TM helices results in ToxR'-mediated activation of a reporter gene encoding chloramphenicol acetyltransferase (CAT) (Figure 5.5.2.1). Activation of the reporter gene results in acquired resistance to the antibiotic chloramphenicol (CAM). Two ways of measuring the extent of TM-induced dimerization in the literature are: a disk diffusion assay (see section 2.7.5), which measures the zone of inhibition resulting from acquired resistance to the antibiotic CAM for each chimera, and a quantitative CAT assay (see section 2.7.6), which measures acetylation of CAM by the CAT enzyme by fluorescence spectroscopy. These assays and other control experiments are detailed below.

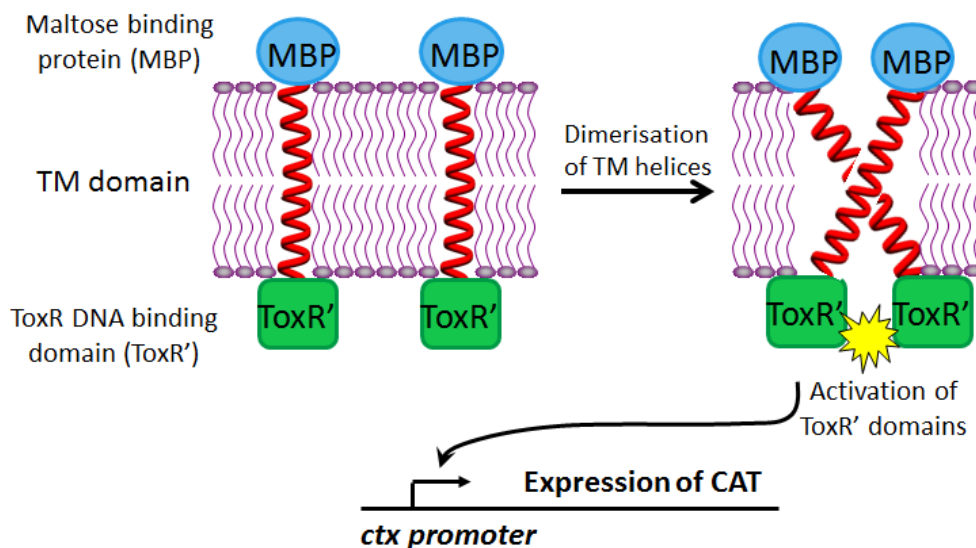


Figure 5.5.2.1: A schematic diagram of the basis for the ToxCAT assay. A chimeric fusion protein is expressed from the *pccKan* plasmid, containing a cytoplasmic ToxR DNA binding domain. Upon dimerisation, the transmembrane domains bring ToxR' domains into close contact, activating them towards binding to the *ctx* promoter to effect expression of CAT enzyme, the level of which can be monitored in the quantitative ToxCAT assay.

To establish whether chimeric fusion proteins were inserting into *E. coli* membranes with the correct topology, a *malE* complementation assay was first conducted (see section 2.7.2). The *pccKan* plasmid containing the VanS TM was transformed into NT326 cells, which lack endogenous MBP. NT326 cells cannot transport maltose into the cytoplasm for metabolism, and therefore cannot grow on maltose/agar plates. However, if the ToxCAT chimerae are correctly inserted into the inner membrane, the periplasmic MBP domain will complement the NT326 *malE*-deficient phenotype and support growth on maltose. All constructs were correctly oriented in the membrane, and grew on maltose plates (Figure 5.5.2.2), unlike NT326 negative controls.

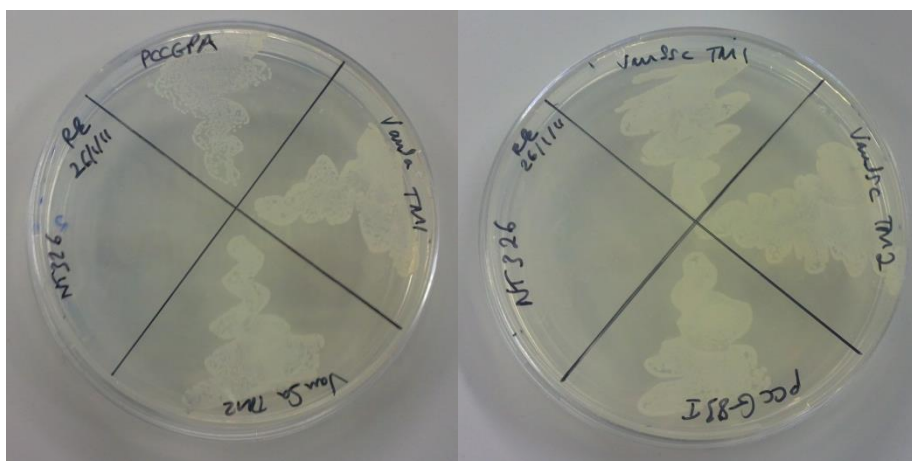


Figure 5.5.2.2: The *malE* complementation assay. NT326 cells transformed with *pccKan* plasmids (expressing chimeric *VanS* fusion proteins) were streaked onto minimal media plates containing only maltose as a carbon source, to provide a check for insertion of the TM domain (TM1/TM2) across the membrane. Untransformed NT326 cells were streaked as a negative control, and a control protein (*GpA*) and its mutant (*G83I*) were also streaked.

The expression level of the chimeric fusion proteins in NT326 cells was also checked (see section 2.7.3). The chimera *ToxR'*-TM-MBP is constitutively expressed at low levels by the *toxR* promoter and differences in the expression levels will affect the relative amount of dimerization, therefore by determining the expression level of the chimerae, ToxCAT data can be normalized relative to expression. To check expression levels, an aliquot of NT326 cells expressing the chimera was taken (diluted to an OD_{600} of 0.3), and pelleted by centrifugation, before resuspending in SDS sample buffer and loading onto a NuPAGE 12% Bis-Tris gel (see section 2.7.3). The gel bands were subsequently transferred to a nitrocellulose membrane, blotted with anti-MBP antibodies and developed (refer to section 2.6.4). The anti-MBP Western blot showing the successful expression and relative levels for each construct is given in Figure 5.5.2.3A.

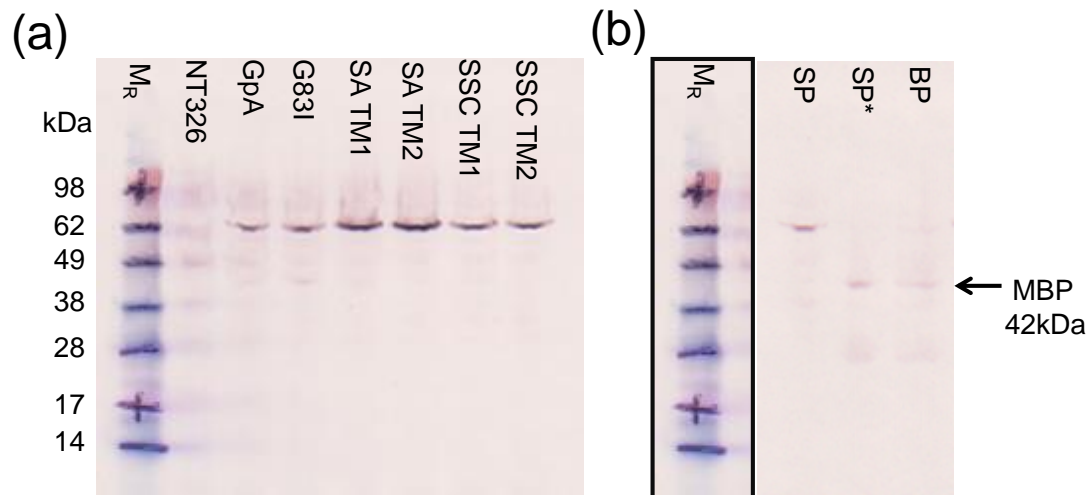


Figure 5.5.2.3: Anti-MBP Western blots showing (a) the expression of chimeric fusion proteins in NT326 cells (normalised by OD_{600}) or (b) a spheroplast assay for one fusion protein. For expression tests a negative control of untransformed NT326 cells was loaded. In the spheroplast assay, fractions collected before (SP) and after proteolysis (SP*), or after cycles of freeze-thawing (BP) are shown. The molecular weight band corresponding to MBP is highlighted by an arrow at ~ 42 kDa.

Next, protease sensitivity assays were conducted, in order to measure the membrane insertion and orientation of the MBP chimerae and verify that interactions within the membrane were responsible for the observed CAT activity (see section 2.7.4). The protease sensitivity of a chimera is assayed in cells that have been stripped of their outer membrane and cell wall (spheroplasts). As anticipated, MBP was detected in the spheroplast fraction ('sp') since it is associated with the inner membrane via TM and ToxR domains, and the addition of proteinase K (protease) excised the MBP domain from the TM domains as it was present on the periplasmic side of the membrane, which can be observed on SDS-PAGE gels of proteolysed spheroplast fractions ('sp*'), as a lower molecular weight fragment (~ 42 kDa) (see Figure 5.5.2.3B).

As a final test of TM-mediated dimerization of different chimerae, prior to quantitative CAT assays, disk diffusion assays were carried out. An aliquot of NT326 cells expressing the chimerae (normalised by optical cell density) was plated on LB/ampicillin plates and allowed to dry, before placing a chloramphenicol soaked disk into the centre of the plate. The diameter of the clear zone of inhibition of growth around the disk was then recorded, and the size of this zone is directly dependent on the strength of TM-dimerisation in the chimera; increased dimerization confers greater CAM resistance, thereby decreasing the diameter of the zone of inhibition. Unsurprisingly GpA had the smallest diameter zone of inhibition, and G83I, the largest, with the VanS TM-containing chimerae displaying inhibition zones in between these values. Three of the plates and their inhibition zones are shown in Figure 5.5.2.4.



Figure 5.5.2.4: The disk diffusion assay. Clear zones of inhibition occur around a chloramphenicol soaked disk on LB/Ampicillin plates transformed with NT326 cells containing chimeric fusion proteins; GpA (left), G83I (center) or VanS_{SC} TM1 (right). The diameter of the inhibition zone is indicated by arrows, and is directly related to the strength of dimerization of the TM domains present in the chimera.

To quantify the strength of TM-dimerisation, CAT activity was measured in cell-free extracts by the quantitative ToxCAT assay. The assay is based on the Invitrogen FAST CAT (deoxy, green) system, using xylene phase extraction to isolate product, as described by Seed & Sheen, (1988), and experimental details as given in section 2.7.6.

In this assay, the rate of transfer of a butyryl group from butyryl-CoA to fluorescent chloramphenicol (CAM) is detected by the rate of color change (at ~520 nm) associated with the reaction of the resulting free coenzyme A with BODIPY-FL-deoxyCAM (Molecular Probes). Each sample containing an expressed chimera was lysed, and incubated with 10 μ l of fluorescent CAM, then 10 μ l of a 5 mg/ml butyryl CoA solution. Samples were centrifuged briefly before terminating reactions by adding 300 μ l xylene and centrifuging to collect the upper phase. This phase was subsequently assayed for fluorescence by excitation at 495 nm, and emission spectra were collected between 500 and 600 nm (see Figure 5.5.2.5).

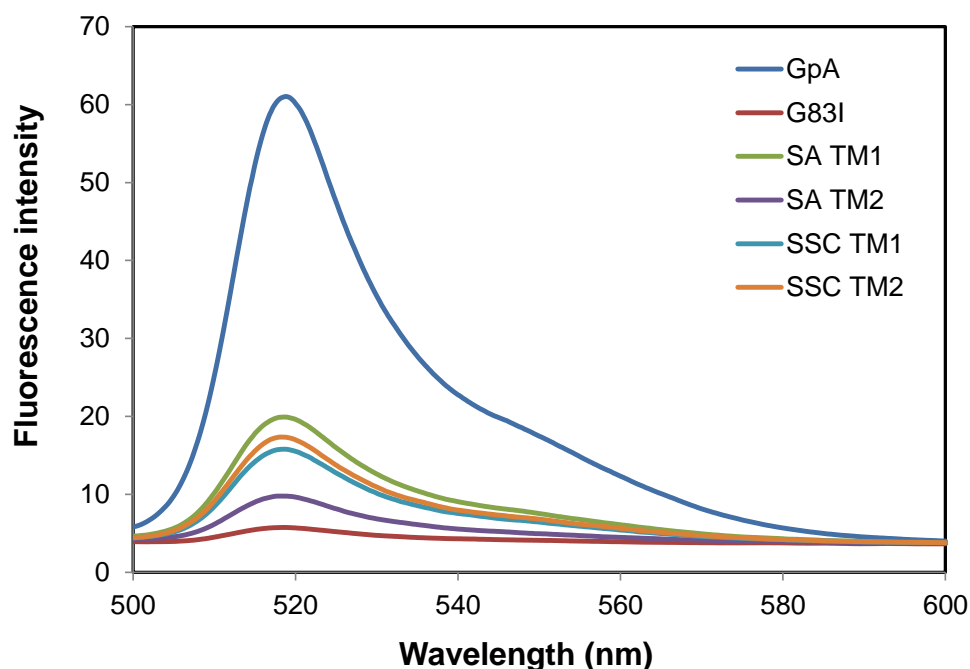


Figure 5.5.2.5: Fluorescence emission spectra collected upon excitation of samples containing chimeric fusion proteins at 495 nm. Each fusion protein is labelled and coloured as follows: blue - GpA, red - G83I, green - VanS_A TM1, purple - VanS_A TM2, cyan - VanS_{SC} TM1 and orange - VanS_{SC} TM2.

As shown in Figure 5.5.2.5, the fluorescence maxima at ~ 520 nm for the TM domains of most VanS proteins display significantly higher intensity than the negative, mutant control G83I. However the fluorescence intensity is still only one third to one quarter of the intensity of the strongly dimerising positive control, GpA. This suggests that whilst there may be

association of TM domain in VanS proteins, the level of dimerization appears to be fairly weak. In order to quantify the relative strengths of dimerization of all chimera, the fluorescence values at 520 nm were recorded and normalised for any concentration differences, against expression levels (by band sizing using the blot in Figure 5.5.2.3A). The positive control (GpA) was plotted and data normalised to this value, and the negative control (G83I) was also plotted, which should show ~ 10% of the strength of dimerization of GpA as a result of the isoleucine mutation (see Figure 5.5.2.6).

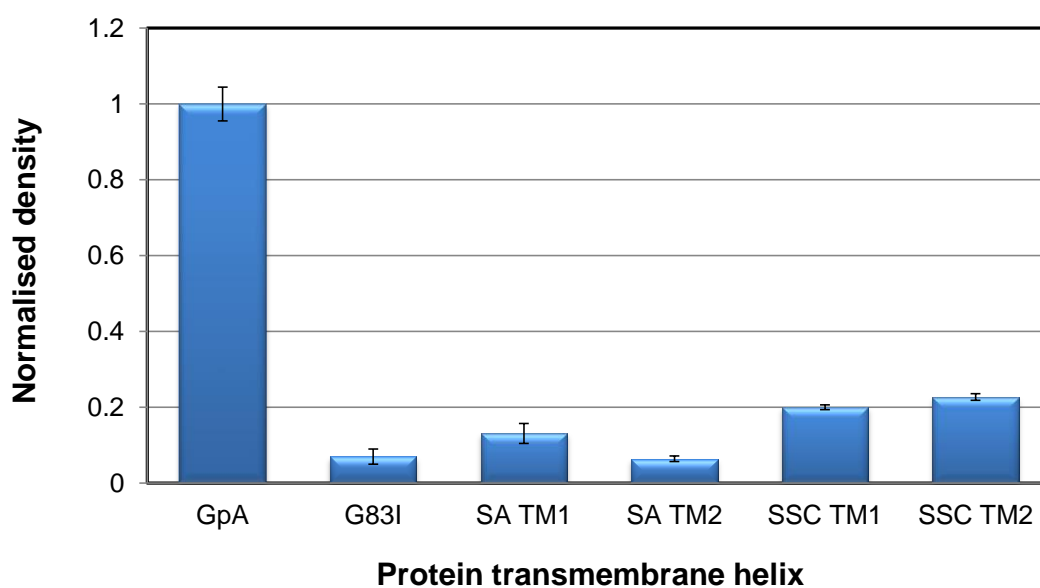


Figure 5.5.2.6: Normalised ToxCAT activity for each chimeric fusion protein. The bar graph shows the CAT activity of each chimera measured by fluorescence at 520 nm and normalised to expression levels, plotted relative to a positive (GpA, 1.0) and a negative control (G83I, ~ 0.1). Error bars are displayed for each chimera, calculated from the standard deviation in the value of fluorescence at 520 nm over three sample repeats.

As a result of the high expression level of VanS_A fusion proteins, when the fluorescence values were normalised to density values in Figure 5.5.2.6, the overall strength of dimerization was diminished, whereas, VanS_{SC} fusion proteins remained relatively unaffected. A comparison to the G83I negative control (density of 0.07), shows that VanS_{SC} TM1 (0.20) and TM2 (0.23) have some propensity to dimerise, but VanS_A TM1 (0.13) and VanS_A TM2 (0.06) are within the error values of the negative control.

The overall strength of oligomerisation for the VanS fusion proteins is relatively low, which implies that TM-TM homo-interactions are weak and may not be a key feature of the signal transduction pathway. However, these TM domains were only predicted, and it is known that optimisation of the lengths of the TM regions within the constructs is often required in order to observe TM-TM association (Brosig & Langosch, 1998). For instance, a previous PhD student at Warwick University (Jenei *et al.*, 2009) working on Carnitine palmitoyltransferase 1A (CPT1A), a mitochondrial membrane protein, found that the optimum CPT1A TM1 length was 24 amino acids, and that reducing to 21 amino acids, resulted in halving the CAT activity. By comparison, the length of CPT1A TM2 used that resulted in CAT activity was 16 amino acids. Interestingly, Jenei *et al.*, (2009) also found that TM1 yielded CAT activities that were equivalent to that of the G83I negative control, whereas the TM2 showed a higher propensity to form homo-oligomers, yielding CAT activities of at around 40% of the level of the positive control, GpA, which is similar to the CAT activity presented here in Figure 5.5.2.6. The CPT1 protein has two membrane-spanning helices and an identical N-in, C-in topology to that of VanS, and based on this data, CAT activity observed for VanS_{SC} TM1 and TM2 in Figure 5.5.2.6 could indicate TM-TM association. Hetero-oligomeric interactions may also occur e.g. TM1-TM2, in the active dimeric form of VanS, which would need to be assessed using another *in vivo* assay; the GALLEX assay (Schneider & Engelman, 2003).

Close examination of the protein TM sequences, finds that there are also several small-xxx-small motifs present (where 'x' is any residue) (Kleiger *et al.*, 2002) which are implicated in helix-helix interactions as they can provide close-packing of TM domains, promoting homo-dimerisation (see Figure 5.5.2.7). The most common of these small-xxx-small motifs is GxxxG (Russ & Engelman, 2000), but other motifs are known such as AxxxA and VxxxV, which can also provide close-packing arrangements of dimer interfaces (Schneider & Engelman, 2004).

It can be seen that there is a G₇₇-xxx-G₈₁ motif in VanS_{SC} TM2, and other motifs, which may increase TM association in VanS_{SC}. In the TM2 helix of some chemotaxis receptors from *R. sphaeroides* bacteria there are also several small-xxx-small motifs (Senes *et al.*, 2006), which increase association strength, suggesting that TM-TM packing interactions are important for function in these and other systems (Hall *et al.*, 2011).

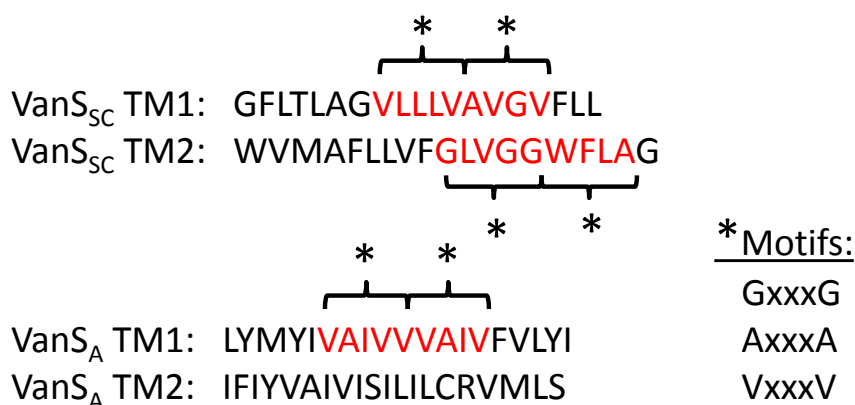


Figure 5.5.2.7: A comparison of the predicted TM sequences for VanS_A and VanS_{SC} proteins, highlighting helix-helix packing motifs. Each small-xxx-small motif is starred and residues are highlighted in red.

As a final note, the strengths of dimerization of VanS TM domains *in vivo* (from normalised density data), correlate well with the Blue-Native PAGE data *in vitro* (in DPC detergent). The BN-PAGE data shows that a higher percentage of VanS_{SC} dimer appears to be stabilised in DPC micelles than VanS_A dimer. This would fit with the higher propensity of VanS_{SC} helices to dimerise, as presented in the ToxCAT data. Although both the BN-PAGE and ToxCAT data need much greater analysis and additional repeats, there may be a correlation between the propensity of VanS proteins to dimerise and their observed antibiotic sensitivity. For instance, increased strength of dimerisation of the VanS protein may result in increased binding of glycopeptide antibiotics, which in turn could affect modulation of signals transduced to the kinase domain.

5.6 Discussion

Both fluorescence techniques involving BODIPY-vancomycin analogues, and NMR-based titration data involving vancomycin antibiotics, indicate that VanS_{SC} and VanS_A proteins appear able to directly interact with vancomycin. This data supports a model for direct interaction between vancomycin antibiotics and VanS proteins derived from *Enterococcus* and *Streptomyces*, and challenges the consensus view that the *Enterococcal* VanS protein should be indirectly activated by vancomycin. Furthermore, a number of significant Chemical Shift Perturbations are observed in the ¹H-¹⁵N HSQC spectra of ¹⁵N-labelled VanS sensor domains, upon addition of vancomycin, which appear to cluster to a particular region of the spectrum, for a range of detergents, and could map to a binding site. The assignment of these peaks requires further optimisation of protein concentration to allow collection of 3D spectra such as TOCSY-HSQC or NOESY-HSQC with improved signal-to-noise.

The role of oligomerisation in VanS activity and signalling mechanisms was also assessed using Native PAGE assays, which showed that purified full-length VanS proteins existed in to some degree in a dimeric state in DPC detergent. In contrast, *in vivo* ToxCAT assays, found that for fusion proteins studied (containing predicted VanS TM helices) only weak homo-oligomeric TM-TM association was observed, and it was concluded that TM-TM association is unlikely to be a major mechanism in the two-component signalling mechanism, although the possibility of hetero-oligomerisation cannot be ruled out.

5.6.1 New evidence for a direct interaction between vancomycin and VanS

BODIPY-vancomycin dyes were chosen as ligands in fluorescence studies based on their previous use within the Warwick group, and showed minimal changes in fluorophore environment in the presence of DPC detergent micelles. Upon addition of VanS proteins to BODIPY-vancomycin solutions, red shifts of 4-5 nm were observed for both proteins (from ~ 510 nm to ~515 nm), similar to that observed on addition of a Lipid II control. This gave an indication that the full-length proteins may be interacting with the vancomycin molecule, and further details of residues involved could be obtained by NMR techniques.

Isotopic ^{15}N -labelling of VanS sensor domains enabled the first known NMR spectra of a VanS sensor domain to be acquired (as detailed in section 4.6). By adding unlabelled vancomycin antibiotics to the labelled VanS proteins, it was possible to determine chemical shift changes during interaction with the antibiotic using a Chemical Shift Perturbation (CSP) analysis. All resolvable peaks in the ^1H - ^{15}N HSQC spectra of ^{15}N -labelled VanS proteins, at each titration point, were picked and tabulated, and enabled a bar graph to be produced of chemical shift perturbation (CSP) vs. peak number (see Figure 5.4.1.5). These CSP analyses were conducted for VanS proteins in different detergent environments upon antibiotic addition, and identified a number of statistically significant peak shifts that represent genuine interactions involving conformational changes in the protein (Figures 5.4.1.6 to 5.4.1.8). Some of these peaks appear to cluster to a particular region of the spectrum, across the range of detergents, which could map to a binding site. However the identity of the residues has not yet been assigned and will require 3D HSQC-TOCSY or HSQC-NOESY NMR techniques, which are currently underway within the Warwick group. There is still a possibility that the changes observed in both the fluorescence and NMR spectra could result from indirect effects, such as the alteration of the micelle structure and dynamics upon binding to vancomycin, which would indirectly affect the chemical shifts of the protein and the fluorescence wavelength rather than being a direct binding effect.

Therefore supporting data is required using other biophysical techniques such as SPR or ITC-based ligand-binding assays (as outlined in section 6.6) to confirm this direct binding between VanS and vancomycin.

In terms of the kinetics, individual peak shifts for the NMR spectra of VanS proteins in the presence of vancomycin (see Figure 5.4.1.9), show a positive correlation between peak chemical shift and vancomycin concentration, which would suggest that vancomycin acts as a direct ligand for VanS. The magnitude of these peak shifts is relatively small (~ 0.05 ppm) indicating a slow or intermediate exchange to the bound state, but this may be expected since the VanS protein is solubilised within a micelle, which could occlude approach of the antibiotic. Indeed, this would correlate with the activity data obtained in Chapter 3, which showed that the presence of detergent micelles hampered the rate of autophosphorylation (as a function of ADP release), increasing the assay time to over two hours in some cases. It would have been useful to have obtained a dissociation constant (K_D) for this binding; by plotting a titration curve of chemical shift change ($\Delta\delta$) vs. ligand concentration, but unfortunately only two points (two ligand concentrations) were tested for each sample. In future a greater number of ligand concentrations should be sampled, in order to qualitatively determine the dissociation constant for the proposed binding of vancomycin to VanS.

An interesting result from NMR binding studies was the identification of a chemical shift perturbation for a tryptophan residue in the VanS_{SC} protein, characterised by a peak for its indole ring NH proton at ~ 10 ppm. This residue must be solvent-exposed, and there is only one exposed Trp residue in the expressed VanS sensor protein (Trp-41), so in the absence of residue assignment data, this peak is proposed to be Trp-41. This residue is one of the four residues (DQWG) predicted to bind directly to vancomycin in studies by Koteva *et al.*, (2010), therefore this data indicates that Trp-41 is involved in binding and supports the view that VanS_{SC} directly interacts with vancomycin at its extracytoplasmic sensor loop *in vivo*.

A number of questions have been raised as a result of these studies, most importantly, the question of whether *Enterococcal* VanS_A proteins do bind directly to vancomycin antibiotics, since biophysical ligand-binding techniques conducted in this thesis appear to show a real interaction, resulting in conformational changes of several residues. This data contradicts the consensus view from previous biochemical assays that VanS_A should be induced indirectly whereas VanS_{SC} should bind directly; since VanS_A can be activated by glycopeptide antibiotics and other structurally unrelated antibiotics. Further research is clearly required to characterise the interaction observed between VanS and vancomycin, including assignment of residues in the sensor domain that show conformational changes upon antibiotic addition.

As a final NMR experiment, HSQC spectra were collected for the full-length VanS proteins, since it was thought that addition of vancomycin to functional, full-length VanS would result in further observable changes in conformation, compared to those of the isolated sensor domain, as interactions could be more productive. However, overlaid NMR spectra of the full-length VanS_A protein against its isolated VanS_A sensor domain (see Figure 5.4.2.1A) showed that most of the peaks implicated in antibiotic binding to the VanS_A sensor domain were either not observed in the spectrum of full-length VanS_A or were not visible due to peak overlap. Of those peaks that did shift, the magnitude of the shift was low, indicating that any interaction of VanS with vancomycin is not altered by the presence of the kinase domain.

5.6.2 The role of transmembrane domains upon signal transduction

It was postulated that transmembrane helix-helix interactions may be involved in oligomerisation of the protein, and may provide a route to transduce signals downstream. For this reason, ToxCAT homo-oligomerisation assays were conducted to study TM-TM interactions as detailed in section 5.5.2. These assays showed that the TM domains of VanS_A proteins did not show any significant oligomerisation, but there was an appreciable association of VanS_{SC} TM domains, and this could be due to differences in the dimerisation

interfaces, since a number of GxxxG close-packing motifs are present in VanS_{SC} TMs.

Overall though the level of association was weak, which suggests that transmembrane association is unlikely to feature in the two-component signalling mechanism (unless hetero-oligomerisation is occurring, which would which require further analysis using GALLEX assays). However, conformational changes in the transmembrane region could still be occurring to transduce signals across the membrane.

Indeed in a number of studies involving the isolated sensor domains of histidine kinases, it has been observed ligand binding at the extracytoplasmic sensor loop causes dimerisation of the sensor complex, and results in structural changes that are transduced through the protein. This includes conformational changes in the form of piston-like movements or rotations of the TM helices (Cheung & Hendrickson, 2010; Zhang & Hendrickson, 2010). For example, NarX is activated by nitrate binding to its isolated sensor loop, which induces a displacement of its N-terminal helices toward the cell membrane, relative to the C-terminal helix (see Figure 5.6.2.1) (Cheung & Hendrickson, 2009). Since these N- and C-terminal helices are expected to connect to TM1 and TM2 respectively, the relative movement of the two helices would push down TM1 or lift up TM2 (see for Figure 5.6.2.1). These piston-like motions are also observed upon ligand binding in Tar HK sensor domain (Falke and Hazelbauer, 2001), but the displacements are in an opposite direction.

Furthermore, the direction of helix movement correlates with HK function: nitrate binding in NarX promotes a phosphorylated state (Williams & Stewart, 1997), and aspartate binding in Tar promotes a dephosphorylated state (Jin & Inouye, 1994). These displacements are shown clearly in the NMR structures of ligand-free and ligand-bound forms of the CitA sensor domain (Sevvana *et al.*, 2008) (see Figure 5.6.2.1). It is found that residues in the β -sheet region curled up to one side towards the citrate ligand binding site which corresponded to an upward movement of the TM2 helices (Sevvana *et al.*, 2008), in the similar manner and direction to that observed for the Tar chemotaxis protein (Falke and Hazelbauer, 2001).

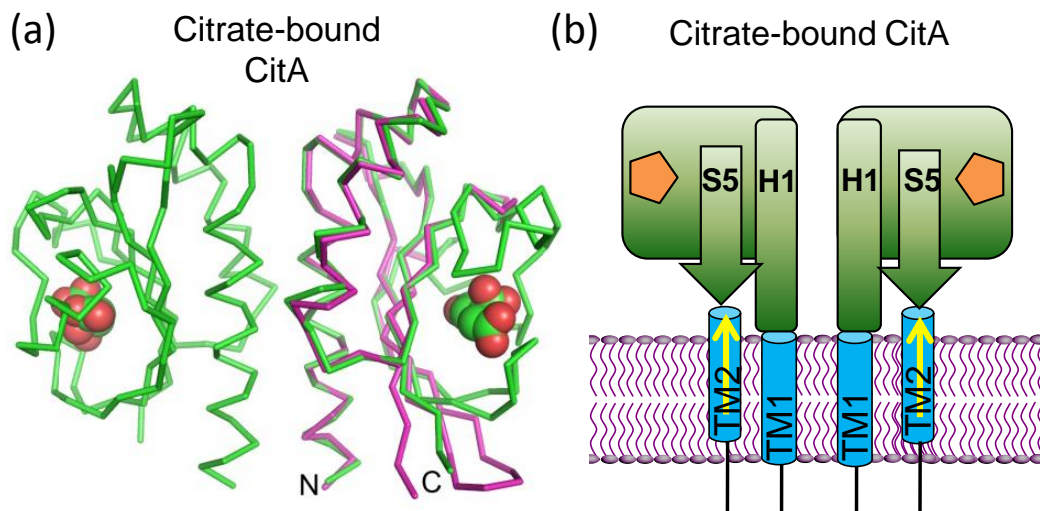


Figure 5.6.2.1: (a) Overlaid backbone structures of CitA ligand-free monomers (magenta) and ligand-bound dimers (green), reproduced from Wang (2012) and (b) the hypothetical model of TM signalling in CitA. In the model in (b), citrate binding causes the PDC domain to contract (as shown in (a) by the β -sheet moving up towards ligand), which triggers a piston-like movement of the TM2 helices, and transduction of the signal to the cytoplasmic side. CitA PDB codes for monomer and ligand-bound dimer are 2J80 and 2V9A.

Therefore displacements or rotations of TM domains is important for signal transduction in histidine kinases and is likely to feature for the VanS kinase, and to a higher degree than signalling from transmembrane helix-helix association during protein dimerisation. It is also interesting to note that in the structures of isolated sensor domains of HKs in the literature e.g. NarX and CitA, the ligand free forms are monomeric, whereas ligand-binding induces dimerisation, as seen in Figure 5.6.2.1. It is therefore possible that similar ligand-induced binding may occur for the isolated VanS sensor domains, and peak shifts observed in the HSQC NMR spectra may reflect conformational changes in the sensor domain upon dimerisation. However, the oligomerisation state of the detergent-extracted and purified sensor domains of each VanS protein was not deeply investigated during these studies, so identification of oligomeric state of both free sensor domain and vancomycin-bound sensor by AUC or Native MS techniques would be required to test this theory.

Overall, the use of Native PAGE and *in vivo* ToxCAT assays have provided an insight into the protein oligomeric state (in NMR-relevant detergents) and the strength of homo-dimerisation of VanS transmembrane helices, which has improved knowledge of the role of oligomerisation in VanS activity and in the signal transduction mechanism.

5.6.3 The role of vancomycin dimerization in ligand binding

It has been shown in a number of NMR studies (Gerhard *et al.*, 1993b; Pearce *et al.*, 1995, Beauregard *et al.*, 1995) that vancomycin and its analogues (e.g. ristocetin, eremomycin) are predominantly dimeric in solution and that there is a correlation between the degree of dimerization of the glycopeptide and its affinity for peptide ligands. Beauregard *et al.*, (1995), calculated from NMR experiments, that dimeric vancomycin increases its affinity for D-Ala-D-Ala cell wall precursors by a factor of 1 to 10 and for cell wall fragments by factors of 2 to 100. This data suggests that dimerization may have a physiological influence in the action of antibiotics of the vancomycin group, and could also affect the extent of their interaction with the VanS sensor kinase.

Vancomycin and other glycopeptide antibiotics are known to form noncovalent dimers (Loll *et al.*, 1998; Lehmann *et al.*, 2002), sometimes referred to as “back-to-back” dimers, in which the dimerization surface is on the opposite side of the molecule from the ligand binding pocket (see Figure 5.6.3.1). X-ray studies of vancomycin shows that this back-to-back dimerisation produces two asymmetric binding sites with different binding affinities, due to the positioning of the sugar moieties in each monomer.

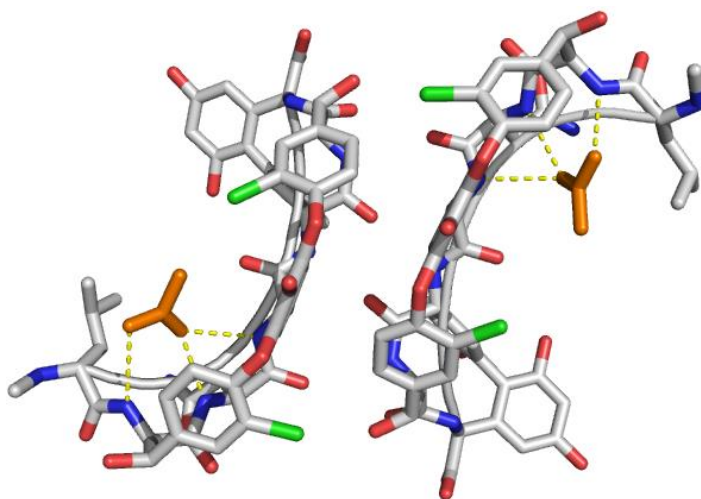


Figure 5.6.3.1: A back-to-back dimer of the vancomycin aglycone induced by an acetate ligand, represented by sticks and a cartoon ribbon. The acetate ligand is shown in orange for simplicity and the crystal structure contains only the aglycone. Four independent monomers of the vancomycin aglycone (PDB: 1GHG) comprise the crystallographic asymmetric unit, forming two asymmetric dimers, one of which is shown. Individual elements are coloured as follows: carbon – white, oxygen – red, nitrogen – blue and chlorine – green.

Most interestingly, in the crystal structure in Figure 5.6.3.1, both binding pockets of the vancomycin aglycone are occupied by bound acetate ions, which mimic binding of the C-terminus of nascent cell wall peptides. This could provide an explanation for the observed magnitudes of CSPs in the HSQC NMR spectra of VanS proteins in the presence of vancomycin in sodium acetate buffer (see Figure 5.4.1.6 and 5.4.1.8), which are larger than those in HEPES buffer (see Figure 5.4.1.7). The acetate ions can increase stabilisation of dimeric vancomycin, which in turn may increase interaction with the VanS sensor domain (provided that the functional state of vancomycin in NMR titrations was dimeric).

Thermodynamic data collected by McPhail & Cooper, (1997) (by calorimetric dilution experiments), calculated the dimerization constant (K_{dim} , Equation 5) for vancomycin ('V') in phosphate buffer at pH 7 and 298K as $475 \text{ dm}^3 \text{ mol}^{-1}$, whereas in acetate buffer a K_{dim} of $860 \text{ dm}^3 \text{ mol}^{-1}$ was calculated for the same conditions. This equates to a requirement of approximately 2.2 mM vancomycin in phosphate buffer in order to form 50% dimer in solution, but in acetate buffer, only 1 mM vancomycin is required.

$$K_{dim} = \frac{[V_2]}{[V]^2} \quad (5)$$

Therefore a higher proportion of dimer can be formed in acetate buffer for the same final concentration of vancomycin, and would have been present during NMR-based titration experiments conducted (e.g. in Figure 5.4.1.6). In fact, in all titration spectra collected, significant changes in the peak chemical shifts of VanS proteins appear to occur upon addition of 0.8-1 mM vancomycin (Figures 5.4.1.6 - 5.4.1.8), which would support a requirement for interaction of VanS with a dimeric form of vancomycin.

In addition to the dimerisation ability of vancomycin, there are reports of hexameric structures of vancomycin, which form when crystallised in the presence of certain cell-wall precursor analogues (e.g. N-acetyl-D-Ala-D-Ala (NAAA) and diacetyl-Lys-D-Ala-D-Ala (DALAA) (Loll *et al.*, 2009), Nitanai *et al.*, 2009). These consist of a trimer of dimers formed by three vancomycin-ligand complexes containing ‘back-to-back’, ‘face-to-face’ and ‘side-to-side’ interactions (see Figure 5.6.3.2) (Lehmann *et al.*, 2002; Nitanai *et al.*, 2009).

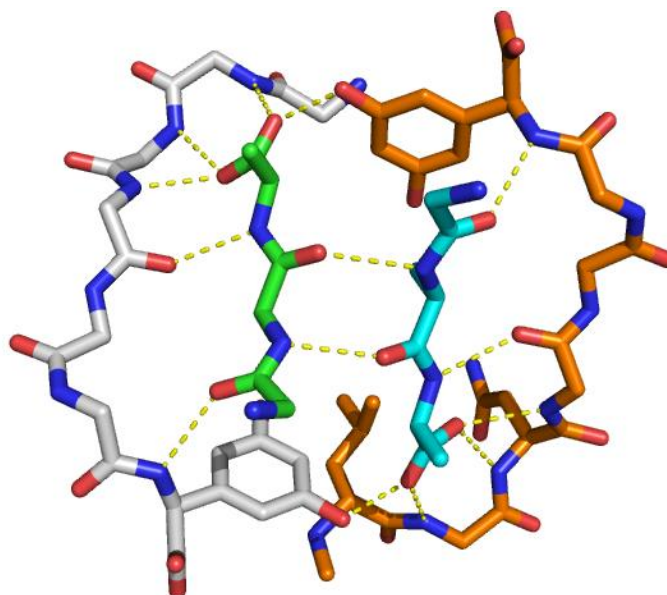


Figure 5.6.3.2: Stereo view of the “face-to-face” dimer present for vancomycins 4 and 6 in a six-vancomycin-asymmetric unit (PDB: 1FVM), with hydrogen bonding to DALAA ligands. Vancomycin is colored in white or orange, and the ligands in green or cyan. The diacetyl-Lys of the ligand chain was removed for clarity.

“Face-to-face” interactions are also observed in balhimycin complexes with cell wall mimetics (Lehmann *et al.*, 2002) and are likely to represent a general mode of oligomerisation for vancomycin complexes with cell wall peptides. Therefore the oligomerisation behaviour of vancomycin may be relevant to its antibacterial mechanism of action, especially as it is expected to recognise two types of muramyl peptide targets *in vivo*; those found on Lipid II and those found on nascent peptidoglycan chains (Loll *et al.*, 2009). The asymmetric nature of vancomycin complexes may also enable interactions with both cell wall precursor peptides and VanS proteins at different interfaces (e.g. face-to-face and back-to-back), as each face has a different degree of ‘openness’. Furthermore, Kwun *et al.*, (2013), stated that although VanS_{SC} proteins should be activated by interaction with a complex of vancomycin bound to its cell wall precursor, they said that they cannot exclude the possibility that VanS senses vancomycin via interactions with its D-Ala-D-Ala binding pocket, of which several could be available in these hexameric structures of vancomycin.

It therefore appears that greater analysis is required to elucidate the oligomerisation state of vancomycin that is present in solution during NMR and fluorescence studies (as presented in this thesis), and its interaction with VanS proteins. Since the addition of cell wall penta-peptide or tri-peptide analogues (which are soluble in aqueous media) are able to induce back-to-back, face-to-face and side-to-side dimeric vancomycin structures, this could provide a new route to study VanS-vancomycin interactions by NMR, without the difficulty of using detergent-solubilised Lipid II in titration experiments. Alternatively, VanS interactions with oligomeric vancomycin molecules, and Lipid II, could be assessed in a more native environment, by reconstituting the proteins into liposomes, which is discussed in more detail in the recommendations for future work (see section 6.6).

6 Summary and Conclusions

6.1 Background and Objectives

The work discussed in Chapters 3 – 5 covers three key areas: structural/mechanistic studies of VanS proteins, antibiotic binding to VanS, and the role of VanS oligomerisation in signal transduction. As a prerequisite to these studies, *vanS* genes from two species were cloned, recombinantly expressed and purified into appropriate membrane mimetics. Proteins were also characterised for their identity, homogeneity and fold, to ensure they would be suitable for structural and ligand binding studies. This section details progress to address the questions highlighted in section 1.7 of the Introduction, using the findings from this research project and outlines the conclusions from these studies.

6.2 Efforts towards Crystallisation or an NMR Structure of a VanS protein

To improve upon previous crystallographic studies of C-His-tagged VanS proteins within the Warwick group (Williams, 2007), crystal trials were conducted using tag-cleaved VanS proteins, which would reduce the possibility of crystallising other histidine-rich impurity proteins expressed in *E. coli* (e.g. AcrB). *vanS* genes were selected from two species (*E. faecium* and *S. coelicolor*) which exhibited different resistance phenotypes to glycopeptide antibiotics. These genes were cloned into pProEx vectors and overexpressed as TEV-cleavable, N-His-tagged VanS proteins. The proteins were able to be purified by IMAC and found to be in a well-folded, homogenous and active state. Attempts were then made to crystallise these VanS proteins, by removing the His-tag, and applying samples to 96-well crystal screens. Additionally, it had been found previously that crystallisation trials in DDM detergent only gave low resolution (8Å) crystals (Williams, 2007), which was proposed to result from the large steric size of its micelles (50-70 kDa).

To select for an appropriate detergent in place of DDM, a detergent screen was conducted, which found that highly soluble, and active VanS protein could be achieved in DPC detergent, which has a smaller micellar size (15-25 kDa) and thereby might improve growth by increasing protein-protein interactions in the crystal. However, despite these efforts, no crystals of the VanS_A protein could be obtained in these studies in DPC or DDM detergents. This is a setback in improving the 8Å resolution of the VanS_A diffraction pattern, but it is clear that crystallisation of VanS_A or another VanS protein requires wider screening and increased collaboration with specialist membrane protein research groups.

Efforts towards elucidation of the VanS structure by NMR spectroscopy required greater optimisation of construct design and expression protocols, since no protocols were available in the literature to overexpress and purify a VanS protein in labelled NMR media. It was decided to initially study the membrane-bound VanS sensor domain, by truncating the C-terminal kinase domain. This had the added advantage that the binding affinity of potential glycopeptide ligands to the extracellular sensor loop could be interrogated, to determine whether a direct binding mechanism was involved, or if binding was indirect as proposed from biochemical assays for inducers of VanS activity.

The isolated sensor domains of VanS_A and VanS_{SC} were obtained through unconventional 'Round-the-horn' PCR techniques to insert an enzymatic cleavage site, for removal of the C-terminal domain, and selective purification of the His-tagged, N-terminal sensor domain. These sensor domains were labelled in ¹⁵N M9 minimal media, using optimised expression protocols and allowed ¹H-¹⁵N HSQC NMR investigations on the sensor domain structure (and antibiotic binding). This has resulted in the first known ¹H-¹⁵N HSQC spectra of VanS proteins from enterococci and *Streptomyces*, and high resolution spectra were achieved by selecting appropriate detergents (e.g. lyso-lipids) and optimising buffer conditions. By using improved sensitivity 3D NMR experiments, it should be possible to assign residues in the sensor domain, and other domains, leading toward an NMR structure for the VanS protein.

6.3 Characterising the Mechanism of VanS autophosphorylation

Autophosphorylation activity of his-tagged VanS proteins was assessed by a combination of ADP release and phosphate release assays, which had been developed by Quigley (2010) and enabled the continuous measurement of VanS ATPase function. These methods provided an alternative route to the use of radiolabelling to track phosphorylation and have been shown in these studies to be applicable to full-length detergent-purified VanS proteins.

The ADP release assays allowed quantification of ATP turnover, showing that ADP is released from VanS after phosphorylation, as proposed by Marina *et al.*, (2005), and before VanR binding occurs. In conjunction with the ADP release assay, an inorganic phosphate release assay demonstrated release of phosphate during autophosphorylation, showing the high lability of the phospho-histidine bond. In comparison to the activity observed for MBP-VanS_AΔ95 by Wright *et al.*, (1993), and full-length VanS_A by Quigley (2010), it appears that phosphorylation reactions in these studies require longer timescales to complete. This may be due to the presence of excess detergent micelles which would hamper the ability of the VanS catalytic domain to phosphorylate its conserved His site.

In addition to increased reaction times, the nmoles of ADP produced in assays was greater than the nmoles of VanS present, and the percentage of phosphorylation (subtracting for phosphate release) over 1 hour was greater than 100%, indicating formation of a secondary product or multiple-site phosphorylation. Quigley (2010) also calculated a value for phosphorylation of VanS_A of >100%, and explained this by demonstrating that VanS_A also synthesises a secondary product, AP₄. Attempts to identify any secondary reaction products by analysing products of a simplified reaction between ATP and VanS over time (without regeneration of ATP) using anion-exchange chromatography were not conclusive and AP₄ formation could not be observed. Anion exchange assays did, however, clearly show the conversion of ATP to ADP, which supports that VanS proteins purified in these studies were

functionally active kinases. Multiple-site phosphorylation was not assessed in the time length of these studies, but approaches to identify phosphorylation sites were discussed and could include site-directed mutagenesis (at the conserved His site) or tandem mass spectrometry techniques (see section 3.13.4).

6.4 Assessing the Binding of Potential Antibiotic Ligands to VanS proteins

Although the general consensus has been that *E. faecium* VanS_A is unlikely to bind directly to glycopeptide antibiotics, as it appears to be induced by several structurally unrelated antibiotics in biochemical assays, no biophysical data has been collected to support this theory, and several assays do not concur on the identities of inducers. By using fluorescence spectroscopic techniques and solution state NMR experiments biophysical data has now been collected which supports a direct interaction between vancomycin and VanS_A (as well as VanS_{SC}). Fluorescence assays were conducted based on the observance of a direct interaction between *S. coelicolor* VanS_{SC} and a fluorescent vancomycin photoaffinity probe (VPP) (Koteva *et al.*, 2010), and it was surmised that this protein could be used as a positive control of vancomycin binding. Furthermore, based on the affinity of vancomycin for the D-Ala-D-Ala N-terminus of cell wall precursors, in-house synthesised Lipid II was added to samples of a fluorescently tagged vancomycin analogue (BODIPY), as a control experiment, to show that the altered vancomycin molecule could still bind its target substrate.

The addition of purified VanS proteins to BODIPY-vancomycin solutions (in the presence of detergent micelles), resulted in red shifts of 4-5 nm of the emission maxima (~ 510 nm to ~515 nm), for both VanS_{SC} and VanS_A, similar to that observed for the Lipid II control. These shifts indicated a change in the environment of the BODIPY fluorophore, resulting from interaction of BODIPY-vancomycin with VanS, presumably at the exposed sensor domain of the protein.

Purified sensor domains of ^{15}N -labelled VanS_A and VanS_{SC} protein samples were then analysed by ^1H - ^{15}N HSQC NMR titration experiments, to test for a direct interaction of vancomycin to the exposed VanS sensor loop. These experiments supported the fluorescence data, showing a number of statistically significant Chemical Shift Perturbations upon addition of vancomycin. Peak shifts appeared to cluster to a particular region of the spectrum for a range of detergents, which could also indicate a binding site. However, the assignment of these peaks could not be achieved during these studies and the kinetics for the binding of vancomycin to VanS (K_D) could not be determined from the NMR titration data collected (as only two ligand concentrations were tested).

It should be noted however that the magnitude of the CSP values was relatively low, compared to systems involving fast exchange to a bound state or binding at a well-defined site. Indeed CSP values in the range obtained have been found by e.g. Morrison *et al.*, (2003), to indicate ligand binding in multiple conformations. Based on the asymmetric conformations of vancomycin binding sites in crystal structures (see section 5.6.3), it is possible that these low CSP values reflect an interaction of vancomycin with VanS through multiple binding modes, although this would require much greater experimental study.

6.5 Assessing the role of TM domain association in Signal transduction

Conformational changes must occur within the transmembrane region to transduce signals to towards the kinase domain (Wang, 2012) and it was postulated that TM helix-helix interactions could provide this route for signal transduction. ToxCAT homo-oligomerisation assays developed in the Warwick group were conducted to study VanS TM-TM interactions as a function of CAT activity, and showed that although VanS_A TM domains did not oligomerise, VanS_{SC} TM domains demonstrated significant association, which is proposed to result from additional dimerisation motifs e.g. GxxxG close-packing motifs.

However, this does not appear to be a major feature in the mechanism of TCS signal transduction, and recent structures of isolated HK sensor domains have shown that ligand binding to the HK sensor loop effects structural changes in the TM region, triggering rotations or piston-like translations of the TM helices. These conformational changes alter the position of the TM helices in the membrane, and activate a kinase or phosphatase state, implying that rotations or displacements are likely to be the key modulators of TCS signal transduction across the membrane. However, one cannot exclude the possibility that signal transduction may also involve hetero-oligomerisation, which could be tested using a GALLEX *in vivo* reporter assay (as mentioned in section 5.1).

As a further observation, the strengths of dimerization of VanS TM domains *in vivo*, correlate well with Native PAGE data collected for full-length VanS proteins *in vitro*. Native PAGE data shows that a higher percentage of VanS_{SC} dimer appears to be stabilised in DPC micelles than the VanS_A dimer. This fits well with the higher propensity of VanS_{SC} helices to dimerise, as presented in the ToxCAT data.

This PhD study has provided increased knowledge of the structure and function of VanS proteins from two different species, and their ligand binding properties. NMR-based titration data has now provided, for the first time, evidence for a direct binding between VanS_A and vancomycin antibiotic, challenging consensus opinion in the literature. As a result of this PhD research, a number of avenues can be explored in future studies, and recommendations for a plan of future work is detailed in section 6.6.

6.6 Recommendations for Future Work

Future work should continue in all of the avenues detailed above (structural/functional elucidation, antibiotic binding and signalling mechanisms). Substantial progress has been made towards obtaining structural data for the VanS proteins using solution state NMR, and this technique indicates for the first time, a direct interaction between vancomycin and the VanS_A protein. It would therefore be pertinent to focus on firstly assigning the residues in the VanS sensor domain involved in binding.

Towards this goal, ¹⁵N-labelled VanS proteins could be assigned without additional labelling by using e.g. 3D HSQC-TOCSY or HSQC-NOESY experiments (Marion *et al.*, 1989a; 1989b; Zuiderweg & Fesik, 1989). These assign proton spin systems to a specific residue and allow assignment of potentially overlapping peaks using a series of 2D ¹H-¹⁵N slices, edited with respect to the frequency of the ¹⁵N heteronucleus, in a third dimension. Increased protein yields (≥ 1 mM) of VanS_A and VanS_{SC} would be required to conduct these experiments, since a resolvable HSQC spectrum must be collected in around one hour, and typically, experiments involve 32 or more individual HSQC slices. Protein yields of VanS_A could be improved by optimising expression protocols, e.g. by further increasing cell density prior to induction (as suggested by Sivashanmugam *et al.*, 2009; see section 4.7.2). For VanS_{SC}, improvements are required in the level of soluble expression, which could be achieved through codon-optimisation of the gene, or using affinity tags that aid solubility such as MBP (e.g. in the pMAL system, see section 4.7.1).

Perhaps a simpler strategy to assign residue types to specific peaks in the VanS HSQC spectra could even be a selective ‘unlabelling’ approach (Krishnarjuna *et al.*, 2011). In this approach, a specific amino acid is ‘unlabelled’ by feeding the host bacteria ¹⁵N-labelled ammonium chloride as the sole source of nitrogen, along with the amino acid to be assigned, in unlabelled form. This leads to the selected amino acids in the protein being unlabelled and

as a result of which, cross-peaks from these residues disappear in the HSQC spectrum. This route could be highly beneficial to selectively ‘unlabel’ the tryptophan residues in the VanS_{SC} sensor domain, to confirm whether the peak shifts observed at ~10 ppm (in Figure 5.4.1.9F) result from interaction of vancomycin with the exposed Trp-41 residue in the VanS_{SC} sensor loop.

Alternatively, if the protein can be expressed with ¹³C and ¹⁵N labels, triple-resonance NMR experiments such as HNCO, HN(CA)CO, HNCA, and HN(CO)CA (Grzesiek & Bax, 1992) could be conducted, which would provide greater sensitivity and complete sequential assignment. The experiments are named according to the nuclei involved in the experiment, and the order of nuclei in the name gives the sequence for the path of magnetisation. For instance the HNCO experiment provides the connectivities between the amide proton of a residue with the carbonyl carbon of the preceding residues. This experiment is often used in tandem with HN(CA)CO, in which the amide resonance of a residue is correlated with the carbonyl carbon of the same residue, as well as that of the preceding residues. In this way, triple-resonance experiments can provide assignment of the residue type (including side-chain resonances) and their connectivity in the protein sequence (often referred to as ‘walking’ along the backbone of the polypeptide).

Assuming that assignment is feasible, the high quality of the HSQC spectra obtained here, opens the door to numerous structural studies of this protein. For example, further in-depth studies could be conducted on the mechanistic details of ligand binding, and its effect upon the structure and dynamics of the protein. This could then allow identification of those structural motifs which can bind to and activate the VanS kinase, leading to production of resistance genes.

In addition, a promising avenue for future work that does not depend on assignment, is the ability to use the NMR titration assay to screen vancomycin-based antibiotics and fragments thereof, e.g. the glycopeptide aglycone, disaccharide moieties, etc. to identify other ligands for this Two-Component System. A titration curve of chemical shift vs. concentration of ligand could be fitted from this data, to obtain a value for the dissociation constant of each ligand (K_D), provided enough ligand concentrations are tested.

Furthermore, to support NMR-based (and fluorescence-based) titration data, other biophysical techniques could also be conducted. For example, SPR and ITC techniques are applicable to membrane proteins, and can provide thermodynamic and kinetic data for ligand binding (Patching, 2014; Rajarathnam & Rösger, 2014). SPR ligand-binding assays are label-free and conventionally involve immobilisation of a receptor (reconstituted in lipid) onto a sensor chip surface whilst an analyte solution containing the interacting molecule flows over the sensor. Binding is detected by measuring small differences in the refractive index due to changes in thickness at the sensor surface (Whelan *et al.*, 2002). Although many experimental procedures exist for SPR measurements, one method to analyse VanS-antibiotic binding could be to apply detergent-solubilised His-tagged VanS proteins to a functionalised nickel surface (Giess *et al.*, 2004) (similar to that in IMAC, see Figure 6.6.1). The detergent solution could then be diluted and exchanged for lipids (to form a bilayer), to study binding to the VanS sensor on addition of an antibiotic-containing analyte solution.

In the case of ITC experiments, the thermodynamics of binding between VanS proteins and antibiotic ligands could be studied in detergent micelles, provided that titrations are controlled to avoid protein-detergent interactions affecting the result. ITC techniques can be powerful tools e.g. Sikora & Turner, (2005), analysed the oligomerisation state of a transmembrane protein, EmrE, which like VanS, is believed to be functionally active as a dimer. However ITC data was able to show that the molar ratio of drug molecules that bound to EmrE was 1:1, and therefore oligomerisation was not a requirement for drug binding.

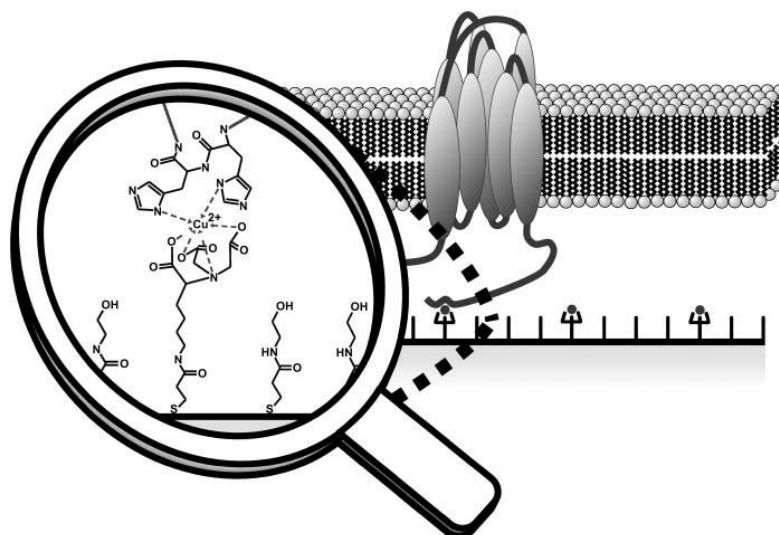


Figure 6.6.1: *Conceptual representation of the protein-tethered lipid bilayer, reproduced from Giess et al., 2004. The interaction between the terminal His-tag of the membrane protein and a Copper-NTA group is magnified at the left side.*

In terms of characterising the functional activity of VanS, the new anti-pHis activity assay developed for histidine kinases by Kee *et al.*, (2013) (see section 3.13.3) shows great promise. This assay could be easily incorporated into the current Western blotting screens, to test for purification of active VanS proteins, prior to structural or ligand binding techniques. Using the ADP/Pi release assays presented here, in conjunction with anti-pHis blotting assays (Kee *et al.*, 2013; Wang *et al.*, 2014), it may also be possible to determine the kinetic parameters for the binding of ATP to VanS such as the Michaelis-Menten constant (K_M), the turnover number of substrate to product (K_{CAT}) and the maximal velocity (V_{Max}).

Furthermore, phosphotransfer and phosphatase assays could be developed based on the ADP/Pi or anti-pHis system, to model the full kinetic profile of the VanRS system.

Finally, the mechanism of signal transduction could be further studied through the use of e.g. GALLEX *in vivo* reporter systems, which analyse the role of hetero-oligomerisation in signal transduction, and allow a second measure of homo-oligomerisation to ToxCAT. It would also be beneficial to couple the observed binding of VanS to vancomycin, with the activation of resistance genes *in vivo*, to assess whether the binding is productive. This could be accomplished by using the *vanH* gene reporter system, developed by Koteva *et al.*, (2010), (as mentioned in section 1.4.2), who previously demonstrated that their vancomycin probe was a bioactive ligand of *S. coelicolor* VanS, as it was able to induce *vanH* gene production.

The new insights gained from these studies into the structure and function of VanS_A and VanS_{SC} proteins, and the recommended plan of future work to support and improve upon this data, should lead to a detailed knowledge of the VanRS two-component system. Further information on the VanRS system could also lead to the rational design of novel inhibitors (like that of amidine vancomycin in section 1.6.2) which, in conjunction with glycopeptide antibiotics, could provide a more targeted therapy against antibiotic resistance mechanisms in these Two-Component Systems.

Bibliography

Aarestrup FM, Kruse H, Tast E, Hammerum AM, Jensen LB (2000)

Associations between the use of antimicrobial agents for growth promotion and the occurrence of resistance among *Enterococcus faecium* from broilers and pigs in Denmark, Finland, and Norway. *Microb Drug Resist* **6**: 63-70

Abraham EP, Chain E (1988) An enzyme from bacteria able to destroy penicillin. 1940. *Rev Infect Dis* **10**: 677-678

Abrahams KA (2011) The enzymology of *Streptococcus pneumoniae* peptidoglycan polymerisation. PhD available via Warwick Research Archive Portal (WRAP), University of Warwick.

Abramoff MD, Magalhaes PJ, Ram SJ (2004) Image Processing with ImageJ. *Biophotonics International* **11**: 36-42

Airola MV, Watts KJ, et al. (2010) Structure of concatenated HAMP domains provides a mechanism for signal transduction. *Structure* **18**: 436-448

Alberts B, Johnson A, Lewis J, et al. (2002) *Membrane Proteins*, 4th Edition edn. New York: Garland Science.

Alekshun MN, Levy SB (2007) Molecular mechanisms of antibacterial multidrug resistance. *Cell* **128**: 1037-1050

Alexandrov A (2001) MBP fusion protein with a viral protease cleavage site: one-step. **30**: 1194-1198

Allen NE, Hobbs JN (1995) Induction of vancomycin resistance in *Enterococcus faecium* by non-glycopeptide antibiotics. *FEMS Microbiology Letters* **132**: 107-114

Arias CA, Murray BE (2009) Antibiotic-Resistant Bugs in the 21st Century — A Clinical Super-Challenge. *New England Journal of Medicine* **360**: 439-443

Arthur M, Depardieu F, et al. (1999) Regulated interactions between partner and non-partner sensors and response regulators that control glycopeptide resistance gene expression in enterococci. *Microbiology* **145** (8): 1849-1858

Arthur M, Depardieu F, Gerbaud G, Courvalin P et al. (1997) The VanS sensor negatively controls VanR-mediated transcriptional activation of glycopeptide resistance genes of Tn1546 and related elements in the absence of induction. *J Bacteriol* **179**: 97-106

- Arthur M, Depardieu F, Molinas C, Reynolds P, Courvalin P (1995)** The vanZ gene of Tn1546 from *Enterococcus faecium* BM4147 confers resistance to teicoplanin. *Gene* **154**: 87-92
- Arthur M, Molinas C, Courvalin P (1992)** The VanS-VanR two-component regulatory system controls synthesis of depsipeptide peptidoglycan precursors in *Enterococcus faecium* BM4147. *J Bacteriol* **174**: 2582-2591
- Arunkumar AI, Kumar TK, Yu C (1997)** Non-specific helix-induction in charged homopolypeptides by alcohols. *Biochim Biophys Acta* **1338**: 69-76
- Ayers RA, Moffat K (2008)** Changes in quaternary structure in the signalling mechanisms of PAS domains. *Biochemistry* **47**: 12078-12086
- Bager F, Madsen M, et al. (1997)** Avoparcin used as a growth promoter is associated with the occurrence of vancomycin-resistant *Enterococcus faecium* on Danish poultry and pig farms. *Prev Vet Med* **31**: 95-112
- Bakheet TM, Doig AJ (2009)** Properties and identification of human protein drug targets. *Bioinformatics* **25**: 451-457
- Ban N, Nissen P, Hansen J, et al. (2000)** The complete atomic structure of the large ribosomal subunit at 2.4 Å resolution. *Science* **289**: 905-20
- Baneyx F (1999)** Recombinant protein expression in *Escherichia coli*. *Curr Opin Biotechnol* **10**: 411-421
- Baptista M, Depardieu F, Courvalin P, Arthur M (1996)** Specificity of induction of glycopeptide resistance genes in *Enterococcus faecalis*. *Antimicrob Agents Chemother* **40**: 2291-2295
- Baptista M, Depardieu F, Reynolds P, Courvalin P, Arthur M (1997)** Mutations leading to increased levels of resistance to glycopeptide antibiotics in VanB-type enterococci. *Mol Microbiol* **25**: 93-105
- Baptista M, Rodrigues P, Depardieu F, et al. (1999)** Single-cell analysis of glycopeptide resistance gene expression in teicoplanin-resistant mutants of a VanB-type *Enterococcus faecalis*. *Mol Microbiol* **32**: 17-28
- Barna J, Williams D, Stone D, et al. (1984)** Structure elucidation of the teicoplanin antibiotics. *Journal of the American Chemical Society* **106**: 4895-4902
- Barreteau H, Kovac A, Boniface A, Sova M, et al. (2008)** Cytoplasmic steps of peptidoglycan biosynthesis. *FEMS Microbiol Rev* **32**: 168-207

- Bates J, Jordens J, Griffiths D (1994)** Farm animals as a putative reservoir for vancomycin-resistant enterococcal infection in man. *J Antimicrob Chemother* **34**: 507-514
- Beauregard DA, Williams DH, Gwynn MN, Knowles DJ (1995)** Dimerization and membrane anchors in extracellular targeting of vancomycin group antibiotics. *Antimicrob Agents Chemother* **39**: 781-785
- Benvenuti M, Mangani S (2007)** Crystallization of soluble proteins in vapor diffusion for x-ray crystallography. *Nat Protocols* **2**: 1633-1651
- Bertani G (2004)** Lysogeny at mid-twentieth century: P1, P2, and other experimental systems. *J Bacteriol* **186**: 595-600
- Berthold DA, (undated)** Top ten tips for producing ¹³C ¹⁵N protein in abundance. *Cambridge Isotopes Laboratory Application Note 15*: 1-4
- Bhairi SM. (1997)** A guide to the properties and uses of detergents in biological systems. Calbiochem-Novabiochem Corporation.
- Bilwes AM, Alex LA, Crane BR, Simon MI (1999)** Structure of CheA, a signal-transducing histidine kinase. *Cell* **96**: 131-141
- Bilwes AM, Quezada CM, Croal LR, Crane BR, Simon MI (2001)** Nucleotide binding by the histidine kinase CheA. *Nat Struct Mol Biol* **8**: 353-360
- Blewett AM (2005)** The Substrate Specificity of Peptidoglycan Biosynthesis Enzymes from *Streptococcus pneumoniae*. Unpublished PhD, University of Warwick.
- Block H, Maertens B, et al. (2009)** Chapter 27 Immobilized-Metal Affinity Chromatography (IMAC): A Review. In *Methods in Enzymology*, Vol. 463, pp 439-473. Academic Press
- Bolanos-Garcia VM, Davies OR (2006)** Structural analysis and classification of native proteins from E. coli commonly co-purified by immobilised metal affinity chromatography. *Biochim Biophys Acta* **1760**: 1304-1313
- Bond PJ, Cuthbertson JM, Deol SS, Sansom MSP, (2004)** MD Simulations of Spontaneous Membrane Protein/Detergent Micelle Formation. *Journal of the American Chemical Society* **126**: 15948-15949
- Boucher HW, Talbot GH, Bradley JS, Edwards JE, et al. (2009)** Bad bugs, no drugs: no ESKAPE! An update from the Infectious Diseases Society of America. *Clin Infect Dis* **48**: 1-12

- Bouhss A, Dementin S, van Heijenoort J, et al. (1999)** Formation of adenosine 5'-tetraphosphate from the acyl phosphate intermediate: a difference between the MurC and MurD synthetases of *Escherichia coli*. *FEBS Lett* **453**: 15-19
- Bouhss A, Trunkfield AE, Bugg TD, Mengin-Lecreulx D (2008)** The biosynthesis of peptidoglycan lipid-linked intermediates. *FEMS Microbiol Rev* **32**: 208-33
- Breukink E, de Kruijff B (2006)** Lipid II as a target for antibiotics. *Nat Rev Drug Discov* **5**: 321-332
- Brosig B, Langosch D (1998)** The dimerization motif of the glycophorin A transmembrane segment in membranes: importance of glycine residues. *Protein Sci* **7**: 1052-1056
- Brumfitt W, Salton MR, Hamilton-Miller JM (2002)** Nisin, alone and combined with peptidoglycan-modulating antibiotics: activity against methicillin-resistant *Staphylococcus aureus* and vancomycin-resistant enterococci. *J Antimicrob Chemother* **50**: 731-734
- Bugg T, Wright G, Dutka-Malen S, Arthur M, et al. (1991)** Molecular basis for vancomycin resistance in *Enterococcus faecium* BM4147: biosynthesis of a depsipeptide peptidoglycan precursor by vancomycin resistance proteins VanH and VanA. *Biochemistry* **30**: 10408-10415
- Bush K (2004)** Antibacterial drug discovery in the 21st century. *Clin Microbiol Infect* **10 Suppl 4**: 10-17
- Butler EK, Davis RM, Bari V, et al. (2013)** Structure-function analysis of MurJ reveals a solvent-exposed cavity containing residues essential for peptidoglycan biogenesis in *Escherichia coli*. *J Bacteriol* **195**: 4639-4649
- Cai M, Huang Y, Sakaguchi K, Clore GM, et al. (1998)** An efficient and cost-effective isotope labeling protocol for proteins expressed in *Escherichia coli*. *J Biomol NMR* **11**: 97-102
- Carpenter EP, Beis K, Cameron AD, Iwata S (2008)** Overcoming the challenges of membrane protein crystallography. *Current Opinion in Structural Biology* **18**: 581-586
- Casino P, Miguel-Romero L, Marina A (2014)** Visualizing autophosphorylation in histidine kinases. *Nat Commun* **5**
- Casino P, Rubio V, Marina A (2009)** Structural insight into partner specificity and phosphoryl transfer in two-component signal transduction. *Cell* **139**: 325-336

- Casino P, Rubio V, Marina A (2010)** The mechanism of signal transduction by two-component systems. *Curr Opin Struct Biol* **20**: 763-771
- CDC. (2013)** Antibiotic resistance threats in the United States, 2013. Centre for Disease Control and Prevention, <http://www.cdc.gov/drugresistance/threat-report-2013/>, Vol. 2013.
- Chain E, Florey HW, Adelaide MB, et al. (1993)** Penicillin as a chemotherapeutic agent. 1940. *Clin Orthop Relat Res*: 3-7
- Champoux JJ (2001)** DNA topoisomerases: structure, function, and mechanism. *Annu Rev Biochem* **70**: 369-413
- Chang S, et al. (2003)** Infection with vancomycin-resistant *Staphylococcus aureus* containing the vanA resistance gene. *N Engl J Med* **348**: 1342-1347
- Chatterjee AN, Perkins HR (1966)** Compounds formed between nucleotides related to the biosynthesis of bacterial cell wall and vancomycin. *Biochem Biophys Res Commun* **24**: 489-494
- Cheung J, Bingman CA, Reingold M, et al. (2008)** Crystal structure of a functional dimer of the PhoQ sensor domain. *J Biol Chem* **283**: 13762-13770
- Cheung J, Hendrickson WA (2009)** Structural analysis of ligand stimulation of the histidine kinase NarX. *Structure* **17**: 190-201
- Cheung J, Hendrickson WA (2010)** Sensor domains of two-component regulatory systems. *Current Opinion in Microbiology* **13**: 116-123
- Clardy J, Fischbach MA, Walsh CT (2006)** New antibiotics from bacterial natural products. *Nat Biotechnol* **24**: 1541-1550
- Cole C, Barber JD, Barton GJ (2008)** The Jpred 3 secondary structure prediction server. *Nucleic Acids Res* **36**: W197-201
- Corey GR, Stryjewski ME, Weyenberg W, et al. (2009)** Telavancin. In *Nat Rev Drug Discov* Vol. 8, pp 929-930. England
- Corrêa DHA, Ramos C, H. I. (2009)** The use of circular dichroism spectroscopy to study protein folding, form and function. *Afr J Biochem Res* **3**: 164-173
- Cymer F, Sanders CR, Schneider D (2013)** Analyzing oligomerization of individual transmembrane helices and of entire membrane proteins in E. coli: A hitchhiker's guide to GALLEX. *Methods Mol Biol* **932**: 259-276
- D'Costa VM, Griffiths E, et al. (2007)** Expanding the soil antibiotic resistome: exploring environmental diversity. *Curr Opin Microbiol* **10**: 481-489

- D'Costa VM, McGrann KM, Hughes DW, Wright GD (2006)** Sampling the antibiotic resistome. *Science* **311**: 374-377
- Damrosch DS (1946)** Chemoprophylaxis and sulfonamide resistant streptococci. *J Am Med Assoc* **130**: 124-128
- Davis BD, Chen LL, Tai PC (1986a)** Misread protein creates membrane channels: an essential step in the bactericidal action of aminoglycosides. *Proc Natl Acad Sci U S A* **83**: 6164-6168
- Davis RL, Smith AL, Koup JR (1986b)** The "red man's syndrome" and slow infusion of vancomycin. *Ann Intern Med* **104**: 285-286
- de Jong LAA, Uges DRA, et al. (2005)** Receptor–ligand binding assays: Technologies and Applications. *Journal of Chromatography B* **829**: 1-25
- De Pascale G, Grigoriadou C, Losi D, et al. (2007)** Validation for high-throughput screening of a VanRS-based reporter gene assay for bacterial cell wall inhibitors. *J Appl Microbiol* **103**: 133-140
- DeDent AC, McAdow M, Schneewind O (2007)** Distribution of protein A on the surface of *Staphylococcus aureus*. *J Bacteriol* **189**: 4473-4484
- Deisenhofer J, Epp O, Miki K, Huber R, Michel H (1985)** Structure of the protein subunits in the photosynthetic reaction centre of *Rhodospseudomonas viridis* at 3 Å resolution. *Nature* **318**: 618-624
- Depardieu F, et al. (2003)** A six amino acid deletion, partially overlapping the VanSB G2 ATP-binding motif, leads to constitutive glycopeptide resistance in VanB-type *Enterococcus faecium*. *Mol Microbiol* **50**: 1069-1083
- Depardieu F, Podglajen I, Leclercq R, et al. (2007)** Modes and modulations of antibiotic resistance gene expression. *Clin Microbiol Rev* **20**: 79-114
- Dephore N, Gould KL, Gygi SP, Kellogg DR (2013)** Mapping and analysis of phosphorylation sites: a quick guide for cell biologists. *Mol Biol Cell* **24**: 535-42
- Diensthuber RP, Bommer M, Gleichmann T, Moglich A (2013)** Full-length structure of a sensor histidine kinase pinpoints coaxial coiled coils as signal transducers and modulators. *Structure* **21**: 1127-1136
- Doyle K (1996)** *Promega Protocols and Applications Guide*, 3rd edn. Madison, WI: Promega Corporation.

- Drew D, Newstead S, Sonoda Y, et al. (2008)** GFP-based optimization scheme for the overexpression and purification of eukaryotic membrane proteins in *Saccharomyces cerevisiae*. *Nat Protocols* **3**: 784-798
- Drlica K, Zhao X (1997)** DNA gyrase, topoisomerase IV, and the 4-quinolones. *Microbiol Mol Biol Rev* **61**: 377-392
- Dutta R, Inouye M (2000)** GHKL, an emergent ATPase/kinase superfamily. *Trends Biochem Sci* **25**: 24-28
- Dutta R, Qin L, Inouye M (1999)** Histidine kinases: diversity of domain organization. *Mol Microbiol* **34**: 633-640
- Eletsky A, Kienhofer A, Pervushin K (2001)** TROSY NMR with partially deuterated proteins. *J Biomol NMR* **20**: 177-180
- Engelman DM, Dixon AM, et al. (2003)** Membrane protein folding: beyond the two stage model. *FEBS Lett* **555**: 122-125
- Evers S, Courvalin P (1996)** Regulation of VanB-type vancomycin resistance gene expression by the VanS(B)-VanR (B) two-component regulatory system in *Enterococcus faecalis* V583. *J Bacteriol* **178**: 1302-1309
- Fabretti F, Theilacker C, Baldassarri L, et al. (2006)** Alanine esters of enterococcal lipoteichoic acid play a role in biofilm formation and resistance to antimicrobial peptides. *Infect Immun* **74**: 4164-4171
- Fagerberg L, Jonasson K, von Heijne G, Uhlen M, Berglund L (2010)** Prediction of the human membrane proteome. *Proteomics* **10**: 1141-1149
- Falke JJ, Hazelbauer GL (2001)** Transmembrane signaling in bacterial chemoreceptors. *Trends Biochem Sci* **26**: 257-265
- FDA. (2008)** Vancomycin Solubility Study. <http://www.fda.gov/downloads/Drugs> Vol. 2013.
- FDA. (2012)** FDA approves first drug to treat multi-drug resistant pulmonary TB. <http://www.fda.gov/NewsEvents/Newsroom/PressAnnouncements> Vol. 2012.
- FDA. (2014)** FDA approves Orbactiv to treat skin infections. <http://www.fda.gov/NewsEvents/Newsroom/PressAnnouncements> Vol. 2014.
- Feldman WH, Hinshaw HC (1948)** Streptomycin; a valuable anti-tuberculosis agent. *Br Med J* **1**: 87-92
- Ferris HU, Dunin-Horkawicz S, Hornig N, Hulko M, et al. (2012)** Mechanism of regulation of receptor histidine kinases. *Structure* **20**: 56-66

- Fielding L (2003)** NMR methods for the determination of protein-ligand dissociation constants. *Curr Top Med Chem* **3**: 39-53
- Fischbach MA, Walsh CT (2009)** Antibiotics for Emerging Pathogens. *Science* **325**: 1089-1093
- Fisher SL, Jiang W, Wanner BL, Walsh CT (1995)** Cross-talk between the histidine protein kinase VanS and the response regulator PhoB. Characterization and identification of a VanS domain that inhibits activation of PhoB. *J Biol Chem* **270**: 23143-23149
- Fisher SL, Kim SK, Wanner BL, Walsh CT (1996)** Kinetic comparison of the specificity of the vancomycin resistance VanS for two response regulators, VanR and PhoB. *Biochemistry* **35**: 4732-4740
- Fleming A (1980)** Classics in infectious diseases: on the antibacterial action of cultures of a penicillium, with special reference to their use in the isolation of *B. influenzae* by Alexander Fleming, Reprinted from the British Journal of Experimental Pathology 10:226-236, 1929. *Rev Infect Dis* **2**: 129-139
- Foury F, Amory A, Goffeau A (1981)** Large-scale purification and phosphorylation of a detergent-treated adenosine triphosphatase complex from plasma membrane of *Saccharomyces cerevisiae*. *Eur J Biochem* **119**: 395-400
- Gao R, Stock AM (2009)** Biological insights from structures of two-component proteins. *Annu Rev Microbiol* **63**: 133-154
- Gao Y (2002)** Glycopeptide antibiotics and development of inhibitors to overcome vancomycin resistance. *Nat Prod Rep* **19**: 100-107
- Garrett DS, Seok YJ, Peterkofsky A, et al. (1997)** Identification by NMR of the binding surface for the histidine-containing phosphocarrier protein HPr on the N-terminal domain of enzyme I of the *Escherichia coli* phosphotransferase system. *Biochemistry* **36**: 4393-4398
- Gasparian ME, Ostapchenko VG, Schulga AA, et al. (2003)** Expression, purification, and characterization of human enteropeptidase catalytic subunit in *Escherichia coli*. *Protein Expression and Purification* **31**: 133-139
- Gautier A, Mott HR, Bostock MJ, et al. (2010)** Structure determination of the seven-helix transmembrane receptor sensory rhodopsin II by solution NMR spectroscopy. *Nat Struct Mol Biol* **17**: 768-774
- Ge M, Kahne D et al. (1999)** Vancomycin derivatives that inhibit peptidoglycan biosynthesis without binding D-Ala-D-Ala. *Science* **284**: 507-511

- Gerding DN (1997)** Is there a relationship between vancomycin-resistant enterococcal infection and Clostridium difficile infection? *Clin Infect Dis* **25 Suppl 2**: S206-210
- Gerhard U (1993a)** Molecular recognition studies on vancomycin group antibiotics. PhD thesis. University of Cambridge.,
- Gerhard U, Mackay JP, Maplestone RA, Williams DH (1993b)** The role of the sugar and chlorine substituents in the dimerization of vancomycin antibiotics. *Journal of the American Chemical Society* **115**: 232-237
- Gidden J, Denson J, Liyanage R, et al. (2009)** Lipid Compositions in *Escherichia coli* and *Bacillus subtilis* During Growth as Determined by MALDI-TOF and TOF/TOF Mass Spectrometry. *Int J Mass Spectrom* **283**: 178-184
- Giegé R, Mikol V (1989)** Crystallogenesi of proteins. *Trends in Biotechnology* **7**: 277-282
- Giess F, Friedrich MG, Heberle J, Naumann RL, Knoll W (2004)** The Protein-Tethered Lipid Bilayer: A Novel Mimic of the Biological Membrane. *Biophysical Journal* **87**: 3213-3220
- Glück JM, Wittlich M, Feuerstein S, Hoffmann et al. (2009)** Integral Membrane Proteins in Nanodiscs Can Be Studied by Solution NMR Spectroscopy. *Journal of the American Chemical Society* **131**: 12060-12061
- Gordeliy VI, Labahn J, et al. (2002)** Molecular basis of transmembrane signalling by sensory rhodopsin II-transducer complex. *Nature* **419**: 484-487
- Gram H (1884)** Über die isolierte Färbung der Schizomyceten in Schnitt- und Trockenpräparaten. *Fortschritte der Medizin* **2**: 185-189
- Grant SG, Jessee J, et al. (1990)** Differential plasmid rescue from transgenic mouse DNAs into *Escherichia coli*. *Proc Natl Acad Sci U S A* **87**: 4645-4649
- Grasberger B, Minton AP, DeLisi C, Metzger H (1986)** Interaction between proteins localized in membranes. *Proc Natl Acad Sci U S A* **83**: 6258-6262
- Grissom-Arnold J, et al. (1997)** Induction of VanA vancomycin resistance genes in *Enterococcus faecalis*: use of a promoter fusion to evaluate glycopeptide and nonglycopeptide induction signals. *Microb Drug Resist* **3**: 53-64
- Grzesiek S, Bax A (1992)** Improved 3D triple-resonance NMR techniques applied to a 31 kDa protein. *Journal of Magnetic Resonance (1969)* **96**: 432-440

- Grzesiek S, Stahl SJ, Wingfield PT, Bax A (1996)** The CD4 determinant for downregulation by HIV-1 Nef directly binds to Nef. Mapping of the Nef binding surface by NMR. *Biochemistry* **35**: 10256-10261
- Gutmann DA, Mizohata E, Newstead S, et al. (2007)** A high-throughput method for membrane protein solubility screening: the ultracentrifugation dispersity sedimentation assay. *Protein Sci* **16**: 1422-1428
- Hajduk PJ, et al. (1997)** One-Dimensional Relaxation- and Diffusion-Edited NMR Methods for Screening Compounds That Bind to Macromolecules. *Journal of the American Chemical Society* **119**: 12257-12261
- Haldimann A, Fisher SL, Daniels LL, et al. (1997)** Transcriptional regulation of the *Enterococcus faecium* BM4147 vancomycin resistance gene cluster by the VanS-VanR two-component regulatory system in *Escherichia coli* K-12. *J Bacteriol* **179**: 5903-5913
- Hall BA, Armitage JP, Sansom MS (2011)** Transmembrane helix dynamics of bacterial chemoreceptors supports a piston model of signalling. *PLoS Comput Biol* **7**: e1002204
- Hall MN, Silhavy TJ (1981)** Genetic analysis of the major outer membrane proteins of *Escherichia coli*. *Annu Rev Genet* **15**: 91-142
- Hanahan D (1983)** Studies on transformation of *Escherichia coli* with plasmids. *J Mol Biol* **166**: 557-580
- Hanahan D (1985)** *DNA Cloning: A Practical Approach*, Vol. 1, Oxford, UK: Oxford University Press.
- Hancock RE, Speert DP (2000)** Antibiotic resistance in *Pseudomonas aeruginosa*: mechanisms and impact on treatment. *Drug Resist Updat* **3**: 247-255
- Handwerger S, Kolokathis A (1990)** Induction of vancomycin resistance in *Enterococcus faecium* by inhibition of transglycosylation. *FEMS Microbiol Lett* **58**: 167-170
- Harbarth S, Samore MH (2005)** Antimicrobial resistance determinants and future control. *Emerg Infect Dis* **11**: 794-801
- Harris CM, Harris TM (1982)** Structure of the glycopeptide antibiotic vancomycin. Evidence for an asparagine residue in the peptide. *Journal of the American Chemical Society* **104**: 4293-4295
- Hastie CJ, McLauchlan HJ, Cohen P (2006)** Assay of protein kinases using radiolabeled ATP: a protocol. *Nat Protocols* **1**: 968-971

- Hauser H (2000)** Short-chain phospholipids as detergents. *Biochimica et Biophysica Acta (BBA) – Biomembranes* **1508**: 164-181
- Havranek JJ, Harbury PB (2003)** Automated design of specificity in molecular recognition. *Nat Struct Biol* **10**: 45-52
- Healy VL, Lessard IA, Roper DI, Knox JR, Walsh CT (2000)** Vancomycin resistance in enterococci: reprogramming of the D-ala-D-Ala ligases in bacterial peptidoglycan biosynthesis. *Chem Biol* **7**: R109-119
- Hefti MH, Francoijs KJ, de Vries SC, Dixon R, Vervoort J (2004)** The PAS fold. A redefinition of the PAS domain based upon structural prediction. *Eur J Biochem* **271**: 1198-1208
- Hiramatsu K (2001)** Vancomycin-resistant *Staphylococcus aureus*: a new model of antibiotic resistance. *Lancet Infect Dis* **1**: 147-155
- Hjelmeland LM, Chrambach A (1984)** Solubilization of functional membrane proteins. *Methods Enzymol* **104**: 305-318
- Hochuli E, Bannwarth W, Dobeli H, Gentz R, Stuber D (1988)** Genetic Approach to Facilitate Purification of Recombinant Proteins with a Novel Metal Chelate Adsorbent. *Nat Biotech* **6**: 1321-1325
- Hochuli E, Döbeli H, Schacher A (1987)** New metal chelate adsorbent selective for proteins and peptides containing neighbouring histidine residues. *Journal of Chromatography A* **411**: 177-184
- Hofmann K, Stoffel W (1993)** TMbase - A database of membrane spanning proteins segments. *Biol Chem Hoppe-Seyler* **374**
- Hong H-J, Hutchings MI, Buttner MJ (2008)** Chapter 14: Vancomycin Resistance VanS/VanR Two Component Systems. In *Bacterial Signal Transduction: Networks and Drug Targets*, Utsumi R (ed), Vol. 631, pp 200-210. New York, USA: Landes Bioscience and Springer Science + Business Media
- Hong HJ, Hutchings MI, Hill LM, Buttner MJ (2005)** The role of the novel Fem protein VanK in vancomycin resistance in *Streptomyces coelicolor*. *J Biol Chem* **280**: 13055-13061
- Hong HJ, Hutchings MI, Neu JM, Wright GD, Paget MS, Buttner MJ (2004)** Characterization of an inducible vancomycin resistance system in *Streptomyces coelicolor* reveals a novel gene (vanK) required for drug resistance. *Mol Microbiol* **52**: 1107-1121

- House of Commons (2009)** Reducing Healthcare Associated Infection in Hospitals in England. UK Parliament, <http://www.publications.parliament.uk> Vol 2013.
- Hsu ST, Breukink E, Tischenko E, de Kruijff B, et al. (2004)** The nisin-lipid II complex reveals a pyrophosphate cage that provides a blueprint for novel antibiotics. *Nat Struct Mol Biol* **11**: 963-967
- Huang P, Liu Q, Scarborough GA, (1998)** Lysophosphatidylglycerol: A Novel Effective Detergent for Solubilizing and Purifying the Cystic Fibrosis Transmembrane Conductance Regulator. *Analytical Biochemistry* **259**: 89-97
- Hulko M, Berndt F, Gruber M, et al. (2006)** The HAMP domain structure implies helix rotation in transmembrane signaling. *Cell* **126**: 929-940
- Hutchings MI, Hong HJ, Buttner MJ (2006)** The vancomycin resistance VanRS two-component signal transduction system of *Streptomyces coelicolor*. *Mol Microbiol* **59**: 923-935
- Huynh TN, Stewart V (2011)** Negative control in two-component signal transduction by transmitter phosphatase activity. *Mol Microbiol* **82**: 275-286
- Iyer HV (2008)** History revisited - Prontosil red. In *J Emerg Med* Vol. 35, pp 209-210. United States
- James RC, Pierce JG, Okano A, Xie J, Boger DL (2012)** Redesign of glycopeptide antibiotics: back to the future. *ACS Chem Biol* **7**: 797-804
- Jansson M, et al. (1996)** High-level production of uniformly ¹⁵N- and ¹³C-enriched fusion proteins in *Escherichia coli*. *J Biomol NMR* **7**: 131-141
- Jeffery CJ, Koshland DE, Jr. (1994)** A single hydrophobic to hydrophobic substitution in the transmembrane domain impairs aspartate receptor function. *Biochemistry* **33**: 3457-3463
- Jenei ZA, Borthwick K, Zammit VA, Dixon AM (2009)** Self-association of transmembrane domain 2 (TM2), but not TM1, in carnitine palmitoyltransferase 1A: role of GXXXG motifs. *J Biol Chem* **284**: 6988-97
- Jin T, Inouye M (1994)** Transmembrane Signaling: Mutational Analysis of the Cytoplasmic Linker Region of Taz1-1, a Tar-EnvZ Chimeric Receptor in *Escherichia coli*. *Journal of Molecular Biology* **244**: 477-481
- Jones DT (1999)** Protein secondary structure prediction based on position-specific scoring matrices. *J Mol Biol* **292**: 195-202
- Jung K, Fried L, Behr S, Heermann R (2012)** Histidine kinases and response regulators in networks. *Curr Opin Microbiol* **15**: 118-124

- Kahne D, Leimkuhler C, Lu W, Walsh C (2005)** Glycopeptide and Lipoglycopeptide Antibiotics. *Chemical Reviews* **105**: 425-448
- Kainosho M (1997)** Isotope labelling of macromolecules for structure determinations. *Nat Struct Biol* **4**: 854-857
- Kapust RB, Waugh DS et al. (2001)** Tobacco etch virus protease: mechanism of autolysis and rational design of stable mutants with wild-type catalytic proficiency. *Protein Eng* **14**: 993-1000
- Kapust RB, Waugh DS (1999)** *Escherichia coli* maltose-binding protein is uncommonly effective at promoting the solubility of polypeptides to which it is fused. *Protein Sci* **8**: 1668-1674
- Kawate T, Gouaux E (2006)** Fluorescence-detection size-exclusion chromatography for precrystallization screening of integral membrane proteins. *Structure* **14**: 673-681
- Kee JM, Oslund RC, et al. (2013)** A pan-specific antibody for direct detection of protein histidine phosphorylation. *Nat Chem Biol* **9**: 416-421
- Kelly SM, Jess TJ, Price NC (2005)** How to study proteins by circular dichroism. *Biochim Biophys Acta* **1751**: 119-139
- Kirst HA, Thompson DG, Nicas TI (1998)** Historical yearly usage of vancomycin. *Antimicrob Agents Chemother* **42**: 1303-1304
- Klare I, Badstubner D et al. (1999)** Decreased incidence of VanA-type vancomycin-resistant enterococci isolated from poultry meat and from fecal samples of humans in the community after discontinuation of avoparcin usage in animal husbandry. *Microb Drug Resist* **5**: 45-52
- Klare I, Heier H, et al. (1995)** *Enterococcus faecium* strains with vanA-mediated high-level glycopeptide resistance isolated from animal foodstuffs and fecal samples of humans in the community. *Microb Drug Resist* **1**: 265-272
- Kleiger G, Grothe R, Mallick P, Eisenberg D (2002)** GXXXG and AXXXA: common alpha-helical interaction motifs in proteins, particularly in extremophiles. *Biochemistry* **41**: 5990-5997
- Koehler J, Sulistijo ES, Sakakura M, Kim HJ, Ellis CD, Sanders CR (2010)** Lysophospholipid micelles sustain the stability and catalytic activity of diacylglycerol kinase in the absence of lipids. *Biochemistry* **49**: 7089-99
- Kohanski MA, Dwyer DJ, Collins JJ (2010)** How antibiotics kill bacteria: from targets to networks. *Nat Rev Microbiol* **8**: 423-435

- Kolb A, Busby S, Buc H, Garges S, Adhya S (1993)** Transcriptional regulation by cAMP and its receptor protein. *Annu Rev Biochem* **62**: 749-795
- Koteva K, Hong H-J, Buttner MJ, Wright GD et al. (2010)** A vancomycin photoprobe identifies the histidine kinase VanSsc as a vancomycin receptor. *Nat Chem Biol* **6**: 327-329
- Krishnamurthy H, Lou H, et al. (2005)** Associative mechanism for phosphoryl transfer: a molecular dynamics simulation of *Escherichia coli* adenylate kinase complexed with its substrates. *Proteins* **58**: 88-100
- Krishnarajuna B, Jaipuria G, Thakur A, D'Silva P, Atreya HS, (2011)** Amino acid selective unlabeled for sequence specific resonance assignments in proteins. *J Biomol NMR* **49**: 39-51
- Krueger-Koplin RD, Sorgen PL, Krueger-Koplin ST et al. (2004)** An evaluation of detergents for NMR structural studies of membrane proteins. *J Biomol NMR* **28**: 43-57
- Kumar A, Schweizer HP (2005)** Bacterial resistance to antibiotics: active efflux and reduced uptake. *Adv Drug Deliv Rev* **57**: 1486-1513
- Kuroda T, Tsuchiya T (2009)** Multidrug efflux transporters in the MATE family. *Biochim Biophys Acta* **1794**: 763-768
- Kwan AH, Mobli M, Gooley PR, King GF, Mackay JP (2011)** Macromolecular NMR spectroscopy for the non-spectroscopist. *FEBS Journal* **278**: 687-703
- Kwun MJ, Novotna G, Hesketh AR, Hill L, Hong HJ (2013)** *In vivo* studies suggest that induction of VanS-dependent vancomycin resistance requires binding of the drug to D-Ala-D-Ala termini in the peptidoglycan cell wall. *Antimicrob Agents Chemother* **57**: 4470-4480
- Laemmli UK (1970)** Cleavage of Structural Proteins during the Assembly of the Head of Bacteriophage T4. *Nature* **227**: 680-685
- Laganowsky A, Reading E, Hopper JTS, Robinson CV (2013)** Mass spectrometry of intact membrane protein complexes. *Nat Protocols* **8**: 639-651
- Lai MH, Kirsch DR (1996)** Induction signals for vancomycin resistance encoded by the vanA gene cluster in *Enterococcus faecium*. *Antimicrob Agents Chemother* **40**: 1645-1648
- Lambert PA (2005)** Bacterial resistance to antibiotics: modified target sites. *Adv Drug Deliv Rev* **57**: 1471-1485
- Larkin MA (2007)** Clustal W and Clustal X version 2.0. **23**: 2947-2948

- Laub MT, Goulian M (2007)** Specificity in two-component signal transduction pathways. *Annu Rev Genet* **41**: 121-145
- Lazar K, Walker S (2002)** Substrate analogues to study cell-wall biosynthesis and its inhibition. *Curr Opin Chem Biol* **6**: 786-793
- Lea WA, Simeonov A (2011)** Fluorescence polarization assays in small molecule screening. *Expert Opin Drug Discov* **6**: 17-32
- Lehmann C, Bunkoczi G, Vertesy L, Sheldrick GM (2002)** Structures of glycopeptide antibiotics with peptides that model bacterial cell-wall precursors. *J Mol Biol* **318**: 723-732
- Letunic I, Copley RR, et al. (2004)** SMART 4.0: towards genomic data integration. *Nucleic Acids Res* **32**: D142-144
- Letunic I, Doerks T, Bork P (2012)** SMART 7: recent updates to the protein domain annotation resource. *Nucleic Acids Res* **40**: D302-305
- Levine DP (2006)** Vancomycin: a history. *Clin Infect Dis* **42 Suppl 1**: S5-12
- Levy SB (2001)** Antibiotic resistance: consequences of inaction. *Clin Infect Dis* **33 Suppl 3**: S124-129
- Levy SB, Marshall B (2004)** Antibacterial resistance worldwide: causes, challenges and responses. *Nat Med* **10**: S122-129
- Lewis K (2013)** Platforms for antibiotic discovery. *Nat Rev Drug Discov* **12**: 371-87
- Liu Y, Manna A, Li R, Martin WE et al. (2001)** Crystal structure of the SarR protein from *Staphylococcus aureus*. *Proceedings of the National Academy of Sciences* **98**: 6877-6882
- Loll PJ, Miller R, Weeks CM, Axelsen PH (1998)** A ligand-mediated dimerization mode for vancomycin. *Chemistry & Biology* **5**: 293-298
- Loll PJ, Shapovalov MV et al. (2009)** Vancomycin forms ligand-mediated supramolecular complexes. *J Mol Biol* **385**: 200-211
- Long AC, Orr DC, Cameron JM, Dunn BM, Kay J (1989)** A consensus sequence for substrate hydrolysis by rhinovirus 3C proteinase. *FEBS Lett* **258**: 75-78
- Lucas LH, Larive CK (2004)** Measuring ligand-protein binding using NMR diffusion experiments. *Concepts in Magnetic Resonance Part A* **20A**: 24-41

- Lukat GS, McCleary WR, Stock AM, Stock JB (1992)** Phosphorylation of bacterial response regulator proteins by low molecular weight phospho-donors. *Proc Natl Acad Sci U S A* **89**: 718-722
- Macfarlane RD (2007)** Analytical Ultracentrifugation: Techniques and Methods Edited by David J. Scott, Stephen E. Harding, and Arthur J. Rowe (University of Nottingham). Royal Society of Chemistry: Cambridge. 2005. *Journal of the American Chemical Society* **129**: 9246-9246
- Mackay JP, Gerhard U, et al. (1994)** Glycopeptide Antibiotic Activity and the Possible Role of Dimerization: A Model for Biological Signaling. *Journal of the American Chemical Society* **116**: 4581-4590
- Maestro B, Novakova L, Lee M et al. (2011)** Recognition of peptidoglycan and beta-lactam antibiotics by the extracellular domain of the Ser/Thr protein kinase StkP from *Streptococcus pneumoniae*. *FEBS Lett* **585**: 357-363
- Mani N, Sancheti P, Jiang ZD et al. (1998)** Screening systems for detecting inhibitors of cell wall transglycosylation in *Enterococcus*. Cell wall transglycosylation inhibitors in *Enterococcus*. *J Antibiot (Tokyo)* **51**: 471-479
- Marina A, Hendrickson WA, Waldburger CD et al. (2001)** Structural and mutational analysis of the PhoQ histidine kinase catalytic domain. Insight into the reaction mechanism. *J Biol Chem* **276**: 41182-41190
- Marina A, Waldburger CD, Hendrickson WA (2005)** Structure of the entire cytoplasmic portion of a sensor histidine-kinase protein. *EMBO J* **24**:4247-59
- Marion D, Driscoll PC, Kay LE, et al. (1989a)** Overcoming the overlap problem in the assignment of proton NMR spectra of larger proteins by use of three-dimensional heteronuclear proton-nitrogen-15 Hartmann-Hahn-multiple quantum coherence and nuclear Overhauser-multiple quantum coherence spectroscopy: application to interleukin 1.β. *Biochemistry* **28**: 6150-6156
- Marion D, Kay LE, Sparks SW, Torchia DA, Bax A (1989b)** Three-dimensional heteronuclear NMR of nitrogen-15 labeled proteins. *Journal of the American Chemical Society* **111**: 1515-1517
- Maris AE, Kaczor-Grzeskowiak M et al. (2005)** Primary and secondary modes of DNA recognition by the NarL two-component response regulator. *Biochemistry* **44**: 14538-14552

- Maris AE, Sawaya MR, Kaczor-Grzeskowiak M, et al. (2002)** Dimerization allows DNA target site recognition by the NarL response regulator. *Nat Struct Biol* **9**: 771-778
- Marley J, Lu M, Bracken C (2001)** A method for efficient isotopic labeling of recombinant proteins. *J Biomol NMR* **20**: 71-75
- Marshall CG, Lessard IA, Park I, Wright GD (1998)** Glycopeptide antibiotic resistance genes in glycopeptide-producing organisms. *Antimicrob Agents Chemother* **42**: 2215-2220
- Martin G, Lazarus A (2000)** Epidemiology and diagnosis of tuberculosis. Recognition of at-risk patients is key to prompt detection. *Postgrad Med* **108**: 42-44, 47-50, 53-44
- Maslennikov I, et al. (2010)** Membrane domain structures of three classes of histidine kinase receptors by cell-free expression and rapid NMR analysis. *Proceedings of the National Academy of Sciences* **107**: 10902-10907
- Mayer M, Meyer B (1999)** Characterization of Ligand Binding by Saturation Transfer Difference NMR Spectroscopy. *Angewandte Chemie International Edition* **38**: 1784-1788
- McCoy CE, Campbell DG, et al. (2005)** MSK1 activity is controlled by multiple phosphorylation sites. *Biochem J* **387**: 507-17
- McPhail D, Cooper A (1997)** Thermodynamics and kinetics of dissociation of ligand-induced dimers of vancomycin antibiotics. *Journal of the Chemical Society, Faraday Transactions* **93**: 2283-2289
- Meyer B, Peters T (2003)** NMR spectroscopy techniques for screening and identifying ligand binding to protein receptors. *Angew Chem Int Ed Engl* **42**: 864-890
- Mir M, Asong J et al. (2011)** The Extracytoplasmic Domain of the *Mycobacterium tuberculosis* Ser/Thr Kinase PknB Binds Specific Muropeptides and Is Required for PknB Localization. *PLoS Pathog* **7**: e1002182
- Miroux B, Walker JE (1996)** Over-production of proteins in *Escherichia coli*: mutant hosts that allow. *J Mol Biol* **260**: 289-298
- Moellering RC, Jr. (2006)** Vancomycin: a 50-year reassessment. *Clin Infect Dis* **42** Suppl 1: S3-4
- Moffatt BA, Studier FW (1987)** T7 lysozyme inhibits transcription by T7 RNA polymerase. *Cell* **49**: 221-227

- Mohammadi T, Bouhss A, de Kruijff B, Breukink E et al. (2011)** Identification of FtsW as a transporter of lipid-linked cell wall precursors across the membrane. *Embo j* **30**: 1425-1432
- Moore JO, Hendrickson WA (2009)** Structural analysis of sensor domains from the TMAO-responsive histidine kinase receptor TorS. *Structure* **17**: 1195-1204
- Morrison J, Yang J-C, Stewart M, Neuhaus D (2003)** Solution NMR Study of the Interaction Between NTF2 and Nucleoporin FxFG Repeats. *Journal of Molecular Biology* **333**: 587-603
- Mulvey MR, Simor AE (2009)** Antimicrobial resistance in hospitals: how concerned should we be? *Cmaj* **180**: 408-415
- Murray BE (2000)** Vancomycin-resistant enterococcal infections. *N Engl J Med* **342**: 710-721
- Möller M, Denicola A (2002)** Study of protein-ligand binding by fluorescence. *Biochemistry and Molecular Biology Education* **30**: 309-312
- Neuhoff V, Arold N, Taube D, Ehrhardt W (1988)** Improved staining of proteins in polyacrylamide gels including isoelectric focusing gels with clear background at nanogram sensitivity using Coomassie Brilliant Blue G-250 and R-250. *Electrophoresis* **9**: 255-262
- Newby ZE (2009)** A general protocol for the crystallization of membrane proteins for X-ray. **4**: 619-637
- Nikaido H (2003)** Molecular basis of bacterial outer membrane permeability revisited. *Microbiol Mol Biol Rev* **67**: 593-656
- Nishikido N (1983)** Estimation of micellar charge or aggregation number from conductivity and counterion-activity measurements. *Journal of Colloid and Interface Science* **92**: 588-591
- Nitanai Y, Kikuchi T, et al. (2009)** Crystal structures of the complexes between vancomycin and cell-wall precursor analogs. *J Mol Biol* **385**: 1422-1432
- Normark BH, Normark S (2002)** Evolution and spread of antibiotic resistance. *J Intern Med* **252**: 91-106
- Novotna G, Hong HJ et al. (2012)** A novel membrane protein, VanJ, conferring resistance to teicoplanin. *Antimicrob Agents Chemother* **56**: 1784-96
- Oliver RC, Lipfert J, Fox DA, Lo RH, Doniach S, Columbus L (2013)** Dependence of Micelle Size and Shape on Detergent Alkyl Chain Length and Head Group. *PLoS ONE* **8**: e62488

- Palumbi SR (2001)** Humans as the world's greatest evolutionary force. *Science* **293**: 1786-1790
- Park JT (1952)** Uridine-5'-pyrophosphate derivatives. II. Isolation from *Staphylococcus aureus*. *J Biol Chem* **194**: 877-884
- Patching SG (2014)** Surface plasmon resonance spectroscopy for characterisation of membrane protein–ligand interactions and its potential for drug discovery. *Biochimica et Biophysica Acta (BBA) - Biomembranes* **1838**: 43-55
- Payne DJ, Gwynn MN, et al. (2007)** Drugs for bad bugs: confronting the challenges of antibacterial discovery. *Nat Rev Drug Discov* **6**: 29-40
- Pearce CM, Gerhard U, Williams DH (1995)** Ligands which bind weakly to vancomycin: studies by ¹³C NMR spectroscopy. *Journal of the Chemical Society, Perkin Transactions 2*: 159-162
- Pereira PM, Filipe SR, Tomasz A, Pinho MG (2007)** Fluorescence ratio imaging microscopy shows decreased access of vancomycin to cell wall synthetic sites in vancomycin-resistant *Staphylococcus aureus*. *Antimicrob Agents Chemother* **51**: 3627-3633
- Perichon B, Courvalin P (2009)** VanA-type vancomycin-resistant *Staphylococcus aureus*. *Antimicrob Agents Chemother* **53**: 4580-4587
- Perry J, Koteva K, Wright G (2011)** Receptor domains of two-component signal transduction systems. *Mol Biosyst* **7**: 1388-1398
- Pirrung MC (1999)** Histidine kinases and two-component signal transduction systems. *Chem Biol* **6**: R167-175
- Podust LM, Ioanoviciu A, Ortiz de Montellano PR (2008)** 2.3 A X-ray structure of the heme-bound GAF domain of sensory histidine kinase DosT of *Mycobacterium tuberculosis*. *Biochemistry* **47**: 12523-12531
- Popieniek PH, Pratt RF (1987)** A fluorescent ligand for binding studies with glycopeptide antibiotics of the vancomycin class. *Analytical Biochemistry* **165**: 108-113
- Porath J, Carlsson JAN et al. (1975)** Metal chelate affinity chromatography, a new approach to protein fractionation. *Nature* **258**: 598-599
- Pryor KD, Leiting B (1997)** High-level expression of soluble protein in *Escherichia coli* using a His6-tag and maltose-binding-protein double-affinity fusion system. *Protein Expr Purif* **10**: 309-319

- Quigley AM (2010)** The Two-Component System Controlling Inducible Glycopeptide Resistance in Enterococci. Unpublished PhD studies, University of Warwick,
- Quintiliani R, Jr., Courvalin P (1996)** Characterization of Tn1547, a composite transposon flanked by the IS16 and IS256-like elements, that confers vancomycin resistance in *Enterococcus faecalis* BM4281. *Gene* **172**: 1-8
- Rajarathnam K, Rosgen J (2014)** Isothermal titration calorimetry of membrane proteins - progress and challenges. *Biochim Biophys Acta* **1838**: 69-77
- Reynolds PE, Courvalin P (2005)** Vancomycin resistance in enterococci due to synthesis of precursors terminating in D-alanyl-D-serine. *Antimicrob Agents Chemother* **49**: 21-25
- Riek R, Fiaux J, Bertelsen EB, et al. (2002)** Solution NMR techniques for large molecular and supramolecular structures. *J Am Chem Soc* **124**: 12144-12153
- Rodger A, Norden B (1997)** *Circular Dichroism and Linear Dichroism*, Oxford, UK: Oxford University Press.
- Rost B, et al. (2004)** The PredictProtein server. *Nucleic Acids Res* **32**: W321-326
- Rubin RP (2007)** A brief history of great discoveries in pharmacology: in celebration of the centennial anniversary of the founding of the American Society of Pharmacology and Experimental Therapeutics. *Pharmacol Rev* **59**: 289-359
- Russ WP, Engelman DM (1999)** TOXCAT: A measure of transmembrane helix association in a biological membrane. *Proceedings of the National Academy of Sciences* **96**: 863-868
- Russ WP, Engelman DM (2000)** The GxxxG motif: a framework for transmembrane helix-helix association. *J Mol Biol* **296**: 911-919
- Russo Krauss I (2013)** An overview of biological macromolecule crystallization. **14**: 11643-11691
- Sachdev D, Chirgwin JM (1998)** Order of fusions between bacterial and mammalian proteins can determine solubility in *Escherichia coli*. *Biochem Biophys Res Commun* **244**: 933-937
- Sambrook J, Fritsch EF, Maniatis T (1989)** *Molecular Cloning: A Laboratory Manual*, Vol. 3, 2nd edn. Cold Spring Harbour, NY: Cold Spring Harbor Laboratory Press.

- Sample I. (2013)** Antibiotic-resistant diseases pose apocalyptic threat. The Guardian, <http://www.theguardian.com/society/2013/jan/23/antibiotic-resistant-diseases-apocalyptic-threat>, Vol. 2013.
- Sauvage E, Kerff F, Terrak M, Ayala JA, Charlier P (2008)** The penicillin-binding proteins: structure and role in peptidoglycan biosynthesis. *FEMS Microbiol Rev* **32**: 234-258
- Schagger H (1991)** Blue native electrophoresis for isolation of membrane protein complexes in. **199**: 223-231
- Schagger H, Cramer WA, von Jagow G (1994)** Analysis of molecular masses and oligomeric states of protein complexes by blue native electrophoresis and isolation of membrane protein complexes by two-dimensional native electrophoresis. *Anal Biochem* **217**: 220-230
- Schatz A, Bugie E, Waksman SA (2005)** Streptomycin, a substance exhibiting antibiotic activity against gram-positive and gram-negative bacteria. 1944. *Clin Orthop Relat Res*: 3-6
- Schleifer KH, Kandler O (1972)** Peptidoglycan types of bacterial cell walls and their taxonomic implications. *Bacteriol Rev* **36**: 407-477
- Schneider D, Engelman DM (2003)** GALLEX, a measurement of heterologous association of transmembrane helices in a biological membrane. *J Biol Chem* **278**: 3105-3111
- Schneider D, Engelman DM (2004)** Motifs of two small residues can assist but are not sufficient to mediate transmembrane helix interactions. *J Mol Biol* **343**: 799-804
- Schumann FH, Riepl H, Maurer T et al. (2007)** Combined chemical shift changes and amino acid specific chemical shift mapping of protein-protein interactions. *J Biomol NMR* **39**: 275-289
- Schwartz RS (2004)** Paul Ehrlich's magic bullets. *N Engl J Med* **350**: 1079-1080
- Sciences NAO. (1980) The Effects on Human Health of Subtherapeutic Use of Antimicrobial Drugs in Animal Feeds.
- Seddon AM (2004)** Membrane proteins, lipids and detergents: not just a soap opera. **1666**: 105-117
- Seed B, Sheen JY (1988)** A simple phase-extraction assay for chloramphenicol acyltransferase activity. *Gene* **67**: 271-277

- Sevvana M, Vijayan V, et al. (2008)** A ligand-induced switch in the periplasmic domain of sensor histidine kinase CitA. *J Mol Biol* **377**: 512-523
- Shah IM, Laaberki MH, Popham DL, Dworkin J (2008)** A eukaryotic-like Ser/Thr kinase signals bacteria to exit dormancy in response to peptidoglycan fragments. *Cell* **135**: 486-496
- Sham LT, Butler EK, Lebar MD, Kahne D et al. (2014)** Bacterial cell wall. MurJ is the flippase of lipid-linked precursors for peptidoglycan biogenesis. *Science* **345**: 220-222
- Sharma A, Schulman SG (1999)** *Introduction to Fluorescence Spectroscopy*, New York: Wiley Interscience.
- Shaw WV (1975)** Chloramphenicol acetyltransferase from chloramphenicol-resistant bacteria. *Methods Enzymol* **43**: 737-755
- Shiraki K, Nishikawa K, Goto Y (1995)** Trifluoroethanol-induced stabilization of the alpha-helical structure of beta-lactoglobulin: implication for non-hierarchical protein folding. *J Mol Biol* **245**: 180-194
- Sikora CW, Turner RJ (2005)** Investigation of Ligand Binding to the Multidrug Resistance Protein EmrE by Isothermal Titration Calorimetry. *Biophysical Journal* **88**: 475-482
- Silva JC, Haldimann A et al. (1998)** In vivo characterization of the type A and B vancomycin-resistant enterococci (VRE) VanRS two-component systems in *Escherichia coli*: a nonpathogenic model for studying the VRE signal transduction pathways. *Proc Natl Acad Sci U S A* **95**: 11951-11956
- Sivashanmugam A, Murray V, Cui C et al. (2009)** Practical protocols for production of very high yields of recombinant proteins using *Escherichia coli*. *Protein Sci* **18**: 936-948
- Skerker JM, Perchuk BS, Siryaporn A et al. (2008)** Rewiring the specificity of two-component signal transduction systems. *Cell* **133**: 1043-1054
- Smith R, Coast J (2013)** The true cost of antimicrobial resistance. *Bmj* **346**: f1493
- Smyth DR, Mrozkiewicz MK, McGrath WJ et al. (2003)** Crystal structures of fusion proteins with large-affinity tags. *Protein Sci* **12**: 1313-1322
- Soloman E, Berg L, Martin D (1999)** *Biology*, 5th Edition edn.: Saunders College Publishing.

- Stock AM, Robinson VL, Goudreau PN (2000)** Two-component signal transduction. *Annu Rev Biochem* **69**: 183-215
- Studier FW (2005)** Protein production by auto-induction in high density shaking cultures. *Protein Expr Purif* **41**: 207-234
- Studier FW, Moffatt BA (1986)** Use of bacteriophage T7 RNA polymerase to direct selective high-level expression. *J Mol Biol* **189**: 113-130
- Sujatha S, Prahraj I (2012)** Glycopeptide resistance in gram-positive cocci: a review. *Interdiscip Perspect Infect Dis* **2012**: 781679
- Szurmant H, White RA, Hoch JA (2007)** Sensor complexes regulating two-component signal transduction. *Curr Opin Struct Biol* **17**: 706-715
- Tanaka T, Saha SK, Tomomori C et al. (1998)** NMR structure of the histidine kinase domain of the E. coli osmosensor EnvZ. *Nature* **396**: 88-92
- Taylor BL, Zhulin IB (1999)** PAS domains: internal sensors of oxygen, redox potential, and light. *Microbiol Mol Biol Rev* **63**: 479-506
- Tian C, Karra MD, Ellis CD, Jacob J et al. (2005)** Membrane protein preparation for TROSY NMR screening. *Methods Enzymol* **394**: 321-334
- Tipper DJ, Strominger JL (1965)** Mechanism of action of penicillins: a proposal based on their structural similarity to acyl-D-alanyl-D-alanine. *Proc Natl Acad Sci U S A* **54**: 1133-1141
- Tomomori C, Tanaka T, Dutta R et al. (1999)** Solution structure of the homodimeric core domain of *Escherichia coli* histidine kinase EnvZ. *Nat Struct Biol* **6**: 729-734
- Towbin H, Staehelin T, Gordon J (1979)** Electrophoretic transfer of proteins from polyacrylamide gels to nitrocellulose. *Proc Natl Acad Sci U S A* **76**: 4350-54
- Trajtenberg F, Grana M, Ruetalo N, Botti H, Buschiazio A (2010)** Structural and enzymatic insights into the ATP binding and autophosphorylation mechanism of a sensor histidine kinase. *J Biol Chem* **285**: 24892-24903
- Treptow NA, Shuman HA (1985)** Genetic evidence for substrate and periplasmic-binding-protein recognition by the. *J Bacteriol* **163**: 654-660
- Ulijasz AT, Falk SP, Weisblum B (2009)** Phosphorylation of the RitR DNA-binding domain by a Ser-Thr phosphokinase: implications for global gene regulation in the streptococci. *Mol Microbiol* **71**: 382-390

- Ulijasz AT, Grenader A, Weisblum B (1996)** A vancomycin-inducible lacZ reporter system in *Bacillus subtilis*: induction by antibiotics that inhibit cell wall synthesis and by lysozyme. *J Bacteriol* **178**: 6305-6309
- Uttley AH, George RC, Naidoo J et al. (1989)** High-level vancomycin-resistant enterococci causing hospital infections. *Epidemiol Infect* **103**: 173-181
- Vannuffel P, Cocito C (1996)** Mechanism of action of streptogramins and macrolides. *Drugs* **51 Suppl 1**: 20-30
- Veesler D, Blangy S, et al. (2008)** There is a baby in the bath water: AcrB contamination is a major problem in membrane-protein crystallization. *Acta Crystallogr Sect F Struct Biol Cryst Commun* **64**: 880-885
- Vollmer W, Blanot D, de Pedro MA (2008)** Peptidoglycan structure and architecture. *FEMS Microbiol Rev* **32**: 149-167
- von Heijne G (1992)** Membrane protein structure prediction. Hydrophobicity analysis and the positive-inside rule. *J Mol Biol* **225**: 487-494
- Wagner S, Klepsch MM et al. (2008)** Tuning *Escherichia coli* for membrane protein overexpression. *Proc Natl Acad Sci U S A* **105**: 14371-14376
- Walsh C (2003)** Where will new antibiotics come from? *Nat Rev Micro* **1**: 65-70
- Walsh CT, Fisher SL, Park IS, Prahalad M, Wu Z (1996)** Bacterial resistance to vancomycin: five genes and one missing hydrogen bond tell the story. *Chem Biol* **3**: 21-28
- Walsh CT, Wencewicz TA (2014)** Prospects for new antibiotics: a molecule-centered perspective. *J Antibiot* **67**: 7-22
- Walsh JP, Bell RM (1986)** sn-1,2-Diacylglycerol kinase of *Escherichia coli*. Structural and kinetic analysis of the lipid cofactor dependence. *J Biol Chem* **261**: 15062-15069
- Wampler DE, Westhead EW (1968)** Two aspartokinases from *Escherichia coli*. Nature of the inhibition and molecular. *Biochemistry* **7**: 1661-1671
- Wang B, Zhao A, Novick RP, Muir TW (2014)** Activation and inhibition of the receptor histidine kinase AgrC occurs through opposite helical transduction motions. *Mol Cell* **53**: 929-940
- Wang J, Soisson SM, Young K et al. (2006)** Platensimycin is a selective FabF inhibitor with potent antibiotic properties. *Nature* **441**: 358-361

- Wang S (2012)** Chapter 15: Protein Phosphorylation in Human Health. In *Bacterial Two-Component Systems: Structures and Signaling Mechanisms*, Huang C (ed). InTech
- Ward A, Rutherford NG, Henderson PJF et al. (2000)** Chapter 6: The amplified expression, identification, purification, assay and properties of histidine-tagged bacterial membrane transport proteins. In *Membrane Transport : A Practical Approach*, Baldwin SA (ed), pp 141-166. Oxford, UK: Oxford University Press
- Wagh DS (2011)** An overview of enzymatic reagents for the removal of affinity tags. *Protein Expr Purif* **80**: 283-293
- Webb MR (1992)** A continuous spectrophotometric assay for inorganic phosphate and for measuring. *Proc Natl Acad Sci U S A* **89**: 4884-4887
- Wegener HC (2003)** Antibiotics in animal feed and their role in resistance development. *Curr Opin Microbiol* **6**: 439-445
- Whelan RJ, Wohland T, Neumann L et al. (2002)** Analysis of biomolecular interactions using a miniaturized surface plasmon resonance sensor. *Anal Chem* **74**: 4570-4576
- Whitmore L, Wallace BA (2004)** DICHROWEB: an online server for protein secondary structure analyses from circular dichroism spectroscopic data. *Nucleic Acids Research* **32**: W668-W673
- WHO. (2014a)** Ebola Virus Disease outbreak - west africa.
http://www.who.int/csr/don/2014_09_04_ebolavirus/en/, Vol. 2014.
- WHO. (2014b)** Antimicrobial resistance: global report on surveillance 2014.
<http://www.who.int/drugresistance/documents/surveillancereport/en> Vol 2014
- Wikström M (2005)** Chapter 14: Inhibitors of Mitochondrial F1-ATPase. In *Biophysical and Structural Aspects of Bioenergetics*, Wikström M (ed), pp 338-339. Cambridge, UK: Royal Society of Chemistry
- Williams DH, Williamson MP et al. (1983)** Detailed binding sites of the antibiotics vancomycin and ristocetin A: determination of intermolecular distances in antibiotic/substrate complexes by use of the time-dependent NOE. *Journal of the American Chemical Society* **105**: 1332-1339
- Williams MR (2007)** An Investigation into the VanA and VanB Two-Component Systems Responsible for Inducible Vancomycin Resistance in Pathogenic Enterococci. Unpublished PhD. University of Warwick.

- Williams SB, Stewart V (1997)** Discrimination between structurally related ligands nitrate and nitrite controls autokinase activity of the NarX transmembrane signal transducer of *Escherichia coli* K-12. *Mol Microbiol* **26**: 911-925
- Williamson MP (2013)** Using chemical shift perturbation to characterise ligand binding. *Prog Nucl Magn Reson Spectrosc* **73**: 1-16
- Williamson MP, Williams DH (1981)** Structure revision of the antibiotic vancomycin. Use of nuclear Overhauser effect difference spectroscopy. *Journal of the American Chemical Society* **103**: 6580-6585
- Williamson RA, Carr MD et al. (1997)** Mapping the binding site for matrix metalloproteinase on the N-terminal domain of the tissue inhibitor of metalloproteinases-2 by NMR chemical shift perturbation. *Biochemistry* **36**: 13882-13889
- Wilson WD (2002)** Tech.Sight. Analyzing biomolecular interactions. *Science* **295**: 2103-2105
- Wimberly BT, Brodersen DE, Clemons WM, Jr., et al. (2000)** Structure of the 30S ribosomal subunit. *Nature* **407**: 327-339
- Wolanin PM, Thomason PA, Stock JB (2002)** Histidine protein kinases: key signal transducers outside the animal kingdom. *Genome Biol* **3**: Reviews3013
- Wong JK, Gunthard HF, Havlir DV et al. (1997)** Reduction of HIV-1 in blood and lymph nodes following potent antiretroviral therapy and the virologic correlates of treatment failure. *Proc Natl Acad Sci U S A* **94**: 12574-12579
- Wright GD (2005)** Bacterial resistance to antibiotics: enzymatic degradation and modification. *Adv Drug Deliv Rev* **57**: 1451-1470
- Wright GD (2011)** Molecular mechanisms of antibiotic resistance. *Chem Commun (Camb)* **47**: 4055-4061
- Wright GD, Holman TR, Walsh CT (1993)** Purification and characterization of VanR and the cytosolic domain of VanS: A two-component regulatory system required for vancomycin resistance in *Enterococcus faecium* BM4147. *Biochemistry* **32**: 5057-5063
- Wright GD, Molinas C, Arthur M et al. (1992)** Characterization of vanY, a DD-carboxypeptidase from vancomycin-resistant *Enterococcus faecium* BM4147. *Antimicrob Agents Chemother* **36**: 1514-1518
- Wüthrich K (1986)** *NMR of Proteins and Nucleic Acids*, New York: Wiley & Sons.

- Xie J, Boger DL et al. (2011)** A redesigned vancomycin engineered for dual D-Ala-D-ala And D-Ala-D-Lac binding exhibits potent antimicrobial activity against vancomycin-resistant bacteria. *J Am Chem Soc* **133**: 13946-13949
- Xu Z, Horwich AL, Sigler PB (1997)** The crystal structure of the asymmetric GroEL-GroES-(ADP)₇ chaperonin complex. *Nature* **388**: 741-750
- Yamada S, Shiro Y (2008)** Structural basis of the signal transduction in the two-component system. *Adv Exp Med Biol* **631**: 22-39
- Yamada S, Sugimoto H, Kobayashi M et al. (2009)** Structure of PAS-linked histidine kinase and the response regulator complex. *Structure* **17**: 1333-1344
- Yildirim MA, Goh KI, Cusick ME, Barabasi AL, Vidal M (2007)** Drug-target network. *Nat Biotechnol* **25**: 1119-1126
- Young K, Jayasuriya H et al. (2006)** Discovery of FabH/FabF inhibitors from natural products. *Antimicrob Agents Chemother* **50**: 519-526
- Zapf J, Sen U, Madhusudan, Hoch JA, Varughese KI (2000)** A transient interaction between two phosphorelay proteins trapped in a crystal lattice reveals the mechanism of molecular recognition and phosphotransfer in signal transduction. *Structure* **8**: 851-862
- Zhang Z, Hendrickson WA (2010)** Structural Characterization of the Predominant Family of Histidine Kinase Sensor Domains. *Journal of Molecular Biology* **400**: 335-353
- Zlotnick A, Lee A, Bourne CR, Johnson JM, Domanico PL, Stray SJ (2007)** *In vitro* screening for molecules that affect virus capsid assembly (and other protein association reactions). *Nat Protoc* **2**: 490-498
- Zuiderweg ERP, Fesik SW (1989)** Heteronuclear three-dimensional NMR spectroscopy of the inflammatory protein C5a. *Biochemistry* **28**: 2387-2391

Appendix

Table A1: A list of detergent classes tested in these studies and their properties (according to data in the literature).

<i>Detergent (abbreviation)</i>	<i>Type</i>	<i>Mean Aggregation number ('a')</i>	<i>CMC (mM)*</i>	<i>Mean Molecular Weight (Da)⁴</i>	<i>Reagent Source</i>	<i>Data Reference</i>
1,2-dihexanoyl- <i>sn</i> -glycero-3-phosphocholine (C₆-DHPC)	Zwitterionic	19-20	15	453.5	Avanti Polar Lipids	Hauser, (2000)
1,2-diheptanoyl- <i>sn</i> -glycero-3-phosphocholine (C₇-DHPC)	Zwitterionic	25-30	1.4	481.6	Avanti Polar Lipids	Hauser, (2000)
<i>n</i> -dodecyl β-D-maltoside (DDM)	Non-ionic	98	0.17-0.3	510.6	Anatrace	Bhairi, (1997)
<i>n</i> -decyl β-D-maltoside (DM)	Non-ionic	69	1.8	482.6	Anatrace	Oliver <i>et al.</i> , (2013)
<i>n</i> -dodecyl phosphocholine (DPC)	Zwitterionic	56	1.1	351.3	Avanti Polar Lipids	Wüthrich, (1986)
1-myristoyl-2-hydroxy- <i>sn</i> -glycero-3-phosphocholine (LMPC-14)	Zwitterionic	108	0.07-0.12	467.6	Avanti Polar Lipids	Oliver <i>et al.</i> , (2013)
1-palmitoyl-2-hydroxy- <i>sn</i> -glycero-3-[phospho-1'- <i>rac</i> -glycerol] (LPPG)	Anionic	160-170	0.018	506.5	Avanti Polar Lipids	Oliver <i>et al.</i> , (2013)
1-myristoyl-2-hydroxy- <i>sn</i> -glycero-3-[phospho-1'- <i>rac</i> -glycerol] (LMPG-14)	Anionic	55	0.16	478.5	Avanti Polar Lipids	Oliver <i>et al.</i> , (2013)
<i>n</i> -octyl β-D-glucoside (OG)	Non-ionic	84	18-20	292.4	Anatrace	Bhairi, (1997)
Sodium dodecyl sulphate (SDS)	Anionic	62	8-14	293.4	Anatrace	Nishikido (1983)
Triton X-100 (Triton)	Non-ionic	100-155	0.2-0.25	625	Anatrace	Bhairi, (1997)

*All CMCs are reported for conditions of detergent in H₂O from data collected at 298K.

⁴ Average molecular weights (Da) are given for detergents composed of mixtures of different chain length

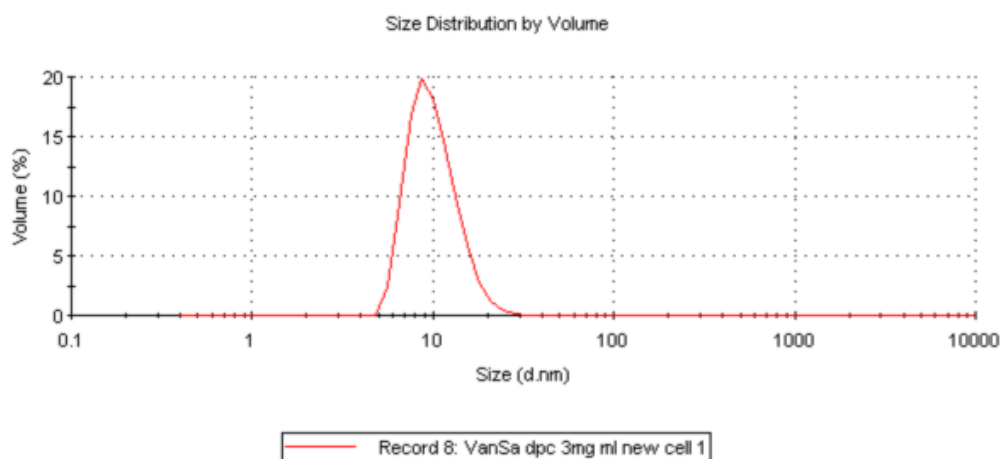


Figure A1: A plot of the volume-size distribution for a sample of VanS_A protein purified in 2 mM DPC detergent, collected at room temperature using a Malvern Nano Zetasizer.

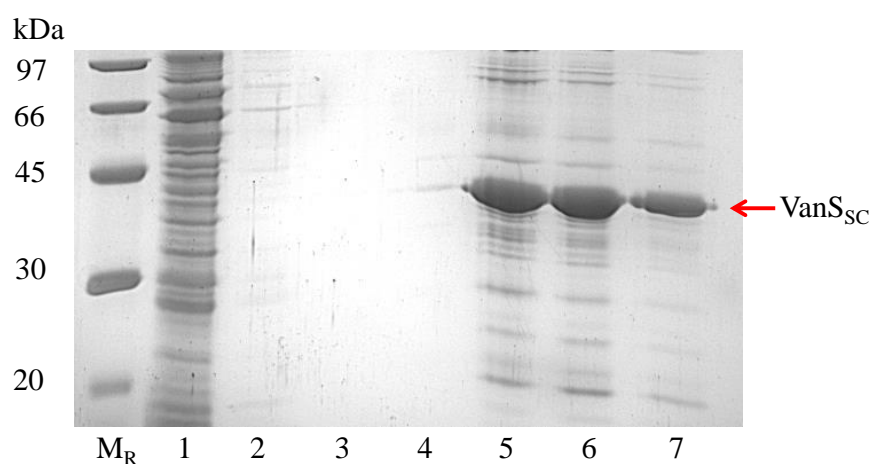


Figure A2: 12% SDS-PAGE gel showing purification of N-His₆-VanS_{sc} by affinity chromatography. Membranes were extracted and solubilised from 6L of expressed cells, in 1% DPC and purified in a buffer containing 0.075% DPC. M_R – Protein ladder (GE), Lane 1 – FT, Lanes 2 – 4 20-40 mM Imidazole wash steps, Lane 5-7 – 300 mM Imidazole elution.

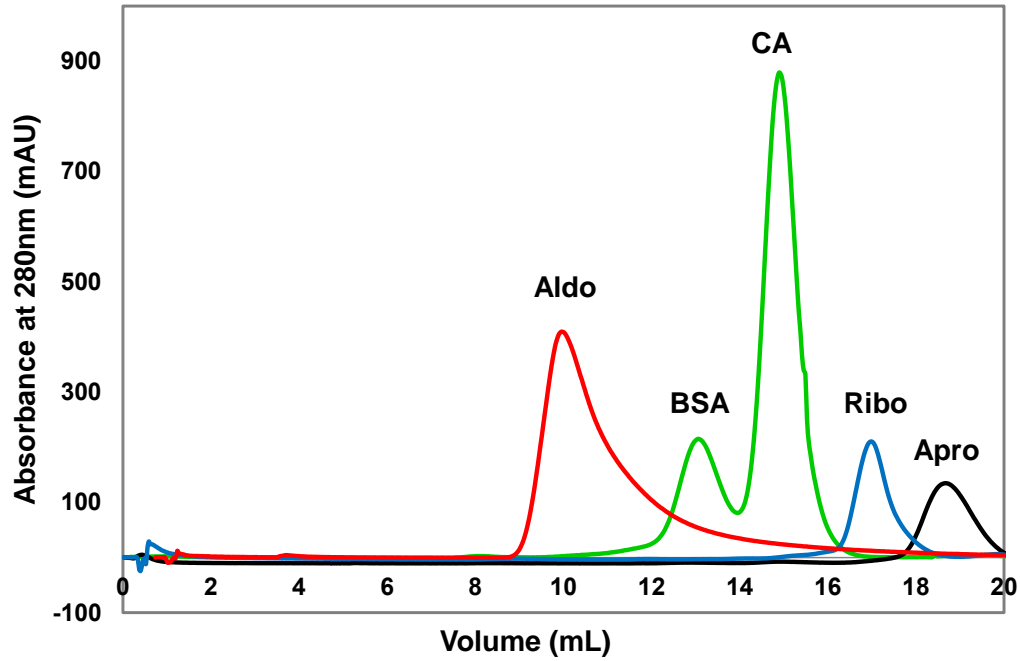


Figure A3: Gel filtration profiles of GE Healthcare standards applied to a Superose 12 10/300GL column, under an isocratic gradient of 100% B. Buffer B: 20 mM HEPES pH 7.8, 300 mM NaCl, 0.075% w/v DPC. Standards were: Aldolase ('Aldo', 158 kDa), Bovine Serum Albumin ('BSA', 66.9 kDa), Carbonic Anhydrase ('CA', 29 kDa), Ribonuclease A ('Ribo', 13.7 kDa) and Aprotinin ('Apro', 6.5 kDa). CA and BSA samples were added in the same sample, all other standards were run separately.

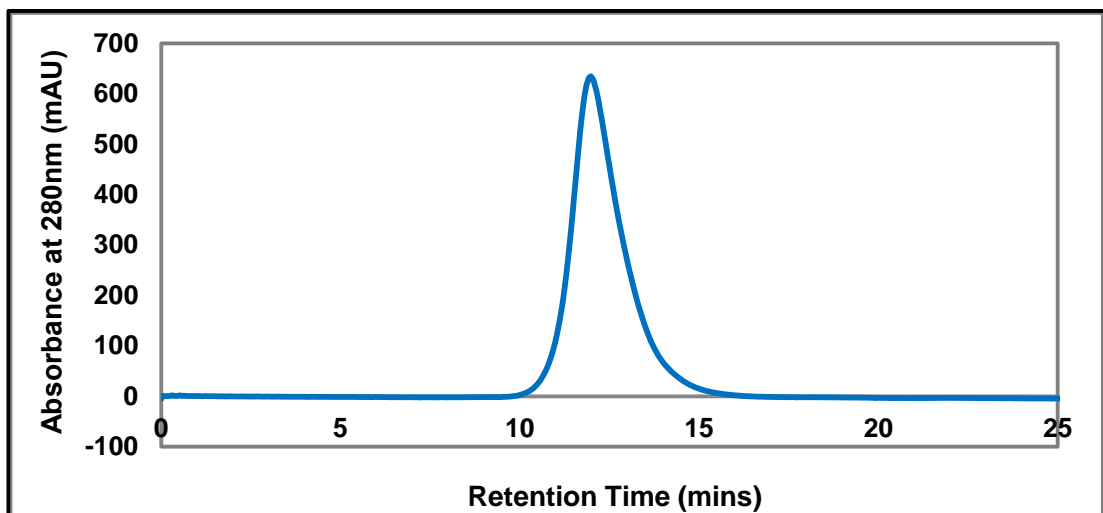


Figure A4: Gel filtration profile of IMAC-purified tag-cleaved Van_SA protein, applied to a Superose 12 10/300 GL column under an isocratic gradient of 100% B. Buffer B: 20 mM HEPES pH 7.8, 300 mM NaCl, 0.075% w/v DPC. The chromatogram shows a single peak and samples were concentrated and used in crystal trials at the SGC (Oxford).

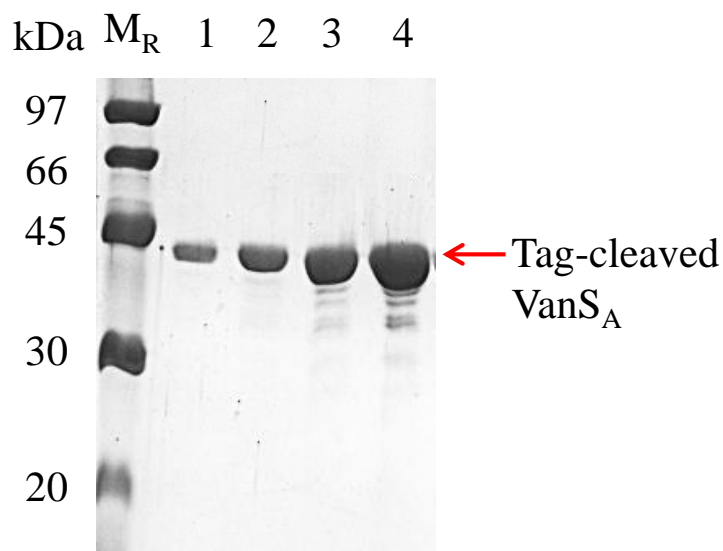


Figure A5: 12% SDS-PAGE gel showing tag-cleaved (wild-type) VanS_A protein after gel filtration and concentration to 200 μ L. Lane 1 – 2 μ g protein, Lane 2 – 4 μ g protein, Lane 3 – 8 μ g, Lane 4 – 12 μ g protein.

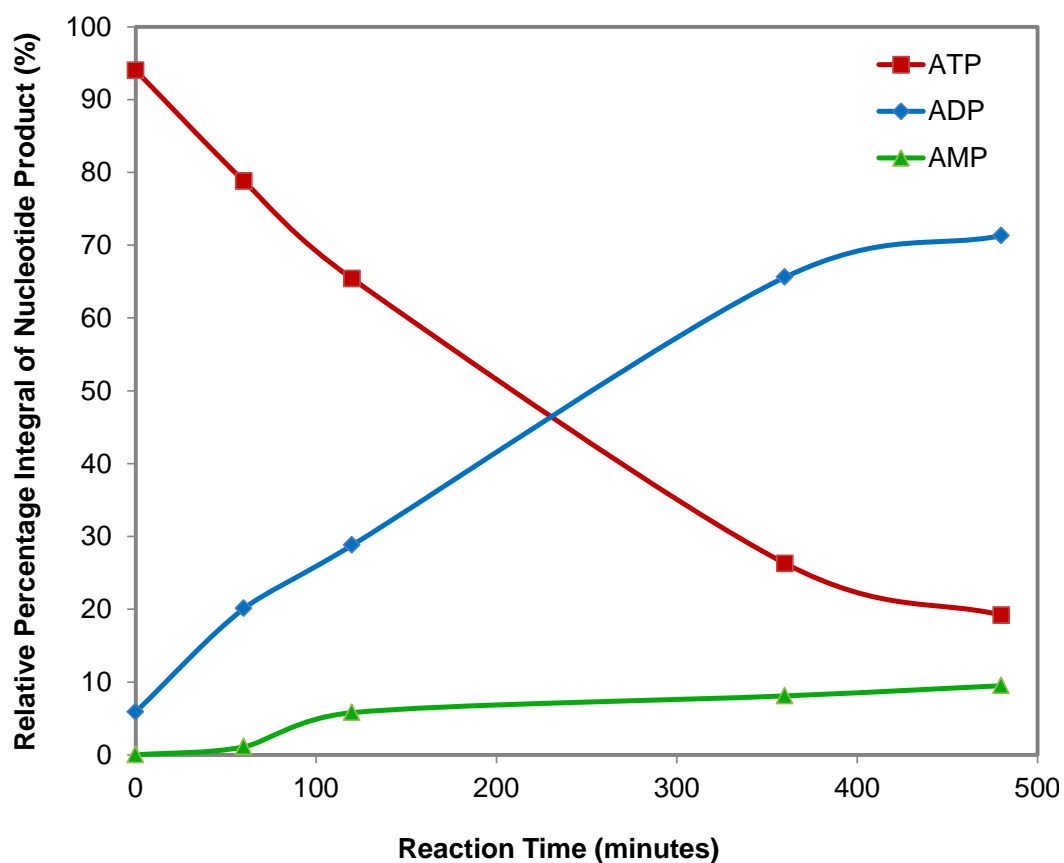


Figure A6: A graph to show the relative percentage of each nucleotide product present over time during turnover of ATP by the VanS_A kinase, plotted from peak integration of anion exchange data. Points were plotted using values in Table 3.11.4.1A and percentage integrals were calculated relative to the total reaction products at each timepoint.

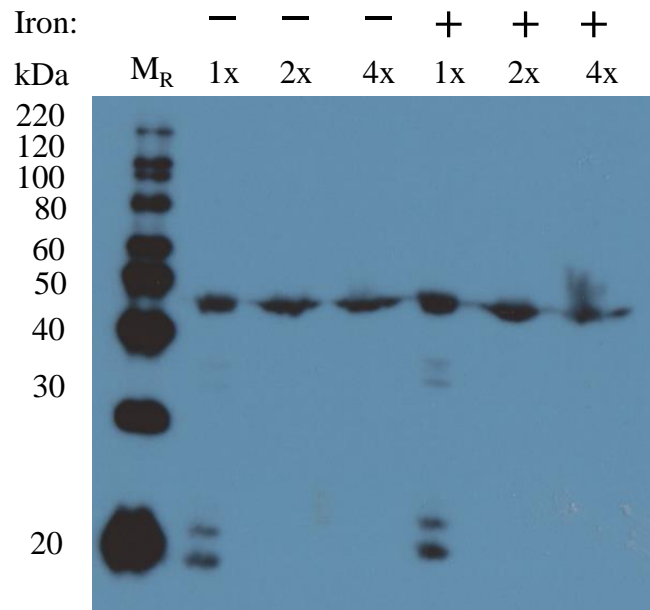


Figure A7: Western blot showing relative expression levels of full-length $VanS_A$ proteins in ^{15}N M9 minimal media. Cell cultures were concentrated (reduced in volume) by a factor of 1x, 2x or 4x, before induction with 0.2 mM IPTG. The effect of adding iron (+) into the minimal media (at 75 μM) was also assessed, against unsupplemented controls (-). M_R – Magic Mark XP His-tagged ladder (Invitrogen).

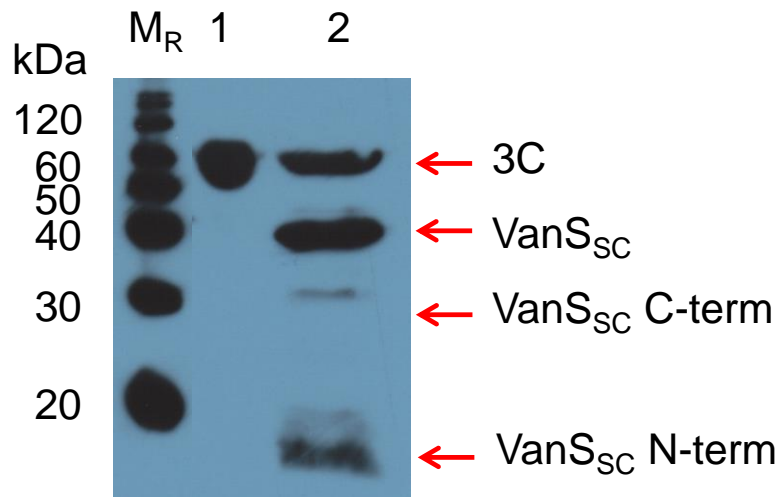


Figure A8: Western blot showing initial digestion products of $VanS_{SC}$ -3C upon 1:1 incubation with 3C protease at room temperature for 4 hours. Key bands are labeled with arrows. M_R - MagicMark XP ladder. Lane 1: 3C protease (~66 kDa), Lane 2: Digestion mixture containing $VanS_{SC}$ -3C and 3C protease.

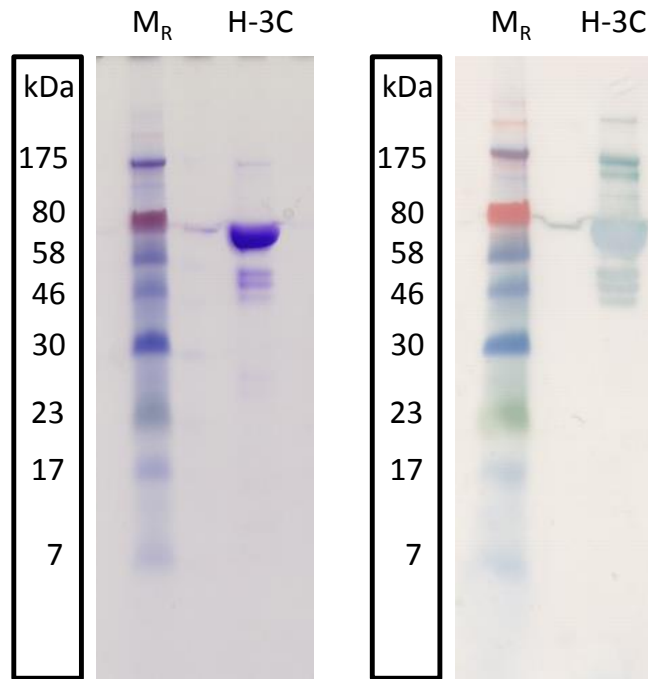


Figure A9: Purified 3C protease applied to a precast 12% Novex Tris-glycine gel (left) and the blotted with anti-MBP (right). M_R - Color Plus Prestained 7-175 kDa Protein (NEB).

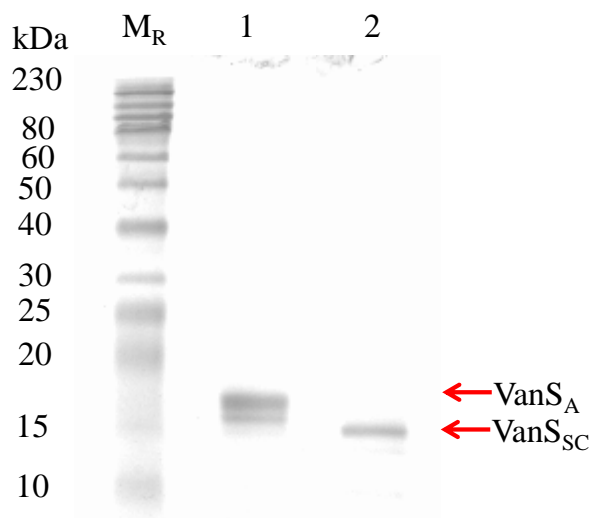


Figure A10: A 12% Tris-glycine gel showing purified N-terminal sensor domains of $VanS_A$ (lane 1) and $VanS_{SC}$ (lane 2) in DPC detergent, after two weeks of NMR analyses at 310K. M_R - ColorPlus Prestained Protein Ladder, Broad Range (10-230 kDa).

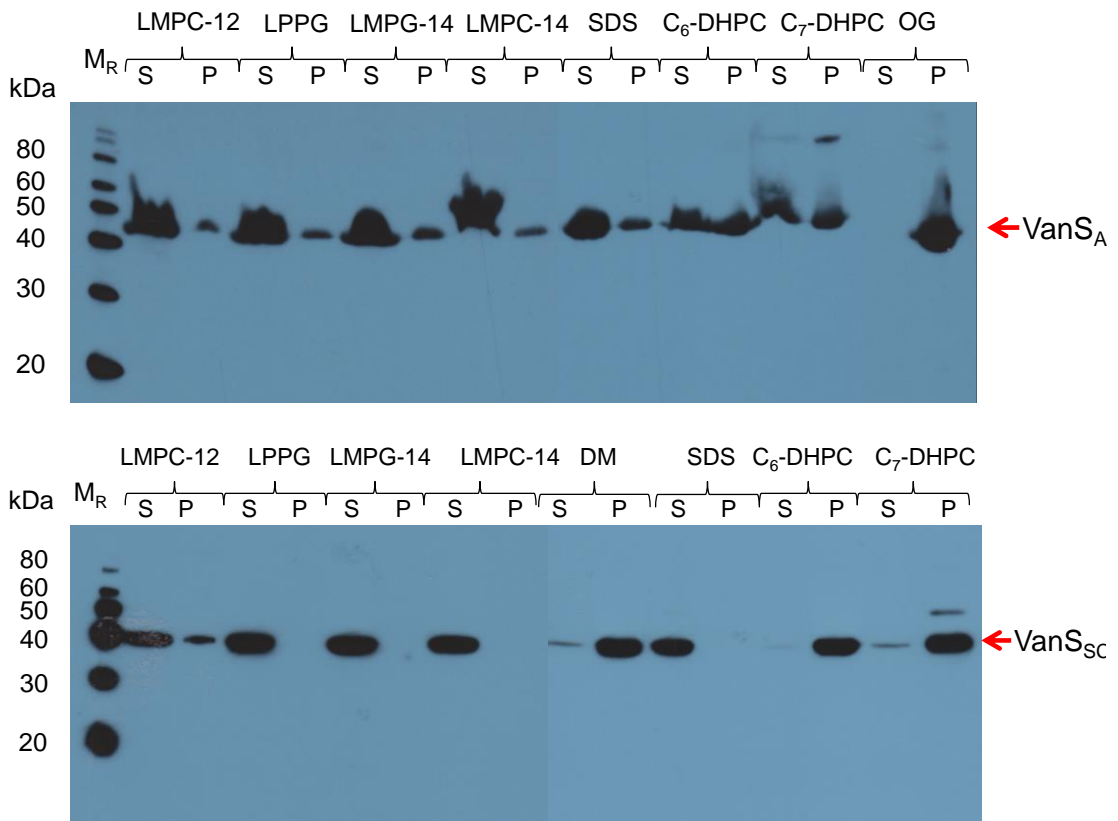


Figure A11: Western blots comparing detergent solubilisation of membrane pellets containing VanS_A (top) or VanS_{SC} (bottom) proteins. All detergents were added to 1% w/v (except OG (1.8%) as it has a higher CMC). S – Soluble supernatant fraction, P – insoluble pellet fraction. VanS band is indicated by a red arrow. M_R – MagicMark ladder (Invitrogen).

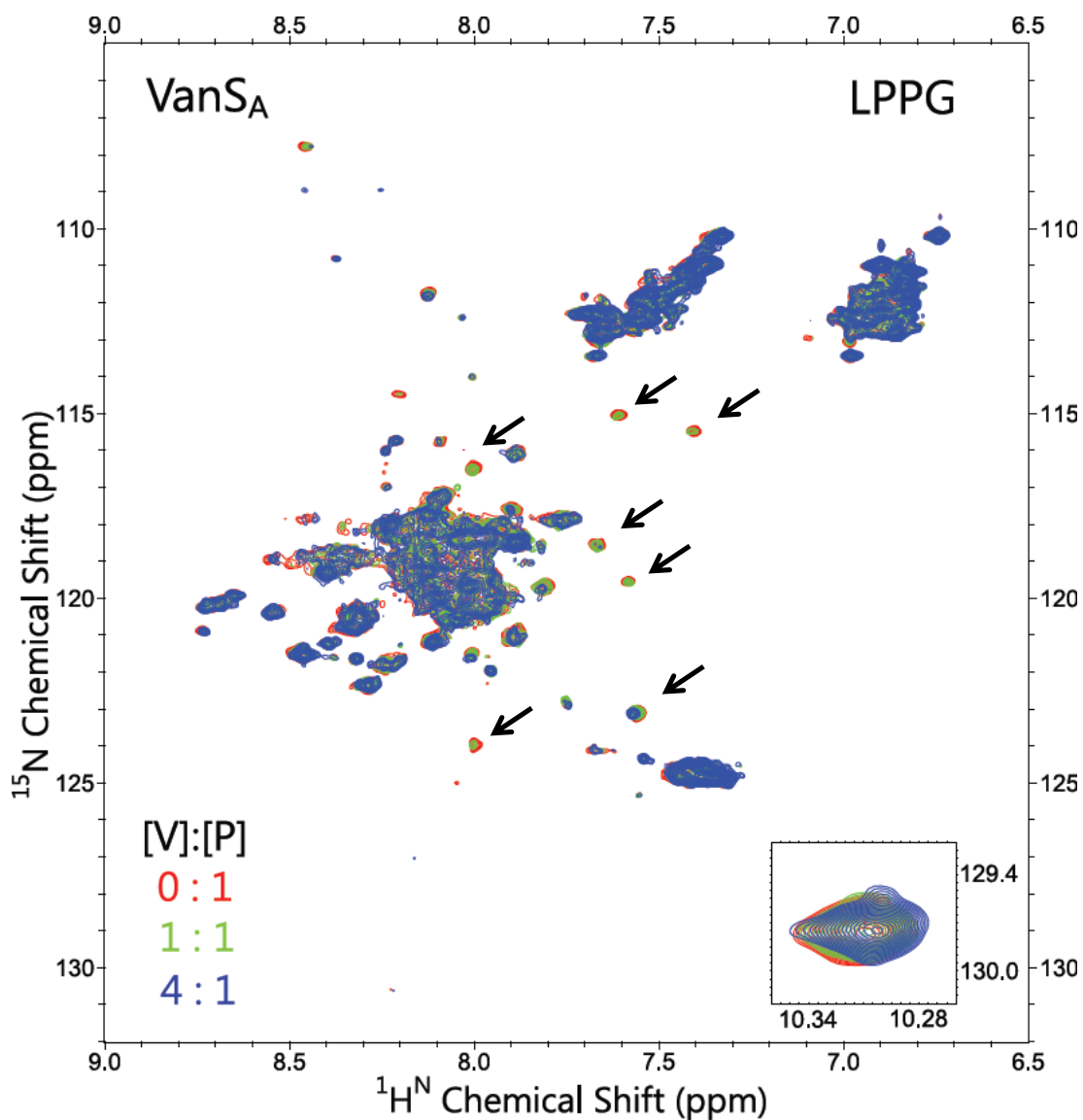


Figure A12: Overlaid 2D ^1H - ^{15}N HSQC of 300 μM VanS_A N-terminal domain solubilised in 50 mM LPPG, 50 mM Sodium acetate pH 4.6, during titration of detergent-solubilised vancomycin. [Vancomycin]:[protein] ratios of 0:1 (red), 1:1 (green), 4:1 (blue). Spectra were collected at 310 K and peaks of interest are highlighted by arrows.

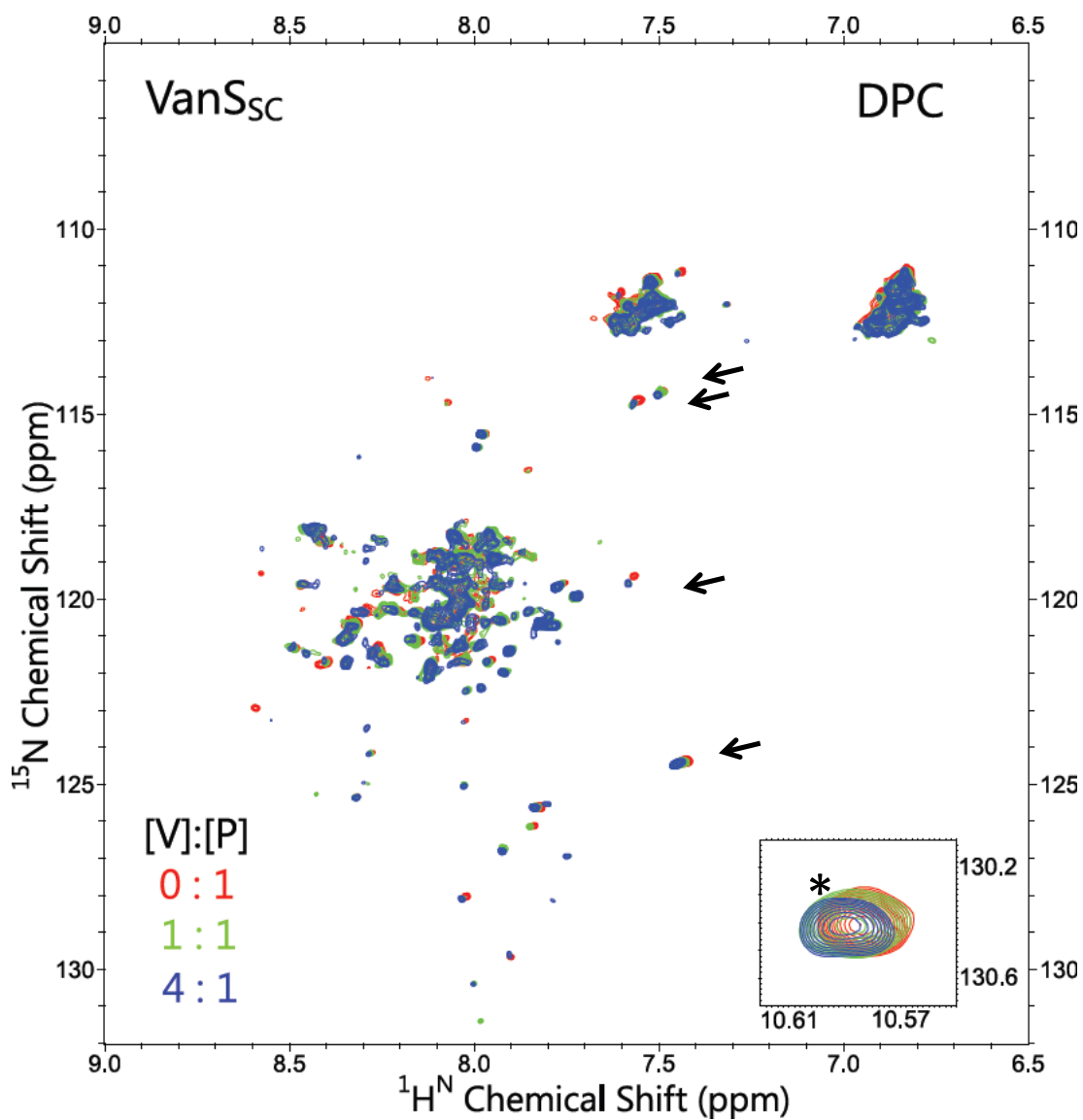


Figure A13: Overlaid 2D ¹H-¹⁵N HSQC spectra of 200 μM VanS_{sc} N-terminal domain solubilised in 50 mM DPC, 20 mM HEPES pH 6.8, during titration of detergent-solubilised vancomycin. [Vancomycin]:[protein] ratios of 0:1 (red), 1:1 (green), 4:1 (blue). Spectra were collected at 310K and peaks of interest are highlighted by arrows.

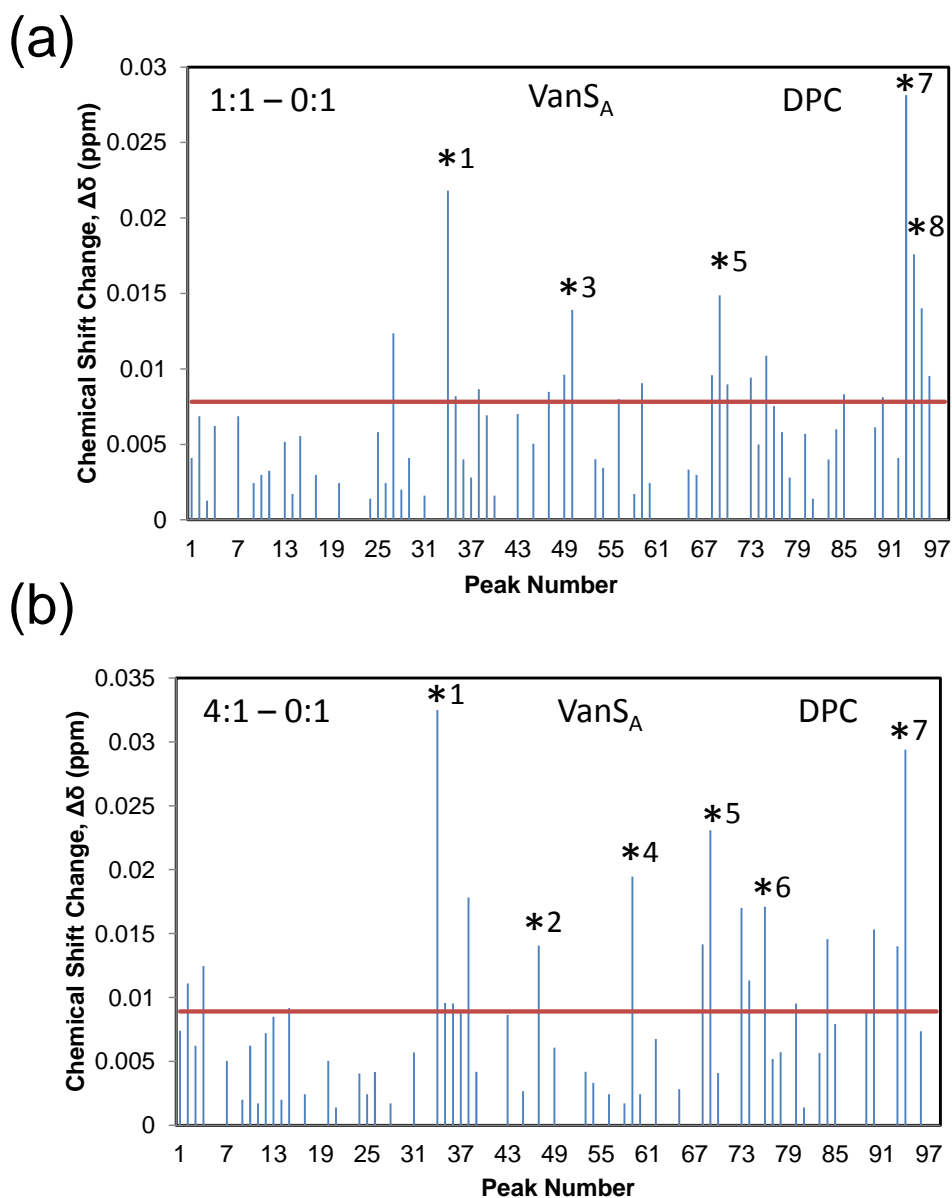


Figure A14: Chemical shift changes for each peak in the ^1H - ^{15}N HSQC spectrum of VanS_A protein in DPC (from Fig. 5.4.1.3A) on addition of vancomycin, represented by a bar chart of peak number (ascending $^1\text{H}^N$) against chemical shift change ($\Delta\delta$). Changes for side-chain and backbone $^1\text{H}^N$ protons were calculated using the equation: $\Delta\delta = \sqrt{0.5 \cdot [\delta_H^2 - (0.14 \cdot \delta_N^2)]}$, against a threshold value (σ , red line). Peaks with significant CSPs are annotated by starring. (A) Chemical shift changes upon adding a 1:1 molar ratio of [vancomycin]:[protein] (B) Chemical shift changes upon adding a 4:1 molar ratio of [vancomycin]:[protein].

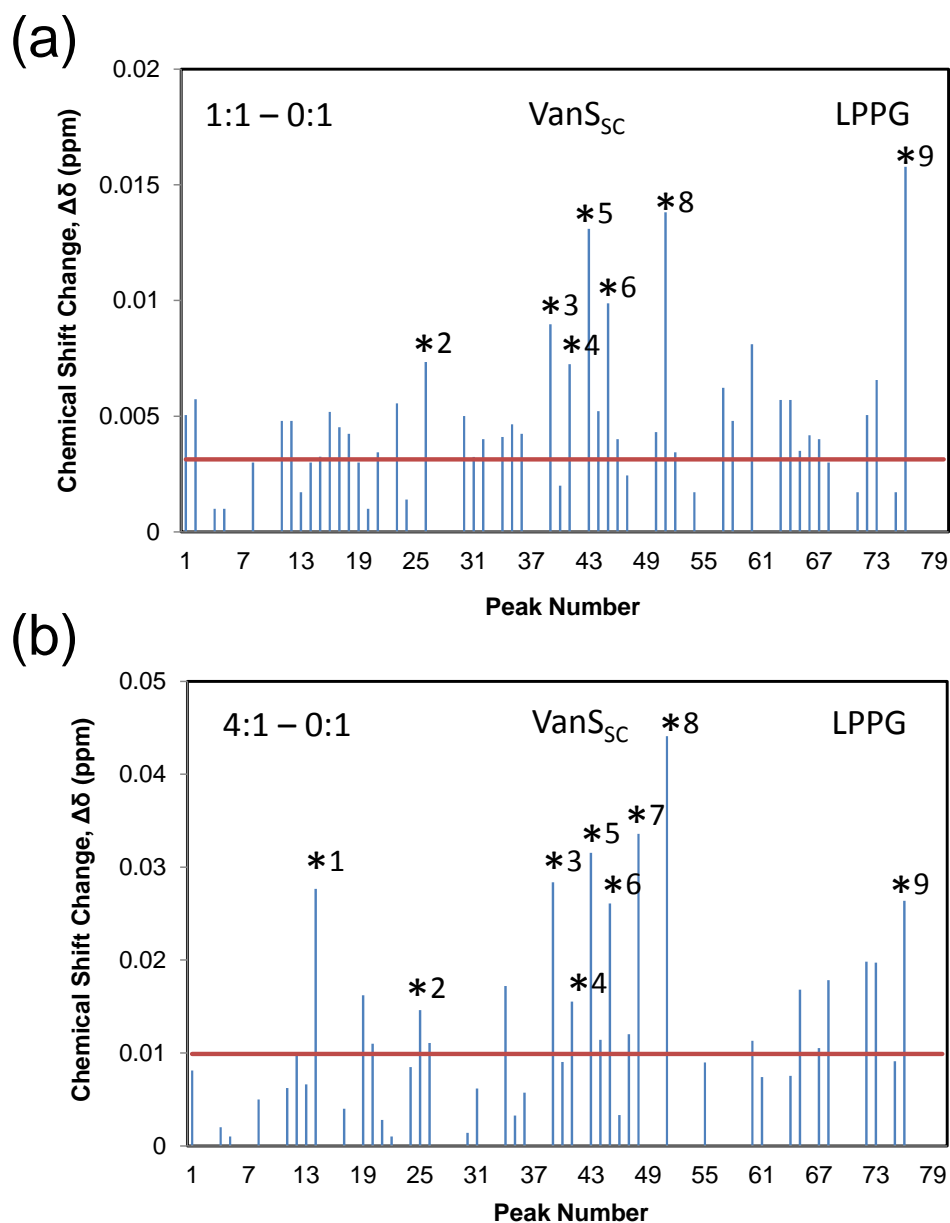


Figure A15: Chemical shift changes for individual peaks in the ^1H - ^{15}N HSQC spectrum of VanS_{SC} protein in LPPG (from Fig. 5.4.1.4) on addition of vancomycin, represented by a bar chart of peak number (ascending $^1\text{H}^{\text{N}}$) against chemical shift change ($\Delta\delta$). Changes for side-chain and backbone $^1\text{H}^{\text{N}}$ protons were calculated using the equation: $\Delta\delta = \sqrt{0.5 \cdot [\delta_{\text{H}}^2 - (0.14 \cdot \delta_{\text{N}}^2)]}$, against a threshold value (σ , red line). Peaks with significant CSPs are annotated by starring. (A) Chemical shift changes upon adding a 1:1 molar ratio of [vancomycin]:[protein] (B) Chemical shift changes upon adding a 4:1 molar ratio of [vancomycin]:[protein].

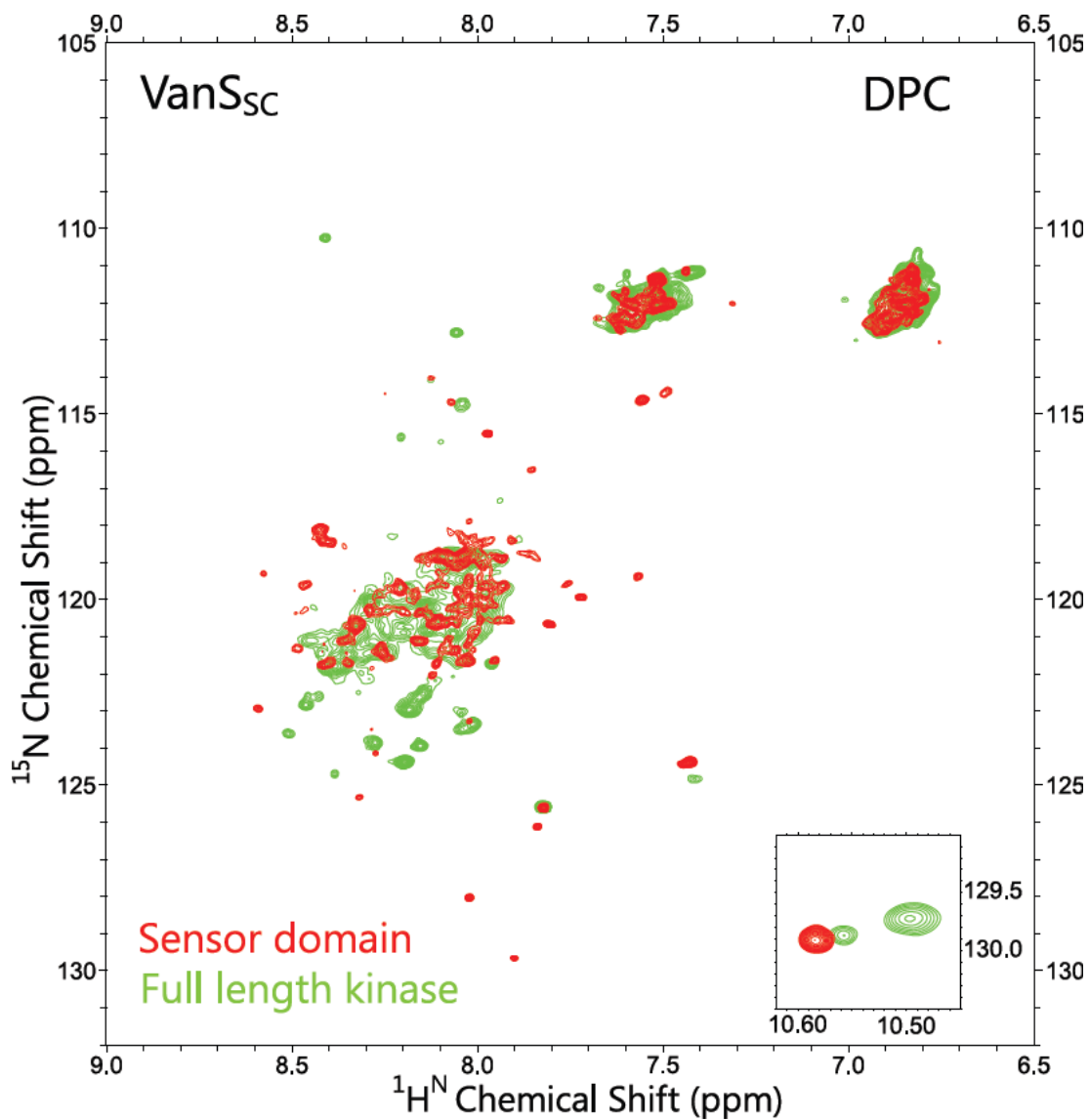


Figure A16: Overlaid 2D ^1H - ^{15}N HSQC of 200 μM VanS_{SC} N-terminal domain (red) or 300 μM full-length protein (green), collected at 310K on a 700 MHz spectrometer. The proteins were both solubilised in 50 mM DPC, 75mM NaCl and 20 mM HEPES pH 6.8.